PATHOMECHANISMS AND TREATMENTS TO PROTECT THE PRETERM, FETAL GROWTH RESTRICTED AND NEONATAL ENCEPHALOPATHIC BRAIN

EDITED BY: Julie Wixey, Tracey Bjorkman, Bobbi Fleiss and Deirdre M. Murray
PUBLISHED IN: Frontiers in Neurology and Frontiers in Pediatrics

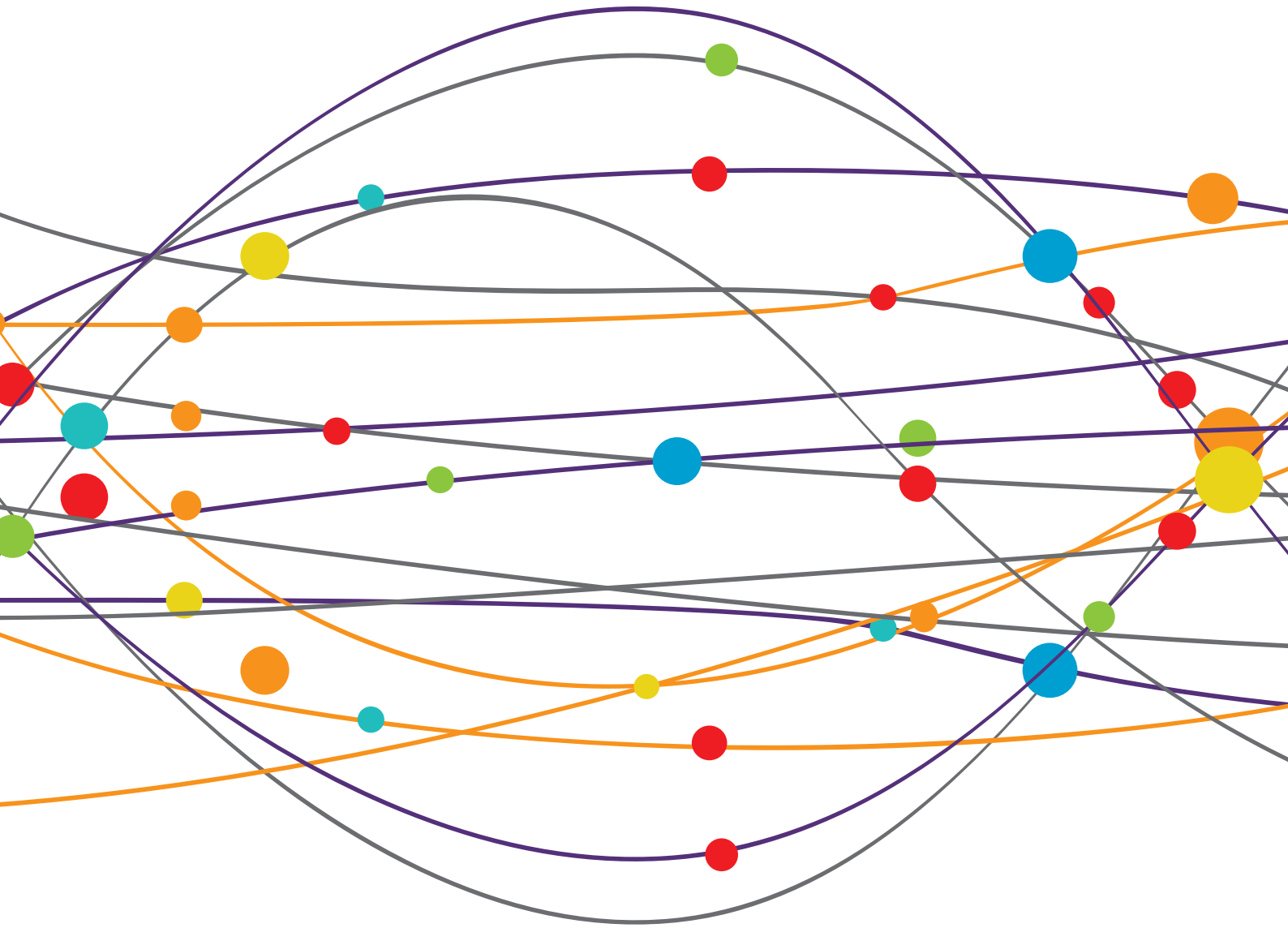

frontiers Research Topics

ISSN 1664-8714
ISBN 978-2-88971-556-5
DOI 10.3389/978-2-88971-556-5

About Frontiers

Frontiers is more than just an open-access publisher of scholarly articles: it is a pioneering approach to the world of academia, radically improving the way scholarly research is managed. The grand vision of Frontiers is a world where all people have an equal opportunity to seek, share and generate knowledge. Frontiers provides immediate and permanent online open access to all its publications, but this alone is not enough to realize our grand goals.

Frontiers Journal Series

The Frontiers Journal Series is a multi-tier and interdisciplinary set of open-access, online journals, promising a paradigm shift from the current review, selection and dissemination processes in academic publishing. All Frontiers journals are driven by researchers for researchers; therefore, they constitute a service to the scholarly community. At the same time, the Frontiers Journal Series operates on a revolutionary invention, the tiered publishing system, initially addressing specific communities of scholars, and gradually climbing up to broader public understanding, thus serving the interests of the lay society, too.

Dedication to Quality

Each Frontiers article is a landmark of the highest quality, thanks to genuinely collaborative interactions between authors and review editors, who include some of the world's best academicians. Research must be certified by peers before entering a stream of knowledge that may eventually reach the public - and shape society; therefore, Frontiers only applies the most rigorous and unbiased reviews.
Frontiers revolutionizes research publishing by freely delivering the most outstanding research, evaluated with no bias from both the academic and social point of view. By applying the most advanced information technologies, Frontiers is catapulting scholarly publishing into a new generation.

What are Frontiers Research Topics?

Frontiers Research Topics are very popular trademarks of the Frontiers Journals Series: they are collections of at least ten articles, all centered on a particular subject. With their unique mix of varied contributions from Original Research to Review Articles, Frontiers Research Topics unify the most influential researchers, the latest key findings and historical advances in a hot research area! Find out more on how to host your own Frontiers Research Topic or contribute to one as an author by contacting the Frontiers Editorial Office: frontiersin.org/about/contact

PATHOMECHANISMS AND TREATMENTS TO PROTECT THE PRETERM, FETAL GROWTH RESTRICTED AND NEONATAL ENCEPHALOPATHIC BRAIN

Topic Editors:
Julie Wixey, The University of Queensland, Australia
Tracey Bjorkman, The University of Queensland, Australia
Bobbi Fleiss, RMIT University, Australia
Deirdre M. Murray, University College Cork, Ireland

Citation: Wixey, J., Bjorkman, T., Fleiss, B., Murray, D. M., eds. (2021). Pathomechanisms and Treatments to Protect the Preterm, Fetal Growth Restricted and Neonatal Encephalopathic Brain. Lausanne: Frontiers Media SA. doi: 10.3389/978-2-88971-556-5

Table of Contents

frontiers in Neurology

EDITORIAL
published: 09 September 2021
doi: 10.3389/fneur.2021.755617

Editorial: Pathomechanisms and Treatments to Protect the Preterm, Fetal Growth Restricted and Neonatal Encephalopathic Brain

Bobbi Fleiss[1], *Deidre M. Murray*[2], *S. Tracey Bjorkman*[3] *and Julie A. Wixey*[3]*

[1] School of Health and Biomedical Sciences, Royal Melbourne Institute of Technology (RMIT) University, Melbourne, VIC, Australia, [2] Department of Paediatric and Child Health, University College Cork, Cork, Ireland, [3] UQ Centre for Clinical Research, Faculty of Medicine, The University of Queensland, Brisbane, QLD, Australia

Keywords: preterm (birth), hypoxic-ischemic encephalopathy, fetal growth restriction (FGR), neuroprotection, mechanisms

Editorial on the Research Topic

Pathomechanisms and Treatments to Protect the Preterm, Fetal Growth Restricted and Neonatal Encephalopathic Brain

Every year, many hundreds of thousands of infants are at high risk of perinatal morbidity, poor neonatal outcomes, and life-long disability because they are exposed to events such as preterm birth, fetal growth restriction, or they present with neonatal encephalopathy. Collectively, these negative perinatal events compromise brain development and the high rate of disabilities include outcomes such as cerebral palsy, learning and attention difficulties, behavioral issues, and psychiatric disorders. There are only very limited treatments available to protect the newborn brain. For instance, we are fortunate to have a therapy for neonatal encephalopathy, therapeutic hypothermia, but this is not completely neuroprotective and is difficult to implement outside high resource health care settings. Nevertheless, hypothermia shows that therapies are possible. As such, there is a critical need for further high-quality research into improved identification, stratification, and care of these infants at risk of poor outcomes.

This Research Topic contains an equal contribution of articles focusing on neonatal encephalopathy related to hypoxia-ischemia (HIE) and prematurity, including three systematic reviews examining differing aspects of detection and prediction of adverse neurological outcomes in the HIE infant.

The first systematic review and article of this Topic (Liu et al.) examines the unmet clinical need for markers to predict outcome in hypothermia-treated infants with HIE. The authors consolidate our current knowledge that the currently available clinical tests magnetic resonance imaging (MRI) and electroencephalopathy (EEG) are useful predictors of adverse outcomes, however continued follow-up of the children is crucial to determine whether their predictive abilities include the ability to predict long-term outcomes.

The second systematic review in this issue examined cerebral near infrared spectroscopy (NIRS) monitoring in term and near-term infants with HIE (Mitra et al.). NIRS monitoring is an important tool in the neonatologist's toolbox, as it can provide information regarding changes in cerebral oxygenation and hemodynamics. The authors demonstrated that monitoring HIE newborns using a combination of NIRS and EEG is not only feasible but may improve prognosis of neurodevelopmental outcome. However, further randomized clinical trials and large observational studies are necessary to assess the utility of NIRS in predicting neurodevelopmental outcome and guiding therapeutic intervention.

Edited and reviewed by:
Jo Madeleine Wilmshurst, University of Cape Town, South Africa

***Correspondence:**
Julie A. Wixey
j.wixey@uq.edu.au

Specialty section:
This article was submitted to Pediatric Neurology, a section of the journal Frontiers in Neurology

Received: *09 August 2021*
Accepted: *20 August 2021*
Published: *09 September 2021*

Citation:
Fleiss B, Murray DM, Bjorkman ST and Wixey JA (2021) Editorial: Pathomechanisms and Treatments to Protect the Preterm, Fetal Growth Restricted and Neonatal Encephalopathic Brain. Front. Neurol. 12:755617. doi: 10.3389/fneur.2021.755617

The importance of defining of a good prognostic marker of adverse neurodevelopmental outcome in HIE babies is also highlighted in the work from Shah et al.. This team showed that in a cohort of HIE babies, increased levels of plasma neurofilament light protein (NfL) were associated with adverse outcomes at 18 months of age in HIE babies who have undergone hypothermia treatment.

A meta-analysis was undertaken to assess the overall strength of the links between birth asphyxia (as determined by pH value of umbilical cord blood) and increased risk of cerebral palsy (CP) by Zhang et al.. This meta-analysis solidified our understanding of the positive association between asphyxia and CP and reassuringly found the available studies are high quality with little publication bias.

The piglet model of HIE has a strong translational value to the human newborn with HIE. In the first of two studies using piglet models of HIE, Pang et al. focus on inflammation sensitized LPS/HIE. They reveal that in the LPS/HIE piglet treated with hypothermia, melatonin, and magnesium, and assessed using magnetic resonance spectroscopy (MRS); that the lactate to N-acetylaspartate (Lac/NAA) ratio is robust outcome predictor—correlating strongly with overall cell death and microglial reactivity.

The second piglet study, (Andelius et al.) induced a relatively mild HIE insult, with a shorter duration of amplitude electroencephalography (aEEG) suppression and duration of hypotension compared to the model from the Robertson team (Pang et al.). Andelius et al. assessed the combined effects of therapeutic hypothermia (TH) and remote ischemic conditioning (RIPC) on HIE. TH itself lowered the lactate to creatine measurement (Lac/Cr) on MRS but there was no additive neuroprotective benefit and additional research in a more severe model is suggested by the authors to fully examine the neuroprotective potential.

We are also provided with specific data on the role of chemokine signaling in driving pathology in LPS-sensitized HIE, using a well-established rat model. Serdar et al., outlined that there is a specific role of NLRP3 upregulation in microglia and the CXCL1/CXCR2 pathway in this model using a battery of gene and protein-based analyses. This pathway may be involved in LPS-sensitized HI brain injury in the newborn and may lead to new treatment options.

A further six articles in this Research Topic examined pathology and mechanisms of brain injury in the preterm born neonate. These are led by an interesting study that supports erythropoietin (EPO) may have neuroprotective abilities for preterm born infants in the context of hyperoxia related injury. Dewan et al. used repeated doses of EPO and showed improvements in short term neuropathology and long-term motor-cognitive outcomes.

Blesa et al. provides evidence for the validity of a novel approach to the analysis of mean diffusivity from 3T MRI, bringing a histogram-based approach validated in adults and showing its promise for assessing preterm born infant brain injury.

Parodi et al. undertook a retrospective cohort study assessing placental and perinatal risk factors for intraventricular hemorrhage (IVH) and cerebellar hemorrhages in preterm infants. Assessing placental pathology may help in understanding mechanisms leading to IVH, though its potential role in predicting cerebellar bleeding needs further investigation.

Although much of the work in this edition focuses on white matter outcomes in preterm born infants, a review from Fleiss et al. outlines the increasingly important evidence for gray matter injury. This review includes a summary of gray matter findings in animal models, how gray matter injury explains neurodevelopmental outcomes and discusses therapeutic targets.

An interesting review presents the hypothesis that in the preterm infant loss of plasma from the circulation results in hypovolemia, and that this is a significant driver of cardiovascular instability and thus poor cerebral oxygenation (Eiby et al.). The authors present their rationale for this hypothesis and how this may be tested in the future.

Further refinements to our imaging arsenal for assessing preterm brain injury were presented by Malova et al.. This retrospective study of 81 patients used susceptibility-weighted imaging (SWI) of punctate white matter lesions in preterm born infants. The study found that are haemosiderin positive SWI lesions occurred more often in infants with lower gestational age and closer to the ventricle. Further research stemming from these interesting findings will hopefully uncover the biological meaning of the observed differences.

Rounding out the edition, is a review from Ross-Munro et al., that proposed that the growth factor midkine may have beneficial roles as a neuroprotectant across forms of perinatal injury. This review brings together a great deal of information on the developmental expression of midkine across species and covers its potential role across a vast number of pathogenic processes.

AUTHOR CONTRIBUTIONS

BF and JW wrote the first draft. DM and SB edited the text. All authors (guest associate editors) read and approved the submitted version of the Editorial for this Research Topic.

ACKNOWLEDGMENTS

We thank all the authors for their valuable contributions to this Research Topic and the referees for taking the time to meticulously review each article.

Conflict of Interest: The authors declare that the research was conducted in the absence of any commercial or financial relationships that could be construed as a potential conflict of interest.

frontiers in Neurology

SYSTEMATIC REVIEW
published: 25 February 2020
doi: 10.3389/fneur.2020.00133

Prognostic Value of Clinical Tests in Neonates With Hypoxic-Ischemic Encephalopathy Treated With Therapeutic Hypothermia: A Systematic Review and Meta-Analysis

Weiqin Liu[1,2†], *Qifen Yang*[3†], *Hong Wei*[1,2], *Wenhui Dong*[1,2], *Ying Fan*[1,2] *and Ziyu Hua*[1,2*]

[1] *Department of Neonatology, Ministry of Education Key Laboratory of Child Development and Disorders, National Clinical Research Center for Child Health and Disorders, China International Science and Technology Cooperation Base of Child Development and Critical Disorders, Children's Hospital of Chongqing Medical University, Chongqing, China,* [2] *Chongqing Key Laboratory of Pediatrics, Children's Hospital of Chongqing Medical University, Chongqing, China,* [3] *School of Life Sciences, SouthWest University, Chongqing, China*

OPEN ACCESS

Edited by:
Deirdre M. Murray,
University College Cork, Ireland

Reviewed by:
Maurizio Elia,
Oasi Research Institute (IRCCS), Italy
Ryan J. Felling,
Johns Hopkins University,
United States

***Correspondence:**
Ziyu Hua
h_ziyu@163.com

[†] *These authors have contributed equally to this work and share first authorship*

Specialty section:
This article was submitted to Pediatric Neurology, a section of the journal Frontiers in Neurology

Received: *21 August 2019*
Accepted: *05 February 2020*
Published: *25 February 2020*

Citation:
Liu W, Yang Q, Wei H, Dong W, Fan Y and Hua Z (2020) Prognostic Value of Clinical Tests in Neonates With Hypoxic-Ischemic Encephalopathy Treated With Therapeutic Hypothermia: A Systematic Review and Meta-Analysis. Front. Neurol. 11:133. doi: 10.3389/fneur.2020.00133

Background and Objective: There remains an unmet clinical need for markers that predict outcomes in the hypothermia-treated (HT) infants with HIE. The aim of this meta-analysis was to investigate the prognostic accuracy of currently available clinical tests performed in the immediate post-natal period for predicting neurological outcomes between 18 months and 3 years of age in HT near-term and term infants with perinatal asphyxia and HIE.

Methods: A comprehensive review of the Embase, Cochrane library, and PubMed databases was performed to identify studies that evaluated the prognostic value of clinical tests for neurological outcomes in HT near-term and term infants with perinatal asphyxia and hypoxic-ischemic encephalopathy. Pooled sensitivity and specificity with corresponding 95% confidence intervals and area under the receiver operating characteristic (ROC) curve (AUC) were calculated.

Results: Of the 1,144 relevant studies, 26 studies describing four clinical tests conducted in 1458 HT near-term or term infants were included. For predicting an unfavorable neurological outcome, of the imaging techniques, MRI within 2 weeks of birth performed best on sensitivity 0.85 (95% *CI* 0.79–0.89), specificity 0.72 (95% *CI* 0.66–0.77), and AUC 0.88; among the neurophysiological tests, multichannel EEG (Electroencephalogram) demonstrated the sensitivity 0.63 (95% *CI* 0.49–0.76), specificity 0.82 (95% *CI* 0.70–0.91), and AUC 0.88, and for aEEG (amplitude-integrated electroencephalography) background pattern pooled sensitivity, specificity and AUC were 0.90 (95% *CI* 0.86–0.94), 0.46 (95% *CI* 0.42–0.51), and 0.78 whereas for SEPs (Somatosensory evoked potentials), pooled sensitivity and specificity were 0.52 (95% *CI* 0.34–0.69), 0.76 (95% *CI* 0.63–0.87), and AUC 0.84, respectively.

Conclusions: In the wake of the era of TH, MRI and neurophysiological tests (aEEG or EEG) were promising predictors of adverse outcomes, while SEPs need high-quality studies to confirm the findings. Continued follow-up of the children and well-designed large prospective studies are essential to determine whether these benefits are maintained in later childhood.

Keywords: therapeutic hypothermia, hypoxic-ischemic encephalopathy, neonates, clinical test, prognosis

INTRODUCTION

Hypoxic-ischemic encephalopathy (HIE) after perinatal asphyxia is the primary cause of death or long-term neurological impairment in infants born at term. Early predictive indicators of neurological outcomes in infants with HIE is essential for making rational clinical decisions. Before the era of therapeutic hypothermia, the prognostic value of MRI (first week) in neonates with HIE has been well-validated. aEEG or EEG recorded within the first 7 days of life in term infants may have potential as a neurophysiologic predicting tests. However, the prognostic value of SEP should be interpreted with caution due to small sample sizes (1).

Therapeutic hypothermia for 72 h provides neuroprotection that significantly improves survival and neurological outcomes in term infants with moderate to severe HIE (2). However, the prognostic capability of these parameters may vary under hypothermic conditions, and there remains an unmet clinical need for markers that predict outcomes in hypothermia-treated (HT) infants (3, 4).

To the authors' knowledge, there are no published meta-analyses that investigate the prognostic capabilities of currently available clinical tests for predicting long-term neurological outcomes in HT term-infants with HIE. Therefore, a meta-analysis was conducted to evaluate the prognostic accuracy of currently available clinical tests performed in the immediate post-natal period for predicting neurological outcomes between 18 months and 3 years of age in HT near-term and term infants with perinatal asphyxia and HIE.

METHODS

Search Strtegy

Three review authors (W.L, Q.Y and Z.H) independently searched the PubMed, Cochrane Library, and Embase databases from 2009 to February 2019 using the following keywords "hypoxic-ischemic encephalopathy" AND "newborn" AND "hypothermia"; "neonatal Encephalopathy" AND "newborn" AND "hypothermia" Searches were limited to literature published in the English language.

Inclusion and Exclusion Criteria

Inclusion criteria were: (1)observational prognostic studies that included infants ≥35 weeks of gestation with perinatal asphyxia and HIE diagnosed according to clearly described criteria; (2) that were treated with therapeutic hypothermia; and (3) that underwent neurological follow-up longitudinally until ≥18 months of age, with outcomes defined as good or adverse.

Exclusion criteria were: (1) reviews, letters, abstracts, or editorials; or (2) studies that reported insufficient data, (3) Non-English language, (4) Uncertain follow-up time and Follow-up time is >18 months.

Study Selection

Three review authors (W.L, Q.Y, and Z.H) independently screened the titles and abstracts identified by the search for potentially relevant studies. Texts were retrieved and reviewed to determine which studies met the inclusion criteria. Disagreements about data extraction were resolved by discussion with a third review author (ZH) until consensus was reached.

Data Extraction

Three review authors (W.D, H.W., and Y.F) independently extracted data from the included studies using a data extraction sheet. The following information was recorded: authors, year of publication, number of study subjects, gestational age, birth weight, Apgar score, blood pH, clinical tests (e.g., imaging, neurophysiological, other), neurological tests, and length of follow-up. If both hypothermic and normothermic infants were included in a study, data about the hypothermic infants were extracted separately. According to the review of the studies, we established the MRI subgroup and the aEEG subgroup.

Statistical Analysis

Statistical analyses were conducted with *RevMan v*5.3 and *Meta-Disc* 1.4. Three review authors (W.L, Q.Y, and Z.H) examined the quality of the included studies using *Quadas* 2, which evaluates four key domains, including patient selection, index test, reference standard, and flow and timing and independently extracted individual patient data from each of the studies into a predefined database. Personal patient data from all studies were pooled to create 2 × 2 tables and pooled sensitivity and specificity with 95% confidence intervals (*CI*s) and area under the receiver operating characteristic curve (AUC) were calculated. Heterogeneity between studies was tested with the inconsistency (I^2) index and χ^2- test. A fixed-effect model was used if there was no evidence of heterogeneity between studies ($I^2 < 50\%$, $P > 0.05$); otherwise, a random-effects model was used.

RESULTS

Study Identification

The searches identified 1,144 articles. Following the removal of duplicates, the titles and abstracts of 925 studies were

screened, and 82 studies were considered potentially eligible for inclusion in this meta-analysis. Full-text articles were retrieved and reviewed; among these, 11 studies were excluded because they were not published in the English language, 27 studies were excluded due to missing data. Fifteen studies were excluded due to uncertain follow-up time and follow-up time is <18 months, and three studies were not analyzed due to small sample size. Finally, 26 reviews were included in the pooled analyses (**Figure 1** and **Supplementary Table 1**).

Characteristics of Included Studies

The characteristics of the included studies are shown in **Tables 1**, **2**. The 26 eligible studies included 1458 HT near-term or term infants with perinatal asphyxia and HIE and follow up available after 18 months of age. Clinical tests performed in the immediate postnatal period included brain magnetic resonance imaging (MRI), EEG, aEEG, SEPs. Neurological examinations were performed between 18 months and 3 years of age.

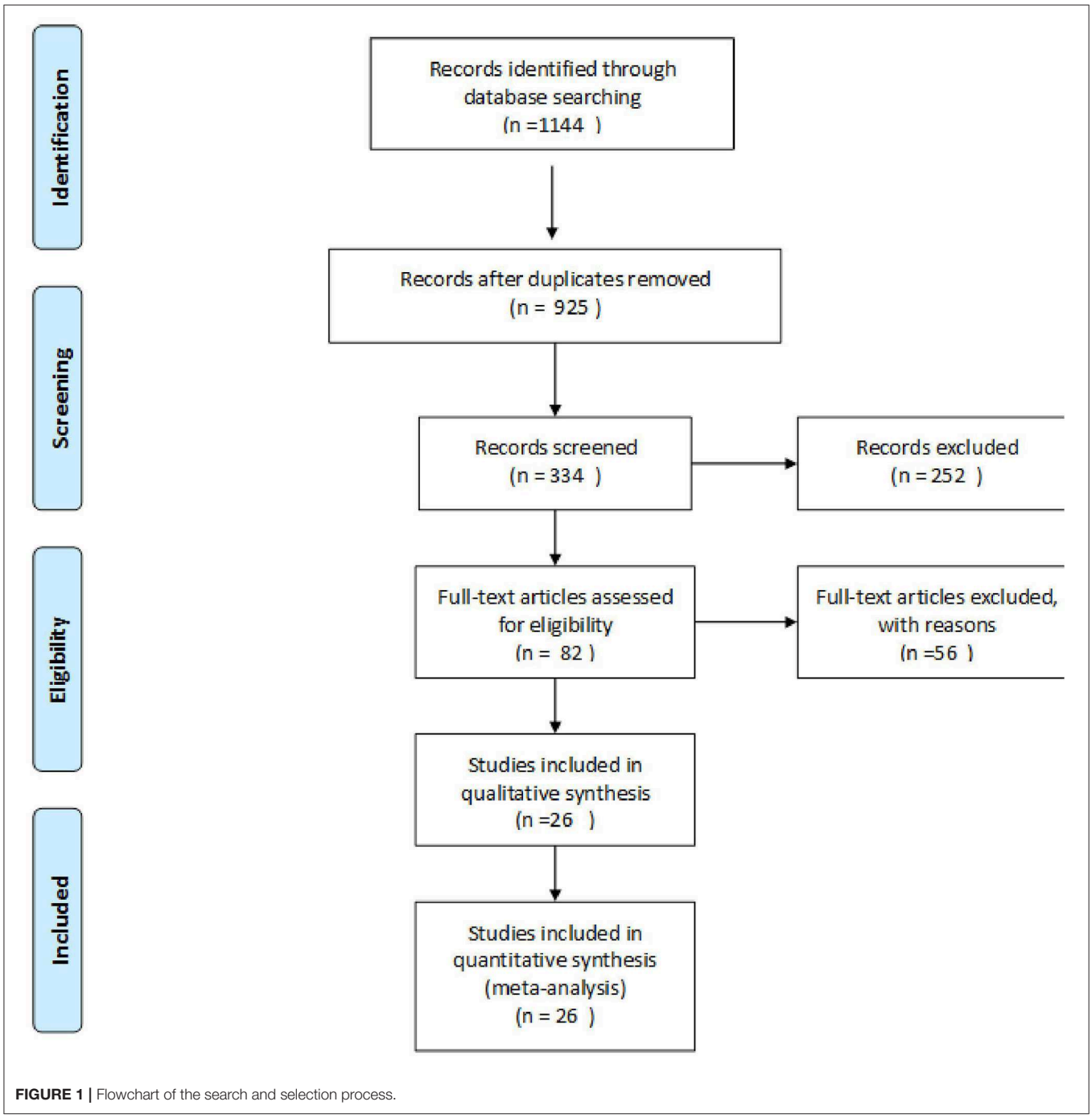

FIGURE 1 | Flowchart of the search and selection process.

TABLE 1 | Characteristics of included studies.

References	Time	Study design	Number of patients (Female/ Male Ratio)	Gestational age (W)	Birth weight (Kg)	Apgar score (1/5/10 min)	Blood pH
Rutherford et al. (5)	2010	P	64 (25/39)	40(39–41)	3.45(2.995–3.863)	4 (3–5) (10min)	Unknown
Thoresen et al. (6)	2010	P	43 (20/23)	40	3.38 (0.80)	5 (3.75) (10 min)	6.95 (0.16)
Shankaran et al. (7)	2011	P	57 (Unknown)	≥36	Unknown	Unknown	6.9 (0.2)
Takenouchi et al. (8)	2011	P	29 (Unknown)	Poor outcome 38 (1.7) Good outcome 39 (1.5)	Poor outcome 3.350 (0.767) Good outcome 3.234 (0.559)	Unknown	Poor outcome 6.91 (0.21) Good outcome 6.84 (0.26)
Shankaran et al. (9)	2012	P	73 (37/36)	39.1 (1.5)	3.328 (0.557)	Unknown	6.9 (0.2)
Cseko et al. (10)	2013	R	70 (28/42)	Poor outcome 39 (37–40) Good outcome 39 (37.5–40)	Poor outcome 3.26 (2.95–3.488) Good outcome 3.3 (2.948–3.558)	Poor outcome 3 (2–4) (5 min) Good outcome 5 (3–6.25) (5 min)	Poor outcome 6.89 (6.82–7.1) Good outcome 7.2 (7.02–7.27)
Lemmers et al. (11)	2013	P	39 (15/24)	Good outcome 40.32 (1.5) Poor outcome 40.21 (1.26)	Good outcome 3.744 (0.644) Poor outcome 3.831 (0.603)	Good outcome 3 (1–6) (5 min) Poor outcome 3 (0–7) (5 min)	Good outcome 6.97 (0.2) Poor outcome 6.90 (0.3)
Li et al. (12)	2013	R	21 (13/8)	Good outcome 38.8 (1.9) Poor outcome 39.2 (1.9)	Good outcome 3.071 (0.507) Poor outcome 2.867 (0.470)	Good outcome 4.2 (2.7) (5 min) Poor outcome 3.5 (2.2) (5 min)	Good outcome 7.07 (0.22) Poor outcome 7.13 (0.26)
Chalak et al. (13)	2014	P	90 (35/55)	39 ± 2	3.43 (0.584)	2 (0–7) (1 min) 4 (0–9) (5 min)	6.97 (0.17)
Azzopardi (14)	2014	P	147 (Unknown)	40 (39–41)	Unknown	3 (1–5) (5 min)	6.9 (6.78–7.01)
Del Balzo et al. (15)	2014	P	20 (Unknown)	≥36	≥1.80	Unknown	Unknown
Garfinkle et al. (16)	2015	R	26 (10/16)	38.8	3.336 (0.606)	4 (3–5) (5 min)	6.96 (0.13)
Alderliesten et al. (17)	2015	P	65 (Unknown)	40.1 (1.6)	3.239 (0.469)	2 (3) (1 min) 5 (2) (5 min)	6.99 (0.18)
Charon et al. (18)	2016	R	43 (Unknown)	Good outcome 39+5 (38+2–40+6) Poor outcome 39+2 (39+4–41)	Good outcome 3.17 (2.775–3.460) Poor outcome 3.6 (3.07–3.872)	Good outcome 4 (3–5) (5 min) Poor outcome 3 (1.5–4.5) (5 min)	Good outcome 7.26 (7.08–7.33) Poor outcome 7.25 (7.12–7.30)
Weeke et al. (19)	2016	P	26 (11/15)	40.4	3.445 (2.261–4.75)	4 (1–10) (5 min)	6.89 (0.20)
Chiang et al. (20)	2016	P	12 (4/8)	Good outcome 39.5 (0.6) Poor outcome 37.9 (1.5)	Good outcome 2.658 (0.465) Poor outcome 3.525 (0.828)	Good outcome 4 (1; 5) (5 min) Poor outcome 4 (3; 7) (5 min)	Good outcome 6.97 (6.73–7.32) Poor outcome 7.02 (6.72–7.43)
Heursen et al. (21)	2017	P	54 (24/30)	39.4 (1.64)	3.323 ± 0.527	2 (0–6) (1 min) 4.5 (0–8) (5 min)	6.93 (0.13)
Ahearne et al. (22)	2017	P	33 (11/22)	Good outcome 40.4 (39.2–41.1) Poor Outcome 40.8 (39.7–41.4)	Good outcome 3.5 (3.2–4.1) Poor Outcome 3.4 (3.1–3.7)	Unknown	Unknown
Cainelli et al. (23)	2018	P	35 (Unknown)	38 (37; 40)	3.280 (2.665; 3.515)	3 (1; 5) (1 min) 5 (4; 6) (5 min) 7 (5; 8) (10 min)	7.0 (6.8; 7.1)
Nevalainen et al. (24)	2017	R	24 (13/11)	39.6 (1.5)	3.350 (0.600)	1 (1 min) 2 (5 min) 3.5 (10 min)	6.9 (0.2)
Trivedi et al. (25)	2017	P	57 (29/28)	38.5 (1.6)	3.166 (0.688)	4 (5 min) 5 (10 min)	7.05 (0.19)
Skranes et al. (26)	2017	P	47 (Unknown)	≥36 weeks	Unknown	Unknown	Unknown
Weeke et al. (27)	2017	P	122 (53/69)	40.0 (2.2)	3.50 (0.858)	3 (5 min)	6.90 (0.25)
Liu et al. (28)	2017	P	165 (62/103)	≥36 weeks	Unknown	Unknown	Unknown
Barta et al. (29)	2018	R	51 (20/31)	Good outcome 39 (38;40) Poor outcome 38 (37;40)	Good outcome 3.261 (0.577) Poor outcome 3.128 (0.537)	Good outcome 5 (4–7) (5 min) Poor outcome 3 (2–4) (5 min)	Good outcome 7.21 (6.98–7.28) (1 h) Poor outcome 7.10 (7.00–7.20) (1 h)
De Wispelaere et al. (30)	2019	R	45 (23/22)	39+6 (38+1–40+4)	3.29 ± 0.612	3 (1–4) (5 min)	6.96 ± 0.24

Prospective study (P) Retrospective study (R). Values represent the mean (SD), median [IQR], or median (range). unless otherwise indicated.

TABLE 2 | Neurological outcomes defined by study.

References	Time	Index test	Abnormal findings	Follow up (m)	Neurodevelopmental assessment (definition of adverse outcome)
Rutherford et al. (5)	2010	MRI	Abnormal signal in the WM, BGT, PLIC, COR, or various combinations of such lesions	18	Bayley II and GMFCS; death or disability (MDI <70, GMFCS level 3–5, or altered vision or hearing)
Thoresen et al. (6)	2010	aEEG	Lower margin ≤5 μV and upper margin>10 μV or <10 μV (voltage classifications) BS, LV, and FT traces (pattern classification)	18	Bayley II and GMFCS; death or disability (MDI <70, GMFCS level 3–5, or altered vision or hearing)
Shankaran et al. (7)	2011	aEEG	BS, LV, and FT traces (pattern classification)	18	Bayley II and GMFCS; death or disability (MDI <85, GMFCS level 2–5, or altered vision or hearing)
Takenouchi et al. (8)	2011	MRI	Abnormal signal in the BGT, severe extensive supratentorial restricted diffusion.	18	Bayley III; death or severe disability (MDI <70 or severe motor deficit restricting
Shankaran et al. (9)	2012	MRI	abnormal signal in the WM, BGT, PLIC, ALIC, COR, or various combinations of such lesions (NICHD brain injury pattern scale)	18–22	Bayley II and GMFCS; death or disability (MDI <85, GMFCS level 2–5, or altered vision or hearing, persistent seizure disorder)
Cseko et al. (10)	2013	aEEG	BS, LV, and FT traces	18–24	Bayley II; death or disability (MDI or PDI <85)
Lemmers et al. (11)	2013	aEEG	BS, LV, and FT traces	18	Griffiths and neurologic examination: Death or DQ <85
Li et al. (12)	2013	MRI EEG	Abnormal signal in the WM, BGT, COR, or various combinations of such lesions Background EEG depression (classification of Watanabe)	24	K-Form Developmental Test: death, CP, hearing impairment, or blindness, DQ < 70
Chalak et al. (13)	2014	MRI	Abnormal signal in the WM, BGT, PLIC, ALIC, COR, or various combinations of such lesions (NICHD brain injury pattern scale)	24	Bayley III; Death, cerebral palsy, Bayley scores >1 SDs from the norm, Bayley<85
Azzopardi (14)	2014	aEEG	Lower margin ≤5 μV and upper margin >10 μV or <10 μV (voltage classifications) BS, LV, and FT traces (pattern classification)	18	Bayley II and GMFCS; death or disability (MDI <70, GMFCS level 3–5, or altered vision or hearing)
Del Balzo et al. (15)	2014	EEG MRI	Classification of EEG background activity (Pressler et al. score) Abnormal signal in the WM, BGT, PLIC, ALIC, COR, or various combinations of such lesions	18	Bayley III; death or severe disability (cognitive development index 3 S.D.s below mean or severe sensorimotor disability)
Garfinkle et al. (16)	2015	SEPs MRI	N19 potentials absent or prolonged (unilaterally or bilaterally) Abnormal cortex and BGT, or various combinations of such lesions(Barkovich score)	24	Bayley III; death or Bayley <80, GMFCS level 2–5, or altered vision or hearing
Alderliesten et al. (17)	2015	MRI	Abnormal cortex and BGT, or various combinations of such lesions (Barkovich score)	18	GMDS; death, CP, or DQ < 85
Charon et al. (18)	2016	MRI	Abnormal cortex and BGT, or various combinations of such lesions(Barkovich score)	18–41	RBL scale and GMFCS: death or disability (DQ < 70 and GMFCS level 3–5)
Weeke et al. (19)	2016	MRI EEG	Abnormal cortex and BGT, or various combinations of such lesions(Barkovich score) Classification of EEG background activity (Pressler et al. score)	24	Bayley III; death, CP, hearing impairment, or blindness, Bayley < 85
Chiang et al. (20)	2016	MRI	Abnormal signal in the WM, BGT, PLIC, or various combinations of such lesions	24	Bayley III; disability(CP, bilateral blindness, or bilateral hearing loss) or Neurodevelopmental delay
Heursen et al. (21)	2017	MRI	Abnormal signals of the BGT or WM, or Near-total injury	24	Bayley III and GMFCS; CP, death or disability GMFCS level 2–5 or altered vision or hearing)
Nevalainen et al. (24)	2017	SEP	Bilaterally absent SEPs	18	Unfavorable outcomes included death or severe neurological sequelae comprising severe epilepsy, tetraparesis or dyskinetic cerebral palsy or severe psychomotor retardation
Trivedi et al. (25)	2017	MRI	Abnormal signals of the subcortical region, or white matter; or cortex, or cerebellum and brainstem	18	Bayley III; death or a Bayley-III score of <85 in any domain
Skranes et al. (26)	2017	aEEG	BS, LV, and FT traces (pattern classification)	24	(Bayley III and GMFCS; CP, death or cognitive or motor scores of <85, GMFCS level 3–5, or altered vision or hearing)
Ahearne et al. (22)	2017	EEG	Classification of EEG background activity (Pressler et al. score)	36–42	Bayley III; death or cognitive, language, and motor scores of < 85, dyskinetic, or spastic quadriplegic cerebral palsy or autism
Weeke et al. (27)	2017	aEEG	BS, LV, and FT traces (pattern classification)	≥24	Bayley III and GMFCS; death, CP, severe hearing, or visual impairments, or an adverse neurodevelopment (Bayley score <85, Griffiths developmental quotient < 88)

(Continued)

TABLE 2 | Continued

References	Time	Index test	Abnormal findings	Follow up (m)	Neurodevelopmental assessment (definition of adverse outcome)
Liu et al. (28)	2017	aEEG	Lower margin ≤5 μV and upper margin >10 μV or <10 μV (voltage classifications) BS, LV, and FT traces (pattern classification)	24	Bayley III and GMFCS; Bayley score <85, GMFCS 3–5, severe visual deficits, or severe bilateral hearing loss
Barta et al. (29)	2018	MRI aEEG	Abnormal cortex and BGT, or various combinations of such lesions(Barkovich score) BS, LV, and FT traces (pattern classification)	24	Bayley III and GMFCS; death or disability (MDI or PDI <85, GMFCS level 2–5, or altered vision or hearing)
Cainelli et al. (23)	2018	EEG SEP	Classification of EEG background activity (Pressler et al. score) N20 OR N13 potentials absent or prolonged (unilaterally or bilaterally)	24	GMDS; death, CP or DQ < 85
De Wispelaere et al. (30)	2019	MRI	Abnormal cortex and BGT, or various combinations of such lesions(Barkovich score)	24	Bayley III and GMFCS; death or disability (MDI or PDI < 85, GMFCS level 2–5, or altered vision or hearing)

BSID-II or BSID-III, Bayley Scales of Infant Development II or III; WPPSI, Wechsler Preschool and Primary Scale of Intelligence III; GMFCS, Gross Motor Function Classification System; GMDS, Griffiths mental development scales; RBL, Revised Brunet-Lezine scale; MDI, Mental Developmental Index; PDI, Psychomotor Developmental Index; CP, Cerebral palsy; DQ, Developmental quotient; SEPs, Somatosensory evoked potentials; EEG, Electroencephalogram; MRI, Magnetic resonance imaging; aEEG, amplitude-integrated electroencephalogram; BGT, basal ganglia and thalamus; ALIC/PLIC, anterior or posterior limb of the internal capsule; WM, white matter; COR, cortex; BS, burst-suppression; LV, low voltage; FT, FT flat trace.

Methodological Quality of Included Studies

The risks of bias in the index test and patient selection were low (**Figures 2**, **3**). Sixteen studies (5, 8, 10, 12, 14–21, 25, 27, 28, 30) did not indicate whether the reference standard results were interpreted without knowledge of the results of the index test. For flow and timing, 14 studies (5, 7, 8, 10, 13, 14, 18–20, 22, 24, 26, 29, 30) did not include all patients in the analyses. Overall, most of the included studies did not have a high risk of bias.

Prognostic Value of Clinical Tests

The results of the meta-analysis are shown in **Table 3** (pooled sensitivities and specificities with confidence intervals) and **Figure 4** (forest plots of sensitivity and specificity as calculated from the original reports).

Imaging: Brain MRI

Fourteen studies (5, 8, 9, 12, 13, 15–17, 19–21, 25, 29, 30) evaluated the prognostic value of brain MRI($I^2 = 47.9\%$, fixed-effect model) for neurological outcomes in HT near-term and term infants with perinatal asphyxia and HIE. Pooled sensitivity and specificity were 0.85 (95% *CI* 0.79–0.89) and 0.69 (95% *CI* 0.64–0.74), and AUC was 0.87 for predicting an unfavorable outcome. Early MRI (≤6 days from birth) ($I^2 = 60\%$, random-effects model) performed best on sensitivity 0.91 (95% *CI* 0.83–0.96). Late MRI (≥7 days from birth) ($I^2 = 33\%$, fixed-effect model) performed best on specificity 0.88 (95% *CI* 0.78–0.94). MRI within 2 weeks ($I^2 = 59.5\%$, random-effects model) of birth performed best on sensitivity 0.85 (95% *CI* 0.79–0.89), specificity 0.72 (95% *CI* 0.66–0.77), and AUC 0.88.

Neurophysiological Tests: aEEG, EEG, and SEPs

Nine studies (6, 7, 10, 11, 14, 26–29) evaluated the prognostic value of aEEG tests for neurological outcomes in HT near-term and term infants with perinatal asphyxia and HIE. For aEEG background patterns ($I^2 = 65.2\%$, random-effects model), pooled sensitivity and specificity were 0.90 (95% *CI* 0.86–0.94) and 0.46 (95% *CI* 0.42–0.51), and AUC was 0.78 for predicting an unfavorable outcome. For aEEG voltage classification ($I^2 = 36.7$, fixed-effect model), pooled sensitivity and specificity were 0.90 (95% *CI* 0.84–0.95) and 0.32 (95% *CI* 0.26–0.39), and AUC was 0.66 for predicting an unfavorable outcome.

Multichannel EEG ($I^2 = 17.7\%$, fixed-effect model) demonstrated the sensitivity 0.63 (95% *CI* 0.49–0.76), specificity 0.82 (95% *CI* 0.70–0.91), and AUC 0.88. Three studies (16, 23, 24) evaluated the prognostic value of SEPs for neurological outcomes in HT near-term and term infants with perinatal asphyxia and HIE. For SEPs ($I^2 = 57.9\%$, random-effects model), pooled sensitivity and specificity were 0.52 (95% *CI* 0.34–0.69) and 0.76 (95% *CI* 0.63–0.87) for predicting an unfavorable outcome, and AUC 0.84.

DISCUSSION

HIE after perinatal asphyxia is a significant cause of mortality and morbidity in newborns, accounting for approximately 20% of cerebral palsy cases (31, 32). Evaluating long-term neurological outcomes based on clinical evaluations in the immediate post-natal period can be challenging. However, a reliable, evidence-based prognosis is essential for parental counseling regarding possible long-term sequelae. Hypothermia is generally accepted as the safest method for reducing neurological morbidity and mortality in infants with perinatal asphyxia and HIE (33, 34). Although the literature is replete with studies evaluating novel but relatively unknown test modalities, to ensure clinical relevance. The present review focused on tests that are widely used in clinical practice and did not attempt to provide an overview of all available procedures (1).

Current MRI injury scoring systems published in the literature include the Barkovich, the National Institutes for Child Health and Development (NICHD) and Rutherford systems (5, 9, 35). Each scoring system has some limitations. The previous does

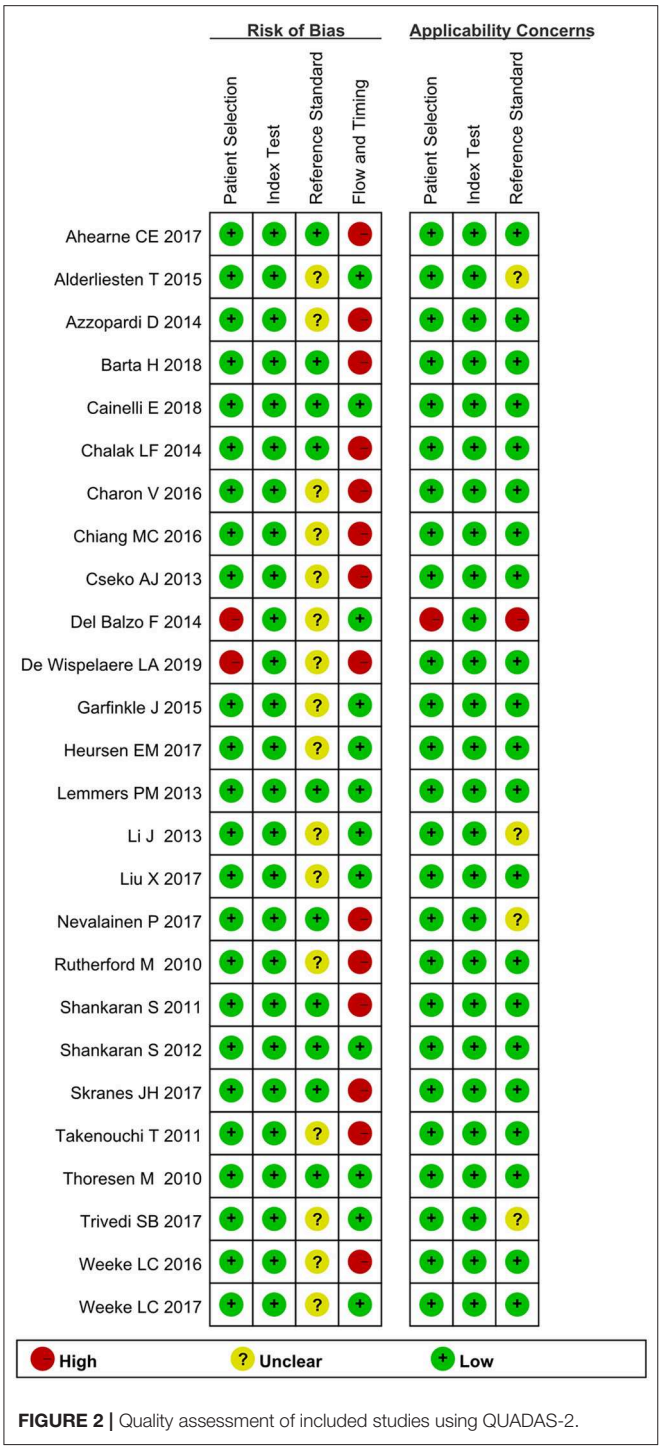

FIGURE 2 | Quality assessment of included studies using QUADAS-2.

not explicitly address posterior limb of the internal capsule injury, whereas the latter two systems do not include diffusion-weighted imaging (DWI) (25), and Clinicians often evaluate the neonatal brain MRI as a whole test rather than specific brain MRI components. So, we considered parenchymal (gray or white matter) abnormalities on T1, T2, and diffuse weighted images to define an abnormal MRI. In the systematic review, brain MRI predicted an unfavorable neurological outcome in HT infants with perinatal asphyxia and HIE with a sensitivity of 0.85. Accordingly, in the TOBY trial, the accuracy of prediction of death or disability to 18 months of age by MRI was 0.84 (0.74–0.94) in HT infants and 0.81 (0.71–0.91) in a normothermic group (5). Evidence suggests that therapeutic hypothermia without affecting the overall predictive value of MRI as a marker of neurological impairment (5, 13).

In the era of predates hypothermia treatment, late MRI (8–30 days) had higher sensitivity but lower specificity than early MRI (1–7 days) (36). However, the current literature does not provide detailed individual data on the time of neonatal brain MRI in HT (37). In the present review, late MRI predicted an unfavorable neurological outcome with a sensitivity and specificity of 0.88 and 0.88, respectively, whereas early MRI showed less specificity of 0.73. However, Charon et al. reported that the specificity of MRI for predicting death or disability to 18 months of age in HT infants with HIE was 96.3% in the first week and 89.3% in the second week (18). The discrepancy between our findings and those reported by Charon et al. might be explained by the various abnormal findings and the thresholds for the index tests. Results from the present meta-analysis indicate that within 2 weeks of birth correctly predict neurological outcomes at 18 months of age in HT infants with HIE (pooled sensitivity, 0.85 [95% *CI*, 0.79–0.89].

Deep gray matter lactate/N-acetyl aspartate (Lac/NAA) peak/area ratio is the most quantitative biomarker for prediction of neurodevelopmental outcomes in magnetic resonance spectroscopy (38). However, the equipment is not widely used in clinical practice, and based on limited available studies, the validity of the results has not been quantified in previous reviews of the literature.

aEEG is the commonly used neurophysiological tests for assessment of HIE severity, for monitoring improvement over time, and for predicting neurological outcomes in infants (39). aEEG can be performed at the bedside, and background patterns and voltage classification have been considered an early predictor of neurological outcomes in HT infants with HIE. In normothermic infants, a persistently abnormal aEEG between 6 and 24 h of age is considered predictive of adverse outcomes (6, 40). However, the predictive value of aEEG for subsequent neurological impairment is altered by hypothermia. In one study, the positive prognostic value of an abnormal aEEG increased from 6 to 48 h of age in HT term infants with HIE. This shift in prognostic accuracy may be explained, at least in part, by the neuroprotective effects of therapeutic hypothermia (41). In the present review, aEEG background pattern predicted an unfavorable neurological outcome with a sensitivity and specificity of 0.90 and 0.46, respectively, and an AUC of 0.78, while aEEG voltage classification was less predictive [sensitivity 0.90 [95% *CI* 0.84–0.95]; specificity 0.32 [95% *CI* 0.26–0.39], AUC 0.66]. Possible explanations are that the sedative drugs and anticonvulsants that are commonly administered to HT infants have prolonged half-lives and increased plasma levels compared to normothermic conditions, causing voltage fluctuations on the EEG signal (12). In accordance with our findings, Shany et al. reported that background pattern was more sensitive than voltage classification for predicting neurological outcomes in infants with

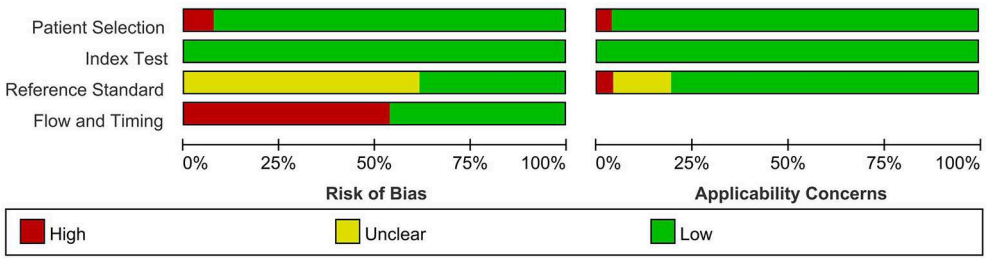

FIGURE 3 | Percentage of the studies with risk of bias and applicability concerns in the different domains of QUADAS-2.

TABLE 3 | Pooled sensitivities and specificities with confidence intervals for tests where pooling was possible.

Test	No. of studies	No. of patients	Pooled sensitivity		Pooled specificity		AUC
			Point Estimate	95% *CI*	Point Estimate	95% *CI*	
MRI	14	605	0.85	0.79–0.89	0.69	0.64–0.74	0.87
Early MRI (≤6 days)	6	269	0.91	0.83–0.96	0.73	0.66–0.79	0.92
late MRI (≥7 days)	5	124	0.88	0.75–0.96	0.88	0.78–0.94	0.94
MRI within 2 weeks	12	506	0.85	0.79–0.89	0.72	0.66–0.77	0.88
aEEG Background classification	9	741	0.90	0.86–0.94	0.46	0.42–0.51	0.78
aEEG voltage classification	3	355	0.90	0.84–0.95	0.32	0.26–0.39	0.66
EEG	5	111	0.63	0.49–0.76	0.82	0.70–0.91	0.88
SEPs	3	84	0.52	0.34–0.69	0.76	0.63–0.87	0.84

HIE, although assessment of background pattern may be more subjective (42).

Multichannel EEG is the gold standard for assessment of the severity of HIE and for monitoring improvement over time (39). In our review, EEG predicted subsequent neurological impairment in HT infants with HIE with a sensitivity of 0.63 (95% *CI*, 0.49–0.76), specificity of 0.82 (95% *CI*, 0.70–0.91), and an AUC of 0.88, yielding a higher specificity than aEEG. However, EEG is a relatively complex technique. Technicians are required to site EEG leads and specialists are needed to interpret neurophysiology, but these resources may not be readily available (39). High seizure burden and sleep-wake cycling have been independently associated with poor outcomes in HT infants with HIE (41). Unfortunately, lack of data meant that these parameters could not be examined in the present meta-analysis.

SEPs assess the deep brain structures such as the thalami and brainstem, which are known to be selectively vulnerable to hypoxia and ischemia (43). Several studies had shown that normal SEPs were strongly predictive of a favorable outcome, and absent SEPs were strongly predictive of an unfavorable outcome (44, 45). In our review, SEPs predicted an unfavorable neurological outcome in HT infants with HIE with a sensitivity of 0.52 (95% *CI*, 0.34–0.69) and a specificity of 0.76 (95% *CI*, 0.63–0.87). Although SEPs may provide complementary prognostic resources to HIE after perinatal asphyxia, the predictive value of SEPs investigated in this review should be interpreted with caution due to small sample sizes.

Although not explored in this review, we propose that a combination of the above prognostic tests performed would provide the greater prognostic accuracy for predicting long-term neurological outcomes in the HIE infants undergoing HT.

Strengths and Weaknesses

To the authors' knowledge, this is the first meta-analysis to investigate the prognostic value of clinical tests performed in the immediate post-natal period as predictors of adverse neurological outcomes in HT near-term and term infants with perinatal asphyxia and HIE. Importantly, to investigate which HIE infants would have neurological sequelae, this review only included studies with long-term follow-up, whereby infants were followed until ≥18 months of age. In our opinion, outcomes couldn't be accurately assessed in infants younger than 18 months as neurological sequelae usually manifest at ≥12 months of age, and mental and behavioral disabilities might appear even later (46).

This meta-analysis has several limitations. First, the sample size was small. Second, this review was restricted to articles published in the English language, which may have led to an overestimation or underestimation of prognostic reliability. Finally, heterogeneity was low to moderate, possibly due to differences in thresholds for the index test, the severity of HIE and the design of the studies. Subgroup analyses were not performed to investigate the source of this heterogeneity. Well-designed more extensive studies are required to determine an accurate estimate of the value of clinical tests performed in

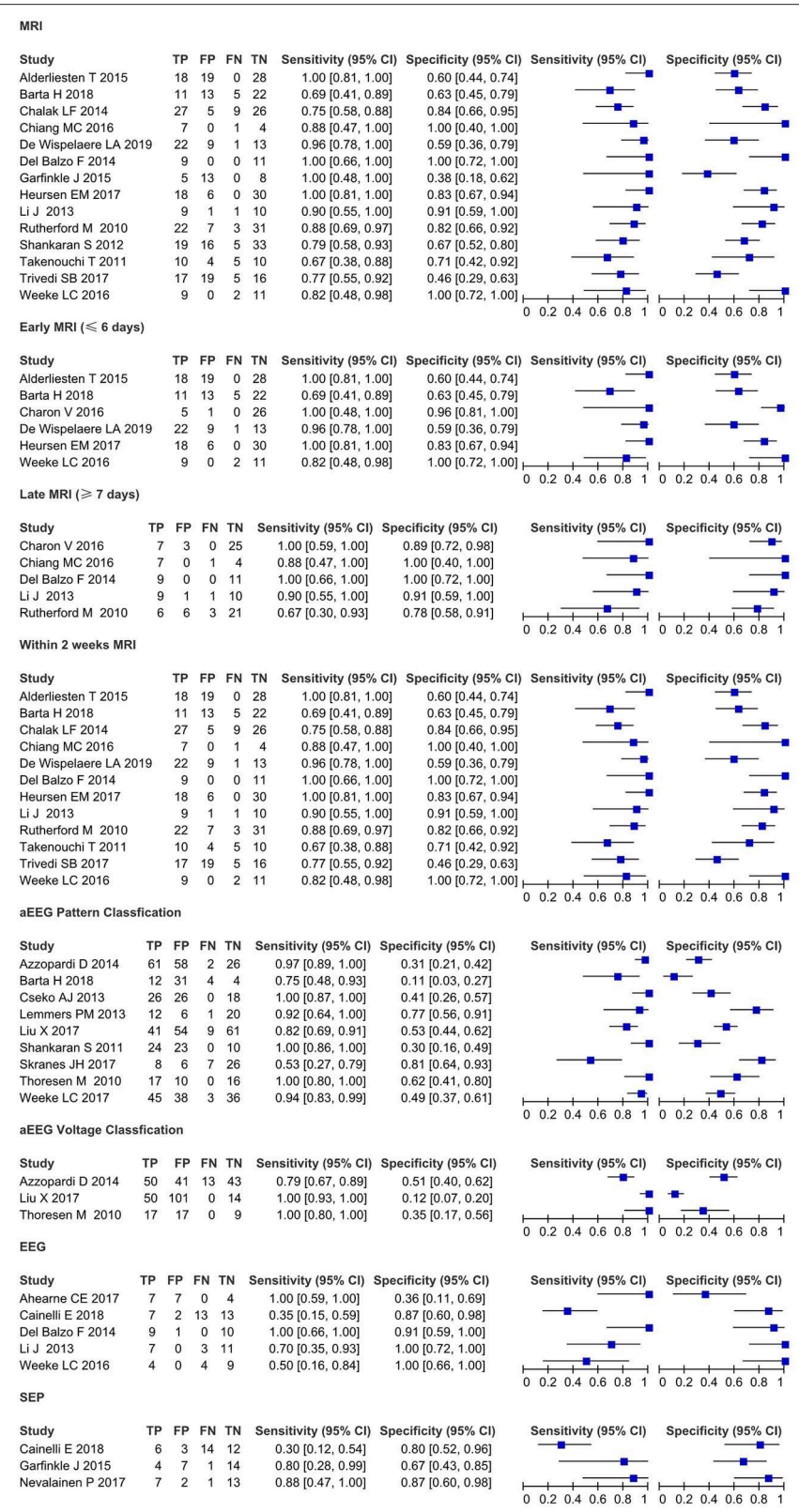

FIGURE 4 | Forest plots of sensitivity and specificity as calculated from the original reports.

the immediate post-natal period for predicting in HT infants with HIE.

CONCLUSIONS

This systematic review and meta-analysis provided insight into the prognostic value of clinical tests performed in the immediate post-natal period as predictors of adverse neurological outcomes in HT near-term and term infants with perinatal asphyxia. MRI and neurophysiological tests (aEEG or EEG) were promising predictors of the adverse outcomes, whereas SEPs need high-quality studies to confirm the findings. Given the heterogeneity in the tests' performance, continued follow-up of the children and well-designed large prospective studies are essential to determine whether these benefits are maintained in later childhood.

DATA AVAILABILITY STATEMENT

All datasets generated for this study are included in the article/**Supplementary Material**.

AUTHOR CONTRIBUTIONS

WL, QY, and ZH performed the screening, extraction of data for included studies, and assessed the quality of study. WD, HW, and YF conducted data extraction of included studies. WL supervises the development of concepts, execution of methodology, analysis, and manuscript writing. All authors reviewed and commented the manuscript.

FUNDING

This study was supported by grants from the Clinical Research Project of Children's Hospital of Chongqing Medical University (YBXM 2019–007).

SUPPLEMENTARY MATERIAL

The Supplementary Material for this article can be found online at: https://www.frontiersin.org/articles/10.3389/fneur.2020.00133/full#supplementary-material

REFERENCES

1. van Laerhoven H, de Haan TR, Offringa M, Post B, van der Lee JH. Prognostic tests in term neonates with hypoxic-ischemic encephalopathy: a systematic review. *Pediatrics.* (2013) 131:88–98. doi: 10.1542/peds.2012-1297
2. Tagin MA, Woolcott CG, Vincer MJ, Whyte RK, Stinson DA. Hypothermia for neonatal hypoxic ischemic encephalopathy: an updated systematic review and meta-analysis. *Arch Pediatr Adolesc Med.* (2012) 166:558–66. doi: 10.1001/archpediatrics.2011.1772
3. Del Río R, Ochoa C, Alarcon A, Arnáez J, Blanco D, García-Alix A. Amplitude integrated electroencephalogram as a prognostic tool in neonates with hypoxic-ischemic encephalopathy: a systematic review. *PLoS ONE.* (2016) 11:e0165744. doi: 10.1371/journal.pone.0165744
4. Edwards AD, Brocklehurst P, Gunn AJ, Halliday H, Juszczak E, Levene M, et al. Neurological outcomes at 18 months of age after moderate hypothermia for perinatal hypoxic ischaemic encephalopathy: synthesis and meta-analysis of trial data. *BMJ.* (2010) 340:c363. doi: 10.1136/bmj.c363
5. Rutherford M, Ramenghi LA, Edwards AD, Brocklehurst P, Halliday H, Levene M, et al. Assessment of brain tissue injury after moderate hypothermia in neonates with hypoxic-ischaemic encephalopathy: a nested substudy of a randomised controlled trial. *Lancet Neurol.* (2010) 9:39–45. doi: 10.1016/S1474-4422(09)70295-9
6. Thoresen M, Hellström-Westas L, Liu X, de Vries LS. Effect of hypothermia on amplitude-integrated electroencephalogram in infants with asphyxia. *Pediatrics.* (2010) 126:e131–9. doi: 10.1542/peds.2009-2938
7. Shankaran S, Pappas A, McDonald SA, Laptook AR, Bara R, Ehrenkranz RA, et al. Predictive value of an early amplitude integrated electroencephalogram and neurologic examination. *Pediatrics.* (2011) 128:e112–20. doi: 10.1542/peds.2010-2036
8. Takenouchi T, Rubens EO, Yap VL, Ross G, Engel M, Perlman JM. Delayed onset of sleep-wake cycling with favorable outcome in hypothermic-treated neonates with encephalopathy. *J Pediatr.* (2011) 159:232–7. doi: 10.1016/j.jpeds.2011.01.006
9. Shankaran S, Barnes PD, Hintz SR, Laptook AR, Zaterka-Baxter KM, McDonald SA, et al. Brain injury following trial of hypothermia for neonatal hypoxic-ischaemic encephalopathy. *Arch Dis Child Fetal Neonatal Ed.* (2012) 97:F398–404. doi: 10.1136/archdischild-2011-301524
10. Cseko AJ, Bangó M, Lakatos P, Kárdási J, Pusztai L, Szabó M. Accuracy of amplitude-integrated electroencephalography in the prediction of neurodevelopmental outcome in asphyxiated infants receiving hypothermia treatment. *Acta Paediatr.* (2013) 102:707–11. doi: 10.1111/apa.12226
11. Lemmers PM, Zwanenburg RJ, Benders MJ, de Vries LS, Groenendaal F, van Bel F, et al. Cerebral oxygenation and brain activity after perinatal asphyxia: does hypothermia change their prognostic value. *Pediatr Res.* (2013) 74:180–5. doi: 10.1038/pr.2013.84
12. Li J, Funato M, Tamai H, Wada H, Nishihara M, Iwamoto H, et al. Predictors of neurological outcome in cooled neonates. *Pediatr Int.* (2013) 55:169–76. doi: 10.1111/ped.12008
13. Chalak LF, DuPont TL, Sánchez PJ, Lucke A, Heyne RJ, Morriss MC, et al. Neurodevelopmental outcomes after hypothermia therapy in the era of Bayley-III. *J Perinatol.* (2014) 34:629–33. doi: 10.1038/jp.2014.67
14. Azzopardi D. Predictive value of the amplitude integrated EEG in infants with hypoxic ischaemic encephalopathy: data from a randomised trial of therapeutic hypothermia. *Arch Dis Child Fetal Neonatal Ed.* (2014) 99:F80–2. doi: 10.1136/archdischild-2013-303710
15. Del Balzo F, Maiolo S, Papoff P, Giannini L, Moretti C, Properzi E, et al. Electroencephalogram and magnetic resonance imaging comparison as a predicting factor for neurodevelopmental outcome in hypoxic ischemic encephalopathy infant treated with hypothermia. *Pediatr Rep.* (2014) 6:5532. doi: 10.4081/pr.2014.5532
16. Garfinkle J, Sant'Anna GM, Rosenblatt B, Majnemer A, Wintermark P, Shevell MI. Somatosensory evoked potentials in neonates with hypoxic-ischemic encephalopathy treated with hypothermia. *Eur J Paediatr Neurol.* (2015) 19:423–8. doi: 10.1016/j.ejpn.2015.03.001
17. Alderliesten T, de Vries LS, Khalil Y, van Haastert IC, Benders MJ, Koopman-Esseboom C, et al. Therapeutic hypothermia modifies perinatal asphyxia-induced changes of the corpus callosum and outcome in neonates. *PLoS ONE.* (2015) 10:e0123230. doi: 10.1371/journal.pone.0123230
18. Charon V, Proisy M, Bretaudeau G, Bruneau B, Pladys P, Beuchée A, et al. Early MRI in neonatal hypoxic-ischaemic encephalopathy treated with hypothermia: prognostic role at 2-year follow-up. *Eur J Radiol.* (2016) 85:1366–74. doi: 10.1016/j.ejrad.2016.05.005
19. Weeke LC, Boylan GB, Pressler RM, Hallberg B, Blennow M, Toet MC, et al. Role of EEG background activity, seizure burden and MRI in predicting neurodevelopmental outcome in full-term infants with hypoxic-ischaemic encephalopathy in the era of therapeutic hypothermia. *Eur J Paediatr Neurol.* (2016) 20:855–64. doi: 10.1016/j.ejpn.2016.06.003
20. Chiang MC, Lien R, Chu SM, Yang PH, Lin JJ, Hsu JF, et al. Serum lactate, brain magnetic resonance imaging and outcome of neonatal hypoxic ischemic encephalopathy after therapeutic hypothermia. *Pediatr Neonatol.* (2016) 57:35–40. doi: 10.1016/j.pedneo.2015.04.008

21. Heursen EM, Zuazo Ojeda A, Benavente Fernández I, Jimenez Gómez G, Campuzano Fernández-Colima R, Paz-Expósito J, et al. Prognostic value of the apparent diffusion coefficient in newborns with hypoxic-ischaemic encephalopathy treated with therapeutic hypothermia. *Neonatology.* (2017) 112:67–72. doi: 10.1159/000456707
22. Ahearne CE, Chang RY, Walsh BH, Boylan GB, Murray DM. Cord blood IL-16 is associated with 3-year neurodevelopmental outcomes in perinatal asphyxia and hypoxic-ischaemic encephalopathy. *Dev Neurosci.* (2017) 39:59–65. doi: 10.1159/000471508
23. Cainelli E, Trevisanuto D, Cavallin F, Manara R, Suppiej A. Evoked potentials predict psychomotor development in neonates with normal MRI after hypothermia for hypoxic-ischemic encephalopathy. *Clin Neurophysiol.* (2018) 129:1300–6. doi: 10.1016/j.clinph.2018.03.043
24. Nevalainen P, Lauronen L, Metsäranta M, Lönnqvist T, Ahtola E, Vanhatalo S. Neonatal somatosensory evoked potentials persist during hypothermia. *Acta Paediatr.* (2017) 106:912–7. doi: 10.1111/apa.13813
25. Trivedi SB, Vesoulis ZA, Rao R, Liao SM, Shimony JS, McKinstry RC, et al. A validated clinical MRI injury scoring system in neonatal hypoxic-ischemic encephalopathy. *Pediatr Radiol.* (2017) 47:1491–9. doi: 10.1007/s00247-017-3893-y
26. Skranes JH, Løhaugen G, Schumacher EM, Osredkar D, Server A, Cowan FM, et al. Amplitude-integrated electroencephalography improves the identification of infants with encephalopathy for therapeutic hypothermia and predicts neurodevelopmental outcomes at 2 years of age. *J Pediatr.* (2017) 187:34–42. doi: 10.1016/j.jpeds.2017.04.041
27. Weeke LC, Vilan A, Toet MC, van Haastert IC, de Vries LS, Groenendaal F. A comparison of the thompson encephalopathy score and amplitude-integrated electroencephalography in infants with perinatal asphyxia and therapeutic hypothermia. *Neonatology.* (2017) 112:24–9. doi: 10.1159/000455819
28. Liu X, Jary S, Cowan F, Thoresen M. Reduced infancy and childhood epilepsy following hypothermia-treated neonatal encephalopathy. *Epilepsia.* (2017) 58:1902–11. doi: 10.1111/epi.13914
29. Barta H, Jermendy A, Kolossvary M, Kozak LR, Lakatos A, Meder U, et al. Prognostic value of early, conventional proton magnetic resonance spectroscopy in cooled asphyxiated infants. *BMC Pediatr.* (2018) 18:302. doi: 10.1186/s12887-018-1269-6
30. De Wispelaere LA, Ouwehand S, Olsthoorn M, Govaert P, Smit LS, de Jonge RC, et al. Electroencephalography and brain magnetic resonance imaging in asphyxia comparing cooled and non-cooled infants. *Eur J Paediatr Neurol.* (2019) 23:181–90. doi: 10.1016/j.ejpn.2018.09.001
31. Nelson KB. Neonatal encephalopathy: etiology and outcome. *Dev Med Child Neurol.* (2005) 47:292. doi: 10.1017/S0012162205000563
32. Badawi N, Felix JF, Kurinczuk JJ, Dixon G, Watson L, Keogh JM, et al. Cerebral palsy following term newborn encephalopathy: a population-based study. *Dev Med Child Neurol.* (2005) 47:293–8. doi: 10.1017/S0012162205000575
33. Gunn AJ, Gluckman PD, Gunn TR. Selective head cooling in newborn infants after perinatal asphyxia: a safety study. *Pediatrics.* (1998) 102(4 Pt 1):885–92. doi: 10.1542/peds.102.4.885
34. Shankaran S, Laptook A, Wright LL, Ehrenkranz RA, Donovan EF, Fanaroff AA, et al. Whole-body hypothermia for neonatal encephalopathy: animal observations as a basis for a randomized, controlled pilot study in term infants. *Pediatrics.* (2002) 110(2 Pt 1):377–85. doi: 10.1542/peds.110.2.377
35. Barkovich AJ, Hajnal BL, Vigneron D, Sola A, Partridge JC, Allen F, et al. Prediction of neuromotor outcome in perinatal asphyxia: evaluation of MR scoring systems. *AJNR Am J Neuroradiol.* (1998) 19:143–9.
36. Thayyil S, Chandrasekaran M, Taylor A, Bainbridge A, Cady EB, Chong WK, et al. Cerebral magnetic resonance biomarkers in neonatal encephalopathy: a meta-analysis. *Pediatrics.* (2010) 125:e382–95. doi: 10.1542/peds.2009-1046
37. Sánchez Fernández I, Morales-Quezada JL, Law S, Kim P. Prognostic value of brain magnetic resonance imaging in neonatal hypoxic-ischemic encephalopathy: a meta-analysis. *J Child Neurol.* (2017) 32:1065–73. doi: 10.1177/0883073817726681
38. Degraeuwe PLj, Jaspers GJ, Robertson NJ, Kessels AG. Magnetic resonance spectroscopy as a prognostic marker in neonatal hypoxic-ischemic encephalopathy: a study protocol for an individual patient data meta-analysis. *Syst Rev.* (2013) 2:96. doi: 10.1186/2046-4053-2-96
39. Martinello K, Hart AR, Yap S, Mitra S, Robertson NJ. Management and investigation of neonatal encephalopathy: 2017 update. *Arch Dis Child Fetal Neonatal Ed.* (2017) 102:F346–58. doi: 10.1136/archdischild-2015-309639
40. Hellström-Westas L, Rosén I, Svenningsen NW. Predictive value of early continuous amplitude integrated EEG recordings on outcome after severe birth asphyxia in full term infants. *Arch Dis Child Fetal Neonatal Ed.* (1995) 72:F34–8. doi: 10.1136/fn.72.1.F34
41. Chandrasekaran M, Chaban B, Montaldo P, Thayyil S. Predictive value of amplitude-integrated EEG (aEEG) after rescue hypothermic neuroprotection for hypoxic ischemic encephalopathy: a meta-analysis. *J Perinatol.* (2017) 37:684–9. doi: 10.1038/jp.2017.14
42. Shany E, Goldstein E, Khvatskin S, Friger MD, Heiman N, Goldstein M, et al. Predictive value of amplitude-integrated electroencephalography pattern and voltage in asphyxiated term infants. *Pediatr Neurol.* (2006) 35:335–42. doi: 10.1016/j.pediatrneurol.2006.06.007
43. Gunn AJ, Bennet L. Fetal hypoxia insults and patterns of brain injury: insights from animal models. *Clin Perinatol.* (2009) 36:579–93. doi: 10.1016/j.clp.2009.06.007
44. Swarte RM, Cherian PJ, Lequin M, Visser GH, Govaert P. Somatosensory evoked potentials are of additional prognostic value in certain patterns of brain injury in term birth asphyxia. *Clin Neurophysiol.* (2012) 123:1631–8. doi: 10.1016/j.clinph.2011.12.009
45. Suppiej A, Cappellari A, Franzoi M, Traverso A, Ermani M, Zanardo V. Bilateral loss of cortical somatosensory evoked potential at birth predicts cerebral palsy in term and near-term newborns. *Early Hum Dev.* (2010) 86:93–8. doi: 10.1016/j.earlhumdev.2010.01.024
46. van Handel M, Swaab H, de Vries LS, Jongmans MJ. Long-term cognitive and behavioral consequences of neonatal encephalopathy following perinatal asphyxia: a review. *Eur J Pediatr.* (2007) 166:645–54. doi: 10.1007/s00431-007-0437-8

Conflict of Interest: The authors declare that the research was conducted in the absence of any commercial or financial relationships that could be construed as a potential conflict of interest.

frontiers in Neurology

ORIGINAL RESEARCH
published: 03 April 2020
doi: 10.3389/fneur.2020.00235

Peak Width of Skeletonized Water Diffusion MRI in the Neonatal Brain

Manuel Blesa[1], Paola Galdi[1], Gemma Sullivan[1], Emily N. Wheater[1], David Q. Stoye[1], Gillian J. Lamb[1], Alan J. Quigley[2], Michael J. Thrippleton[3,4], Mark E. Bastin[3] and James P. Boardman[1,3]*

[1] MRC Centre for Reproductive Health, University of Edinburgh, Edinburgh, United Kingdom, [2] Department of Radiology, Royal Hospital for Sick Children, Edinburgh, United Kingdom, [3] Centre for Clinical Brain Sciences, University of Edinburgh, Edinburgh, United Kingdom, [4] Edinburgh Imaging, University of Edinburgh, Edinburgh, United Kingdom

Preterm birth is closely associated with cognitive impairment and generalized dysconnectivity of neural networks inferred from water diffusion MRI (dMRI) metrics. Peak width of skeletonized mean diffusivity (PSMD) is a metric derived from histogram analysis of mean diffusivity across the white matter skeleton, and it is a useful biomarker of generalized dysconnectivity and cognition in adulthood. We calculated PSMD and five other histogram based metrics derived from diffusion tensor imaging (DTI) and neurite orientation and dispersion imaging (NODDI) in the newborn, and evaluated their accuracy as biomarkers of microstructural brain white matter alterations associated with preterm birth. One hundred and thirty five neonates (76 preterm, 59 term) underwent 3T MRI at term equivalent age. There were group differences in peak width of skeletonized mean, axial, and radial diffusivities (PSMD, PSAD, PSRD), orientation dispersion index (PSODI) and neurite dispersion index (PSNDI), all $p < 10^{-4}$. PSFA did not differ between groups. PSNDI was the best classifier of gestational age at birth with an accuracy of $81 \pm 10\%$, followed by PSMD, which had $77 \pm 9\%$ accuracy. Models built on both NODDI metrics, and on all dMRI metrics combined, did not outperform the model based on PSNDI alone. We conclude that histogram based analyses of DTI and NODDI parameters are promising new image markers for investigating diffuse changes in brain connectivity in early life.

Keywords: diffusion MRI, PSMD, preterm, neonate, NODDI, DTI

OPEN ACCESS

Edited by:
Deirdre M. Murray, University College Cork, Ireland

Reviewed by:
Daniel Edward Lumsden, Guy's and St. Thomas' NHS Foundation Trust, United Kingdom
Diego Iacono, Biomedical Research Institute of New Jersey, United States

****Correspondence:***
Manuel Blesa
manuel.blesa@ed.ac.uk

Specialty section:
This article was submitted to Pediatric Neurology, a section of the journal Frontiers in Neurology

Received: *03 December 2019*
Accepted: *11 March 2020*
Published: *03 April 2020*

Citation:
Blesa M, Galdi P, Sullivan G, Wheater EN, Stoye DQ, Lamb GJ, Quigley AJ, Thrippleton MJ, Bastin ME and Boardman JP (2020) Peak Width of Skeletonized Water Diffusion MRI in the Neonatal Brain. Front. Neurol. 11:235. doi: 10.3389/fneur.2020.00235

1. INTRODUCTION

Preterm birth is closely associated with a phenotype that includes cognitive impairment in childhood and cerebral white matter disease. White matter disease is apparent as diffuse changes in signal intensity on conventional MRI (1, 2), and alterations in diffusion MRI parameters based on the diffusion tensor [fractional anisotropy (FA), and mean, axial, and radial diffusivities, (MD, AD, RD)], and more recently, metrics based on biophysical models, such as neurite orientation and dispersion imaging (NODDI) (3, 4). These metrics have proven useful for making inferences about microstructural alteration of white matter that characterizes dysmaturity associated with preterm birth, for investigating upstream pathways to typical / atypical brain development, and for studying the anatomical bases of subsequent cognitive function in early life (5–13). However, deriving whole brain estimations of these parameters is often computationally expensive, there are uncertainties about which metric or combination of metrics best captures generalized white matter disease associated with preterm birth, and which is likely to be most useful for prognosis.

Peak width of skeletonized mean diffusivity (PSMD) is associated with processing speed—a foundational competence of cognition—in patients with small cerebral vessel disease, patients with Alzheimer's disease, healthy adults, and with a broader set of cognitive impairment (14, 15). In addition, it is a marker of widespread white matter tissue damage in multiple sclerosis (16). It works by calculating the width of the histogram of mean diffusivity of the skeletonized white matter (WM) tracts, thereby largely eliminating cerebrospinal fluid (CSF) contamination and focusing on the core of the main WM tracts. The framework is readily extensible to other DTI metrics (FA, RD, and AD) and to NODDI metrics.

Peak width of skeletonized DTI and NODDI metrics have potential to be useful biomarkers of preterm brain dysmaturation because several are known to be altered throughout white matter in association with preterm birth. Specifically, low FA and increased MD occur throughout the white matter in preterm infants at term equivalent age compared with term-born infants (4, 17–20), and NDI at term equivalent age it is negatively correlated with gestational age at birth (8). Additional advantages are that this framework is fully automated, only requires a single diffusion MRI acquisition, is computationally inexpensive, and has high inter-scanner reproducibility so could be used in clinical settings and for multi-center clinical trials (14).

In this work, we first optimized the PSMD pipeline described by Baykara et al. (14) for application to neonatal data in order to calculate values for PS- MD, FA, RD, AD, NDI, and ODI in early life. Next, based on the generalized dysconnectivity phenotype associated with preterm birth, we tested the hypothesis that infants born preterm would have differences in one or more of the histogram based metrics compared with infants born at term. Finally, we investigated the utility of these metrics by studying their relationship with gestational age at birth and testing their predictive ability in a classification task to discriminate between preterm and term brain images.

2. METHODS

2.1. Participants and Data Acquisition

Participants were recruited as part of a longitudinal study designed to investigate the effects of preterm birth on brain structure and long term outcome (www.tebc.ed.ac.uk) (21). One hundred and thirty-five neonates underwent MRI at term equivalent age at the Edinburgh Imaging Facility: Royal Infirmary of Edinburgh, University of Edinburgh, UK.

A Siemens MAGNETOM Prisma 3 T MRI clinical scanner (Siemens Healthcare Erlangen, Germany) and 16-channel phased-array pediatric head coil were used to acquire: 3D T2-weighted SPACE (T2w) (voxel size = 1 mm isotropic) with TE 409 ms and TR 3,200 ms; and axial dMRI. dMRI was acquired in two separate acquisitions: the first acquisition consisted of 8 baseline volumes (b = 0 s/mm^2 [b0]) and 64 volumes with b = 750 s/mm^2, the second consisted of 8 b0, 3 volumes with b = 200 s/mm^2, 6 volumes with b = 500 s/mm^2 and 64 volumes with b = 2,500 s/mm^2; an optimal angular coverage for the sampling scheme was applied (22). In addition, an acquisition of 3 b0 volumes with an inverse phase encoding direction was performed. All dMRI images were acquired using single-shot spin-echo echo planar imaging (EPI) with 2-fold simultaneous multislice and 2-fold in-plane parallel imaging acceleration and 2 mm isotropic voxels; all three diffusion acquisitions had the same parameters (TR/TE 3,400/78.0 ms). Images affected by motion artifact were re-acquired multiple times as required; dMRI acquisitions were repeated if signal loss was seen in 3 or more volumes.

Infants were fed and wrapped and allowed to sleep naturally in the scanner. Pulse oximetry, electrocardiography and temperature were monitored. Flexible earplugs and neonatal earmuffs (MiniMuffs, Natus) were used for acoustic protection. All scans were supervised by a doctor or nurse trained in neonatal resuscitation. Structural images were reported by an experienced pediatric radiologist (A.J.Q.) using the system described in Leuchter et al. (23), the exclusion criteria were the evidence of focal parenchymal injury (post-hemorrhagic ventricular dilatation, porencephalic cyst or cystic periventricular leukomalacia), or central nervous system malformation.

2.2. Data Pre-processing

All DICOM (Digital Imaging and Communication On Medicine) image files (dMRI and sMRI) were converted to the NIFTI (Neuroimaging Informatics Technology Initiative) format (24). Diffusion MRI processing was performed as follows: for each subject the two dMRI acquisitions were first concatenated and then denoised using a Marchenko-Pastur-PCA-based algorithm (25–27); eddy current, head movement and EPI geometric distortions were corrected using outlier replacement and slice-to-volume registration (28–32); bias field inhomogeneity correction was performed by calculating the bias field of the mean b0 volume and applying the correction to all the volumes (33). From the diffusion images we calculated the tensor (FA, MD, AD, and RD) and the NODDI (intracellular volume fraction [NDI] and the overall orientation dispersion index [ODI_{TOT}]) maps (3, 34–36).

2.3. Atlas Construction

Images from 50 term born infants were used to create a multi-modality template (including T1w, T2w, FA, and tensor templates in addition to different parcellation schemes and tissue probability maps) using established methods (37). The final atlas is the Edinburgh Neonatal Atlas 50 (ENA50) (38). Prior to template creation, the structural images were processed using the minimal processing pipeline of the developing human connectome project (39, 40). To obtain the parcellation schemes, different neonatal atlases were registered to the T2w (38, 41–45). The mean b0 of each subject was co-registered to the T2w (46) and the inverse transformation was used to move all the maps to diffusion space (label maps, T1w and T2w).

The template was constructed using DTI-TK. In summary, it performs white alignment using a non-parametric, highly deformable, diffeomorphic registration method that incrementally estimates the displacement field using a tensor-based registration formulation (37). The resulting transformations were then applied to all the modalities. The final templates were obtained by averaging all the images of the same

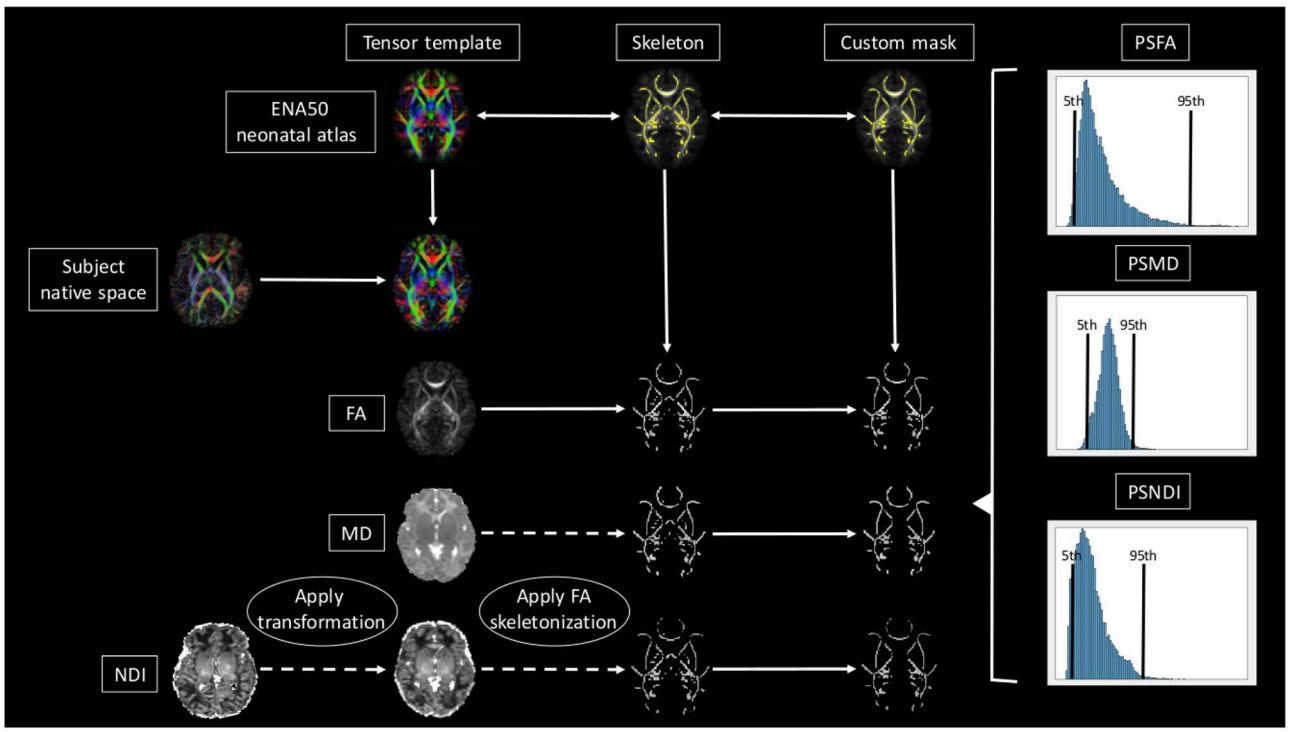

FIGURE 1 | Overview of the full pipeline. For simplicity only NDI, MD, and FA are shown. The subject is registered to the ENA50 using a tensor registration. Then the DTI derived maps are generated and the transformation applied to the NODDI maps. Using FA as a conductor, the images are skeletonized, and finally, all images are multiplied by the custom mask.

modality registered to the template space. For the parcellation maps, majority voting was used (47).

2.4. Peak Width of Skeletonized Water Diffusion MRI Derived Maps Calculation

All the subjects were registered to the tensor atlas using DTI-TK (48, 49). The tensor derived maps of each subject were calculated after registration and the NODDI metrics were propagated using the computed transformation. Then, the main skeleton of the FA template was created (50) by thresholding at 0.15, and individual FA maps were projected into this skeleton. Driven by the FA, the rest of the maps were projected onto the WM skeleton.

A custom mask was created by editing the skeleton mask to remove CSF and GM contaminated areas, and removing tracts passing through the cerebellum, the brainstem and the subcortical GM areas using ITK-Snap (51), using as a reference the custom mask created by Baykara et al. (14). The resulting skeletonized maps were then multiplied by the custom mask. Finally, the peak width of the histogram of values computed within the skeletonized maps was calculated as the difference between the 95th and 5th percentiles (14).

A brief overview of the full pipeline can be seen in **Figure 1**.

2.5. Statistical Analysis

In the following analyses, metrics were adjusted for age a scan by fitting a liner model of each metric on GA at scan and retaining the residuals. We report Pearson's correlations between each of the residualized metrics and GA at birth in the whole sample. A D'Agostino and Pearson's test was used to assess the normality of the residualized imaging metrics. Group comparisons of residualized PS-MD, AD, RD, FA, NDI, and ODI were made using two-sample *t*-test for normally distributed variables and the Mann-Whitney U test for variables that did not have a normal distribution. Reported *p*-values were adjusted for the false discovery rate (FDR) using the Benjamini–Hochberg procedure. We then used the residualized metrics as predictors in a logistic regression model to discriminate between preterm and term born infants. We compared the performance of each metric individually and of three multivariate models including all the metrics, only DTI metrics and only NODDI metrics, respectively. We measured classification accuracy using a 30-repeated 10-fold cross validation, meaning that in each of 30 repetitions data are randomly split in 10-folds of which one in turn is used as a test set to assess the generalization ability of the model trained on the remaining 9-folds. Folds were stratified to preserve the proportion of term and preterm subjects of the whole sample. Accuracy was computed as the percentage of correctly classified subjects across folds and repetitions.

3. RESULTS

Table 1 shows summary statistics of demographic characteristics of the study group.

TABLE 1 | Demographic characteristics of the study group.

	Preterm ($N = 76$)	Term ($N = 59$)	Term template ($N = 50$)
Male:Female	43:33	31:28	25:25
Mean GA at birth/weeks (range)	29.48 (23.42–32)*	39.48 (36.42–42)	39.49 (37–42)
Mean GA at scan/weeks (range)	40.97 (38–44.56) *	41.84 (38.28–43.84)	41.89 (38.28–43.84)

*Values marked with * are significantly different in preterm subjects with p<0.01 after FDR correction.*

TABLE 2 | Summary statistics for all metrics.

	PSMD	PSFA	PSAD	PSRD	PSNDI	PSODI
TERM						
Median	0.50	0.32	0.70	0.62	0.22	0.26
25%	0.48	0.31	0.68	0.57	0.21	0.25
75%	0.54	0.33	0.72	0.66	0.23	0.27
Min	0.38	0.29	0.61	0.48	0.18	0.23
Max	0.66	0.37	0.80	0.77	0.25	0.35
PRETERM						
Median	0.60	0.32	0.75	0.72	0.24	0.27
25%	0.56	0.32	0.72	0.67	0.23	0.27
75%	0.65	0.34	0.78	0.76	0.25	0.28
Min	0.45	0.28	0.63	0.54	0.19	0.24
Max	0.82	0.37	0.91	0.89	0.28	0.45

TABLE 3 | Mean 5th and 95th percentiles of imaging metrics in preterm and term groups.

	MD	FA	AD	RD	NDI	ODI
TERM						
5%	1.04	0.15	1.37	0.77	0.07	0.02
95%	1.55	0.48	2.07	1.38	0.29	0.28
PRETERM						
5%	1.05	0.13*	1.37	0.79	0.05*	0.02
95%	1.65*	0.46*	2.12*	1.50*	0.29	0.29*

*Values marked with * are significantly different in preterm subjects with p<0.01 after FDR correction.*

Table 2 shows the median, 25th and 75th percentiles, minimum and maximum values for each of the six histogram based metrics grouped by term and preterm categories, and **Table 3** shows the mean 5th and 95th percentiles for the original metrics separated by group. **Figure 2** shows the variation of each histogram based metric with respect to GA at birth and correlations between the metrics and GA at birth are reported in **Table 4**, together with results of group comparisons. With the exception of PSFA, all metrics were correlated with GA at birth ($p < 0.01$) and showed group differences in the term vs. preterm comparison ($p < 0.01$).

Table 4 reports the cross-validation accuracy of each metric in the classification task (term vs. preterm). Four out of six metrics achieved at least 70% accuracy, with the exception of PSFA (60 ± 5%) and PSODI (67 ± 17%). PSMD and PSNDI obtained the best results among the DTI and NODDI metrics, respectively. Combining the metrics in a multivariate model increased only slightly the prediction accuracy: using all DTI metrics: 79 ± 9% accuracy; using all NODDI metrics: 81 ± 7% accuracy; using all metrics: 79 ± 7% accuracy.

4. DISCUSSION

We developed a pipeline for calculating peak width of skeletonized diffusion MRI derived metrics of the developing brain, and we show that five of these histogram based markers detect generalized white matter microstructural alteration associated with preterm birth. Calculation of these image markers is fully automated and computationally inexpensive, so peak width of skeletonized water diffusion metrics could have high value for research designed to investigate generalized dysconnectivity phenotypes in early life.

The NODDI and tensor derived metrics have been applied to different populations including healthy and aging adults (52, 53), patients with amyotrophic lateral sclerosis and Alzheimer's disease patients (54, 55), and to preclinical models (56, 57). In the neonatal MRI field, tensor derived metrics have been widely used to study the effects of prematurity on the brain (5), and several other factors, such as chronic lung disease, nutrition, prenatal drug exposure, among others (11, 13, 19, 58). In recent years NODDI metrics have been applied to neonatal data because of the added inference they offer with respect to microstructural organization and characteristics (59). They have revealed new insights into cortical maturation in perinatal life, and identified dysmaturation in newborns with congenital heart disease (59, 60). Recently, the tensor derived and NODDI metrics have been used together in integrated approaches, such as morphometric similarity networks (12, 61), but to our knowledge, this is the first time that DTI and NODDI metrics have been used within the peak width skeletonized framework for studying the developing brain.

We found that all the PS metrics with exception of the PSFA were higher for preterm infants at term equivalent age compared with values calculated from infants born at full term, meaning that the range of values was wider for the preterm population. However, the behavior of the metrics was different, which enables an inference about underlying tissue microstructure. For example MD has the same 5th percentile in term and preterm infants at term equivalent age but the 95th percentile is much higher in preterm group, whereas for NDI the opposite is true: both groups have the same 95th percentile, but the 5th percentile is much lower in preterm infants. Taken together, the metrics indicate

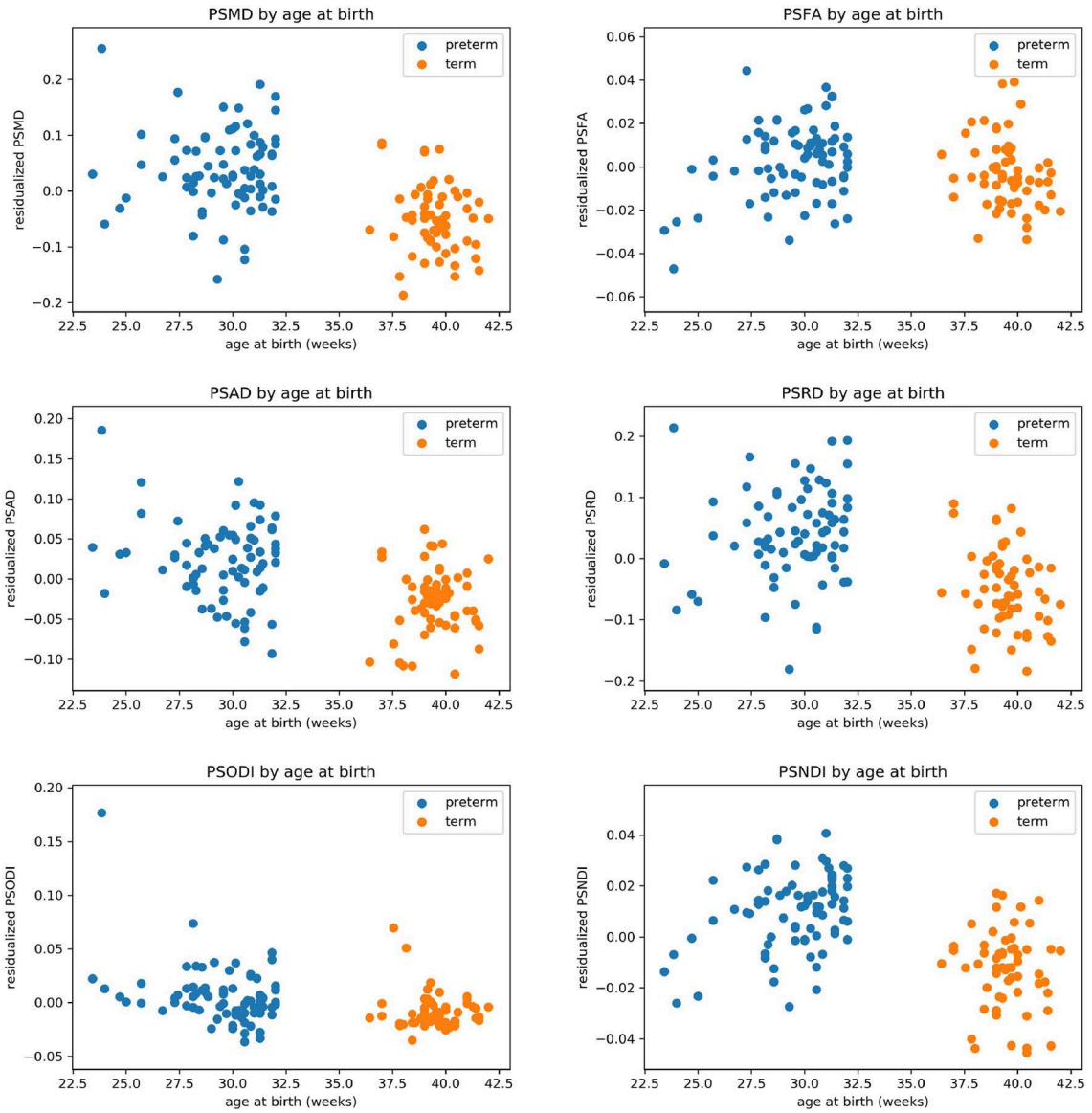

FIGURE 2 | Scatter plots showing the relationship between each of the metric and gestational age at birth.

TABLE 4 | Results for the correlation with GA and the classification task.

Metric	Correlation with GA at birth	Group comparison	Classification accuracy
PSMD	$r = -0.52, p = 2.72 \times 10^{-10}$	$t = 7.59,\ p = 2.80 \times 10^{-11}$	0.77 ± 0.09
PSFA	$r = -0.11, p = 0.233$	$t = 2.02,\ p = 0.052$	0.60 ± 0.05
PSAD	$r = -0.49, p = 4.95 \times 10^{-9}$	$t = 6.40,\ p = 5.60 \times 10^{-9}$	0.73 ± 0.11
PSRD	$r = -0.50, p = 2.257 \times 10^{-09}$	$t = 7.45,\ p = 4.78 \times 10^{-11}$	0.75 ± 0.09
PSNDI	$r = -0.51, p = 8.50 \times 10^{-10}$	$t = 8.55,\ p = 4.56 \times 10^{-13}$	0.81 ± 0.10
PSODI	$r = -0.37, p = 1.39 \times 10^{-05}$	$u = 3272, p = 7.86 \times 10^{-06}$	0.67 ± 0.17

higher variability in water content (toward higher values) and in intra-axonal volume (toward lower values) in preterm infant. This is consistent with lower myelination in preterm infants and/or less coherent WM organization (62), which is suggested by an overall higher PSODI for the preterm population. For RD the values in 95th and 5th percentile are higher in preterm than term, but the difference is much more accentuated in the 95th percentile, in agreement with PSMD. Increased PSAD in preterm

infants at term equivalent age is consistent with altered axonal integrity, which is a feature of white matter disease in preterm infants. PSFA was the only metric that did not show a significant difference between groups, although there was a histogram shift (**Table 3**) such that term infants do have higher mean FA across the skeleton, which is a consistent finding across studies (4).

All the metrics, with exception of the PSFA and PSODI, achieved high accuracy (≥70%) in the classification task of preterm vs. term brain images. PSMD and PSNDI performed with greatest accuracy (**Table 3**), and this was not enhanced by combining multiple features in the same model. Different methods for preterm vs. term classification have been proposed with varying accuracy: 80% (63) or 92% (12). However, previous methods usually require long acquisitions and/or complicated processing frameworks. The main advantage of the histogram based framework is that it is possible to calculate measures from standard diffusion MRI acquisition and with relatively simple processing, making it suitable for large scale multi-site studies (14).

Application of histogram based methods to neonatal data required some modifications to the original framework proposed by Baykara et al. First, we optimized the method to operate in a specific neonatal space, as opposed to the MNI152 co-ordinate system (64). For doing this, a neonatal template was created (ENA50) and used as a common space for the whole process. The registration method was also changed: the original method uses FNIRT (65) because it is based in the main TBSS framework (50). Due the nature of the tensor-based neonatal atlas, we are able to use a tensor-based registration (48, 49) with a three-step registration, adding a rigid step at the beginning (19). This method has been shown to improve the alignment of WM tracts in neonatal data (10, 19, 66). One of the main advantages of the proposed framework, is that due to the multi-modal nature of the ENA50 (FA, T1-weighted, T2-weighted and tensor templates) the pipeline can be easily modified to change the registration process for any of the available intensity-based algorithms (41, 65, 67–69).

Histogram based analyses of DTI and NODDI metrics offer tractable markers that could be used to investigate generalized white matter connectivity in other neonatal populations at risk of atypical brain development and the extensible nature of the framework means that it could be applied to other myelin sensitive metrics not derived from diffusion, such as T1w/T2w (70) or g-ratio (71). Future work could investigate the utility of histogram based metrics for assessing the impact of perinatal exposures and co-morbidities on brain tissue development, and their predictive value for cognitive and behavioral outcomes in children at risk of impairment. Furthermore, their possible utility in clinical settings, providing summary information about WM microstructure from MRI datasets acquired on different scanners, and as potential biomarkers in neuroprotection trials should be evaluated.

5. CONCLUSION

In this work, we introduce an age-specific pipeline for calculation of peak width of skeletonized MD, RD, AD, FA, NDI, and ODI of the neonatal brain. We found that these histogram based metrics, which represent generalized water content, myelination, and complexity of dendrites and axons across the WM skeleton, are altered in association with preterm birth. PSMD and PSNDI appear to be the most promising biomarkers due to their relative ease of computation compared with other methods, and their comparable accuracy.

DATA AVAILABILITY STATEMENT

The atlas with templates can be found at https://git.ecdf.ed.ac.uk/jbrl/ena and the code necessary to calculate histogram based metrics is at https://git.ecdf.ed.ac.uk/jbrl/psmd. Reasonable requests for original image data will be considered through the BRAINS governance process: www.brainsimagebank.ac.uk (72).

ETHICS STATEMENT

The studies involving human participants were reviewed and approved by UK National Research Ethics Service. Written informed consent to participate in this study was provided by the participants' legal guardian/next of kin.

AUTHOR CONTRIBUTIONS

MB and PG designed the experiments and wrote the first draft of the manuscript. MB processed the data. PG did the statistical analyses. GS, DS, GL, AQ, and MT acquired the data. EW contributed to the analysis of data. JB and MEB provided help with the interpretation and wrote the manuscript. All authors revised and commented on the manuscript.

FUNDING

This work was supported by Theirworld (www.theirworld.org). MT was supported by NHS Lothian Research and Development Office. The work was undertaken in the MRC Centre for Reproductive Health, which was funded by MRC Centre Grant (MRC G1002033).

ACKNOWLEDGMENTS

Participants were scanned in the University of Edinburgh Imaging Research MRI Facility at the Royal Infirmary of Edinburgh which was established with funding from The Wellcome Trust, Dunhill Medical Trust, Edinburgh and Lothians Research Foundation, Theirworld, The Muir Maxwell Trust, and other sources.

Individual parcellated templates and structural MRI images from the M-CRIB atlas (45) were supplied by the Murdoch Children's Research Institute.

We were grateful to the families who consented to take part in the study and to all the University's imaging research staff for providing the infant scanning.

REFERENCES

1. Dyet LE, Kennea N, Counsell SJ, Maalouf EF, Ajayi-Obe M, Duggan PJ, et al. Natural history of brain lesions in extremely preterm infants studied with serial magnetic resonance imaging from birth and neurodevelopmental assessment. *Pediatrics.* (2006) 118:536–48. doi: 10.1542/peds.2005-1866
2. Woodward LJ, Anderson PJ, Austin NC, Howard K, Inder TE. Neonatal MRI to predict neurodevelopmental outcomes in preterm infants. *N Engl J Med.* (2006) 355:685–94. doi: 10.1056/NEJMoa053792
3. Zhang H, Schneider T, Wheeler-Kingshott CA, Alexander DC. NODDI: practical *in vivo* neurite orientation dispersion and density imaging of the human brain. *Neuroimage.* (2012) 61:1000–16. doi: 10.1016/j.neuroimage.2012.03.072
4. Pecheva D, Kelly C, Kimpton J, Bonthrone A, Batalle D, Zhang H, et al. Recent advances in diffusion neuroimaging: applications in the developing preterm brain. *F1000Res.* (2018) 7:F1000 Faculty Rev-1326. doi: 10.12688/f1000research.15073.1
5. Counsell SJ, Edwards AD, Chew ATM, Cowan FM, Boardman JP, Allsop JM, et al. Specific relations between neurodevelopmental abilities and white matter microstructure in children born preterm. *Brain.* (2008) 131:3201–8. doi: 10.1093/brain/awn268
6. van Kooij BJM, van Pul C, Benders MJNL, van Haastert IC, de Vries LS, Groenendaal F. Fiber tracking at term displays gender differences regarding cognitive and motor outcome at 2 years of age in preterm infants. *Pediatr Res.* (2011) 70:626–32. doi: 10.1203/PDR.0b013e318232a963
7. Anblagan D, Pataky R, Evans MJ, Telford EJ, Serag A, Sparrow S, et al. Association between preterm brain injury and exposure to chorioamnionitis during fetal life. *Sci Rep.* (2016) 6:37932. doi: 10.1038/srep37932
8. Batalle D, Hughes EJ, Zhang H, Tournier JD, Tusor N, et al. Early development of structural networks and the impact of prematurity on brain connectivity. *Neuroimage.* (2017) 149:379–92. doi: 10.1016/j.neuroimage.2017.01.065
9. Telford EJ, Cox SR, Fletcher-Watson S, Anblagan D, Sparrow S, Pataky R, et al. A latent measure explains substantial variance in white matter microstructure across the newborn human brain. *Brain Struct Funct.* (2017) 222:4023–33. doi: 10.1007/s00429-017-1455-6
10. Barnett ML, Tusor N, Ball G, Chew A, Falconer S, Aljabar P, et al. Exploring the multiple-hit hypothesis of preterm white matter damage using diffusion MRI. *Neuroimage Clin.* (2018) 17:596–606. doi: 10.1016/j.nicl.2017.11.017
11. Blesa M, Sullivan G, Anblagan D, Telford EJ, Quigley AJ, Sparrow SA, et al. Early breast milk exposure modifies brain connectivity in preterm infants. *Neuroimage.* (2019) 184:431–9. doi: 10.1016/j.neuroimage.2018.09.045
12. Galdi P, Blesa M, Stoye DQ, Sullivan G, Lamb GJ, Quigley AJ, et al. Neonatal morphometric similarity mapping for predicting brain age and characterizing neuroanatomic variation associated with preterm birth. *Neuroimage Clin.* (2020) 25:102195. doi: 10.1016/j.nicl.2020.102195
13. Boardman JP, Counsell SJ. Factors associated with atypical brain development in preterm infants: insights from magnetic resonance imaging. *Neuropathol Appl Neurobiol.* (2019). doi: 10.1111/nan.12589
14. Baykara E, Gesierich B, Adam R, Tuladhar AM, Biesbroek JM, Koek HL, et al. A novel imaging marker for small vessel disease based on skeletonization of white matter tracts and diffusion histograms. *Ann Neurol.* (2016) 80:581–92. doi: 10.1002/ana.24758
15. Deary IJ, Ritchie SJ, Muñoz Maniega S, Cox SR, Valdés Hernández MC, Luciano M, et al. Brain peak width of skeletonized mean diffusivity (PSMD) and cognitive function in later life. *Front Psychiatry.* (2019) 10:524. doi: 10.3389/fpsyt.2019.00524
16. Vinciguerra C, Giorgio A, Zhang J, Donato ID, Stromillo ML, Brocci RT, et al. Peak width of skeletonized mean diffusivity (PSMD) as marker of widespread white matter tissue damage in multiple sclerosis. *Mult Scler Relat Disord.* (2019) 27:294–7. doi: 10.1016/j.msard.2018.11.011
17. Partridge SC, Mukherjee P, Henry RG, Miller SP, Berman JI, Jin H, et al. Diffusion tensor imaging: serial quantitation of white matter tract maturity in premature newborns. *Neuroimage.* (2004) 22:1302–14. doi: 10.1016/j.neuroimage.2004.02.038
18. Anjari M, Srinivasan L, Allsop JM, Hajnal JV, Rutherford MA, Edwards AD, et al. Diffusion tensor imaging with tract-based spatial statistics reveals local white matter abnormalities in preterm infants. *Neuroimage.* (2007) 35:1021–7. doi: 10.1016/j.neuroimage.2007.01.035
19. Ball G, Counsell SJ, Anjari M, Merchant N, Arichi T, Doria V, et al. An optimised tract-based spatial statistics protocol for neonates: applications to prematurity and chronic lung disease. *Neuroimage.* (2010) 53:94–102. doi: 10.1016/j.neuroimage.2010.05.055
20. Thompson DK, Inder TE, Faggian N, Johnston L, Warfield SK, Anderson PJ, et al. Characterization of the corpus callosum in very preterm and full-term infants utilizing MRI. *Neuroimage.* (2011) 55:479–90. doi: 10.1016/j.neuroimage.2010.12.025
21. Boardman JP, Hall J, Thrippleton MJ, Reynolds RM, Bogaert D, Davidson DJ, et al. Impact of preterm birth on brain development and long-term outcome: protocol for a cohort study in Scotland. *BMJ open.* (2020) 10:e035854.
22. Caruyer E, Lenglet C, Sapiro G, Deriche R. Design of multishell sampling schemes with uniform coverage in diffusion MRI. *Magn Reson Med.* (2013) 69:1534–40. doi: 10.1002/mrm.24736
23. Leuchter RHV, Gui L, Poncet A, Hagmann C, Lodygensky GA, Martin E, et al. Association between early administration of high-dose erythropoietin in preterm infants and brain MRI abnormality at term-equivalent age. *JAMA.* (2014) 312:817–24. doi: 10.1001/jama.2014.9645
24. Li X, Morgan PS, Ashburner J, Smith J, Rorden C. The first step for neuroimaging data analysis: DICOM to NIfTI conversion. *J Neurosci Methods.* (2016) 264:47–56. doi: 10.1016/j.jneumeth.2016.03.001
25. Veraart J, Fieremans E, Novikov DS. Diffusion MRI noise mapping using random matrix theory. *Magn Reson Med.* (2016) 76:1582–93. doi: 10.1002/mrm.26059
26. Veraart J, Novikov DS, Christiaens D, Ades-aron B, Sijbers J, Fieremans E. Denoising of diffusion MRI using random matrix theory. *Neuroimage.* (2016) 142:394–406. doi: 10.1016/j.neuroimage.2016.08.016
27. Tournier JD, Smith RE, Raffelt DA, Tabbara R, Dhollander T, Pietsch M, et al. MRtrix3: a fast, flexible and open software framework for medical image processing and visualisation. *NeuroImage.* (2019) 202:116137. doi: 10.1101/551739
28. Andersson JLR, Skare S, Ashburner J. How to correct susceptibility distortions in spin-echo echo-planar images: application to diffusion tensor imaging. *Neuroimage.* (2003) 20:870–88. doi: 10.1016/S1053-8119(03)00336-7
29. Smith SM, Jenkinson M, Woolrich MW, Beckmann CF, Behrens TEJ, Johansen-Berg H, et al. Advances in functional and structural MR image analysis and implementation as FSL. *Neuroimage.* (2004) 23:S208–19. doi: 10.1016/j.neuroimage.2004.07.051
30. Andersson JLR, Sotiropoulos SN. An integrated approach to correction for off-resonance effects and subject movement in diffusion MR imaging. *Neuroimage.* (2016) 125:1063–78. doi: 10.1016/j.neuroimage.2015.10.019
31. Andersson JLR, Graham MS, Zsoldos E, Sotiropoulos SN. Incorporating outlier detection and replacement into a non-parametric framework for movement and distortion correction of diffusion MR images. *Neuroimage.* (2016) 141:556–72. doi: 10.1016/j.neuroimage.2016.06.058
32. Andersson JLR, Graham MS, Drobnjak I, Zhang H, Filippini N, Bastiani M. Towards a comprehensive framework for movement and distortion correction of diffusion MR images: within volume movement. *Neuroimage.* (2017) 152:450–66. doi: 10.1016/j.neuroimage.2017.02.085
33. Tustison NJ, Avants BB, Cook PA, Zheng Y, Egan A, Yushkevich PA, et al. N4ITK: improved N3 bias correction. *IEEE Trans Med Imaging.* (2010) 29:1310–20. doi: 10.1109/TMI.2010.2046908
34. Basser PJ, Pierpaoli C. Microstructural and physiological features of tissues elucidated by quantitative-diffusion-tensor MRI. *J Magn Reson.* (2011) 213:560–70. doi: 10.1016/j.jmr.2011.09.022

35. Tariq M, Schneider T, Alexander DC, Wheeler-Kingshott CAG, Zhang H. Bingham-NODDI: mapping anisotropic orientation dispersion of neurites using diffusion MRI. *Neuroimage.* (2016) 133:207–23. doi: 10.1016/j.neuroimage.2016.01.046
36. Hernandez-Fernandez M, Reguly I, Jbabdi S, Giles M, Smith S, Sotiropoulos SN. Using GPUs to accelerate computational diffusion MRI: from microstructure estimation to tractography and connectomes. *Neuroimage.* (2019) 188:598–615. doi: 10.1016/j.neuroimage.2018.12.015
37. Zhang H, Yushkevich PA, Rueckert D, Gee JC. Unbiased white matter atlas construction using diffusion tensor images. In: Ayache N, Ourselin S, Maeder A, editors. *Medical Image Computing and Computer-Assisted Intervention-MICCAI 2007*. Berlin; Heidelberg: Springer Berlin Heidelberg (2007). p. 211–8.
38. Blesa M, Serag A, Wilkinson AG, Anblagan D, Telford EJ, Pataky R, et al. Parcellation of the healthy neonatal brain into 107 regions using atlas propagation through intermediate time points in childhood. *Front Neurosci.* (2016) 10:220. doi: 10.3389/fnins.2016.00220
39. Makropoulos A, Aljabar P, Wright R, Hüning B, Merchant N, et al. Regional growth and atlasing of the developing human brain. *Neuroimage.* (2016) 125:456–78. doi: 10.1016/j.neuroimage.2015.10.047
40. Makropoulos A, Robinson EC, Schuh A, Wright R, Fitzgibbon S, et al. The developing human connectome project: a minimal processing pipeline for neonatal cortical surface reconstruction. *Neuroimage.* (2018) 173:88–112. doi: 10.1016/j.neuroimage.2018.01.054
41. Avants BB, Epstein CL, Grossman M, Gee JC. Symmetric diffeomorphic image registration with cross-correlation: Evaluating automated labeling of elderly and neurodegenerative brain. *Med Image Anal.* (2008) 12:26–41. doi: 10.1016/j.media.2007.06.004
42. Shi F, Yap PT, Wu G, Jia H, Gilmore JH, Lin W, et al. Infant brain atlases from neonates to 1- and 2-year-olds. *PLoS ONE.* (2011) 6:e18746. doi: 10.1371/journal.pone.0018746
43. Oishi K, Mori S, Donohue PK, Ernst T, Anderson L, Buchthal S, et al. Multi-contrast human neonatal brain atlas: application to normal neonate development analysis. *Neuroimage.* (2011) 56:8–20. doi: 10.1016/j.neuroimage.2011.01.051
44. Wang H, Suh JW, Das SR, Pluta JB, Craige C, Yushkevich PA. Multi-atlas segmentation with joint label fusion. *IEEE Trans Pattern Anal Mach Intell.* (2013) 35:611–23. doi: 10.1109/TPAMI.2012.143
45. Alexander B, Murray AL, Loh WY, Matthews LG, Adamson C, Beare R, et al. A new neonatal cortical and subcortical brain atlas: the Melbourne Children's Regional Infant Brain (M-CRIB) atlas. *Neuroimage.* (2017) 147:841–51. doi: 10.1016/j.neuroimage.2016.09.068
46. Greve DN, Fischl B. Accurate and robust brain image alignment using boundary-based registration. *Neuroimage.* (2009) 48:63–72. doi: 10.1016/j.neuroimage.2009.06.060
47. Heckemann RA, Hajnal JV, Aljabar P, Rueckert D, Hammers A. Automatic anatomical brain MRI segmentation combining label propagation and decision fusion. *Neuroimage.* (2006) 33:115–26. doi: 10.1016/j.neuroimage.2006.05.061
48. Zhang H, Yushkevich PA, Alexander DC, Gee JC. Deformable registration of diffusion tensor MR images with explicit orientation optimization. *Med Image Anal.* (2006) 10:764–85. doi: 10.1016/j.media.2006.06.004
49. Zhang H, Avants BB, Yushkevich PA, Woo JH, Wang S, McCluskey LF, et al. High-dimensional spatial normalization of diffusion tensor images improves the detection of white matter differences: an example study using amyotrophic lateral sclerosis. *IEEE Trans Med Imaging.* (2007) 26:1585–97. doi: 10.1109/TMI.2007.906784
50. Smith SM, Jenkinson M, Johansen-Berg H, Rueckert D, Nichols TE, Mackay CE, et al. Tract-based spatial statistics: voxelwise analysis of multi-subject diffusion data. *Neuroimage.* (2006) 31:1487–505. doi: 10.1016/j.neuroimage.2006.02.024
51. Yushkevich PA, Piven J, Cody Hazlett H, Gimpel Smith R, Ho S, Gee JC, et al. User-guided 3D active contour segmentation of anatomical structures: significantly improved efficiency and reliability. *Neuroimage.* (2006) 31:1116–28. doi: 10.1016/j.neuroimage.2006.01.015
52. Cox SR, Ritchie SJ, Tucker-Drob EM, Liewald DC, Hagenaars SP, Davies G, et al. Ageing and brain white matter structure in 3,513 UK biobank participants. *Nat Commun.* (2016) 7:13629. doi: 10.1038/ncomms13629
53. Kodiweera C, Alexander AL, Harezlak J, McAllister TW, Wu YC. Age effects and sex differences in human brain white matter of young to middle-aged adults: a DTI, NODDI, and q-space study. *Neuroimage.* (2016) 128:180–92. doi: 10.1016/j.neuroimage.2015.12.033
54. Wen Q, Mustafi SM, Li J, Risacher SL, Tallman E, Brown SA, et al. White matter alterations in early-stage Alzheimer's disease: a tract-specific study. *Alzheimers Dement.* (2019) 11:576–87. doi: 10.1016/j.dadm.2019.06.003
55. Broad RJ, Gabel MC, Dowell NG, Schwartzman DJ, Seth AK, Zhang H, et al. Neurite orientation and dispersion density imaging (NODDI) detects cortical and corticospinal tract degeneration in ALS. *J Neurol Neurosurg Psychiatry.* (2019) 90:404–11. doi: 10.1136/jnnp-2018-318830
56. Colgan N, Siow B, O'Callaghan JM, Harrison IF, Wells JA, Holmes HE, et al. Application of neurite orientation dispersion and density imaging (NODDI) to a tau pathology model of Alzheimer's disease. *Neuroimage.* (2016) 125:739–44. doi: 10.1016/j.neuroimage.2015.10.043
57. Yi SY, Barnett BR, Torres-Velázquez M, Zhang Y, Hurley SA, Rowley PA, et al. Detecting microglial density with quantitative multi-compartment diffusion MRI. *Front Neurosci.* (2019) 13:81. doi: 10.3389/fnins.2019.00081
58. Monnelly VJ, Anblagan D, Quigley A, Cabez MB, Cooper ES, Mactier H, et al. Prenatal methadone exposure is associated with altered neonatal brain development. *Neuroimage Clin.* (2018) 18:9–14. doi: 10.1016/j.nicl.2017.12.033
59. Batalle D, O'Muircheartaigh J, Makropoulos A, Kelly CJ, Dimitrova R, Hughes EJ, et al. Different patterns of cortical maturation before and after 38 weeks gestational age demonstrated by diffusion MRI *in vivo*. *Neuroimage.* (2019) 185:764–75. doi: 10.1016/j.neuroimage.2018.05.046
60. Kelly CJ, Christiaens D, Batalle D, Makropoulos A, Cordero-Grande L, Steinweg JK, et al. Abnormal microstructural development of the cerebral cortex in neonates with congenital heart disease is associated with impaired cerebral oxygen delivery. *J Am Heart Assoc.* (2019) 8:e009893. doi: 10.1161/JAHA.118.009893
61. Fenchel D, Dimitrova R, Seidlitz J, Robinson EC, Batalle D, Hutter J, et al. Development of microstructural and morphological cortical profiles in the neonatal brain. *bioRxiv.* (2020). Available online at: https://www.biorxiv.org/content/early/2020/01/16/2020.01.14.906206
62. Hinojosa-Rodríguez M, Harmony T, Carrillo-Prado C, Horn JDV, Irimia A, Torgerson C, et al. Clinical neuroimaging in the preterm infant: diagnosis and prognosis. *Neuroimage Clin.* (2017) 16:355–68. doi: 10.1016/j.nicl.2017.08.015
63. Ball G, Aljabar P, Arichi T, Tusor N, Cox D, Merchant N, et al. Machine-learning to characterise neonatal functional connectivity in the preterm brain. *Neuroimage.* (2016) 124:267–75. doi: 10.1016/j.neuroimage.2015.08.055
64. Grabner G, Janke AL, Budge MM, Smith D, Pruessner J, Collins DL. Symmetric atlasing and model based segmentation: an application to the hippocampus in older adults. In: Larsen R, Nielsen M, Sporring J, editors. *Medical Image Computing and Computer-Assisted Intervention-MICCAI 2006.* Berlin; Heidelberg: Springer Berlin Heidelberg (2006). p. 58–66.
65. Andersson JLR, Jenkinson M, Smith S. High resolution nonlinear registration with simultaneous modelling of intensities. *bioRxiv.* (2019). Available online at: https://www.biorxiv.org/content/early/2019/05/22/646802
66. Bach M, Laun FB, Leemans A, Tax CMW, Biessels GJ, Stieltjes B, et al. Methodological considerations on tract-based spatial statistics (TBSS). *Neuroimage.* (2014) 100:358–69. doi: 10.1016/j.neuroimage.2014.06.021
67. Rueckert D, Sonoda LI, Hayes C, Hill DLG, Leach MO, Hawkes DJ. Nonrigid registration using free-form deformations: application to breast MR images. *IEEE Trans Med Imaging.* (1999) 18:712–21. doi: 10.1109/42.796284
68. Klein A, Andersson J, Ardekani BA, Ashburner J, Avants B, Chiang MC, et al. Evaluation of 14 nonlinear deformation algorithms applied to human brain MRI registration. *Neuroimage.* (2009) 46:786–802. doi: 10.1016/j.neuroimage.2008.12.037
69. Ou Y, Sotiras A, Paragios N, Davatzikos C. DRAMMS: deformable registration via attribute matching and mutual-saliency weighting. *Med Image Anal.* (2011) 15:622–39. doi: 10.1016/j.media.2010.07.002

70. Glasser MF, Van Essen DC. Mapping human cortical areas *in vivo* based on myelin content as revealed by T1- and T2-weighted MRI. *J Neurosci.* (2011) 31:11597–616. doi: 10.1523/JNEUROSCI.2180-11.2011
71. Stikov N, Campbell JSW, Stroh T, Lavelée M, Frey S, Novek J, et al. *In vivo* histology of the myelin g-ratio with magnetic resonance imaging. *Neuroimage.* (2015) 118:397–405. doi: 10.1016/j.neuroimage.2015.05.023
72. Job DE, Dickie DA, Rodriguez D, Robson A, Danso S, Pernet C, et al. A brain imaging repository of normal structural MRI across the life course: brain images of normal subjects (BRAINS). *Neuroimage.* (2017) 144:299–304. doi: 10.1016/j.neuroimage.2016.01.027

Conflict of Interest: The authors declare that the research was conducted in the absence of any commercial or financial relationships that could be construed as a potential conflict of interest.

frontiers in Neurology

SYSTEMATIC REVIEW
published: 27 May 2020
doi: 10.3389/fneur.2020.00393

Cerebral Near Infrared Spectroscopy Monitoring in Term Infants With Hypoxic Ischemic Encephalopathy—A Systematic Review

Subhabrata Mitra[1], Gemma Bale[2], Judith Meek[1], Ilias Tachtsidis[2] and Nicola J. Robertson[1]*

[1] Neonatology, Institute for Women's Health, University College London, London, United Kingdom, [2] Medical Physics and Biomedical Engineering, University College London, London, United Kingdom

OPEN ACCESS

Edited by:
Julie Wixey,
University of Queensland, Australia

Reviewed by:
Flora Wong,
Monash University, Australia
Eugene Dempsey,
University College Cork, Ireland

***Correspondence:**
Subhabrata Mitra
subhabrata.mitra.13@ucl.ac.uk

Specialty section:
This article was submitted to Pediatric Neurology, a section of the journal Frontiers in Neurology

Received: *07 February 2020*
Accepted: *17 April 2020*
Published: *27 May 2020*

Citation:
Mitra S, Bale G, Meek J, Tachtsidis I and Robertson NJ (2020) Cerebral Near Infrared Spectroscopy Monitoring in Term Infants With Hypoxic Ischemic Encephalopathy—A Systematic Review. Front. Neurol. 11:393. doi: 10.3389/fneur.2020.00393

Background: Neonatal hypoxic ischemic encephalopathy (HIE) remains a significant cause of mortality and morbidity worldwide. Cerebral near infrared spectroscopy (NIRS) can provide cot side continuous information about changes in brain hemodynamics, oxygenation and metabolism in real time.

Objective: To perform a systematic review of cerebral NIRS monitoring in term and near-term infants with HIE.

Search Methods: A systematic search was performed in Ovid EMBASE and Medline database from inception to November 2019. The search combined three broad categories: measurement (NIRS monitoring), disease condition [hypoxic ischemic encephalopathy (HIE)] and subject category (newborn infants) using a stepwise approach as per PRISMA guidance.

Selection Criteria: Only human studies published in English were included.

Data Collection and Analysis: Two authors independently selected, assessed the quality, and extracted data from the studies for this review.

Results: Forty-seven studies on term and near-term infants following HIE were identified. Most studies measured multi-distance NIRS based cerebral tissue saturation using monitors that are referred to as cerebral oximeters. Thirty-nine studies were published since 2010; eight studies were published before this. Fifteen studies reviewed the neurodevelopmental outcome in relation to NIRS findings. No randomized study was identified.

Conclusion: Commercial NIRS cerebral oximeters can provide important information regarding changes in cerebral oxygenation and hemodynamics following HIE and can be particularly helpful when used in combination with other neuromonitoring tools. Optical measurements of brain metabolism using broadband NIRS and cerebral blood flow using

diffuse correlation spectroscopy add additional pathophysiological information. Further randomized clinical trials and large observational studies are necessary with proper study design to assess the utility of NIRS in predicting neurodevelopmental outcome and guiding therapeutic interventions.

Keywords: neonate, hypoxic ischemic encephalopathy, oxygenation, metabolism, near infrared spectroscopy

INTRODUCTION

The current practice of therapeutic hypothermia (TH) has reduced the disability rates and the severity spectrum of cerebral palsy in newborn infants with hypoxic ischaemic encephalopathy (HIE). Infants with HIE are routinely monitored in the neonatal intensive care unit (NICU) with electroencephalography (EEG) or amplitude integrated EEG (aEEG) and cranial ultrasound (CrUSS) during TH to detect seizures, investigate the severity of the injury and inform prognosis. Brain magnetic resonance imaging (MRI) and spectroscopy (MRS) are gold standard tools for prognostication of injury and are optimally performed after completion of TH. However, these current technologies do not offer all the necessary physiological information that is needed for a continuous assessment of the changes in the newborn brain.

Following perinatal hypoxia-ischaemia, significant cerebral haemodynamic and metabolic derangements evolve over time (1–3). This evolution is associated with changes in the brain energy state and underlying neurochemical and neurotoxic state. Following acute hypoxia ischaemia (HI), brain high energy metabolites decrease with a reduction in CBF. Oxidative metabolism appears to recover after resuscitation along with improvement in brain perfusion but a period of hypoperfusion persists in the latent phase (up to 24 h following injury). Without any intervention, mitochondrial failure and cell death start in the secondary phase (persisting for days after birth) together with a state of hyperperfusion. Over the next few weeks and months, cerebral hemodynamic and metabolic abnormalities gradually normalize despite pathological processes persisting in this tertiary phase of injury. The degree of deranged cerebral oxidative metabolism following HIE can be identified using magnetic resonance spectroscopy (MRS) (4, 5).

Cerebral NIRS has several advantages as a neuromonitoring tool in the neonatal intensive care unit (NICU) and can be combined with aEEG/EEG monitoring. Its application is easy and quick. The monitoring can be continuous over a long period of time. NIRS can continuously monitor CBF, oxygenation, and metabolism at the cot side from the early stages after birth, with the potential to provide information on the severity of the evolving injury and outcome. NIRS uses the relative transparency of biological tissue in the near infrared (NIR) region of light (700–1,000 nm). In comparison to adults and older children, the thinner skin and skull thickness in newborn infants allows a better depth penetration of brain tissue and make the technique an ideal neuromonitoring tool for newborn infants. Hemoglobin is one of the compounds (chromophores) in the human body that absorbs light. The absorption spectra of oxygenated and de-oxygenated hemoglobin (HbO_2 and HHb) are different in the near-infrared region, allowing changes in concentration to be individually monitored using NIRS. Total hemoglobin (HbT = HbO_2 + HHb) and hemoglobin difference (HbD = HbO_2-HHb) are derived parameters and have been used to represent changes in cerebral blood volume (CBV) and cerebral oxygenation, respectively. Most commercially available NIRS systems measure cerebral oxygenation or tissue saturation (StO_2, $rScO_2$, TOI, rSO_2), which is the percentage ratio of HbO_2 to HbT (HbO_2/HbT); these systems are often referred to as brain oximeters, with different manufactures implementing different NIRS techniques to derive brain tissue saturation (6–9). We will use the term cerebral oxygenation in this review and this measurement will be discussed in further detail later under "NIRS devices and methodology." In healthy term infants, irrespective of the mode of delivery, cerebral oxygenation is lowest at birth (between 40 and 56%) (6–10) and gradually increases to reach ∼78% (±7.9%) in the first 24 h (11). It stabilizes over the next few weeks between 55 and 85% (12–14). Using the combined measurement of cerebral oxygenation and peripheral arterial oxygen saturation one can estimate fractional tissue oxygen extraction (FTOE = SaO_2 – cerebral oxygenation/SaO_2). It represents the balance between oxygen delivery and oxygen consumption, a proxy marker of cerebral metabolism (15). An increase in FTOE indicates an increased extraction of oxygen by brain tissue, suggesting a higher oxygen consumption in relation to oxygen delivery. A decrease of FTOE, on the other hand suggests reduced use of oxygen by brain tissue in relation to supply. Neither cerebral oxygenation nor FTOE accurately reflects the cerebral metabolic rate of oxygen consumption ($CMRO_2$).

Beyond the NIRS measurements of hemoglobin oxygenation, another NIR chromophore is cytochrome c oxidase (CCO). It is the terminal electron acceptor in the electron transport chain (ETC) and is responsible for more than 90% of ATP production, thus providing important information related to the changes in mitochondrial oxidative metabolism. The absorption spectra of the CCO will depend on its redox state, which in turn will depend on oxygen and energetic substrate availability. The NIRS measurements of CCO attracted a great deal of attention in the 1980's (16–19) but accurate measurement of CCO proved challenging due to its low *in vivo* concentration. However, recent developments in optical methods have enabled this measurement in the NICU, as will be discussed later under "NIRS devices and methodology."

We performed a systematic review of NIRS measurements in term or near-term newborn infants with HIE. Although several NIRS reviews in the preterm population have been published (6, 20), there is no comprehensive review of NIRS in term

infants with HIE. The aim of this work is to review the potential benefits of cerebral NIRS monitoring in newborn infants with HIE and the utility of different NIRS variables to prognosticate outcome (short term or long term). We present a review of different optical measurements: how these indices evolve over time and their relationship with outcome, monitoring of cerebral autoregulation using NIRS and the use of NIRS together with other neuromonitoring tools. A brief description of the basic methodology and technology used for cerebral NIRS is presented along with emerging technologies in this area.

METHODS

A stepwise approach was taken to identify articles from databases following the guidance from the Preferred Items for Systematic Reviews and Meta-analysis (PRISMA) statement (21).

SEARCH STRATEGY

Published articles were identified using a systematic search of Medline database and Ovid EMBASE from inception to November 2019. Articles were filtered with publications in English only. The search focused on publications related to cerebral oxygenation, perfusion and metabolism using single or multiple site NIRS in infants with HIE. The retrieved articles were further examined for any other relevant published reports. Websites of manufacturers of NIRS monitors were also screened during the search to capture any articles that might have been overlooked.

The search combined three broad categories: measurement (NIRS monitoring), disease condition [hypoxic ischemic encephalopathy (HIE)] and subject category (newborn infants). Search term included: brain metabolism, brain function, tissue metabolism, cerebral metabolism or oxygenation or hemodynamic or blood flow or volume, near infrared, near infrared spectroscopy, brain hypoxia or anoxia, perinatal hypoxia or ischemia, asphyxia neonatorum, brain ischemia, brain injury or damage, encephalopathy, neonatal encephalopathy, newborn(s), newborn babies, infant(s) and neonate, neonates and neonatal.

The search strategies for the review is presented in **Table 1**.

STUDY SELECTION

Publications were included in the review if they presented original data discussing the use of NIRS in newborn term or near-term infants with HIE. The articles identified from the databases were screened for duplicity and were then evaluated using the publication title and abstracts. Full texts were examined where uncertainty was noted at this stage. Articles with preclinical studies and abstract-only publications (where a full-length article was not published in a peer-reviewed journal) were excluded. Studies on human infants were included for the final analysis. Full texts were assessed for the remaining articles and publications were excluded if they did not present original data in the term newborn population (review articles, commentaries, and studies in preterm population). Studies included for the final review were then assessed for data collection.

RESULTS

The initial search identified 3,144 articles. After excluding duplicate articles, preclinical studies and abstract only publications, 66 articles were identified, all of which discussed NIRS measurement in human newborn infants after HIE. Full texts of these articles were reviewed, and a further 14 articles were excluded (review papers:11, and studies in preterm population: 3), leading to final inclusion of 52 original research studies on the term and near-term infants following HIE. Five studies presented changes in NIRS variables specifically during seizures following HIE and were excluded from this review leaving 47 studies for the final review. The PRISMA chart detailing the searching and inclusion of the articles for the review is presented in **Figure 1**. Basic characteristics and brief details of the studies are presented in **Table 2**. Thirty-nine studies have been published since 2010, compared to eight studies before 2010. Most of the studies (thirty-five) investigated the changes in cerebral oxygenation. Other optical indices were FTOE, CBF, $CMRO_2$, HbD, HbT, oxCCO, markers of haemodynamic reactivity and metabolic reactivity. Fifteen different devices were used in these studies and eleven of them were commercially available (**Figure 2**). Eight recent studies used broadband NIRS (BNIRS) to investigate changes in cerebral metabolism using direct measurement of changes in the oxidation state of cytochrome c oxidase (oxCCO). Fifteen studies presented MRI or MRS evidence of injury as short term outcome for comparing with NIRS makers while an equivalent number of studies presented neurodevelopmental follow up data. Eight studies used combined neuromonitoring using NIRS and aEEG/EEG.

DISCUSSION

Over the last decade, there has been increasing focus on NIRS monitoring at the cot side in babies with HIE and how it can inform clinical management and prognosis (**Table 2**).

NIRS DEVICES AND METHODOLOGY

Fifteen different NIRS instruments were used in the included studies, of which 11 instruments were commercially available. Among the non-commercial systems, a BNIRS system was used in eight studies (25–28, 46, 51–53), purpose-built to monitor concentration changes in oxCCO and hemoglobin parameters. A frequency-domain near-infrared spectroscopy (FD-NIRS) protocol in a customized commercial FD oximeter was used to measure cerebral oxygenation (35). This was also coupled with a diffuse correlation spectroscopy (DCS) system to measure an additional index of tissue CBF (41). Huang et al. used a prototype instrument (TSNIR-3, using SRS technology) to

TABLE 1 | Search strategy for the systamtic review on EMBASE.

Search strategy used for systematic review:
1. ("exp brain metabolism") or ("brain function") or ("tissue metabolism") or ([cerebr* adj3 (metabol* or oxygenation or hemodynamic* or "blood flow" or volume*)].mp. [mp=title, abstract, heading word, drug trade name, original title, device manufacturer, drug manufacturer, device trade name, keyword, floating subheading word, candidate term word]) or ("near infrared spectroscopy") or ((near infrared adj3 spectroscop*).mp. [mp=title, abstract, heading word, drug trade name, original title, device manufacturer, drug manufacturer, device trade name, keyword, floating subheading word, candidate term word]). (Result: 169743)
2. ("brain hypoxia") or ("exp brain ischemia") or [((cerebr* or brain*) adj3 ("brain damage" or encephalopath*)].mp. [mp=title, abstract, heading word, drug trade name, original title, device manufacturer, drug manufacturer, device trade name, keyword, floating subheading word, candidate term word]) or [((hypoxi* or anoxi*) adj3 ("brain damage*" or "brain injur*" or encephalopath*)].mp. [mp=title, abstract, heading word, drug trade name, original title, device manufacturer, drug manufacturer, device trade name, keyword, floating subheading word, candidate term word]) or ("perinatal asphyxia") or [(asphyxia* adj3 (newborn or baby or babies or infan* or neonat*)].mp. [mp=title, abstract, heading word, drug trade name, original title, device manufacturer, drug manufacturer, device trade name, keyword, floating subheading word, candidate term word]) or ((encephalopath* adj3 neonat*).mp. [mp=title, abstract, heading word, drug trade name, original title, device manufacturer, drug manufacturer, device trade name, keyword, floating subheading word, candidate term word]). (Result: 228291)
3. ('newborn') or ((newborn or baby or babies or infan* or neonat*).mp. [mp=title, abstract, heading word, drug trade name, original title, device manufacturer, drug manufacturer, device trade name, keyword, floating subheading word, candidate term word]). (Result: 1475873)
4. 1 and 2 and 3. (Result: 1671)

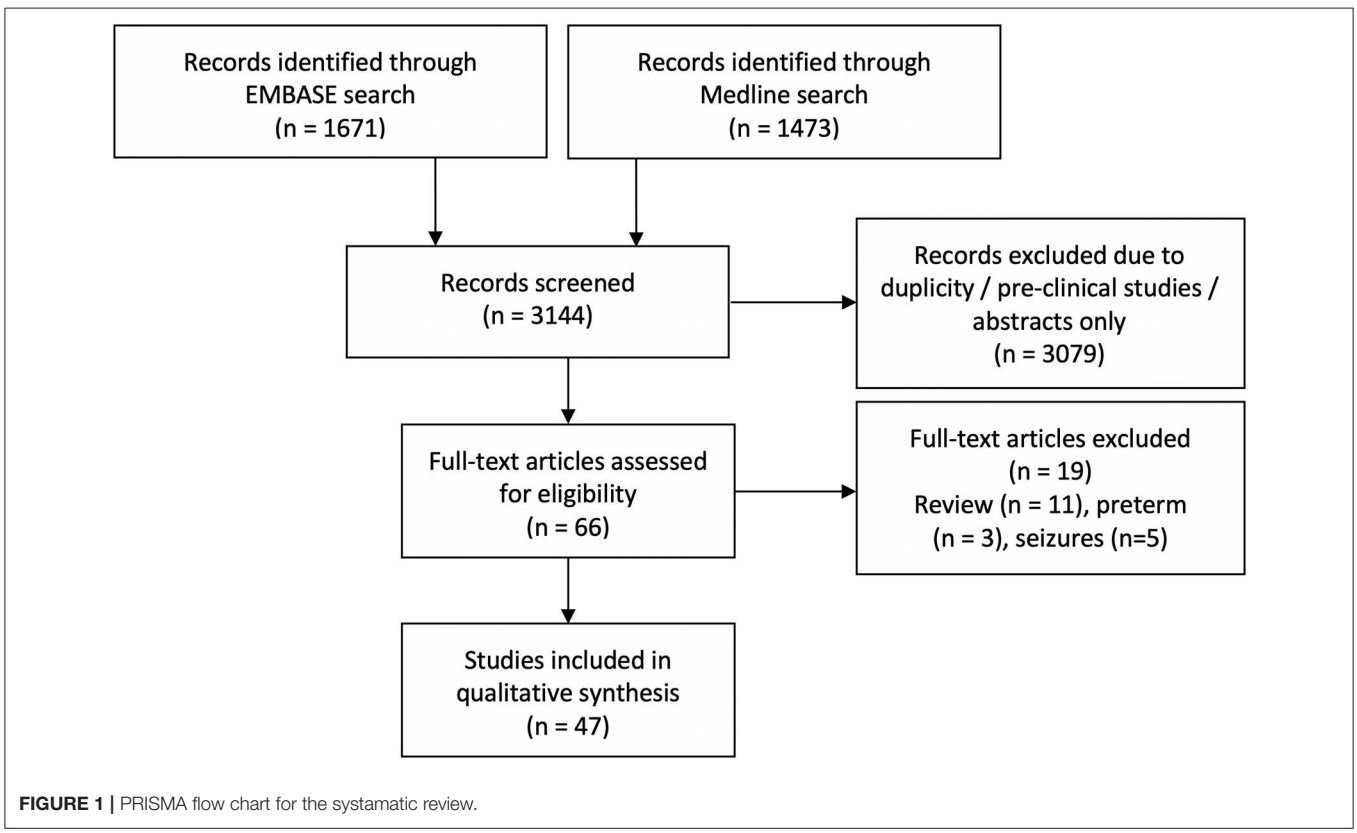

FIGURE 1 | PRISMA flow chart for the systamatic review.

compare cerebral oxygenation between healthy controls and HIE infants (44).

Three different modes of NIRS have been developed and used in systems in clinical settings—continuous wave, time resolved, and frequency domain NIRS.

Continuous wave (CW) instruments were the earliest NIRS instruments to be developed and are the most commonly used. They use 2–4 discrete wavelength continuous sources [either laser or light-emitting diode (LED)] and measure the transmitted or reflected intensity through tissue. CW-NIRS systems are unable to separate attenuation of light due to absorption and scattering, so instead monitor changes in attenuation, and assume these are all due to absorption and that scattering remains stable within the measurement period. Using the modified Beer-Lambert law (66), these devices calculate changes in HbO_2 and HHb concentration from an arbitrary baseline. Therefore, CW-NIRS protocols typically rely on variations in the signals or responses to specific (physiological or functional) stimuli.

In frequency domain NIRS (FD-NIRS) systems, the intensity of the emitted light is modulated at a particular frequency

TABLE 2 | Study characteristics.

First author, Year (Ref.)	Study design	Gestation (weeks)	No of subjects	Study aim	NIRS device, sensor	Optode placement on head	Duration of study	Result
Ancora et al. (22)	Observational	39	1	To evaluate the time course of aEEG and NIRS data before, during and after cool cap treatment	NIRO 200	Forehead		Early significant increase in THI and TOI before TH. TOI improved with TH and remained stable during the rewarming period
Ancora et al. (23)	Observational	≥36	12	To evaluate the prognostic value NIRS data in asphyxiated cooled infants	NIRO 200	Forehead	72 h	Mean TOI at 12h of life is significantly higher in infants who develop a poor neurological outcome than in those with normal outcome
Arriaga-Redondo et al. (24)	Observational	≥36	23	To assess the variability of cerebral tissue oxygenation over time in infants with HIE	Invos 5100	Forehead	100 h	$rScO_2$ values >90% and a lack of variability over time in infants with HIE during cooling were associated with poor outcome
Bale et al. (25)	Observational	≥38	6	Feasibility study to assess the potential of cytochrome c oxidase monitoring in NE	Broadband NIRS	Frontal bilateral	Up to 5 days	Mean values for HbD and oxCCO consistently decreased during desaturation and HbT increased.
Bale et al. (26)	Prospective observational	>35	11	To investigate the dynamic changes in cerebral metabolism in response to systemic changes, as a marker of injury	Broadband NIRS	Frontal	3 h on day 3 of TH	Strong relationship between oxCCO and systemic variables during TH on day 3 indicated severe injury following HI
Bale et al. (27)	Prospective observational	>36	50	To determine whether broadband NIRS can distinguish injury severity in HIE in the first 4 days after birth	Broadband NIRS	Frontal	Up to day 4	A strong relationship between cerebral metabolism [broadband NIRS-measured cytochrome-c-oxidase (CCO)] and cerebral oxygenation was associated with unfavorable outcome during spontaneous desaturation episodes during TH.
Bale et al. (28)	Observational	>36	11	To use changes in cerebral oxygenation and peripheral oxygen saturation during spontaneous desaturation for determination of CBF	Broadband NIRS	Frontal	Up to day 4	Infants with severe HIE had significantly lower CBF compared with infants with moderate HIE on the day of birth
Burton et al. (29)	Observational	≥35	19	To assess the relationship between autoregulation during TH and neurodevelopmental outcomes at 2 years of age	INVOS 5100	Forehead	84 h	Children with developmental impairments at 2 years, had higher MAP_{OPT} values, spent more time with MABP below MAP_{OPT}, and had greater MABP deviation below MAP_{OPT} during rewarming. Greater MABP deviation above MAP_{OPT} during rewarming was associated with less disability and higher cognitive scores
Campbell et al. (30)	Observational	>36	27	Whether infants with autonomic dysfunction after HIE have aberrant physiological responses to care events	NIRO-200NX	Right and left frontotemporal	2.58–8 h	Infants with depressed heart rate (HR) variability had different physiological responses [post event changes in cerebral blood flow (HbD) and cerebral blood volume (HbT)] compared to infants with intact HR variability
Chalak et al. (31)	Observational	≥36	10	To develop an approach to assess cerebral hemodynamics across multiple time scales during first 72 h of life	INVOS 4100–5100	left frontoparietal	72 h	multiple-timescale correlations between oscillations in MAP and $SctO_2$ in the first 72 hrs, indicating impairment of cerebral hemodynamics

(Continued)

TABLE 2 | Continued

First author, Year (Ref.)	Study design	Gestation (weeks)	No of subjects	Study aim	NIRS device, sensor	Optode placement on head	Duration of study	Result
Chalak et al. (32)	Observational	≥36	10	To quantify neurovascular coupling (NVC) using wavelet analysis of the dynamic coherence between aEEG and $SctO_2$ in NE	INVOS 4100–5100	Bilateral parietal area	60 ± 6 h	High coherence, intact NVC between the oscillations of $SctO_2$ and aEEG in the frequency range of 0.00025–0.001 Hz in the non-encephalopathic newborns. NVC coherence was significantly decreased in encephalopathic newborns who were cooled vs. non- encephalopathic controls and was significantly lower in those with abnormal 2 year outcomes relative to those with normal outcomes
Chen et al. (33)	Observational	>35.7	44	To evaluate the evoked CBO response to neuronal activation in newborns with HIE and compare with the response in healthy infants	NIRO 500	Forehead	Between day 1–3	Infants with HIE have decreased rCBF in the frontal lobes during auditory stimulation, (decrease of HbO_2 and HbT) compared to normal infants
Chock et al. (34)	Retrospective chart review	≥36	38	To review cerebral and renal tissue saturation during TH	INVOS 5100C	Lateral forehead	110 h	Renal tissue saturation was lower than cerebral tissue saturation during TH
Dehaes et al. (35)	Observational	≥36	27	To assess cerebral hemodynamics and oxygen metabolism during and after TH	Hybrid FDNIRS–DCS system	Left, middle, and right frontal	10–16 sec 3 times/ location during TH, rewarming, and post-TH	$CMRO_{2i}$ and CBF lower in neonates with HIE during TH compared with post –TH and controls
Forman et al. (36)	Prospective observational	>35	20	To assess the feasibility and reliability cerebral perfusion monitoring in NE	INVOS, neonatal sensors	Center of the forehead	84 h	$SctO_2$ increased over first 30 h of TH and stayed high for the remainder of the study
Gagnon and Wintermark (37)	Case series	>38	3	To examine the impact of PPHN on cerebral oxygenation in infants on TH after HIE	FORE-SIGHT	Forehead (bilateral)	86 h	Periods of pulmonary hypertensive crisis were associated with significant drop in cerebral saturation, indicating that PPHN can independently cause further injury
Goeral et al. (38)	Prospective observational	>36	32	To assess the predictive values of aEEG and NIRS parameters and the respective cut-off values regarding short-term outcomes in HIE	INVOS 5100C	Frontoparietal	102 h	No significant differences in NIRS values were observed between groups (normal and abnormal MRI). Combined score of BP, aEEG and NIRS increased the accuracy of early outcome prediction
Govindan et al. (39)	Observational	n.r.	4	To identify the efficacy of a modified approach to quantify the pressure passivity	NIRO 200	Bilateral fronto-temporal areas	n.r.	A modified coherence estimation approach over every 30 s epochs identified better the association between HbD and MABP (pressure passivity index).
Govindan et al. (40)	Observational	≥38	4	To review the efficacy of a novel method to quantify neuro-vascular coupling (NVC) using NIRS and EEG	NIRO 200	Bilateral fronto-temporal areas	n.r.	Two infants who survived, revealed the emergence of NVC during TH. Other 2 infants who did not survive, lacked this feature.
Grant et al. (41)	Observational	≥33	43	Whether StO2, CBV, and $rCMRO_2$ have the potential to distinguish between neonates with brain injury (HIE and other etiologies) and healthy controls	FDNIRS	5 ± 3 locations. Primary location –forehead, also temporal and parietal	n.r.	No significant difference in StO_2 between brain-injured and normal neonates. However, CBV and estimates of $rCMRO_2$ were significantly increased in the brain injured group compared with all other clinical groups

(Continued)

TABLE 2 | Continued

First author, Year (Ref.)	Study design	Gestation (weeks)	No of subjects	Study aim	NIRS device, sensor	Optode placement on head	Duration of study	Result
Gucuyener et al. (42)	Observational	≥36	8	Investigate the correlations between aEEG and NIRS monitoring and outcome following HIE	NIRO 200	Parietal	30 min each before cooling, at 34°C during TH and after rewarming	Detection of context-sensitive changes in TOI and FTOE can be helpful especially while monitoring the effects of a therapy, in conjunction with other cerebral trend monitors
Howlett et al. (43)	Observational	>37	24	To describe the relationship between autoregulation during TH and brain injury on MRI after HIE	INVOS, Neonatal sensor	Forehead	84 h	Optimal MABP identified using HVx (running correlation between HbT and MAP). Infants with evidence of brain injury on MRI spent longer time below MAP_{OPT} during rewarming than neonates with no or mild injury. Neonates with moderate/severe injury on MRI had greater MAP deviation below MAP_{OPT} during rewarming than neonates without injury
Huang et al. (44)	Observational	≥37	41	To find out the clinically useful parameters for the assessment of HIE using NIRS	TSNIR-3	n.r.	n.r.	rSO_2 in quiet condition and rSO2, HbO_2 and Hb during the inhalation of oxygen may be helpful for HIE infants. rSO2 for the healthy group increased rapidly, with the increase 7 ± 2.3%, compared to 3 ± 1.5% in HIE infants
Jain et al. (45)	Prospective observational	>36	21	To examine the value of $CrSO_2$	INVOS	Midfrontal	48 h	Higher absolute $CrSO_2$ values during TH correlates with subcortical injury on MRI and poor neurodevelopmental outcome
Kovacsova et al. (46)	Observational	>36	55	To investigate the SRS algorithm using a multi-distance broadband NIRS device to derive tissue saturation	Broadband NIRS	Frontal	14 h	A broadband NIRS multi-distance device can provide additional information to improve the robustness of the SRS estimation of cerebral tissue saturation
Lee et al. (47)	Prospective observational		64	To examine whether optimizing cerebral autoregulation is associated with decreased brain injury	INVOS 5100	Bilateral forehead	90 h	Blood pressure deviation from the optimal vasoreactivity was associated with evidence of brain injury on MRI, independent of initial birth asphyxia
Lemmers et al. (48)	Observational	≥36	39	To re-evaluate the early predictive value of $rScO_2$, cFTOE and aEEG background pattern for outcome	INVOS 4100–5100, with adult sensor	Frontoparietal	84 h	Higher $rScO_2$ values and lower aEEG background pattern scores in neonates with adverse neurodevelopmental outcome
Massaro et al. (49)	Prospective observational	>36	10	To assess cerebral perfusion and oxygenation differences after HIE	FORE-SIGHT	n.r.	84 h	Cerebral FTOE values were significantly reduced after rewarming in infants with evidence of injury on MR imaging
Massaro et al. (50)	Observational	≥35	36	To investigate if the duration and magnitude of the pressure passivity during TH were related to outcome	NIRO 200	Fronto-temporal	84 h	Higher PPI in both hemispheres and high gain on right hemisphere were associated with poor outcome
Meek et al. (2)	Observational	≥36	27	To measure changes in cerebral hemodynamics during the first 24 hrs of life after perinatal asphyxia, and relate them to outcome	NIRO1000 or NIRO500	n.r.	1–4 occasions between 2 and 72 h of age	increase in CBV on the 1st day of life is a sensitive predictor of adverse outcome. A reduction in CBVR is almost universally seen following asphyxia, but is not significantly correlated with severity of adverse outcome

(Continued)

TABLE 2 | Continued

First author, Year (Ref.)	Study design	Gestation (weeks)	No of subjects	Study aim	NIRS device, sensor	Optode placement on head	Duration of study	Result
Mitra et al. (51)	Prospective observational	≥35	14	To assess the cerebral metabolic and hemodynamic changes during the rewarming period after TH	Broadband NIRS	Frontal	14 h	The relationship between mitochondrial metabolism and oxygenation became impaired with rising Lac/NAA. Cardiovascular parameters remained stable during rewarming.
Mitra et al. (52)	Prospective observational	>34	23	To investigate the effects of disturbances in brain metabolism following HIE on outcome, using a wavelet based metabolic reactivity index between oxCCO and MABP	Broadband NIRS	Frontal	1 h	Pressure passive changes in brain metabolism were associated with injury severity and outcome following HIE. oxCCO-MABP semblance as a metabolic reactivity index correlated with MRS derived Lac/NAA. It also differed among groups of mild to moderate and severe injury based on MRI score and neuro-developmental outcome at 1 yr of age.
Mitra et al. (53)	Prospective observational	>36	14	To assess the changes in brain hemodynamics and metabolism following HIE in relation to initial degree on injury on EEG	Broadband NIRS	Frontal	12.5 h	Significant difference noted in derangement of brain oxygenation and metabolism between infants with mild and moderate to severe EEG abnormality
Nakamura et al. (54)	Observational	>35	11	To find the influence of CBV and ScO_2 on clinical outcome	TRS-10	Parietal	72 h	Early postnatal CBV and ScO_2 elevations were predictive of a poor outcome based on MRI injury
Niezen et al. (55)	Retrospective observational study	≥37	39	To determine the predictive value of aEEG and NIRS alone, and in combination, during the first 4 days after HIE	INVOS 5100C	left or right frontoparietal	96 h	After 48 h of TH, a higher $rcSO_2$ was associated with a severely abnormal outcome
Peng et al. (56)	Observational	>=36	18	To assess whether NIRS Identifies the newborns during TH, who later develop brain injury	FORE-SIGHT	Forehead	79 h	rSO2 was consistently higher in newborns who developed brain injury on MRI and was significantly higher on day 1 compared to infants who did not develop injury on brain MRI.
Shellhaas et al. (57)	Observational	≥37	21	To evaluate the utility of aEEG and rSO_2 for short-term outcome	INVOS 5100C	bilateral parietal regions, also one sensor over thigh	90 h	During day 3 of cooling and during rewarming, loss of physiologic variability (by systemic NIRS) was the best predictor of poor short-term outcome. Cerebral rSO2 variability was independent from short-term outcome
Shellhaas et al. (58)	Observational	≥35	4	To evaluate the variability of cerebral oxygen metabolism in sleep-wake states among sick neonates	INVOS 5100C	bilateral parietal-occipital regions	11.7 h	Cerebral oxygenation (sSO_2) and FTOE significantly differ between wakefullness and sleep stages
Shellhaas et al. (59)	Observational	"term neonates"	18	To identify systemic and cerebral risk factors for adverse long-term neuro-developmental outcome following HIE	INVOS 5100C	Bilateral parietal regions, neonatal sensors	72 h	Mean cerebral rSO_2 was not different between those with favorable vs. adverse 18-months outcomes, but those with favorable outcomes had higher systemic rSO_2 variability during hours 48–72 of cooling
Tax et al. (60)	Observational	>34	38	To investigate peripheral oxygenation and perfusion in the first 48 h after perinatal asphyxia	NIRO 300	Left calf	n.r.	Peripheral oxygenation and perfusion are compromised with worsening degree of acidosis on cord blood gas

(Continued)

TABLE 2 | Continued

First author, Year (Ref.)	Study design	Gestation (weeks)	No of subjects	Study aim	NIRS device, sensor	Optode placement on head	Duration of study	Result
Tekes et al. (61)	Observational	≥35	27	To assess whether lower ADC values on MRI would correlate with worse autoregulatory status measured by NIRS	INVOS	Forehead bilateral	n.r.	Lower ADC scalars in the PCS, PLIC and PP correlated with blood pressure deviation below MAP_{OPT} during hypothermia and rewarming
Tian et al. (62)	Observational	≥36	9	Quantitative evaluation of cerebral autoregulation	INVOS 4100-5100, neonatal sensor	Frontoparietal	72 h	Cerebral autoregulation was time-scale –dependant. Both in phase and anti-phase coherence were related to worse outcome
Toet et al. (15)	Observational	>37	18	To determine the value of rSO_2, FTOE measured by NIRS, and aEEG in relation to neuro-developmental outcome	INVOS 4100	Left parietal	48 h	rSO_2 values remained normal and stable in infants with a normal outcome with values between 50 and 70% 30,33 but increased to supranormal values after 24 h in the infants with an adverse outcome. From 24 h onward, the values of rSO_2 of the infants with an adverse outcome were significantly higher as compared with those with a favorable outcome
Van Bel et al. (18)	Observational	>35	31	To investigate whether cerebral perfusion and metabolism drops following hypoxia	Radiometer	Source on ant. fontanel, detector on Fronto-parietal	4–6 h	CBV, HbO, HbR, and $Cytaa_3$ decreased in the first 12 hs of life in severely asphyxiated neonates who subsequently developed neurologic abnormalities
Wintermark et al. (63)	Observational	≥36	7	To determine the correlation between measurements of brain perfusion by NIRS and by MRI	FORE-SIGHT Cerebral Oximeter	Forehead	84 h	$SctO_2$ and CBF increase from days 1 to 2 in all, despite TH. $SctO_2$ and CBF are highly correlated in newborns with severe encephalopathy. Newborns with severe encephalopathy have lower CBF than newborns with moderate encephalopathy. Newborns developing brain HI injury have higher $SctO_2$ than newborns not developing brain injury
Wu et al. (64)	Retrospective cohort study	≥36	20	To review the cerebral hemodynamic response during rewarming following TH	INVOS 5100C	Frontal region	14 h	$CrSO_2$ and cerebral FTOE remained unchanged during rewarming
Zaramella et al. (65)	Case control study	≥36	22	To assess the diagnostic and prognostic value of TOI and ΔCBV in HIE	NIRO 300	Fronto-temporal	Duration n.r., study on day 1	Increased TOI on day 1 suggested abnormal outcome at 1 year of age

ADC, Apparent diffusion coefficient; aEEG, Amplitude integrated electroencephalogram; HIE, Hypoxic-ischemic encephalopathy; CBO, Cerebral blood oxygenation; CBV, Cerebral blood volume; CCVR, Cerebral blood volume response; $CrSO_2$, Cerebral regional oxygen saturation; Cytaa3, Cytochrome oxidase; DCS, Diffusion correlation spectroscopy; EEG, Electroencephalography; FDNIRS, Frequency-domain near-infrared spectroscopy; FTOE, Fractional tissue oxygen extraction; HbO, Oxy-hemoglobin; HbR, Deoxy-hemoglobin; MABP, Mean arterial blood pressure; MRI, Magnetic resonance imaging; MRS, Magnetic resonance spectroscopy; NE, Neonatal encephalopathy; NIRS, Near Infrared spectroscopy; NVC, Neurovascular coupling; oxCCO, Oxidation state of cytochrome c oxidase; PCS, Posterior centrum semiovale; PLIC, Posterior limb of internal capsule; PP, Putamen and globus pallidus; $rCMRO_2$, Relative cerebral metabolic rate of oxygen consumption; rSO_2, Regional oxygen saturation; $rScO_2$, Regional cerebral tissue oxygen saturation; $SctO_2$, Regional cerebral tissue oxygen saturation; StO_2, Cerebral tissue oxygenation; TH, Therapeutic hypothermia; TOI, Tissue oxygenation index; TH, Therapeutic hypothermia; THI, Total hemoglobin index.

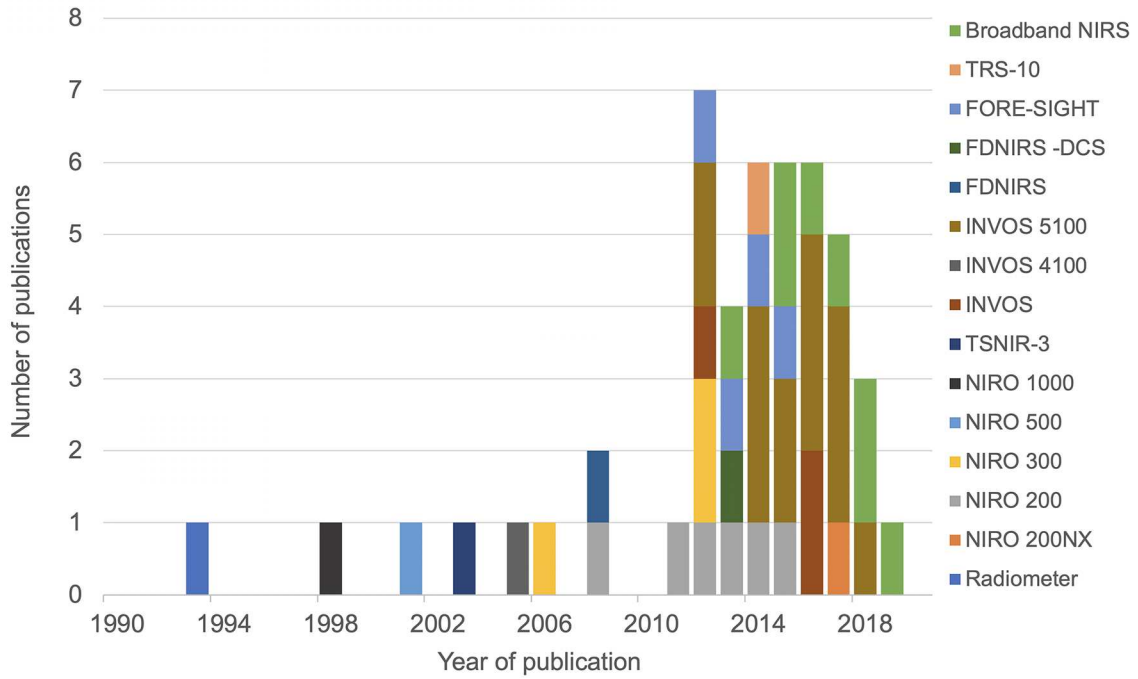

FIGURE 2 | Different NIRS devices used in the studies with their year of publication.

and the transmitted light attenuation and the frequency phase shift are measured. Observations of phase shift relate to tissue scattering, so FD-NIRS systems can derive absolute chromophore concentrations by decoupling absorption from scattering. This gives FD-NIRS a theoretical advantage of a more consistent quantitative measurement which can be important for cerebral NIRS.

The most complex NIRS mode, time domain NIRS (TD-NIRS) uses ultrashort pulses of light and measures the time of flight through the tissue with a photon counting device. This enables quantification of scattering and chromophore concentrations absolutely. An additional advantage of time resolved NIRS is the ability to gate the signal to obtain depth resolution. The disadvantages of this technology are the large instrument size and higher cost, although technological advances make up for these drawbacks (67). Both FD-NIRS and TD-NIRS systems appear to have superior depth sensitivity compared to CW-NIRS system (68).

The most common use of NIRS in the neonatal intensive care is a variation on CW-NIRS or FD-NIRS called cerebral oximetry, which allows the quantification of the oxygen saturation within tissue as a percentage using multi-distance approaches. These enable the recovery of scaled absolute measurements using a variety of different techniques (most commercial methods are not published). The NIRO series brain oximeter devices from Hamamatsu implements the spatially resolved spectroscopy (SRS) algorithm with their multi-distance measurements (69, 70). The multi-distance designs are less sensitive to changes in the extracerebral layers, giving more brain-specific measurements (71). Cerebral oxygenation represents the combined oxygen saturation of the arterial and venous vascular compartments, weighted by their volume (ratio of arterial and venous vessels in cerebral tissue is ∼25:75%). The simplicity of the reading as an absolute number, small size and low weight of the instrument as well as the high sampling rate makes it ideal for bedside monitoring.

Most commercially available NIRS instruments only measure brain tissue light attenuation at 2–4 wavelengths to resolve hemoglobin oxygenation. However, broadband NIRS devices measure brain tissue light attenuation over a wide range of NIR wavelengths, allowing enhanced spectroscopic information and the possibility to resolve multiple chromophores. Broadband NIRS systems are particularly useful for monitoring changes in CCO (53) together with tissue saturation (46, 72). Due to the relatively low concentration of CCO *in vivo*, the selection of the specific wavelengths and number of wavelengths becomes an important factor for monitoring CCO. Broadband NIRS devices are able to accurately quantify changes in the oxidation state of CCO (oxCCO) by using over 100 wavelengths to improve the optical signal and extract the relatively low concentration changes (19).

DCS measures the microvascular blood flow in the biological tissue. It uses a NIR laser to measure temporal fluctuations in the detected laser intensity which are directly proportional to the speed of scatterers (mainly red blood cells) within the tissue. DCS has been used in combination with a multidistance FD-NIRS system to measure an index of the cerebral metabolic rate of oxygen ($CMRO_2$) (35).

MONITORING CEREBRAL OXYGENATION

Thirty-five studies used cerebral oximetry measurements to describe changes in cerebral tissue oxygen saturation. Different oximetry terminologies have been described in **Table 2**. Seven studies have also used hemoglobin difference (HbD) as a marker of tissue oxygenation. Although cerebral oximetry presents an absolute value, HbD is measured as a change in concentration (27, 52).

Studies conducted continuously over the period of TH and rewarming revealed a difference in cerebral oxygenation between the groups of infants with good and poor outcome (56, 61). Cerebral oxygenation drops in the first 4–6 h of life following HI injury and recovers by 18–20 h (56). This post-HI drop in cerebral oxygenation was less evident in infants who subsequently develop brain injury (61). Peng et al. described a significant difference in cerebral oxygenation from birth till first 12 h of life between groups with evidence or absence of injury on MRI (56), while Lemmers et al. indicated a significant difference from 24 h onwards between groups of favorable and adverse neurodevelopmental outcomes at 2 years of age (48). The sensitivity and specificity of cerebral oxygenation to predict the adverse outcome within the first 10 h of TH were 100 and 83% in the study by Peng et al. (56). Lemmers et al. identified the highest predictive value at 24–30 h of life with a sensitivity of 92% and specificity of 64% (48). Higher cerebral oxygenation between 24 and 36 h of life also significantly increased the odds of having moderate to severe injury on MRI (45). This increased cerebral oxygenation is likely to be related to mitochondrial dysfunction or injury, reflected by decreased oxygen utilization. In addition, vasoparesis and luxury perfusion in the "secondary energy failure" stage, with cerebral perfusion exceeding the metabolic demand results in higher cerebral oxygenation in infants with severe injury.

Van Bel et al. reviewed cerebral hemodynamics and oxygenation responses in babies with HIE (18) in the pre-hypothermic era - CBV, HbO_2, and HbR (deoxy-hemoglobin) decreased in the first 12 h of life in severely asphyxiated infants with the parameters becoming more stable between 12 and 24 h of life. Meek et al. also noted increased CBF and CBV on the 1st day of life in infants with severe HIE at presentation (Sarnat stage III) (2). These findings were further supported by the study from Nakamura et al. (54). CBV was significantly higher in the poor outcome group (three cooled and two non-cooled infants) at 6 h of age and by 24 h of age, cerebral oxygenation was significantly higher in the same group when compared to the infants with favorable outcome based on MRI findings. Cerebral oxygenation together with CBV at 24 h had a sensitivity, specificity, PPV and NPV of 100% for the predictive ability for neurological outcome based on MRI findings between 7 and 14 days after birth.

MONITORING MITOCHONDRIAL OXIDATIVE METABOLISM

Jöbsis in his seminal paper in Science (17) reported a new optical method (NIRS) intended to monitor changes in concentration of cytochrome c oxidase along with changes in oxy- and deoxy-hemoglobin for use as a clinical tool. Using a commercial NIRS system (radiometer using four wavelengths—904, 845, 805, and 775 nm) van Bel et al. described a decrease in $Cytaa_3$ (cytochrome oxidase) with increasing postnatal age in infants with severe HIE in the pre-TH era. Recently, the UCL group monitored Δ[oxCCO] in a preclinical model using a broadband NIRS (BNIRS) and described a significant correlation between the indicators of brain energy state on phosphorus (^{31}P) MRS [phosphocreatine/exchangeable phosphate pool (PCr/epp) and total nucleotide triphosphate/exchangeable phosphate pool (NTP/epp)] and Δ[oxCCO] during and after HI insult (73). Bale et al. subsequently described a new BNIRS instrument for clinical research (CYRIL, using 136 wavelengths, 770–906 nm) (25) and investigated how the relationship between the changes in [oxCCO] and systemic physiology was associated with injury severity (26). Mitra et al. presented a metabolic reactivity index using wavelet analysis (wavelet semblance or phase relationship between two variables) between [oxCCO] and MABP at 48 h of life during TH following HIE that differentiated between infants with good and poor outcome (based on MRI scores, thalamic MRS outcome biomarker (Lactate/N-acetyl aspartate) and neurodevelopmental outcome) (52). The relationship between cerebral oxygen delivery and mitochondrial oxidative metabolism also indicated injury severity during TH (27) and rewarming (51, 53). Findings from these studies using broadband NIRS are consistent with known pathophysiological changes following HIE and indicate deranged oxidative metabolism resulting from mitochondrial injury and altered hemodynamics associated with the neurochemical cascade effects on cerebrovascular tone.

Fractional tissue oxygen extraction (FTOE, five studies) and cerebral metabolic rate of oxygen consumption ($CMRO_2$, two studies) have also been used to monitor cerebral oxidative metabolism. FTOE decreased from 24 h of age in the adverse outcome group as compared with the favorable outcome group in two studies from the Utrecht group in the cooling and pre-cooling era (15, 48), indicating an inability to utilize available oxygen due to more severe mitochondrial injury. Using an FD-NIRS–DCS system, the Harvard group (35, 41) successfully monitored CBF and calculated $CMRO_2$ using Fick's principle. Increased $CMRO_2$ and CBV were more sensitive markers of evolving neuronal injury compared to brain tissue oxygenation in a cohort of infants with evidence of brain injury on ultrasound and MRI following HIE (3 cases) and other etiologies in the pre-cooling era (41). A subsequent study from the same group in a cohort of infants undergoing TH (10 infants with HIE and 17 matched control infants) (35) presented lower $CMRO_2$ and CBF and high CBV in infants during TH compared to control infants and post-TH values. The reason for difference in findings of $CMRO_2$ was not clear, but $CMRO_2$ depends on CBF which was also low in the second study and was not recorded in the first study. In the first study, all three infants had a severe injury (intensive care withdrawn in two cases and the third case developed significant impairment), but in the second study, eight infants had a comparatively milder injury (either normal MRI or decreased apparent diffusion coefficient (ADC) in the cortex and white matter). The neurodevelopmental outcome in the second study at 18 months of age (56.6% normal outcome)

was similar to those reported in the literature. The findings in the different neurodevelopmental groups were not explored in this study. Elevated CBV during TH was noted (consistent with previous studies) although CBF was decreased. Possible effects of medications (e.g., dopamine) and deranged cerebral autoregulation following HIE were discussed as possible factors contributing to these findings.

MONITORING CEREBRAL AUTOREGULATION

Cerebral autoregulation refers to the physiological ability of the healthy brain to maintain a steady cerebral blood flow (CBF) during changes in cerebral perfusion pressure (CPP). In view of the difficulty in direct measurement of invasive CPP, mean arterial blood pressure (MABP) is used as a proxy marker in neonatal studies. The relationship between cerebral oxygenation (as a marker of changes in CBF) or total hemoglobin concentration (as a marker of total blood volume) and MABP has been used to determine the autoregulatory capacity of the newborn brain both in time and frequency domain analysis. Cerebral vasoparesis following perinatal hypoxia ischaemia is associated with impaired pressure autoregulation leading to poor outcome (2). Failure to regulate CBF during changes in MABP following HIE can lead to the uncoupling of the tight relationship between CBF and cerebral energy metabolism and results in further injury during secondary energy failure.

Nine studies investigated changes in different cerebrovascular reactivity indices in relation to outcome. Massaro et al. (49) used spectral coherence that quantifies the relationship between changes in MABP and changes in HbD to identify pressure-passive cerebrovascular circulation indicated by increased coherence between the two physiological signals. Pressure passivity index (PPI) and gain were used for quantification of the duration and magnitude of cerebral pressure passivity, respectively. Infants with poor outcome (evidence of injury on MRI) exhibited higher PPI and gain, indicating longer duration and higher magnitude of cerebral pressure passivity following hypoxia-ischemia. Howlett et al. used a time domain-based reactivity index between hemoglobin volume and MABP (HVx) to identify an optimal blood pressure (MAP_{OPT}) where vasoreactivity is greatest (43). A greater severity of brain injury was associated with more time spent with MABP below MAP_{OPT} during rewarming, while neonates with evidence of no or mild injury spent more time with MABP within or above MAP_{OPT}. Burton et al. used the same index (HVx) and followed up 19 infants to 2 years of age (29). Infants with poor outcome at 2 years had higher MAP_{OPT} values, spent more time with MABP below MAP_{OPT} and had greater MABP deviation below MAP_{OPT} during rewarming. Also, infants with greater MABP deviation above MAP_{OPT} had lesser disability and higher cognitive scores. Lee et al. from the same group reviewed the role of HVx in a larger cohort of 64 infants and confirmed that greater duration and deviation of MABP below MAP_{OPT} were associated with greater injury in the white matter and paracentral gyri on MRI. MABP within MAP_{OPT} was associated with lesser injury in the white matter, putamen and globus pallidus, and brain stem (47). Restricted diffusion (characterized by low ADC values) in the posterior centrum semiovale and the posterior limb of the internal capsule correlated with MABP deviation below the MAP_{OPT} during hypothermia was also observed (61). Lower ADC scalars in the basal ganglia correlated with worse autoregulation during rewarming after TH.

Chalak et al. reviewed the dynamic and multiple-time-scale properties of cerebral autoregulation with a moving time window correlation between cerebral oxygenation and MABP and demonstrated the presence of large spontaneous fluctuations in MABP during TH in the infants with abnormal outcome (31). Both in-phase and antiphase correlations were associated with poor outcome. Tian et al. from the same group used wavelet analysis to understand and characterize the cerebrovascular reactivity in both time and frequency domain (62). The time-scale dependent nature of dynamic cerebral autoregulation was described with both in-phase and anti-phase coherence between the spontaneous oscillations in MABP and cerebral oxygenation. Findings were similar to their previous study (31). Mitra et al. presented a refined wavelet analysis technique and described a metabolic and haemodynamic reactivity index (wavelet semblance or phase difference between [oxCCO] and MABP or [HbD] and MABP]) in relation to outcome (52).

These findings highlight the importance of appropriate haemodynamic management following HIE for the prevention of secondary brain injury. This potential benefit of optimizing haemodynamic management using NIRS based reactivity indices requires validation.

CEREBRAL NIRS MARKERS AND NEURODEVELOPMENTAL OUTCOME

Fifteen studies have included a neurodevelopmental follow up data to compare the NIRS based indices for outcome prognostication. Meek et al. followed up a cohort of infants following HIE to 1 year of age and noted a raised CBV in the adverse outcome group on day 1 (2). Toet et al. followed up their cohort up to 5 years of age using the Griffiths Mental Developmental Scale to identify the favorable and unfavorable groups in the pre-TH era (15). The same group has subsequently reviewed the prognostic value of cerebral oxygenation and FTOE in the cooling era in a cohort of 39 infants and noted significant differences in both cerebral oxygenation and FTOE between the good and adverse outcome groups (48). These findings have been discussed previously. Interestingly, in a study cohort of 18 infants (57), no definite relationship was noted by Shellhaas et al. between cerebral oxygenation and neurodevelopmental outcome at 18 months. Differences of these findings compared to previous studies can be related to: (a) smaller sample size; (b) decisions to withdraw intensive care were different; in the other two studies (15, 48) as most infants with a predicted adverse outcome died after redirection of care during the neonatal period; (c) use of different neurodevelopmental assessment tools—Shellhass et al.

used Bayley Scales of Infant Development, Lemmers et al. and Toet et al. both used Griffiths Mental Developmental scales; and (d) use of different NIRS sensors—neonatal sensors were used by Shellhass et al. while the other studies used pediatric sensors. Different NIRS sensors are known to cause differences in absolute values of cerebral oxygenation (74, 75). Neonatal sensors tend to record tissue saturations higher than adult sensor (in case of INVOS NIRS monitors, this is ∼10%). As most monitors have the upper limit set to 95%, higher values recorded by neonatal sensors can present in a straight line over time, without much variability.

Ancora et al. (23) noted a significantly higher cerebral oxygenation value at 12 h of age in infants with the adverse outcome on a 1-year Griffiths assessment. A trend toward higher values in the adverse outcome group was also observed at 6- and 24-h during TH. Similar findings were reported also by Zaramella et al. using the Amiel-Tison score at 1 year of age (65). Two recent studies (52, 62) using wavelet analysis also noted a clear difference in NIRS biomarkers between good and poor outcome infants based on their neurodevelopment assessment scores.

NIRS MONITORING WITH OTHER NEUROMONITORING TOOLS

Fifteen studies combined NIRS monitoring with structural and haemodynamic changes on MRI and metabolic derangement on thalamic ^{1}H MRS while eight studies reviewed background electrical activity on aEEG together with NIRS.

Shellhas et al. (57), Peng et al. (56), and Mitra et al. (52) used different MRI scores to review the relationship between NIRS biomarkers with short term outcome. Massaro et al. (49) compared a measurement of CBF on Arterial spin labeling (ASL) MR imaging between 7 and 10 days with FTOE on day 1 (during cooling) and on day 4 (after rewarming) in infants with HIE and healthy controls. Infants with HIE had lower FTOE on both days (significantly lower after rewarming). Regional CBF on ASL in the basal ganglia thalamic (BGT) region and anterior white matter (AWM) was higher in the HIE cohort. However, CBF in BGT area in infants with no evidence of injury on MR imaging or watershed type of injury following HIE was higher in comparison to infants with confirmed evidence of injury in basal ganglia and focal/multifocal injury in the WM. The lack of hyperperfusion was thought to be related to the pseudonormalisation of CBF and low metabolic demand after the development of an irreversible injury. Wintermark et al. (63) further investigated the relationship between brain perfusion measured by NIRS and ASL-MRI. A strong correlation was noted between cerebral oxygenation and CBF measured with ASL MRI (mean CBF from both frontal lobes) in infants with severe HIE, although no significant correlation was found when both groups of infants with moderate and severe HIE were combined together. This study also demonstrated that infants with severe HIE had lower CBF and lower oxygen extraction compared to those with moderate HIE.

Tekes et al. reviewed the relationship between a NIRS marker of cerebrovascular reactivity (HVx) with diffusion weighted MR imaging (61). Blood pressure deviation from $MABP_{OPT}$ (using HVx) was associated with low ADC scalers in the posterior limb of internal capsule (PLIC) and posterior centrum semiovale on MRI performed on day 10 of life or later. Howlett et al. used the same index to identify the optimal blood pressure that relates to outcome based on MRI findings (43). Mitra et al. used wavelet based NIRS reactivity indices to describe the relationship with proton (^{1}H) MRS derived thalamic Lac/NAA (52).

The first study combining NIRS and aEEG monitoring was reported by Ancora et al. (22). A persistently abnormal aEEG at 24 h of life was not predictive of the adverse outcome but the recovery of electrical activity within this period was associated with good outcome (23). In comparison, high cerebral oxygenation at 12 h indicated poor neurodevelopmental outcome. In two Dutch studies (15, 48), higher cerebral oxygenation and lower aEEG background scores both were subsequently associated with poor outcome. Lemmers et al. were the first to evaluate a combined NIRS (cerebral oxygenation) and aEEG score for the prediction of neurodevelopmental outcome (48). The combined score had a significantly improved positive predictive value (91%) compared to individual monitoring (cerebral oxygenation 67%, aEEG 62%). This combined score helped to predict the outcome as early as 12 h of age (sensitivity 100%, specificity 87%). Improvement in predicting outcome using a combined score was also described by Goeral et al. (38) and Neizen et al. (55). Chalak et al. introduced an estimation of neurovascular coupling (NVC) using wavelet analysis of cerebral oxygenation and aEEG. A few examples were presented as case studies where this wavelet index of NVC was related to outcome (32).

Shellhaas et al. compared cerebral and somatic oxygenation on NIRS and aEEG with a composite score of short-term outcome (using Thompson scores on neurological examination after rewarming and MRI scores) (58). Absolute values of cerebral and somatic oxygenation, as well as the aEEG variables before and during rewarming did not correlate with short term outcome. However, the variability of systemic oxygenation was a good predictor of the short-term outcome, Variability of cerebral oxygenation was not related to outcome. The study presented only the analysis of data 6 h before rewarming and during the rewarming period (6 h), although their monitoring included the entire period of TH, rewarming period and 12 h of normothermia after completion of rewarming. It would have been useful to identify the trend of cerebral oxygenation on days 1–3 during TH in relation to this new short-term outcome composite score. The authors speculated that the multiorgan dysfunction resulting from HIE was reflected in low systemic oxygenation variability.

FUTURE DIRECTION

Ideally, an optical neuromonitor in neonatal intensive care should provide continuous information regarding cerebral oxidative metabolism, oxygenation and blood flow in real-time at the cot side. Current studies using commercial NIRS oximeter systems can measure only cerebral oxygenation and in combination with other systemic measurements attempt to

derive markers of metabolism. However, recent advances in NIRS technology and techniques have allowed the emergence of new directions in optical monitoring that promise to present a better insight into the degree of neural injury. New NIRS monitors that can monitor cerebral oxygenation and blood flow [Babylux: combining DCS and time-resolved reflectance spectroscopy (TRS) (76), Metaox: combining FD-NIRS and DCS (77)], Cyril: monitoring of CCO (BNIRS) and Florence: monitoring of CCO and blood flow together (combining BNIRS and DCS, currently being used by UCL group) are encouraging innovations in this area. There is continued research in the optical community to investigate the validity of existing tissue oximetry algorithms, especially regarding their precision and reproducibility (46, 78). New approaches, such as using broadband spectra (72) or novel combinations of spectral and multidistance techniques (79), are being developed to obtain more robust measurements of cerebral oxygenation. Advances in the optical developments to improve the accuracy of the measurement will increase acceptance within the clinical practice. The combination of (as opposed to the individual) measurements of brain tissue mitochondrial function, blood flow, oxygenation, and oxygen consumption will lead to a better assessment of neonatal hypoxic-ischaemic brain injury and most likely to offer enhanced prognostic value. An optical instrument that can deliver these measurements in real-time, non-invasively at the cot-side is necessary, with appropriate analysis techniques that will allow integration of these measurements toward the derivation of clinical information.

A small sample size often limits the validity of the findings of many NIRS studies. Future studies in this field need to be designed with sample size appropriate to answer the clinically relevant questions using measurable outcome parameters. This will provide further confidence in the clinical translation of this technology. Multicenter randomized controlled studies in the preterm population to review the benefit of NIRS monitoring have demonstrated the benefits of the cerebral oximetry monitoring (14), but no similar study has been published for HIE. One of the other complex issues is the use of different NIRS sensors and algorithms used by different manufacturers to measure cerebral oxygenation. Despite the difference in techniques and algorithms, most of the commercial monitors have shown a reasonable correlation between the measured tissue saturation values (74, 80–84) but without a uniform terminology, readers struggle to correlate the findings from different studies. Several manufacturers have developed smaller and flexible neonatal sensors but the use of different sensors with the same brain oximeter can produce different measurements, as pointed out by Lemmers et al. and colleagues (6, 74, 75). So, it is important to specify the type of NIRS oximeter sensor used with their reference values in each study. Finally, quantification of cerebral autoregulation using NIRS and systemic variables can offer a good insight of brain health; however, authors should consider the use of advanced signal processing techniques (e.g., wavelet analysis) to better quantify changes in the context of the dynamic nature of cerebral autoregulation.

LIMITATIONS

We only reviewed human studies to focus on the assessment of this neuromonitoring technique in the clinical environment. This is a limitation of this review as some important work in preclinical models were not included. The use of the English language as a filter during the search and literature search using two medical databases might have resulted in the omission of some studies, although the chance of missing any major publication in this field will be low.

There are also some inherent limitations of NIRS technology. Any strong light (e.g., halogen spotlight attached to the incubator or a standing spotlight) can cause interference with NIRS monitoring. Hair can also sometimes pose an issue as it can absorb a lot of light, although this is unlikely in newborn infants. Hematoma and significant edema in the layers between skin and the scalp can also cause problems with NIRS recording as they will contribute to the measured signals, reducing the amount of information detected from the brain. Movement artifacts can also be an issue if not carefully documented.

CONCLUSION

Significant effort has been made over the last decade to examine the role of cerebral NIRS monitoring in HIE. Commercially available cerebral NIRS parameters can identify cerebral hyperoxygenation, increased cerebral perfusion and loss of cerebral autoregulation in infants with severe HIE. Changes in NIRS variables in HIE are associated with subsequent neurodevelopmental outcome. Combined clinical neuromonitoring using NIRS and aEEG/EEG monitoring is feasible and appears to improve the prognostication of the neurodevelopmental outcome. Although the evidence from the currently available studies indicates a positive role for NIRS based neuromonitoring for infants with HIE, these findings need to be reviewed in larger prospective cohorts before translation to clinical practice.

AUTHOR CONTRIBUTIONS

SM completed the initial literature search. SM and NR assessed the papers and drafted the first review. SM, GB, JM, IT, and NR contributed to the final version.

FUNDING

The Wellcome Trust (219610/Z/19/Z) and Medical Research Council (MR/S003134/1).

ACKNOWLEDGMENTS

The authors would like to acknowledge the help from Simon Coats, Clinical Support librarian in UCL medical library for this systematic review.

REFERENCES

1. Azzopardi D, Wyatt JS, Cady EB, Delpy DT, Baudin J, Stewart AL, et al. Prognosis of newborn infants with hypoxic-ischemic brain injury assessed by phosphorus magnetic resonance spectroscopy. *Pediatr Res*. (1989) 25:445–51. doi: 10.1203/00006450-198905000-00004
2. Meek JH, Elwell CE, McCormick DC, Edwards AD, Townsend JP, Stewart AL, et al. Abnormal cerebral hemodynamics in perinatally asphyxiated neonates related to outcome. *Arch Dis Child Fetal Neonatal Ed*. (1999) 81:F110–F5. doi: 10.1136/fn.81.2.F110
3. Hassell KJ, Ezzati M, Alonso-Alconada D, Hausenloy DJ, Robertson NJ. New horizons for newborn brain protection: enhancing endogenous neuroprotection. *Arch Dis Child Fetal Neonatal Ed*. (2015) 100:F541–52. doi: 10.1136/archdischild-2014-306284
4. Mitra S, Kendall GS, Bainbridge A, Sokolska M, Dinan M, Uria-Avellanal C, et al. Proton magnetic resonance spectroscopy lactate/N-acetylaspartate within 2 weeks of birth accurately predicts 2-year motor, cognitive and language outcomes in neonatal encephalopathy after therapeutic hypothermia. *Arch Dis Child Fetal Neonatal Ed*. (2019) 104:F424–32. doi: 10.1136/archdischild-2018-315478
5. Lally PJ, Montaldo P, Oliveira V, Soe A, Swamy R, Bassett P, et al. Marble consortium. Magnetic resonance spectroscopy assessment of brain injury after moderate hypothermia in neonatal encephalopathy: a prospective multicentre cohort study. *Lancet Neurol*. (2019) 18:35–45. doi: 10.1016/S1474-4422(18)30325-9
6. Dix LM, van Bel F, Lemmers PM. Monitoring cerebral oxygenation in neonates: an update. *Front Pediatr*. (2017) 5:46. doi: 10.3389/fped.2017.00046
7. Garvey AA, Dempsey EM. Applications of near infrared spectroscopy in the neonate. *Curr Opin Pediatr*. (2018) 30:209–15. doi: 10.1097/MOP.0000000000000599
8. Almaazmi M, Schmid MB, Havers S, Reister F, Lindner W, Mayer B, et al. Cerebral near-infrared spectroscopy during transition of healthy term new-borns. *Neonatology*. (2013) 103:246–51. doi: 10.1159/000345926
9. Urlesberger B, Kratky E, Rehak T, Pocivalnik M, Avian A, Czihak J, et al. Regional oxygen saturation of the brain during birth transition of term infants: comparison between elective cesarean and vaginal deliveries. *J Pediatr*. (2011) 159:404–8. doi: 10.1016/j.jpeds.2011.02.030
10. Baik N, Urlesberger B, Schwaberger B, Schmolzer GM, Mileder L, Avian A, et al. Reference ranges for cerebral tissue oxygen saturation index in term neonates during immediate neonatal transition after birth. *Neonatology*. (2015) 108:283–6. doi: 10.1159/000438450
11. Bailey SM, Hendricks-Munoz KD, Mally P. Cerebral, renal, and splanchnic tissue oxygen saturation values in healthy term newborns. *Am J Perinatol*. (2014) 31:339–44. doi: 10.1055/s-0033-1349894
12. McNeill S, Gatenby JC, McElroy S, Engelhardt B. Normal cerebral, renal and abdominal regional oxygen saturations using near-infrared spectroscopy in preterm infants. *J Perinatol*. (2011) 31:51–7. doi: 10.1038/jp.2010.71
13. Roche-Labarbe N, Carp SA, Surova A, Patel M, Boas DA, Grant PE, et al. Noninvasive optical measures of CBV, StO_2, CBF index, and $rCMRO_2$ in human premature neonates brains in the first six weeks of life. *Hum Brain Mapp*. (2010) 31:341–52. doi: 10.1002/hbm.20868
14. Hyttel-Sorensen S, Pellicer A, Alderliesten T, Austin T, van Bel F, Benders M, et al. Cerebral near infrared spectroscopy oximetry in extremely preterm infants: phase II randomised clinical trial. *BMJ*. (2015) 350:g7635. doi: 10.1136/bmj.g7635
15. Toet MC, Lemmers PMA, van Schelven LJ, van Bel F. Cerebral oxygenation and electrical activity after birth asphyxia: their relation to outcome. *Pediatrics*. (2006) 117:333–9. doi: 10.1542/peds.2005-0987
16. Edwards AD, Brown GC, Cope M, Wyatt JS, McCormick DC, Roth SC, et al. Quantification of concentration changes in neonatal human cerebral oxidized cytochrome oxidase. *J Appl Physiol*. (1985) 71:1907–13. doi: 10.1152/jappl.1991.71.5.1907
17. Jöbsis FF. Noninvasive, infrared monitoring of cerebral and myocardial oxygen sufficiency and circulatory parameters. *Science*. (1977) 198:1264–7. doi: 10.1126/science.929199
18. Van Bel F, Dorrepaal CA, Benders MJNL, Zeeuwe PEM, Van de Bor M, Berger HM. Changes in cerebral hemodynamics and oxygenation in the first 24 hours after birth asphyxia. *Pediatrics*. (1993) 92:365–72.
19. Bale G, Elwell CE, Tachtsidis I. From Jöbsis to the present day: a review of clinical near-infrared spectroscopy measurements of cerebral cytochrome-c-oxidase. *J Biomed Opt*. (2016) 21:099801. doi: 10.1117/1.JBO.21.9.099801
20. Korček P, Stranák Z, Širc J, Naulaers G. The role of near-infrared spectroscopy monitoring in preterm infants. *J Perinatol*. (2017) 37:1070–77. doi: 10.1038/jp.2017.60
21. Liberati A, Altman DG, Tetzlaff J, Mulrow C, Gøtzsche PC, Ioannidis JP, et al. The PRISMA statement for reporting systematic reviews and meta-analyses of studies that evaluate healthcare interventions: explanation and elaboration. *PLoS Med*. (2009) 6:e1000100. doi: 10.1371/journal.pmed.1000100
22. Ancora G, Maranella E, Locatelli C, Pierantoni L, Faldella G. Changes in cerebral hemodynamics and amplitude integrated EEG in an asphyxiated newborn during and after cool cap treatment. *Brain Dev*. (2009) 31:442–4. doi: 10.1016/j.braindev.2008.06.003
23. Ancora G, Maranella E, Grandi S, Sbravati F, Coccolini E, Savini S, et al. Early predictors of short term neurodevelopmental outcome in asphyxiated cooled infants. A combined brain amplitude integrated electroencephalography and near infrared spectroscopy study. *Brain Dev*. (2013) 35:26–31. doi: 10.1016/j.braindev.2011.09.008
24. Arriaga-Redondo M, Arnaez J, Benavente-Fernández I, Lubián-López S, Hortigüela M, Vega-Del-Val C, et al. Lack of variability in cerebral oximetry tendency in infants with severe hypoxic-ischemic encephalopathy under hypothermia. *Ther Hypothermia Temp Manag*. (2019) 9:243–50. doi: 10.1089/ther.2018.0041
25. Bale G, Mitra S, Meek J, Robertson N, Tachtsidis I. A new broadband near-infrared spectroscopy system for *in-vivo* measurements of cerebral cytochrome-c-oxidase changes in neonatal brain injury. *Biomed Opt Express*. (2014) 5:3450–66. doi: 10.1364/BOE.5.003450
26. Bale G, Mitra S, de Roever I, Chan M, Caicedo-Dorado A, Meek J, et al. Interrelationship between broadband NIRS measurements of cerebral cytochrome C oxidase and systemic changes indicates injury severity in neonatal encephalopathy. *Adv Exp Med Biol*. (2016) 923:181–6 doi: 10.1007/978-3-319-38810-6_24
27. Bale G, Mitra S, de Roever I, Sokolska M, Price D, Bainbridge A, et al. Oxygen dependency of mitochondrial metabolism indicates outcome of newborn brain injury. *J Cereb Blood Flow Metab*. (2018) 39, 2035–2047. doi: 10.1177/0271678X18777928
28. Bale G, Taylor N, Mitra S, Sudakou A, de Roever I, Meek J, et al. Near-infrared spectroscopy measured cerebral blood flow from spontaneous oxygenation changes in neonatal brain injury. *Adv Exp Med Biol*. (2020) 1232:3–9. doi: 10.1007/978-3-030-34461-0_1
29. Burton VJ, Gerner G, Cristofalo E, Chung SE, Jennings JM, Parkinson C, et al. A pilot cohort study of cerebral autoregulation and 2-year neurodevelopmental outcomes in neonates with hypoxic-ischemic encephalopathy who received therapeutic hypothermia. *BMC Neurology*. (2015) 15:209. doi: 10.1186/s12883-015-0464-4
30. Campbell H, Govindan RB, Kota S, Al-Shargabi T, Metzler M, Andescavage N, et al. Autonomic dysfunction in neonates with hypoxic ischemic encephalopathy undergoing therapeutic hypothermia impairs physiological responses to routine care events. *J Pediatr*. (2018) 196:38–44. doi: 10.1016/j.jpeds.2017.12.071
31. Chalak LF, Tian F, Tarumi T, Zhang R. Cerebral hemodynamics in asphyxiated newborns undergoing hypothermia therapy: pilot findings using a multiple-time-scale analysis. *Pediatr. Neurol*. (2016) 55:30–6. doi: 10.1016/j.pediatrneurol.2015.11.010
32. Chalak LF, Tian F, Adams-Huet B, Vasil D, Laptook A, Tarumi T, et al. Novel wavelet real time analysis of neurovascular coupling in neonatal encephalopathy. *Sci Rep*. (2017) 7:45958. doi: 10.1038/srep45958
33. Chen S, Sakatani K, Lichty W, Ning P, Zhao S, Zuo H. Auditory-evoked cerebral oxygenation changes in hypoxic-ischemic encephalopathy of newborn infants monitored by near infrared spectroscopy. *Early Hum Dev*. (2002) 67:113–21. doi: 10.1016/S0378-3782(02)00004-X

34. Chock VY, Frymoyer A, Yeh CG, Van Meurs KP. Renal saturation and acute kidney injury in neonates with hypoxic ischemic encephalopathy undergoing therapeutic hypothermia.*J Pediatr*. (2018) 200:232–9.e1. doi: 10.1016/j.jpeds.2018.04.076
35. Dehaes M, Aggarwal A, Lin PY, Rosa Fortuno C, Fenoglio A, Roche-Labarbe N, et al. Cerebral oxygen metabolism in neonatal hypoxic ischemic encephalopathy during and after therapeutic hypothermia. *J Cerebr Blood Flow Metab*. (2014) 34:87–94. doi: 10.1038/jcbfm.2013.165
36. Forman E, Breatnach CR, Ryan S, Semberova J, Miletin J, Foran A, et al. Noninvasive continuous cardiac output and cerebral perfusion monitoring in term infants with neonatal encephalopathy: assessment of feasibility and reliability. *Pediatr Res*. (2017) 82:789–95. doi: 10.1038/pr.2017.154
37. Gagnon MH, Wintermark P. Effect of persistent pulmonary hypertension on brain oxygenation in asphyxiated term newborns treated with hypothermia. *J Matern Fetal Neonatal Med*. (2016) 29:2049–55. doi: 10.3109/14767058.2015.1077221
38. Goeral K, Urlesberger B, Giordano V, Kasprian G, Wagner M, Schmidt L, et al. Prediction of outcome in neonates with hypoxic-ischemic encephalopathy II: role of amplitude-integrated electroencephalography and cerebral oxygen saturation measured by near-infrared spectroscopy. *Neonatology*. (2017) 112:193–202. doi: 10.1159/000468976
39. Govindan RB, AN Massaro N, Andescavage NN, Chang T, du Plesis A. Cerebral pressure passivity in newborns with encephalopathy undergoing therapeutic hypothermia. *Front Hum Neurosci*. (2014) 8:266. doi: 10.3389/fnhum.2014.00266
40. Govindan RB, Massaro A, Chang T, Vezina G, du Plessis A. A novel technique for quantitative bedside monitoring of neurovascular coupling. *J Neurosci Methods*. (2016) 259:135–42. doi: 10.1016/j.jneumeth.2015.11.025
41. Grant PE, Roche-Labarbe N, Surova A, Themelis G, Selb J, Warren EK, et al. Increased cerebral blood volume and oxygen consumption in neonatal brain injury. *J Cerebr Blood Flow Metab*. (2009) 29:1704–13. doi: 10.1038/jcbfm.2009.90
42. Gucuyener K, Beken S, Ergenekon E, Soysal S, Hirfanoglu T, Turan O, et al. Use of amplitude-integrated electroencephalography (aEEG) and near infrared spectroscopy findings in neonates with asphyxia during selective head cooling. *Brain Dev*. (2012) 34:280–6. doi: 10.1016/j.braindev.2011.06.005
43. Howlett JA, Northington FJ, Gilmore MM, Tekes A, Huisman TAGM, Parkinson C, et al. Cerebrovascular autoregulation and neurologic injury in neonatal hypoxic-ischemic encephalopathy. *Pediatr Res*. (2013) 74:525–35. doi: 10.1038/pr.2013.132
44. Huang L, Ding H, Hou X, Zhou C, Wang G, Tian F. Assessment of the hypoxic-ischemic encephalopathy in neonates using non-invasive near-infrared spectroscopy. *Physiol Meas*. (2004) 25:749–61. doi: 10.1088/0967-3334/25/3/014
45. Jain SV, Pagano L, Gillam-Krakauer M, Slaughter JC, Pruthi S, Engelhardt B. Cerebral regional oxygen saturation trends in infants with hypoxic-ischemic encephalopathy. *Early Hum Dev*. (2017) 113:55–61. doi: 10.1016/j.earlhumdev.2017.07.008
46. Kovacsova Z, Bale G, Mitra S, Meek J, Robertson N, Tachtsidis I. Investigation of confounding factors in measuring tissue saturation with NIRS spatially resolved spectroscopy. *Adv Exp Med Biol*. (2018) 1072:307–12. doi: 10.1007/978-3-319-91287-5_49
47. Lee JK, Poretti A, Perin J, Huisman TAGM, Parkinson C, Chavez-Valdez R, et al. Optimizing cerebral autoregulation may decrease neonatal regional hypoxic-ischemic brain injury. *Dev Neurosci*. (2017) 39:248–56. doi: 10.1159/000452833
48. Lemmers PMA, Zwanenburg RJ, Benders MJNL, De Vries LS, Groenendaal F, Van Bel F, et al. Cerebral oxygenation and brain activity after perinatal asphyxia: does hypothermia change their prognostic value? *Pediatr Res*. (2013) 74:180–5. doi: 10.1038/pr.2013.84
49. Massaro AN, Bouyssi-Kobar M, Chang T, Vezina LG, Du Plessis AJ, Limperopoulos C. Brain perfusion in encephalopathic newborns after therapeutic hypothermia. *Am J Neuroradiol*. (2013) 34:1649–55. doi: 10.3174/ajnr.A3422
50. Massaro AN, Govindan RB, Vezina G, Chang T, Andescavage NN, Wang Y, et al. Impaired cerebral autoregulation and brain injury in newborns with hypoxic-ischemic encephalopathy treated with hypothermia. *J Neurophysiol*. (2015) 114:818–24. doi: 10.1152/jn.00353.2015
51. Mitra S, Bale G, Meek J, Uria-Avellanal C, Robertson NJ, Tachtsidis I. Relationship between cerebral oxygenation and metabolism during rewarming in newborn infants after therapeutic hypothermia following hypoxic-ischemic brain injury. *Adv Exp Med Biol*. (2016) 923:245–51. doi: 10.1007/978-3-319-38810-6_33
52. Mitra S, Bale G, Highton D, Gunny R, Uria-Avellanal C, Bainbridge A, et al. Pressure passivity of cerebral mitochondrial metabolism is associated with poor outcome following perinatal hypoxic ischemic brain injury. *J Cereb Blood Flow Metab*. (2017) 1:271678X17733639. doi: 10.1177/0271678X17733639
53. Mitra S, Bale G, de Roever I, Meek J, Robertson NJ, Tachtsidis I. Changes in brain tissue oxygenation and metabolism during rewarming after neonatal encephalopathy are related to electrical abnormality. *Adv Exp Med Biol*. (2020) 1232:25–31. doi: 10.1007/978-3-030-34461-0_4
54. Nakamura S, Koyano K, Jinnai W, Hamano S, Yasuda S, Konishi Y, et al. Simultaneous measurement of cerebral hemoglobin oxygen saturation and blood volume in asphyxiated neonates by near-infrared time-resolved spectroscopy. *Brain Dev*. (2015) 37:925–32. doi: 10.1016/j.braindev.2015.04.002
55. Niezen CK, Bos AF, Sival DA, Meiners LC, Ter Horst HJ. Amplitude-integrated EEG and cerebral near-infrared spectroscopy in cooled, asphyxiated infants. *Am J Perinatol*. (2018) 35:904–10. doi: 10.1055/s-0038-1626712
56. Peng S, Boudes E, Tan X, Saint-Martin C, Shevell M, Wintermark P. Does near-infrared spectroscopy identify asphyxiated newborns at risk of developing brain injury during hypothermia treatment? *Am J Perinatol*. (2015) 32:555–64. doi: 10.1055/s-0034-1396692
57. Shellhaas RA, Thelen BJ, Bapuraj JR, Burns JW, Swenson AW, Christensen MK, et al. Limited short-term prognostic utility of cerebral NIRS during neonatal therapeutic hypothermia. *Neurology*. (2013) 81:249–55. doi: 10.1212/WNL.0b013e31829bfe41
58. Shellhaas RA, Burns JW, Wiggins SA, Christensen MK, Barks JD, Chervin RD. Sleep-wake cycling and cerebral oxygen metabolism among critically ill neonates. *J Child Neurol*. (2014) 29:530–3. doi: 10.1177/0883073812470972
59. Shellhaas RA, Kushwaha JS, Plegue MA, Selewski DT, Barks JD. An evaluation of cerebral and systemic predictors of 18-month outcomes for neonates with hypoxic ischemic encephalopathy. *J Child Neurol*. (2015) 30:1526–31. doi: 10.1177/0883073815573319
60. Tax N, Urlesberger B, Binder C, Pocivalnik M, Morris N, Pichler G. The influence of perinatal asphyxia on peripheral oxygenation and perfusion in neonates. *Early Hum Dev*. (2013) 89:483–6. doi: 10.1016/j.earlhumdev.2013.03.011
61. Tekes A, Poretti A, Scheurkogel MM, Huisman TAGM, Howlett JA, Alqahtani E, et al. Apparent diffusion coefficient scalars correlate with near-Infrared spectroscopy markers of cerebrovascular autoregulation in neonates cooled for perinatal hypoxic-Ischemic injury. *Am J Neuroradiol*. (2015) 36:188–93. doi: 10.3174/ajnr.A4083
62. Tian F, Tarumi T, Liu H, Zhang R, Chalak L. Wavelet coherence analysis of dynamic cerebral autoregulation in neonatal hypoxic-ischemic encephalopathy. *NeuroImage: Clin*. (2016) 11:124–32. doi: 10.1016/j.nicl.2016.01.020
63. Wintermark P, Hansen A, Warfield SK, Dukhovny D, Soul JS. Near-infrared spectroscopy versus magnetic resonance imaging to study brain perfusion in newborns with hypoxic-ischemic encephalopathy treated with hypothermia. *NeuroImage*. (2014) 85:287–93. doi: 10.1016/j.neuroimage.2013.04.072
64. Wu TW, Tamrazi B, Soleymani S, Seri I, Noori S. Hemodynamic changes during rewarming phase of whole-body hypothermia therapy in neonates with hypoxic-ischemic encephalopathy.*J Pediatr*. (2018) 197:68–74.e2 doi: 10.1016/j.jpeds.2018.01.067
65. Zaramella P, Saraceni E, Freato F, Falcon E, Suppiej A, Milan A, et al. Can tissue oxygenation index (TOI) and cotside neurophysiological variables predict outcome in depressed/asphyxiated newborn infants? *Early Hum Dev*. (2007) 83:483–9. doi: 10.1016/j.earlhumdev.2006.09.003
66. Scholkmann F, Kleiser S, Metz AJ, Zimmermann R, Pavia JM, Wolf U, et al. A review on continuous wave functional near-infrared spectroscopy and imaging instrumentation and methodology. *Neuroimage*. (2014) 85:6–27. doi: 10.1016/j.neuroimage.2013.05.004
67. Buttafava M, Martinenghi E, Tamborini D, Contini D, Dalla Mora A, Renna M, et al. A compact two-wavelength time-domain NIRS system

based on SiPM and pulsed diode lasers. *IEEE Photonics J*. (2017) 9:1–14. doi: 10.1109/JPHOT.2016.2632061
68. Gunadi S, Leung TS, Elwell CE, Tachtsidis I. Spatial sensitivity and penetration depth of three cerebral oxygenation monitors. *Biomed Opt Express*. (2014) 5:2896–12. doi: 10.1364/BOE.5.002896
69. Matcher SJ, Elwell CE, Cooper CE, Cope M, Delpy DT. Performance comparison of several published tissue near-infrared spectroscopy algorithms. *Anal Biochem*. (1995) 227:54–68. doi: 10.1006/abio.1995.1252
70. Suzuki S, Takasaki S, Ozaki T, Kobayashi Y. Tissue oxygenation monitor using NIR spatially resolved spectroscopy. *Proc. SPIE 3597, Optical Tomography and Spectroscopy of Tissue III* San Hose, CA (1999). doi: 10.1117/12.356862
71. Al-Rawi PG, Smielewski P, Kirkpatrick PJ. Evaluation of a near-infrared spectrometer (NIRO 300) for the detection of intracranial oxygenation changes in the adult head. *Stroke*. (2001) 32:2492–500. doi: 10.1161/hs1101.098356
72. Yeganeh HZ, Toronov V, Elliott JT, Diop M, Lee TY, St. Lawrence K. Broadband continuous-wave technique to measure baseline values and changes in the tissue chromophore concentrations. *Biomed Opt Express*. (2012) 3:2761–70. doi: 10.1364/BOE.3.002761
73. Bainbridge A, Tachtsidis I, Faulkner SD, Price D, Zhu T, Baer E, et al. Brain mitochondrial oxidative metabolism during and after cerebral hypoxia–ischemia studied by simultaneous phosphorus magnetic-resonance and broadband near-infrared spectroscopy. *Neuroimage*. (2014) 102:173–83. doi: 10.1016/j.neuroimage.2013.08.016
74. Lemmers PM, Dix LM, Toet MC, van Bel F. Limited short-term prognostic utility of cerebral NIRS during neonatal therapeutic hypothermia. *Neurology*. (2014) 82:1480–1. doi: 10.1212/01.wnl.0000446829.77267.81
75. Dix LM, van Bel F, Baerts W, Lemmers PM. Comparing near-infrared spectroscopy devices and their sensors for monitoring regional cerebral oxygen saturation in the neonate. *Pediatr Res*. (2013) 74:557–63. doi: 10.1038/pr.2013.133
76. Giovannella M, Contini D, Pagliazzi M, Pifferi A, Spinelli L, Erdmann R, et al. BabyLux device: a diffuse optical system integrating diffuse correlation spectroscopy and time-resolved near-infrared spectroscopy for the neuromonitoring of the premature newborn brain. *Neurophoton*. (2019) 6:025007. doi: 10.1117/1.NPh.6.2.025007
77. Jain V, Buckley EM, Licht DJ, Lynch JM, Schwab PJ, Naim MY, et al. Cerebral oxygen metabolism in neonates with congenital heart disease quantified by MRI and optics. *J Cereb Blood Flow Metab*. (2014) 34:380–8. doi: 10.1038/jcbfm.2013.214
78. Kleiser S, Nasseri N, Andresen B, Greisen G, Wolf M. Comparison of tissue oximeters on a liquid phantom with adjustable optical properties. *Biomed Opt Express*. (2016) 7:2973–92. doi: 10.1364/BOE.7.002973
79. Kovácsová Z, Bale G, Veesa JD, Dehghani H, Tachtsidis I. A broadband multi-distance approach to measure tissue oxygen saturation with continuous wave near-infrared spectroscopy. *Proc. SPIE 11074, Diffuse Optical Spectroscopy and Imaging VII, 110740P*. Munich (2019). doi: 10.1117/12.2527180
80. Thavasothy M, Broadhead M, Elwell C, Peters M, Smith M. A comparison of cerebral oxygenation as measured by the NIRO 300 and the INVOS 5100 near-infrared spectrophotometers. *Anaesthesia*. (2002) 57:999–1006. doi: 10.1046/j.1365-2044.2002.02826.x
81. Nagdyman N, Ewert P, Peters B, Miera O, Fleck T, Berger F. Comparison of different near-infrared spectroscopic cerebral oxygenation indices with central venous and jugular venous oxygen-ation saturation in children. *Paediatr Anaesth*. (2008) 18:160–6. doi: 10.1111/j.1460-9592.2007.02365.x
82. Grubhofer G, Tonninger W, Keznickl P, Skyllouriotis P, Ehrlich M, Hiesmayr M, et al. A comparison of the monitors INVOS 3100 and NIRO 500 in detecting changes in cerebral oxygenation. *Acta Anaesthesiol Scand*. (1999) 43:470–5. doi: 10.1034/j.1399-6576.1999.430417.x
83. Cho H, Nemoto EM, Sanders M, Fernandez K, Yonas H. Comparison of two commercially available near-infrared spectroscopy instruments for cerebral oximetry. *Technical note. J Neurosurg*. (2000) 93:351–4. doi: 10.3171/jns.2000.93.2.0351
84. Yoshitani K, Kawaguchi M, Tatsumi K, Kitaguchi K, Furuya H. A comparison of the INVOS 4100 and the NIRO 300 near-infrared spectrophotometers. *Anesth Analg*. (2002) 94:586–90. doi: 10.1097/00000539-200203000-00020

Conflict of Interest: The authors declare that the research was conducted in the absence of any commercial or financial relationships that could be construed as a potential conflict of interest.

frontiers in Pediatrics

ORIGINAL RESEARCH
published: 26 June 2020
doi: 10.3389/fped.2020.00299

No Added Neuroprotective Effect of Remote Ischemic Postconditioning and Therapeutic Hypothermia After Mild Hypoxia-Ischemia in a Piglet Model

Ted C. K. Andelius[1†], Mette V. Pedersen[1], Hannah B. Andersen[1], Mads Andersen[1], Vibeke E. Hjortdal[2], Michael Pedersen[3], Steffen Ringgaard[4], Lærke H. Hansen[1], Tine B. Henriksen[1] and Kasper J. Kyng[1]*

[1] Department of Pediatrics, Aarhus University Hospital, Aarhus, Denmark, [2] Department of Cardiothoracic and Vascular Surgery, Aarhus University Hospital, Aarhus, Denmark, [3] Comparative Medicine Lab, Aarhus University Hospital, Aarhus, Denmark, [4] The MR Research Centre, Aarhus University Hospital, Aarhus, Denmark

Introduction: Hypoxic ischemic encephalopathy (HIE) is a major cause of death and disability in children worldwide. Apart from supportive care, the only established treatment for HIE is therapeutic hypothermia (TH). As TH is only partly neuroprotective, there is a need for additional therapies. Intermittent periods of limb ischemia, called remote ischemic postconditioning (RIPC), have been shown to be neuroprotective after HIE in rats and piglets. However, it is unknown whether RIPC adds to the effect of TH. We tested the neuroprotective effect of RIPC with TH compared to TH alone using magnetic resonance imaging and spectroscopy (MRI/MRS) in a piglet HIE model.

Methods: Thirty-two male and female piglets were subjected to 45-min global hypoxia-ischemia (HI). Twenty-six animals were randomized to TH or RIPC plus TH; six animals received supportive care only. TH was induced through whole-body cooling. RIPC was induced 1 h after HI by four cycles of 5 min of ischemia and 5 min of reperfusion in both hind limbs. Primary outcome was Lac/NAA ratio at 24 h measured by MRS. Secondary outcomes were NAA/Cr, diffusion-weighted imaging (DWI), arterial spin labeling, aEGG score, and blood oxygen dependent (BOLD) signal measured by MRI/MRS at 6, 12, and 24 h after the hypoxic-ischemic insult.

Results: All groups were subjected to a comparable but mild insult. No difference was found between the two intervention groups in Lac/NAA ratio, NAA/Cr ratio, DWI, arterial spin labeling, or BOLD signal. NAA/Cr ratio at 24 h was higher in the two intervention groups compared to supportive care only. There was no difference in aEEG score between the three groups.

OPEN ACCESS

Edited by:
Julie Wixey, The University of Queensland, Australia

Reviewed by:
Ivo Bendix, Essen University Hospital, Germany
Nicola Jayne Robertson, University College London, United Kingdom

***Correspondence:**
Ted C. K. Andelius
ted.andelius@clin.au.dk

†ORCID:
Ted C. K. Andelius
orcid.org/0000-0003-4438-4686

Specialty section:
This article was submitted to Pediatric Neurology, a section of the journal Frontiers in Pediatrics

Received: *31 January 2020*
Accepted: *11 May 2020*
Published: *26 June 2020*

Citation:
Andelius TCK, Pedersen MV, Andersen HB, Andersen M, Hjortdal VE, Pedersen M, Ringgaard S, Hansen LH, Henriksen TB and Kyng KJ (2020) No Added Neuroprotective Effect of Remote Ischemic Postconditioning and Therapeutic Hypothermia After Mild Hypoxia-Ischemia in a Piglet Model. Front. Pediatr. 8:299. doi: 10.3389/fped.2020.00299

Conclusion: Treatment with RIPC resulted in no additional neuroprotection when combined with TH. However, insult severity was mild and only evaluated at 24 h after HI with a short MRS echo time. In future studies more subtle neurological effects may be detected with increased MRS echo time and post mortem investigations, such as brain histology. Thus, the possible neuroprotective effect of RIPC needs further evaluation.

Keywords: neonatal encephalopathy, neuroprotection, remote ishemic postconditioning, piglet model, magnetic resonance imaging, magnetic resonance spectroscopy

INTRODUCTION

Neonatal hypoxic ischemic encephalopathy (HIE) is a major cause of death and impairment in children (1). Treatment with therapeutic hypothermia (TH) has improved outcome in neonates with moderate to severe HIE, but morbidity and mortality remain high (2). Treatment with TH is limited by a narrow therapeutic time window and further limited to tertiary centers due to technical requirements and the need for specially trained staff. Accordingly, there is a need for neuroprotective strategies that can be combined with TH to improve outcome.

In 1986, Murry et al. showed in dogs that infarction size after coronary occlusion was reduced if the acute myocardial injury was preceded by short ischemic periods—preconditioning (3). Through short periods ischemia applied to a hind limp after the insult, the similar tissue protective effect was later demonstrated in a stroke model in adult rats—remote ischemic postconditioning (RIPC) (4). The tissue protective mechanism of RIPC remains to be fully elucidated together with the optimal timing, number, and duration of remote ischemic cycles. In a review of RIPC for cardio and neuro protection, clinical studies used 5-min cycles of RIPC (5, 6). RIPC has been proposed as a novel neuroprotective intervention for HIE and proven to be neuroprotective in both smaller and larger animal models (7). RIPC reduced infarct volume in rat pups compared to untreated controls (8). Another study in rat pups found improved long-term motor sensory deficits in animals treated with RIPC 24 h after the insult (9). When applied in a larger animal model of HIE, Ezzati et al. found reduced white matter Lac/NAA ratio, higher levels of whole brain ATP, and reduced histological white matter damage with 10 min cycles of RIPC (10). RIPC has also been shown to reduce nitrosative stress in piglets with HIE (11). We have recently shown reduced Lac/NAA ratio in the basal ganglia in piglets treated with 5-min cycles of RIPC compared to piglets who received supportive care only (12). RIPC is a low-tech, readily available intervention and therefore holds potential as a novel neuroprotectant for neonates with HIE. However, it is unknown whether RIPC in combination with TH will improve neuroprotection beyond that of TH alone (13).

We therefore investigated whether there is an added neuroprotective effect of combining RIPC with TH compared to TH alone using magnetic resonance imaging and spectroscopy (MRI/MRS).

MATERIALS AND METHODS

The study was approved by the Danish Animal Experiments Inspectorate (Permission nr. 2016-15-0201-01052). This study is reported in accordance with the ARRIVE guidelines (ARRIVE checklist in **Supplementary Material 1**) (14). Details on this piglet model of HIE have previously been given (12, 15).

Anesthesia

Newborn Danish Landrace piglets (<12 h old) were used in this study. Animals were transported directly from the farm to the experimental facilities. Piglets were anesthetized using inhalation of 2–4% sevoflurane. Peripheral intravenous access was acquired through an ear vein. A bolus of propofol 10 mg/kg, fentanyl 30 μg/kg, and rocuronium 1 mg/kg was given and the piglet was intubated and ventilated. Anesthesia was maintained through an infusion of propofol 4–10 mg/kg/h and fentanyl 5–12 μg/kg/h. Anesthetics were reduced to the lowest relevant dose to minimize any possible effect on the aEEG and neurological outcomes. The ventilator was adjusted to an end-tidal CO_2 of 4.5–5.5 kPa. Under sterile conditions, umbilical venous and arterial catheters were placed. $SatO_2$%, heart rate, mean arterial blood pressure (MABP), core temperature, and electrocardiogram were continuously recorded and downloaded to a computer (Datex Ohmeda S/5 Collect, Finland). Core temperature was measured through a rectal thermometer placed ∼5 cm into the rectum. A single-channel amplitude-integrated electroencephalogram (aEEG) was recorded continuously (Natus Medical Incorporated, CA, USA). Two electrodes were placed on the left and the right side, one behind each eye (approximately equivalent to the parietal 3 and 4 electrodes used in a human neonate). A reference electrode was placed at the base of the snout and a ground electrode on the most caudal part of the head. Piglets received i.v. gentamicin 5 mg/kg once every 24 h and ampicillin 30 mg/kg every 12 h. Blood glucose and electrolytes were monitored and kept within the normal range through infusion of 5–10 ml/kg/h of NeoKNaG (Na^+: 15 mmol/L, K^+: 10 mmol/L, Cl^-: 25 mmol/L, glucose: 505 mmol/L). We aimed to keep MABP >40 mmHg. If hypotension occurred, anesthetics were reduced to the minimum relevant dose and the following treatment given: first, a bolus of saline (10 ml/kg) was administered, followed by infusion of noradrenaline (0.25–1.5 μg/kg/min) and/or dopamine (5–15 μg/kg/min) and/or adrenalin (0.1–1.5 μg/kg/min) and/or dobutamine (2–20 μg/kg/min) (16). For refractory hypotension a bolus of hydrocortisone 2.5 mg/kg was administered.

Hypoxic-Ischemic Insult

During a 45-min period, piglets were ventilated at an FiO_2 of 2–10% to mimic the generalized hypoxia neonates may experience during birth. To ensure maximal survival combined with a clinically relevant insult, FiO_2 was titrated to a target aEEG ($< 7\mu V$) combined with a target MABP ($< 70\%$ of baseline MABP) for at least 5 min. FiO_2 was briefly increased if HR < 80 min^{-1} or aEEG $< 3\ \mu V$. After 45 min of hypoxia the piglets were resuscitated at an FiO_2 of 21%. If needed, FiO_2 was increased to keep $SatO_2 > 90\%$.

Therapeutic Hypothermia

TH was achieved through whole-body cooling with a target temperature of 33.5–34.0°C. TH was induced by active cooling with 5°C water bags directly placed on the piglet until target temperature was reached and then maintained through passive cooling with ambient air. TH was commenced 90 min after HI and continued for 24 h.

Remote Ischemic Postconditioning

Sixty minutes after the HI insult, RIPC was induced by four conditioning cycles of 5 min of ischemia and 5 min of reperfusion on both hind limbs. Total occlusion of blood flow was induced by two plastic strips around the proximal part of the hind limbs, and absence/presence of blood flow was verified by ultrasound with Doppler. 5-min periods of ischemia/reperfusion have been found cardio- and neuroprotective in adults (5, 6). In accordance with this, we have previously found reduced brain Lac/NAA ratios in piglets treated with 5 min of RIPC compared to untreated controls (12). Thus, to ensure comparability, 5 min of ischemia/reperfusion were chosen for this study.

Magnetic Resonance Imaging and Spectroscopy (MRI/MRS)

MRI/MRS was performed with a 3 T MR scanner using a knee transmit/receive coil (Skyra, Siemens, Erlangen, Germany). Axial and coronal T2-weighted images were acquired [fast spin echo, repetition and echo time (TR/TE) 6,430/74 ms, slice thickness 2 mm, matrix 320 × 240, field of view (FOV) 160 × 160 mm^2]. Diffusion-weighted images (DWI) were acquired (single-shot EPI, TR/TE 3,300/108 msec, slice thickness 3 mm, matrix 196 × 190, FOV 213 × 206 mm^2, b-value 800 s/mm^2) and apparent diffusion coefficient (ADC) values were calculated in a region of interest (ROI) in the right thalamus. Perfusion-weighted images were acquired using an arterial spin labeling (ASL) sequence (PICORE Q2T, single-shot EPI, TR/TE 3,200/25.6 ms, slice thickness 5 mm, 84 × 84 matrix, FOV 144 × 144 mm^2), and whole brain perfusion was calculated in three slices and averaged. Due to low signal-to-noise ratio, ASL data may be negative; all negative values were manually removed before final analysis. A multiecho gradient echo (MGRE) sequence was used for obtaining T2* maps (11 echoes TR/TE 431/3.67–49 ms, slice thickness 4 mm, 192 × 126 matrix, FOV 180 × 118 mm^2). ROIs were drawn on the thalamus in two slices and values were averaged. The researcher performing the MRI data analysis was blinded to treatment allocation in the two intervention groups, but not to the group receiving supportive care only. Images were analyzed with Horos software (Annapolis, MD, USA) version 3.3.5. A representative image is provided in **Supplementary Material 2**. Single voxel proton MRS (PRESS, TR/TE 2,000/135 ms, voxel size 8 × 8 × 8 mm^3, 1,024 sample points, spectral width (SW) 1,200 Hz, 128 averages) was acquired in the right side of thalamus, subcortical right-side white matter at the centrum semiovale level, and frontal and occipital cortex. N-acetylaspartate (NAA, 2.02 ppm), lactate (Lac, 1.33 ppm), choline (Cho, 3.2 ppm), and creatine (Cr, 3.02 ppm) were identified. Spectroscopy data were analyzed with LCModel (Stephen Provencher, Oakville, ON, Canada) version 6.3-1L, and Lac/NAA and NAA/Cr ratios were calculated. Thalamic MRS was acquired in two planes and averaged. An image illustrating voxel location and graph can be found in **Supplementary Material 2**.

Electroencephalographic Analysis

Amplitude integrated EEG (aEEG) recordings were obtained continuously throughout the study. During transport and acquisition of MRI/MRS, electrodes were removed and recordings were paused. aEEG was recorded for all animals during the HI insult. Due to equipment limitations, aEEG was recorded in only half of the animals during the observation period after the HI insult. aEEG recordings were analyzed and scored from 0 to 4 depending on severity as previously described (17, 18). aEEG recordings (0; flat trace, 1; continuous low voltage, 2; burst suppression, 3; discontinuous normal voltage, and 4; normal voltage) were analyzed for each hour after the HI insult and then averaged at 1, 6, 12, 18, and 24 h. Animals were selected randomly for continuous aEEG recording, and the researchers calculating the aEEG score were blinded to the intervention.

Experimental Protocol

A total of 26 piglets were subjected to 45 min of global hypoxia-ischemia (HI) and randomized to RIPC + TH (RIPC + TH group) or TH alone (TH group). The experimental protocol was carried out in two piglets from the same litter on each experimental day. After the HI insult one piglet was randomized to one of the intervention groups, while the other was automatically allocated to the other. Six piglets served as controls and were subjected to the HI insult, received supportive care only, and were kept normothermic (NT group). Animals were observed for 24 h and MRI/MRS was performed at 6, 12, and 24 h of observation. After 24 h, piglets were euthanized by a lethal pentobarbital (80 mg/kg) injection.

Statistics

Based on the data from Zhou et al., a reduction in infarction size from 31 to 22% in RIPC treated animals, and assuming an alpha level of 5 and 90% power, we estimated that 11 animals were sufficient to detect an effect in this study (8). With an expected mortality of 10%, 13 animals were enrolled in each treatment group. Statistical analysis was performed using GraphPad Prism® v8 software. Use of inotropes was registered hourly as infusion rate and then averaged for the 24-h observation period. Number of animals receiving inotropes was reported, the average infusion rate was calculated in the animals that received inotropes. Non-parametric MRS data

were log transformed (y=log(y+(1/6)). MRI/MRS and EEG data were tested by mixed-effect model analysis with assumed sphericity and randomly missing values, corrected for multiple comparisons and post-tested with Tukeys test. Demographic- and insult-severity data, inotrope infusion, blood-gas values, and vital parameters were compared with one-way ANOVA for parametric data and Kruskal-Wallis test for non-parametric data. A two-sided p-value < 0.05 was considered statistically significant. Demographic- and insult-severity data, inotrope infusion, blood-gas values, and vital parameters are presented as median with interquartile range (IQR). MRI/MRS data are presented as scatter plots with superimposed median and interquartile range.

RESULTS

Insult Severity and Survival

Four animals in the TH group, three animals in the RIPC + TH group, and one animal in the NT group died after the HI insult. All died from refractory hypotension except for the one death in the NT group which was caused by mechanical ventilator failure. Thus, nine animals in the TH group, ten animals in the RIPC+TH group, and five animals in the NT group completed the whole study (**Table 1**). All three groups received a comparable insult with regard to duration of aEEG depression, hypotension, and metabolic acidosis (**Tables 2**, **3**). The two intervention groups received more dopamine than the NT group (**Table 2**). One animal in the TH and two animals in the TH + RIPC group received a bolus of hydrocortisone. One animal in the NT group received infusion with adrenaline (0.01 μg/kg/min) and dobutamine (0.42 μg/kg/min). Temperature from before to 1 h after the insult was slightly increased but within normal range (**Table 3**). TH was successfully induced in both intervention groups and resulted in a decreased heart rate (**Table 3**).

Magnetic Resonance Spectroscopy

MRS showed no difference between the three groups with regards to Lac/NAA ratio at any time point (**Figure 1**). MRS showed decreased NAA/Cr ratio in the occipital cortex and thalamus 24 h after the insult in the NT group compared to the TH and TH + RIPC group (**Figure 2**) and the NAA/Cr ratio in the occipital cortex was lower in the TH + RIPC group compared to the TH group (**Figure 2**). NAA/Cr ratio was stable over time in the two intervention groups, while the NAA/Cr ratio decreased with time in the NT group (**Figure 2**).

Magnetic Resonance Imaging

Cerebral edema measured by DWI showed no difference between the three groups (**Figure 3**). Although not statistically significant, animals in the NT group had lower cerebral oxygenation 6 and 12 h after the HI insult as assessed from by BOLD measurements (**Figure 3**). There was no difference between the two intervention groups with regard to cerebral oxygenation. After a quality check of the ASL data one scan was removed from the TH+RIPC group and two from the NT group. CBF measured by ASL was similar in the three groups (**Figure 3**).

aEEG Analysis

aEEG was available for three animals in the NT group, six animals in the TH group, and seven animals in the TH+RIPC group. aEEG data were missing during the first 6 h in two animals in the TH + RIPC group. Early EEG recovery (continuous aEEG reached by the 2nd hour) was seen in two of the three animals in the NT group, four of the six animals in the TH group, and two of the five in the TH+RIPC group. Seizures and brief rhythmic discharges were detected in 0 out of three animals in the NT group, two of the six animals in the TH group, and

TABLE 1 | Survival and gender distribution in the three groups and number of animals who were scanned at the three time points.

	Time point			
Group and sex [*n*, (f/m)]	**Baseline**	**6-h scan**	**12-h scan**	**24-h scan**
NT	6 (4/2)	5 (4/1)	5 (4/1)	5 (4/1)
TH	13 (6/7)	12 (5/7)	10 (4/6)	9 (4/5)
RIPC + TH	13 (6/7)	11 (4/7)	11 (4/7)	10 (3/7)

Seven animals died after the hypoxic ischemic insult at different timepoints. One animal in the NT group was excluded after a secondary hypoxic insult due to ventilator failure. NT, no treatment; TH, therapeutic hypothermia; RIPC, remote ischemic postconditioning.

TABLE 2 | Demographic- and insult-severity data for piglets subjected to a HI insult and subsequently treated with TH, TH + RIPC, or supportive care only.

Weight (kg)	
NT	1.8 (1.6–2.4)
TH	1.8 (1.6–1.9)
RIPC + TH	1.7 (1.7–1.9)
Time < 7 uV aEEG (min)	
NT	26.8 (23.0–29.7)
TH	26.5 (19.4–29.9)
RIPC + TH	28.9 (20.3–37.1)
Time with MABP < 70% of baseline (min)	
NT	7.8 (4.3–11.3)
TH	7.5 (1.0–14.0)
RIPC + TH	6.8 (2.2–12.8)
Noradrenaline infusion (μg/kg/min)	
NT	2/6 [0.39 (0.19–0.60)]
TH	7/13 [0.39 (0.26–0.94)]
RIPC + TH	7/13 [0.40 (0.06–0.75)]
Dopamine infusion (μg/kg/min)	
NT	0/6
TH	4/13 [4.17 (3.08–5.00)] #
RIPC + TH	4/13 [4.75 (1.90–7.82)] #

*Use of inotropes was registered hourly as infusion rate and then averaged for the 24-h observation period. Number of animals receiving inotropes was reported and for those who received inotropes the average infusion rate calculated. Data are median with interquartile range. One-way ANOVA and Kruskal-Wallis test. # indicates significance vs. NT. * Indicates significance vs. TH or TH + RIPC. HI, hypoxia ischemia; TH, therapeutic hypothermia; NT, no treatment; RIPC, remote ischemic postconditioning; aEEG, amplitude integrated electroencephalography; MABP, Mean arterial blood pressure.*

TABLE 3 | Arterial blood-gas values and vital parameters at baseline, during hypoxia, and in recovery in piglets subjected to a hypoxic-ischemic insult and subsequently treated with TH, TH + RIPC, or supportive care only.

	Baseline	Hypoxia			Recovery					
		15 min	30 min	45 min	1 h	2 h	4 h	6 h	12 h	24 h
pH										
NT	7.54 (7.51–7.56)	7.40 (7.38–7.42)	7.12 (7.10–7.22)	6.97 (6.90–7.06)	7.31 (7.14–7.42)	7.46 (7.35–7.53)	7.43 (7.40–7.50)	7.43 (7.39–7.49)	7.56 (7.49–7.57)	7.45 (7.38–7.49)
TH	7.52 (7.50–7.57)	7.38 (7.33–7.42)	7.22 (7.04–7.28)	7.01 (6.90–7.13)	7.37 (7.25–7.46)	7.44 (7.36–7.48)	7.43 (7.39–7.53)	7.51 (7.40–7.53)	7.51 (7.43–7.57)	7.47 (7.38–7.52)
TH + RIPC	7.55 (7.51–7.58)	7.36 (7.28–7.44)	7.16 (7.09–7.25)	7.06 (6.96–7.11)	7.39 (7.31–7.47)	7.47 (7.40–7.53)	7.49 (7.46–7.52)	7.53 (7.46–7.57)	7.46 (7.45–7.58)	7.49 (7.44–7.54)
pCO_2 (kPa)										
NT	4.86 (4.28–5.49)	5.38 (4.58–5.69)	5.46 (4.84–6.01)	5.68 (5.11–6.67)	4.73 (3.94–6.42)	4.59 (4.04–5.63)	5.54 (4.89–5.90)	5.78 (5.49–6.52)	4.85 (3.88–4.97)	5.72 (5.18–5.99)
TH	4.91 (4.35–5.14)	4.99 (4.68–5.54)	5.61 (4.00–6.16)	5.72 (4.40–6.59)	4.34 (3.84–5.39)	4.99 (4.46–5.37)	4.91 (4.32–6.19)	5.09 (4.61–5.53)	4.63 (3.98–5.95)	4.96 (4.51–5.42)
TH + RIPC	4.68 (4.35–5.26)	5.67 (4.26–6.28)	5.42 (4.94–6.24)	5.10 (4.80–6.67)	4.12 (3.66–5.43)	4.49 (4.31–5.69)	5.12 (4.55–5.40)	5.26 (4.11–5.73)	4.70 (4.46–5.75)	5.41 (5.18–5.66)
pO_2 (kPa)										
NT	12.70 (10.88–14.13)	2.06 (1.79–2.26)	2.48 (2.29–4.25)	3.49 (3.14–4.41)	15.35 (13.63–17.48)	15.60 (14.70–19.68)	15.85 (15.35–16.65)	15.70 (11.16–18.78)	16.00 (13.25–17.45)	13.40 (11.85–15.35)
TH	11.70 (10.40–13.30)	1.94 (1.72–2.24)	2.29 (1.99–2.84)	2.68 (2.03–3.90)	12.40 (10.85–14.50)	12.45 (11.43–15.68)	11.80 (10.60–14.00)	11.50 (10.30–13.90)	**11.70 (10.10–13.00) #**	12.20 (10.98–14.53)
TH + RIPC	12.05 (11.35–13.50)	1.90 (1.76–2.60)	2.45 (1.85–3.23)	3.35 (3.08–4.32)	13.80 (11.15–15.85)	**12.35 (9.46–13.45) #**	**10.10 (9.39–12.80) #**	12.30 (11.10–13.50)	**11.40 (10.60–13.60) #**	10.10 (8.79–13.90)
Lactate (mmol/L)										
NT	1.70 (0.85–2.15)	9.00 (7.80–10.83)	16.50 (14.73–18.25)	20.50 (19.25–23.50)	11.00 (9.50–13.55)	4.10 (3.40–5.65)	1.45 (1.15–2.50)	1.25 (1.05–1.43)	1.10 (0.85–1.65)	0.90 (0.65–2.20)
TH	1.30 (0.95–1.45)	8.90 (5.70–9.75)	14.30 (12.05–18.00)	19.00 (15.30–23.00)	10.80 (7.45–14.00)	2.90 (1.38–9.00)	0.90 (0.50–1.60)	0.60 (0.60–1.30)	0.90 (0.80–1.40)	0.65 (0.48–0.95)
TH + RIPC	1.40 (1.10–1.68)	9.20 (7.40–9.85)	15.00 (13.70–16.50)	18.00 (17.50–21.00)	9.80 (6.75–11.60)	3.80 (2.70–4.60)	1.10 (0.70–1.90)	0.90 (0.70–1.10)	0.80 (0.70–1.70)	0.90 (0.70–1.18)
Base Excess (mmol/L)										
NT	7.75 (4.98–13.65)	−1.80 (−3.05 to −1.53)	−15.00 (−16.25 to −12.33)	−22.75 (−23.85 to −18.05)	−7.05 (−14.00 to −3.05)	0.00 (−3.70 to −6.80)	4.50 (0.48–6.58)	5.35 (0.18–10.05)	6.70 (1.85–9.45)	6.50 (−1.45–8.50)
TH	6.40 (4.65–9.10)	−2.10 (−5.70 to −0.45)	−12.00 (−16.50 to −10.35)	−20.80 (−25.00 to −16.50)	−6.50 (−12.5 to −2.10)	1.00 (−4.73 to −4.25)	3.70 (0.00–5.10)	6.30 (4.10–7.40)	5.20 (3.00–6.40)	3.25 (1.13–6.73)
TH + RIPC	7.80 (6.65–10.23)	−1.80 (−5.30–0.75)	−12.10 (−15.95 to −10.45)	−18.70 (−20.35 to −16.65)	−3.80 (−6.45 to −1.40)	3.35 (−1.55 to −4.50)	5.70 (4.40–7.40)	6.20 (5.10–9.40)	6.00 (3.30–8.70)	8.70 (4.80–10.45)
Glucose (mmol/L)										
NT	6.90 (5.65–7.78)	8.15 (7.33–9.10)	11.05 (9.30–13.03)	12.45 (9.98–14.13)	8.75 (5.70–9.83)	6.75 (5.00–7.83)	6.95 (5.80–7.35)	7.10 (6.10–7.55)	4.70 (3.90–5.35)	6.10 (3.85–8.80)
TH	7.10 (5.95–8.80)	6.50 (5.40–7.35)	**8.20 (6.25–9.43) #**	**7.60 (6.20–9.15) #**	7.50 (6.15–8.85)	6.95 (5.30–8.38)	6.70 (5.30–10.00)	6.50 (5.30–11.00)	7.60 (6.90–9.10)	7.95 (3.83–10.08)
TH + RIPC	7.30 (6.85–9.85)	6.90 (6.30–9.90)	8.30 (7.30–11.15)	8.90 (7.45–11.60)	6.80 (6.20–8.50)	6.40 (4.60–6.60)	6.10 (5.00–8.90)	5.70 (5.10–9.10)	**9.80 (6.10–12.20) #**	8.40 (6.45–12.65)
Heart rate (bpm)										
NT	112 (115–167)	182 (159–210)	157 (131–218)	166 (135–204)	172 (141–218)	184 (152–250)	214 (154–250)	213 (173–250)	189 (155–224)	190 (156–219)
TH	136 (127–149)	207 (197–222)	176 (163–197)	182 (156–218)	182 (169–213)	143 (122–179)	**126 (92–180) #**	**127 (110–175) #**	**120 (117–148) #**	157 (127–169)
TH + RIPC	134 (125–142)	200 (187–225)	180 (167–200)	165 (147–222)	181 (169–200)	162 (143–174)	**125 (85–143) #**	**116 (91–165) #**	**118 (90–156) #**	**126 (99–158) #**
Mean arterial blood pressure (mmHg)										
NT	56 (50–60)	59 (52–59)	39 (34–48)	42 (31–52)	51 (47–57)	51 (43–59)	54 (47–55)	50 (47–56)	53 (46–59)	45 (40–51)
TH	48 (45–57)	50 (47–63)	36 (31–43)	37 (29–50)	47 (44–53)	45 (40–51)	44 (42–51)	45 (41–46)	48 (37–53)	47 (42–50)
TH + RIPC	47 (43–51)	49 (42–56)	39 (31–41)	33 (27–35)	45 (39–49)	45 (43–49)	44 (42–50)	46 (43–49)	48 (44–51)	47 (38–55)
Rectal temperature (°C)										
NT	38.6 (37.0–39.2)				39.6 (38.6–40.0)	38.9 (38.5–39.4)	39.3 (38.2–39.5)	39.0 (38.3–39.8)	39.1 (38.2–39.5)	39.0 (38.6–39.6)
TH	38.6 (38.3–39.0)				39.4 (39.0–39.6)	**37.0 (36.2–37.8) #**	**33.9 (33.7–34.1) #**	**33.8 (33.4–34.3) #**	**33.8 (33.7–34.0) #**	**33.8 (33.2–34.0) #**
TH + RIPC	38.5 (38.4–38.9)				39.3 (39.0–39.7)	**37.1 (36.5–37.5) #**	**34.0 (33.7–34.1) #**	**33.9 (33.7–34.3) #**	**34.0 (33.9–34.3) #**	**33.7 (33.6–34.2) #**

*Data are median with interquartile range. One-way ANOVA and Kruskal-Wallis test. Values with significant in-group differences are bold. # indicates significance vs. NT. *indicates significance vs. TH or TH + RIPC. TH, therapeutic hypothermia; NT, no treatment; RIPC, remote ischemic postconditioning.*

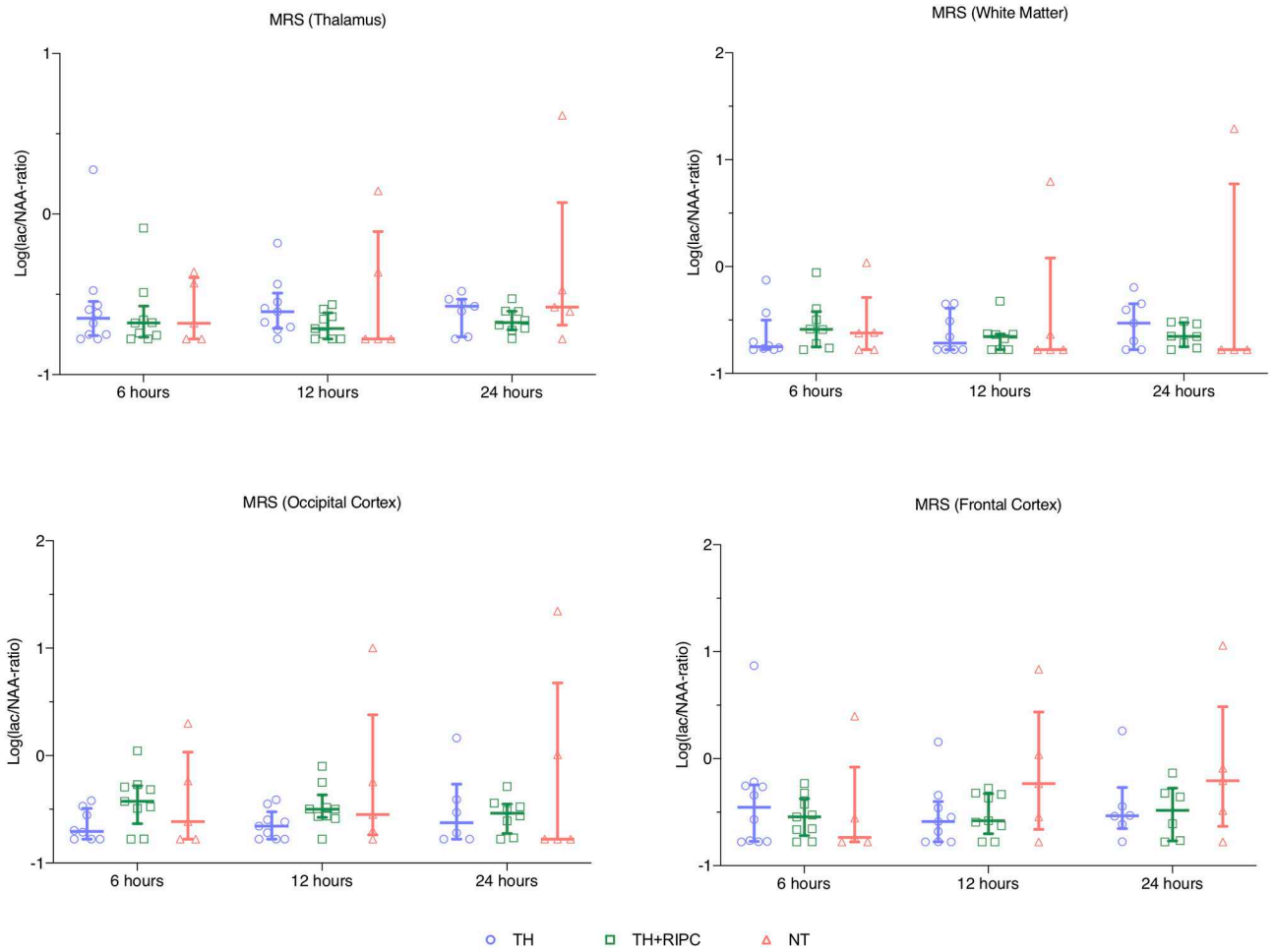

FIGURE 1 | Magnetic resonance spectroscopy in piglets subjected to a HI insult and treated with therapeutic hypothermia (TH), TH and remote ischemic postconditioning (TH + RIPC), or supportive care only (NT). Scans were performed at 6, 12, and 24 h after the insult. Lac, lactate; NAA, N-acetylaspartate. Data are scatter plots with superimposed median and interquartile range. Mixed-effect model analysis, *p < 0.05.

three of the seven animals in the TH + RIPC group. There was no overall difference in aEEG score between the three groups (**Figure 4**).

DISCUSSION

This is the first study to assess RIPC in addition to TH in neonatal HIE. Overall, adding RIPC to TH resulted in no additional neuroprotective effect. When comparing duration of aEEG suppression and duration of hypotension from this study with data from a similar study in piglets, the insult severity acquired in this study should be regarded as mild rather than severe (19). Indeed, most of our animals presented with rapid recovery and normalization of aEEG after HI (**Figure 4**). To ensure survival and substantial neural damage, titration of the insult is essential as too extensive HI results in death and too little HI results in absence of damage (20). Insult titration also ensures that the animal is subjected not only to a period of hypoxia but also to a predetermined period of hypotension. Hypotension combined with hypoxia has been shown to be essential to produce a more severe insult (19). This is in accordance with our own observations in a previous study where severely damaged animals had aEEG suppression of at least 40 min combined with a period of hypotension (12). The importance of cerebral hypoperfusion in the pathology of brain injury is further underlined by other studies in which universal hypoxia was combined with carotid clamping (21). It would therefore be relevant in future studies to investigate the neuroprotective effect of RIPC when combined with TH after a severe insult.

Despite the mild insult, the NT group showed a lower NAA/Cr ratio at 24 h than was seen in the other groups. N-acetylaspartate is an amino acid present in healthy neurons and oligodendrocytes-type 2 astrocyte progenitor cells (22, 23), and a reduction in NAA after a HI insult is due to neural damage and reduction in progenitor cells. Peak-area ratio of NAA/Cr and [NAA] measured by MRS has high prognostic accuracy for neonates with HIE (24, 25). This is in accordance with our results as peak-area ratio of NAA/Cr was reduced as early 24 h after the

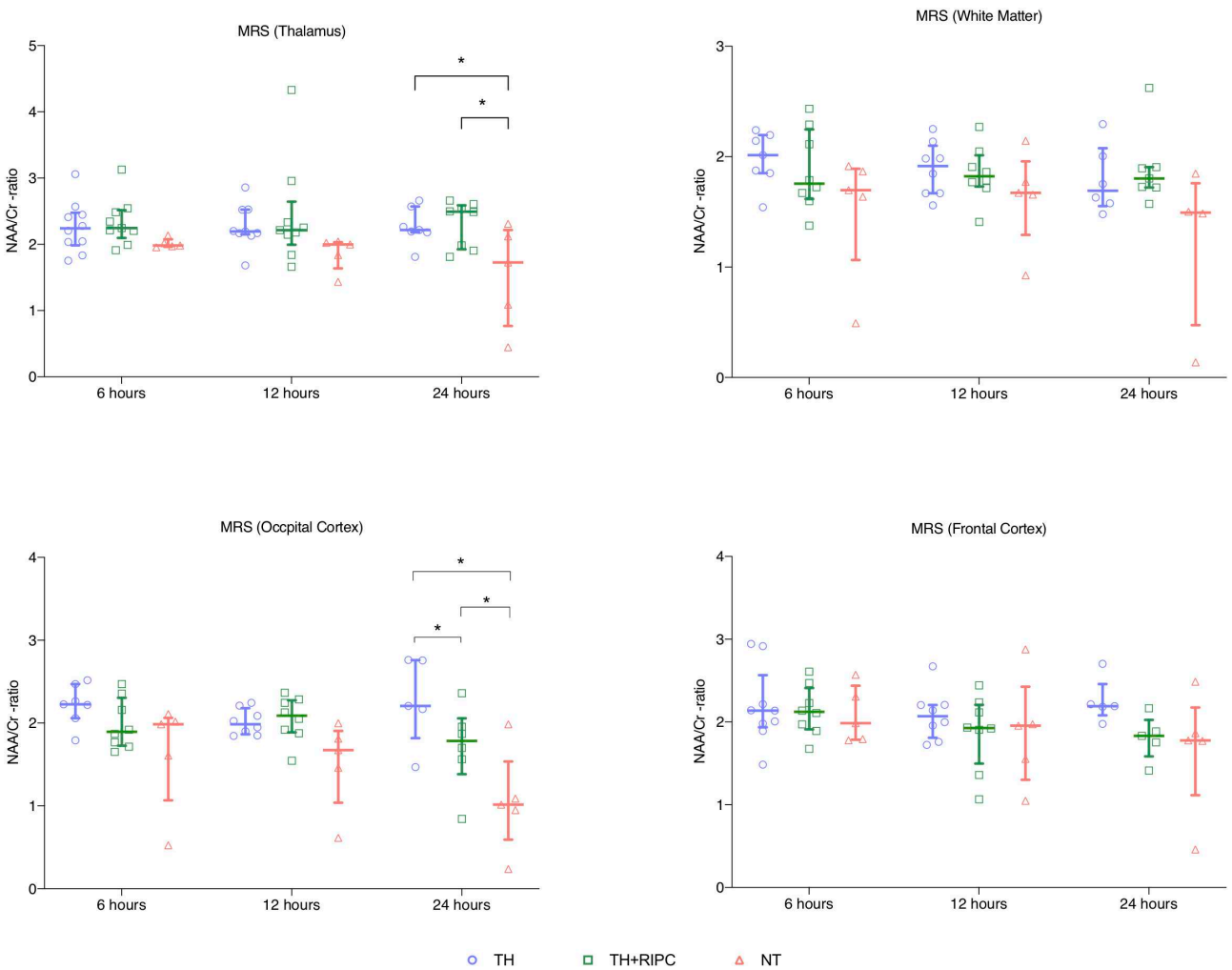

FIGURE 2 | Magnetic resonance spectroscopy in piglets subjected to a HI insult and treated with therapeutic hypothermia (TH), TH and remote ischemic postconditioning (TH + RIPC), or supportive care only (NT). Scans were performed at 6, 12, and 24 h after the insult. NAA, N-acetyl aspartate; Cr, creatinine. Data are scatter plots with superimposed median and interquartile range. Mixed-effect model analysis, $^*p < 0.05$.

insult in the NT group. This finding underline one of the possible neuroprotective mechanisms of TH.

Cerebral edema measured by diffusion weighted imaging (DWI) has been proposed as a biomarker of brain injury in neonates with HIE (26). Compared to MRS, DWI has been shown to underestimate the extent of damage when acquired on day 1 (27). McKinstry et al. found that edema measured by diffusion tensor imaging also underestimates the neural damage when performed on day 1 compared to images acquired on day 2–4 (28). In keeping with this, in our study we found no difference between the three groups on ADC maps acquired within the first 24 h after the HI insult.

BOLD measured by MRI is based on the paramagnetic properties of deoxyhemoglobin. Increased concentration of deoxyhemoglobin will result in decreased T2* relaxation time and signal loss (29). In this study, BOLD measurements were performed in the thalamus after the HI insult and compared local differences in oxygenation. Although not statistically significant, animals in the NT group had lower T2* values after 6 and 12 h and reached the same levels as did the TH and TH+RICP groups by 24 h. TH is known to reduce cerebral metabolism (30). The decreased T2* values could indicate an increased turnover of oxyhemoglobin to deoxyhemoglobin due to relatively high metabolism immediately after the HI insult. Increased oxygen consumption is coupled to regional changes in blood flow, and T2* values have been correlated to CBF measured by ASL (31). Surprisingly, change in blood flow was not demonstrated in our study as the NT group presented with CBF values comparable to the two intervention groups despite lower T2* values.

Several of the animals that received TH developed hypotension after the HI insult. Ethical standards for animal

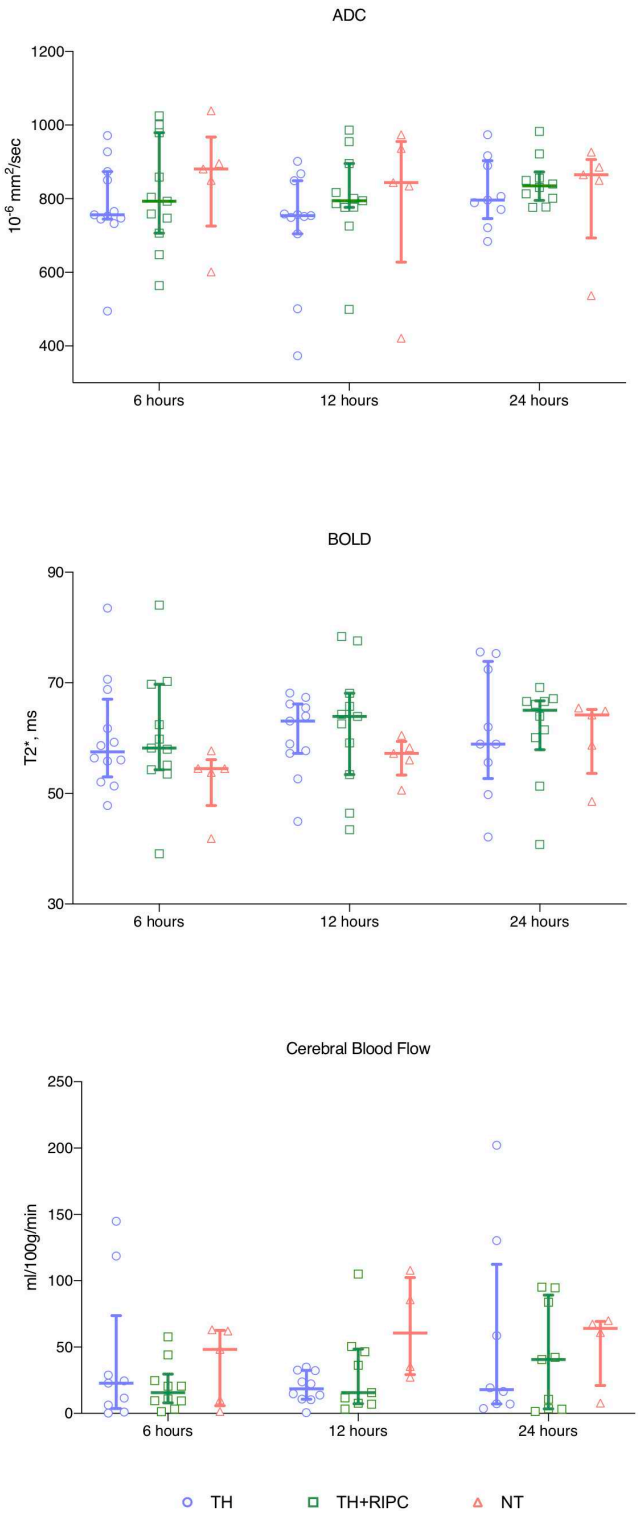

FIGURE 3 | Magnetic resonance imaging in piglets subjected to a HI insult and treated with therapeutic hypothermia (TH), TH and remote ischemic postconditioning (TH + RIPC), or supportive care only (NT). Scans were performed at 6, 12, and 24 h after the insult. ADC, apparent diffusion imaging; BOLD, blood oxygenation level dependent. Data are scatter plots with superimposed median and interquartile range. Mixed-effect model analysis, $*p < 0.05$.

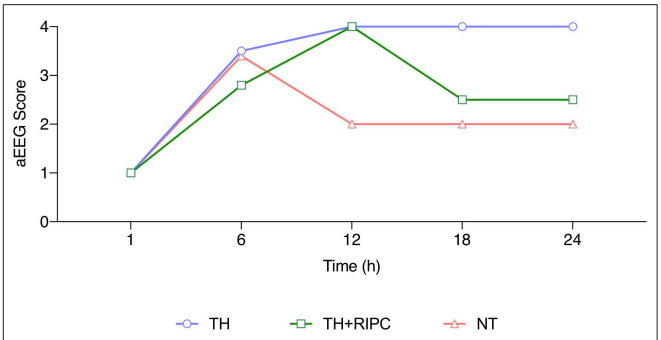

FIGURE 4 | aEEG score for piglets subjected to a HI insult and treated with therapeutic hypothermia (TH), TH and remote ischemic postconditioning (TH + RIPC), or supportive care only (NT). aEEG were scored every hour and averaged for 6, 12, 18, and 24 h. Data are median. Mixed-effect model analysis. #TH vs. NT, *TH vs. TH + RIPC, §NT vs. TH + RIPC.

studies require pain relief and sedation. A side effect of propofol is reduced cardiac output and hypotension, which may be more severe when propofol is combined with opioids (32). In addition, drug metabolism may be impaired after HI due to liver and kidney failure and then be further reduced by TH because it alters drug metabolism (33, 34). Cardiac function might also be compromised due to TH (35). This was apparent in our study, as piglets in the two TH-treated groups required more inotropes and died from refractory hypotension more often than piglets that received supportive care only. The comparison between the two TH-treated groups should, however, still be valid. The increased mortality due to this complication is unlikely to influence the overall conclusion of this study because the majority of MRI/MRS data were similar between the two TH-treated groups.

LIMITATIONS

Piglets received intravenous infusion with fentanyl and propofol to ensure pain relief and sedation. One of the proposed mechanisms of RIPC is through opioid receptor activation (8). Since both intervention groups received fentanyl, the additional neuroprotective effect of RIPC may have been reduced.

Another limitation is spatial resolution of the MRI data. RIPC was shown to predominantly protect white matter measured by MRS in a previous piglet study (10). Due to limited spatial resolution in the MRI data we were unable to perform DWI, BOLD, and ADC measurements on white matter specifically.

An echo time (TE) of 135 ms was chosen as this is part of the MRS protocol used in our clinical MR Centre. A TE of 135 ms also allows for easy lactate-peak identification due to peak inversion. However, a prolonged TE of 288 ms will increase PRESS detection (36). Lactate peak identification with a TE of 135 ms in a 3T scanner is possibly further complicated by anomalous J-modulation (37). To ensure high spatial resolution,

a 8 × 8 × 8 mm voxel was used despite the decrease in signal-to-noise ratio. However, the low signal-to-noise ratio and short TE may have obscured the detection of lactate peaks in some animals. Accordingly, in future studies an TE of 288 ms and a larger voxel size might identify more subtle differences.

We examined MRI/MRS 24 h after HI based on times-series pilot studies that showed significant lactate accumulation detectable early in normothermic piglets. This timing would coincide with the secondary energy failure phase. Clinical data on early MRI/MRS suggest that moderate-severe HIE can be identified at this time (38). However, TH augments and delays neuropathological processes and the possible protective effect of RIPC may not manifest until later as neurological injury after HI is a dynamic process that evolves over time (39). Thus, longer running studies are required to evaluate the full extent of neural damage. We opted to focus on outcome measures available in the clinical setting. However, histological analysis was not performed, but could contribute with valuable information on the more subtle neural damage present at this early stage.

CONCLUSION

We found no additional neuroprotective effect when RIPC was added to TH after mild HI. However, despite the mild trauma, the neuroprotective effect of TH was detectable by a reduction in peak-area ratio of NAA/Cr. Our results suggest that future studies may benefit from more severe insults, prolonged TE on MRS, less sedation, histological analysis, and outcomes measured at a later time point after HI.

DATA AVAILABILITY STATEMENT

The datasets generated for this study are available on request to the corresponding author.

ETHICS STATEMENT

The animal study was reviewed and approved by the Danish Animal Experiments Inspectorate (Permission nr. 2016-15-0201-01052). This study is reported in accordance with the ARRIVE guidelines (ARRIVE checklist in **Supplementary Material 1**).

AUTHOR CONTRIBUTIONS

TA, KK, VH, MP, SR, and TH designed the study. TA, MVP, MA, and HA undertook the experiments. TA, SR, LH, and MP performed data analysis. TA drafted the manuscript. All authors have critically reviewed the drafted manuscript and have approved the final manuscript and agree to be accountable for all aspects of the work.

FUNDING

This study was funded by The Lundbeck Foundation (grant no: R20 8-2015-3647), Aarhus University, The Ludvig and Sara Elsass Foundation (grant no: 19-3-0288), and Young Investigator START-UP Award by the European Society for Pediatric Research.

ACKNOWLEDGMENTS

The authors would like to acknowledge the staff at the animal facilities at Institute of Clinical Medicine at Aarhus University.

SUPPLEMENTARY MATERIAL

The Supplementary Material for this article can be found online at: https://www.frontiersin.org/articles/10.3389/fped.2020.00299/full#supplementary-material

REFERENCES

1. Douglas-Escobar M, Weiss MD. Hypoxic-ischemic encephalopathy A review for the clinician. *JAMA Pediatr.* (2015) 169:397–403. doi: 10.1001/jamapediatrics.2014.3269
2. Jacobs SE, Berg M, Hunt R, Tarnow-Mordi WO, Inder TE, Davis PG. Cooling for newborns with hypoxic ischaemic encephalopathy. *Cochrane Database Syst Rev.* (2013) 2013:CD003311. doi: 10.1002/14651858.CD003311.pub3
3. Murry CE, Jennings RB, Reimer KA. Preconditioning with ischemia : injury delay of lethal cell ischemic myocardium. *Circulation.* (1986) 74:1224–136. doi: 10.1161/01.CIR.74.5.1124
4. Ren C, Yan Z, Wei D, Gao X, Chen X, Zhao H. Limb remote ischemic postconditioning protects against focal ischemia in rats. *Brain Res.* (2009) 1288:88–94. doi: 10.1016/j.brainres.2009.07.029
5. Zhao JJ, Xiao H, Zhao WB, Zhang XP, Xiang Y, Ye ZJ, et al. Remote ischemic postconditioning for ischemic stroke: a systematic review and meta-analysis of randomized controlled trials. *Chin Med J. (*2018) 131:956–65. doi: 10.4103/0366-6999.229892
6. Pickard JMJ, Bøtker HE, Crimi G, Davidson B, Davidson SM, Dutka D, et al. Remote ischemic conditioning: from experimental observation to clinical application: report from the 8th Biennial Hatter Cardiovascular Institute Workshop. *Basic Res Cardiol.* (2015) 110:453. doi: 10.1007/s00395-014-0453-6
7. Hassell KJ, Ezzati M, Alonso-Alconada D, Hausenloy DJ, Robertson NJ. New horizons for newborn brain protection: enhancing endogenous neuroprotection. *Arch Dis Child Fetal Neonatal Ed.* (2015) 100:F541–51. doi: 10.1136/archdischild-2014-306284
8. Zhou Y, Fathali N, Lekic T, Ostrowski RP, Chen C, Martin RD, et al. Remote limb ischemic postconditioning protects against neonatal hypoxic-ischemic brain injury in rat pups by the opioid receptor/akt pathway. *Stroke.* (2011) 42:439–44. doi: 10.1161/STROKEAHA.110.592162
9. Drunalini Perera PN, Hu Q, Tang J, Li L, Barnhart M, Doycheva DM, et al. Delayed remote ischemic postconditioning improves long term sensory motor deficits in a neonatal hypoxic ischemic rat model. *PLoS ONE.* (2014) 9:e90258. doi: 10.1371/journal.pone.0090258
10. Ezzati M, Bainbridge A, Broad KD, Kawano G, Oliver-Taylor A, Rocha-Ferreira E, et al. Immediate remote ischemic postconditioning after hypoxia ischemia in piglets protects cerebral white matter but not grey matter. *J Cereb Blood Flow Metab.* (2016) 36:1396–411. doi: 10.1177/0271678X15608862
11. Rocha-Ferreira E, Rudge B, Hughes MP, Rahim AA, Hristova M, Robertson NJ. Immediate remote ischemic postconditioning reduces brain nitrotyrosine formation in a piglet asphyxia model. *Oxid Med Cell Longev.* (2016) 2016:5763743. doi: 10.1155/2016/5763743
12. Kyng KJ, Kerrn-Jespersen S, Bennedsgaard K, Skajaa T, Pedersen M, Holm IE, et al. Short-term outcomes of remote ischemic postconditioning 1 h after perinatal hypoxia-ischemia in term piglets. *Pediatr Res.* (2020). doi: 10.1038/s41390-020-0878-6. [Epub ahead of print].

13. Adstamongkonkul D, Hess DC. Ischemic Conditioning and neonatal hypoxic ischemic encephalopathy: a literature review. *Cond Med*. (2017) 1:9–16.
14. Kilkenny C, Browne WJ, Cuthill IC, Emerson M, Altman DG. The ARRIVE guidelines checklist animal research : reporting *in vivo* experiments. *Br J Pharmacol*. (2010) 8:8–9. doi: 10.1371/journal.pbio.1000412
15. Kyng KJ, Skajaa T, Kerrn-Jespersen S, Andreassen CS, Bennedsgaard K, Henriksen TB. A piglet model of neonatal hypoxic-ischemic encephalopathy. *J Vis Exp*. (2015) e52454. doi: 10.3791/52454
16. Nachar RA, Booth EA, Friedlich P, Borzage M, Soleymani S, Wider MD, et al. Dose-dependent hemodynamic and metabolic effects of vasoactive medications in normotensive, anesthetized neonatal piglets. *Pediatr Res*. (2011) 70:473–9. doi: 10.1203/PDR.0b013e31822e178e
17. Hellström-Westas L, Rosen I, de Vries LS, Greisen G. Amplitude-integrated EEG classification and interpretation in preterm and term infants. *Neoreviews*. (2006) 7:e76–87. doi: 10.1542/neo.7-2-e76
18. Robertson NJ, Martinello K, Lingam I, Avdic-Belltheus A, Meehan C, Alonso-Alconada D, et al. Melatonin as an adjunct to therapeutic hypothermia in a piglet model of neonatal encephalopathy: a translational study. *Neurobiol Dis*. (2019) 121:240–51. doi: 10.1016/j.nbd.2018.10.004
19. Foster KA, Colditz PB, Lingwood BE, Burke C, Dunster KR, Roberts MS. An improved survival model of hypoxia / ischaemia in the piglet suitable for neuroprotection studies. *Brain Res*. (2001) 919:122–31. doi: 10.1016/S0006-8993(01)03011-6
20. Björkman ST, Foster KA, O'driscoll SM, Healy GN, Lingwood BE, Burke C, et al. Hypoxic/Ischemic models in newborn piglet: comparison of constant FiO_2 versus variable FiO_2 delivery. *Brain Res*. (2006) 1100:110–7. doi: 10.1016/j.brainres.2006.04.119
21. Munkeby BH, De Lange C, Emblem KE, Bjornerud A, Kro GAB, Andresen J, et al. A piglet model for detection of hypoxic-ischemic brain injury with magnetic resonance imaging. *Acta Radiol*. (2008) 49:1049–57. doi: 10.1080/02841850802334224
22. Urenjak J, Williams SR, Gadian DG, Noble M. Proton nuclear magnetic resonance spectroscopy unambiguously identifies different neural cell types. *J Neurosci*. (1993) 13:981–9. doi: 10.1523/JNEUROSCI.13-03-00981.1993
23. Urenjak J, Williams SR, Gadian DG, Noble M. Specific expression of N-acetylaspartate in neurons, oligodendrocyte-type-2 astrocyte progenitors, and immature oligodendrocytes *in vitro*. *J Neurochem*. (1992) 59:55–61. doi: 10.1111/j.1471-4159.1992.tb08875.x
24. Cheong JLY, Cady EB, Penrice J, Wyatt JS, Cox IJ, Robertson NJ. Proton MR spectroscopy in neonates with perinatal cerebral hypoxic-ischemic injury: metabolite peak-area ratios, relaxation times, and absolute concentrations. *Am J Neuroradiol*. (2006) 27:1546–54.
25. Lally PJ, Montaldo P, Oliveira V, Soe A, Swamy R, Bassett P, et al. Magnetic resonance spectroscopy assessment of brain injury after moderate hypothermia in neonatal encephalopathy: a prospective multicentre cohort study. *Lancet Neurol*. (2019) 18:35–45. doi: 10.1016/S1474-4422(18)30325-9
26. van Laerhoven H, de Haan TR, Offringa M, Post B, van der Lee JH. Prognostic tests in term neonates with hypoxic-ischemic encephalopathy: a systematic review. *Pediatrics*. (2013) 131:88–98. doi: 10.1542/peds.2012-1297
27. Barkovich AJ, Westmark KD, Bedi HS, Partridge JC, Ferriero DM, Vigneron DB. Proton spectroscopy and diffusion imaging on the first day of life after perinatal asphyxia: preliminary report. *Am J Neuroradiol*. (2001) 22:1786–94.
28. McKinstry RC, Miller JH, Snyder AZ, Mathur A, Schefft GL, Almli CR, et al. A prospective, longitudinal diffusion tensor imaging study of brain injury in newborns. *Neurology*. (2002) 59:824–33. doi: 10.1212/WNL.59.6.824
29. Thulborn KR, Waterton JC, Matthews PM, Radda GK. Oxygenation dependence of the transverse relaxation time of water protons in whole blood at high field. *Biochim Biophys Acta*. (1982) 714:265–70. doi: 10.1016/0304-4165(82)90333-6
30. Laptook AR, Corbett RJT, Sterett R, Garcia D, Tollefsbol G. Quantitative relationship between brain temperature and energy utilization rate measured *in vivo* using 31P and 1H magnetic resonance spectroscopy. *Pediatr Res*. (1995) 38:919–25. doi: 10.1203/00006450-199512000-00015
31. Christen T, Schmiedeskamp H, Straka M, Bammer R, Zaharchuk G. Measuring brain oxygenation in humans using a multiparametric quantitative blood oxygenation level dependent MRI approach. *Magn Reson Med*. (2012) 68:905–11. doi: 10.1002/mrm.23283
32. Skues MA, Prys-Roberts C. The pharmacology of propofol. *J Clin Anesth*. (1989) 1:387–400. doi: 10.1016/0952-8180(89)90080-9
33. Shah P, Riphagen S, Beyene J, Perlman M. Multiorgan dysfunction in infants with post-asphyxial hypoxic-ischaemic encephalopathy. *Arch Dis Child Fetal Neonatal Ed*. (2004) 89:F152–5. doi: 10.1136/adc.2002.023093
34. van den Broek MPH, Groenendaal F, Egberts ACG, Rademaker CMA. Effects of hypothermia on pharmacokinetics and pharmacodynamics. *Clin Pharmacokinet*. (2010) 49:277–94. doi: 10.2165/11319360-000000000-00000
35. Giesinger RE, Bailey LJ, Deshpande P, McNamara PJ. Hypoxic-ischemic encephalopathy and therapeutic hypothermia: the hemodynamic perspective. *J Pediatr*. (2017) 180:22–30.e2. doi: 10.1016/j.jpeds.2016.09.009
36. Robertson NJ, Thayyil S, Cady BE, Raivich G. Magnetic resonance spectroscopy biomarkers in term perinatal asphyxial encephalopathy: from neuropathological correlates to future clinical applications. *Curr Pediatr Rev*. (2014) 10:37–47. doi: 10.2174/157339631001140408120613
37. Lange T, Dydak U, Roberts TPL, Rowley HA, Bjeljac M, Boesiger P. Pitfalls in lactate measurements at 3T. *Am J Neuroradiol*. (2006) 27:895–901.
38. Lucke AM, Shetty AN, Hagan JL, Walton A, Stafford TD, Chu ZD, et al. Early proton magnetic resonance spectroscopy during and after therapeutic hypothermia in perinatal hypoxic–ischemic encephalopathy. *Pediatr Radiol*. (2019) 49:941–50. doi: 10.1007/s00247-019-04383-8
39. Davidson JO, Dean JM, Fraser M, Wassink G, Andelius TC, Dhillon SK, et al. Perinatal brain injury: mechanisms and therapeutic approaches. *Front Biosci*. (2018) 23:2204–26. doi: 10.2741/4700

Conflict of Interest: The authors declare that the research was conducted in the absence of any commercial or financial relationships that could be construed as a potential conflict of interest.

frontiers in Neurology

REVIEW
published: 14 July 2020
doi: 10.3389/fneur.2020.00575

Cortical Gray Matter Injury in Encephalopathy of Prematurity: Link to Neurodevelopmental Disorders

Bobbi Fleiss[1,2,3,4], *Pierre Gressens*[2,3,4] *and Helen B. Stolp*[4,5]*

[1] School of Health and Biomedical Sciences, RMIT University, Bundoora, VIC, Australia, [2] Université de Paris, NeuroDiderot, Inserm, Paris, France, [3] PremUP, Paris, France, [4] Centre for the Developing Brain, School of Biomedical Engineering and Imaging Sciences, King's College London, London, United Kingdom, [5] Comparative Biomedical Sciences, Royal Veterinary College, London, United Kingdom

Preterm-born infants frequently suffer from an array of neurological damage, collectively termed encephalopathy of prematurity (EoP). They also have an increased risk of presenting with a neurodevelopmental disorder (e.g., autism spectrum disorder; attention deficit hyperactivity disorder) later in life. It is hypothesized that it is the gray matter injury to the cortex, in addition to white matter injury, in EoP that is responsible for the altered behavior and cognition in these individuals. However, although it is established that gray matter injury occurs in infants following preterm birth, the exact nature of these changes is not fully elucidated. Here we will review the current state of knowledge in this field, amalgamating data from both clinical and preclinical studies. This will be placed in the context of normal processes of developmental biology and the known pathophysiology of neurodevelopmental disorders. Novel diagnostic and therapeutic tactics required integration of this information so that in the future we can combine mechanism-based approaches with patient stratification to ensure the most efficacious and cost-effective clinical practice.

Keywords: preterm, brain injury, development, inflammation, synaptopathy, MRI, functional activity, neuropathology

OPEN ACCESS

Edited by:
Silvia Noemi Tenembaum, Garrahan Hospital, Argentina

Reviewed by:
Carlotta Spagnoli, Santa Maria Nuova Hospital, Italy
Thalia Harmony, National Autonomous University of Mexico, Mexico

***Correspondence:**
Helen B. Stolp
hstolp@rvc.ac.uk

Specialty section:
This article was submitted to Pediatric Neurology, a section of the journal Frontiers in Neurology

Received: *07 April 2020*
Accepted: *19 May 2020*
Published: *14 July 2020*

Citation:
Fleiss B, Gressens P and Stolp HB (2020) Cortical Gray Matter Injury in Encephalopathy of Prematurity: Link to Neurodevelopmental Disorders. Front. Neurol. 11:575. doi: 10.3389/fneur.2020.00575

INTRODUCTION

Preterm birth is defined as delivery before 37 completed weeks of gestation, and although the shorter the gestation, the higher risk of mortality and morbidity, even the late preterm-born infants are vulnerable to injury, including to the brain. The hallmarks of brain injury to the preterm born infant are: neuroinflammation, oligodendrocyte maturation arrest and hypomyelination, axonopathy, reduced fractional anisotropy and cortical volume determined by magnetic resonance imaging (MRI), and eventually, significant cognitive deficits (1). Collectively the brain damage associated with preterm birth is called encephalopathy of prematurity (EoP).

As long-term cognitive and behavioral consequences of preterm birth are increasingly recognized, neuropathological studies have focused on gray matter (GM), in addition to white matter (WM). It was initially thought that cortical GM injury only occurred in preterm infants in cases of very severe injury. Increased understanding of cortical development and more detailed post-mortem studies revealed that this not the case (2, 3). Over the past few years, work has increasingly indicated a widespread subtle neuronal injury in infants born preterm, that in some cases, such as interneuron deficits, may be independent of WM injury (4). Further than this, swathes

of clinical and preclinical studies indicate that the cortical GM injury found in preterm infants significantly contributes to their increased risk of neurodevelopmental disorders (NNDs), such as autism spectrum disorder (ASD), attention deficit hyperactivity disorder (ADHD), and other learning and behavioral disorders.

The large and long running EPICURE (UK), EPIPAGE (France), and ELGAN (U.S.A.) studies have provided invaluable data on the incidence of neurological injury following very premature birth [e.g., (5–7)]. Together, these epidemiological studies confirm that preterm infants have a 25–30% incidence of neurological disorder, with as many as 40% of affected individuals having more than one diagnosable disorder (5–7). In all studies, incidence of cerebral palsy was 5–8% of preterm children, consistent between 2, 6, and 10 years of age (5, 6, 8). In addition, more than 40% of children at 2 years were below threshold for communication, motor, problem solving, and social skills (7), and 30% of children were diagnosed with cognitive impairment at 6 years of age (5), while at school age (10–11 years), 7–8% of preterm born children were diagnosed with ASD, 11% with ADHD, and 10% with emotional disorders, such as anxiety (8, 9). Using latent profile analysis in school age preterm born children (10 years of age), 25% of children were shown to have impaired executive functioning across a range of cognitive domains, while 41% of children fell into a "low-normal" category, where impairment was related to reasoning and working memory (10).

ENVIRONMENTAL CONTRIBUTORS TO EoP AND MECHANISMS OF INJURY

The maternal fetal membranes surrounding the amniotic cavity represent the boundaries of a sort of "black box," inside which we struggle to know and understand the processes preceding preterm birth. This is due to technical difficulties in safely monitoring the biochemical processes ongoing in the uterine space. However, processes causing brain injury in the preterm born infants certainly begin before delivery, as indicated by a small study of brain functional connectivity in fetuses who went on to be born preterm (11) and an increasingly number of studies showing predictive biomarkers in maternal blood months before preterm birth (12–14). Numerous events and antenatal exposures have also been associated with preterm birth and EoP via epidemiological study and verified with preclinical studies. These include placental abruption or twin–twin transfusion, preeclampsia, or placental insufficiency (potentially contributing to a hypoxic-ischemic-like insult and/or intrauterine growth retardation) and, less commonly, complications linked to oligohydramnios and maternal substance abuse (15). A predominant role of hypoxia in EoP with no other complications (such as those described above) is not supported by clinical data (16). Chorioamnionitis, leading to a maternal–fetal inflammatory response, is a chief driver of the process of early parturition leading to preterm birth, demonstrated across clinical and preclinical studies (17–19). Maternal–fetal inflammatory response not only precipitates preterm birth, but a wealth of epidemiological and clinical studies have shown that, although it is often clinically silent, it is a major driver of EoP (20, 21) and its associated long-term neurological and behavioral/psychiatric deficits [see reviews (22, 23)]. While EoP can be initiated prenatally, there is evidence of continued disruption of the brain post-natally, which could be driven by a mixture of pre- and post-natal factors. For instance, Bouyssi-Kobar et al. (24) show reduced brain growth trajectories in preterm born infants compared to age-matched *in utero* controls that were associated with (antenatal) chorioamnionitis, as well as post-natal sepsis. Inflammatory drivers include pre- and post-natal events and conditions: chorioamnionitis, funisitis, early and late onset sepsis, and necrotizing enterocolitis. Other, non-inflammatory, post-natal contributors to EoP may include hyperoxia (25), as the *ex utero* environment is relatively high in oxygen compared to the *in utero* environment (26), and reduced exposure to maternal hormones, such as estrogen and other neuroactive precursors (27). While there has been little follow up on the estrogen hypothesis clinically (28), recent animal models have suggested a potential protective effect (4, 29, 30). That hyperoxia plays a role in EoP is also supported by animal studies (31–33).

CELLULAR MEDIATORS OF BRAIN INJURY

How, specifically, do these perinatal events lead to EoP? In the case of maternal–fetal inflammation, systemic inflammation drives changes in the brain after either crossing directly through the endothelial cells making up the blood–brain barrier (BBB) or by stimulating, via receptors for cytokines, such as interleukin-1 (IL-1), production of pro-inflammatory molecules by the endothelial cells that are secreted into the brain parenchyma (34, 35). It is currently unclear whether these immune mediators act directly on neurons or have their actions performed via stimulated glial cells, such as microglia and astrocytes, though it is likely that both processes occur. Inflammation has been shown in the fetal brain to reduce neurogenesis in embryonic proliferative zones (36) or to increase neurogenesis in the SVZ and dentate gyrus (37), which has been linked to microglia activity in some cases [reviewed in (38–40)]. The timing of the exposure of neurons to inflammatory stimuli is undoubtedly critical. The exact timing of events impacting EoP is not clear, though it is likely that events occurring in the third trimester are most influential. Although the vast amount of proliferation is complete in the third trimester, there are specific cell types, interneurons of note, that are still being born and migrating in this period and that are increasingly demonstrated to be vulnerable in preterm born infants and animal models (41, 42). Susceptibility of processes, such as neuronal arborization and synapse formation may be even more important, given the intersect between injury

Abbreviations: ADHD, attention deficit hyperactivity disorder; ASD, autism spectrum disorder; EEG, electroencephalogram; EoP, encephalopathy of prematurity; GM, gray matter; FA, fractional anisotropy; IVH, intraventricular hemorrhage; MRI, magnetic resonance imaging; NDD, neurodevelopmental disorder; PVL, periventricular leukomalacia; WM, white matter.

events sensitizing to EoP and the developmental timetable of the brain (discussed in more detail below).

Over the past decade, the importance of microglial activation has been exhaustively demonstrated in human preterm-born infant post-mortem brain samples and in models of perinatal brain injury [reviewed in (43, 44)]. These studies have included experimental evidence that microglia are necessary for the evolution of injury in the developing brain (45, 46), but conversely, that microglia also play protective roles in perinatal brain injury (47, 48). Microglia are also activated by other modulators of brain injury, such as hypoxia or hypoxia-ischemia, as these events lead to cell injury and the release of damage-associated messenger proteins (DAMPS) and/or the production of toxic metabolites that also activate microglia directly (49, 50). Microglia establish territories in the developing brain from early in embryonic life and are intimately involved in the processes of brain building. Thus, microglia activation to an immune responsive state leads to EoP via a double hit, whereby there is production of toxic factors for neighboring neural cells and loss of normal microglial functions to shape axonal connectivity and synaptic elimination/function. This has been well-described in the WM (51–54). There is substantially less information on the specific effects of activated microglia on the GM, including synapses and interneurons, which are relevant to EoP. However, as increasing evidence shows that microglial dysfunction persists for weeks to years after insult (55–58), the importance of this phenomena may become more apparent with further study. It is also plausible that the GM and WM are differentially vulnerable, as microglia in these tissues have differing gene expression patterns in the basal state and after injury, based on studies in adults (59, 60). However, nothing is known of this difference in a model relevant to EoP. As such, although we can speculate that there may be specific soluble factors or regulators (micoRNAs, cytokines, etc.) released (possible via vesicles) from GM microglia that influence GM development in ways that would offer therapeutic avenues (61, 62), evidence is still required.

Reactive astrogliosis is also observed in some forms of human perinatal WM injury (63, 64) and is associated with deleterious effects mediated by agents, including hyaluronic acid (65), bone morphogenic protein (66), cycloxygenase-2 induction and associated prostaglandin E2 production (64), and endothelin-1 (67), which can impair oligodendrocyte precursor cell maturation. Clinical and experimental studies have shown a role for GFAP-positive astrocytes in WM injury in preterm born infants, but specifically in older preterm born infants [>32 weeks; (68, 69)] and during equivalent stages of rodent development [5 post-natal days plus; (70)]. In the GM, astrocytes increase in number with gestational age. Compared to the WM, GFAP positive cells represent a far smaller proportion of cells (<1%) (71) and the response of the populations a whole to injury is under-studied. In preterm-born infants, a small increase in the number of GM astrocytes was reported in a study of infants with cystic periventricular leukomalacia (cPVL; severe injury), but as the control group had a significantly lower gestational age, this effect did not survive correcting for development (72). However, studies in animals support the hypothesis that astrocytic dysfunction proceeds neuronal damage in at least some injury paradigms (73).

DEVELOPMENTAL EVENTS SUSCEPTIBLE TO INJURY IN THE PRETERM BRAIN

When assessing how pre- and post-natal factors contribute to EoP, it is necessary to consider what developmental events happen during the preterm period that may be affected by preterm birth. The prenatal period most associated with EoP (from 23 to 32 weeks) is characterized by the final stages of neurogenesis in the human telencephalon, neuronal migration, differentiation and maturation, and the very early stages of cortical myelination. Neurogenesis peaks very early in gestation (8–12 weeks), but continues both in the ventricular zone of the dorsal cortex and within the ganglionic eminences for up to 29 weeks (41). The cortical plate forms around 11 weeks into gestation [reviewed in (74)] until shortly after the end of neurogenesis. Excitatory neurons primarily come from the progenitors in the ventricular zone of the dorsal cortex and migrate radially to the cortical plate [reviewed in (74)], while inhibitory cortical neurons derive from the ganglionic eminences and migrate tangentially to the cortical plate [reviewed in (75)]. Once neurons reach their final positions in the cortical plate, they start to mature—a process which includes extending dendritic arbors and forming synapses, detectable form 19–23 weeks gestation (76). At the same time, radial projections of the neural progenitors are lost, and tangential extension of subcortical and cortico-cortical projections continues. These processes continue through the prenatal and post-natal period of brain development, with an extensive period of synaptic modulation and pruning throughout the first year of life. Local electrical activity and connectivity between neurons can be detected early, undergoing numerous changes over development, and don't appear to find a mature state until early adolescence [reviewed by (77)]. Details of these events and many of the mechanisms underlying them are reviewed extensively in Molnar et al. (78) and Volpe (79). On top of these microstructural changes is a general increase in cortical thickness and a semi-stereotypical pattern of cortical folding, with primary sulci forming from 16 to 19 weeks gestation, and secondary and tertiary sulci formation starting from 32 to 36 weeks, respectively (80).

The real-time development of the brain, including the increasing complexity in the cortical structure, can be detected with non-invasive imaging methods, such as T1/T2 or diffusion-weighted MRI [(81–83); reviewed by (84)] and these techniques have allowed the detection of delayed or impaired cortical development in preterm born infants. However, given the relatively low resolution and integrated nature of diffusion MRI signal, interpreting the specific structural changes in relation to neurodevelopmental processes is difficult. Techniques are in development to scale match MRI and histological data [e.g., (85)], though changes in diffusion MRI are currently interpreted through comparison with standard histological measures. There is evidence that preterm birth can result in changes to all the processes of cortical development

described above, including reduced progenitor proliferation, arborization, and myelination, as well as direct injury outcomes, such as cell death. The rest of this review will discuss a number of these in detail, including potential mechanisms of injury, overlap with neurodevelopmental disorders (NDDs), and potential therapeutics.

MACROSCALE ALTERATIONS IN CORTICAL GM

Many elegant neuroimaging studies have begun to correlate both typical and pathological behavior with specific brain areas or functional readouts. Based on these, we know that many brain regions contribute to the diverse array of neurological disorders presented by preterm-born children. In particular, the important role of cortical dysfunction underlying these cognitive disorders (but not so prominently in motor disorders) is increasingly clear. Rathbone et al. (86), in their study of cortical growth (cerebral volume and cortical surface area) in the 20 weeks between birth and term-equivalent age in preterm infants, showed that slow rates of cortical growth correlated directly with neurocognitive ability at 2 and 6 years of age. In particular, impaired cortical surface area growth correlated with poorer scores in numerous features of executive function, learning, memory, and attention, as well as social ability. However, there was a clear lack of correlation between cortical growth and motor abilities (86). Numerous neuroimaging studies using different post-imaging assessment methods have shown reductions in cortical GM volumes in preterm infants, both in the preterm population as a whole (87–89) or specifically those with periventricular leukomalacia [PVL; (90, 91)] and in very preterm born children [assessed at 7 years; (92)] and adolescence [assessed at 15 years; (93, 94)]. Reductions in volume of the deep GM have also been reported (95, 96); changes in thalamic volume were found to be a predictor of reduced cortical GM volume and alterations in diffusivity within the thalamocortical networks (95) were found to correlate with cognitive performance at 2 years of age, though they only accounted for 11% of the variance (97).

Importantly, Bora et al. (98) showed that very preterm infants had a 13%-increased risk of inattention and hyperactivity behavior at school age (4, 6, and 9 years), which correlated with decreased GM volumes, particularly within the prefrontal region. Increased anxiety-like behavior has also been associated with preterm born infants with reduced GM volume (99). In a small study group, very preterm infants that went on to have a diagnosis of ASD were found to have increased incidence of cystic WM lesions, and reduced cerebellar volume, but no changes in GM volume (100). However, only eight children in the cohort (4.7%) were diagnosed with ASD by the age of 7 years, so the study may have been underpowered for detecting more subtle changes in cortical GM.

In animal models, mimicking changes in these cortical volume parameters is difficult, due to differences in the relative GM and WM volumes in experimental species and the differences in the size/complexity of the individual regions relative to one another. Sheep are used in studies of perinatal brain injury, with advantages regarding physiological and neurological similarities to preterm humans, including gray–white ratios [discussed in (101)]. Dean et al. (102) have studied intra-amniotic LPS in sheep, a paradigm able to cause cystic WM injury. This inflammatory exposure caused no obvious cell loss in the GM, but reduced cortical volume by ∼18%. In further work in sheep models, Dean et al. (103) also showed a reduction in cortical GM volume after *in utero* hypoxia-ischemia, in which there was again no cortical cell loss. Interestingly, there was no early reduction in cortical volume (+7 days) but these became increasingly apparent with time after injury [starting at 2 weeks and at least up to 4 weeks; (103)]. In a mouse model of maternal immune activation using poly I:C, subtle decreases in GM volumes were observed throughout development (104), though changes in cortical volumes were not specifically reported.

In addition to alterations in GM volume, complex changes in cortical architecture have also been identified. For instance, Zhang et al. (92) determined that there was a decrease in cortical surface area and the gyrification index of 7-years-old following very preterm birth compared to term-born controls. Maps of cortical folding patterns in neonates suggest that preterm infants have fewer and shallower sulci than term equivalent controls (105). Data suggested that the lower gyrification index and cortical surface area in preterm-born neonates was likely to be due to a combination of altered *in utero* and post-natal growth, and it was a finding independent of reduced total brain volume (105, 106). Reduced cortical folding has also been associated with increased incidence of NDDs later in life (106), matching, at least partly with data from specific disorder cohorts (107–110), though the data are not substantial here, as existing studies are small.

Collectively, these data point to the possibility that alterations in cortical folding are driven by numerous age-specific microstructural changes. The theories behind cortical folding are many, and include processes such as the rate of neurogenesis, of tangential migration and neuronal arborization [reviewed by (111–113)]; currently no single one is sufficient to explain the biological underpinning to normal or abnormal cortical folding. Numerous aspects of the *in utero* environment and preterm injury have been associated with changes in cortical folding [reviewed by (114)], though the mechanism by which this injury is produced is still unclear. Recent work by Garcia et al. (115) has shown regional differences in cortical growth rate between post-menstrual age 30 and term equivalent age (based on 2–4 MRI scans over this period in preterm-born infants), which are disrupted in preterm-born infants with gross injury, such as intraventricular hemorrhage (IVH). Their work suggests that severe injury in preterm born infants may alter local cortical growth and subsequently cortical folding (115), supporting the hypothesis that cortical folding may result from mechanical instability as the GM grows faster than underlying WM (116). Alternatively, recent compelling evidence also shows that the extracellular matrix is essential in normal cortical folding (117), likely contributing to the mechanical tension within the brain. The link between these highly reductionist *ex vivo* studies and EoP is currently unclear, though they have suggested that hyaluronic acid can inhibit cortical folding (117), and increases in hyaluronic acid have been found within the preterm brain (118).

GRAY MATTER NEUROPATHOLOGY ASSOCIATED WITH EoP

There are few neuropathological studies of GM injury in preterm-born infants, compared to the number of studies of WM injury. Complicating matters, due to the difficulties of defining appropriate controls, GM studies typically use evidence of WM injury as a starting point in the assessment of the GM, rather than searching for independent patterns of injury. We have created **Table 1**, which summarizes studies performed on human preterm-born, post-mortem tissue that have included GM analyses. From this, we can generalize that in studies of infants with severe and contemporaneously uncommon WM injury (cystic PVL), there are reductions in neuronal number and increased neuronal cell death (where assessed; 6/6 studies). However, in studies of infants predominantly with diffuse WM injury, global reductions in cell number are less frequently reported (1/5 studies), but interneurons seem to be a vulnerable subpopulation (present in 3/3 studies) and dysmaturation in cerebellar lamination are reported (1 study). Interestingly, there are complex subtle changes in interneurons in cases with non-cystic WM injury vs. controls (42) and when comparing very preterm infants to less preterm infants [irrespective of WM injury; (4)]. It is necessary to note that of the 12 studies identified, 6 of these were performed on archival tissue collected between 1993 and 2007 from the Department of Pathology at the Children's Hospital Boston. An additional observation study was not included in the table, as the data were expanded upon in a later study (127). It is not possible from the published details of the Boston group's work to determine whether cases in these studies have been reused. Thus, reports of cell death across regions in these studies may be interdependent, due to case severity in this center, and studies of other centers and in more contemporaneous cohorts are needed to determine the state of neuronal injury in preterm born infants more generally.

ANIMAL MODELS OF GM PATHOLOGY

Severe Injury

Severe brain injury, including cystic lesions and severe IVH, occurs in very few preterm-born infants [<5% cystic lesions, <5% IVH; (128)]. Historically, the proportion of infants with these forms of injury was much higher. It was also once considered that hypoxia-ischemia was the leading (possibly the predominant) cause of perinatal injury, including in preterm-born infants. Because of these historical trends and (now updated) ideas, much of the data that we have on GM injury in EoP is from animal models of gross clastic lesion (30–80% hemispheric ablation). This initial wave of data suggested that of the cortical layers, the subplate was most susceptible to hypoxic-ischemic injury at preterm equivalent ages (129), possibly due to its relatively early birth and maturation. However, subsequent studies agree that the extent of cortical injury is dependent on the severity of the insult, and all lower cortical layers have the capacity for cell loss after severe hypoxia-ischemia (130). In a study of partial uterine artery occlusion, modeling hypoxia-ischemia in the fetal sheep, immediate low level necrotic cell death was found throughout the deep and cortical GM, followed by extensive apoptosis in both the GM and WM at 3 h post-injury (131). Other studies of *in utero* hypoxia-ischemia in sheep have shown some increase in pyknotic cells and activated caspase-3 staining from 24 h up to 4 weeks in the caudate nucleus and subplate (132, 133), reduced NeuN and somatostatin positive neurons in the caudate and putamen (134), specific loss of glutamate decarboxylase interneurons (a marker of GABAergic neurons) and their perineuronal nets in the cortex (135), along with reduced arborization complexity and spine density in both the caudate, hippocampus, and cortex (103, 132–134, 136).

Moderate/Mild Injury

Improvements in antenatal and post-natal care, including the use of prenatal steroids and post-natal surfactants and improved respiratory support, have collectively led to the decrease in severe brain injury, so that now the vast majority of infants suffer from diffuse WM injury (118). This has inspired the revision/creation of animal models focused on modeling white matter dysmaturation. A number of these new(er) models providing insights into the role of contemporaneously relevant insults to GM injury are described. A landmark study in our understanding of the GM injury induced by preterm birth came from the team led by Sandra Rees (137), wherein they delivered baboons preterm and held them in a NICU environment for 2 weeks. This important study isolated the roles of prematurity itself from exogenous/precipitating factors (such as chorioamnionitis and sepsis). WM injury and hemorrhage were most common in preterm baboons, but there were significant pockets of necrosis in layer IV/V cortical neurons (4/16 cases) and in the head of the caudate (1/16 cases). One of the first attempts to nail down the cellular substrate of GM injury was the analysis of the effects of intrauterine hypoxia-ischemia on the fetal sheep (103). Although it can be debated whether hypoxia-ischemia is particularly relevant to the majority of cases of EoP (16), this team used cutting edge combinations of high-field MRI and detailed neuropathological assessments of cell number and structure to reveal novel insights into brain injury. The team found that overall reductions in GM volume were not precipitated by neuronal cell loss, but that there were frank changes in dendritic arborizations [length, number, intersections; (103)].

Sheep models of moderate inflammatory injury are also providing important information. Exposure to intra-amniotic inflammation prior to preterm birth, was used to reveal the evolution of *in utero* inflammatory brain injury (138). Interestingly, sheep were all exposed to inflammation on the same gestational day, but sub-groups were culled every 24 h providing a detailed time course of events. Cleave caspase-3 positive cells were increased in number in the hippocampus at 2, 4, 8, and 15 days following LPS exposure, and in the cortex (at 8 days only), along with increases in MAP2 staining in both GM regions. Strikingly, there was only moderate WM injury (few cleaved caspase-3 positive cells, microgliosis, and mild demyelination) suggesting that neurons may be vulnerable to injury in the absence of overt WM damage. Reduced cortical neurons were found in another

TABLE 1 | Summary of post-mortem studies of preterm-born infants, including analysis of the GM, highlighting the case characteristics, regions of interest, and the GM and WM injuries described.

Reference / *Study location* / **Years of sample collection**	Number of cases (n) / *Gestational age at birth* / **Survival time**	Pathologists description of injury / *Post-mortem delay*	Nature of cases designated as controls	Regions of interest	Gray matter pathology (description of what was analyzed)	White matter pathology (description of what was analyzed)
Andiman et al. (119) / *Dept. of Pathology, Children's Hospital Boston, MA, USA* / **1993–2007**	20 WMI, 15 controls / *WMI = 33.9 ± 4.3, Control = 33.1 ± 6.2* / **WMI = 5.9 ± 14.0 weeks, Controls = 13.2 ± 23.6 (NS diff)**	PVL or diffuse WMI as diagnosed by a histopathologist / *Post-mortem delay not reported*	Prematurity with respiratory distress syndrome, $n = 4$; congenital heart disease, $n = 2$; primary pulmonary hypertension, $n = 1$; hydrops fetalis due to placental chorioangiomas, $n = 1$; hydrops fetalis, $n = 1$; sacral teratoma, $n = 1$; cystic lymphatic malformation of the neck, $n = 1$; Werdnig–Hoffmann disease, $n = 1$; foreign body aspiration, $n = 1$; Blackfan–Diamond syndrome, $n = 1$ and bronchiolitis, $n = 1$ No difference in mean Apgar scores at 5 min (6.8 for both groups) or in other disorders / confounders	In the WMI cases, the cortex overlying WMI and compared it to similar cortical areas in control cases	No sig. difference in the presence of fractin-immunopositive neurons in any cortical layer No sig. difference in the incidence of the percent of MAP2-stained pyramidal cells in layer V or obvious cortical anomalies. Significant reduction (67%) in the density (MAP2) of layer V pyramidal neurons No sig. difference in the cortical or laminar thickness (MAP2, H&E)	Periventricular focal necrosis in the deep white matter with surrounding diffuse reactive gliosis and microglial activation (previous neuropathologic studies)
Haynes and van Leyen (120) 12 / 15-Lipoxygenase / *Dept. of Pathology, Children's Hospital Boston, MA, USA* / **Collection epoch not reported**	13 PVL, 17 controls / *PVL −29 to 43 PC weeks (median = 35.5) and 0–8 PN weeks (median = 1.5), Controls −20 to 43 PC weeks (median = 33.5) and 0–2.5 PN weeks (median = 1)* / **Survival time not reported**	PVL as diagnosed by a histopathologist / *PVL = 6–25 h, Control = 4–25 h*	Control cases did not have PVL or other significant brain pathology upon standard histologic examination. Autopsy reports were reviewed for major clinical findings, systemic autopsy diagnoses, and neuropathologic findings	Subcortical white matter and the cortex overlying WMI and compared it to similar cortical areas in control cases	No increase in 12/15-LOX expression in neurons of the cerebral cortex in PVL. Cell death or total cell number not assessed in the gray matter	PVL had "focal" necrotic component in the periventricular region, and "diffuse" component characterized by reactive gliosis and activated microglia in the surrounding white matter Increased 12/15-LOX expression in large round $CD68^+$ cells, lectin double positive and O4 double positive cells and scattered TUNEL- positive cells
Haynes et al. (121) Diffuse axonal / *Dept. of Pathology, Children's Hospital Boston, MA* / **Collection epoch not reported**	13 PVL, 17 Control (spread across acute and later stages) / *Mean gestational age (wks) PVL =36 ± 3, Controls = 32 ± 7* / **Mean postnatal age (wks)—PVL = 7.5 ± 17, Control = 10.5 ± 27**	PVL as diagnosed by a histopathologist / *PVL = 6–44 h (median = 17), Controls = 1.5–132 h (median = 14)*	Control cases did not have PVL or other significant brain pathology upon standard histologic examination. Causes of death included Noonan's syndrome 1, Fetal hydrops 1, Neonatal hepatic disease 1, Immune thrombocytopenia 1, Possible mitochondrial disorder 1, Sudden unexplained death in childhood, 1, Trisomy 21 1, Unexplained stillbirth	The area of study for axonal damage in PVL was distant from the infarct, i.e., in a separate section with no overlying cortical damage	Approximately 1/3rd PVL cases had thalamic gliosis, neuronal loss, and / or microinfarcts as determined by conventional histopathologic examination. Visually appreciable neuronal loss was present in the overlying cerebral cortex in 15% of the PVL cases. None of the non-PVL, non-axonal controls examined showed evidence of thalamic and / or cerebral cortical damage	PVL based on histopathologic criteria—periventricular focal necrosis in association with diffuse reactive gliosis and microglial activation Diffuse axonal injury, as determined by the apoptotic marker fraction, in the gliotic (non-necrotic) cerebral white matter in the acute and organizing stages of focal PVL
Ligam et al. (122) / *Dept. of Pathology, Children's Hospital Boston, MA, USA* / **Collection epoch not reported**	22 PVL, 16 non-PVL / *Gestational age in PVL = 32.5 ± 4.8 gw, Controls = 36.7 ± 5.2 gw, Sig dif in gw.* / **PVL = ∼4 weeks, Controls = ∼20 weeks (*P* = 0.07)**	PVL as diagnosed by a histopathologist / *Post-mortem delay not described*	Control cases did not demonstrate white matter features. Lower rates of NEC and sepsis in controls than in PVL	Thalamic sections were analyzed at one of the following levels: I (anterior), level of the mammillary bodies; II (mid), level of the red nucleus; and III (posterior), level of the lateral geniculate nucleus	Increased thalamic pathology via neuropathologist assessment (H&E) Trend to decreased neuronal density with H&E ($p = 0.07$)—criteria for neuronal discrimination not described Increased density of reactive astrocytes (GFAP) in the mediodorsal nucleus and the lateral posterior nucleus No significant increase in the density of CD68 + cells and numbers overall low No difference in the density of MDA-immunopositive neurons or percent of MDA-immunopositive neurons	Histopathology to confirm (or not) PVL, with "focal" necrotic component in the periventricular region, and "diffuse" component characterized by reactive gliosis and activated microglia in the surrounding white matter

(Continued)

TABLE 1 | Continued

Reference / *Study location* / **Years of sample collection**	Number of cases (n) / *Gestational age at birth* / **Survival time**	Pathologists description of injury / *Post-mortem delay*	Nature of cases designated as controls	Regions of interest	Gray matter pathology (description of what was analyzed)	White matter pathology (description of what was analyzed)
Kinney et al. (123) / *Dept. of Pathology, Children's Hospital Boston, MA, USA* / **1998–2012**	15 PVL, 10 controls / *The mean gestational age PVL = 32.8 ± 4.1 weeks in the, Control = 30.1 ± 5.9 weeks* / **PVL = 34 ± 4.6 postconceptional weeks, Controls = 31.6 ± 6.6 postconceptional weeks**	PVL as diagnosed by a histopathologist / *Causes of death in PVL: respiratory distress syndrome (n = 7); congenital heart disease (n = 3); primary skeletal disorders (n = 2); congenital diaphragmatic hernia (n = 1); inborn error of metabolism (n = 1) and VOGM (n = 1)* / *PVL = median 14 h, Control = median 16.5 h*	Controls did not demonstrate white matter abnormalities Causes of death in controls respiratory distress syndrome ($n = 5$); congenital heart disease ($n = 1$); hydrops fetalis due to placental chorioangiomas ($n = 1$); hydrops fetalis due to parvovirus ($n = 1$); primary pulmonary hypertension ($n = 1$); and bronchiolitis ($n = 1$)	Neurons in the ventricular/ subventricular region, periventricular white matter, central white matter, and subplate region in PVL cases and controls—including five subtypes of subcortical neurons: granular, unipolar, bipolar, inverted pyramidal, and multipolar	The neuronal density of the granular neurons in each of the four regions was 54–80% lower ($p \leq 0.01$) in the PVL cases compared to controls adjusted for age and post-mortem interval The overall densities of unipolar, bipolar, multipolar, and inverted pyramidal neurons did not differ significantly between the PVL cases and controls	Analysis grouped neurons in the subplate and white matter collectively PVL was characterized by necrotic foci in the periventricular and/ or central white matter; and diffuse astrogliosis and microglial activation in the surrounding white matter
Pierson et al. (72) / *Dept. of Pathology, Children's Hospital Boston, MA, USA* / **1997–1999**	17 PVL, 17 DWMI, 7 Negative (controls) / *PVL = 3.7 ± 4.1 (median = 2.3), DWMI = 3.4 ± 14.0 (median = 1.2), Negative = 0.8 ± 1.2 (n = number of samples)*	PVL or diffuse white matter gliosis (DWMG) without necrosis / *Post-mortem delay not described*	"Negative" white matter group with no diffuse gliosis or focal periventricular necrosis in the cerebral white matter	Seventeen gray matter regions, across the limbic system, cerebral cortex, deep gray nuclei, cerebellum and relay nuclei Seven white matter regions—frontal lobe, temporal lobe, parietal lobe, occipital lobe, corpus callosum, internal capsule and cerebellum	Sig increased neuronal injury in the cerebellar cortex and frontal cortex of PVL compared with DWMI or Negatives (H&E) No increase in astrogliosis (GFAP)	Focal periventricular necrosis; diffuse white matter gliosis
Haldipur et al. (124) / *National Brain Research Centre, Manesar, India* / **2007–2010**	40 cases / *Across the window of 28 weeks of gestation to 8 postnatal months* / **4 controls with 0 days survival and 32 cases of varying age at birth and survival**	All cases are those in which the autopsy indicated minimum or no damage to the brain and cerebellum in particular / *Delay = <24 h*	Still birth cases—with no obvious signs of injury as per cases with postnatal survival	Cerebellum	EGL cell density significantly increased by preterm birth EGL thickness reduced by preterm birth	None described
Marin-Padilla (3) / *Paediatric Autopsy Service, Dartmouth-Hitchcock Medical Center, Hannover, New Hampshire, USA (via ref 23)* / **Collection epoch not reported**	33 cases total / *5 cases born preterm who all had short survival time* / **3 months through to 5 years survival**	PVL as diagnosed by a histopathologist / *Post-mortem delay not described*	No controls—description of changes over time after WM injury only	Gray matter overlying frank WM injury	No changes visible in the acute cases—which were the pre-term born infants In the cases surviving longer—late term and term born infants, no change in the upper cortical layer vascular and cellular distribution and morphology (H&E, Golgi) Axomatoised pyramidal neurons change from being long projecting to being local-circuit (Golgi). These cells have increased circuitry and altered neuronal morphology—populations of larger and smaller cells with altered distributions (Golgi, H&E, GFAP)	Cystic white matter lesions
Stolp et al. (42) / *Perinatal Pathology Department, Imperial Health Care Trust, London,*	Non-WMI group, $n = 7$, WMI group, $n = 6$ / *Non-WMI group = 23 + 2 to 28 + 1 gw, WMI group 26 + 5 to 29 + 3*	Evidence of diffuse (non-cystic) white matter injury (WMI cases) including white matter gliosis and focal lesions / *1–3 days—bodies stored at 4°C*	Seven cases showed no significant brain pathology, non-neuropathologic controls (no WMI cases)	Interneurons of the frontal cortex and underlying white matter	No change in the total number of cortical neurons, identified by HuC/ HuD immunoreactivity, with 53,104 ± 11,009 immunopositive cells/ mm2 found in the control brains ($n = 5$)	No statistical differences in the number of SST or NPY subpopulations in the white matter between preterm infants with or without white matter injury. Significant decrease in the

(Continued)

TABLE 1 | Continued

Reference / *Study location* / **Years of sample collection**	Number of cases (n) / *Gestational age at birth* / **Survival time**	Pathologists description of injury / *Post-mortem delay*	Nature of cases designated as controls	Regions of interest	Gray matter pathology (description of what was analyzed)	White matter pathology (description of what was analyzed)
UK / **Collection epoch not reported**	*gw* / **Non-WMI group = 5 min to 43 h. WMI group 1 min to 5 weeks (comparison $p = 0.002$)**				and 52,120 ± 6,327 cells/mm2 in the cortex of the white matter injury cases ($n = 4$) Significant decrease in the cortical calretinin+ cells Calbindin- and parvalbumin-positive cells were observed in low numbers in both cases, insufficient for determining statistically significant changes. Somatostatin and Neuropeptide Y only found in the white matter	arborization of Somatostatin and Neuropeptide Y interneurons in both of these interneuron classes As previously reported (125)
Panda et al. (4) / *New York Medical College and Albert Einstein College of Medicine, USA* / **2002–2016**	Fetuses: 20–22 gw, $n = 5$, Infants: 23–28 gw, $n = 5$, Inafnat: 29–34 gw, $n = 5$ / *20–40 gestational weeks (gw): 26–27 gw infants surviving for 4–6 weeks were compared with 32–33 gw infants who lived for ∼3 days. Therefore, both had PMA33 gw at their death*	Excluded = moderate to severe intraventricular hemorrhage, major congenital anomalies, history of neurogenetic disorder, chromosomal defects, culture-proven sepsis, meningitis, or hypoxic–ischemic encephalopathy and infants receiving extracorporeal membrane oxygenation treatment / *post-mortem interval of ∼18 h*	None. Comparisons of effects of varying degrees of prematurity	Cortex (cortical plate), white matter (embryonic intermediate layer), and ganglionic eminences, which were cut at the level of the head of caudate nucleus	More prematurely born infants have fewer GAD67+ neurons in upper and not lower cortical layers More prematurely born infants have fewer Parvalbumin+ neurons in upper and not lower cortical layers More prematurely born infants have greater numbers of Somatostatin+ neurons in upper and not lower cortical layers Calretinin+ and neuropeptide Y+ interneurons not effected by preterm birth	No analysis undertaken.
Vontell et al. (125) / *Perinatal Pathology Department, Imperial Health Care Trust, London, UK* / **Collection epoch not reported**	7 WMI and 7 controls / *All <32 weeks' gestational age, vaginally delivered* / **Survival time not reported**	Cerebral white matter gliosis, lipid-laden macrophages, and focal lesions with evidence of WMI on pathologic examination (WMI cases) / *1–3 days—bodies stored at 4°C*	Also, extremely preterm, but with no significant brain pathology on gross and microscopic examination from post-mortem examination and had no visible brain abnormalities on post-mortem magnetic resonance imaging	Thalamus (medial dorsal (MD) nucleus, ventral lateral posterior (VLp) nucleus, ventral posterior lateral (VPL) nucleus) White matter [posterior limb of the internal capsule (PLIC) adjacent to the VLp (PLIC-VLp) and PLIC adjacent to the VPL (PLIC-VPL)]	No difference in the total average cell density in thalamic regions (H&E) Significant decrease in neurons in WMI cases in the MD, VLp, and VPL (HuC/HuD) Significant increase in the ratio of astrocytes (GFAP+) to total cell count in thalamic regions in WMI cases, compared with MD ($p < 0.01$) and VLp ($p < 0.01$)—but not VPL Significant increase in IBA1+ cells in WMI cases in the MD, VLp, and VPL.	No difference in the average total cell density in white matter regions Significant increases in neurons in PLIC-VPL but not in PLIC-VLp Significant increase in IBA1+ cells in the PLIC-VPL ($p < 0.05$), but not in PLIC-VLp
Pogledic et al. (126) / *Hôpital Robert Debré, Paris, France* / **Collection epoch not reported**	Cystic (c)-WMI, $n = 7$, Controls, $n = 18$ / *c-WMI = 24 + 4 to 27 gw, controls = 24 + 2 to 34 gw* / **c-WMI = 0–4 weeks and 1 day, Control = 0–11 days**	Cystic cases including focal lesions with macroscopic cysts associated or not with necrosis and / or calcifications surrounded by diffuse pallor / *post-mortem interval <48 h*	Non-cystic cases without tissue loss displayed pallor and gliosis (18/18 cases) associated with microscopic necrotic foci in a few cases (4/18 cases) and were considered to consist of diffuse lesions	Cortical regions located in the posterior part of the superior, middle and inferior frontal gyri and sulci, and the precentral gyrus and central sulcus corresponding to corresponding to the presumptive premotor and motor areas (areas 8-6-4) and contiguous prefrontal areas	Significantly increased cortical plate and subplate astrogliosis (GFAP) in c-WMI vs. control preterm WMI (no change in very preterm cystic and control cases) No increase in cortical plate and subplate microgliosis (IBA1) in c-WMI vs. control preterm WMI (for very preterm or just preterm cases)	White matter cysts were confined to the white matter without extending into superficial layers of the cerebral wall, such as the subplate and cortical plate

WM injury provided as context for overall injury severity.

Of the 12 studies identified, those highlighted in yellow (n = 6) report studies performed on tissues drawn from the same pool of post-mortem samples between the years of 1993–2007. It is unclear, and undeterminable from the case reports, how many times a single case appears across the six studies, and as such, how co-dependent the findings are. 12/15-LOX, 12/15-lipoxygenase; DWMI, diffuse white matter injury; EGL, external granule cell layer; h, hours; GAD67, glutamate decarboxylase 67; GFAP, glial fibrillary protein; gw, gestational weeks; H&E, hematoxylin and eosin; MAP2, microtubule associated protein 2; MD, Medial dorsal nucleus (thalamus); MDA, malondialdehyde; NEC, necrotising enterocolitis; PC, post-conceptional; PLIC, posterior limb of the internal capsule; PVL, periventricular leukomalacia; TUNEL, terminal deoxynucleotidyl transferase dUTP nick end labeling; WMI, white matter injury; VLp, ventral lateral, posterior (thalamus); vPL, Ventral posterolateral nucleus (thalamus).

study exposing the developing sheep to LPS (139), 7 days after a single LPS challenge. In these experiments there was no difference in either astrogliosis or microgliosis at the time point analyzed compared with the previous sheep study (138) in which microgliosis was present, but astrogliosis was not.

Rodent models are by far the most common for studying potential neuropathology of EoP. In a rat model of inflammatory exposure (maternal LPS exposure at the end of gestation), significant post-natal reduction in brain and body weight were observed, and a small increase in cell death in the striatum and germinal matrix (140). In a milder injury model of prolonged induction of systemic inflammation [using systemic IL-1β exposure; (52)], there was no gross body weight change, no evidence of caspase-3 positive dying cells or alteration in the number of NeuN-positive neurons in the neocortex. However, in this injury model, there were numerous changes in gene expression for synaptic and neurotransmission related genes (141). In this same animal model, and similar to data reported in human cases, a specific alteration in interneuron number was identified in the neocortex (42)—a finding supported by a number of other early-life inflammatory exposure models (142, 143) and preterm birth models (4). It is likely that the migration and differentiation of these cell populations is affected, though many studies show that injury reduces or repairs in adult mice, following early-life inflammation (42, 143). The important advantage of rodent models is the potential for behavioral testing, where aspects of human clinical disease can be recapitulated. In the inflammatory injury models just described, behavioral dysfunction has been reported, including reduced social interaction (143), short and long-term memory deficits (46, 52), attention-shifting deficits, and anxiety-like behavior (142). These behaviors are commonly found in preterm infants, as described above, and in other NDDs, thus supporting the face validity of these models. This is further supported by an extensive body of work showing reduction in GABAergic interneurons or expression of parvalbumin (as distinct from a reduction in cell number) in clinical ASD cases (144–146) and genetic models of NDDs (147–149).

EoP AS A SYNAPTOPATHY

A synaptopathy is a disease or disorder caused by dysfunction of synapses. This dysfunction can arise due to a mutation in a gene encoding a synaptic-related protein, such as an ion channel, a neurotransmitter receptor, or a protein involved in neurotransmitter release; alternatively, a synaptopathy may be due to structural deficits in extension of neuronal arbors and synaptic process. Whether EoP can be defined as synaptopathy requires further study, but we suggest that this is likely to be an important part of the neuropathology of this condition. The changes in EoP of gross GM volume changes, variations in growth rate, and patterns of cortical folding discussed above all reflect a combination of microstructural deficits (150) and connectivity (97, 151, 152) including delayed acquisition of the default mode network, as assessed by MRI techniques. Additionally, there is the fact that EoP predisposes to strikingly increased odds of a diagnosis of a NDD that are clearly recognized as synaptopathies, such as: ASD, up to 17-fold increased rates (9, 153); attention deficit disorder, up to 2.5-fold increased rates (154, 155); epilepsy, up to 5-fold increased rates (156, 157); and decreases in IQ directly proportional to the severity of their preterm birth (158, 159).

Considering the developmental events happening during the period of preterm birth, it may be expected that alterations should be found in patterns of neuronal migration, time frames and degrees of arborization, axon extension, and synapse formation. On this subject, the recent study by Petrenko et al. (160), provides a number of important insights. In a highly reductionist model of selective neuronal apoptosis in layer 5 of the cortex, induced by diphtheria toxin (161), the authors showed a progressive loss of ∼20% of neurons within the cortex over a 14-days period. While this degree of neuronal loss is unlikely to occur in EoP, the pre- and post-apoptosis changes to the brain have interesting correlates for the injury observed in EoP. Specifically, there was an associated increasing presence of astro- and microgliosis, retraction of dendritic arbors in dying neurons (days 3–5), and increased arborization (branch number and length) in the surviving neurons [day 14; (160)]. Alterations in dendritic arborization have been found in the GM in a number of experimental studies, many of which have already been referred to above [e.g., (103, 138)]. Additionally, a model of intrauterine growth restriction in pig, initiated at 100 days of pregnancy and assessed 22 days later, showed a loss of MAP2 staining in the parietal cortex and hippocampus, which was interpreted as disrupted somatodendritic neurites (162). Intrauterine growth restriction is an important contributor to poor perinatal outcomes, particularity in preterm born infants [see (163)]. Reduced dendritic branching and spine immaturity have also been reported in the CA1 region of hippocampus in a model of preterm birth in rabbit kits (30) and in the granular layer of the dentate gyrus in a maternal inflammatory activation (using i.p. poly I:C exposure) model in mice (164). These assessments are harder to perform in neuropathology on clinical samples, though reduced dendritic complexity (branch number and length) have been described for somatostatin and neuropeptide Y-positive neurons in the subcortical WM of preterm born infants with WM injury (42). Dendritic arborization, and relatedly, synapse formation [something also disrupted in these models; (42, 102, 165)], are essential developmental events for ensuring appropriate connectivity in the brain, and disruption in these processes have been implicated in a number of functional disorders of the brain (discussed below). The vulnerability of synapse structure in preterm born infants is clearly shown in a study that revealed a relationship between brain injury in preterm born infants and single nucleotide polymorphism (SNP) variants in the gene for the post-synaptic protein 95 [PSD-95, *DLG4*; (166)]. This work focused on a novel role for PSD-95 expressed specifically by microglia in early development in EoP, but the patient SNP data also suggest a wider vulnerability of synapse structure in preterm-born infants.

While evidence of EoP as a synaptopathy inevitable comes from neuropathological studies, our best capacity to clinical recognize disease, stratify patients for treatment, and monitor progress comes from neuroimaging. When relating *in vivo* imaging to pathology, the study by Petrenko et al. (160) suggested that (a) neurons loss could be detected by decrease in N-acetylaspartate and N-acetylaspartylglutamate and astrogliosis with reduced Glutamate/Glycine ratio, using magnetic resonance spectroscopy within 3 days of injury; and (b) diffusion MRI could also detect microstructural injury within 3 days of cell death induction, starting with increased water diffusivity (mean diffusivity) and extending to reduced factional anisotropy (FA) due to altered dendritic arrangement. Ball et al. (150) have shown a developmental decrease in FA in the cortex over the preterm period, with preterm born infants lagging behind term born infants in this maturational process, i.e., with a higher FA at term equivalent age. Modeling by Dean et al. (103) supports the idea that this increased FA value is due to delays in the normal dendritic arborization of the cortical neurons over this period. Vinall et al. (167), studied variation in diffusion MRI values between two scans in a cohort of very preterm infants. Their work showed that increased FA in the cortical GM at scan two was independently associated with reduced gestational age, birth weight, and slow weight gain. In addition, changes in FA were related to the second and third eigenvector direction, rather than the primary eigenvector direction. Collectively, these data imply that delays in cortical maturation were most likely driven by delays in neuronal process formation, or cell loss, and that cortical maturation was associated primarily with the phase of neonatal growth (167). Structural connectivity studies, typically based on the integrity of WM tracts using diffusion MRI, have shown a topographically dependent timetable of connectivity developing brain, which is impaired in the preterm brain (168, 169), and which is altered in nature over time, but persists in some form to adulthood (170). While these measures are not directly assessing cortical GM injury, it is likely that an interplay between WM and GM development occurs and that altered connectivity maps will reflect changes in GM development. These structural alterations are also likely to have functional consequences that reflect both local and global connectivity.

INTERPLAY OF STRUCTURAL AND FUNCTIONAL DEFICITS IN EoP

Altered structural and functional connectivity can be identified in the brains of preterm infants at term equivalent age, using combined diffusion and functional MRI (171). Aside from studies testing passive function, including touch and auditory stimulation, the majority of functional MRI studies in preterm infants have investigated resting states. Collectively, these resting state studies suggest that there is modular organization of the connectivity of the preterm brain, as is seen in the mature brain, but that integration between networks is altered (172–174). In these studies, there is evidence for disruption in both cortico-cortical and cortico-subcortical networks (172, 174), and reduced connectivity between areas associated with motor function, cognition, language, and executive function (173).

The electroencephalogram (EEG) is a clinical tool that has been shown to have some potential to monitor and predict severity and outcome of EoP. EEG waveforms are immature in the preterm brain, but appear to have some characteristic changes that can be used as a biomarker, including seizures, EEG suppression, and mechanical delta brush activity (175–178). The rate of spontaneous activity transients on EEG in preterm born infants with or without GM-IVH, measured over the first 48 h of life, was associated with cortical GM volume growth, increased gyrification index, and increased FA in WM tracts (179). Additional studies of the association between early EEG and cortical growth have revealed very specific band frequency relationships and with spontaneous activity transients (SATs) (180). As we begin to understand the biological drivers of these events, it will provide further information of the structure function relationship of the EEG recordings. Whitehead et al. (181), using EEG, showed that gross injury initially disrupts signal recruitment from cortical circuits. Signal recruitment appears to eventually be reinstated following injury but remains different from individuals without gross injury. Importantly, EEG abnormalities assessed shortly after birth (a week to a month after birth) were able to predict both developmental delay and cerebral palsy at 18–24 months (182, 183).

In animal models, fMRI has not been used, but EEG has been used extensively in sheep models of *in utero* hypoxic ischemic injury (more closely modeling hypoxic-ischemic encephalopathy) and shows reduced maturation of the EEG signal over time, seizure susceptibility, and microscale epileptiform events in the latent phase (up to 7 h post-injury) prior to seizure onset that correlates with cell death (184, 185). Following intrauterine inflammatory exposure in fetal sheep, changes in developmental patterns in alpha and beta power (reduced) and delta power (increased) have also been reported (186). However, while there is widespread evidence of altered EEG parameters in both clinical and preclinical studies, it is not clear how well these changes related to the neuropathology and how predictive they are for outcome. This work is only just beginning in clinical populations [e.g., (181–183)], but in pre-clinical studies, a number of studies have found a disconnect between EEG results and activity and arousal (187) or neuropathology (188, 189). However, it should be noted that the pathology examined in the study by Galinsky et al. (189) was largely focused on WM, rather than GM, features, and therefore may provide a limited understanding the pathological correlates of EEG. Van den Heuij et al. (185), for instance, have reported improved EEG findings together with reduced cortical and deep GM damage following intrauterine artery occlusion in the fetal sheep. In rodent models, EEG studies are less common, due to the size of the post-natal brain. Using *ex vivo* multi-electrode arrays, Mordel et al. (190) showed that inflammation and hypoxia, alone or together, increased the excitability of cortical neurons, in a glutamate receptor dependent manner. Interestingly, this research group has also shown that inflammation-induced alterations in cortical neuron spontaneous burst activity subsequently results in an increase in

apoptosis in the same cell population (191). The work of Mordel et al. (190) suggests that altered electrical activity in the cortex occurs only in the first few weeks after injury and that it recovers in adulthood. However, long-term alterations in spontaneous and mini-inhibitory post-synaptic currents, a more subtle measure of neuronal activity, was found specifically for parvalbumin-positive interneurons following fetal exposure to inflammation (142). Electrophysiological studies in the preterm sheep have shown altered excitability in subplate neurons (133), as well as reductions in intrinsic excitability, altered polarization dynamics and reduced long-term synaptic plasticity in the hippocampus, following hypoxia-ischemia and hypoxia alone (136).

The relationship with structure and function is complex and needs to be understood better at a (sub-)cellular level in the context of EoP. However, the study of Zaslavsky et al. (192) in iPSCs from ASD patients shows increased dendritic arborization and synaptic connectivity associated with a significant increase in sESPC frequency, supporting suggestions that altered neuronal morphology does change cellular function (rather than being compensated for in the function of the cellular communications pathway). This link between structure and function, the capacity for one to affect the other, and the plasticity for recovery is a particularly important point to consider when exploring new therapeutic targets, and optimal periods of treatment, for EoP and NDDs. This concept has recently been supported in a study of genetically encoded epilepsy, where timely treatment with Bumetanide altered long-term neuronal activity and network formation (193).

POTENTIAL THERAPIES FOR EoP

Gray Matter Targets

The most obvious change in the GM of preterm born infants are reductions in volumes on MRI, changes that persist with increasing age. These gross changes are likely mediated by limited but significant cell death, changes in sub-classes of interneurons, and, across neuronal classes, reductions in arborization and/or synaptic number. There are no therapies designed to target GM injury in the preterm specifically. Given that there are striking similarities between the GM changes in EoP and NDDs, it would seem appropriate to consider if any therapeutic candidates from the NDD field might have efficacy in EoP. Current pharmacological strategies for the treatment of ADHD focus on normalizing, but not repairing, disturbances in synaptic transmission and activity (194), and the same is the case for the various forms of epilepsy (195, 196). For ASD, therapy focuses on treating the symptoms of the disorder, such as risperidone, to reduce irritability via antagonism of central type 2 serotonergic (5-HT2) receptors and central dopamine D2 receptors (197). There are no therapies for ASD to treat the underlying deficits in social abilities. Other NDDs, such as intellectual disability and learning disorders (dyslexia and dyscalculia), together with ASD and ADHD, are successfully treated with behavioral interventions. It is believed that these therapies do rewire the brain (198), but whether they are capable of repair is not at all established.

A recent review of the drugs under investigation review for ASD highlighted that potential therapies fall into several clear classes—GABA/glutamate modulators, neuropeptides, immunologics, and dietary supplementation (199). The only therapies whose specific underlying premise is to permanently alter the structure of the brain are immunological therapies; although, neurotransmitter modulators given at the optimal stage of development may normalize aspects of structural and functional development—something that needs to be considered in future research. That immunological therapies might enable repair is based on the underlying idea that, in the brains of people with ASD, there is a persistent immunological dysfunction that itself is the cause of the core social deficits. As such, removing this dysfunction allows the brain to return to a normal structural and functional state. A very similar process of persisting and damaging inflammation is hypothesized to occur in the brain after perinatal brain injury (200) that evidence begins to accrue, which, in this context, it is also a valid therapeutic target (57, 201).

Another exploratory area of understanding and treating ASD and other NDDs is the gut–microbiome–brain axis (202, 203). Gene mutations associated with autism pathogenesis impair brain and gut function and contribute to core and comorbid symptoms reported in autism (204, 205). The gut and brain share cellular structures, molecular pathways and processes that likely cause shared vulnerability to processes leading to autism (203). For instance, gut and brain synaptic structure and function are similarly vulnerable to disturbances in structural proteins, such as neuroligins, post-synaptic density proteins, and Shanks (166, 206–210). An inexorable production of gut microbe-derived neuroactive metabolites influences gastrointestinal function, and these also traverse the BBB to exert potent effects on the brain (211–213). Importantly, microbiome-mediated gut and brain crosstalk even alters early brain development (214, 215) via dysbiosis, which impairs the function of the brain's chief "building managers" and resident immune cells—microglia. Microbe-derived metabolites also regulate the function of the BBB itself (216) demonstrating the integral nature of the microbiome-gut-brain axis in brain health. As such, research investigating factors modulating the gut–microbiome axis in NDDs may uncover novel mechanisms for treatment (217, 218).

Considering the options from the classes of drugs already being tested in models of EoP, we find that, despite many compounds being tested (with mixed results), most have not considered outcomes in the GM. There are some notable exceptions, such as $MgSO_4$ pre-treatment in a rat model of preterm HI (modeling antenatal treatment in at-risk mothers), significantly reduced tissue loss in the hippocampus and striatum and were associated with reduced neurological injury score (219). $MgSO_4$ has also been tested in a sheep model of perinatal asphyxia, reporting reduced seizure burden, but worse WM outcomes and no GM neuropathology (189). Clinically, $MgSO_4$ has a number to treat of 54 (220), though due to the nature of pre-treatment of at risk individuals, the exact efficacy is difficult to determine; a Cochrane review of four trials of antenatal treatment of at-risk women showed no significant effect on mortality or neurological outcome

(220). Erythropoietin in this environment has not been shown to be protective for qualitative WM or GM injury when administered as three doses of 25 μg/kg within the first 2 days of birth in preterm infants (221). This is despite positive GM outcomes in rodent (188, 222) and sheep models (223). Robinson et al. (222) showed that 2,000 U/kg erythropoietin (∼17 μg/kg), administered post-natally following intrauterine occlusion, was beneficial for both WM and GM, ameliorating behavioral deficits in gait and social interaction and fractional anisotropy changes in the WM, hippocampus, and striatum. In their study of perinatal injury, hypoxia-ischemia in the post-natal day-3 rat, van de Looij et al. (188) showed that erythropoietin improved somatosensory-evoked potentials and diffusion parameters in the WM, when measured with MRI, but didn't prevent cortical tissue loss. Wassink et al. (223) assessed neuronal number and cell death in the caudate, showing a significant improvement with erythropoietin (5,000 IU loading dose, followed by 832 IU/h) in the preterm sheep, as well as reduced seizure burden. More positive data on erythropoietin have been found for WM injury [reviewed in (79, 224)], supporting the numerous on-going clinical trials for this drug; however, it is clear that additional therapeutic agents need to be tested for GM efficacy.

LINKS BETWEEN EoP AND NEURODEVELOPMENTAL DISEASES

It has been unequivocally established that preterm born infants have increased rates of diagnosis for NDDs, including ASD, ADHD, and generalized learning disorders (5, 7–9, 225). It is also clear that, in the brains of people who suffered from EoP and those with NDDs (and from their matched preclinical models), there are a striking number of shared pathomechanisms. In this section, we will highlight key phenotypic, macrostructural, genetic, cellular, and sub-cellular processes shared with EoP and in cases of NDD. We will focus on the GM; but, we wish to highlight that for the WM these links between EoP and NDD are more established, such as shared deficits in corpus callosum structure in people after EoP and those with ASD and ADHD (226).

Recent work has assessed in detail the specific characteristics of behavioral disturbances in people born preterm with NDD, compared with people born at-term with an NDD [see reviews (227, 228)]. In general, in preterm vs. term NDD, the phenotypic presentations are similar. However, there are important differences. For instance, in people born at term, there is a higher rate of ADHD in males compared with females; but, this sex difference in not observed in people with ADHD who were born preterm (229). For ASD, a greater proportion of preterm (vs. term-born) males reported comorbidities (sleep apnea, seizure disorders, and ADHD) and people born preterm (particularly females) were more often non-verbal (230). Another recent small study of children with ASD demonstrated that, compared to term children, the preterm children had higher quality peer relationships and socioemotional reciprocity, but poorer non-verbal behaviors that regulate social communication (231). None of the current literature has indicated a problem with diagnosing those born preterm using the current diagnostic criteria. However, we speculate that just as autism has been expanded and refined into a complex spectrum of disorders that, in the future, ASD phenotypes specific to preterm born infants may be defined.

With increased MRI analyses of the GM in individuals with EoP, we begin to see a clear pattern of similarities in changes in brain structure in people with ASD and those born preterm—there are shared changes in the orbitofrontal regions, the amygdala, the basal ganglia, the hippocampus, and the cerebellum [reviewed in (227, 232)]. There is also a parallel with the altered cortical growth in preterm born infants and equivalent findings in ASD and ADHD patients. In MRI studies of ASD and ADHD, decreased GM volume has been associated with both conditions (233–237). In ASD, decreases have particularly been found in areas related to social behavior networks (233, 235, 237), while regions associated with inhibitory control (234) were changed in ADHD. In both cases, it is clear that patterns of GM deficits alter through the disease course (235, 238). Changes in the volume of GM in preterm infants/children/adolescents have been found in many of these regions [e.g., (91, 92, 239)], but are typically more widespread. Variation between studies has, of course, been reported, with not all studies finding cortical GM volume changes or associating them with neurological outcome. However, these are in the minority, and it has been suggested that these may be due to difficulties in accurately recognizing the gray-white matter boundary in the developing brain (240). Interestingly, in addition to this overlap in affected brain areas in both EoP and NDDs, MRI studies are also showing alterations in cortical networks [e.g., (236, 241)] in ASD and ADHD that warrant further exploration, and may come from as similar anatomical basis as in the EoP studies.

A newer avenue to link EoP and NDDs are genetic studies, such as genome-wide association studies (GWAS), copy number variant (CNV) studies, SNP, and haplotype studies, and these are revealing common risk factors. For instance, we have recently uncovered that an SNP in the gene for PSD95 is associated with poorer outcome for preterm born infants (166), mentioned above, as genetic variation in polymorphisms for PSD95 is a known risk factor for ASD (242). Common genetic variants and methylation patterns have been revealed in focused studies of people with ASD, with and without prior history of preterm birth (243). Changes uncovered by these targeted studies include tyrosine-protein kinase Met (*MET*), Neuregulin 3 (*NRG3*), and serotonin transporter (*SLC6A4*). A great deal can also be learned from comparing findings from studies of NDDs and studies of prematurity and EoP. For NDDs, there are numerous genes associated with synapse formation identified from GWAS studies including Shanks, Neuroregulin, Neurexin, and Contactins [reviewed by (244, 245)]. Many of these genes also associate with preterm birth or outcomes after preterm birth. Of note, neuregulin is found associated with infant outcome, with polymorphisms increasing mRNA levels in patients associated with better outcomes in babies born preterm (246).

A key vulnerable neuronal subpopulation in EoP is interneurons, although it is still unclear which populations are the most vulnerable at which time point and in what regions based on the human and preclinical studies (4, 42). Research into neuropathology in NDD, via post-mortem studies and animal models of NDD, also conclusively illustrates changes in interneurons (146). Quite strikingly, in a synaptic protein knockout model of ASD (PTEN KO), interneuron transplantation rescues social behavior deficits (247). This study also questions the established idea that interneuron deficits associate with NDDs due to negative effects on inhibitory circuit activation (248), as, although interneuron transplantation rescued the behavioral phenotype, there were no improvements in circuit function.

No discussion of the similarities between NDD and EoP could be complete with highlighting the shared common pathological process of neuroinflammation, which has, at its core, the aberrant activation of microglia. Indeed, across NDD and EoP models and human studies, evidence shows that microglial activities are altered [thoroughly reviewed in (22, 249–251)]. A chief function of microglia during development, but also throughout life, is regulation of connectivity via refinement of synaptic number [(252–254); and reviewed in (255–257)]. Based on all the evidence for the role of microglia and the presence of inflammation (both systemic and central) in EoP and NDD it is clear that microglia (and their effects on synapses and neurogenesis) are an important starting point in understanding GM pathology across NDDs and EoP and also a shared target for neurorepair.

We outlined above the reasons that EoP can be considered a synaptopathy, including genetic associations between injury severity and synaptic genes, connectivity deficits, and that preclinical studies show synaptic immaturity plus arborization deficits. These characteristics are also common among NDDs, and NDDs are clearly characterized as synaptopathies (258–261). For example, about half of the genes identified as candidate genes in people with ASD code synaptic proteins (262). Additionally, animal models of abnormal synaptic pruning induced by abnormal microglial function (227), or via genetic perturbation of synaptic structure (263), have cognitive and behavioral deficits reminiscent of NDDs. Thus, perhaps it is the collective change in these functional units of the neuron that give rise to the shared gross volumetric changes and pervasive behavioral problems in people with NDDs and due to EoP. Though it should also be said that a great many children and adults who were born preterm and who had EoP have typical neurodevelopmental profiles, potentially and interaction of genetics and environmental challenges in these case lead to structurally resilient synapses. There is clearly need for a better understanding of the vulnerabilities leading to NDDs and negative consequences after EoP.

CONCLUSIONS

Imaging and neuropathological studies indicate changes in GM are a subtle but substantial contributor to EoP. The full nature of this injury is probably only just being discovered and would benefit from more longitudinal MRI studies, with closer integration of both patient genetics data and neuropathology where possible. Given the link between GM injury and long-term cognitive and behavioral disorders, it is important to therapeutically target this injury, distinct from the WM injury aspects of EoP. In particular, while preterm birth and EoP increase the risk of NDD in later life, the current evidence suggests that preterm born infants may make up a specific subset of cases in these disorder spectrums and could benefit from a distinct treatment paradigm. In terms of what this therapeutic paradigm might look like, it is likely that a combination of ameliorating (e.g., anti-inflammatory or growth supporting) agents and restorative agents (e.g., drugs facilitating normal structural-functional development) will be required. If these treatments are delivered at optimal periods of brain development, it may be possible to limit the need for life-long symptom controlling medication. In this regard, it is necessary to focus more research on the synaptopathic aspects of EoP. Current research in this area is only the tip of the iceberg, particularly lacking in clinical studies, and increased understanding of the injury mechanisms and plasticity during the post-natal period may identify new therapeutic targets. Our great hope is actually that this proposed work becomes redundant. We hope that our highly skilled and motivated counterparts working on prediction and prevention of preterm birth have major breakthroughs. However, pragmatically, even major breakthroughs will take decades to make it across high and middle/low economic settings, meaning that millions more babies are going to need us to better understand the GM and its changes after EoP.

AUTHOR CONTRIBUTIONS

All authors listed have made a substantial, direct and intellectual contribution to the work, and approved it for publication.

FUNDING

The authors of this work are supported by grants from Sparks Children's Medical Research (15KCL05); King's Health Partners (R170506); the Medical Research Council (MR/K006355/1); Inserm, Université de Paris, Horizon 2020 Framework Program of the European Union (grant agreement no. 874721/PREMSTEM); Investissement d'Avenir (ANR-11-INBS-0011, NeurATRIS), Fondation de France; Fondation pour la Recherche sur le Cerveau, Fondation Grace de Monaco; Action Medical Research; the Australian National Health and Medical Research Council; and the Cerebral Palsy Alliance Research Foundation Australia. BF's research was also supported by a Vice Chancellor's Research Fellowship from RMIT University.

ACKNOWLEDGMENTS

We wish to acknowledge the support of the Department of Perinatal Imaging & Health, King's College London. In addition,

the authors acknowledge financial support from the National Institute for Health Research (NIHR) Biomedical Research Centre based at Guy's and St Thomas' NHS Foundation Trust and King's College London. The views expressed are those of the author(s) and not necessarily those of the NHS, the NIHR or the Department of Health.

REFERENCES

1. Volpe JJ. The encephalopathy of prematurity–brain injury and impaired brain development inextricably intertwined. *Semin Pediatr Neurol.* (2009) 16:167–78. doi: 10.1016/j.spen.2009.09.005
2. Kostovic I, Judas M, Petanjek Z, Simic G. Ontogenesis of goal-directed behavior: anatomo-functional considerations. *Int J Psychophysiol.* (1995) 19:85–102. doi: 10.1016/0167-8760(94)00081-O
3. Marin-Padilla M. Developmental neuropathology and impact of perinatal brain damage. II: white matter lesions of the neocortex. *J Neuropathol Exp Neurol.* (1997) 56:219–35. doi: 10.1097/00005072-199703000-00001
4. Panda S, Dohare P, Jain S, Parikh N, Singla P, Mehdizadeh R, et al. Estrogen treatment reverses prematurity-induced disruption in cortical interneuron population. *J Neurosci.* (2018) 38:7378–91. doi: 10.1523/JNEUROSCI.0478-18.2018
5. Marlow N, Wolke D, Bracewell MA, Samara M, Group EPS. Neurologic and developmental disability at six years of age after extremely preterm birth. *N Engl J Med.* (2005) 352:9–19. doi: 10.1056/NEJMoa041367
6. O'Shea TM, Allred EN, Dammann O, Hirtz D, Kuban KC, Paneth N, et al. The ELGAN study of the brain and related disorders in extremely low gestational age newborns. *Early Hum Dev.* (2009) 85:719–25. doi: 10.1016/j.earlhumdev.2009.08.060
7. Pierrat V, Marchand-Martin L, Arnaud C, Kaminski M, Resche-Rigon M, Lebeaux C, et al. Neurodevelopmental outcome at 2 years for preterm children born at 22 to 34 weeks' gestation in France in 2011: EPIPAGE-2 cohort study. *BMJ.* (2017) 358:j3448. doi: 10.1136/bmj.j3448
8. Hirschberger RG, Kuban KCK, O'Shea TM, Joseph RM, Heeren T, Douglass LM, et al. Co-occurrence and severity of neurodevelopmental burden (cognitive impairment, cerebral palsy, autism spectrum disorder, and epilepsy) at age ten years in children born extremely preterm. *Pediatr Neurol.* (2018) 79:45–52. doi: 10.1016/j.pediatrneurol.2017.11.002
9. Johnson S, Hollis C, Kochhar P, Hennessy E, Wolke D, Marlow N. Psychiatric disorders in extremely preterm children: longitudinal finding at age 11 years in the EPICure study. *J Am Acad Child Adolesc Psychiatry.* (2010) 49:453–63 e451. doi: 10.1097/00004583-201005000-00006
10. Heeren T, Joseph RM, Allred EN, O'Shea TM, Leviton A, Kuban KCK. Cognitive functioning at the age of 10 years among children born extremely preterm: a latent profile approach. *Pediatr Res.* (2017) 82:614–9. doi: 10.1038/pr.2017.82
11. Thomason ME, Scheinost D, Manning JH, Grove LE, Hect J, Marshall N, et al. Weak functional connectivity in the human fetal brain prior to preterm birth. *Sci Rep.* (2017) 7:39286. doi: 10.1038/srep39286
12. Nunthapiwat S, Sekararithi R, Wanapirak C, Sirichotiyakul S, Tongprasert F, Srisupundit K, et al. Second trimester serum biomarker screen for fetal aneuploidies as a predictor of preterm delivery: a population-based study. *Gynecol Obstet Invest.* (2019) 84:326–33. doi: 10.1159/000495614
13. Souza RT, McKenzie EJ, Jones B, de Seymour JV, Thomas MM, Zarate E, et al. Trace biomarkers associated with spontaneous preterm birth from the maternal serum metabolome of asymptomatic nulliparous women–parallel case-control studies from the SCOPE cohort. *Sci Rep.* (2019) 9:13701. doi: 10.1038/s41598-019-50252-7
14. Leow SM, Di Quinzio MKW, Ng ZL, Grant C, Amitay T, Wei Y, et al. Preterm birth prediction in asymptomatic women at mid-gestation using a panel of novel protein biomarkers: the Prediction of PreTerm Labor (PPeTaL) study. *Am J Obstet Gynecol.* (2020) 2:100084. doi: 10.1016/j.ajogmf.2019.100084
15. Ananth CV, Vintzileos AM. Medically indicated preterm birth: recognizing the importance of the problem. *Clin Perinatol.* (2008) 35:53–67, viii. doi: 10.1016/j.clp.2007.11.001
16. Gilles F, Gressens P, Dammann O, Leviton A. Hypoxia-ischemia is not an antecedent of most preterm brain damage: the illusion of validity. *Dev Med Child Neurol.* (2018) 60:120–5. doi: 10.1111/dmcn.13483
17. Kaga N, Katsuki Y, Obata M, Shibutani Y. Repeated administration of low-dose lipopolysaccharide induces preterm delivery in mice: a model for human preterm parturition and for assessment of the therapeutic ability of drugs against preterm delivery. *Am J Obstet Gynecol.* (1996) 174:754–9. doi: 10.1016/S0002-9378(96)70460-X
18. Romero R, Gomez R, Chaiworapongsa T, Conoscenti G, Kim JC, Kim YM. The role of infection in preterm labour and delivery. *Paediatr Perinat Epidemiol.* (2001) 15:41–56. doi: 10.1046/j.1365-3016.2001.00007.x
19. Fidel P, Ghezzi F, Romero R, Chaiworapongsa T, Espinoza J, Cutright J, et al. The effect of antibiotic therapy on intrauterine infection-induced preterm parturition in rabbits. *J Matern Fetal Neonat Med.* (2003) 14:57–64. doi: 10.1080/jmf.14.1.57.64
20. Dammann O, Leviton A. Maternal intrauterine infection, cytokines, and brain damage in the preterm newborn. *Pediatr Res.* (1997) 42:1–8. doi: 10.1203/00006450-199707000-00001
21. Lau J, Magee F, Qiu Z, Hoube J, Von Dadelszen P, Lee SK. Chorioamnionitis with a fetal inflammatory response is associated with higher neonatal mortality, morbidity, and resource use than chorioamnionitis displaying a maternal inflammatory response only. *Am J Obstet Gynecol.* (2005) 193:708–13. doi: 10.1016/j.ajog.2005.01.017
22. Hagberg H, Mallard C, Ferriero DM, Vannucci SJ, Levison SW, Vexler ZS, et al. The role of inflammation in perinatal brain injury. *Nat Rev Neurol.* (2015) 11:192–208. doi: 10.1038/nrneurol.2015.13
23. Kuban KC, O'Shea TM, Allred EN, Fichorova RN, Heeren T, Paneth N, et al. The breadth and type of systemic inflammation and the risk of adverse neurological outcomes in extremely low gestation newborns. *Pediatr Neurol.* (2015) 52:42–8. doi: 10.1016/j.pediatrneurol.2014.10.005
24. Bouyssi-Kobar M, du Plessis AJ, McCarter R, Brossard-Racine M, Murnick J, Tinkleman L, et al. Third trimester brain growth in preterm infants compared with *in utero* healthy fetuses. *Pediatrics.* (2016) 138:e20161640. doi: 10.1542/peds.2016-1640
25. Wellmann S, Buhrer C, Schmitz T. Focal necrosis and disturbed myelination in the white matter of newborn infants: a tale of too much or too little oxygen. *Front Pediatr.* (2014) 2:143. doi: 10.3389/fped.2014.00143
26. Manley BJ, Owen LS, Hooper SB, Jacobs SE, Cheong JLY, Doyle LW, et al. Towards evidence-based resuscitation of the newborn infant. *Lancet.* (2017) 389:1639–48. doi: 10.1016/S0140-6736(17)30547-0
27. Shaw JC, Berry MJ, Dyson RM, Crombie GK, Hirst JJ, Palliser HK. Reduced neurosteroid exposure following preterm birth and its' contribution to neurological impairment: a novel avenue for preventative therapies. *Front Physiol.* (2019) 10:599. doi: 10.3389/fphys.2019.00599
28. Hunt R, Davis PG, Inder T. Replacement of estrogens and progestins to prevent morbidity and mortality in preterm infants. *Cochrane Database Syst Rev.* (2004) CD003848. doi: 10.1002/14651858.CD003848.pub2
29. Tibrewal M, Cheng B, Dohare P, Hu F, Mehdizadeh R, Wang P, et al. Disruption of interneuron neurogenesis in premature newborns and reversal with estrogen treatment. *J Neurosci.* (2018) 38:1100–13. doi: 10.1523/JNEUROSCI.1875-17.2017
30. Klebe D, Tibrewal M, Sharma DR, Vanaparthy R, Krishna S, Varghese M, et al. Reduced hippocampal dendrite branching, spine density and neurocognitive function in premature rabbits, and reversal with estrogen or TrkB agonist treatment. *Cereb Cortex.* (2019) 29:4932–47. doi: 10.1093/cercor/bhz033
31. Vottier G, Pham H, Pansiot J, Biran V, Gressens P, Charriaut-Marlangue C, et al. Deleterious effect of hyperoxia at birth on white matter damage in the newborn rat. *Dev Neurosci.* (2011) 33:261–9. doi: 10.1159/000327245

32. Schmitz T, Endesfelder S, Reinert MC, Klinker F, Muller S, Buhrer C, et al. Adolescent hyperactivity and impaired coordination after neonatal hyperoxia. *Exp Neurol.* (2012) 235:374–9. doi: 10.1016/j.expneurol.2012.03.002
33. Scheuer T, Brockmoller V, Blanco Knowlton M, Weitkamp JH, Ruhwedel T, Mueller S, et al. Oligodendroglial maldevelopment in the cerebellum after postnatal hyperoxia and its prevention by minocycline. *Glia.* (2015) 63:1825–39. doi: 10.1002/glia.22847
34. Banks WA, Kastin AJ, Broadwell RD. Passage of cytokines across the blood-brain barrier. *Neuroimmunomodulation.* (1995) 2:241–8. doi: 10.1159/000097202
35. Verma S, Nakaoke R, Dohgu S, Banks WA. Release of cytokines by brain endothelial cells: a polarized response to lipopolysaccharide. *Brain Behav Immun.* (2006) 20:449–55. doi: 10.1016/j.bbi.2005.10.005
36. Stolp HB, Turnquist C, Dziegielewska KM, Saunders NR, Anthony DC, Molnar Z. Reduced ventricular proliferation in the foetal cortex following maternal inflammation in the mouse. *Brain.* (2011) 134:3236–48. doi: 10.1093/brain/awr237
37. Pang Y, Dai X, Roller A, Carter K, Paul I, Bhatt AJ, et al. Early postnatal lipopolysaccharide exposure leads to enhanced neurogenesis and impaired communicative functions in rats. *PLoS ONE.* (2016) 11:e0164403. doi: 10.1371/journal.pone.0164403
38. Sato K. Effects of microglia on neurogenesis. *Glia.* (2015) 63:1394–405. doi: 10.1002/glia.22858
39. Fan L-W, Pang Y. Dysregulation of neurogenesis by neuroinflammation: key differences in neurodevelopmental and neurological disorders. *Neural Regen Res.* (2017) 12:366–71. doi: 10.4103/1673-5374.202926
40. Prins JR, Eskandar S, Eggen BJL, Scherjon SA. Microglia, the missing link in maternal immune activation and fetal neurodevelopment; and a possible link in preeclampsia and disturbed neurodevelopment? *J Reprod Immunol.* (2018) 126:18–22. doi: 10.1016/j.jri.2018.01.004
41. Malik S, Vinukonda G, Vose LR, Diamond D, Bhimavarapu BB, Hu F, et al. Neurogenesis continues in the third trimester of pregnancy and is suppressed by premature birth. *J Neurosci.* (2013) 33:411–23. doi: 10.1523/JNEUROSCI.4445-12.2013
42. Stolp HB, Fleiss B, Arai Y, Supramaniam V, Vontell R, Birtles S, et al. Interneuron Development is disrupted in preterm brains with diffuse white matter injury: observations in mouse and human. *Front Physiol.* (2019) 10:955. doi: 10.3389/fphys.2019.00955
43. Mallard C, Tremblay ME, Vexler ZS. Microglia and neonatal brain injury. *Neuroscience.* (2019) 405:68–76. doi: 10.1016/j.neuroscience.2018.01.023
44. McNamara NB, Miron VE. Microglia in developing white matter and perinatal brain injury. *Neurosci Lett.* (2020) 714:134539. doi: 10.1016/j.neulet.2019.134539
45. Dommergues MA, Plaisant F, Verney C, Gressens P. Early microglial activation following neonatal excitotoxic brain damage in mice: a potential target for neuroprotection. *Neuroscience.* (2003) 121:619–28. doi: 10.1016/S0306-4522(03)00558-X
46. Van Steenwinckel J, Schang AL, Krishnan ML, Degos V, Delahaye-Duriez A, Bokobza C, et al. Decreased microglial Wnt/β-catenin signalling drives microglial pro-inflammatory activation in the developing brain. *Brain.* (2019) 142:3806–33. doi: 10.1093/brain/awz319
47. Faustino JV, Wang X, Johnson CE, Klibanov A, Derugin N, Wendland MF, et al. Microglial cells contribute to endogenous brain defenses after acute neonatal focal stroke. *J Neurosci.* (2011) 31:12992–3001. doi: 10.1523/JNEUROSCI.2102-11.2011
48. Fernández-López D, Faustino J, Klibanov AL, Derugin N, Blanchard E, Simon F, et al. Microglial cells prevent hemorrhage in neonatal focal arterial stroke. *J Neurosci.* (2016) 36:2881. doi: 10.1523/JNEUROSCI.0140-15.2016
49. Lafemina MJ, Sheldon RA, Ferriero DM. Acute hypoxia-ischemia results in hydrogen peroxide accumulation in neonatal but not adult mouse brain. *Pediatr Res.* (2006) 59:680–3. doi: 10.1203/01.pdr.0000214891.35363.6a
50. Gao Z, Tsirka SE. Animal models of MS reveal multiple roles of microglia in disease pathogenesis. *Neurol Res Int.* (2011) 2011:383087. doi: 10.1155/2011/383087
51. Pang Y, Campbell L, Zheng B, Fan L, Cai Z, Rhodes P. Lipopolysaccharide-activated microglia induce death of oligodendrocyte progenitor cells and impede their development. *Neuroscience.* (2010) 166:464–75. doi: 10.1016/j.neuroscience.2009.12.040
52. Favrais G, van de Looij Y, Fleiss B, Ramanantsoa N, Bonnin P, Stoltenburg-Didinger G, et al. Systemic inflammation disrupts the developmental program of white matter. *Ann Neurol.* (2011) 70:550–65. doi: 10.1002/ana.22489
53. Scafidi J, Hammond TR, Scafidi S, Ritter J, Jablonska B, Roncal M, et al. Intranasal epidermal growth factor treatment rescues neonatal brain injury. *Nature.* (2014) 506:230–4. doi: 10.1038/nature12880
54. Xie D, Shen F, He S, Chen M, Han Q, Fang M, et al. IL-1beta induces hypomyelination in the periventricular white matter through inhibition of oligodendrocyte progenitor cell maturation via FYN/MEK/ERK signaling pathway in septic neonatal rats. *Glia.* (2016) 64:583–602. doi: 10.1002/glia.22950
55. Ramlackhansingh AF, Brooks DJ, Greenwood RJ, Bose SK, Turkheimer FE, Kinnunen KM, et al. Inflammation after trauma: microglial activation and traumatic brain injury. *Ann Neurol.* (2011) 70:374–83. doi: 10.1002/ana.22455
56. Loane DJ, Kumar A, Stoica BA, Cabatbat R, Faden AI. Progressive neurodegeneration after experimental brain trauma: association with chronic microglial activation. *J Neuropathol Exp Neurol.* (2014) 73:14–29. doi: 10.1097/NEN.0000000000000021
57. Mattei D, Ivanov A, Ferrai C, Jordan P, Guneykaya D, Buonfiglioli A, et al. Maternal immune activation results in complex microglial transcriptome signature in the adult offspring that is reversed by minocycline treatment. *Transl Psychiatry.* (2017) 7:e1120. doi: 10.1038/tp.2017.80
58. Frost PS, Barros-Aragao F, da Silva RT, Venancio A, Matias I, Lyra ESNM, et al. Neonatal infection leads to increased susceptibility to Abeta oligomer-induced brain inflammation, synapse loss and cognitive impairment in mice. *Cell Death Dis.* (2019) 10:323. doi: 10.1038/s41419-019-1529-x
59. Lawson LJ, Perry VH, Dri P, Gordon S. Heterogeneity in the distribution and morphology of microglia in the normal adult mouse brain. *Neuroscience.* (1990) 39:151–70. doi: 10.1016/0306-4522(90)90229-W
60. Hart AD, Wyttenbach A, Perry VH, Teeling JL. Age related changes in microglial phenotype vary between CNS regions: grey versus white matter differences. *Brain Behav Immun.* (2012) 26:754–65. doi: 10.1016/j.bbi.2011.11.006
61. Verderio C, Muzio L, Turola E, Bergami A, Novellino L, Ruffini F, et al. Myeloid microvesicles are a marker and therapeutic target for neuroinflammation. *Ann Neurol.* (2012) 72:610–24. doi: 10.1002/ana.23627
62. Lener T, Gimona M, Aigner L, Borger V, Buzas E, Camussi G, et al. Applying extracellular vesicles based therapeutics in clinical trials–an ISEV position paper. *J Extracell Vesicles.* (2015) 4:30087. doi: 10.3402/jev.v4.30087
63. Back SA, Miller SP. Brain injury in premature neonates: a primary cerebral dysmaturation disorder? *Ann Neurol.* (2014) 75:469–86. doi: 10.1002/ana.24132
64. Shiow LR, Favrais G, Schirmer L, Schang AL, Cipriani S, Andres C, et al. Reactive astrocyte COX2-PGE2 production inhibits oligodendrocyte maturation in neonatal white matter injury. *Glia.* (2017) 65:2024–37. doi: 10.1002/glia.23212
65. Preston M, Gong X, Su W, Matsumoto SG, Banine F, Winkler C, et al. Digestion products of the PH20 hyaluronidase inhibit remyelination. *Ann Neurol.* (2013) 73:266–80. doi: 10.1002/ana.23788
66. Wang Y, Cheng X, He Q, Zheng Y, Kim DH, Whittemore SR, et al. Astrocytes from the contused spinal cord inhibit oligodendrocyte differentiation of adult oligodendrocyte precursor cells by increasing the expression of bone morphogenetic proteins. *J Neurosci.* (2011) 31:6053. doi: 10.1523/JNEUROSCI.5524-09.2011
67. Hammond TR, Gadea A, Dupree J, Kerninon C, Nait-Oumesmar B, Aguirre A, et al. Astrocyte-Derived Endothelin-1 Inhibits Remyelination through Notch Activation. *Neuron.* (2014) 81:588–602. doi: 10.1016/j.neuron.2013.11.015
68. Gelot A, Villapol S, Billette de Villemeur T, Renolleau S, Charriaut-Marlangue C. Astrocytic demise in the developing rat and human brain after hypoxic-ischemic damage. *Dev Neurosci.* (2009) 31:459–70. doi: 10.1159/000232564

69. Verney C, Pogledic I, Biran V, Adle-Biassette H, Fallet-Bianco C, Gressens P. Microglial reaction in axonal crossroads is a hallmark of noncystic periventricular white matter injury in very preterm infants. *J Neuropathol Exp Neurol.* (2012) 71:251–64. doi: 10.1097/NEN.0b013e3182496429
70. Tahraoui SL, Marret S, Bodenant C, Leroux P, Dommergues MA, Evrard P, et al. Central role of microglia in neonatal excitotoxic lesions of the murine periventricular white matter. *Brain Pathol.* (2001) 11:56–71. doi: 10.1111/j.1750-3639.2001.tb00381.x
71. Roessmann U, Gambetti P. Astrocytes in the developing human brain. *Acta Neuropathol.* (1986) 70:308–13. doi: 10.1007/BF00686089
72. Pierson CR, Folkerth RD, Billiards SS, Trachtenberg FL, Drinkwater ME, Volpe JJ, et al. Gray matter injury associated with periventricular leukomalacia in the premature infant. *Acta Neuropathol.* (2007) 114:619–31. doi: 10.1007/s00401-007-0295-5
73. Sullivan SM, Bjorkman ST, Miller SM, Colditz PB, Pow DV. Structural remodeling of gray matter astrocytes in the neonatal pig brain after hypoxia/ischemia. *Glia.* (2010) 58:181–94. doi: 10.1002/glia.20911
74. Sidman RL, Rakic P. Neuronal migration, with special reference to developing human brain: a review. *Brain Res.* (1973) 62:1–35. doi: 10.1016/0006-8993(73)90617-3
75. Marin O. Cellular and molecular mechanisms controlling the migration of neocortical interneurons. *Eur J Neurosci.* (2013) 38:2019–29. doi: 10.1111/ejn.12225
76. Huttenlocher PR. Synaptic density in human frontal cortex–developmental changes and effects of aging. *Brain Res.* (1979) 163:195–205. doi: 10.1016/0006-8993(79)90349-4
77. Kilb W, Kirischuk S, Luhmann HJ. Electrical activity patterns and the functional maturation of the neocortex. *Eur J Neurosci.* (2011) 34:1677–86. doi: 10.1111/j.1460-9568.2011.07878.x
78. Molnar Z, Clowry GJ, Sestan N, Alzu'bi A, Bakken T, Hevner RF, et al. New insights into the development of the human cerebral cortex. *J Anat.* (2019) 235:432–51. doi: 10.1111/joa.13055
79. Volpe JJ. Dysmaturation of premature brain: importance, cellular mechanisms, and potential interventions. *Pediatr Neurol.* (2019) 95:42–66. doi: 10.1016/j.pediatrneurol.2019.02.016
80. Armstrong E, Schleicher A, Omran H, Curtis M, Zilles K. The ontogeny of human gyrification. *Cereb Cortex.* (1995) 5:56–63. doi: 10.1093/cercor/5.1.56
81. Neil JJ, Shiran SI, McKinstry RC, Schefft GL, Snyder AZ, Almli CR, et al. Normal brain in human newborns: apparent diffusion coefficient and diffusion anisotropy measured by using diffusion tensor MR imaging. *Radiology.* (1998) 209:57–66. doi: 10.1148/radiology.209.1.9769812
82. McKinstry RC, Mathur A, Miller JH, Ozcan A, Snyder AZ, Schefft GL, et al. Radial organization of developing preterm human cerebral cortex revealed by non-invasive water diffusion anisotropy MRI. *Cereb Cortex.* (2002) 12:1237–43. doi: 10.1093/cercor/12.12.1237
83. Batalle D, O'Muircheartaigh J, Makropoulos A, Kelly CJ, Dimitrova R, Hughes EJ, et al. Different patterns of cortical maturation before and after 38 weeks gestational age demonstrated by diffusion MRI *in vivo*. *Neuroimage.* (2019) 185:764–75. doi: 10.1016/j.neuroimage.2018.05.046
84. Lodygensky GA, Vasung L, Sizonenko SV, Huppi PS. Neuroimaging of cortical development and brain connectivity in human newborns and animal models. *J Anat.* (2010) 217:418–28. doi: 10.1111/j.1469-7580.2010.01280.x
85. Stolp HB, Ball G, So PW, Tournier JD, Jones M, Thornton C, et al. Voxel-wise comparisons of cellular microstructure and diffusion-MRI in mouse hippocampus using 3D bridging of optically-clear histology with neuroimaging data (3D-BOND). *Sci Rep.* (2018) 8:4011. doi: 10.1038/s41598-018-22295-9
86. Rathbone R, Counsell SJ, Kapellou O, Dyet L, Kennea N, Hajnal J, et al. Perinatal cortical growth and childhood neurocognitive abilities. *Neurology.* (2011) 77:1510–7. doi: 10.1212/WNL.0b013e318233b215
87. Boardman JP, Counsell SJ, Rueckert D, Kapellou O, Bhatia KK, Aljabar P, et al. Abnormal deep grey matter development following preterm birth detected using deformation-based morphometry. *Neuroimage.* (2006) 32:70–8. doi: 10.1016/j.neuroimage.2006.03.029
88. Ajayi-Obe M, Saeed N, Cowan FM, Rutherford MA, Edwards AD. Reduced development of cerebral cortex in extremely preterm infants. *Lancet.* (2000) 356:1162–3. doi: 10.1016/S0140-6736(00)02761-6
89. Makropoulos A, Aljabar P, Wright R, Huning B, Merchant N, Arichi T, et al. Regional growth and atlasing of the developing human brain. *Neuroimage.* (2016) 125:456–78. doi: 10.1016/j.neuroimage.2015.10.047
90. Inder TE, Huppi PS, Warfield S, Kikinis R, Zientara GP, Barnes PD, et al. Periventricular white matter injury in the premature infant is followed by reduced cerebral cortical gray matter volume at term. *Ann Neurol.* (1999) 46:755–60. doi: 10.1002/1531-8249(199911)46:5<755::AID-ANA11>3.0.CO;2-0
91. Zubiaurre-Elorza L, Soria-Pastor S, Junque C, Segarra D, Bargallo N, Mayolas N, et al. Gray matter volume decrements in preterm children with periventricular leukomalacia. *Pediatr Res.* (2011) 69:554–60. doi: 10.1203/PDR.0b013e3182182366
92. Zhang Y, Inder TE, Neil JJ, Dierker DL, Alexopoulos D, Anderson PJ, et al. Cortical structural abnormalities in very preterm children at 7 years of age. *Neuroimage.* (2015) 109:469–79. doi: 10.1016/j.neuroimage.2015.01.005
93. Nosarti C, Al-Asady MH, Frangou S, Stewart AL, Rifkin L, Murray RM. Adolescents who were born very preterm have decreased brain volumes. *Brain.* (2002) 125:1616–23. doi: 10.1093/brain/awf157
94. Nosarti C, Giouroukou E, Healy E, Rifkin L, Walshe M, Reichenberg A, et al. Grey and white matter distribution in very preterm adolescents mediates neurodevelopmental outcome. *Brain.* (2008) 131:205–17. doi: 10.1093/brain/awm282
95. Ball G, Boardman JP, Rueckert D, Aljabar P, Arichi T, Merchant N, et al. The effect of preterm birth on thalamic and cortical development. *Cereb Cortex.* (2012) 22:1016–24. doi: 10.1093/cercor/bhr176
96. Bjuland KJ, Rimol LM, Lohaugen GC, Skranes J. Brain volumes and cognitive function in very-low-birth-weight (VLBW) young adults. *Eur J Paediatr Neurol.* (2014) 18:578–90. doi: 10.1016/j.ejpn.2014.04.004
97. Ball G, Pazderova L, Chew A, Tusor N, Merchant N, Arichi T, et al. Thalamocortical connectivity predicts cognition in children born preterm. *Cereb Cortex.* (2015) 25:4310–8. doi: 10.1093/cercor/bhu331
98. Bora S, Pritchard VE, Chen Z, Inder TE, Woodward LJ. Neonatal cerebral morphometry and later risk of persistent inattention/hyperactivity in children born very preterm. *J Child Psychol Psychiatry.* (2014) 55:828–38. doi: 10.1111/jcpp.12200
99. Rogers CE, Barch DM, Sylvester CM, Pagliaccio D, Harms MP, Botteron KN, et al. Altered gray matter volume and school age anxiety in children born late preterm. *J Pediatr.* (2014) 165:928–35. doi: 10.1016/j.jpeds.2014.06.063
100. Ure AM, Treyvaud K, Thompson DK, Pascoe L, Roberts G, Lee KJ, et al. Neonatal brain abnormalities associated with autism spectrum disorder in children born very preterm. *Autism Res.* (2016) 9:543–52. doi: 10.1002/aur.1558
101. Jantzie LL, Robinson S. Preclinical models of encephalopathy of prematurity. *Dev Neurosci.* (2015) 37:277–88. doi: 10.1159/000371721
102. Dean JM, van de Looij Y, Sizonenko SV, Lodygensky GA, Lazeyras F, Bolouri H, et al. Delayed cortical impairment following lipopolysaccharide exposure in preterm fetal sheep. *Ann Neurol.* (2011) 70:846–56. doi: 10.1002/ana.22480
103. Dean JM, McClendon E, Hansen K, Azimi-Zonooz A, Chen K, Riddle A, et al. Prenatal cerebral ischemia disrupts MRI-defined cortical microstructure through disturbances in neuronal arborization. *Sci Transl Med.* (2013) 5:168ra167. doi: 10.1126/scitranslmed.3004669
104. Crum WR, Sawiak SJ, Chege W, Cooper JD, Williams SCR, Vernon AC. Evolution of structural abnormalities in the rat brain following *in utero* exposure to maternal immune activation: a longitudinal *in vivo* MRI study. *Brain Behav Immun.* (2017) 63:50–9. doi: 10.1016/j.bbi.2016.12.008
105. Engelhardt E, Inder TE, Alexopoulos D, Dierker DL, Hill J, Van Essen D, et al. Regional impairments of cortical folding in premature infants. *Ann Neurol.* (2015) 77:154–62. doi: 10.1002/ana.24313
106. Kersbergen KJ, Makropoulos A, Aljabar P, Groenendaal F, de Vries LS, Counsell SJ, et al. Longitudinal regional brain development and clinical risk factors in extremely preterm infants. *J Pediatr.* (2016) 178:93–100 e106. doi: 10.1016/j.jpeds.2016.08.024

107. Wolosin SM, Richardson ME, Hennessey JG, Denckla MB, Mostofsky SH. Abnormal cerebral cortex structure in children with ADHD. *Hum Brain Mapp*. (2009) 30:175–84. doi: 10.1002/hbm.20496
108. Kohli JS, Kinnear MK, Fong CH, Fishman I, Carper RA, Muller RA. Local cortical gyrification is increased in children with autism spectrum disorders, but decreases rapidly in adolescents. *Cereb Cortex*. (2019) 29:2412–23. doi: 10.1093/cercor/bhy111
109. Kohli JS, Kinnear MK, Martindale IA, Carper RA, Muller RA. Regionally decreased gyrification in middle-aged adults with autism spectrum disorders. *Neurology*. (2019) 93:e1900–5. doi: 10.1212/WNL.0000000000008478
110. Libero LE, Schaer M, Li DD, Amaral DG, Nordahl CW. A longitudinal study of local gyrification index in young boys with autism spectrum disorder. *Cereb Cortex*. (2019) 29:2575–87. doi: 10.1093/cercor/bhy126
111. Bayly PV, Taber LA, Kroenke CD. Mechanical forces in cerebral cortical folding: a review of measurements and models. *J Mech Behav Biomed Mater*. (2014) 29:568–81. doi: 10.1016/j.jmbbm.2013.02.018
112. Striedter GF, Srinivasan S, Monuki ES. Cortical folding: when, where, how, and why? *Annu Rev Neurosci*. (2015) 38:291–307. doi: 10.1146/annurev-neuro-071714-034128
113. Llinares-Benadero C, Borrell V. Deconstructing cortical folding: genetic, cellular and mechanical determinants. *Nat Rev Neurosci*. (2019) 20:161–76. doi: 10.1038/s41583-018-0112-2
114. Quezada S, Castillo-Melendez M, Walker DW, Tolcos M. Development of the cerebral cortex and the effect of the intrauterine environment. *J Physiol*. (2018) 596:5665–74. doi: 10.1113/JP277151
115. Garcia KE, Robinson EC, Alexopoulos D, Dierker DL, Glasser MF, Coalson TS, et al. Dynamic patterns of cortical expansion during folding of the preterm human brain. *Proc Natl Acad Sci USA*. (2018) 115:3156–61. doi: 10.1073/pnas.1715451115
116. Van Essen DC, Donahue CJ, Coalson TS, Kennedy H, Hayashi T, Glasser MF. Cerebral cortical folding, parcellation, and connectivity in humans, nonhuman primates, and mice. *Proc Natl Acad Sci USA*. (2019) 116:26173–80. doi: 10.1073/pnas.1902299116
117. Long KR, Newland B, Florio M, Kalebic N, Langen B, Kolterer A, et al. Extracellular matrix components HAPLN1, lumican, and collagen I cause hyaluronic acid-dependent folding of the developing human neocortex. *Neuron*. (2018) 99:702–19 e706. doi: 10.1016/j.neuron.2018.07.013
118. Buser JR, Maire J, Riddle A, Gong X, Nguyen T, Nelson K, et al. Arrested preoligodendrocyte maturation contributes to myelination failure in premature infants. *Ann Neurol*. (2012) 71:93–109. doi: 10.1002/ana.22627
119. Andiman SE, Haynes RL, Trachtenberg FL, Billiards SS, Folkerth RD, Volpe JJ, et al. The cerebral cortex overlying periventricular leukomalacia: analysis of pyramidal neurons. *Brain Pathol*. (2010) 20:803–14. doi: 10.1111/j.1750-3639.2010.00380.x
120. Haynes RL, van Leyen K. 12/15-lipoxygenase expression is increased in oligodendrocytes and microglia of periventricular leukomalacia. *Dev Neurosci*. (2013) 35:140–54. doi: 10.1159/000350230
121. Haynes RL, Billiards SS, Borenstein NS, Volpe JJ, Kinney HC. Diffuse axonal injury in periventricular leukomalacia as determined by apoptotic marker fractin. *Pediatr Res*. (2008) 63:656–61. doi: 10.1203/PDR.0b013e31816c825c
122. Ligam P, Haynes RL, Folkerth RD, Liu L, Yang M, Volpe JJ, et al. Thalamic damage in periventricular leukomalacia: novel pathologic observations relevant to cognitive deficits in survivors of prematurity. *Pediatr Res*. (2009) 65:524–9. doi: 10.1203/PDR.0b013e3181998baf
123. Kinney HC, Haynes RL, Xu G, Andiman SE, Folkerth RD, Sleeper LA, et al. Neuron deficit in the white matter and subplate in periventricular leukomalacia. *Ann Neurol*. (2012) 71:397–406. doi: 10.1002/ana.22612
124. Haldipur P, Bharti U, Alberti C, Sarkar C, Gulati G, Iyengar S, et al. Preterm delivery disrupts the developmental program of the cerebellum. *PLoS ONE*. (2011) 6:e23449. doi: 10.1371/journal.pone.0023449
125. Vontell R, Supramaniam V, Wyatt-Ashmead J, Gressens P, Rutherford M, Hagberg H, et al. Cellular mechanisms of toll-like receptor-3 activation in the thalamus are associated with white matter injury in the developing brain. *J Neuropathol Exp Neurol*. (2015) 74:273–85. doi: 10.1097/NEN.0000000000000172
126. Pogledic I, Kostovic I, Fallet-Bianco C, Adle-Biassette H, Gressens P, Verney C. Involvement of the subplate zone in preterm infants with periventricular white matter injury. *Brain Pathol*. (2014) 24:128–41. doi: 10.1111/bpa.12096
127. Haynes RL, Folkerth RD, Keefe RJ, Sung I, Swzeda LI, Rosenberg PA, et al. Nitrosative and oxidative injury to premyelinating oligodendrocytes in periventricular leukomalacia. *J Neuropathol Exp Neurol*. (2003) 62:441–50. doi: 10.1093/jnen/62.5.441
128. Ancel PY, Livinec F, Larroque B, Marret S, Arnaud C, Pierrat V, et al. Cerebral palsy among very preterm children in relation to gestational age and neonatal ultrasound abnormalities: the EPIPAGE cohort study. *Pediatrics*. (2006) 117:828–35. doi: 10.1542/peds.2005-0091
129. McQuillen PS, Sheldon RA, Shatz CJ, Ferriero DM. Selective vulnerability of subplate neurons after early neonatal hypoxia-ischemia. *J Neurosci*. (2003) 23:3308–15. doi: 10.1523/JNEUROSCI.23-08-03308.2003
130. Okusa C, Oeschger F, Ginet V, Wang WZ, Hoerder-Suabedissen A, Matsuyama T, et al. Subplate in a rat model of preterm hypoxia-ischemia. *Ann Clin Transl Neurol*. (2014) 1:679–91. doi: 10.1002/acn3.97
131. Goni-de-Cerio F, Alvarez A, Caballero A, Mielgo VE, Alvarez FJ, Rey-Santano MC, et al. Early cell death in the brain of fetal preterm lambs after hypoxic-ischemic injury. *Brain Res*. (2007) 1151:161–71. doi: 10.1016/j.brainres.2007.03.013
132. McClendon E, Chen K, Gong X, Sharifnia E, Hagen M, Cai V, et al. Prenatal cerebral ischemia triggers dysmaturation of caudate projection neurons. *Ann Neurol*. (2014) 75:508–24. doi: 10.1002/ana.24100
133. McClendon E, Shaver DC, Degener-O'Brien K, Gong X, Nguyen T, Hoerder-Suabedissen A, et al. Transient hypoxemia chronically disrupts maturation of preterm fetal ovine subplate neuron arborization and activity. *J Neurosci*. (2017) 37:11912–29. doi: 10.1523/JNEUROSCI.2396-17.2017
134. Ardalan M, Svedin P, Baburamani AA, Supramaniam VG, Ek J, Hagberg H, et al. Dysmaturation of somatostatin interneurons following umbilical cord occlusion in preterm fetal sheep. *Front Physiol*. (2019) 10:563. doi: 10.3389/fphys.2019.00563
135. Fowke TM, Galinsky R, Davidson JO, Wassink G, Karunasinghe RN, Prasad JD, et al. Loss of interneurons and disruption of perineuronal nets in the cerebral cortex following hypoxia-ischaemia in near-term fetal sheep. *Sci Rep*. (2018) 8:17686. doi: 10.1038/s41598-018-36083-y
136. McClendon E, Wang K, Degener-O'Brien K, Hagen MW, Gong X, Nguyen T, et al. Transient hypoxemia disrupts anatomical and functional maturation of preterm fetal ovine CA1 pyramidal neurons. *J Neurosci*. (2019) 39:7853–71. doi: 10.1523/JNEUROSCI.1364-19.2019
137. Dieni S, Inder T, Yoder B, Briscoe T, Camm E, Egan G, et al. The pattern of cerebral injury in a primate model of preterm birth and neonatal intensive care. *J Neuropathol Exp Neurol*. (2004) 63:1297–309. doi: 10.1093/jnen/63.12.1297
138. Gussenhoven R, Westerlaken RJJ, Ophelders D, Jobe AH, Kemp MW, Kallapur SG, et al. Chorioamnionitis, neuroinflammation, and injury: timing is key in the preterm ovine fetus. *J Neuroinflammation*. (2018) 15:113. doi: 10.1186/s12974-018-1149-x
139. Stojanovska V, Atik A, Nitsos I, Skiöld B, Barton SK, Zahra VA, et al. Effects of intrauterine inflammation on cortical gray matter of near-term lambs. *Front Pediatr*. (2018) 6:145. doi: 10.3389/fped.2018.00145
140. Rousset CI, Chalon S, Cantagrel S, Bodard S, Andres C, Gressens P, et al. Maternal exposure to LPS induces hypomyelination in the internal capsule and programmed cell death in the deep gray matter in newborn rats. *Pediatr Res*. (2006) 59:428–33. doi: 10.1203/01.pdr.0000199905.08848.55
141. Fleiss B, Tann CJ, Degos V, Sigaut S, Van Steenwinckel J, Schang AL, et al. Inflammation-induced sensitization of the brain in term infants. *Dev Med Child Neurol*. (2015) 57:17–28. doi: 10.1111/dmcn.12723
142. Canetta S, Bolkan S, Padilla-Coreano N, Song LJ, Sahn R, Harrison NL, et al. Maternal immune activation leads to selective functional deficits in offspring parvalbumin interneurons. *Mol Psychiatry*. (2016) 21:956–68. doi: 10.1038/mp.2015.222
143. Vasistha NA, Pardo-Navarro M, Gasthaus J, Weijers D, Muller MK, Garcia-Gonzalez D, et al. Maternal inflammation has a profound effect on cortical interneuron development in a stage and subtype-specific manner. *Mol Psychiatry*. (2019). doi: 10.1038/s41380-019-0539-5. [Epub ahead of print].

144. Zikopoulos B, Barbas H. Altered neural connectivity in excitatory and inhibitory cortical circuits in autism. *Front Hum Neurosci.* (2013) 7:609. doi: 10.3389/fnhum.2013.00609
145. Adorjan I, Ahmed B, Feher V, Torso M, Krug K, Esiri M, et al. Calretinin interneuron density in the caudate nucleus is lower in autism spectrum disorder. *Brain.* (2017) 140:2028–40. doi: 10.1093/brain/awx131
146. Lunden JW, Durens M, Phillips AW, Nestor MW. Cortical interneuron function in autism spectrum condition. *Pediatr Res.* (2019) 85:146–54. doi: 10.1038/s41390-018-0214-6
147. Yekhlef L, Breschi GL, Lagostena L, Russo G, Taverna S. Selective activation of parvalbumin- or somatostatin-expressing interneurons triggers epileptic seizurelike activity in mouse medial entorhinal cortex. *J Neurophysiol.* (2015) 113:1616–30. doi: 10.1152/jn.00841.2014
148. Lauber E, Filice F, Schwaller B. Dysregulation of parvalbumin expression in the Cntnap2$^{-/-}$ mouse model of autism spectrum disorder. *Front Mol Neurosci.* (2018) 11:262. doi: 10.3389/fnmol.2018.00262
149. Wiebe S, Nagpal A, Truong VT, Park J, Skalecka A, He AJ, et al. Inhibitory interneurons mediate autism-associated behaviors via 4E-BP2. *Proc Natl Acad Sci USA.* (2019) 116:18060–7. doi: 10.1073/pnas.1908126116
150. Ball G, Srinivasan L, Aljabar P, Counsell SJ, Durighel G, Hajnal JV, et al. Development of cortical microstructure in the preterm human brain. *Proc Natl Acad Sci USA.* (2013) 110:9541–6. doi: 10.1073/pnas.1301652110
151. Ball G, Boardman JP, Aljabar P, Pandit A, Arichi T, Merchant N, et al. The influence of preterm birth on the developing thalamocortical connectome. *Cortex.* (2013) 49:1711–21. doi: 10.1016/j.cortex.2012.07.006
152. Pandit AS, Robinson E, Aljabar P, Ball G, Gousias IS, Wang Z, et al. Whole-brain mapping of structural connectivity in infants reveals altered connection strength associated with growth and preterm birth. *Cereb Cortex.* (2014) 24:2324–33. doi: 10.1093/cercor/bht086
153. Limperopoulos C, Bassan H, Sullivan NR, Soul JS, Robertson RL Jr, Moore M, et al. Positive screening for autism in ex-preterm infants: prevalence and risk factors. *Pediatrics.* (2008) 121:758–65. doi: 10.1542/peds.2007-2158
154. Delobel-Ayoub M, Arnaud C, White-Koning M, Casper C, Pierrat V, Garel M, et al. Behavioral problems and cognitive performance at 5 years of age after very preterm birth: the EPIPAGE study. *Pediatrics.* (2009) 123:1485–92. doi: 10.1542/peds.2008-1216
155. Lindstrom K, Lindblad F, Hjern A. Preterm birth and attention-deficit/hyperactivity disorder in schoolchildren. *Pediatrics.* (2011) 127:858–65. doi: 10.1542/peds.2010-1279
156. Hagberg B, Hagberg G, Olow I, von Wendt L. The changing panorama of cerebral palsy in Sweden. VII. Prevalence and origin in the birth year period 1987–90. *Acta Paediatr.* (1996) 85:954–60. doi: 10.1111/j.1651-2227.1996.tb14193.x
157. Crump C, Sundquist K, Winkleby MA, Sundquist J. Preterm birth and risk of epilepsy in Swedish adults. *Neurology.* (2011) 77:1376–82. doi: 10.1212/WNL.0b013e318231528f
158. Wood NS, Costeloe K, Gibson AT, Hennessy EM, Marlow N, Wilkinson AR, et al. The EPICure study: associations and antecedents of neurological and developmental disability at 30 months of age following extremely preterm birth. *Arch Dis Child Fetal Neonatal Ed.* (2005) 90:F134–140. doi: 10.1136/adc.2004.052407
159. Costeloe KL, Hennessy EM, Haider S, Stacey F, Marlow N, Draper ES. Short term outcomes after extreme preterm birth in England: comparison of two birth cohorts in 1995 and 2006 (the EPICure studies). *BMJ.* (2012) 345:e7976. doi: 10.1136/bmj.e7976
160. Petrenko V, van de Looij Y, Mihhailova J, Salmon P, Huppi PS, Sizonenko SV, et al. Multimodal MRI imaging of apoptosis-triggered microstructural alterations in the postnatal cerebral cortex. *Cereb Cortex.* (2018) 28:949–62. doi: 10.1093/cercor/bhw420
161. Petrenko V, Mihhailova J, Salmon P, Kiss JZ. Apoptotic neurons induce proliferative responses of progenitor cells in the postnatal neocortex. *Exp Neurol.* (2015) 273:126–37. doi: 10.1016/j.expneurol.2015.08.010
162. Kalanjati VP, Wixey JA, Miller SM, Colditz PB, Bjorkman ST. GABAA receptor expression and white matter disruption in intrauterine growth restricted piglets. *Int J Dev Neurosci.* (2017) 59:1–9. doi: 10.1016/j.ijdevneu.2017.02.004
163. Fleiss B, Wong F, Brownfoot F, Shearer IK, Baud O, Walker DW, et al. Knowledge gaps and emerging research areas in intrauterine growth restriction-associated brain injury. *Front Endocrinol (Lausanne).* (2019) 10:188. doi: 10.3389/fendo.2019.00188
164. Li WY, Chang YC, Lee LJH, Lee LJ. Prenatal infection affects the neuronal architecture and cognitive function in adult mice. *Dev Neurosci.* (2014) 36:359–70. doi: 10.1159/000362383
165. Balakrishnan B, Dai H, Janisse J, Romero R, Kannan S. Maternal endotoxin exposure results in abnormal neuronal architecture in the newborn rabbit. *Dev Neurosci.* (2013) 35:396–405. doi: 10.1159/000353156
166. Krishnan ML, Van Steenwinckel J, Schang AL, Yan J, Arnadottir J, Le Charpentier T, et al. Integrative genomics of microglia implicates DLG4 (PSD95) in the white matter development of preterm infants. *Nat Commun.* (2017) 8:428. doi: 10.1038/s41467-017-00422-w
167. Vinall J, Grunau RE, Brant R, Chau V, Poskitt KJ, Synnes AR, et al. Slower postnatal growth is associated with delayed cerebral cortical maturation in preterm newborns. *Sci Transl Med.* (2013) 5:168ra168. doi: 10.1126/scitranslmed.3004666
168. Pannek K, Hatzigeorgiou X, Colditz PB, Rose S. Assessment of structural connectivity in the preterm brain at term equivalent age using diffusion MRI and T2 relaxometry: a network-based analysis. *PLoS ONE.* (2013) 8:e68593. doi: 10.1371/journal.pone.0068593
169. Batalle D, Hughes EJ, Zhang H, Tournier JD, Tusor N, Aljabar P, et al. Early development of structural networks and the impact of prematurity on brain connectivity. *Neuroimage.* (2017) 149:379–92. doi: 10.1016/j.neuroimage.2017.01.065
170. Karolis VR, Froudist-Walsh S, Brittain PJ, Kroll J, Ball G, Edwards AD, et al. Reinforcement of the brain's rich-club architecture following early neurodevelopmental disruption caused by very preterm birth. *Cereb Cortex.* (2016) 26:1322–35. doi: 10.1093/cercor/bhv305
171. Arichi T, Counsell SJ, Allievi AG, Chew AT, Martinez-Biarge M, Mondi V, et al. The effects of hemorrhagic parenchymal infarction on the establishment of sensori-motor structural and functional connectivity in early infancy. *Neuroradiology.* (2014) 56:985–94. doi: 10.1007/s00234-014-1412-5
172. Ball G, Aljabar P, Arichi T, Tusor N, Cox D, Merchant N, et al. Machine-learning to characterise neonatal functional connectivity in the preterm brain. *Neuroimage.* (2016) 124:267–75. doi: 10.1016/j.neuroimage.2015.08.055
173. Gozdas E, Parikh NA, Merhar SL, Tkach JA, He L, Holland SK. Altered functional network connectivity in preterm infants: antecedents of cognitive and motor impairments? *Brain Struct Funct.* (2018) 223:3665–80. doi: 10.1007/s00429-018-1707-0
174. Bouyssi-Kobar M, De Asis-Cruz J, Murnick J, Chang T, Limperopoulos C. Altered functional brain network integration, segregation, and modularity in infants born very preterm at term-equivalent age. *J Pediatr.* (2019) 213:13–21 e11. doi: 10.1016/j.jpeds.2019.06.030
175. Ranasinghe S, Or G, Wang EY, Ievins A, McLean MA, Niell CM, et al. Reduced cortical activity impairs development and plasticity after neonatal hypoxia ischemia. *J Neurosci.* (2015) 35:11946–59. doi: 10.1523/JNEUROSCI.2682-14.2015
176. Song J, Xu F, Wang L, Gao L, Guo J, Xia L, et al. Early amplitude-integrated electroencephalography predicts brain injury and neurological outcome in very preterm infants. *Sci Rep.* (2015) 5:13810. doi: 10.1038/srep13810
177. Pavlidis E, Lloyd RO, Boylan GB. EEG–a valuable biomarker of brain injury in preterm infants. *Dev Neurosci.* (2017) 39:23–35. doi: 10.1159/000456659
178. Whitehead K, Pressler R, Fabrizi L. Characteristics and clinical significance of delta brushes in the EEG of premature infants. *Clin Neurophysiol Pract.* (2017) 2:12–8. doi: 10.1016/j.cnp.2016.11.002
179. Tataranno ML, Claessens NHP, Moeskops P, Toet MC, Kersbergen KJ, Buonocore G, et al. Changes in brain morphology and microstructure in relation to early brain activity in extremely preterm infants. *Pediatr Res.* (2018) 83:834–42. doi: 10.1038/pr.2017.314

180. Benders MJ, Palmu K, Menache C, Borradori-Tolsa C, Lazeyras F, Sizonenko S, et al. Early brain activity relates to subsequent brain growth in premature infants. *Cereb Cortex.* (2015) 25:3014–24. doi: 10.1093/cercor/bhu097
181. Whitehead K, Jones L, Laudiano-Dray MP, Meek J, Fabrizi L. Altered cortical processing of somatosensory input in pre-term infants who had high-grade germinal matrix-intraventricular haemorrhage. *Neuroimage Clin.* (2020) 25:102095. doi: 10.1016/j.nicl.2019.102095
182. Hayashi-Kurahashi N, Kidokoro H, Kubota T, Maruyama K, Kato Y, Kato T, et al. EEG for predicting early neurodevelopment in preterm infants: an observational cohort study. *Pediatrics.* (2012) 130:e891–897. doi: 10.1542/peds.2012-1115
183. Reynolds LC, Pineda RG, Mathur A, Vavasseur C, Shah DK, Liao S, et al. Cerebral maturation on amplitude-integrated electroencephalography and perinatal exposures in preterm infants. *Acta Paediatr.* (2014) 103:e96–100. doi: 10.1111/apa.12485
184. Abbasi H, Drury PP, Lear CA, Gunn AJ, Davidson JO, Bennet L, et al. EEG sharp waves are a biomarker of striatal neuronal survival after hypoxia-ischemia in preterm fetal sheep. *Sci Rep.* (2018) 8:16312. doi: 10.1038/s41598-018-34654-7
185. van den Heuij LG, Fraser M, Miller SL, Jenkin G, Wallace EM, Davidson JO, et al. Delayed intranasal infusion of human amnion epithelial cells improves white matter maturation after asphyxia in preterm fetal sheep. *J Cereb Blood Flow Metab.* (2019) 39:223–9. doi: 10.1177/0271678X17729954
186. Keogh MJ, Bennet L, Drury PP, Booth LC, Mathai S, Naylor AS, et al. Subclinical exposure to low-dose endotoxin impairs EEG maturation in preterm fetal sheep. *Am J Physiol Regul Integr Comp Physiol.* (2012) 303:R270–8. doi: 10.1152/ajpregu.00216.2012
187. Plomgaard AM, Andersen AD, Petersen TH, van de Looij Y, Thymann T, Sangild PT, et al. Structural brain maturation differs between preterm and term piglets, whereas brain activity does not. *Acta Paediatr.* (2019) 108:637–44. doi: 10.1111/apa.14556
188. van de Looij Y, Chatagner A, Quairiaux C, Gruetter R, Hüppi PS, Sizonenko SV. Multi-modal assessment of long-term erythropoietin treatment after neonatal hypoxic-ischemic injury in rat brain. *PLoS ONE.* (2014) 9:e95643. doi: 10.1371/journal.pone.0095643
189. Galinsky R, Draghi V, Wassink G, Davidson JO, Drury PP, Lear CA, et al. Magnesium sulfate reduces EEG activity but is not neuroprotective after asphyxia in preterm fetal sheep. *J Cereb Blood Flow Metab.* (2017) 37:1362–73. doi: 10.1177/0271678X16655548
190. Mordel J, Sheikh A, Tsohataridis S, Kanold PO, Zehendner CM, Luhmann HJ. Mild systemic inflammation and moderate hypoxia transiently alter neuronal excitability in mouse somatosensory cortex. *Neurobiol Dis.* (2016) 88:29–43. doi: 10.1016/j.nbd.2015.12.019
191. Nimmervoll B, White R, Yang JW, An S, Henn C, Sun JJ, et al. LPS-induced microglial secretion of TNFalpha increases activity-dependent neuronal apoptosis in the neonatal cerebral cortex. *Cereb Cortex.* (2013) 23:1742–55. doi: 10.1093/cercor/bhs156
192. Zaslavsky K, Zhang WB, McCready FP, Rodrigues DC, Deneault E, Loo C, et al. (2019). SHANK2 mutations associated with autism spectrum disorder cause hyperconnectivity of human neurons. *Nat Neurosci.* 22:556–64. doi: 10.1038/s41593-019-0365-8
193. Marguet SL, Le-Schulte VT, Merseburg A, Neu A, Eichler R, Jakovcevski I, et al. Treatment during a vulnerable developmental period rescues a genetic epilepsy. *Nat Med.* (2015) 21:1436–44. doi: 10.1038/nm.3987
194. Mattingly GW, Wilson J, Rostain AL. A clinician's guide to ADHD treatment options. *Postgrad Med.* (2017) 129:657–66. doi: 10.1080/00325481.2017.1354648
195. Goldenberg MM. Overview of drugs used for epilepsy and seizures: etiology, diagnosis, and treatment. *P T.* (2010) 35:392–415.
196. De Crescenzo F, Cortese S, Adamo N, Janiri L. Pharmacological and non-pharmacological treatment of adults with ADHD: a meta-review. *Evid Based Mental Health.* (2017) 20:4. doi: 10.1136/eb-2016-102415
197. Heylen SL, Gelders YG. Risperidone, a new antipsychotic with serotonin 5-HT2 and dopamine D2 antagonistic properties. *Clin Neuropharmacol.* (1992) 15:180A−1A. doi: 10.1097/00002826-199201001-00095
198. Stavropoulos KK-M. Using neuroscience as an outcome measure for behavioral interventions in autism spectrum disorders (ASD): a review. *Res Autism Spectr Disord.* (2017) 35:62–73. doi: 10.1016/j.rasd.2017.01.001
199. Hong MP, Erickson CA. Investigational drugs in early-stage clinical trials for autism spectrum disorder. *Expert Opin Invest Drugs.* (2019) 28:709–18. doi: 10.1080/13543784.2019.1649656
200. Fleiss B, Gressens P. Tertiary mechanisms of brain damage: a new hope for treatment of cerebral palsy? *Lancet Neurol.* (2012) 11:556–66. doi: 10.1016/S1474-4422(12)70058-3
201. Han M, Zhang JC, Yao W, Yang C, Ishima T, Ren Q, et al. Intake of 7,8-dihydroxyflavone during juvenile and adolescent stages prevents onset of psychosis in adult offspring after maternal immune activation. *Sci Rep.* (2016) 6:36087. doi: 10.1038/srep36087
202. Iannone LF, Gomez-Eguilaz M, Citaro R, Russo E. The potential role of interventions impacting on gut-microbiota in epilepsy. *Expert Rev Clin Pharmacol.* (2020) 1:423–35. doi: 10.1080/17512433.2020.1759414
203. Hill-Yardin EL, McKeown SJ, Novarino G, Grabrucker AM. Extracerebral dysfunction in animal models of autism spectrum disorder. *Adv Anat Embryol Cell Biol.* (2017) 224:159–87. doi: 10.1007/978-3-319-52498-6_9
204. Hosie S, Ellis M, Swaminathan M, Ramalhosa F, Seger GO, Balasuriya GK, et al. Gastrointestinal dysfunction in patients and mice expressing the autism-associated R451C mutation in neuroligin-3. *Autism Res.* (2019) 12:1043–56. doi: 10.1002/aur.2127
205. Lasheras I, Seral P, Latorre E, Barroso E, Gracia-Garcia P, Santabarbara J. Microbiota and gut-brain axis dysfunction in autism spectrum disorder: evidence for functional gastrointestinal disorders. *Asian J Psychiatr.* (2020) 47:101874. doi: 10.1016/j.ajp.2019.101874
206. Sauer AK, Bockmann J, Steinestel K, Boeckers TM, Grabrucker AM. Altered intestinal morphology and microbiota composition in the autism spectrum disorders associated SHANK3 mouse model. *Int J Mol Sci.* (2019) 20:2134. doi: 10.3390/ijms20092134
207. Burrows EL, Laskaris L, Koyama L, Churilov L, Bornstein JC, Hill-Yardin EL, et al. A neuroligin-3 mutation implicated in autism causes abnormal aggression and increases repetitive behavior in mice. *Mol Autism.* (2015) 6:62. doi: 10.1186/s13229-015-0055-7
208. Hosie S, Malone DT, Liu S, Glass M, Adlard PA, Hannan AJ, et al. Altered amygdala excitation and CB1 receptor modulation of aggressive behavior in the neuroligin-3R451C mouse model of autism. *Front Cell Neurosci.* (2018) 12:234. doi: 10.3389/fncel.2018.00234
209. Matta SM, Hill-Yardin EL, Crack PJ. The influence of neuroinflammation in autism spectrum disorder. *Brain Behav Immun.* (2019) 79:75–90. doi: 10.1016/j.bbi.2019.04.037
210. Lee CYQ, Franks AE, Hill-Yardin EL. Autism-associated synaptic mutations impact the gut-brain axis in mice. *Brain Behav Immun.* (2020). doi: 10.1016/j.bbi.2020.05.072. [Epub ahead of print].
211. Hsiao EY, McBride SW, Hsien S, Sharon G, Hyde ER, McCue T, et al. Microbiota modulate behavioral and physiological abnormalities associated with neurodevelopmental disorders. *Cell* (2013) 155:1451–63. doi: 10.1016/j.cell.2013.11.024
212. Sharon G, Cruz NJ, Kang DW, Gandal MJ, Wang B, Kim YM, et al. Human gut microbiota from autism spectrum disorder promote behavioral symptoms in mice. *Cell.* (2019) 177:1600–18.e17. doi: 10.1016/j.cell.2019.05.004
213. Sgritta M, Dooling SW, Buffington SA, Momin EN, Francis MB, Britton RA, et al. Mechanisms underlying microbial-mediated changes in social behavior in mouse models of autism spectrum disorder. *Neuron.* (2019) 101:246–59.e6. doi: 10.1016/j.neuron.2018.11.018
214. Erny D, Hrabe de Angelis AL, Jaitin D, Wieghofer P, Staszewski O, David E, et al. Host microbiota constantly control maturation and function of microglia in the CNS. *Nat Neurosci.* (2015) 18:965–77. doi: 10.1038/nn.4030
215. Matcovitch-Natan O, Winter DR, Giladi A, Vargas Aguilar S, Spinrad A, Sarrazin S, et al. Microglia development follows a stepwise program to regulate brain homeostasis. *Science.* (2016) 353:aad8670. doi: 10.1126/science.aad8670
216. Hoyles L, Snelling T, Umlai U-K, Nicholson JK, Carding SR, Glen RC, et al. Microbiome-host systems interactions: protective effects of propionate upon the blood-brain barrier. *Microbiome* (2018) 6:55. doi: 10.1186/s40168-018-0439-y
217. Swiderski K, Bindon R, Trieu J, Naim T, Schokman S, Swaminathan M, et al. Spatiotemporal mapping reveals regional gastrointestinal dysfunction

in MDX dystrophic mice ameliorated by oral L-arginine supplementation. *J Neurogastroenterol Motil.* (2019).
218. Nithianantharajah J, Balasuriya GK, Franks AE, Hill-Yardin EL. Using animal models to study the role of the gut–brain axis in autism. *Curr Dev Disord Rep.* (2017) 4:28–36. doi: 10.1007/s40474-017-0111-4
219. Koning G, Lyngfelt E, Svedin P, Leverin AL, Jinnai M, Gressens P, et al. Magnesium sulphate induces preconditioning in preterm rodent models of cerebral hypoxia-ischemia. *Int J Dev Neurosci.* (2018) 70:56–66. doi: 10.1016/j.ijdevneu.2018.01.002
220. Doyle LW, Crowther CA, Middleton P, Marret S. Magnesium sulphate for women at risk of preterm birth for neuroprotection of the fetus. *Cochrane Database Syst Rev*. (2007) 68:CD004661. doi: 10.1002/14651858.CD004661.pub2
221. Leuchter RH, Gui L, Poncet A, Hagmann C, Lodygensky GA, Martin E, et al. Association between early administration of high-dose erythropoietin in preterm infants and brain MRI abnormality at term-equivalent age. *JAMA*. (2014) 312:817–24. doi: 10.1001/jama.2014.9645
222. Robinson S, Corbett CJ, Winer JL, Chan LAS, Maxwell JR, Anstine CV, et al. Neonatal erythropoietin mitigates impaired gait, social interaction and diffusion tensor imaging abnormalities in a rat model of prenatal brain injury. *Exp Neurol.* (2018) 302:1–13. doi: 10.1016/j.expneurol.2017.12.010
223. Wassink G, Davidson JO, Dhillon SK, Fraser M, Galinsky R, Bennet L, et al. Partial white and grey matter protection with prolonged infusion of recombinant human erythropoietin after asphyxia in preterm fetal sheep. *J Cereb Blood Flow Metab.* (2017) 37:1080–94. doi: 10.1177/0271678X16650455
224. Fleiss B, Gressens P. Neuroprotection of the preterm brain. *Handb Clin Neurol.* (2019) 162:315–28. doi: 10.1016/B978-0-444-64029-1.00015-1
225. Sucksdorff M, Lehtonen L, Chudal R, Suominen A, Joelsson P, Gissler M, et al. Preterm birth and poor fetal growth as risk factors of attention-deficit/hyperactivity disorder. *Pediatrics.* (2015) 136:e599–608. doi: 10.1542/peds.2015-1043
226. Indredavik MS, Skranes JS, Vik T, Heyerdahl S, Romundstad P, Myhr GE, et al. Low-birth-weight adolescents: psychiatric symptoms and cerebral MRI abnormalities. *Pediatr Neurol.* (2005) 33:259–66. doi: 10.1016/j.pediatrneurol.2005.05.002
227. Bokobza C, Van Steenwinckel J, Mani S, Mezger V, Fleiss B, Gressens P. Neuroinflammation in preterm babies and autism spectrum disorders. *Pediatr Res.* (2019) 85:155–65. doi: 10.1038/s41390-018-0208-4
228. Fitzallen GC, Taylor HG, Bora S. What do we know about the preterm behavioural phenotype? A narrative review. *Front Psychiatry*. (2020) 11:154. doi: 10.3389/fpsyt.2020.00154
229. Elgen I, Sommerfelt K, Markestad T. Population based, controlled study of behavioural problems and psychiatric disorders in low birthweight children at 11 years of age. *Arch Dis Child Fetal Neonatal Ed.* (2002) 87:F128–32. doi: 10.1136/fn.87.2.F128
230. Bowers K, Wink LK, Pottenger A, McDougle CJ, Erickson C. Phenotypic differences in individuals with autism spectrum disorder born preterm and at term gestation. *Autism.* (2015) 19:758–63. doi: 10.1177/1362361314547366
231. Chen LW, Wang ST, Wang LW, Kao YC, Chu CL, Wu CC, et al. Behavioral characteristics of autism spectrum disorder in very preterm birth children. *Mol Autism.* (2019) 10:32. doi: 10.1186/s13229-019-0282-4
232. Batalle D, Edwards AD, O'Muircheartaigh J. Annual research review: not just a small adult brain: understanding later neurodevelopment through imaging the neonatal brain. *J Child Psychol Psychiatry.* (2017) 59:350–71. doi: 10.1111/jcpp.12838
233. McAlonan GM, Cheung V, Cheung C, Suckling J, Lam GY, Tai KS, et al. Mapping the brain in autism. A voxel-based MRI study of volumetric differences and intercorrelations in autism. *Brain.* (2005) 128:268–76. doi: 10.1093/brain/awh332
234. Batty MJ, Liddle EB, Pitiot A, Toro R, Groom MJ, Scerif G, et al. Cortical gray matter in attention-deficit/hyperactivity disorder: a structural magnetic resonance imaging study. *J Am Acad Child Adolesc Psychiatry.* (2010) 49:229–38. doi: 10.1097/00004583-201003000-00006
235. Greimel E, Nehrkorn B, Schulte-Ruther M, Fink GR, Nickl-Jockschat T, Herpertz-Dahlmann B, et al. Changes in grey matter development in autism spectrum disorder. *Brain Struct Funct.* (2013) 218:929–42. doi: 10.1007/s00429-012-0439-9
236. Griffiths KR, Grieve SM, Kohn MR, Clarke S, Williams LM, Korgaonkar MS. Altered gray matter organization in children and adolescents with ADHD: a structural covariance connectome study. *Transl Psychiatry.* (2016) 6:e947. doi: 10.1038/tp.2016.219
237. Sato W, Kochiyama T, Uono S, Yoshimura S, Kubota Y, Sawada R, et al. Reduced gray matter volume in the social brain network in adults with autism spectrum disorder. *Front Hum Neurosci.* (2017) 11:395. doi: 10.3389/fnhum.2017.00395
238. Nakao T, Radua J, Rubia K, Mataix-Cols D. Gray matter volume abnormalities in ADHD: voxel-based meta-analysis exploring the effects of age and stimulant medication. *Am J Psychiatry.* (2011) 168:1154–63. doi: 10.1176/appi.ajp.2011.11020281
239. Lawrence EJ, Froudist-Walsh S, Neilan R, Nam KW, Giampietro V, McGuire P, et al. Motor fMRI and cortical grey matter volume in adults born very preterm. *Dev Cogn Neurosci.* (2014) 10:1–9. doi: 10.1016/j.dcn.2014.06.002
240. Keunen K, Isgum I, van Kooij BJ, Anbeek P, van Haastert IC, Koopman-Esseboom C, et al. Brain volumes at term-equivalent age in preterm infants: imaging biomarkers for neurodevelopmental outcome through early school age. *J Pediatr.* (2016) 172:88–95. doi: 10.1016/j.jpeds.2015.12.023
241. Ecker C, Ronan L, Feng Y, Daly E, Murphy C, Ginestet CE, et al. Intrinsic gray-matter connectivity of the brain in adults with autism spectrum disorder. *Proc Natl Acad Sci USA.* (2013) 110:13222–7. doi: 10.1073/pnas.1221880110
242. Coley AA, Gao WJ. PSD95: a synaptic protein implicated in schizophrenia or autism? *Prog Neuropsychopharmacol Biol Psychiatry.* (2018) 82:187–94. doi: 10.1016/j.pnpbp.2017.11.016
243. Sajdel-Sulkowska EM, Makowska-Zubrycka M, Czarzasta K, Kasarello K, Aggarwal V, Bialy M, et al. Common genetic variants link the abnormalities in the gut-brain axis in prematurity and autism. *Cerebellum.* (2019) 18:255–65. doi: 10.1007/s12311-018-0970-1
244. Guang S, Pang N, Deng X, Yang L, He F, Wu L, et al. Synaptopathology involved in autism spectrum disorder. *Front Cell Neurosci.* (2018) 12:470. doi: 10.3389/fncel.2018.00470
245. Rylaarsdam L, Guemez-Gamboa A. Genetic causes and modifiers of autism spectrum disorder. *Front Cell Neurosci.* (2019) 13:385. doi: 10.3389/fncel.2019.00385
246. Hoffmann I, Bueter W, Zscheppang K, Brinkhaus MJ, Liese A, Riemke S, et al. Neuregulin-1, the fetal endothelium, and brain damage in preterm newborns. *Brain Behav Immun.* (2010) 24:784–91. doi: 10.1016/j.bbi.2009.08.012
247. Southwell DG, Seifikar H, Malik R, Lavi K, Vogt D, Rubenstein JL, et al. Interneuron transplantation rescues social behavior deficits without restoring wild-type physiology in a mouse model of autism with excessive synaptic inhibition. *J Neurosci.* (2020) 40:2215–27. doi: 10.1523/JNEUROSCI.1063-19.2019
248. Pizzarelli R, Cherubini E. Alterations of GABAergic signaling in autism spectrum disorders. *Neural Plast.* (2011) 2011:297153. doi: 10.1155/2011/297153
249. Bilbo SD, Smith SH, Schwarz JM. A lifespan approach to neuroinflammatory and cognitive disorders: a critical role for glia. *J Neuroimmune Pharmacol.* (2012) 7:24–41. doi: 10.1007/s11481-011-9299-y
250. Petrelli F, Pucci L, Bezzi P. Astrocytes and microglia and their potential link with autism spectrum disorders. *Front Cell Neurosci.* (2016) 10:21. doi: 10.3389/fncel.2016.00021
251. Vezzani A, Balosso S, Ravizza T. Neuroinflammatory pathways as treatment targets and biomarkers in epilepsy. *Nat Rev Neurol.* (2019) 15:459–72. doi: 10.1038/s41582-019-0217-x
252. Paolicelli RC, Bolasco G, Pagani F, Maggi L, Scianni M, Panzanelli P, et al. Synaptic pruning by microglia is necessary for normal brain development. *Science.* (2011) 333:1456–8. doi: 10.1126/science.1202529
253. Zhan Y, Paolicelli RC, Sforazzini F, Weinhard L, Bolasco G, Pagani F, et al. Deficient neuron-microglia signaling results in impaired functional brain connectivity and social behavior. *Nat Neurosci.* (2014) 17:400–6. doi: 10.1038/nn.3641

254. Mallya AP, Wang HD, Lee HNR, Deutch AY. Microglial pruning of synapses in the prefrontal cortex during adolescence. *Cereb Cortex.* (2019) 29:1634–43. doi: 10.1093/cercor/bhy061
255. Schafer DP, Lehrman EK, Kautzman AG, Koyama R, Mardinly AR, Yamasaki R, et al. Microglia sculpt postnatal neural circuits in an activity and complement-dependent manner. *Neuron.* (2012) 74:691–705. doi: 10.1016/j.neuron.2012.03.026
256. Bilimoria PM, Stevens B. Microglia function during brain development: new insights from animal models. *Brain Res.* (2015) 1617:7–17. doi: 10.1016/j.brainres.2014.11.032
257. Tay TL, Savage JC, Hui CW, Bisht K, Tremblay ME. Microglia across the lifespan: from origin to function in brain development, plasticity and cognition. *J Physiol.* (2017) 595:1929–45. doi: 10.1113/JP272134
258. Won H, Mah W, Kim E. Autism spectrum disorder causes, mechanisms, and treatments: focus on neuronal synapses. *Front Mol Neurosci.* (2013) 6:19. doi: 10.3389/fnmol.2013.00019
259. Ebrahimi-Fakhari D, Sahin M. Autism and the synapse: emerging mechanisms and mechanism-based therapies. *Curr Opin Neurol.* (2015) 28:91–102. doi: 10.1097/WCO.0000000000000186
260. Lepeta K, Lourenco MV, Schweitzer BC, Martino Adami PV, Banerjee P, Catuara-Solarz S, et al. Synaptopathies: synaptic dysfunction in neurological disorders–a review from students to students. *J Neurochem.* (2016) 138:785–805. doi: 10.1111/jnc.13713
261. Luo J, Norris RH, Gordon SL, Nithianantharajah J. Neurodevelopmental synaptopathies: insights from behaviour in rodent models of synapse gene mutations. *Prog Neuropsychopharmacol Biol Psychiatry.* (2018) 84:424–39. doi: 10.1016/j.pnpbp.2017.12.001
262. Delorme R, Ey E, Toro R, Leboyer M, Gillberg C, Bourgeron T. Progress toward treatments for synaptic defects in autism. *Nat Med.* (2013) 19:685–94. doi: 10.1038/nm.3193
263. Giovedí S, Corradi A, Fassio A, Benfenati F. Involvement of synaptic genes in the pathogenesis of autism spectrum disorders: the case of synapsins. *Front Pediatr.* (2014) 2:94. doi: 10.3389/fped.2014.00094

Conflict of Interest: The authors declare that the research was conducted in the absence of any commercial or financial relationships that could be construed as a potential conflict of interest.

frontiers in Neurology

SYSTEMATIC REVIEW
published: 16 July 2020
doi: 10.3389/fneur.2020.00704

Birth Asphyxia Is Associated With Increased Risk of Cerebral Palsy: A Meta-Analysis

Shan Zhang[1], *Bingbing Li*[1], *Xiaoli Zhang*[1], *Changlian Zhu*[1,2,3] *and Xiaoyang Wang*[1,4*]

[1] Henan Key Laboratory of Child Brain Injury, Third Affiliated Hospital and Institute of Neuroscience of Zhengzhou University, Zhengzhou, China, [2] Center for Brain Repair and Rehabilitation, Institute of Neuroscience and Physiology, Sahlgrenska Academy, University of Gothenburg, Gothenburg, Sweden, [3] Department of Women's and Children's Health, Karolinska Institutet, Stockholm, Sweden, [4] Center of Perinatal Medicine and Health, Institute of Neuroscience and Physiology, Sahlgrenska Academy, University of Gothenburg, Gothenburg, Sweden

Objective: To assess the association between birth asphyxia—as defined by the pH of umbilical cord blood—and cerebral palsy in asphyxiated neonates ≥35 weeks' gestation.

Methods: Two reviewers independently selected English-language studies that included data on the incidence of cerebral palsy in asphyxiated neonates ≥35 weeks' gestation. Studies were searched from the Embase, Google Scholar, PubMed, and Cochrane Library databases up to 31 December 2019, and the references in the retrieved articles were screened.

Results: We identified 10 studies that met the inclusion criteria for our meta-analysis, including 8 randomized controlled trials and 2 observational studies. According to a random effects model, the pooled rate of cerebral palsy in the randomized controlled trials was 20.3% (95% CI: 16.0–24.5) and the incidence of cerebral palsy in the observational studies was 22.2% (95% CI: 8.5–35.8). Subgroup analysis by treatment for hypoxic ischemic encephalopathy in asphyxiated neonates showed that the pooled rates of cerebral palsy were 17.3% (95% CI: 13.3–21.2) and 23.9% (95% CI: 18.1–29.7) for the intervention group and non-intervention group, respectively.

Conclusion: Our findings suggest that the incidence of cerebral palsy in neonates (≥35 weeks' gestation) with perinatal asphyxia is significantly higher compared to that in the healthy neonate population. With the growing emphasis on improving neonatal neurodevelopment and reducing neurological sequelae, we conclude that the prevention and treatment of perinatal asphyxia is essential for preventing the development of cerebral palsy.

Keywords: birth asphyxia, cerebral palsy, erythropoietin, hypothermia, meta-analysis

OPEN ACCESS

Edited by:
Bobbi Fleiss,
RMIT University, Australia

Reviewed by:
Sandra E. Juul,
University of Washington, United States
Thalia Harmony,
National Autonomous University of Mexico, Mexico

***Correspondence:**
Xiaoyang Wang
xiaoyang.wang@fysiologi.gu.se

Specialty section:
This article was submitted to Pediatric Neurology, a section of the journal Frontiers in Neurology

Received: *11 April 2020*
Accepted: *09 June 2020*
Published: *16 July 2020*

Citation:
Zhang S, Li B, Zhang X, Zhu C and Wang X (2020) Birth Asphyxia Is Associated With Increased Risk of Cerebral Palsy: A Meta-Analysis. Front. Neurol. 11:704. doi: 10.3389/fneur.2020.00704

INTRODUCTION

Cerebral palsy (CP) is a group of syndromes caused by non-progressive brain injury in the fetus or infant and leads to lifelong disability (1). The prevalence of CP is 2.11 per 1,000 live births globally (2), which remained relatively stable from 1950 to 1980, but increased moderately between 1980 and 1990, probably due to the increased survival of very premature infants as a result of improvements in perinatal care (3, 4). The etiology of CP is complex and multifactorial (5). Although premature

birth is a risk factor, the causes of CP for children born at term remain unclear (6–8). Birth asphyxia has been involved, but its contribution to CP is debatable. Evidence has suggested that most cases of CP are caused by prenatal factors and that the role of birth asphyxia is relatively small (<10% of cases) (9, 10). However, other studies have shown that birth asphyxia is one of the main causes of CP, accounting for more than 30% of cases (11–13).

Birth asphyxia is one of the important causes of neonatal morbidity and mortality (14, 15). Birth asphyxia refers to interruption of the blood flow to the placenta, leading to hypoxia and ischemia. When hypoxia–ischemia persists long enough, it will cause permanent neurologic injury, which may eventually develop into neurodevelopmental disorders such as developmental delay and CP (16, 17). The inconsistencies in the diagnosis of birth asphyxia contribute to variation in the prognosis of birth asphyxia. A previous study found that in studies with different diagnostic criteria of birth asphyxia, the proportion of CP cases with birth asphyxia ranged from <3% to over 50% (18). Metabolic acidosis in the umbilical cord has been recognized internationally as a necessary criterion for defining intrapartum hypoxia (19, 20) and has been used as the definition of asphyxia (21). Thus, the pH value of umbilical cord blood was used as the diagnostic criteria of birth asphyxia for conducting a meta-analysis of human studies to investigate the case exposure rates linking birth asphyxia to CP.

METHODS

Literature Search

Relevant studies were searched from the PubMed, Google Scholar, Embase, and Cochrane Library databases up to 31 December 2019. The search was performed using keywords and subject terms related to "birth asphyxia." The keywords and subject terms related to "cerebral palsy" or "neurodevelopmental outcome" were used to acquire studies related to CP. We combined the two parts of the search terms using "AND" to retrieve the studies (**Supplementary Table 1**). In order to supplement the electronic searches, we also searched the reference lists of previous reviews, key papers, and other relevant literature screened by the electronic search. Two investigators independently reviewed the titles, abstracts, and full-text publications.

Inclusion Criteria

Eligible studies were limited to research focusing on the following: (1) newborn infants who were born at ≥35 weeks' gestation, (2) evidence of birth asphyxia based on a pH ≤ 7.0 and/or a base deficit ≥12 mmol/L in an umbilical cord blood sample during the first hour after birth, and (3) clinical hypoxic ischemic encephalopathy (HIE) manifestation as well as neurodevelopmental outcomes that included data on CP. Additionally, when multiple studies based on the same population were published, only the most complete one was included.

Exclusion Criteria

The following exclusion criteria were applied: (1) reviews, meta-analyses, or case reports, (2) studies not published in English, (3) studies using evidence for birth asphyxia that was inconsistent with our inclusion criteria described above, and (4) studies reporting overlapping data.

Data Extraction

Information relating to data extraction was gathered individually from each identified article, including the name of the first author, study design, publication year, the size of sample, gestational age, asphyxiation criteria, follow-up period, and neurodevelopmental outcome regarding CP.

Quality Assessment

Of the included studies, eight were randomized controlled trials and two were observational studies. The Newcastle-Ottawa Scale was used to evaluate the quality of the observational studies (22) (**Supplementary Table 2**), including the choice of the research population (0–4 points), the study comparability (0–2 points), and the evaluation of exposure factor and outcome (0–3 points). The Cochrane collaboration's tool for assessing risk of bias, which is based on the important elements of reducing bias, including selection bias, performance bias, detection bias, attrition bias, reporting bias, and other biases, was used to assess the quality of the randomized controlled trials (23) (**Supplementary Figure 1**).

Statistical Analysis

Stata software version 12.0 (Stata Corporation, College Station, TX, US) was used for data analysis. The combined rate of CP and 95% confidence intervals (CIs) were calculated for all predetermined groups. A random effects model was used to give a pooled estimate of prevalence because of the small number of studies and the heterogeneity across studies in this meta-analysis. Heterogeneity was estimated by the Q statistic and the I^2 statistic. Sensitivity analyses were performed to identify any potential influence between the included studies on the pooled prevalence of CP. Possible publication bias was tested by Egger's and Begg's tests. The significance level of Q statistic for the heterogeneity test was set to 0.10 and p <0.05 were considered statistically significant.

RESULTS

Search Results

The electronic database searches initially yielded 5,671 studies, and 5,616 studies were deleted due to either repetition or lack of relevance. A total of 55 full-text studies were retrieved and critically appraised. Of these articles, 45 did not satisfy the inclusion criteria (9 studies performed secondary analyses on the same study populations, 17 studies did not report the neurodevelopment outcomes, 4 studies did not have data for the pH of umbilical cord blood, and 15 studies were excluded due to unusable data such as articles that reported the prevalence of CP between those with birth asphyxia and those without birth asphyxia and articles for which the exact association between asphyxia and CP could not be determined). Of the remaining

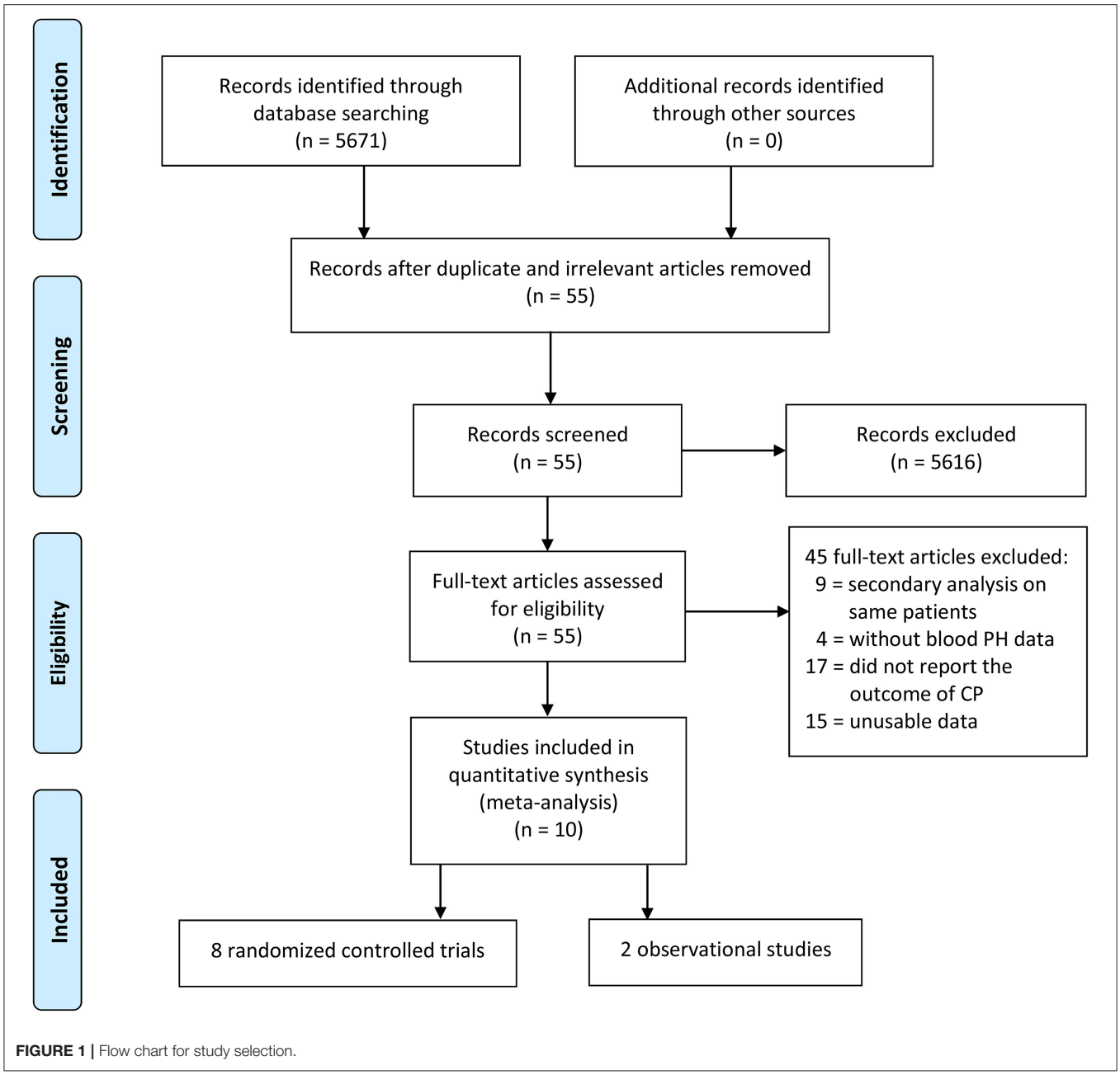

FIGURE 1 | Flow chart for study selection.

10 acceptable studies, 8 studies were randomized controlled trials and 2 studies were observational studies (**Figure 1**).

Characteristics of the Studies

We compiled a dataset of 1,665 infants from the 10 studies. All of the neonates in the included studies meeting the asphyxia criteria were diagnosed as HIE. Of the eight randomized controlled trials (24–31), six studies used moderate hypothermia as a treatment for HIE in asphyxiated neonates, one used erythropoietin treatment in asphyxiated neonates, and one used a combination of moderate hypothermia and topiramate treatment in asphyxiated neonates. The two observational studies (32, 33) investigated the neurodevelopment outcomes in asphyxiated neonates without any interventions. The characteristics of included trials were summarized in **Table 1**.

Sensitivity Analysis and Publication Bias

Sensitivity analysis was conducted on the eight randomized controlled trials, and none of them had a significant impact on the results of the meta-analysis, suggesting that this study had good stability (**Supplementary Figure 2**). Publication bias was evaluated by Egger's ($P = 0.134$) and Begg's ($P = 0.536$) tests (**Supplementary Figure 3**). The pooled results demonstrated that there was no significant publication bias.

TABLE 1 | Characteristics of the included studies.

Study	Publication year	Study design	*N*	Gestational age, weeks	Umbilical cord blood pH value	Number of CP cases	Follow-up period
Carli et al. (32)	2004	Cohort study	43	≥37	pH < 7.00 or BD ≥ 12 mmol/L	13	12–36 months
Gluckman et al. (24)	2005	RCT	218	≥36	pH < 7.00 or BD > 16 mmol/L	52	18 months
Shankaran et al. (25)	2005	RCT	205	≥36	pH ≤ 7.00 or BD ≥ 16 mmol/L	34	18–22 months
Azzopardi et al. (26)	2009	RCT	323	≥36	pH < 7.00 or BD ≥ 16 mmol/L	81	18 months
Simbruner et al. (27)	2010	RCT	111	≥36	pH < 7.00 or BD > 16 mmol/L	14	18–21 months
Jacobs et al. (28)	2011	RCT	208	≥35	pH < 7.00 or BD ≥ 12 mmol/L	38	24 months
Perez et al. (33)	2013	Cohort study	68	≥36	pH < 7.1 and BD < −10 mmol/L	11	8.2–15.7 years
Filippi et al. (29)	2017	RCT	42	≥36	pH < 7.00 and/or BD > 16 mmol/L	13	18–24 months
Malla et al. (30)	2017	RCT	100	≥37	pH ≤ 7.00 and/or BD ≥ 16 mmol/L	29	19 months
Shankaran et al. (31)	2017	RCT	347	≥36	pH ≤ 7.00 or BD ≥ 16 mmol/L	47	18–22 months

BD, base deficit.

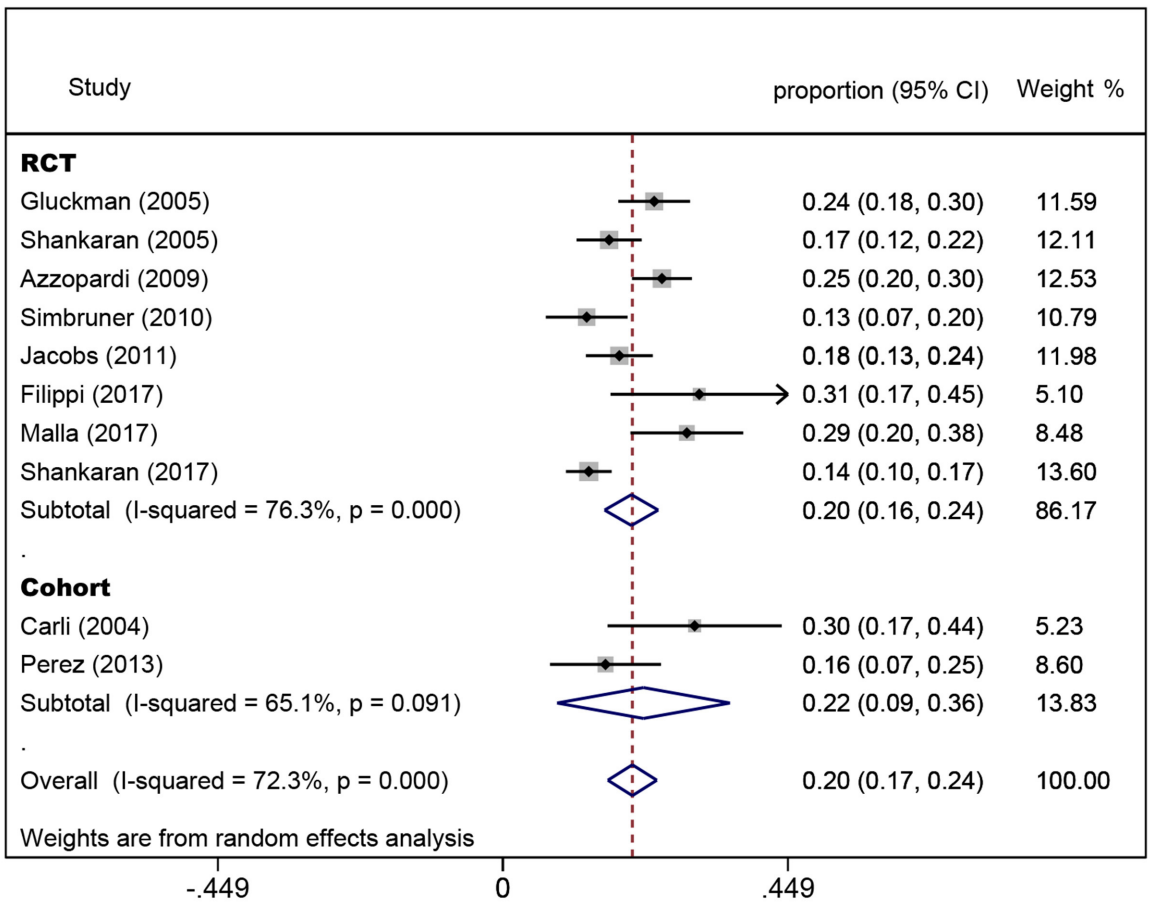

FIGURE 2 | Forest plot of the pooled rate of cerebral palsy. The solid diamonds and horizontal solid lines represent the proportions and 95% CIs of each included study. The size of the gray area indicates the study-specific statistical weight. The hollow diamonds show the pooled proportions and 95% CIs of each group and the overall population. The vertical red dotted line shows the combined effect estimate.

Pooled Rate of CP

In the eight randomized controlled trials, the number of infants with CP was 308 for a pooled rate of 20.3% (95% CI: 16.0–24.5, I^2 = 76.3%). In the two observational studies, the number of infants with CP was 24 and the combined incidence was 22.2% (95% CI: 8.5–35.8, I^2 = 65.1%) (**Figure 2**). In the randomized controlled trials, the infants were divided into intervention and non-intervention groups. The number of infants with CP was 166

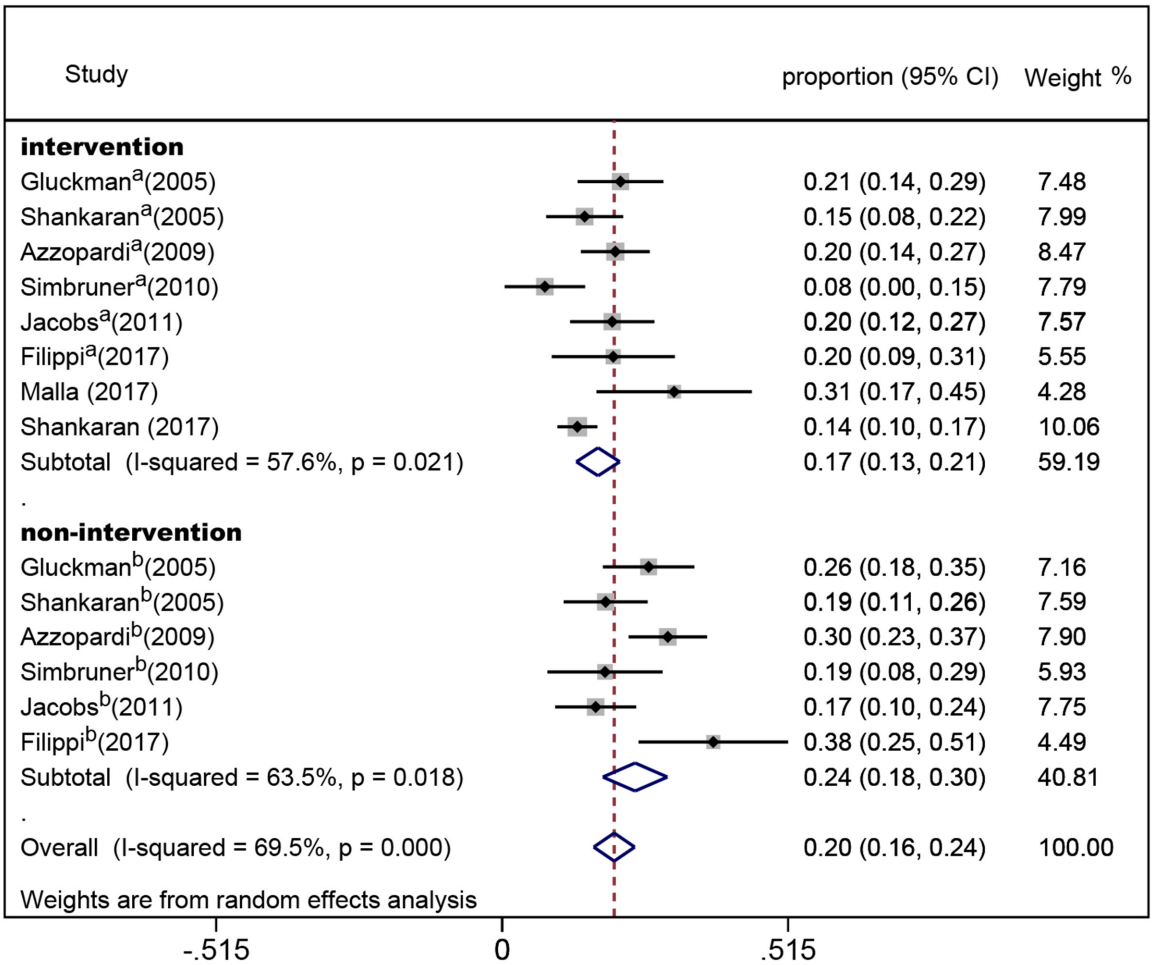

FIGURE 3 | Forest plot of the pooled rate of cerebral palsy in the intervention and non-intervention groups in randomized controlled trials. The solid diamonds and horizontal solid lines represent the proportions and 95% CIs of each included study. The size of the gray area indicates the study-specific statistical weight. The hollow diamonds show the pooled proportions and 95% CIs of each subgroup and the overall population. The vertical red dotted line shows the combined effect estimate.

in the intervention group and was 142 in the non-intervention group. The pooled rate of CP was 17.3% (95% CI: 13.3–21.2, $I^2 = 57.6\%$) in the intervention group and was 23.9% (95% CI: 18.1–29.7, $I^2 = 63.5\%$) in the non-intervention group (**Figure 3**), indicating that whether interventions were performed or not led to the high heterogeneity between studies.

DISCUSSION

To our knowledge, this is the first evaluation of the link between birth asphyxia and CP using the pH value of umbilical cord blood as a diagnostic criterion for birth asphyxia in addition to clinical HIE manifestations. The results of this meta-analysis indicated that birth asphyxia is associated with CP in both term and near-term infants.

Birth asphyxia might affect the outcomes of neurodevelopment in infants through a variety of mechanisms. Prolonged or intense asphyxia will cause energy depletion in tissues that depend on aerobic metabolism, such as the central nervous system (34, 35). Lack of energy can lead to the failure of ATP-dependent pumps resulting in the loss of neuronal transmembrane potential (36), and thus the most sensitive areas of the brain will die (37–39). In areas that are more resistant, excessive excitability of neurons, abundant ionic calcium influx, free radical generation, and changes in mitochondrial metabolism (40–42) might cause secondary energy exhaustion and programmed neuronal death (43, 44). Thus, these irreversible brain injuries during early brain development might ultimately result in CP.

The accurate diagnosis of birth asphyxia is still a challenge worldwide, resulting in an unclear correlation between asphyxia and CP. Birth asphyxia is predicated by fetal metabolic acidosis, as measured by umbilical cord pH at birth (21, 45), and a recent study showed that a low umbilical cord pH was associated with the occurrence of CP but failed to prove that there was a link between the degree of acidosis and the prevalence or severity of CP (46). In two studies an umbilical arterial pH $\leq$

7.00 was referred to pathological or severe fetal acidemia in which the risk of adverse neurological sequelae was increased (47, 48). Furthermore, different consensus statements have mentioned the diagnosis of intrapartum asphyxia since 1992. These statements point out that metabolic acidosis (pH $<$ 7.0 and base deficit of 12 mmol/L or more) is the essential criterion for the diagnosis of asphyxia (49, 50). Therefore, an umbilical arterial pH $\leq$ 7.00 and/or a base deficit of 12 mmol/L or more was used as the standard of acidosis to diagnose birth asphyxia in this meta-analysis in addition to neonatal clinical HIE manifestations.

The American Academy of Pediatrics and the Society of Obstetrics and Gynecology suggests that infants suffering from "asphyxiation" near delivery, which is severe enough to result in acute neurologic injury, should meet the following criteria: (1) severe metabolic or mixed acidemia (pH $<$ 7.00) on an umbilical arterial blood sample, (2) an Apgar score of 0 to 3 for longer than 5 min, (3) neurologic manifestation such as seizure, coma, or hypotonia, and (4) evidence of multiorgan dysfunction (51). However, it is difficult to measure all of the diagnostic criteria in the clinic, and currently the Apgar score system is most commonly used. Neither Apgar score nor umbilical arterial pH $\leq$ 7.00 and/or a base deficit $\geq$ 12 mmol/L as the diagnostic criterion of asphyxia is a complete definition of birth asphyxia, and fetal severe acidosis is instead considered to be a fairer and more objective standard (52).

The evidence reported in previous studies was unable to support a clear association between birth asphyxia and CP (9, 53). However, our pooled analysis of 1,665 infants in 10 studies showed that the CP incidence was 20.3% (95% CI: 16.0–24.5, I^2 = 76.3%) in the randomized controlled trials and 22.2% (95% CI: 8.5–35.8, I^2 = 65.1%) in the observational studies, which means a more relevant association between birth asphyxia and CP. With the popularization of blood gas analysis, the detection of umbilical arterial pH value at birth is easier to perform (54). Our results suggest that blood gas analysis should be used along with Apgar score in daily clinic work when there is the possibility of birth asphyxia. Considering that preterm birth is a risk factor of CP (6, 7), we only included studies with newborn infants who were born at term or near term. Some of the patients were treated with hypothermia and/or drugs in randomized controlled trials, so we divided these patients into intervention and non-intervention groups. The results showed that the incidence of CP in the intervention group had a slight decrease compared to that in the non-intervention group, which was consistent with the conclusion that hypothermia therapy can reduce the risk of neurological impairment in infants with HIE (55). Further treatment should be considered to prevent CP after hypothermia in the acute phase (56).

Previous analysis the association of birth asphyxia and CP showed a large variation from 3 to 50% (18). Other researchers also indicated that <12% of children who have CP were exposed to perinatal asphyxia, which contradicts our results (57–59). For such inconsistent results linking birth asphyxia and CP, the differences in the diagnosis criteria of birth asphyxia were probably the main problems (5, 60). The critical criteria might affect our results to a certain extent. Nevertheless, we still hope to emphasize the importance of severe acidosis as one of necessary criteria of asphyxia in clinical application through the results in this meta-analysis.

Our meta-analysis has some other limitations. First, we only searched literature published in English. Second, publication bias and incomplete ascertainment of published literature might exist. Third, the number of studies in our analysis was small, and the selection of the diagnostic criteria of birth asphyxia might have caused a selection bias in our study. Therefore, the results of this study should be interpreted with caution. Furthermore, some of the included studies used interventions, so measurement bias existed and some heterogeneity was inevitable.

In conclusion, our meta-analysis provides evidence that birth asphyxia is associated with CP in children. Thus, the prevention and treatment of birth asphyxia is of great significance for reducing the prevalence of CP.

DATA AVAILABILITY STATEMENT

All datasets presented in this study are included in the article/ **Supplementary Material**.

AUTHOR CONTRIBUTIONS

SZ and BL searched the databases, screened the articles, and collected the data. SZ wrote the first draft of the manuscript. BL and XZ were responsible for the statistical analysis and interpretation of the data. XW coordinated and supervised the data collection. SZ, CZ, and XW participated in study conception and design. XZ, CZ, and XW critically reviewed and revised the manuscript. All authors contributed to and approved the final version. All authors contributed to the article and approved the submitted version.

FUNDING

This work was supported by the National Nature Science Foundation of China (U1704281, 31761133015, and 81771418), the Department of Science and Technology of Henan Province, China (171100310200), VINNMER–Marie Curie (VINNOVA, 2015-04780), the Swedish Research Council (2018-02267), and Swedish Governmental grants to scientists working in health care of Gothenburg, Sweden (ALFGBG-717791).

SUPPLEMENTARY MATERIAL

The Supplementary Material for this article can be found online at: https://www.frontiersin.org/articles/10.3389/fneur.2020.00704/full#supplementary-material

REFERENCES

1. Graham HK, Rosenbaum P, Paneth N, Dan B, Lin JP, Damiano DL, et al. Cerebral palsy. *Nat Rev Dis Primers.* (2016) 2:15082. doi: 10.1038/nrdp.2015.82
2. Oskoui M, Coutinho F, Dykeman J, Jette N, Pringsheim T. An update on the prevalence of cerebral palsy: a systematic review and meta-analysis. *Dev Med Child Neurol.* (2013) 55:509–19. doi: 10.1111/dmcn.12080
3. Paneth N, Hong T, Korzeniewski S. The descriptive epidemiology of cerebral palsy. *Clin Perinatol.* (2006) 33:251–67. doi: 10.1016/j.clp.2006.03.011
4. Bhushan V, Paneth N, Kiely JL. Impact of improved survival of very low birth weight infants on recent secular trends in the prevalence of cerebral palsy. *Pediatrics.* (1993) 91:1094–100.
5. MacLennan AH, Lewis S, Moreno-De-Luca A, Fahey M, Leventer RJ, McIntyre S, et al. Genetic or other causation should not change the clinical diagnosis of cerebral palsy. *J Child Neurol.* (2019) 34:472–6. doi: 10.1177/0883073819840449
6. Nelson KB, Blair E. Prenatal factors in singletons with cerebral palsy born at or near term. *N Engl J Med.* (2015) 373:946–53. doi: 10.1056/NEJMra1505261
7. Moster D, Lie RT, Markestad T. Long-term medical and social consequences of preterm birth. *N Engl J Med.* (2008) 359:262–73. doi: 10.1056/NEJMoa0706475
8. Song J, Sun H, Xu F, Kang W, Gao L, Guo J, et al. Recombinant human erythropoietin improves neurological outcomes in very preterm infants. *Ann Neurol.* (2016) 80:24–34. doi: 10.1002/ana.24677
9. Jacobsson B, Hagberg G. Antenatal risk factors for cerebral palsy. *Best Pract Res Clin Obstet Gynaecol.* (2004) 18:425–36. doi: 10.1016/j.bpobgyn.2004.02.011
10. Blair E, Stanley FJ. Intrapartum asphyxia: a rare cause of cerebral palsy. *J Pediatr.* (1988) 112:515–9. doi: 10.1016/S0022-3476(88)80161-6
11. Erkin G, Delialioglu SU, Ozel S, Culha C, Sirzai H. Risk factors and clinical profiles in Turkish children with cerebral palsy: analysis of 625 cases. *Int J Rehabil Res.* (2008) 31:89–91. doi: 10.1097/MRR.0b013e3282f45225
12. Venkateswaran S, Shevell MI. Etiologic profile of spastic quadriplegia in children. *Pediatr Neurol.* (2007) 37:203–8. doi: 10.1016/j.pediatrneurol.2007.05.006
13. Anwar S, Chowdhury J, Khatun M, Mollah AH, Begum HA, Rahman Z, et al. Clinical profile and predisposing factors of cerebral palsy. *Mymensingh Med J.* (2006) 15:142–5. doi: 10.3329/mmj.v15i2.32
14. Lawn JE, Cousens S, Zupan J. 4 million neonatal deaths: when? Where? Why? *Lancet.* (2005) 365:891–900. doi: 10.1016/S0140-6736(05)71048-5
15. Zhu C, Kang W, Xu F, Cheng X, Zhang Z, Jia L, et al. Erythropoietin improved neurologic outcomes in newborns with hypoxic-ischemic encephalopathy. *Pediatrics.* (2009) 124:e218–26. doi: 10.1542/peds.2008-3553
16. Perlman JM. Interruption of placental blood flow during labor: potential systemic and cerebral organ consequences. *J Pediatr.* (2011) 158(Suppl. 2):e1–4. doi: 10.1016/j.jpeds.2010.11.003
17. Rainaldi MA, Perlman JM. Pathophysiology of birth asphyxia. *Clin Perinatol.* (2016) 43:409–22. doi: 10.1016/j.clp.2016.04.002
18. Ellenberg JH, Nelson KB. The association of cerebral palsy with birth asphyxia: a definitional quagmire. *Dev Med Child Neurol.* (2013) 55:210–6. doi: 10.1111/dmcn.12016
19. Low JA. The role of blood gas and acid-base assessment in the diagnosis of intrapartum fetal asphyxia. *Am J Obstet Gynecol.* (1988) 159:1235–40. doi: 10.1016/0002-9378(88)90456-5
20. Goodwin TM, Belai I, Hernandez P, Durand M, Paul RH. Asphyxial complications in the term newborn with severe umbilical acidemia. *Am J Obstet Gynecol.* (1992) 167:1506–12. doi: 10.1016/0002-9378(92)91728-S
21. Ruth VJ, Raivio KO. Perinatal brain damage: predictive value of metabolic acidosis and the Apgar score. *BMJ.* (1988) 297:24–7. doi: 10.1136/bmj.297.6640.24
22. Stang A. Critical evaluation of the Newcastle-Ottawa scale for the assessment of the quality of nonrandomized studies in meta-analyses. *Eur J Epidemiol.* (2010) 25:603–5. doi: 10.1007/s10654-010-9491-z
23. Higgins JP, Altman DG, Gotzsche PC, Juni P, Moher D, Oxman AD, et al. The cochrane collaboration's tool for assessing risk of bias in randomised trials. *BMJ.* (2011) 343:d5928. doi: 10.1136/bmj.d5928
24. Gluckman PD, Wyatt JS, Azzopardi D, Ballard R, Edwards AD, Ferriero DM, et al. Selective head cooling with mild systemic hypothermia after neonatal encephalopathy: multicentre randomised trial. *Lancet.* (2005) 365:663–70. doi: 10.1016/S0140-6736(05)17946-X
25. Shankaran S, Laptook AR, Ehrenkranz RA, Tyson JE, McDonald SA, Donovan EF, et al. Whole-body hypothermia for neonates with hypoxic-ischemic encephalopathy. *N Engl J Med.* (2005) 353:1574–84. doi: 10.1056/NEJMcps050929
26. Azzopardi DV, Strohm B, Edwards AD, Dyet L, Halliday HL, Juszczak E, et al. Moderate hypothermia to treat perinatal asphyxial encephalopathy. *N Engl J Med.* (2009) 361:1349–58. doi: 10.1056/NEJMoa0900854
27. Simbruner G, Mittal RA, Rohlmann F, Muche R. Systemic hypothermia after neonatal encephalopathy: outcomes of neo.nEURO.network RCT. *Pediatrics.* (2010) 126:e771–8. doi: 10.1542/peds.2009-2441
28. Jacobs SE, Morley CJ, Inder TE, Stewart MJ, Smith KR, McNamara PJ, et al. Whole-body hypothermia for term and near-term newborns with hypoxic-ischemic encephalopathy: a randomized controlled trial. *Arch Pediatr Adolesc Med.* (2011) 165:692–700. doi: 10.1001/archpediatrics.2011.43
29. Filippi L, Fiorini P, Catarzi S, Berti E, Padrini L, Landucci E, et al. Safety and efficacy of topiramate in neonates with hypoxic ischemic encephalopathy treated with hypothermia (NeoNATI): a feasibility study. *J Matern Fetal Neonatal Med.* (2018) 31:973–80. doi: 10.1080/14767058.2017.1304536
30. Malla RR, Asimi R, Teli MA, Shaheen F, Bhat MA. Erythropoietin monotherapy in perinatal asphyxia with moderate to severe encephalopathy: a randomized placebo-controlled trial. *J Perinatol.* (2017) 37:596–601. doi: 10.1038/jp.2017.17
31. Shankaran S, Laptook AR, Pappas A, McDonald SA, Das A, Tyson JE, et al. Effect of depth and duration of cooling on death or disability at age 18 months among neonates with hypoxic-ischemic encephalopathy: a randomized clinical trial. *JAMA.* (2017) 318:57–67. doi: 10.1001/jama.2017.7218
32. Carli G, Reiger I, Evans N. One-year neurodevelopmental outcome after moderate newborn hypoxic ischaemic encephalopathy. *J Paediatr Child Health.* (2004) 40:217–20. doi: 10.1111/j.1440-1754.2004.00341.x
33. Perez A, Ritter S, Brotschi B, Werner H, Caflisch J, Martin E, et al. Long-term neurodevelopmental outcome with hypoxic-ischemic encephalopathy. *J Pediatr.* (2013) 163:454–9. doi: 10.1016/j.jpeds.2013.02.003
34. Wassink G, Gunn ER, Drury PP, Bennet L, Gunn AJ. The mechanisms and treatment of asphyxial encephalopathy. *Front Neurosci.* (2014) 8:40. doi: 10.3389/fnins.2014.00040
35. Johnston MV, Fatemi A, Wilson MA, Northington F. Treatment advances in neonatal neuroprotection and neurointensive care. *Lancet Neurol.* (2011) 10:372–82. doi: 10.1016/S1474-4422(11)70016-3
36. Sanderson TH, Reynolds CA, Kumar R, Przyklenk K, Huttemann M. Molecular mechanisms of ischemia-reperfusion injury in brain: pivotal role of the mitochondrial membrane potential in reactive oxygen species generation. *Mol Neurobiol.* (2013) 47:9–23. doi: 10.1007/s12035-012-8344-z
37. Circu ML, Aw TY. Reactive oxygen species, cellular redox systems, and apoptosis. *Free Radic Biol Med.* (2010) 48:749–62. doi: 10.1016/j.freeradbiomed.2009.12.022
38. Redza-Dutordoir M, Averill-Bates DA. Activation of apoptosis signalling pathways by reactive oxygen species. *Biochim Biophys Acta.* (2016) 1863:2977–92. doi: 10.1016/j.bbamcr.2016.09.012
39. Wu Y, Song J, Wang Y, Wang X, Culmsee C, Zhu C. The potential role of ferroptosis in neonatal brain injury. *Front Neurosci.* (2019) 13:115. doi: 10.3389/fnins.2019.00115
40. Ahearne CE, Denihan NM, Walsh BH, Reinke SN, Kenny LC, Boylan GB, et al. Early cord metabolite index and outcome in perinatal asphyxia and hypoxic-ischaemic encephalopathy. *Neonatology.* (2016) 110:296–302. doi: 10.1159/000446556
41. Denihan NM, Boylan GB, Murray DM. Metabolomic profiling in perinatal asphyxia: a promising new field. *Biomed Res Int.* (2015) 2015:254076. doi: 10.1155/2015/254076
42. Sun Y, Li T, Xie C, Zhang Y, Zhou K, Wang X, et al. Dichloroacetate treatment improves mitochondrial metabolism and reduces brain injury in neonatal mice. *Oncotarget.* (2016) 7:31708–22. doi: 10.18632/oncotarget.9150
43. Xie C, Ginet V, Sun Y, Koike M, Zhou K, Li T, et al. Neuroprotection by selective neuronal deletion of Atg7 in neonatal brain injury. *Autophagy.* (2016) 12:410–23. doi: 10.1080/15548627.2015.1132134

44. Li K, Li T, Wang Y, Xu Y, Zhang S, Culmsee C, et al. Sex differences in neonatal mouse brain injury after hypoxia-ischemia and adaptaquin treatment. *J Neurochem.* (2019) 150:759–75. doi: 10.1111/jnc.14790
45. Fahey J, King TL. Intrauterine asphyxia: clinical implications for providers of intrapartum care. *J Midwifery Womens Health.* (2005) 50:498–506. doi: 10.1016/j.jmwh.2005.08.007
46. Malin GL, Morris RK, Khan KS. Strength of association between umbilical cord pH and perinatal and long term outcomes: systematic review and meta-analysis. *BMJ.* (2010) 340:c1471. doi: 10.1136/bmj.c1471
47. Sehdev HM, Stamilio DM, Macones GA, Graham E, Morgan MA. Predictive factors for neonatal morbidity in neonates with an umbilical arterial cord pH less than 7.00. *Am J Obstet Gynecol.* (1997) 177:1030–4. doi: 10.1016/S0002-9378(97)70008-5
48. Goldaber KG, Gilstrap LC III, Leveno KJ, Dax JS, McIntire DD. Pathologic fetal acidemia. *Obstet Gynecol.* (1991) 78:1103–7.
49. MacLennan A. A template for defining a causal relation between acute intrapartum events and cerebral palsy: international consensus statement. *BMJ.* (1999) 319:1054–9. doi: 10.1136/bmj.319.7216.1054
50. Hankins GD, Speer M. Defining the pathogenesis and pathophysiology of neonatal encephalopathy and cerebral palsy. *Obstet Gynecol.* (2003) 102:628–36. doi: 10.1016/S0029-7844(03)00574-X
51. Committee on Fetus and Newborn, American Academy of Pediatrics, Committee on Obstetric Practice, American College of Obstetricians and Gynecologists. Use and abuse of the Apgar score. *Pediatrics*. (1996) 98:141–2.
52. Perlman JM. Pathogenesis of hypoxic-ischemic brain injury. *J Perinatol.* (2007) 27:S39–46. doi: 10.1038/sj.jp.7211716
53. Graham EM, Ruis KA, Hartman AL, Northington FJ, Fox HE. A systematic review of the role of intrapartum hypoxia-ischemia in the causation of neonatal encephalopathy. *Am J Obstet Gynecol.* (2008) 199:587–95. doi: 10.1016/j.ajog.2008.06.094
54. Armstrong L, Stenson BJ. Use of umbilical cord blood gas analysis in the assessment of the newborn. *Arch Dis Child Fetal Neonatal Ed.* (2007) 92:F430–4. doi: 10.1136/adc.2006.099846
55. Edwards AD, Brocklehurst P, Gunn AJ, Halliday H, Juszczak E, Levene M, et al. Neurological outcomes at 18 months of age after moderate hypothermia for perinatal hypoxic ischaemic encephalopathy: synthesis and meta-analysis of trial data. *BMJ.* (2010) 340:c363. doi: 10.1136/bmj.c363
56. Fleiss B, Gressens P. Tertiary mechanisms of brain damage: a new hope for treatment of cerebral palsy? *Lancet Neurol.* (2012) 11:556–66. doi: 10.1016/S1474-4422(12)70058-3
57. Pappas A, Korzeniewski SJ. Long-term cognitive outcomes of birth asphyxia and the contribution of identified perinatal asphyxia to cerebral palsy. *Clin Perinatol.* (2016) 43:559–72. doi: 10.1016/j.clp.2016.04.012
58. Nelson KB, Ellenberg JH. Apgar scores as predictors of chronic neurologic disability. *Pediatrics.* (1981) 68:36–44.
59. Nelson KB, Ellenberg JH. Antecedents of cerebral palsy. Multivariate analysis of risk. *N Engl J Med.* (1986) 315:81–6. doi: 10.1056/NEJM198607103150202
60. Sun L, Xia L, Wang M, Zhu D, Wang Y, Bi D, et al. Variants of the OLIG2 gene are associated with cerebral palsy in Chinese Han infants with hypoxic-ischemic encephalopathy. *Neuromol Med.* (2019) 21:75–84. doi: 10.1007/s12017-018-8510-1

Conflict of Interest: The authors declare that the research was conducted in the absence of any commercial or financial relationships that could be construed as a potential conflict of interest.

frontiers in Neurology

ORIGINAL RESEARCH
published: 12 August 2020
doi: 10.3389/fneur.2020.00804

Repetitive Erythropoietin Treatment Improves Long-Term Neurocognitive Outcome by Attenuating Hyperoxia-Induced Hypomyelination in the Developing Brain

*Monia Vanessa Dewan[1], Meray Serdar[1], Yohan van de Looij[2,3], Mirjam Kowallick[1], Martin Hadamitzky[4], Stefanie Endesfelder[5], Joachim Fandrey[6], Stéphane V. Sizonenko[2], Josephine Herz[1], Ursula Felderhoff-Müser[1] and Ivo Bendix[1]**

[1] Department of Paediatrics I, Neonatology and Experimental Perinatal Neurosciences, University Hospital Essen, University Duisburg-Essen, Essen, Germany, [2] Division of Child Development and Growth, Department of Paediatrics, School of Medicine, University of Geneva, Geneva, Switzerland, [3] Center for Biomedical Imaging, Animal Imaging and Technology, Ecole Polytechnique Fédérale de Lausanne, Lausanne, Switzerland, [4] Institute of Medical Psychology and Behavioural Immunobiology, University Hospital Essen, University Duisburg-Essen, Essen, Germany, [5] Department of Neonatology, Charité-Universitätsmedizin Berlin, Berlin, Germany, [6] Institute of Physiology, University Hospital Essen, University Duisburg-Essen, Essen, Germany

OPEN ACCESS

Edited by:
Deirdre M. Murray,
University College Cork, Ireland

Reviewed by:
Carlotta Spagnoli,
Santa Maria Nuova Hospital, Italy
Dinesh Upadhya,
Manipal Academy of Higher Education, India

***Correspondence:**
Ivo Bendix
ivo.bendix@uk-essen.de

Specialty section:
This article was submitted to Pediatric Neurology, a section of the journal Frontiers in Neurology

Received: 30 March 2020
Accepted: 29 June 2020
Published: 12 August 2020

Citation:
Dewan MV, Serdar M, van de Looij Y, Kowallick M, Hadamitzky M, Endesfelder S, Fandrey J, Sizonenko SV, Herz J, Felderhoff-Müser U and Bendix I (2020) Repetitive Erythropoietin Treatment Improves Long-Term Neurocognitive Outcome by Attenuating Hyperoxia-Induced Hypomyelination in the Developing Brain. Front. Neurol. 11:804. doi: 10.3389/fneur.2020.00804

Introduction: Preterm infants born before 28 weeks of gestation are at high risk of neurodevelopmental impairment in later life. Cerebral white and gray matter injury is associated with adverse outcomes. High oxygen levels, often unavoidable in neonatal intensive care, have been identified as one of the main contributing factors to preterm brain injury. Thus, preventive and therapeutic strategies against hyperoxia-induced brain injury are needed. Erythropoietin (Epo) is a promising and also neuroprotective candidate due to its clinical use in infants as erythropoiesis-stimulating agent.

Objective: The objective of this study was to investigate the effects of repetitive Epo treatment on the cerebral white matter and long-term motor-cognitive outcome in a neonatal rodent model of hyperoxia-induced brain injury.

Methods: Three-day old Wistar rats were exposed to hyperoxia (48 h, 80% oxygen). Four doses of Epo (5,000 IU/kg body weight per day) were applied intraperitoneally from P3-P6 with the first dose at the onset of hyperoxia. Oligodendrocyte maturation and myelination were evaluated via immunohistochemistry and Western blot on P11. Motor-cognitive deficits were assessed in a battery of complex behavior tests (Open Field, Novel Object Recognition, Barnes maze) in adolescent and fully adult animals. Following behavior tests animals underwent post-mortem diffusion tensor imaging to investigate long-lasting microstructural alterations of the white matter.

Results: Repetitive treatment with Epo significantly improved myelination deficits following neonatal hyperoxia at P11. Behavioral testing revealed attenuated hyperoxia-induced cognitive deficits in Epo-treated adolescent and adult rats.

Conclusion: A multiple Epo dosage regimen protects the developing brain against hyperoxia-induced brain injury by improving myelination and long-term cognitive outcome. Though current clinical studies on short-term outcome of Epo-treated prematurely born children contradict our findings, long-term effects up to adulthood are still lacking. Our data support the essential need for long-term follow-up of preterm infants in current clinical trials.

Keywords: erythropoietin, neuroprotection, preterm brain injury, white matter injury, hyperoxia, myelination

INTRODUCTION

Extremely preterm born infants (<28 weeks of gestation) are at high risk for neurodevelopmental impairment. Around 50% of survivors suffer from neurological or developmental disabilities ranging from various motor, cognitive and sensory impairments to behavioral and emotional disorders in later life (1–3). Cerebral magnetic resonance imaging (MRI) studies at term equivalent age revealed that most survivors show cerebral gray and white matter abnormalities, which are associated with adverse outcome (4). The high risk of neurodevelopmental disabilities is caused by the high vulnerability of the immature brain to the extra-uterine environment in a period of enormous brain growth and maturation (5).

Clinical and pre-clinical studies suggested that the developing brain is particularly vulnerable to chronic exposure to high oxygen levels resulting in subtle and diffuse brain injury (6, 7). Rodent models of hyperoxia-induced brain injury demonstrated that supraphysiologic oxygen-levels induce oxidative stress, inflammation and cellular degeneration, leading to hypomyelination and long-term cognitive deficits (7–10). Despite these findings, oxygen remains an indispensable therapeutic agent in neonatal intensive care. Therefore, neuroprotective agents preventing oxygen-induced brain injury are urgently needed.

One of these promising neuroprotective candidates is Erythropoietin (Epo) (11), an endogenous hormone, which in its recombinant form has been used for the prevention of anemia of prematurity for almost three decades (12). Besides its hematopoietic effects, Epo is suggested to be a neurotrophic and neuroprotective factor in the developing brain, where it is expressed by different cell types such as neurons, oligodendrocytes and astrocytes from early gestation on (13–15). Several studies in experimental models of neonatal brain injury have confirmed its neuroprotective effects (16–19). However, findings from clinical studies are inconsistent: While some retro- and prospective studies revealed improved neurocognitive outcome and white matter development in MRI studies (20–22), recent results from two large randomized controlled trials could not confirm these findings at the corrected age of 2 years (23, 24).

In the rodent model of hyperoxia-induced brain injury, we have previously shown that a single bolus application of 20,000 IE/kg body weight of Epo at the onset of hyperoxia leads to long-lasting improvement of neurocognitive development up to adolescent and adult age (25). Suggested mechanisms include a reduction of oxidative stress, cellular degeneration and inflammation, as well as modulation of autophagy signaling and improvement of synaptic plasticity (16, 25–27). Although bolus Epo-application resulted in a reduced degeneration of oligodendrocytes in our previous study, myelination or white matter development were not changed (25). These results were in contrast to findings in other experimental settings and in clinical studies using multiple dosage regimes (21, 28–30).

Taking into account that in clinical settings, a single-dose Epo regimen is uncommon and that safety-studies have already proven good tolerability of even larger doses (31), the aim of this study was to investigate effects of a repetitive Epo treatment in a model of hyperoxia-induced perinatal brain injury. We hypothesized that repetitive Epo applications protect the developing brain against hyperoxia-induced hypomyelination as well as microstructural alterations of the white matter and ameliorate long-term neurodevelopmental deficits.

MATERIALS AND METHODS

Animals and Experimental Design

All animal procedures were approved by the local animal welfare committee and performed according to the guidelines of the University Hospital Essen. Three-day old (P3) Wistar rat pups were exposed to 80% oxygen for 48 h in an oxygen chamber (OxyCycler, BioSpherix, Lacona, NY, USA). The control group was kept under normoxic conditions (21% oxygen, room-air). In both groups, pups were with their lactating dams. After the first 24 h, dams were exchanged in order to avoid prolonged exposition to hyperoxia. From P3 to P6 animals received daily intraperitoneal (i.p.) injections of 5,000 IU/kg body weight Epo (Epo, NeoRecormon®, Boehringer-La Roche, Grenzach, Germany) culminating in a total dose of 20,000 IU/kg body weight. The first Epo dose was administered at the onset of hyperoxia. Control animals received an equal amount of saline (10 mL/kg body weight).

In total, 132 pups derived from 14 litters were enrolled in this study. Pups per litter were randomly assigned to all treatment groups considering sex–and weight. Increase of bodyweight was monitored daily until P11 and once a week afterwards. No differences were observed between the study groups throughout the entire experiments. Behavioral studies were performed in adolescent (1–2 months old) and adult (4 months old) rats. Pups were sacrificed on P11 (88 pups, 10 litters) and at the age of 5 months (44 pups, 4 litters). Animals sacrificed on P11 were evaluated for subacute white matter injury via Western blot analysis and immunohistochemistry. Pups sacrificed at fully adult

age (5 months), which were subjected to behavioral assessment, were evaluated for microstructural changes via diffusion tensor imaging (DTI).

For Western blot analysis, animals were decapitated following transcardial perfusion with phosphate buffered saline. Hemispheres (excluding cerebellum) were snap frozen in liquid nitrogen and stored at 80°C until further processing. For histological and DTI studies, pups were transcardially perfused with phosphate buffered saline followed by 4% paraformaldehyde (PFA, Sigma-Aldrich, Munich, Germany). Brains were post-fixed in 4% PFA overnight at 4°C and embedded in paraffin or sent for DTI.

Immunoblotting

Snap-frozen brain tissues were homogenized in ice-cooled radioimmunoprecipitation assay (RIPA, Sigma-Aldrich) buffer, phenylmethanesulfonyl fluoride (PMFS, Sigma-Aldrich), complete Mini, EDTA-free (Roche, Basel, Switzerland) and sodium orthovanadate. Homogenates were centrifuged at 17,000 g for 20 min at 4°C. Protein concentrations of the cytosolic fraction were determined using the BCA assay kit (Thermo Fisher Scientific, Dreieich, Germany). Western blotting was performed with 30 μg lysate per sample. Proteins were separated in 15% sodium dodecyl sulfate polyacrylamide gels and transferred to 0.2 μm pore nitrocellulose membranes (Sigma-Aldrich). To control for equal protein transfer, membranes were stained with Ponceau S solution (Sigma Aldrich). Blocking of non-specific protein binding in 5% non-fat dry milk in Tris buffered saline/0.1% Tween 20 (TBS-T) for 60 min at room temperature was followed by primary antibody incubation in 2.5 or 5% non-fat dry milk in TBST at 4°C overnight. The following primary antibodies were used: monoclonal mouse anti-myelin basic protein (MBP) (1:1000, Covance, Münster, Germany), monoclonal mouse anti-oligodendrocyte transcription factor 2 (Olig2) (1:1000, Merck Millipore, Darmstadt, Germany), monoclonal mouse anti-2', 3'-cyclic nucleotide 3'-phosphodiesterase (CNPase) (1:1000, Merck Millipore) and monoclonal rabbit anti-Glycerinaldehyd-3-phosphat-Dehydrogenase (GAPDH) (1:5000, Cell Signaling, Frankfurt, Germany). To detect primary antibody binding, membranes were incubated for 1 h at room temperature with horseradish peroxidase-conjugated secondary anti-mouse (1:5000, Dako, Hamburg, Germany) or anti-rabbit (1:2000, Dako) antibody. Antibody binding was detected by using enhanced chemiluminescence (GE Healthcare Life Sciences, Munich, Germany) and visualized by the ChemiDoc XRS+ imaging system. ImageLab software (Bio-Rad, Munich, Germany) was used for densitometric analysis. Density ratios between the protein of interest and the reference protein GAPDH were calculated for each sample. These ratios were normalized to the control group NO.

Immunohistochemistry

Ten micrometre coronal sections (−3.72 ± 0.7 mm from bregma) were deparaffinized and rehydrated followed by antigen-retrieval in preheated 10 mM sodium-citrate buffer (pH 6.0) for 30 min. After blocking with 1% bovine serum albumin and 0.3% cold fish skin gelatine in TBST (Sigma-Aldrich) slides were incubated with primary antibodies at 4°C overnight. The following primary antibodies were used: polyclonal rabbit anti-Olig2 (1:100, Millipore), monoclonal rat anti-MBP (1:200, abcam, Berlin, Germany) and monoclonal mouse anti-adenomatous polyposis coli clone CC1 (APC-CC1, 1:100, Merck Millipore). This was followed by incubation with appropriate secondary antibodies for 1 h at room temperature [anti-mouse Alexa Fluor 488, anti-rat Alexa Fluor 555 and anti-rabbit Alexa Fluor 647 (all 1:500, Invitrogen, Darmstadt, Germany)]. Sections were counterstained with 4,6-diamidino-2-phenylindole (DAPI) (1 μg/mL, Invitrogen, Karlsruhe, Germany).

For image acquisition four laser lines (laser diode, 405 nm; Ar laser, 514 nm; G-HeNe laser, 543 nm; Rn Laser 639 nm) and four different filters (450/50-405 LP, 515/20-540 LP, and 585/65-640 LP) were used. Confocal z-stacks of 10 μm thickness (z-plane distance 1 μm) large-scale images of complete hemispheres were acquired with a 10× objective. From each animal two slides of a total hemisphere were assessed. Data were acquired and analyzed by investigators blinded to treatment.

For analysis of triple-positive cells ($Olig2^+$/APC-$CC1^+$/$DAPI^+$) nine regions of interest (ROIs) were selected: three specific ROIs in the white matter, three in the cortex and three in the thalamus (each 500 × 500 μm). The 3D-images were converted to maximal intensity projections and converted to Tiff-images followed by analysis with the cell counter plugin of ImageJ (National Institutes of Health, Java 1.8.0). Data are expressed as average positive cells per mm^2 in the white matter, the cortex and the thalamus.

For analysis of MBP, the positively stained area was analyzed with the binary tool of the NIS AIR software using the NIS Elements AR software 4.0 (Nikon, Germany). Data are presented as percentage of MBP-positive area per hemisphere.

Behavioral Studies

From P22 on, animals were habituated to the blinded investigator and the inverse 12-h light-dark cycle. Behavioral testing was performed in adolescent animals from P35 to P49 and repeated in adult animals from P137 to P145 (32). Paradigms were chosen as they proved high reliability and validity in our recent studies (10, 25).

One day of open field was followed by 4 days of novel object recognition and further 4 days of Barnes maze test. The open field test (33) assesses anxiety-related behavior and spontaneous motor-activity. For this test, animals were placed into the center of an open field arena (50 × 50 × 40 cm for adolescent or 75 × 75 × 40 cm for adult animals) placed upon an infrared lightbox (emitted light 850 nm, TSE Systems, Bad Homburg, Germany). General motor activity (traveled distance and velocity) was assessed for 5 min. For the novel object recognition test, animals were placed into the center of a Y-maze (arm length: 60 cm; width: 26 cm; wall height: 56 cm) under red light. No external cues were visible from inside the maze. The first day, animals were habituated to the empty arena. On day two and three, they were familiarized with three identical objects (cones), placed at the end of the

maze arms. On day four, a familiar object was replaced by a novel one (cylinder). The time spent with the familiar and novel object was recorded. Each session lasted 5 min while only the first 2 min were used for evaluation (34). Spatiotemporal memory was assessed by the Barnes maze (35) as described previously (10). Briefly, animals were placed into the center of the maze (1.22 m width, 0.8 m height, 20 holes at the border, TSE Systems) under red light followed by bright light to allow the animal to recognize extra-maze cues. Animals were expected to explore the maze and find the escape box within 120 s, where they were kept for 1 min. Animals who did not find the escape box were gently placed into it for 1 min. To avoid intra-maze cues due to odor the escape box was rotated clockwise for every other animal, with the same escape location for each animal as on the three training days. On the fourth day of the experiment, all holes were closed and the latency to find the trained escape box was measured (36). All mazes were cleaned with 70% ethanol between trials to eliminate possible odor cues of previous animals. Data were recorded using an automatic tracking system, Ethovision 14 (Noldus, Wageningen, Netherlands).

Diffusion Tensor Imaging

At the age of 5 months (P151), behavior tested animals were sacrificed and fixed brains were scanned with diffusion tensor imaging. *Ex-vivo* MRI experiments were performed on an actively shielded 9.4T/31cm magnet (Agilent) equipped with 12-cm gradient coils (400 mT/m, 120 μs) with a 2.5 cm diameter birdcage coil. Diffusion weighted images were acquired using a spin-echo sequence with the following parameters: FOV = 23 × 18 mm^2, matrix size = 128 × 92, 15 slices of 0.6 mm thickness in the axial plane, 3 averages with TE/TR = 45/2000 ms. A total of 36 diffusion weighted images were acquired, 15 of them as b_0 reference images. The remaining 21 directions were uniformly distributed and non-collinear with a *b*-value = 1,750 s/mm^2. The diffusion tensor (DT) was computed using DTI-TK (37). The regions of interest (ROI) were manually delineated DTI derived color maps.

ROIs were selected in two different structures of the brain [corpus callosum (CC) and external capsule (EC)] in six different image-planes of the brain from the genu to the splenium of the corpus callosum.

Statistical Analysis

Statistical analysis was performed with Prism 6 (GraphPad Software, San Diego, CA, USA). Graphical data are presented as median values with boxplots including the 25% and the 75% percentile. Differences between groups were determined by one-way analysis of variance (one-way ANOVA) followed by Bonferroni *post hoc* test for multiple comparison. For DTI results, non-parametric Mann–Whitney *U*-test were used. $p \leq 0.05$ were considered as statistically significant.

RESULTS

A Repetitive Application of Epo Ameliorates Subacute Hyperoxia-Induced Hypomyelination

MRI studies revealed white matter changes in preterm born infants later in life (4). From our previous experimental studies we know that hyperoxia is one factor causing hypomyelination in the developing brain (8–10, 25). Recently we have shown that a single Epo dose of 20,000 IU/kg body weight led to an improved oligodendrocyte survival acutely after hyperoxia but failed to prevent hypomyelination. According to the clinical setting (23, 24), where repetitive application regimens are common, we adopted our rat model of hyperoxia-induced brain injury and applied 4 × 5,000 IU/kg body weight from P3 to P6. The first dose was administered at the onset of hyperoxia (80% oxygen, 48 h). To analyse the influence of repetitive Epo applications on the developing white matter at P11, we performed immunohistochemical staining for MBP (**Figure 1A**), APC-CC1, a marker for mature oligodendrocytes, and the pan oligodendrocyte marker Olig2. We found a significant decrease in MBP-expression after hyperoxia, which was attenuated following repetitive Epo treatment (**Figure 1B**). Analysis of Olig2 and APC-CC1 showed no difference between the 4 study groups (**Figure 2**). These findings were confirmed by protein analysis via Western blot: While hyperoxia led to a significant decrease of MBP-expression, repetitive Epo-applications reversed this effect in the hyperoxia group (HO + Epo) (**Figure 1C**). No differences were observed for oligodendrocyte-associated markers Olig2 and CNPase (**Figures 1D,E**).

Epo-Treatment Attenuates Neonatal Hyperoxia-Induced Cognitive Deficits in Adolescent and Adult Rats Without Obvious Long-Term Microstructural Alterations in the White Matter

We showed that repetitive Epo-applications of 4 × 5000 IU/kg body weight in neonatal rats (P3–P6) led to a significant improvement of hyperoxia-induced hypomyelination. To evaluate whether improved myelination on P11 was associated with improved long-term motor-cognitive function we performed a battery of motor-cognitive behavior tests. Anxiety-related behavior and general motor activity were analyzed in the open field test and cognitive function was assessed in the novel object recognition and the Barnes maze test. **Figure 3A** shows the results of the open field test with the parameters "traveled distance" and "velocity" as indicators of anxiety-related behavior and general motor-activity in adolescent and adult rats. No significant differences were found between study groups. The novel object recognition test is based on the observation, that rats show a preference to novel objects (34). As depicted in **Figure 3B**, adolescent control animals (NO and NO + Epo) spent significantly more time with the novel object, whereas animals in the hyperoxia group (HO) did not show a clear preference to any object. However, upon Epo-treatment we

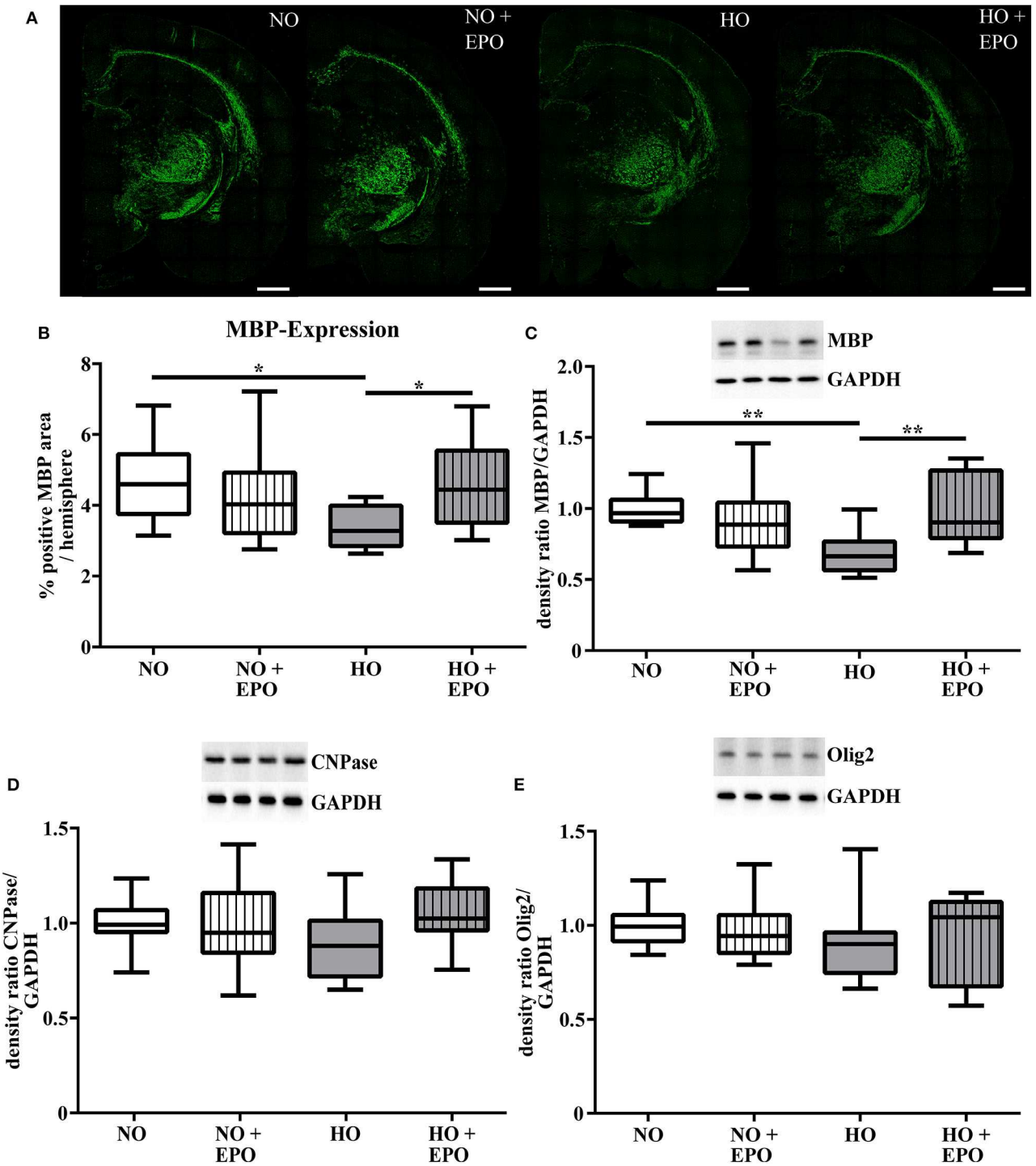

FIGURE 1 | A repetitive application of Erythropoietin (Epo) ameliorates hyperoxia-mediated hypomyelination. Animals were exposed to either normoxia (NO, 21% oxygen) or hyperoxia (HO, 80% oxygen for 48 h from P3 to P5) and were either treated with Epo (4 × 5000 IU/kg body weight per day from P3 to P6) or with an equal amount of normal saline. Analysis of myelination and oligodendrocyte-associated proteins were assessed at P11. **(A)** Representative immunhistochemical images of MBP (green) in coronal brain sections (−3.72 ± 0.7 mm from bregma) on P11. Scale bar = 100 μm **(B)** Analysis of MBP-immunohistochemistry. Data are presented as percentage of MBP-positive area per hemisphere. $n = 10–11$ **(C)** Western blot analysis of MBP-, **(D)** CNPase- and **(E)** Olig2-expression in protein lysates of brain hemispheres (excluding cerebellum). $^{*}p < 0.05$, $^{**}p < 0.01$, $n = 11–12$ rats/group.

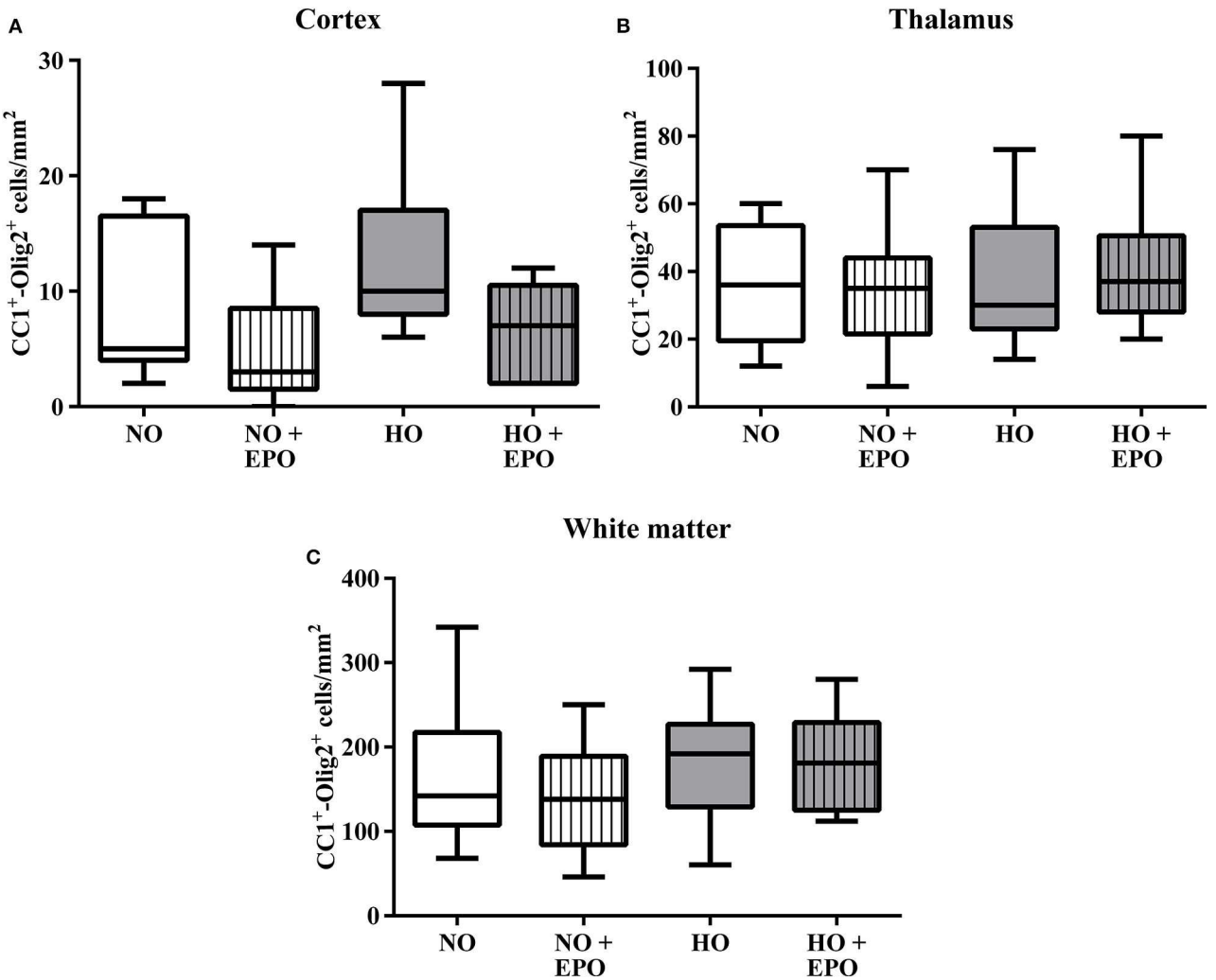

FIGURE 2 | Mature oligodendrocytes were not modulated by hyperoxia and Epo-treatment. The amount of mature oligodendrocytes was analysed via immunohistochemistry for Olig2 and APC-CC1. Triple-positive cells ($Olig2^+$/APC-$CC1^+$/$DAPI^+$) were determined in brain sections from 11-day old rats after exposure to either normoxia [21% oxygen (NO)] or hyperoxia [48 h 80% oxygen (HO)] from P3-P5. Rats were either treated with Epo (4 × 5000 IU/kg body weight per day from P3 to P6) or with an equal amount of normal saline. The average amount of triple-positive cells in **(A)** the cortex, **(B)** the thalamus, and **(C)** the white matter are expressed as cells per mm^2. $n = 10–11$ rats/group.

detected normalized preference for the new, unfamiliar object in adolescent rats. Adult rats exposed to hyperoxia (HO) spent significantly less time with the novel object than the control group (NO and NO + Epo) and the Epo-treated hyperoxic group (HO + Epo). In the Barnes maze, adolescent and adult animals exposed to hyperoxia needed significantly more time to find the trained escape box, while Epo-treatment significantly improved latency to find the box (**Figure 3C**).

To investigate whether improved cognitive outcome might be associated with microstructural alterations of the white matter, post-mortem diffusion tensor imaging was performed in brains of animals that underwent behavioral testing. Analyzing the corpus callosum (CC), we found decreased mean diffusivity (MD) and radial diffusivity (RD, $D_{D\perp}$) in the hyperoxic Epo-treated group (HO + Epo) as well as decreased axial diffusivity (AD, $D_{//}$) in the normoxic Epo-treated group (NO + Epo) compared to controls (NO). Nevertheless, no significant differences for fractional anisotropy (FA) as a marker for white matter integrity (38) were found between study groups. Likewise, no differences for MD, AD, RD, or FA were detected in the external capsule (**Figure 4**).

DISCUSSION

The present study investigated the effect of a repetitive Epo dosage regimen on myelination and neurocognitive outcome in a rodent model of hyperoxia-induced brain-injury. With the first application given at the onset of hyperoxia (oxygen 80%, 48 h), a repetitive Epo-treatment with 5,000 IU/kg body weight per day (P3 to P6) improved hyperoxia-induced hypomyelination

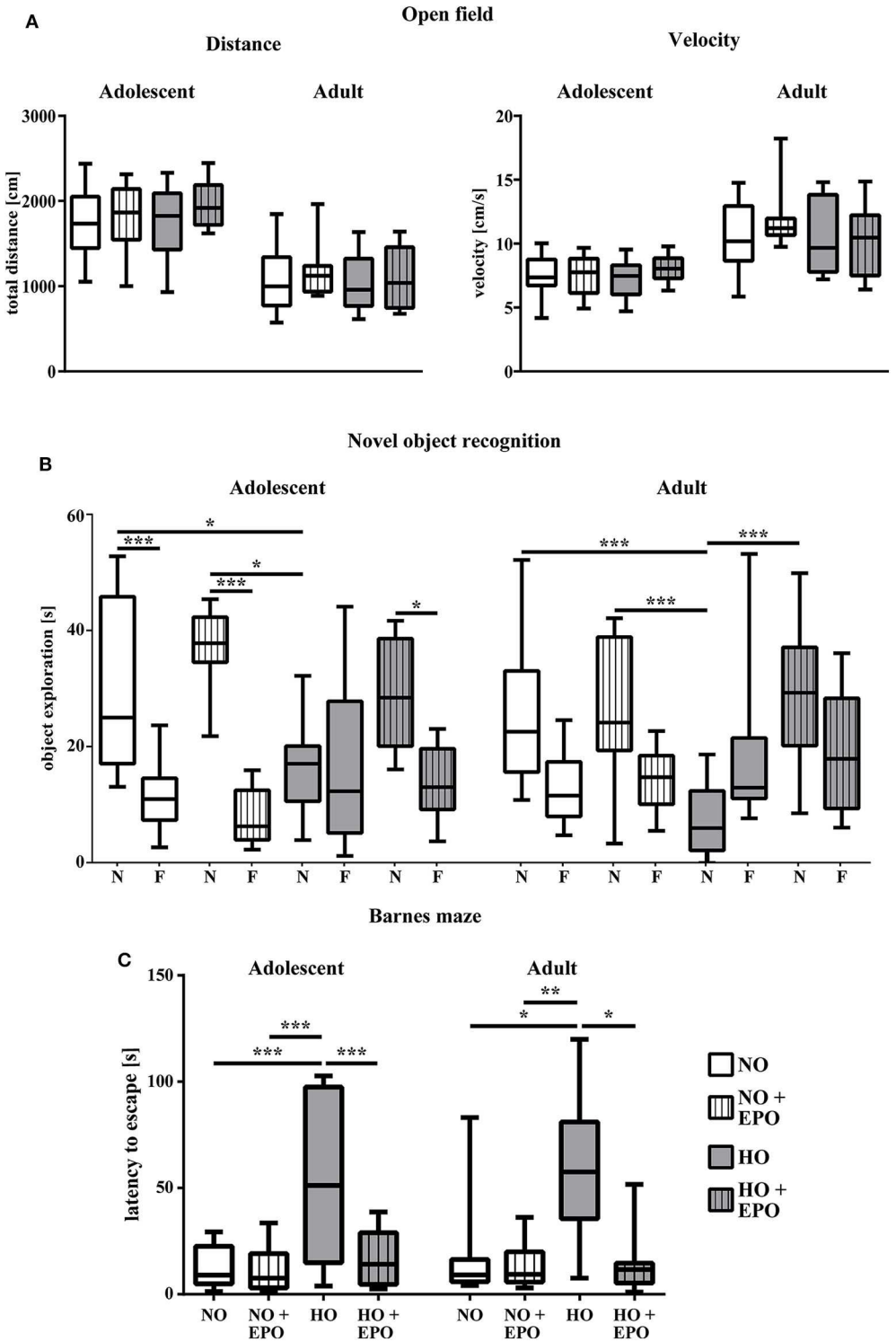

FIGURE 3 | Repetitive Epo treatment improved cognitive function in adolescent and adult rats after neonatal hyperoxia-induced brain-injury. Animals were exposed to either normoxia (NO, 21% oxygen) or hyperoxia (HO, 80% oxygen for 48 h from P3 to P5) and were either treated with Epo (4 × 5000 IU/kg body weight per day from P3 to P6) or with an equal amount of normal saline. Neurodevelopmental outcome was assessed at the age of 2 months (adolescent) and 4 months (adult) **(A)** General motor activity and anxiety-related behavior was tested in the open field, where animals were placed in the maze for 5 min. Movement was assessed by automated video tracking. Motor activity is expressed by the mean velocity and the total distance of the animals. **(B)** Cognitive function was analyzed in the novel object recognition task presented as the exploration time (s) at the novel object (N) vs. familiar objects (F). **(C)** Memory function was determined in the Barnes maze test expressed as the latency to find the trained escape hole after a 3-day training period. $^{*}p < 0.05$, $^{**}p < 0.01$, and $^{***}p < 0.001$, $n = 10$-12 rats/group.

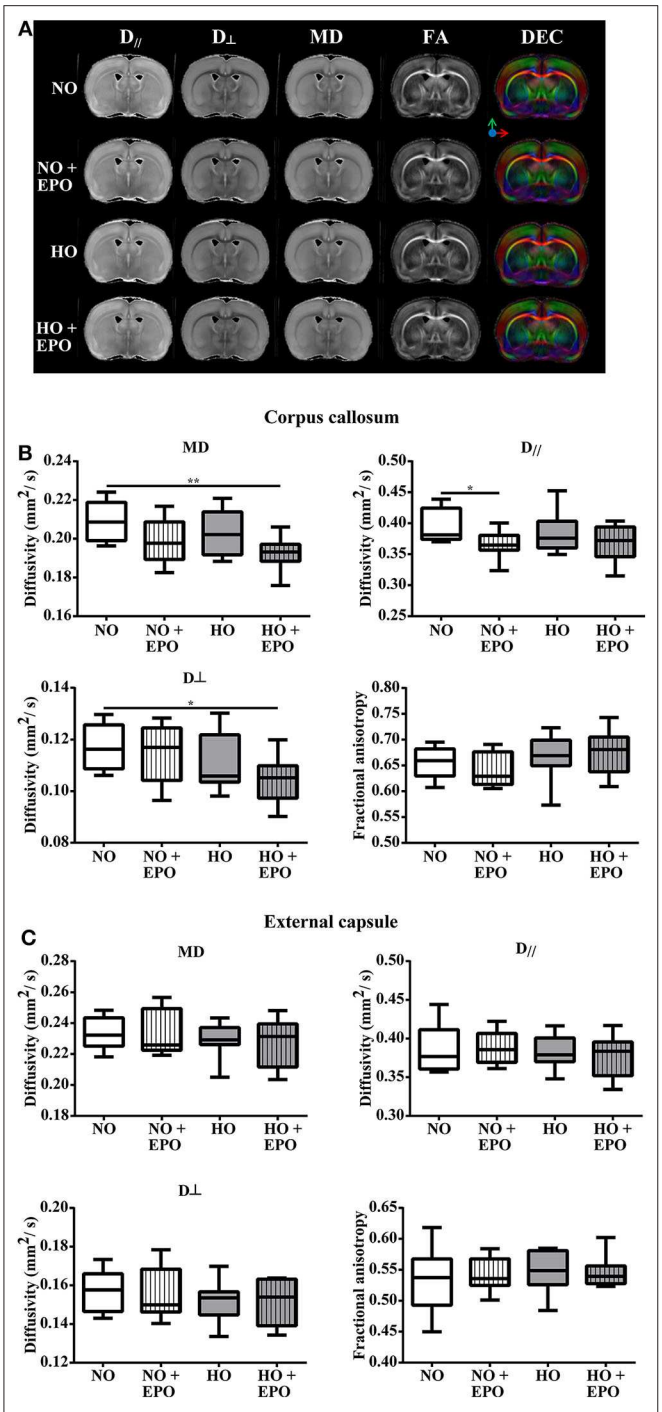

FIGURE 4 | Long-term microstructural development after neonatal hyperoxia-induced brain-injury. Diffusion tensor imaging (DTI) was performed in 5 months old rats, which were exposed to behavior tests at the age of 2 and 4 months. From P3 to P5, rats were either exposed to normoxia [21% oxygen (NO)] or hyperoxia (80% oxygen (HO)] and treated with Epo (4 × 5000 IU/kg body weight per day from P3 to P6) or with an equal amount of normal saline. **(A)** For each treatment group, representative maps for axial diffusivity (AD, $D_{//}$), radial diffusivity (RD, $D_{\perp}$), mean diffusivity (MD), fractional anisotropy (FA) and direction encoded colour maps (DEC) derived from DTI are shown. Diffusivity values for MD, AD ($D_{//}$), RD ($D_{\perp}$) and FA are displayed for **(B)** corpus callosum, and **(C)** external capsule. $^{*}p < 0.05$, $^{**}p < 0.01$, $n = 8$ rats/group.

at term-equivalent age (P11) and long-term neurocognitive outcome in adolescent and adult rats.

The positive effects of Epo on neurocognitive outcome and white matter development have already been described in other models of perinatal brain injury such as hypoxia-ischemia (17, 28, 39, 40). In the preterm model of hyperoxia-induced brain injury, we recently showed that a single Epo application of 20,000 IU/kg bodyweight at the onset of hyperoxia improved neurocognitive outcome in adolescent and adult rats. Nevertheless, in this previous study Epo did not modulate hyperoxia-induced hypomyelination or long-term white matter integrity (25). In the present study, a repetitive Epo application not only improved neurocognitive outcome, but also increased myelination at P11. Clinical studies in preterm infants also showed improved white matter integrity in MRI studies at term-equivalent age (21, 41). It has already been described that Epo promotes maturation and differentiation of oligodendrocytes (19, 29, 42). A direct interaction between oligodendrocytes and Epo may be possible, as oligodendrocytes of all maturation levels have been described to express Epo-receptors (43).

The different effects between a single and repetitive Epo application on myelination on P11 highlight the importance of dosing and timing of Epo-treatment, which varies both in experimental and clinical studies. In the present work, the dosage regimen of 4 × 5,000 IU/kg body weight was based on our previous studies, where the same total amount (20,000 IU/kg body weight) was administered as single bolus application (25, 27). Furthermore, a single dose of 5,000 IU/kg corresponds to a dose of 1,000 IU/kg body weight in preterm infants (44), which is in the range that is commonly used in clinical trials (500–3,000 IU/kg). Improved outcome observed in the present work are supported by a previous study in a model of hypoxic-ischemic brain injury demonstrating that a repetitive dose of 5,000 IU/kg body weight was superior to high-dose Epo treatment regimens in neonatal rats (45). In clinical studies, different treatment regimens have been used, which might explain inconsistent results with regard to Epo's neuroprotective effects in preterm infants. Compared to the placebo group, less moderate to severe disabilities were found by Song et al. in preterm infants < 32 weeks of gestation, who received 500 IU/kg body weight at 72 h after birth followed by daily injections for 2 weeks (46). Another important randomized control trial studied the effect of 3 × 3,000 IU/kg Epo, administered within 3 h after birth, at 12 to 18 h and at 36 to 42 h after birth in preterm infants between 26+0 and 31+6 weeks of gestation. Despite promising findings on MRI at term-equivalent age (reduced risk of brain injury and increased structural brain connectivity) in a sub-cohort of this study (21, 47), the Swiss Epo Neuroprotection Trial did not find improved outcome at the age of 2 and 5 years (23, 48). Both studies were part of a recent meta-analysis of four randomized, controlled trials with 1,133 very preterm infants revealing a decreased risk of Mental Developmental Index < 70 at the age 18 to 24 months (49). A combined regimen of high dose (6 × 1,000 IU/kg every 48 h) and a chronic application (400 IU/kg until 32 completed weeks of gestation) was used by Juul et al. in a large

randomized placebo-controlled trial including only extremely preterm infants (< 28 weeks of gestation). Neurodevelopment assessed at the age of 2 years revealed no beneficial effects of Epo treatment (24). However, further follow up at school age and beyond is necessary, to finally evaluate the role of Epo as neuroprotective agent. Neurodevelopmental testing with the Bayley Scales of Infant Development at this early age can predict motor outcome, however it is poorly predictive of later neurocognitive outcome (50). This is in line with the retrospective study by Neubauer et al. indicating improved neurodevelopmental outcome in extremely low birth infants at school age (20). Our pre-clinical results confirm these long-term effects with improved cognitive outcome even at adulthood. Taking these concerns into account, the Swiss study group has already planned a prospective follow-up study aiming to test executive function in their cohort at the age of 7–12 (48, 51). In addition to dosage, timing of Epo applications might be a further explanation for inconsistent study results. This seems to be supported by our findings demonstrating improved myelination at term-equivalent age after repetitive treatment but not after a single bolus administration of the same cumulative dose (25). However, it needs to be considered that compared to our previous study, we also changed the timing of hyperoxia with an earlier onset at P3. We intended to adopt our model to the group of extremely preterm infants (< 28 weeks of gestation), as they are most vulnerable to white matter injury. In rats, this period is around P3 and characterized by the abundance of oligodendrocyte progenitors. Around P6 immature oligodendrocytes, which are less vulnerable, are predominant (52). These differences in maturation possibly explain the different effect on myelination between this study and our previous work (25).

Several studies have described that hyperoxia induces acute cell death with a reduction of immature and mature oligodendrocytes in the developing brain (7, 9, 53). Nevertheless, this reduction–as well as the reduction of MBP–is likely to be transient. In mice exposed to 48 h hyperoxia (80% oxygen) from P6 to P8, Schmitz et al. have described recovery of total and mature oligodendrocyte populations 4 days after insult while MBP-values were still reduced (54). This might explain our findings with reduced MBP-values on P11, which were not accompanied by a decreased number of mature oligodendrocytes and associated proteins. Neonatal hyperoxia induces long-term microstructural alterations of the white matter as previously shown in pre-clinical DTI studies. These studies revealed a reduced fractional anisotropy in different white matter structures (e.g., corpus callosum, external capsule) indicating disturbed white matter integrity (9, 25, 54). Interestingly, we could not replicate these findings in the present study even though animals exposed to neonatal hyperoxia showed long-term impaired cognitive function. The fact that the animals in this study were older (P151) compared to previous studies might have contributed to these results. Nevertheless, normal white matter integrity on DTI does not exclude abnormalities on the cellular level. Ultrastructural changes assessed via electron microscopy including disturbed long-term axon-oligodendrocyte integrity after neonatal hyperoxia-induced brain injury have been described (55, 56).

Limitations of our study include that we did not investigate long-term abnormalities of the white matter beyond the microstructural level. Future studies should more specifically analyse alterations at the cellular level. Though we detected changes regarding cellular degeneration and survival factors in previous studies (16, 25–27, 57), detailed molecular analyses should be addressed to better understand the mechanisms underlying the neuroprotective effect of Epo in this experimental setting. Furthermore, due to study design no detailed immunohistochemical analysis of oligodendrocyte degeneration or different oligodendrocyte populations was performed immediately after hyperoxia. Thus, we can only speculate that our findings (similar numbers of mature oligodendrocytes in both control and hyperoxia group) are the result of recovery processes (54). Recovery processes might also explain our DTI results as studies investigating earlier time points found an altered microstructure (9, 10, 25). Although in this study we focused on long-term outcome, serial MRI studies could provide this information in subsequent studies. A further limitation is that we only investigated cerebral structures, despite evidence from animal studies that hyperoxia has detrimental effects on the developing cerebellum (58, 59). As impaired neurocognitive outcome of preterm infants is associated with cerebellar injury (60), the effects of Epo on the cerebellum need to be elucidated in the future.

Nevertheless, the findings of this study are of importance, given that the exposure of extremely preterm infants to hyperoxia is almost unavoidable during their treatment in the neonatal intensive care unit. Hyperoxia increases their risk of long-term neurodevelopmental impairment in later life. Thus, understanding of the pathophysiology of hyperoxia-induced brain injury is required as well as the investigation of potential preventive or treatment options such as Epo. Despite disappointing results in first clinical trials (23, 24) our results underline the importance of long-term follow-up studies for neurocognitive outcome in these cohorts.

To conclude, the objective of this study was to investigate the effect of repetitive Epo treatment on cerebral white matter and motor-cognitive outcome in a rodent model of hyperoxia-induced brain injury. We found that a dosage regimen close to clinical application improved myelination and long-term neurocognitive outcome. Despite inconsistent results from recent clinical studies, Epo remains a promising neuroprotective agent in the prevention and therapy of preterm brain injury. The results of the long-term follow-up of recent clinical trials have to be awaited.

DATA AVAILABILITY STATEMENT

The raw data supporting the conclusions of this article will be made available by the authors, without undue reservation.

ETHICS STATEMENT

The animal study was reviewed and approved by State Agency for Nature, Environment and Consumer Protection (LANUV), North Rhine-Westphalia.

AUTHOR CONTRIBUTIONS

MD, MS, JF, UF-M, and IB: conceptualization. MD, MS, SE, JH, and IB: data curation. MD, MS, YL, and IB: formal analysis. MD, UF-M, IB, and YL: funding acquisition. MD, MS, MK, MH, YL, and IB: investigation. MD, MS, MK, MH, YL, and IB: methodology. MD, MS, JF, SS, JH, and IB: validation. All authors contributed to manuscript preparation, read, and approved the submitted version.

FUNDING

The IFORES clinician scientist stipend program of the Medical Faculty of the University Duisburg-Essen, Germany (D/107-40950 to MD); the C. D.-Stiftung (to UF-M and IB); the Swiss National Fund No. 33CM30-124101/140334 and the Fondation pour Recherches Médicales, Geneva; the Center for Biomedical Imaging (CIBM) of the UNIL, UNIGE, HUG, CHUV, and EPFL, and the Leenaards and Jeantet Foundations (to YL).

ACKNOWLEDGMENTS

The authors gratefully thank Karina Kempe, Mandana Rizazad, and Christian Köster for their excellent technical assistance.

REFERENCES

1. Wood NS, Marlow N, Costeloe K, Gibson AT, Wilkinson AR. Neurologic and developmental disability after extremely preterm birth. EPICure Study Group. *N Engl J Med*. (2000) 343:378–84. doi: 10.1056/NEJM200008103430601
2. Marlow N, Wolke D, Bracewell MA, Samara M. Neurologic and developmental disability at six years of age after extremely preterm birth. *N Engl J Med*. (2005) 352:9–19. doi: 10.1056/NEJMoa041367
3. Doyle LW, Anderson PJ. Adult outcome of extremely preterm infants. *Pediatrics*. (2010) 126:342–51. doi: 10.1542/peds.2010-0710
4. Woodward LJ, Anderson PJ, Austin NC, Howard K, Inder TE. Neonatal MRI to predict neurodevelopmental outcomes in preterm infants. *N Engl J Med*. (2006) 355:685–94. doi: 10.1056/NEJMoa053792
5. Dobbing J, Sands J. Quantitative growth and development of human brain. *Arch Dis Child*. (1973) 48:757–67. doi: 10.1136/adc.48.10.757
6. Collins MP, Lorenz JM, Jetton JR, Paneth N. Hypocapnia and other ventilation-related risk factors for cerebral palsy in low birth weight infants. *Pediatr Res*. (2001) 50:712–9. doi: 10.1203/00006450-200112000-00014
7. Felderhoff-Mueser U, Bittigau P, Sifringer M, Jarosz B, Korobowicz E, Mahler L, et al. Oxygen causes cell death in the developing brain. *Neurobiol Dis*. (2004) 17:273–82. doi: 10.1016/j.nbd.2004.07.019
8. Gerstner B, DeSilva TM, Genz K, Armstrong A, Brehmer F, Neve RL, et al. Hyperoxia causes maturation-dependent cell death in the developing white matter. *J Neurosci*. (2008) 28:1236–45. doi: 10.1523/JNEUROSCI.3213-07.2008
9. Brehmer F, Bendix I, Prager S, van de Looij Y, Reinboth BS, Zimmermanns J, et al. Interaction of inflammation and hyperoxia in a rat model of neonatal white matter damage. *PLoS ONE*. (2012) 7:e49023. doi: 10.1371/journal.pone.0049023
10. Serdar M, Herz J, Kempe K, Lumpe K, Reinboth BS, Sizonenko SV, et al. Fingolimod protects against neonatal white matter damage and long-term cognitive deficits caused by hyperoxia. *Brain Behav Immun*. (2016) 52:106–19. doi: 10.1016/j.bbi.2015.10.004
11. Juul S. Neuroprotective role of erythropoietin in neonates. *J Matern Neonatal Med*. (2012) 25(Suppl. 4):105–7. doi: 10.3109/14767058.2012.715025
12. Maier RF, Obladen M, Scigalla P, Linderkamp O, Duc G, Hieronimi G, et al. The effect of epoetin beta (recombinant human erythropoietin) on the need for transfusion in very-low-birth-weight infants. *N Engl J Med*. (1994) 330:1173–8. doi: 10.1056/NEJM199404283301701
13. Juul SE, Anderson DK, Li Y, Christensen RD. Erythropoietin and erythropoietin receptor in the developing human central nervous system. *Pediatr Res*. (1998) 43:40–9. doi: 10.1203/00006450-199801000-00007
14. Dame C, Bartmann P, Wolber EM, Fahnenstich H, Hofmann D, Fandrey J. Erythropoietin gene expression in different areas of the developing human central nervous system. *Dev Brain Res*. (2000) 125:69–74. doi: 10.1016/S0165-3806(00)00118-8
15. Chen ZY, Asavaritikrai P, Prchal JT, Noguchi CT. Endogenous erythropoietin signaling is required for normal neural progenitor cell proliferation. *J Biol Chem*. (2007) 282:25875–83. doi: 10.1074/jbc.M701988200
16. Kaindl AM, Sifringer M, Koppelstaetter A, Genz K, Loeber R, Boerner C, et al. Erythropoietin protects the developing brain from hyperoxia-induced cell death and proteome changes. *Ann Neurol*. (2008) 64:523–34. doi: 10.1002/ana.21471
17. Liu W, Shen Y, Plane JM, Pleasure DE, Deng W. Neuroprotective potential of erythropoietin and its derivative carbamylated erythropoietin in periventricular leukomalacia. *Exp Neurol*. (2011) 230:227–39. doi: 10.1016/j.expneurol.2011.04.021
18. Fan X, van Bel F, van Der Kooij MA, Heijnen CJ, Groenendaal F. Hypothermia and erythropoietin for neuroprotection after neonatal brain damage. *Pediatr Res*. (2013) 73:18–23. doi: 10.1038/pr.2012.139
19. Jantzie LL, Corbett CJ, Firl DJ, Robinson S. Postnatal erythropoietin mitigates impaired cerebral cortical development following subplate loss from prenatal hypoxia-ischemia. *Cereb Cortex*. (2015) 25:2683–95. doi: 10.1093/cercor/bhu066
20. Neubauer AP, Voss W, Wachtendorf M, Jungmann T. Erythropoietin improves neurodevelopmental outcome of extremely preterm infants. *Ann Neurol*. (2010) 67:657–66. doi: 10.1002/ana.21977
21. Leuchter RH-V, Gui L, Poncet A, Hagmann C, Lodygensky GA, Martin E, et al. Association between early administration of high-dose erythropoietin in preterm infants and brain MRI abnormality at term-equivalent age. *JAMA*. (2014) 312:817–24. doi: 10.1001/jama.2014.9645
22. Ohls RK, Cannon DC, Phillips J, Caprihan A, Patel S, Winter S, et al. Preschool assessment of preterm infants treated with darbepoetin and erythropoietin. *Pediatrics*. (2016) 137:e20153859. doi: 10.1542/peds.2015-3859
23. Natalucci G, Latal B, Koller B, Rüegger C, Sick B, Held L, et al. Effect of early prophylactic high-dose recombinant human erythropoietin in very preterm infants on neurodevelopmental outcome at 2 years a randomized clinical trial. *JAMA*. (2016) 315:2079–85. doi: 10.1001/jama.2016.5504
24. Juul SE, Comstock BA, Wadhawan R, Mayock DE, Courtney SE, Robinson T, et al. A randomized trial of erythropoietin for neuroprotection in preterm infants. *N Engl J Med*. (2020) 382:233–43. doi: 10.1056/NEJMoa1907423
25. Hoeber D, Sifringer M, Van De Looij Y, Herz J, Sizonenko S V., Kempe K, et al. Erythropoietin restores long-term neurocognitive function involving mechanisms of neuronal plasticity in a model of hyperoxia-induced preterm brain injury. *Oxid Med Cell Longev*. (2016) 2016:9247493. doi: 10.1155/2016/9247493
26. Sifringer M, Genz K, Brait D, Brehmer F, Löber R, Weichelt U, et al. Erythropoietin attenuates hyperoxia-induced cell death by modulation of inflammatory mediators and matrix metalloproteinases. *Dev Neurosci*. (2009) 31:394–402. doi: 10.1159/000232557
27. Bendix I, Schulze C, von Haefen C, Gellhaus A, Endesfelder S, Heumann R, et al. Erythropoietin modulates autophagy signaling in the developing

rat brain in an *in vivo* model of oxygen-Toxicity. *Int J Mol Sci.* (2012) 13:12939–51. doi: 10.3390/ijms131012939
28. Fan X, Heijnen CJ, van Der Kooij MA, Groenendaal F, van Bel F. Beneficial effect of erythropoietin on sensorimotor function and white matter after hypoxia-ischemia in neonatal mice. *Pediatr Res*. (2011) 69:56–61. doi: 10.1203/PDR.0b013e3181fcbef3
29. Iwai M, Stetler RA, Xing J, Hu X, Gao Y, Zhang W, et al. Enhanced oligodendrogenesis and recovery of neurological function by erythropoietin after neonatal hypoxic/ischemic brain injury. *Stroke*. (2010) 41:1032–7. doi: 10.1161/STROKEAHA.109.570325
30. van de Looij Y, Chatagner A, Quairiaux C, Gruetter R, Hüppi PS, Sizonenko SV. Multi-modal assessment of long-term erythropoietin treatment after neonatal hypoxic-ischemic injury in rat brain. *PLoS ONE*. (2014) 9:e95643. doi: 10.1371/journal.pone.0095643
31. Fauchère JC, Koller BM, Tschopp A, Dame C, Ruegger C, Bucher HU, et al. Safety of early high-dose recombinant erythropoietin for neuroprotection in very preterm infants. *J Pediatr*. (2015) 167:52–7.e1–3. doi: 10.1016/j.jpeds.2015.02.052
32. Semple BD, Blomgren K, Gimlin K, Ferriero DM, Noble-Haeusslein LJ. Brain development in rodents and humans: identifying benchmarks of maturation and vulnerability to injury across species. *Prog Neurobiol*. (2013) 106–107:1–16. doi: 10.1016/j.pneurobio.2013.04.001
33. Defries JC, Hegmann JP, Morton W. Open-field behavior in mice: evidence for a major gene effect mediated by the visual system. *Science*. (1966) 154:1577–9. doi: 10.1126/science.154.3756.1577
34. Chambon C, Wegener N, Gravius A, Danysz W. A new automated method to assess the rat recognition memory: validation of the method. *Behav Brain Res*. (2011) 222:151–7. doi: 10.1016/j.bbr.2011.03.032
35. Barnes CA. Memory deficits associated with senescence: a neurophysiological and behavioral study in the rat. *J Comp Physiol Psychol*. (1979) 93:74–104. doi: 10.1037/h0077579
36. O'Leary TP, Savoie V, Brown RE. Learning, memory and search strategies of inbred mouse strains with different visual abilities in the Barnes maze. *Behav Brain Res*. (2011) 216:531–42. doi: 10.1016/j.bbr.2010.08.030
37. Zhang H, Yushkevich PA, Alexander DC, Gee JC. Deformable registration of diffusion tensor MR images with explicit orientation optimization. *Med Image Anal*. (2006) 10:764–85. doi: 10.1016/j.media.2006.06.004
38. Chang EH, Argyelan M, Aggarwal M, Chandon TSS, Karlsgodt KH, Mori S, et al. The role of myelination in measures of white matter integrity: combination of diffusion tensor imaging and two-photon microscopy of CLARITY intact brains. *Neuroimage*. (2017) 147:253–61. doi: 10.1016/j.neuroimage.2016.11.068
39. Demers EJ, McPherson RJ, Juul SE. Erythropoietin protects dopaminergic neurons and improves neurobehavioral outcomes in juvenile rats after neonatal hypoxia-ischemia. *Pediatr Res*. (2005) 58:297–301. doi: 10.1203/01.PDR.0000169971.64558.5A
40. Lan KM, Tien LT, Cai Z, Lin S, Pang Y, Tanaka S, et al. Erythropoietin ameliorates neonatal hypoxia-ischemia-induced neurobehavioral deficits, neuroinflammation, and hippocampal injury in the juvenile rat. *Int J Mol Sci*. (2016) 17:289. doi: 10.3390/ijms17030289
41. O'Gorman RL, Bucher HU, Held U, Koller BM, Hüppi PS, Hagmann CF. Tract-based spatial statistics to assess the neuroprotective effect of early erythropoietin on white matter development in preterm infants. *Brain*. (2015) 138:388–97. doi: 10.1093/brain/awu363
42. Kaneko N, Kako E, Sawamoto K. Enhancement of ventricular-subventricular zone-derived neurogenesis and oligodendrogenesis by erythropoietin and its derivatives. *Front Cell Neurosci*. (2013) 7:235. doi: 10.3389/fncel.2013.00235
43. Sugawa M, Sakurai Y, Ishikawa-Ieda Y, Suzuki H, Asou H. Effects of erythropoietin on glial cell development; oligodendrocyte maturation and astrocyte proliferation. *Neurosci Res*. (2002) 44:391–403. doi: 10.1016/S0168-0102(02)00161-X
44. Juul SE, McPherson RJ, Bauer LA, Ledbetter KJ, Gleason CA, Mayock DE. A phase I/II trial of high-dose erythropoietin in extremely low birth weight infants: pharmacokinetics and safety. *Pediatrics*. (2008) 122:383–91. doi: 10.1542/peds.2007-2711
45. Kellert BA, McPherson RJ, Juul SE. A comparison of high-dose recombinant erythropoietin treatment regimens in brain-injured neonatal rats. *Pediatr Res*. (2007) 61:451–5. doi: 10.1203/pdr.0b013e3180332cec
46. Song J, Sun H, Xu F, Kang W, Gao L, Guo J, et al. Recombinant human erythropoietin improves neurological outcomes in very preterm infants. *Ann Neurol*. (2016) 80:24–34. doi: 10.1002/ana.24677
47. Jakab A, Ruegger C, Bucher HU, Makki M, Huppi PS, Tuura R, et al. Network based statistics reveals trophic and neuroprotective effect of early high dose erythropoetin on brain connectivity in very preterm infants. *NeuroImage Clin*. (2019) 22:533901. doi: 10.1101/533901
48. Natalucci G, Latal B, Koller BM, Rüegger C, Sick B, Held L, et al. Neurodevelopmental outcome at preschool age after early high-dose recombinant human erythropoietin in very preterm born children: results of a randomized, placebo-controlled, double-blind trial. *Pediatr Res*. (2019) 86:1–64. doi: 10.1038/s41390-019-0521-6
49. Fischer HS, Reibel NJ, Bührer C, Dame C. Prophylactic early erythropoietin for neuroprotection in preterm infants: a meta-analysis. *Pediatrics*. (2017) 139:e20164317. doi: 10.1542/peds.2016-4317
50. Luttikhuizen dos Santos ES, de Kieviet JF, Königs M, van Elburg RM, Oosterlaan J. Predictive value of the Bayley scales of infant development on development of very preterm/very low birth weight children: a meta-analysis. *Early Hum Dev*. (2013) 89:487–96. doi: 10.1016/j.earlhumdev.2013.03.008
51. Wehrle FM, Held U, Gorman RTO, Disselhoff V, Schnider B, Fauchère J, et al. Long-term neuroprotective effect of erythropoietin on executive functions in very preterm children (EpoKids): protocol of a prospective follow- up study. (2018) 8:e022157. doi: 10.1136/bmjopen-2018-022157
52. Craig A, Luo NL, Beardsley DJ, Wingate-Pearse N, Walker DW, Hohimer AR, et al. Quantitative analysis of perinatal rodent oligodendrocyte lineage progression and its correlation with human. *Exp Neurol*. (2003) 181:231–40. doi: 10.1016/S0014-4886(03)00032-3
53. Yiş U, Kurul SH, Kumral A, Cilaker S, Tugyan K, Genç S, et al. Hyperoxic exposure leads to cell death in the developing brain. *Brain Dev*. (2008) 30:556–62. doi: 10.1016/j.braindev.2008.01.010
54. Schmitz T, Ritter J, Mueller S, Felderhoff-Mueser U, Chew LJ, Gallo V. Cellular changes underlying hyperoxia-induced delay of white matter development. *J Neurosci*. (2011) 31:4327–44. doi: 10.1523/JNEUROSCI.3942-10.2011
55. Ritter J, Schmitz T, Chew LJ, Bührer C, Möbius W, Zonouzi M, et al. Neonatal hyperoxia exposure disrupts axon-oligodendrocyte integrity in the subcortical white matter. *J Neurosci*. (2013) 33:8990–9002. doi: 10.1523/JNEUROSCI.5528-12.2013
56. Serdar M, Herz J, Kempe K, Winterhager E, Jastrow H, Heumann R, et al. Protection of oligodendrocytes through neuronal overexpression of the small GTPase ras in hyperoxia-induced neonatal brain injury. *Front Neurol*. (2018) 9:175. doi: 10.3389/fneur.2018.00175
57. Sifringer M, Brait D, Weichelt U, Zimmerman G, Endesfelder S, Brehmer F, et al. Erythropoietin attenuates hyperoxia-induced oxidative stress in the developing rat brain. *Brain Behav Immun*. (2010) 24:792–9. doi: 10.1016/j.bbi.2009.08.010
58. Scheuer T, Brockmöller V, Blanco Knowlton M, Weitkamp JH, Ruhwedel T, Mueller S, et al. Oligodendroglial maldevelopment in the cerebellum after postnatal hyperoxia and its prevention by minocycline. *Glia*. (2015) 63:1825–39. doi: 10.1002/glia.22847
59. Scheuer T, Sharkovska Y, Tarabykin V, Marggraf K, Brockmöller V, Bührer C, et al. Neonatal hyperoxia perturbs neuronal development in the cerebellum. *Mol Neurobiol*. (2018) 55:3901–15. doi: 10.1007/s12035-017-0612-5
60. Limperopoulos C, Chilingaryan G, Sullivan N, Guizard N, Robertson RL, Du Plessis AJ. Injury to the premature cerebellum: outcome is related to remote cortical development. *Cereb Cortex*. (2014) 24:728–36. doi: 10.1093/cercor/bhs354

Conflict of Interest: The authors declare that the research was conducted in the absence of any commercial or financial relationships that could be construed as a potential conflict of interest.

frontiers in Neurology

ORIGINAL RESEARCH
published: 14 August 2020
doi: 10.3389/fneur.2020.00761

Placental Pathology Findings and the Risk of Intraventricular and Cerebellar Hemorrhage in Preterm Neonates

Alessandro Parodi[1], Laura Costanza De Angelis[1], Martina Re[1], Sarah Raffa[1,2], Mariya Malova[1], Andrea Rossi[3,4], Mariasavina Severino[3], Domenico Tortora[3], Giovanni Morana[3], Maria Grazia Calevo[5], Maria Pia Brisigotti[6], Francesca Buffelli[6], Ezio Fulcheri[6,7] and Luca Antonio Ramenghi[1,2]*

[1] Neonatal Intensive Care Unit, Department Mother and Child, IRCCS Istituto Giannina Gaslini, Genoa, Italy, [2] Department of Neurosciences, Rehabilitation, Ophthalmology, Genetics, Maternal and Child Health (DINOGMI), University of Genoa, Genoa, Italy, [3] Neuroradiology Unit, IRCCS Istituto Giannina Gaslini, Genoa, Italy, [4] Department of Health Sciences (DISSAL), University of Genoa, Genoa, Italy, [5] Epidemiology and Biostatistics Unit, IRCCS Istituto Giannina Gaslini, Genoa, Italy, [6] Gynaecologic and Fetal-Perinatal Pathology Centre, IRCCS Istituto Giannina Gaslini, Genoa, Italy, [7] Division of Pathology, Department of Surgical Sciences (DISC), University of Genoa, Genoa, Italy

OPEN ACCESS

Edited by:
Deirdre M. Murray, University College Cork, Ireland

Reviewed by:
Carlotta Spagnoli, Santa Maria Nuova Hospital, Italy
Maurizio Elia, Oasi Research Institute (IRCCS), Italy

***Correspondence:**
Laura Costanza De Angelis
lallade@gmail.com

Specialty section:
This article was submitted to Pediatric Neurology, a section of the journal Frontiers in Neurology

Received: *07 March 2020*
Accepted: *19 June 2020*
Published: *14 August 2020*

Citation:
Parodi A, De Angelis LC, Re M, Raffa S, Malova M, Rossi A, Severino M, Tortora D, Morana G, Calevo MG, Brisigotti MP, Buffelli F, Fulcheri E and Ramenghi LA (2020) Placental Pathology Findings and the Risk of Intraventricular and Cerebellar Hemorrhage in Preterm Neonates. Front. Neurol. 11:761. doi: 10.3389/fneur.2020.00761

Placental pathology as a predisposing factor to intraventricular hemorrhage remains a matter of debate, and its contribution to cerebellar hemorrhage development is still largely unexplored. Our study aimed to assess placental and perinatal risk factors for intraventricular and cerebellar hemorrhages in preterm infants. This retrospective cohort study included very low-birth weight infants born at the Gaslini Children's Hospital between January 2012 and October 2016 who underwent brain magnetic resonance with susceptibility-weighted imaging at term-equivalent age and whose placenta was analyzed according to the Amsterdam Placental Workshop Group Consensus Statement. Of the 286 neonates included, 68 (23.8%) had intraventricular hemorrhage (all grades) and 48 (16.8%) had a cerebellar hemorrhage (all grades). After correction for gestational age, chorioamnionitis involving the maternal side of the placenta was found to be an independent risk factor for developing intraventricular hemorrhage, whereas there was no association between maternal and fetal inflammatory response and cerebellar hemorrhage. Among perinatal factors, we found that intraventricular hemorrhage was significantly associated with cerebellar hemorrhage (odds ratio [OR], 8.14), mechanical ventilation within the first 72 h (OR, 2.67), and patent ductus arteriosus requiring treatment (OR, 2.6), whereas cesarean section emerged as a protective factor (OR, 0.26). Inotropic support within 72 h after birth (OR, 5.24) and intraventricular hemorrhage (OR, 6.38) were independent risk factors for cerebellar hemorrhage, whereas higher gestational age was a protective factor (OR, 0.76). Assessing placental pathology may help in understanding mechanisms leading to intraventricular hemorrhage, although its possible role in predicting cerebellar bleeding needs further evaluation.

Keywords: placenta, intraventricular hemorrhage, cerebellar hemorrhage, preterm infant, chorioamnionitis, maternal malperfusion, magnetic resonance imaging

INTRODUCTION

Despite significant improvements in the perinatal care of preterm infants, intraventricular hemorrhage (GMH-IVH), and cerebellar hemorrhage (CBH) still represent the most frequent lesions occurring during the very first few days of life (1–3). Besides ultrasonography, the implementation of magnetic resonance imaging (MRI) with susceptibility-weighted image (SWI) sequences as a diagnostic tool for preterm brain lesions has improved the accuracy in detecting minor forms of both supratentorial and infratentorial hemorrhages (4–7).

Both GMH-IVH and CBH have a multifactorial etiology (8–10), in which gestational age and perinatal factors seem to play a major role, although they have never been considered together in relation to placental risk factors. In the last decades, several studies have explored the contribution of the prenatal environment to the development of preterm brain lesions (11). In particular, the role of placental pathology in prematurity-related complications has been widely investigated but is still a matter of debate (12, 13). The heterogeneous results in different studies could be explained by the multiplicity of both placental lesion definition and classification.

In addition, whereas the majority of research has focused on GMH-IVH, to date, the contribution of placental pathology to CBH development is still largely unexplored. The aim of our study was to evaluate the role of placental histopathological features in the risk of developing GMH-IVH and CBH, which was diagnosed with brain MRIs performed at term-equivalent age (TEA) in a consecutive cohort of very low-birth weight (VLBW) infants. We hypothesized that the use of both a uniform and detailed placental histopathology classification and the use of brain MRI with SWI sequences to detect even minor forms of brain hemorrhage might better clarify the contribution of placental pathology for the development of both GMH-IVH and CBH in VLBW infants.

MATERIALS AND METHODS

The study was a retrospective analysis of a prospectively collected cohort of all preterm infants born with a birth weight of <1,500 g at Gaslini Children's Hospital (Genoa, Italy) between January 2012 and October 2016. Neonates were included if they underwent a brain MRI at TEA and had a placental pathology performed at birth. We excluded neonates with genetic syndromes, congenital malformations, and brain malformations. For GMH-IVH risk factor analysis, the case group included infants with MRI showing any grade of GMH-IVH, and for CBH risk factor analysis, the case group included infants with punctate (≤4 mm), limited (>4 mm but less than one-third of the cerebellar hemisphere), and massive (more than one-third of the cerebellar hemisphere) hemorrhage.

Clinical Data Collection

Demographic and perinatal clinical data, including known risk factors for prematurity-related brain lesions, were collected by chart review. Prenatal variables included preeclampsia, number of fetuses, twin-to-twin transfusion, intrauterine growth restriction, antenatal steroids (two doses), gestational diabetes, and type of delivery (vaginal delivery or elective/emergent cesarean section). Neonatal variables included gestational age, gender, birth weight, 1′ and 5′ Apgar scores, surfactant administration, neonatal sepsis (early and late onset), necrotizing enterocolitis, and patent ductus arteriosus (PDA) requiring surgical or at least pharmacological treatment. Intubation, mechanical ventilation, pneumothorax, and inotropic treatments were recorded if they occurred within the first 72 h of life.

Brain MRI

Brain MRI scans were obtained at TEA (between 39 and 41 weeks of corrected gestational age) according to our internal VLBW follow-up protocol. Scans were performed on a 1.5-Tesla system (Intera Achieva; Philips, Best, The Netherlands) using a pediatric dedicated head/spine coil. The exam was performed during natural sleep using the "feed and wrap" technique, whereas oral midazolam (0.1 mcg/kg) was used for mild sedation to prevent head motion in selected cases, according to the infant's state of arousal and image quality after the first sequence. Hearing protection was provided for all patients. Heart rate and oxygen saturation were monitored by pulse oximetry throughout the examination. MRI scans of the brain included 3-mm-thick axial T2- and T1-weighted images, 3-mm-thick coronal T2-weighted images, 3-mm-thick sagittal T1-weighted images, axial diffusion-weighted images (b value: 1,000 s/mm^2), and axial SWIs. Informed consent that included statements about the significance and limitations of MRI at TEA was obtained in all cases.

In order to assess the presence of GMH-IVH and CBH, all images were reviewed by three neuroradiologists experienced in neonatal neuroimaging (DT, GM, and MS), who were unaware of perinatal history and placental pathology. Foci of signal loss on SWI alongside lateral ventricle walls or in the caudothalamic notch, without continuity suggestive of veins, were interpreted as intraventricular or subependymal hemosiderin depositions, consistent with previous GMH-IVH. Foci of signal loss on SWI within the cerebellum, without continuity suggestive of veins, were interpreted as hemosiderin depositions, consistent with previous CBH. Similar SWI findings within the fourth ventricle, potentially consistent with intraventricular blood of supratentorial origin, were not interpreted as CBH.

Placental Pathology

Macroscopic examination results of each placenta were collected from the electronic database of our pathology department, and data about the presence of twin monochorionic placenta, velamentous placental cord insertion, and retroplacental hematoma were obtained from placental examination reports. Three experienced placental pathologists (EF, FB, and MB) reviewed placental sections for the microscopic analysis. The following formalin-fixed sections of placental parenchyma, of 3–5 μm thickness and stained with hematoxylin and eosin, were analyzed for every patient: two or more sections of extraplacental membrane roll, three cross sections of the umbilical cord, and 12 full-thickness sections of villous tissue, including one adjacent to the umbilical cord insertion site.

Maternal and fetal stromal–vascular lesions were classified according to the Amsterdam Placental Workshop Group Consensus Statement (14), and the degree of maternal and fetal inflammatory response in ascending intrauterine infection was scored according to Redline et al. (15) and confirmed by the Amsterdam Placental Workshop Group Consensus Statement (14). Maternal inflammatory responses were classified as stage 1 (acute subchorionitis: patchy diffuse accumulations of neutrophils in the subchorionic plate and/or membranous chorionic trophoblast layer), stage 2 (acute chorioamnionitis: more than a few scattered neutrophils in the chorionic plate or membranous chorionic connective tissue and/or the amnion), or stage 3 (necrotizing chorioamnionitis: degenerating neutrophils, thickened eosinophilic amniotic basement membrane, and at least focal amnionic epithelial degeneration). Fetal inflammatory responses were classified as stage 1 (chorionic vasculitis/umbilical phlebitis: neutrophils in the wall of any chorionic plate vessel or the umbilical vein), stage 2 (umbilical vasculitis: neutrophils in one or both umbilical arteries and vein), or stage 3 (necrotizing funisitis or concentric umbilical perivasculitis: neutrophils, cellular debris, eosinophilic precipitate, and/or mineralization arranged in a concentric band, ring, or halo around one or more umbilical vessels) (**Figure 1**). Grade/intensity for both maternal and fetal inflammatory response was not included in the analysis.

Maternal vascular malperfusion was defined by the presence of the following microscopic features: accelerated villous maturation, distal villous hypoplasia, villous infarction, and decidual arteriopathy. Fetal vascular malperfusion was reported in cases of thrombosis, segmental avascular villi, intramural fibrin deposition, and villous stromal–vascular karyorrhexis. The presence of villitis of unknown etiology (multiple foci on more than one section, at least one of which showing inflammation affecting more than 10 contiguous villi) and delayed villous maturation (monotonous villous population with reduced numbers of vasculosyncytial membranes) were recorded.

STATISTICAL ANALYSIS

Descriptive statistics were generated for the whole cohort, and data were expressed as mean and standard deviation for continuous variables. Median value and range were calculated and reported, as were absolute or relative frequencies for categorical variables. Demographic and clinical characteristics were compared using the χ^2 or Fisher's exact test and the Student t-test for categorical and continuous variables, respectively. Univariate analysis was carried out to determine which demographic, perinatal, and placental characteristics were significantly more frequent among the patients with a specific lesion (GMH-IVH or CBH). Logistic regression analyses were used for each variable, and the results were reported as odds ratio (OR) with their 95% confidence intervals (CIs). The absence of exposure to the factor or the variable that was less likely to be associated with the risk of the lesion was used as the reference for each analysis. Multivariate analysis was then performed, and only variables that proved to be statistically or borderline significant in univariate analysis ($P < 0.08$) were included in the model. The model showing the best fit was based on backward stepwise selection procedures, and each variable was removed if it did not contribute significantly. In the final model, a $P <$

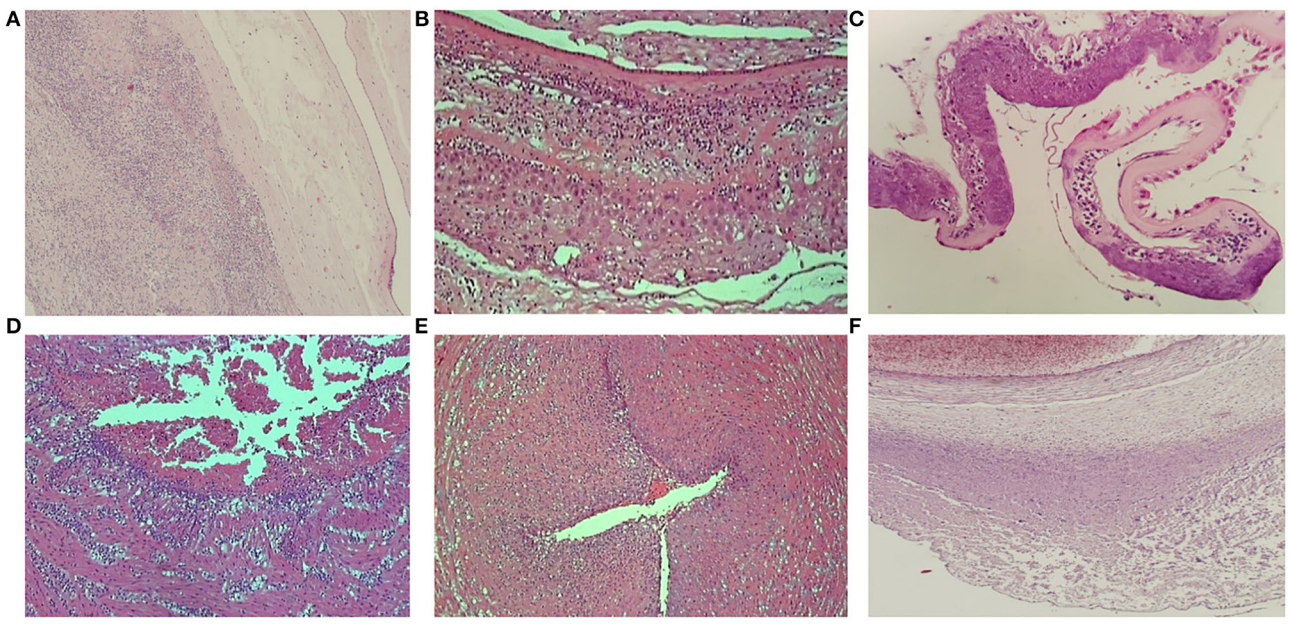

FIGURE 1 | Placental sections showing the three stages of maternal and fetal inflammatory response. **(A)** Maternal inflammatory response—stage 1. **(B)** Maternal inflammatory response—stage 2. **(C)** Maternal inflammatory response—stage 3. **(D)** Fetal inflammatory response—stage 1. **(E)** Fetal inflammatory response—stage 2. **(F)** Fetal inflammatory response—stage 3.

0.05 was considered statistically significant, and all *P*-values were based on two-tailed tests. Statistical analysis was performed using Statistical Package for the Social Sciences (SPSS) for Windows (SPSS Inc, Chicago, IL).

RESULTS

A total of 348 VLBW infants were identified across the study period. Of these, 26 (7.5%) patients died before reaching the TEA and one (0.3%) patient was excluded from the study because of the absence of brain MRI. Pathological examination of the placenta was not performed in 35 (10%) cases. The remaining 286 (82.2%) subjects were included in the study. Of the 286 patients in the final study population, 135 were male (47.2%). Mean gestational age was 28.2 weeks (standard deviation, *SD* ± 2.2 weeks), and mean birth weight was 1,040 g (*SD* ± 264 g). Median 1′ and 5′ Apgar scores were 6 (range, 0–9) and 8 (range, 0–10). GMH-IVH of any grade was detected in 68 patients (23.8%), whereas CHB was identified in 48 patients (16.8%). Of note, 50/68 infants (73.5%) with MRI-diagnosed GMH-IVH had already been diagnosed with cranial ultrasound, and the majority of them (47/50, 94%) received the diagnosis within the first 72 h of life. In addition, in the group of patients excluded because of the absence of placental examination, we found no significant difference in the incidence of GMH-IVH (10/35, 28.6%) nor CBH (4/35, 11.4%) compared to the study population ($p = 0.677$ and 0.626, respectively).

Risk Factors for GMH-IVH

Demographic and perinatal clinical data are shown in **Table 1**. Mean gestational age (27 ± 2.2 vs. 28.6 ± 2.1 weeks; $P = 0.001$) and birth weight (908 ± 250 vs. 1,080 ± 255 g; $P = 0.001$) were significantly lower in patients who developed GMH-IVH. In the univariate analysis, infants with GMH-IVH were less likely to be exposed to preeclampsia and delivered by cesarean section ($P = 0.04$ and $P \leq 0.0001$, respectively). Infants with GMH-IVH had a significantly higher frequency of 5′ Apgar score lower than five, intubation, mechanical ventilation, and inotropic support within the first 72 h, surfactant, late-onset sepsis, and medically and surgically treated PDA (**Table 1**). In addition, the contemporary presence of CBH was significantly more frequent in this population ($P = 0.0001$).

Placental findings of the two populations are shown in **Table 1**. Across the spectrum of histological chorioamnionitis, in the univariate analysis, severe maternal inflammatory response (stage 3) and fetal inflammatory response (stage 2) were associated with GMH-IVH ($P = 0.007$ and $P = 0.04$, respectively). Conversely, maternal vascular malperfusion was more frequent in infants without this lesion ($P = 0.05$).

As shown in **Table 2**, risk factors for GMH-IVH identified by multivariate analysis adjusted for gestational age were the presence of CBH (OR, 8.14; 95% CI, 3.63–18.24), mechanical ventilation within the first 72 h (OR, 2.67; 95% CI, 1.23–5.79), and pharmacologically treated PDA (OR, 2.6; 95% CI, 1.16–5.83). In our cohort, both mild (stage 1) and severe (stage 3) maternal inflammatory responses were found to be an independent risk factor for developing GMH-IVH (OR, 2.92; 95% CI, 1.04–8.19 and OR, 4; 95% CI, 1.24–12.9, respectively). Cesarean section was a protective factor (OR, 0.26; 95% CI, 0.11–0.58).

Risk Factors for Cerebellar Hemorrhage

Mean gestational age (26.6 ± 2 vs. 28.6 ± 2.1 weeks) and birth weight (904 ± 254 vs. 1,067 ± 258 g) were significantly lower in neonates with CBH ($P = 0.0001$). By univariate analysis, intubation, mechanical ventilation, surfactant, hemodynamically significant PDA, inotropic support, late-onset sepsis, and GMH-IVH were significantly more frequent (**Table 3**). Among placental factors, neither maternal or fetal vascular malperfusion nor histologic chorioamnionitis (both maternal and fetal sides) was associated with this lesion in our cohort. In the multivariate analysis (**Table 4**), lower gestational age, inotropic support within 72 h after birth (OR, 5.24; 95% CI, 1.88–14.6), and the contemporary presence of GMH-IVH (OR, 6.38; 95% CI, 3.02–13.5) emerged as independent risk factors for CBH.

DISCUSSION

Over the last decades, advances in perinatal care have contributed to a consistent reduction in severe forms of prematurity-related brain injuries such as periventricular leukomalacia (16). Nevertheless, the same efforts have not been as effective in reducing the incidence of GMH-IVH, which remains a common brain lesion in preterm infants, affecting about one-third of neonates of <32 weeks' gestation (17, 18). Extremely preterm infants are also prone to CBH, and after implementation of MRI for studying neonatal brain, the reported prevalence of CBH in low-birth weight infants went from 2% to a maximum of nearly 20% (6, 19, 20). Both lesions have a significant negative impact on neurodevelopmental outcome in preterm infants (21), although the diagnosis of minor forms of hemorrhage is often challenging with ultrasound and conventional MRI (4, 22) and how these lesions affect neurodevelopment is still a matter of debate (23, 24).

The multifactorial etiology and the relatively small development time frame of GMH-IVH and CBH make their prevention extremely challenging (25). For this reason, many efforts have been made to deeply understand their etiopathology as well as their associated risk factors. A complex interaction between environmental and genetic factors contributes to intraventricular hemorrhage in preterm infants (26). The role of genetic factors has recently gained interest, although the association with the development of GMH-IVH still remains unclear (27). Studies investigating the role of thrombophilic disorders increasing the risk of developing GMH-IVH are consistent with the phenomenon of thrombosis in germinal matrix vessels as a "primum movens" (10, 28–31), although conflicting results have been also published (32). At the same time, many studies found an increased risk of GMH-IVH in neonates with gene polymorphisms of pro-inflammatory cytokines, including IL-1β, IL-6, and TNF-α and of genes associated with the regulation of systemic blood pressure and cerebral blood flow, such as endothelial nitric oxide synthase (33) and type IV collagen genes (34).

TABLE 1 | Demographic information, clinical characteristics, and placental findings of neonates with and without intraventricular hemorrhage (GMH-IVH).

	Study population (*N* = 286)	GMH-IVH (*N* = 68)	No GMH-IVH (*N* = 218)	*P*-value
	N (%)	*N* (%)	*N* (%)	
Prenatal data				
Male	135 (47.2)	36 (52.9)	99 (45.4)	0.33
Intrauterine growth restriction	78 (27.3)	15 (22.1)	63 (28.9)	0.35
Antenatal corticosteroids	224 (78.6)	48 (70.6)	176 (80.7)	0.09
Gestational diabetes	11 (3.8)	2 (2.9)	9 (4.1)	1
Preeclampsia	64 (22.4)	9 (13.2)	55 (27.1)	**0.04**
Twin pregnancy	113 (39.5)	28 (41.2)	85 (39.0)	0.78
Twin to twin transfusion	22 (7.7)	5 (7.4)	17 (7.8)	1
Cesarean section	227 (79.4)	43 (63.2)	184 (84.4)	**≤0.0001**
Postnatal data				
Gestational age at birth mean (*SD*), weeks	28.2 ± 2.2	27 ± 2.2	28.6 ± 2.1	0.001
Birth weight mean (*SD*), g	1040 ± 264	908 ± 250	1080 ± 255	0.001
1′ Apgar ≤ 5	114 (39.9)	34 (50)	80 (36.7)	0.06
5′ Apgar ≤ 5	11 (3.8)	7 (10.3)	4 (1.8)	**0.005**
Intubation within the first 72 h	205 (71.7)	61 (89.7)	144 (66.1)	**<0.0001**
Mechanical ventilation within the first 72 h	149 (52.1)	49 (72.1)	100 (45.9)	**<0.0001**
Surfactant administration	200 (69.9)	59 (86.8)	141 (64.7)	**<0.0001**
Pneumothorax within the first 72 h	11 (3.8)	4 (5.9)	7 (3.2)	0.29
Inotropic support within the first 72 h	24 (8.4)	10 (14.7)	14 (6.4)	**0.04**
Early-onset sepsis	10 (3.5)	3 (4.4)	7 (3.2)	0.71
Late-onset sepsis	131 (45.8)	39 (57.4)	92 (42.2)	**0.03**
>1 late-onset sepsis	44 (15.4)	17 (25)	27 (12.4)	**0.02**
Necrotizing enterocolitis	17 (5.9)	5 (7.4)	12 (5.5)	0.56
Surgically treated necrotizing enterocolitis	10 (3.5)	4 (5.9)	6 (2.8)	0.25
Treated patent ductus arteriosus	174 (60.8)	51 (75)	123 (56.4)	**0.007**
Surgically treated patent ductus arteriosus	31 (10.8)	16 (23.5)	15 (6.9)	**<0.0001**
Cerebellar hemorrhage	48 (16.8)	30 (44.1)	18 (8.3)	**0.0001**
Placental findings				
Twin monochorionic placenta	38 (13.3)	7 (10.3)	31(14.2)	0.54
Velamentous placental cord insertion	27 (9.4)	5 (7.4)	22 (10.1)	0.64
Fetal inflammatory response—stage 1	23 (8)	9 (13.2)	14 (6.4)	0.09
Fetal inflammatory response—stage 2	9 (3.1)	5 (7.4)	4 (1.8)	**0.04**
Fetal inflammatory response—stage 3	23 (8)	6 (8.8)	17 (7.8)	0.80
Maternal inflammatory response—stage 1	29 (10.1)	11 (16.2)	18 (8.3)	0.06
Maternal inflammatory response—stage 2	37 (12.9)	8 (11.8)	29 (13.3)	0.84
Maternal inflammatory response—stage 3	22 (7.7)	11 (16.2)	11 (5)	**0.007**
Villitis of unknown etiology	31 (10.8)	10 (14.7)	21 (9.6)	0.26
Maternal vascular malperfusion	165 (57.7)	32 (47.1)	133 (61)	**0.05**
Fetal vascular malperfusion	11 (3.8)	3 (4.4)	8 (3.7)	0.73
Delayed villous maturation	44 (15.4)	8 (11.8)	36 (16.5)	0.26
Retroplacental hematoma	52 (18.2)	12 (17.6)	40 (18.3)	1

Statistically significant differences ($p < 0.05$) are highlighted in bold.

Gestational age and birth weight play a major role in the development of GMH-IVH and CBH, and the lower the weight and gestational age, the higher their incidence (19, 35). Our study showed a strong relationship between low gestational age at birth and CBH, in which the risk of this lesion was reduced at higher gestational ages.

The fetal environment is likely to influence the development of GMH-IVH and CBH because of the precocity of their occurrence. As placental macroscopic and histologic features reflect the quality of intrauterine life, several studies have focused on placental pathology in order to assess whether an association exists between placental lesions and the risk of developing

TABLE 2 | Logistic regression analysis of potential risk factors for intraventricular hemorrhage (GMH-IVH).

	GMH-IVH (*N* = 68)	No GMH-IVH (*N* = 218)	OR (95% CI)	*P*-value
	N (%)	*N* (%)		
Cesarean section	43 (63.2)	184 (84.4)	0.26 (0.11–0.58)	**<0.001**
Maternal inflammatory response—stage 1	11 (16.2)	18 (8.3)	2.92 (1.04–8.19)	**0.04**
Maternal inflammatory response—stage 3	11 (16.2)	11 (5)	4 (1.24–12.9)	**0.02**
Treated patent ductus arteriosus	51 (75)	123 (56.4)	2.6 (1.16–5.83)	**0.02**
Mechanical ventilation within the first 72 h	49 (72.1)	100 (45.9)	2.67 (1.23–5.79)	**0.01**
Cerebellar hemorrhage	30 (44.1)	18 (8.3)	8.14 (3.63–18.24)	**<0.001**

OR, odds ratio; CI, confidence interval. Statistically significant differences ($p < 0.05$) are highlighted in bold.

neonatal brain injuries (12). Intrauterine inflammation/infection (chorioamnionitis) is among the most studied placental lesions associated with preterm birth and potentially with preterm-related complications (36).

The relationship between chorioamnionitis and the development of GMH-IVH is still a matter of debate. A study in 2012 failed to find any association (37), whereas the meta-analysis of Villamor-Martinez et al. (13) showed that both clinical and histological chorioamnionitis constitute an independent risk factor for GMH-IVH. In 2018, Granger et al. demonstrated the same association, although after adjustment for perinatal variables, this association disappeared (38). In the same year, a multicenter study on 350 preterm infants found no association between histological chorioamnionitis and GMH-IVH diagnosed with early postnatal brain MRI (39). Heterogeneous methodology of the studies, different criteria for chorioamnionitis and brain damage diagnosis and staging, and continuous improvement in the clinical care of preterm infants (e.g., the introduction of antenatal steroid prophylaxis) could be possible explanations for this discrepancy (40).

We observed that both mild and severe (stages 1 and 3) histopathologic chorioamnionitis involving the maternal side of the placenta were independent risk factors for the development of GMH-IVH. We observed that both stage 1 and stage 3 histopathologic chorioamnionitis were independent risk factors for the development of GMH-IVH, while stage 2 chorioamnionitis did not show any significant association with GMH-IVH in our cohort.

Besides, fetal inflammatory response, characterized by chorionic vasculitis and different stages of funisitis, was significantly more frequent in the GMH-IVH group only in moderate forms (stage 2 fetal inflammatory response), but this association disappeared in the multivariate analysis. The causal relationship between chorioamnionitis and GMH-IVH is still unclear (41, 42), although plausible mechanisms include the direct effect of pro-inflammatory cytokines on the brain (43, 44), the increased permeability of the brain–blood barrier (45), and the augmented cerebral oxygen consumption associated with antenatal infection/inflammation (46–48).

In our study, the maternal component of intrauterine infection seemed to play a major role in enhancing the risk of GMH-IVH regardless of the presence of fetal inflammatory response. Our finding is consistent with the meta-analysis of Villamor Martinez et al., who evaluated the effect of funisitis on the development of intraventricular hemorrhage. In an analysis of 13 studies regarding infants with histological chorioamnionitis with or without funisitis, the authors did not find a significant difference in GMH-IVH risk between these two groups (13).

Maternal vascular malperfusion is a common placental finding in preterm birth (49) and may be associated with preeclampsia, stillbirth, intrauterine growth retardation, systemic lupus erythematosus, and antiphospholipid antibody syndrome (50). The placenta of nearly half of the VLBW infants in our cohort showed signs of maternal vascular malperfusion. In the univariate analysis, infants with GMH-IVH were less likely to present with this placental feature, but after correction for gestational age, this association disappeared.

In our cohort, histopathologic lesions of the placenta were not associated with a higher risk of CBH. The lack of association between cerebellar insult and chorioamnionitis is consistent with a recent meta-analysis, which included five studies in which clinically diagnosed chorioamnionitis was evaluated as a possible risk factor for CBH (51).

Although predisposition to GMH-IVH and CBH may potentially follow common perinatal patterns, it is possible that a different vascular anatomy may partly modify the factors, making these two brain regions predisposed to hemorrhage. Although subependymal vein anatomy may facilitate venous congestion leading to GMH-IVH (52), cerebellar vascular anatomy has not been investigated in detail as a potential factor contributing to CBH. In addition, human cerebellar development extends from the early first trimester to final circuit maturity, which is achieved by the end of the second postnatal year (53). The protracted nature of human cerebellar development renders this organ particularly vulnerable to developmental injury after birth, in which postnatal preterm-related complications may heavily impact its occurrence (4, 54), while antenatal placental disturbances may not significantly predispose infants to this lesion.

Among perinatal and postnatal risk factors, we found that cesarean section exerts a protective role on the development of

TABLE 3 | Demographic information, clinical characteristics, and placental findings of neonates with and without cerebellar hemorrhage (CBH).

	Study patients (*N* = 286)	CBH (*N* = 48)	No CBH (*N* = 238)	*P*-value
	N (%)	*N* (%)	*N* (%)	
Prenatal data				
Male	135 (47.2)	26 (54.2)	109 (45.8)	0.34
Intrauterine growth restriction	78 (27.3)	8 (16.7)	70 (29.4)	0.08
Antenatal steroids	224 (78.6)	32 (66.7)	192 (80.7)	**0.04**
Gestational diabetes	11 (3.8)	1 (2.1)	10 (4.2)	0.70
Preeclampsia	55 (19.2)	8 (16.7)	56 (23.5)	0.35
Twin pregnancy	110 (38.5)	19 (39.6)	91 (38.2)	0.87
Twin-to-twin transfusion	227 (79.4)	35 (72.9)	192 (80.7)	0.24
Cesarean section				
Postnatal data				
Gestational age at birth mean (*SD*), weeks	28.2 ± 2.2	26.6 ± 2	28.6 ± 2.1	**0.0001**
Birth weight mean (*SD*), g	1040 ± 264	904 ± 254	1067 ± 258	**0.0001**
1′ Apgar ≤ 5	114 (39.9)	23 (47.9)	91 (38.2)	0.26
5′ Apgar ≤ 5	11 (3.8)	3 (6.2)	8 (3.4)	0.40
Intubation within the first 72 h	205 (71.7)	43 (89.6)	162 (68.1)	**0.002**
Mechanical ventilation within the first 72 h	149 (52.1)	32 (66.7)	117 (49.2)	**0.03**
Surfactant administration	200 (69.9)	43 (89.6)	157 (66)	**0.001**
Pneumothorax within the first 72 h	11 (3.8)	3 (6.2)	8 (3.4)	0.40
Inotropic support within the first 72 h	24 (8.4)	13 (27.1)	11 (4.6)	**0.0001**
Early-onset sepsis	10 (3.5)	3 (6.2)	7 (2.9)	0.38
Late-onset sepsis	131 (45.8)	34 (70.8)	97 (40.8)	**0.0001**
>1 late-onset sepsis	44 (15.4)	14 (29.2)	30 (12.6)	**0.007**
Necrotizing enterocolitis	17 (5.9)	3 (6.2)	14 (5.9)	1
Surgically treated necrotizing enterocolitis	10 (3.5)	3 (6.2)	7 (2.9)	0.38
Treated patent ductus arteriosus	174 (60.8)	32 (66.7)	142 (59.7)	0.42
Surgically treated patent ductus arteriosus	31 (10.8)	13 (27.1)	18 (7.6)	**0.0001**
GMH-IVH	68 (23.8)	30 (62.5)	38 (18)	**0.0001**
Placental findings				
Twin monochorionic placenta	38 (13.3)	4 (8.3)	34(14.3)	0.35
Velamentous cord insertion	27 (9.4)	1 (2.1)	26 (10.9)	0.06
Fetal inflammatory response—stage 1	23 (8)	4 (8.3)	19 (8)	1
Fetal inflammatory response—stage 2	9 (3.1)	2 (4.2)	7 (2.9)	0.65
Fetal inflammatory response—stage 3	23 (8)	7 (14.6)	16 (6.7)	0.08
Maternal inflammatory response—stage 1	29 (10.1)	8 (16.7)	21 (8.8)	0.12
Maternal inflammatory response—stage 2	37 (12.9)	8 (16.7)	29 (12.2)	0.48
Maternal inflammatory response—stage 3	22 (7.7)	6 (12.5)	16 (6.7)	0.23
Villitis of unknown etiology	31 (10.8)	4 (8.3)	27 (11.3)	0.80
Fetal vascular malperfusion	11 (3.8)	1 (2.1)	10 (4.2)	0.70
Maternal vascular malperfusion	11 (3.8)	1 (2.1)	10 (4.2)	0.70
Delayed villous maturation	44 (15.4)	7 (14.6)	37 (15.5)	1
Retroplacental hematoma	52 (18.2)	11 (22.9)	41 (17.2)	0.41

Statistically significant differences ($p < 0.05$) are highlighted in bold.

both GMH-IVH and CBH compared to vaginal delivery. The same conclusion regarding GMH-IVH has emerged from two recent studies, in which elective cesarean section was found to reduce the rates of GMH-IVH in large cohorts of preterm infants born before 32 weeks' gestation (11, 55). At the same time, emergent cesarean section seems to increase the risk of CBH (19, 56). Elective cesarean section improving preterm neonatal outcome may be explained by the advantages related to a planned preterm birth, including an increased chance to administer a complete corticosteroid and antibiotic prophylaxes before birth, more attentive monitoring of fetal conditions, and perhaps, a more efficient preparation of the neonatal resuscitation team

TABLE 4 | Logistic regression analysis of potential risk factors for cerebellar hemorrhage (CBH) in our cohort.

	CBH (*N* = 48)	No CBH (*N* = 238)	OR (95% CI)	*P*-value
	N (%)	*N* (%)		
Gestational age	26.6 ± 2	28.6 ± 2.1	0.76 (0.63–0.91)	**0.003**
Inotropic support within the first 72 h	13 (27.1)	11 (4.6)	5.24 (1.88–14.6)	**0.002**
GMH-IVH	30 (62.5)	38 (18)	6.38 (3.02–13.5)	**0.0001**

OR, odds ratio; CI, confidence interval. Statistically significant differences ($p < 0.05$) are highlighted in bold.

(57, 58). Nevertheless, as we included both emergent and elective sections, we are not able to confirm these associations.

Both circulatory and respiratory complications soon after birth predispose infants to GMH-IVH. In very preterm infants, cardiopulmonary resuscitation (35, 59–62), an increased number of intubation attempts in the delivery room (63), and mechanical ventilation (11, 64) were found to be risk factors for severe GMH-IVH. In addition, several studies have reported that neonatal hypotension increases the risk of both GMH-IVH and CBH in extremely preterm infants in the 1st day of life (65–67), possibly because of the immature cerebral autoregulation that may affect the preterm brain (68). Our study confirmed that a difficult adaptation to extrauterine life, demonstrated by a 5′ Apgar score <5, the presence of hemodynamic instability caused by patency of ductus arteriosus, hypotension requiring inotropic support, and the need for surfactant administration, and intubation and mechanical ventilation in the 1st days of life are likely to predispose the infant to both GMH-IVH and CBH. As reported in previous studies on very preterm and extremely preterm infants (11, 69), postnatal sepsis predisposed infants to both GMH-IVH and CBH in our cohort, although its effect was mitigated when corrected for gestational age. In the multivariate analysis, pharmacologically treated PDA and mechanical ventilation within the first 72 h remained significant factors predisposing infants to GMH-IVH, whereas hypotension requiring inotropic support within the first 72 h of life was an independent risk factor for CBH.

Although predisposing factors for GMH-IVH and CBH appear to be slightly different between our cohort and previous studies (56), the chance to have both lesions is high (OR of having a GMH-IVH in presence of CBH was 6.38 in our population and OR of having a CBH in case of GMH-IVH was 8.14 in our population). We suggest that preterm infants at risk for one lesion should be monitored for both GMH-IVH and CBH; interestingly, cerebral and cerebellar anatomical origins of the bleeding share a similar function (3), germinal matrix for GMH-IVH, and external granular layer for CBH, areas where neurons are produced prior to take their final migratory destiny. Of note, the major part of neuronal migration has already taken place in the germinal matrix when GMH-IVH may occur, whereas the external granular layer remains active in healthy infants until a few months after birth (53, 70).

A strength of our study was the use of MRI with SWI sequences to detect even minor forms of hemorrhage that may escape detection not only by ultrasonography but also by conventional magnetic resonance studies (71). In addition, we considered both forms of hemorrhage, GMH-IVH and CBH. As there is an urgent need for standardizing placental findings, we reviewed placental sections of every neonate included according to the recent histologic classification of the Amsterdam Placental Workshop Group Consensus Statement (14), which provides a detailed and comprehensive description of macroscopic and microscopic placental lesions.

Limitations of our study were its retrospective nature and the exclusion of all the patients who died before undergoing brain MRI at TEA or without a placental histologic examination performed at birth. This may have excluded the most preterm and sick neonates in which high-grade GMH-IVH and CBH are common complications. Due to the retrospective nature of the study, we could not identify the reasons why the placental examination was not performed. However, the prevalence of both GMH-IVH and CBH in this subgroup of subjects excluded from the analysis was similar to the prevalence we found in the study population.

Our study stresses the importance of postnatal care in the early neonatal period in reducing the risk of GMH-IVH and CBH. In addition, our data confirm that the presence of intrauterine infection/inflammation may play a significant role in predisposing preterm infants to GMH-IVH and reinforce the importance of preventing prenatal infections. Furthermore, to our knowledge, this is the first study exploring the possible association between placental pathology and hemorrhages like GMH-IVH and CBH, diagnosed, and considered together with SWI sequences. Despite the intuitive role of prenatal influence in early neonatal lesions such as GMH-IVH and CBH, the multifactorial etiology of these lesions and the strong influence of early postnatal factors may modulate individual effects of the prenatal environment on the subsequent risk of GMH-IVH and CBH. We believe that the best way to discover more significant risk factors differentiating the origin of the two lesions should rely on prospective and multicenter studies comparing selected cases of GMH-IVH (in the absence of CBH) to the even fewer isolated CBH.

DATA AVAILABILITY STATEMENT

All datasets generated for this study are included in the article/supplementary material.

ETHICS STATEMENT

The studies involving human participants were reviewed and approved by Giannina Gaslini Hospital, Genoa, Italy. Written informed consent to participate in this study was provided by the participants' legal guardian/next of kin.

AUTHOR CONTRIBUTIONS

AP, LR, and EF contributed to conception and design of the study. AP, MR, SR, and LD organized the database. DT, AR, GM, and MS reviewed the MRI scans. EF, MB, and FB performed the placental analysis. MC performed the statistical analysis. AP and MR wrote the first draft of the manuscript. LD, FB, MC, MM, and LR wrote the sections of the manuscript. All authors contributed to manuscript revision, read, and approved the submitted version.

FUNDING

Funding from Eu-Brain non-profit association supported the present study.

REFERENCES

1. Ancel P-Y, Goffinet F, EPIPAGE-2 Writing Group, Kuhn P, Langer B, Matis J, et al. Survival and morbidity of preterm children born at 22 through 34 weeks' gestation in france in 2011: results of the epipage-2 cohort study. *JAMA Pediatr.* (2015) 169:230–8. doi: 10.1001/jamapediatrics.2014.3351
2. Brouwer AJ, Groenendaal F, Benders MJ, de Vries LS. Early and late complications of germinal matrix-intraventricular haemorrhage in the preterm infant: what is new? *Neonatology.* (2014) 106:296–303. doi: 10.1159/000365127
3. Fumagalli M, Bassi L, Sirgiovanni I, Mosca F, Sannia A, Ramenghi LA. From germinal matrix to cerebellar haemorrhage. *J Matern Fetal Neonatal Med.* (2015) 8:2280–5. doi: 10.3109/14767058.2013.796168
4. Parodi A, Morana G, Severino MS, Malova M, Natalizia AR, Sannia A, et al. Low-grade intraventricular hemorrhage: is ultrasound good enough? *J Matern Fetal Neonatal Med.* (2015) 28:2261–4. doi: 10.3109/14767058.2013.796162
5. Rutherford MA, Supramaniam V, Ederies A, Chew A, Bassi L, Groppo M, et al. Magnetic resonance imaging of white matter diseases of prematurity. *Neuroradiology.* (2010) 52:505–21. doi: 10.1007/s00234-010-0700-y
6. Tam EW, Rosenbluth G, Rogers EE, Ferriero DM, Glidden D, Goldstein RB, et al. Cerebellar hemorrhage on magnetic resonance imaging in preterm newborns associated with abnormal neurologic outcome. *J Pediatr.* (2011) 158:245–50. doi: 10.1016/j.jpeds.2010.07.049
7. Nandigam RN, Viswanathan A, Delgado P, Skehan ME, Smith EE, Rosand J, et al. MR imaging detection of cerebral microbleeds: effect of susceptibility-weighted imaging, section thickness, and field strength. *Am J Neuroradiol.* (2009) 30:338–43. doi: 10.3174/ajnr.A1355
8. Tam EWY. Cerebellar injury in preterm infants. *Handb Clin Neurol.* (2018) 155:49–59. doi: 10.1016/B978-0-444-64189-2.00003-2
9. Volpe JJ. Cerebellum of the premature infant: rapidly developing, vulnerable, clinically important. *J Child Neurol.* (2009) 24:1085–104. doi: 10.1177/0883073809338067
10. Ramenghi LA, Fumagalli M, Groppo M, Consonni D, Gatti L, Bertazzi PA, et al. Germinal matrix hemorrhage: intraventricular hemorrhage in very-low-birth-weight infants: the independent role of inherited thrombophilia. *Stroke.* (2011) 42:1889–93. doi: 10.1161/STROKEAHA.110.590455
11. Poryo M, Boeckh JC, Gortner L, Zemlin M, Duppré P, Daniel Ebrahimi-Fakhari D, et al. Antenatal, perinatal and postnatal factors associated with intraventricular hemorrhage in very premature infants. *Early Hum Dev.* (2018) 116:1–8. doi: 10.1016/j.earlhumdev.2017.08.010
12. Catov JM, Scifres CM, Caritis SN, Bertolet M, Larkin J, Parks WT. Neonatal outcomes following preterm birth classified according to placental features. *Am J Obstet Gynecol.* (2017) 216:411.e1–14. doi: 10.1016/j.ajog.2016.12.022
13. Villamor-Martinez E, Fumagalli M, Mohammed Rahim O, Passera S, Cavallaro G, Degraeuwe P, et al. Chorioamnionitis is a risk factor for intraventricular hemorrhage in preterm infants: a systematic review and meta-analysis. *Front Physiol.* (2018) 9:1253. doi: 10.3389/fphys.2018.01253
14. Khong TY, Mooney EE, Ariel I, Balmus NCM, Boyd TK, Brundler M, et al. Sampling and definitions of placental lesions, amsterdam placental workshop group consensus statement. *Arch Pathol Lab Med.* (2016) 140:698–713. doi: 10.5858/arpa.2015-0225-CC
15. Redline Rw, Faye-Petersen O, Heller D, Qureshi F, Van Savell V, Vogler C. Amniotic infection syndrome: nosology and reproducibility of placental reaction patterns. *Pediatr Dev Pathol.* (2003) 6:435–48. doi: 10.1007/s10024-003-7070-y
16. Cheong JLY, Anderson PJ, Burnett AC, Roberts G, Davis N, Hickey L, et al. Changing neurodevelopment at 8 years in children born extremely preterm since the 1990s. *Pediatrics.* (2017) 139:e20164086. doi 10.1542/peds.2016-4086
17. Ramenghi LA. Germinal matrix-intraventricular haemorrhage: still a very important brain lesion in premature infants! *J Matern Fetal Neonatal Med.* (2015) 28:2259–60. doi: 10.3109/14767058.2013.1031952
18. Stoll BJ, Hansen NI, Bell EF, Walsh MC, Carlo WA, Shankaran S, et al. Eunice kennedy shriver national institute of child health and human development. Neonatal Research Network. Trends in care practices, morbidity, and mortality of extremely preterm neonates, 1993–2012. *JAMA.* (2015) 314:1039–51. doi: 10.1001/jama.2015.10244
19. Limperopoulos C, Benson CB, Bassan H, Disalvo DN, Kinnamon DD, Moore M, et al. Cerebellar hemorrhage in the preterm infant: ultrasonographic findings and risk factors. *Pediatrics.* (2005) 116:717–24. doi: 10.1542/peds.2005-0556
20. Steggerda SJ, Leijser LM, Wiggers-de Bruïne FT, van dG, Walther FJ, van Wezel-Meijler G. Cerebellar injury in preterm infants: incidence and findings on US and MR images. *Radiology.* (2009) 252:190–9. doi: 10.1148/radiol.2521081525
21. Mukerji A, Shah V, Shah PS. Periventricular/Intraventricular hemorrhage and neurodevelopmental outcomes: a meta-analysis. *Pediatrics.* (2015) 136:1132–143. doi: 10.1542/peds.2015-0944
22. Parodi A, Rossi A, Severino M, Morana G, Sannia A, Calevo MG, et al. Accuracy of ultrasound in assessing cerebellar haemorrhages in very low birthweight babies. *Arch Dis Child Fetal Neonatal Ed.* (2015) 100:F289–92. doi: 10.1136/archdischild-2014-307176
23. Bolisetty S, Dhawan A, Abdel-Latif M, Bajuk B, Stack J, Lui K, et al. Intraventricular hemorrhage and neurodevelopmental outcomes in extreme preterm infants. *Pediatrics.* (2014) 133:55–62. doi: 10.1542/peds.2013-0372
24. Boswinkel V, Steggerda SJ, Fumagalli M, Parodi A, Ramenghi LA, Groenendaal F, et al. The CHOPIn study: a multicenter study on cerebellar hemorrhage and outcome in preterm infants. *Cerebellum.* (2019) 18:989–98. doi: 10.1007/s12311-019-01053-1
25. Sannia A, Natalizia AR, Parodi A, Malova M, Fumagalli M, Rossi A, et al. Different gestational ages and changing vulnerability of the premature brain. *J Matern Fetal Neonatal Med.* (2015) 28:2268–72. doi: 10.3109/14767058.2013.796166
26. Ment LR, Ådén U, Bauer CR, Bada HS, Carlo WA, Kaiser JR, et al. Genes and environment in neonatal intraventricular hemorrhage. *Semin Perinatol.* (2015) 39:592–603. doi: 10.1053/j.semperi.2015.09.006
27. Szpecht D, Szymankiewicz M, Seremak-Mrozikiewicz A, Gadzinowski J. The role of genetic factors in the pathogenesis of neonatal intraventricular hemorrhage. *Folia Neuropathol.* (2015) 53:1–7. doi: 10.5114/fn.2015.49968
28. Paneth N, Rudelli R, Kazam, Monte W. The pathology of germinal matrix/intraventricular hemmorhage. In: Paneth N, Rudelli R, Kazam, Monte W,

editors. *Brain Damage in the Preterm Infant. Clinics in Developmental Medicine. No. 131*. 1st ed. London: Mac Keith Press (1994). p. 23–53.
29. Ghazi-Birry HS, Brown WR, Moody DM, Challa VR, Block SM, Reboussin DM. Human germinal matrix: venous origin of hemorrhage and vascular characteristics. *AJNR Am J Neuroradiol*. (1997) 18:219–29.
30. Petäjä J, Hiltunen L, Fellman V. Increased risk of intraventricular hemorrhage in preterm infants with thrombophilia. *Pediatr Res.* (2001) 49:643–6. doi: 10.1203/00006450-200105000-00006
31. Ramenghi LA, Gill BJ, Tanner SF, Martinez D, Arthur R, Levene MI. Cerebral venous thrombosis, intraventricular haemorrhage and white matter lesions in a preterm newborn with factor V (Leiden) mutation. *Neuropediatrics*. (2002) 33:97–9. doi: 10.1055/s-2002-32370
32. Hartel C, Konig I, Koster S, Kattner E, Kuhls E, Kuster H, et al. Genetic polymorphisms of hemostasis genes and primary outcome of very low birth weight infants. *Pediatrics*. (2006) 118:683–9. doi: 10.1542/peds.2005-2670
33. Szpecht D, Wiak K, Braszak A, Szymankiewicz M, Gadzinowski J. Role of selected cytokines in the etiopathogenesis of intraventricular hemorrhage in preterm newborns. *Childs Nerv Syst.* (2016) 32:2097–103. doi: 10.1007/s00381-016-3217-9
34. Bilguvar K, DiLuna ML, Bizzarro MJ, Bayri Y, Schneider KC, Lifton RP, et al. COL4A1 mutation in preterm intraventricular hemorrhage. *J Pediatr*. (2009) 155:743–45 doi: 10.1016/j.jpeds.2009.04.014
35. Lu H, Wang Q, Lu J, Zhang Q, Kumar P. Risk factors for intraventricular hemorrhage in preterm infants born at 34 weeks of gestation or less following preterm premature rupture of membranes. *J Stroke Cerebrovasc Dis*. (2016) 25:807–12. doi: 10.1016/j.jstrokecerebrovasdis.2015.12.011
36. Soraisham AS, Singhal N, McMillan DD, Sauve RS, Lee SK, Canadian Neonatal Network. A multicenter study on the clinical outcome of chorioamnionitis in preterm infants. *Am J Obstet Gynecol*. (2009) 200:372.e1–372.e3726. doi: 10.1016/j.ajog.2008.11.034
37. Ylijoki M, Ekholm E, Haataja L, Lehtonen L, PIPARI study group. Is chorioamnionitis harmful for the brain of preterm infants? A clinical overview. *Acta Obstet Gynecol Scand*. (2012) 91:403–19. doi: 10.1111/j.1600-0412.2012.01349.x
38. Granger C, Spittle AJ, Walsh J, Pyman J, Anderson PJ, Thompson DK, et al. Histologic chorioamnionitis in preterm infants: correlation with brain magnetic resonance imaging at term equivalent age. *BMC Pediatr*. (2018) 18:63. doi: 10.1186/s12887-018-1001-6
39. Bierstone D, Wagenaar N, Gano DL, Guo T, Georgio G, Groenendaal F, et al. Association of histologic chorioamnionitis with perinatal brain injury and early childhood neurodevelopmental outcomes among preterm neonates. *JAMA Pediatr*. (2018) 172:534–41. doi: 10.1001/jamapediatrics.2018.0102
40. Chau V, McFadden DE, Poskitt KJ, Miller SP. Chorioamnionitis in the pathogenesis of brain injury in preterm infants. *Clin Perinatol*. (2014) 41:83–103. doi: 10.1016/j.clp.2013.10.009
41. Edwards AD, Tan S. Perinatal infections, prematurity and brain injury. *Curr Opin Pediatr*. (2006) 18:119–24. doi: 10.1097/01.mop.0000193290.02270.30
42. Gantert M, Been JV, Gavilanes AW, Garnier Y, Zimmermann LJ, Kramer BW. Chorioamnionitis: a multiorgan disease of the fetus? *J Perinatol*. (2010) 30:S21–30. doi: 10.1038/jp.2010.96
43. Viscardi RM, Muhumuza CK, Rodriguez A, Fairchild KD, Sun CCJ, Gross GW, et al. Inflammatory markers in intrauterine and fetal blood and cerebrospinal fluid compartments are associated with adverse pulmonary and neurologic outcomes in preterm infants. *Pediatr Res*. (2004) 55:1009–17. doi: 10.1203/01.pdr.0000127015.60185.8a
44. Lawrence SM, Wynn JL. Chorioamnionitis, IL-17A, and fetal origins of neurologic disease. *Am J Reprod Immunol*. (2018) 79:e12803. doi: 10.1111/aji.12803
45. Stolp HB, Ek CJ, Johansson PA, Dziegielewska KM, Bethge N, Wheaton BJ, et al. Factors involved in inflammation-induced developmental white matter damage. *Neurosci Lett*. (2009) 451:232–6. doi: 10.1016/j.neulet.2009.01.021
46. Stark MJ, Hodyl NA, Belegar VK, Andersen CC. Intrauterine inflammation, cerebral oxygen consumption and susceptibility to early brain injury in very preterm newborns. *Arch Dis Child Fetal Neonatal Ed*. (2015) 101:F137–42. doi: 10.1136/archdischild-2014-306945
47. Yanowitz TD, Potter DM, Bowen A, Baker RW, Roberts JM. Variability in cerebral oxygen delivery is reduced in premature neonates exposed to chorioamnionitis. *Pediatr Res*. (2006) 59:299–304. doi: 10.1203/01.pdr.0000196738.03171.f1
48. Kissack CM, Garr R, Wardle SP, Weindling AM. Postnatal changes in cerebral oxygen extraction in the preterm infant are associated with intraventricular hemorrhage and hemorrhagic parenchymal infarction but not periventricular leukomalacia. *Pediatr Res*. (2004) 56:111–6. doi: 10.1203/01.PDR.0000128984.03461.42
49. Kelly R, Holzman C, Senagore P, Wang J, Tian Y, Rahbar MH, et al. Placental vascular pathology findings and pathways to preterm delivery. *Am J Epidemiol*. (2009) 170:148–58. doi: 10.1093/aje/kwp131
50. Ernst LM. Maternal vascular malperfusion of the placental bed. *APMIS*. (2018) 126:551–60. doi: 10.1111/apm.12833
51. Villamor-Martinez E, Fumagalli M, Alomar YI, Passera S, Cavallaro G, Mosca F, et al. Cerebellar hemorrhage in preterm infants: a meta-analysis on risk factors and neurodevelopmental outcome. *Front Physiol*. (2019) 10:800. doi: 10.3389/fphys.2019.00800
52. Tortora D, Severino M, Malova M, Parodi A, Morana G, Sedlacik J, et al. Differences in subependymal vein anatomy may predispose preterm infants to GMH-IVH. *Arch Dis Child Fetal Neonatal Ed*. (2018) 103:F59–F65. doi: 10.1136/archdischild-2017-312710
53. Haldipur P, Dang D, Millen KJ. Embryology. *Handb Clin Neurol*. (2018) 154:29–44. doi: 10.1016/B978-0-444-63956-1.00002-3
54. Limperopoulos C, Soul JS, Gauvreau K, Warfield SK, Bassan H, Robertson RL, et al. Late gestation cerebellar growth is rapid and impeded by premature birth. *Pediatrics*. (2005) 115:688–95. doi: 10.1542/peds.2004-1169
55. Humberg A, Härtel C, Paul P, Hanke K, Bossung V, Hartz A, et al. Delivery mode and intraventricular hemorrhage risk in very-low-birth-weight infants: observational data of the german neonatal network. *Eur J Obstet Gynecol Reprod Biol*. (2017) 212:144–9. doi: 10.1016/j.ejogrb.2017.03.032
56. Vesoulis ZA, Herco M, Mathur AM. Divergent risk factors for cerebellar and intraventricular hemorrhage. *J Perinatol*. (2018) 38:278–84. doi: 10.1038/s41372-017-0010-x
57. Malloy MH. Impact of cesarean section on neonatal mortality rates among very preterm infants in the United States, 2000-2003. *Pediatrics*. (2008) 122:285–92. doi: 10.1542/peds.2007-2620
58. Dani C, Poggi C, Bertini G, Pratesi S, Di Tommaso M, Scarselli G, et al. Method of delivery and intraventricular haemorrhage in extremely preterm infants. *J Matern Fetal Neonatal Med*. (2010) 23:1419–23. doi: 10.3109/14767051003678218
59. Wyckoff MH, Salhab WA, Heyne RJ, Kendrick D, Stoll BJ, Laptook AR, et al. Outcome of extremely low birth weight infants who received delivery room cardiopulmonary resuscitation. *J Pediatr*. (2012) 160:239–44.e2. doi: 10.1016/j.jpeds.2011.07.041
60. Handley SC, Sun Y, Wyckoff MH, Lee HC. Outcomes of extremely preterm infants after delivery room cardiopulmonary resuscitation in a population-based cohort. *J Perinatol*. (2017) 35:379–83. doi: 10.1038/jp.2014.222
61. Arnon S, Dolfin T, Reichman B, Regev RH, L Lerner-Geva L, Boyko V, et al. Delivery room resuscitation and adverse outcomes among very low birth weight preterm infants. *J Perinatol*. (2017) 37:1010–6. doi: 10.1038/jp.2017.99
62. Roberts JC, Javed MJ, Hocker JR, Wang H, Tarantino MD. Risk factors associated with intraventricular hemorrhage in extremely premature neonates. *Blood Coagul Fibrinolysis*. (2018) 29:25–9. doi: 10.1097/MBC.0000000000000661
63. Sauer CW, Kong JY, Vaucher YE, Finer N, Proudfoot JA, Boutin MA, et al. Intubation attempts increase the risk for severe intraventricular hemorrhage in preterm infants-a retrospective cohort study. *J Pediatr*. (2016) 177:108–13. doi: 10.1016/j.jpeds.2016.06.051
64. Helwich E, Rutkowska M, Bokiniec R, Gulczynska E, Hozejowski R. Intraventricular hemorrhage in premature infants with respiratory distress syndrome treated with surfactant: incidence and risk factors in the prospective cohort study. *Dev Period Med*. (2017) 21:328–35.
65. Faust K, Härtel C, Preuß M, Rabe H, Roll C, Emeis M, et al. Short-term outcome of very-low-birthweight infants with arterial hypotension in the first 24 h of life. *Arch Dis Child Fetal Neonatal Ed*. (2015) 100:F388. doi: 10.1136/archdischild-2014-306483
66. Fanaroff AA, Fanaroff JM. Short- and long-term consequences of hypotension in ELBW infants. *Semin Perinatol*. (2006) 30:151. doi: 10.1053/j.semperi.2006.04.006

67. Vesoulis ZA, Herco M, El Ters NM, Whitehead HV, Mathur A. Cerebellar hemorrhage: a 10-year evaluation of risk factors. *J Matern Fetal Neonatal Med.* (2019) 1:1–9. doi: 10.1080/14767058.2019.1583729
68. Vesoulis ZA, Mathur AM. cerebral autoregulation, brain injury, and the transitioning premature infant. *Front Pediatr.* (2017) 5:64. doi: 10.3389/fped.2017.00064
69. Khanafer-Larocque I, Soraisham A, Stritzke A, Al Awad E, Thomas S, Murthy P, et al. Intraventricular hemorrhage: risk factors and association with patent ductus arteriosus treatment in extremely preterm neonates. *Front Pediatr.* (2019) 7:408. doi: 10.3389/fped.2019.00408
70. Botkin ND, Kovtanyuk AE, Turova VL, Sidorenko IN, Lampe R. Direct modeling of blood flow through the vascular network of the germinal matrix. *Comput Biol Med.* (2018) 92:147–55. doi: 10.1016/j.compbiomed.2017.11.010
71. Intrapiromkul J, Northington F, Huisman TA, Izbudak I, Meoded A, Tekes A. Accuracy of head ultrasound for the detection of intracranial hemorrhage in preterm neonates: comparison with brain MRI and susceptibility-weighted imaging. *J Neuroradiol.* (2013) 40:81–88. doi: 10.1016/j.neurad.2012.03.006

Conflict of Interest: The authors declare that the research was conducted in the absence of any commercial or financial relationships that could be construed as a potential conflict of interest.

frontiers in Neurology

ORIGINAL RESEARCH
published: 04 September 2020
doi: 10.3389/fneur.2020.00883

Proton Magnetic Resonance Spectroscopy Lactate/N-Acetylaspartate Within 48 h Predicts Cell Death Following Varied Neuroprotective Interventions in a Piglet Model of Hypoxia–Ischemia With and Without Inflammation-Sensitization

Raymand Pang[1], *Kathryn A. Martinello*[1], *Christopher Meehan*[1], *Adnan Avdic-Belltheus*[1], *Ingran Lingam*[1], *Magda Sokolska*[2], *Tatenda Mutshiya*[1], *Alan Bainbridge*[2], *Xavier Golay*[3] *and Nicola J. Robertson*[1]*

[1] *Department of Neonatology, Institute for Women's Health, University College London, London, United Kingdom,* [2] *Medical Physics and Engineering, University College London NHS Foundation Trust, London, United Kingdom,* [3] *Department of Brain Repair and Rehabilitation, Institute of Neurology, University College London, London, United Kingdom*

OPEN ACCESS

Edited by:
Deirdre M. Murray, University College Cork, Ireland

Reviewed by:
Yohan van de Looij, Université de Genève, Switzerland
Diego Iacono, Biomedical Research Institute of New Jersey, United States

***Correspondence:**
Nicola J. Robertson
n.robertson@ucl.ac.uk

Specialty section:
This article was submitted to Pediatric Neurology, a section of the journal Frontiers in Neurology

Received: *21 January 2020*
Accepted: *10 July 2020*
Published: *04 September 2020*

Citation:
Pang R, Martinello KA, Meehan C, Avdic-Belltheus A, Lingam I, Sokolska M, Mutshiya T, Bainbridge A, Golay X and Robertson NJ (2020) Proton Magnetic Resonance Spectroscopy Lactate/N-Acetylaspartate Within 48 h Predicts Cell Death Following Varied Neuroprotective Interventions in a Piglet Model of Hypoxia–Ischemia With and Without Inflammation-Sensitization. Front. Neurol. 11:883. doi: 10.3389/fneur.2020.00883

Despite therapeutic hypothermia, survivors of neonatal encephalopathy have high rates of adverse outcome. Early surrogate outcome measures are needed to speed up the translation of neuroprotection trials. Thalamic lactate (Lac)/N-acetylaspartate (NAA) peak area ratio acquired with proton (^{1}H) magnetic resonance spectroscopy (MRS) accurately predicts 2-year neurodevelopmental outcome. We assessed the relationship between MR biomarkers acquired at 24–48 h following injury with cell death and neuroinflammation in a piglet model following various neuroprotective interventions. Sixty-seven piglets with hypoxia–ischemia, hypoxia alone, or lipopolysaccharide (LPS) sensitization were included, and neuroprotective interventions were therapeutic hypothermia, melatonin, and magnesium. MRS and diffusion-weighted imaging (DWI) were acquired at 24 and 48 h. At 48 h, experiments were terminated, and immunohistochemistry was assessed. There was a correlation between Lac/NAA and overall cell death [terminal deoxynucleotidyl transferase dUTP nick end labeling (TUNEL)] [mean Lac/NAA basal ganglia and thalamus (BGT) voxel $r = 0.722$, white matter (WM) voxel $r = 0.784$, $p < 0.01$] and microglial activation [ionized calcium-binding adapter molecule 1 (Iba1)] (BGT $r = -0.786$, WM $r = -0.632$, $p < 0.01$). Correlation with marker of caspase-dependent apoptosis [cleaved caspase 3 (CC3)] was lower (BGT $r = -0.636$, WM $r = -0.495$, $p < 0.01$). Relation between DWI and TUNEL was less robust (mean diffusivity BGT $r = -0.615$, fractional anisotropy BGT $r = 0.523$).

Overall, Lac/NAA correlated best with cell death and microglial activation. These data align with clinical studies demonstrating Lac/NAA superiority as an outcome predictor in neonatal encephalopathy (NE) and support its use in preclinical and clinical neuroprotection studies.

Keywords: neonatal encephalopathy, magnetic resonance spectroscopy, hypoxia–ischemia, piglet, therapeutic hypothermia, neuroprotection

INTRODUCTION

Neonatal encephalopathy (NE) secondary to intrapartum hypoxia–ischemia is a significant cause of brain injury in term infants affecting 2–3 per 1,000 live births in the UK (1). Therapeutic hypothermia (HT) has reduced mortality and disability in survivors of NE [relative risk (RR) 0.75, 95% CI 0.68–0.83, number needed to treat (NNT) = 7] (2). However, despite treatment, there remains a 24–30% mortality rate and 22–44% risk of moderate to severe disability at 18 months following moderate to severe NE (3, 4). NE has a complex and multifactorial etiology; however, over the last decade, preclinical (5) and clinical (6) studies suggest that coexisting infection and inflammation with hypoxia–ischemia (HI) exacerbate brain injury. A strong association exists between fetal infection/inflammation (e.g., chorioamnionitis, funisitis), perinatal brain damage, and neurodisability (7).

In single (8) and multicenter (9) studies of NE babies who have been cooled, the ^{1}H magnetic resonance spectroscopy (MRS) thalamic lactate (Lac)/N-acetylaspartate (NAA) peak area ratio acquired within 15 days of birth accurately predicts neurodevelopmental outcomes. Refinements in the spectral fitting including threonine (Thr) and N-acetylaspartylglutamate (NAAG) in the fitting function can improve the analysis of the spectrum in the regions close to Lac and NAA, respectively, and better signal to noise at 3 Tesla (3T) have optimized the predictive accuracy of Lac/NAA (8). Using a threshold of 0.39, the sensitivity and specificity of BGT Lac/NAA for 2-year motor outcome was 100% and 97%, cognition 90% and 97% and language 81% and 97%, respectively (8). In the TOBY Xenon early-phase clinical neuroprotection trial, adverse outcomes were correctly identified in 95.65% of cases by basal ganglia and thalamus (BGT) Lac/NAA, whereas prediction of adverse outcome using fractional anisotropy (FA) was 78.79% (10). Using Lac/NAA peak area ratio as a qualified biomarker in the clinical context in a small proof-of-concept neuroprotection trial therefore avoids substantial financial and opportunity costs associated with large randomized controlled trials (RCTs).

Over the last two decades, we have used BGT and white matter (WM) Lac/NAA as one of our primary outcome markers in neuroprotection studies of adjunct therapies with HT in our piglet model (11–15). The piglet model allows for regional assessment of brain immunohistochemistry at 48 h with analyses including quantification of terminal deoxynucleotidyl transferase dUTP nick end labeling (TUNEL)-positive cells, assessment of neuroinflammation [ionized calcium-binding adapter molecule 1 (Iba1) ramification index], and quantification of cleaved caspase 3 (CC3), a marker of caspase-dependent apoptosis.

Given the importance of MRI biomarkers in neonatal clinical neuroprotection trials and the translational pathway from preclinical to clinical RCTs, our aim was to assess: (i) the relationship between MR biomarkers [^{1}H MRS metabolite ratios, mean diffusivity (MD), FA], acquired at 24 and 48 h following injury, and brain cell death and neuroinflammation at 48 h in the piglet following various neuroprotective interventions; (ii) brain immunohistochemistry differences related to the Lac/NAA peak area ratio clinical threshold of 0.39 (this ratio accurately predicts 2-year motor, cognitive, and language outcomes in babies with NE) (8). In this study, we included retrospective data from different injuries (hypoxia–ischemia, hypoxia, inflammation-sensitization) and neuroprotective interventions (HT alone and with magnesium or melatonin) to assess the relation between MR biomarkers and immunohistochemistry in the piglet model.

METHODS

Animal Experiments, Surgical Preparation, and Intensive Care Management

All animal experiments were approved by the UCL Ethics Committee and performed according to UK Home Office Guidelines [Animals (Scientific Procedures) Act, 1986]. The study complies with Animal Research: Reporting of *in vivo* Experiments (ARRIVE) guidelines.

Piglets were anesthetized and surgically prepared as described previously (11, 13, 14, 16, 17). In brief, all piglets were sedated with intramuscular midazolam and anesthetized with inhaled 3–4% v/v isoflurane. A tracheostomy was performed, and piglets were intubated (Smiths Medical, Ashford, Kent, UK) and ventilated (SLE 2000 Infant Ventilator, Surrey UK) for the duration of the experiment. Carotid vascular occluders (OC2A, *in vivo* Metric, Healdsburg, CA, USA) were sited for all studies, except study 3. Umbilical venous and arterial access were obtained (arterial catheter Vygon 2.5Fr, venous catheter—2Fr

Abbreviations: 3T, 3-Tesla; ADC, apparent diffusion coefficient; ANLS, astrocyte neuron lactate shuttle; AUC, area under the curve; BGT, basal ganglia, thalamus; CC3, cleaved caspase 3; Cho, choline; Cr, creatine; DGM, Deep gray matter; DWI, diffusion-weighted imaging; FA, fractional anisotropy; HI, hypoxia–ischemia; HT, therapeutic hypothermia; Iba1, ionized calcium-binding adapter molecule 1; Lac/NAA, lactate/N-acetylaspartate; Lac, lactate; LPS, lipopolysaccharide; MD, mean diffusivity; MRS, magnetic resonance spectroscopy; NAA, N-acetylaspartate; NAAG, N-acetylaspartylglutamate; NAD, nicotinamide adenine dinucleotide; NE, neonatal encephalopathy; RCT, randomized controlled trial; ROI, region of interest; T2W, T2 weighted; Thr, threonine; TUNEL, terminal deoxynucleotidyl transferase dUTP nick end labeling; WM, white matter.

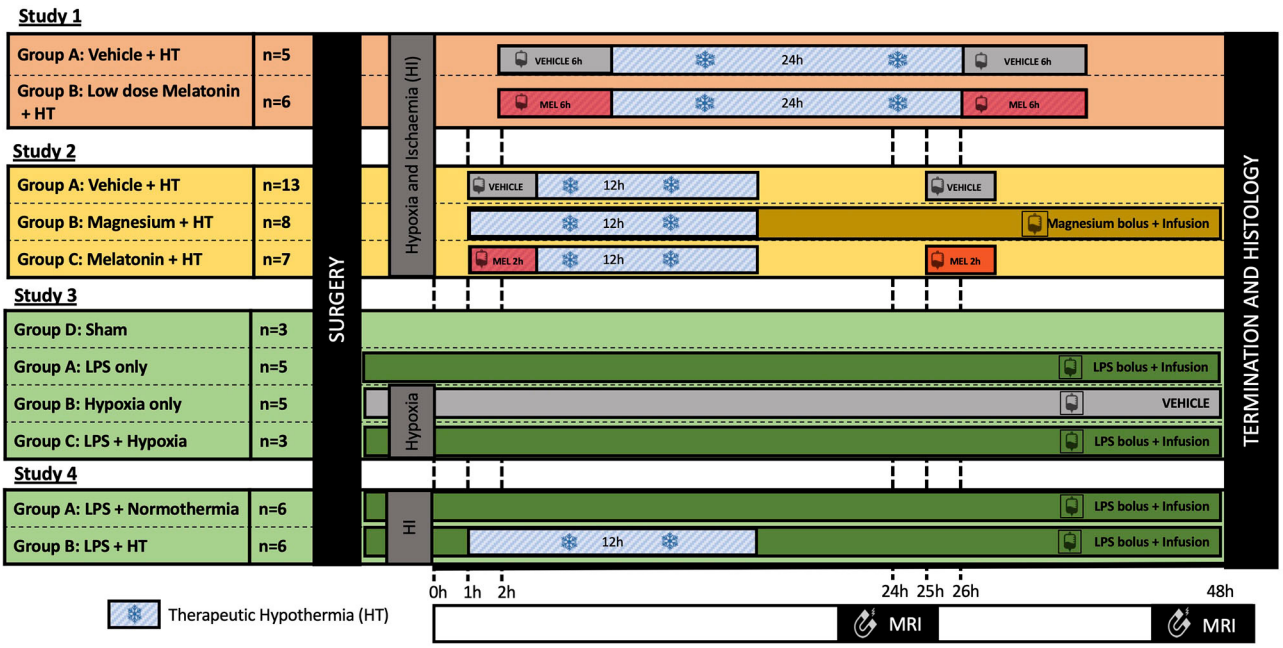

FIGURE 1 | Summary of the experimental protocols. All experiments were 48 h in length; however, cerebral insults and neuroprotective interventions varied between studies. In all studies, 3T–^{1}H magnetic resonance spectroscopy (MRS) was acquired at 24 and 48 h after insult, and immunohistochemistry was assessed at 48 h. Study 1 (11): Piglets were subjected to a transient hypoxia–ischemia (HI) followed by therapeutic hypothermia (HT) for 24 h, started at 2 h after insult. Piglets were randomized to either: (i) vehicle infusion or (ii) melatonin infusion over 6 h at 2 h after HI, repeated at 26 h. Study 2 (13, 17): Piglets were subjected to HI insult followed by cooling for 12 h started 1 h after insult. Piglets were randomized to: (i) vehicle infusion; (ii) magnesium bolus 1 h post insult followed by continuous infusion over 48 h; or (iii) melatonin infused over 2 h at 1 h and 25 h after insult. Study 3 (14): Piglets were randomized to: (i) control (saline bolus and infusion), (ii) lipopolysaccharide (LPS) (bolus followed by a continuous infusion); (iii) hypoxia; or (iv) LPS and hypoxia 4 h after bolus. Study 4: All piglets were subjected to LPS bolus 4 h prior to HI and continuous infusion over 52 h. Animals were then randomized to either normothermia or 12 h HT from 1 to 13 h after insult.

double lumen), and a peripherally inserted central venous catheter (Vygon 2Fr Nutriline) was sited in the proximal forelimb for infusion of intravenous drugs. Piglets were transferred onto a specialized incubator following surgery where continuous vital signs, multichannel electroencephalography (EEG) (Nicolet EEG, Natus), and cerebral near-infrared spectroscopy (NIRS) were monitored. Sedation was maintained with infusion of fentanyl (4 μg/kg/h) and inhaled isoflurane.

Piglets were cared for in accordance with local neonatal intensive care guidelines throughout the experiment. Following insult, maintenance fluid was restricted to 40 ml/kg/day. Ventilation settings were titrated according to arterial blood gas measurements. Mean arterial blood pressure (MABP) was maintained >35 mmHg using infusions of dopamine, dobutamine, noradrenaline, and adrenaline as required. Electrolytes, urea and creatinine, and blood glucose were monitored. All piglets received benzylpenicillin and gentamicin. 10% calcium gluconate (0.5 ml/kg) and salbutamol (4 μg/kg) were used to treat hyperkalemia. Seizures were treated with intravenous phenobarbitone followed by phenytoin if persistent.

Study Selection and Variations in Study Design

This study was a retrospective, secondary analysis of four preclinical neuroprotection piglet studies (11, 13, 14, 17). The study protocols evolved, reflecting optimization and development of study designs over the years, and are shown in **Figure 1**. For full details of the study methodology and results, please refer to publications (11, 13, 14, 17).

All studies lasted 48 h; however, studies varied according to brain injury protocols, duration of HT, and neuroprotective agents used. Primary outcome measures for all studies were identical; MRS was acquired at 24 and 48 h after insult, and immunohistochemistry was assessed at 48 h using the same methodology. Acquisition using the clinical 3T scanner (Philips Achieva) was introduced during study 1 to enhance the translational relevance of our preclinical model. Prior to this, ^{1}H MRS was acquired using a 9.4T MRI scanner. Only piglets with MRS data at 3T and immunohistochemistry data were included in this secondary analysis. Piglets scanned at 9.4T or with no 3T MRS data were excluded.

Brain Injury

Piglets in studies 1 (11) and 2 (13, 17) were subjected to HI. Carotid artery occluders were inflated to induce brain ischemia and the fraction of inspired oxygen (FiO_2) was reduced to 4% and titrated according to response. The HI insult for study 1 was conducted within the bore of a 9.4T MRI. During HI, the ^{31}P MRS β-NTP peak height was continuously monitored, and the FiO_2 was titrated to keep the β-NTP peak height between 30 and 40% of its original height for a period of 12.5 min. The insults for studies 2–4 were conducted outside the MRI. For

these studies, insult duration and FiO_2 titration were determined by MABP (target between 26 and 30 mmHg), duration of flat EEG, arterial blood gas measurements (target lactate between 10 and 12), and NIRS oxidized-cytochrome C levels. Persistent severe hypotension (MABP < 25 mmHg) or bradycardia was an indication to terminate the insult.

Piglets in studies 3 (14) and 4 underwent inflammation-sensitization with *Escherichia coli* liposaccharide (LPS) (Sigma O55:B5) prior to cerebral injury. A bolus of 2 μg/kg LPS followed by an infusion 1 μg/kg/h for the duration of the experiment was given. At 4 h after infusion, piglets in study 3 were subjected to a hypoxia-only insult by reducing FiO_2 to 4%. In study 4, piglets were subjected to an HI insult as described in studies 1 and 2.

Neuroprotective Interventions

All piglets in studies 1 and 2 were cooled to 33.5°C using a servo-controlled water mattress (Tecotherm); however, protocols varied between the studies. In study 1, piglets were cooled from 2 h after HI over a duration of 24 h. Piglets in study 2 were cooled from 1 h after HI for a total duration for 12 h. No piglets in study 3 received HT. In study 4, piglets in the HT treatment arm were cooled for 12 h. All piglets that received HT were rewarmed at a controlled rate of 0.5°C/h to the target temperature of 38°C. Normothermia at 38.5°C was maintained by the water mattress.

Various neuroprotective agents were used in these studies. Piglets in study 1 received either an intravenous melatonin infusion at 2 and 26 h after HI at 5 mg/kg over 6 h or vehicle at the same volume and infusion rate. In study 2, piglets received (i) magnesium as a loading bolus of 180 mg/kg followed by continuous infusion 8 mg/kg/h at 1 h after HI; (ii) melatonin at 18 mg/kg over 2 h at 1 h and 25 h after HI; or (iii) vehicle at the same volume and rate. No additional agents were used in studies 3 or 4.

Magnetic Resonance Imaging

Piglets were transferred to the 3T MRI scanner at 24 and 48 h post insult. Imaging was performed with similar protocols as those used in NE babies on the same 3T scanner (8). ^{1}H MRS was acquired with 8 × 8 matrix and 8 mm^3 × 8 mm^3 × 10 mm^3 voxels with TR/TE 2,000 ms/288 ms. The spectral width was 2 kHz with 2,048 points. MRS data for the BGT (left thalamus) and WM voxels (left subcortical WM at the level of centrum semiovale level) were selected (**Figure 2A**) and processed using Tarquin with threonine included in the basis set. Lipids and macromolecules were excluded. The ratio of Lac/NAA was calculated from the amplitude of the fitted components (Lac+Thr/NAA+NAAG). Other metabolite peaks obtained include choline (Cho), and creatine (Cr) to give Lac/Cho, Lac/Cr, NAA/Cho, NAA/Cr, and Cho/Cr ratios.

Diffusion-weighted imaging (DWI) was acquired using a protocol similar to clinical studies (**Figure 2B**) (8). DWI was acquired with diffusion sensitizing gradient in 16 directions, with b-value of 750 s/mm^2, echo planar imaging (EPI) readout: TR = 9,000 ms, TE = 61 ms, slice thickness = 2 mm, in-plane resolution 2.0 mm^2 × 2.0 mm^2, slice thickness = 2 mm, 20 slices. Postprocessing of the data was carried out using FSL brain imaging software library (8). Brain tissue was manually segmented using ITK-SNAP (18), and DWI volumes were corrected for eddy current-induced distortions with FSL-EDDY tool. Deep gray matter (DGM) and WM regions were identified automatically by atlas (19) labels propagation. First, high-resolution structural template scans were co-registered to each piglet structural scan that was resampled to isotropic voxel size. DWI data and structural scans were then co-registered, and a combination of transformations was used to propagate and down sample labels using nearest neighbor interpolation. Finally, basal ganglia nuclei and thalami were combined into a single DGM region, and MD and FA were calculated within DGM, internal capsule, and whole-brain masks.

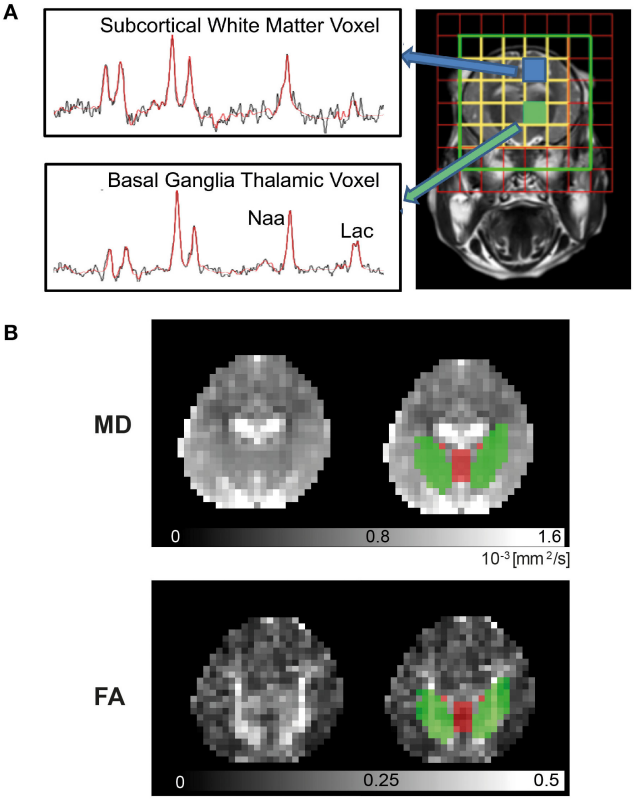

FIGURE 2 | 3T Magnetic Resonance Imaging. Piglets were scanned at 24 and 48 h in the Philips Achieva clinical magnet. ^{1}H- Magnetic Resonance Spectroscopy (MRS) **(A)** was acquired using chemical shift imaging (CSI) with 8 × 8 matrix and 8 × 8 × 10 mm^3 voxels, TR/TE was 2,000 ms/288 ms. The spectral width was 2 kHz with 2,048 points. Voxels selected were over the left thalamus [basal ganglia, thalamus (BGT)] and left subcortical white matter (WM) at the level of the centrum semiovale. Spectra were processed with Tarquin included in basis set, and the ratio of lactate (Lac)/N-acetylaspartate (NAA) was calculated from the amplitude of the fitted components (Lac+Thr/NAA+NAAG). For diffusion-weighted imaging (DWI) **(B)**, regional of interest (ROI) for mean diffusivity (MD) and fractional anisotropy (FA) in the deep gray matter (DGM) (red) and WM (green) were automatically identified by atlas label propagation. The internal capsule was selected to represent WM, and the caudate, putamen, globus pallidus, thalamus, and hypothalamus were used for DGM.

Histology

Brain histology and immunohistochemistry samples were prepared as previously described (11, 12). In brief, experiments were terminated 48 h post HI, and the piglets were euthanized with pentobarbital. Following this, piglets underwent cold

phosphate buffered saline (PBS) cardiac perfusion and tissue fixation with 4% paraformaldehyde (PFA). The brain was dissected and stored in 2% PFA. Then, 5-mm coronal slices were made from the right hemisphere, embedded in paraffin, and cut into 8-μm sections. Two slices were selected for use for histology analysis: R0 at the level of the optic chiasm and R1 at the level of the hippocampus. These were dehydrated in xylene and rehydrated in graded ethanol solution (100–70%) prior to immunohistochemistry to stain cell death (TUNEL), microglia activation (Iba1), and apoptosis (CC3).

TUNEL was used to assess cell death. As previously described (12), slices were treated with 3% hydrogen peroxide followed by predigestion with protease K (Promega, Southampton, UK) and finally incubated in TUNEL solution for 2 h (Roche, Burgess Hill, UK). To visualize the biotin residues, slices were incubated in avidin-biotinylated horseradish peroxidase complex (ABC, Vector Laboratories) followed by diaminobenzidine/H_2O_2 (Sigma) with $CoCl_2$ and $NiCl_2$. A hematoxylin–eosin counterstain was applied, and slices were mounted on coverslips with dibutylphthalate polystyrene xylene (DPX).

For each piglet, eight regions of the brain were examined. In seven regions, TUNEL-positive nuclei were counted (**Figure S1**) from three fields in each of the R0 and R1 slices at 40× magnification. The hippocampus was present in the R1 section only. The counts were converted into cell counts per mm^2.

To assess microglia activation, slides were prepared as previously described by Martinello et al. (14) and Ito et al. (20). Brain sections were pretreated in Ventana CC1 (950-124) and incubated in primary rabbit antibody anti-Iba1 polyclonal antibody (1:250) (WAKO 019-19741) for 4 h followed by incubation in secondary swine anti-rabbit immunoglobulin (DAKO E0343) for a further 1 h. Slices were mounted with Vectrashield + 4',6-diamidino-2-phenylindole (DAPI) aqueous mounting media. The Iba1-positive microglia cell bodies and branch density were calculated using a 0.049 mm × 0.049 mm square grid under 40× magnification. The number of cell bodies was counted within the grid (C), and the average number of branches crossing the three horizontal and vertical grid lines (B) was counted to give a microglial ramification index (B^2/C).

For CC3 immunohistochemistry, brain sections were pretreated as for Iba1 staining, incubated in rabbit anti-CC3 (1:100) (Cell Signaling 9661L) for 32 min followed by swine anti-rabbit immunoglobulin for 44 min. Sections were mounted on Vectrashield + DAPI as described above. CC3 cells were counted at 20× magnification in three fields per brain region and converted to counts per mm^2.

Data and Statistical Analysis

Data analysis was carried out using SPSS Statistics 24 (IBM). The overall whole-brain TUNEL-positive cell counts, CC3-positive cell counts, and Iba1 ramification index were deduced from the sum of the average counts in eight regions of the brain (**Figure S1**).

The 24 and 48 h MRS data were collected for each of the BGT and WM regions and separately correlated with average whole-brain TUNEL, CC3, and Iba1 counts. In addition, the overall mean MRS FA and MD values were deduced from the 24 and 48 h scans and compared with the three immunohistochemistry markers.

The MRS, DWI, and histology count values were $\log_{10}$ transformed to normalize the distribution. The correlation was assessed using Pearson's rank coefficient, and scatter plots were created with GraphPad Prism v8 to illustrate the trend. *P*-values were calculated with two-tailed test to indicate statistical significance. As we compared multiple independent tests, the threshold for statistical significance was corrected to preserve a type 1 error rate (where $p < 0.05$ is significant) using Bonferonni correction. A $p < 0.01$ denotes statistical significance. Logistic regression modeling in infants with NE identified Lac/NAA of 0.39 as the optimal cutoff value for sensitivity and specificity to predict adverse neurodevelopmental outcomes at 18 months (8). Using this clinical Lac/NAA value, the mean $\log_{10}$ TUNEL, Iba1, and CC3 counts were deduced, and significance was compared using independent *t*-test.

RESULTS

Sixty-seven male large white piglets were recruited from four neuroprotection studies including 11 (16.4%) from Robertson et al. (11); 28 (41.8%) from Robertson et al. (17), and Lingam et al. (13); and 16 (23.9%) from Martinello et al. (14). Twelve piglets were included from an unpublished study. Twenty-seven piglets were excluded as no 3T MRS data were available. There was a larger proportion of piglets excluded from study 1 (n = 17/27, 60.7%) as scans at 3T were introduced later in this study. MRS data at both the 24 and 48 h MRI scans were complete for 54 piglets (80.6%). The remaining 13 piglets had either 24 h scan (n = 8) or 48 h scan ($n = 5$) available. Reasons for incomplete data include piglet death prior to the 48 h scan ($n = 4$), 3T scanner not available due to technical issues ($n = 3$), or issues with the spectral fit processing ($n = 6$).

Figure 1 summarizes the treatment regimens across the four studies. In total, 59 of 67 (88.1%) piglets were subjected to cerebral injury. The remaining eight animals were either naive ($n = 3$, 4.5%) or LPS inflammation sensitized without cerebral injury ($n = 5$, 7.5%). Cerebral injury included: HI (39/67, 58.2%), LPS inflammation sensitized hypoxic injury (8/67, 11.9%), and LPS inflammation sensitized HI injury (12/67, 17.9%).

Neuroprotective interventions also varied with 45 of 67 (67.2%) piglets receiving HT for either 12 h (34/67, 50.7%) or 24 h (n = 11/67, 16.4%). Melatonin was given to 11 (16.4%) animals, and magnesium was given to eight (11.9%) piglets.

Lactate/N-Acetylaspartate to Terminal Deoxynucleotidyl Transferase dUTP Nick End Labeling

Mean Lac/NAA and TUNEL-positive cell counts of the whole brain correlated in the BGT ($r = 0.722$, $p < 0.001$) and WM voxel ($r = 0.784$, $p < 0.001$) (**Figures 3A,B**). The positive correlation was present at both 24 and 48 h (**Table 1**).

Lac/NAA ≥0.39 was associated with significantly higher TUNEL-positive cells in the whole brain across both voxels and both the 24 and 48 h scans (**Table 2**, **Figures 3G,J**) ($p <$ 0.001) [mean BGT Lac/NAA ≥0.39, mean TUNEL count = 103

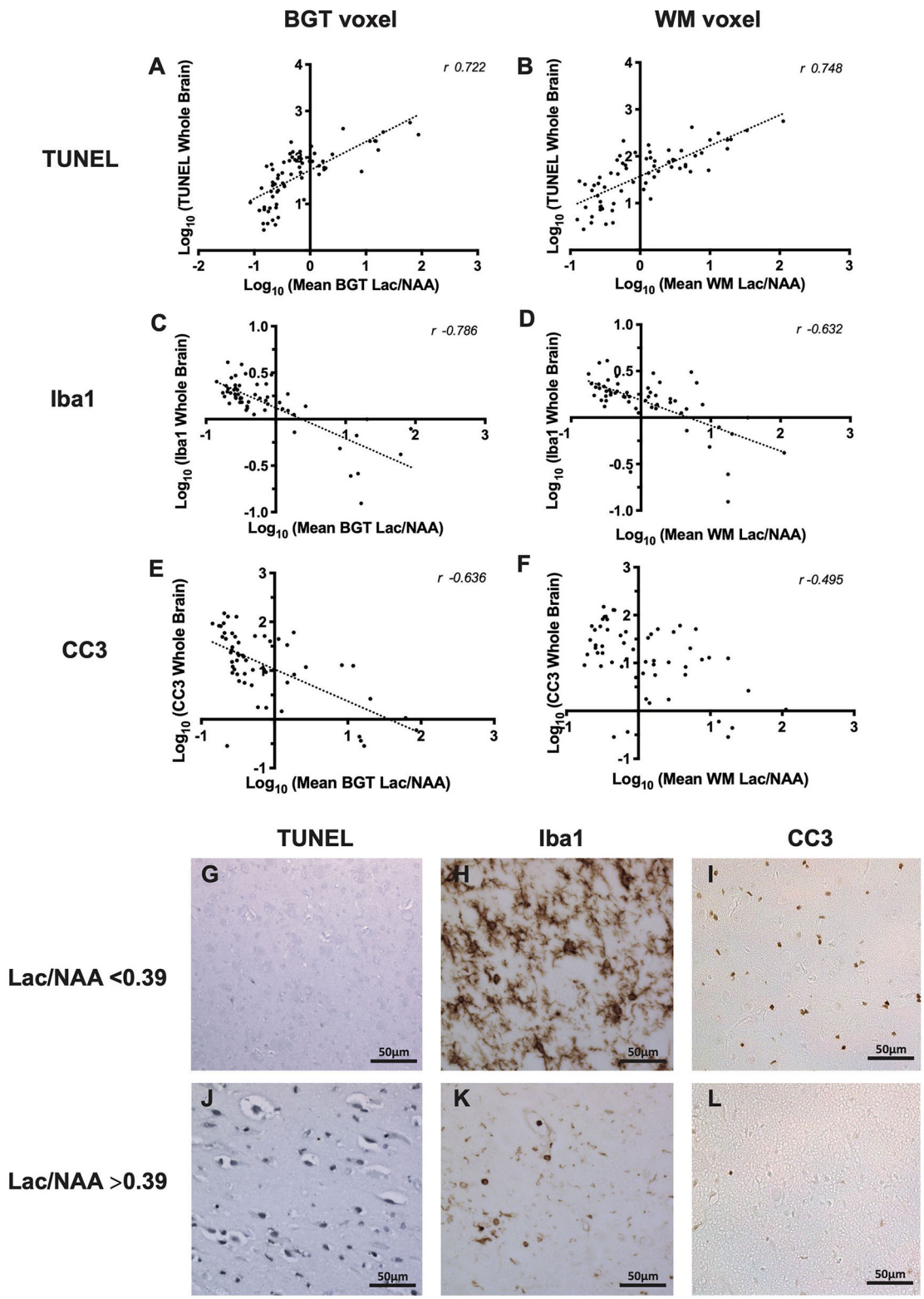

FIGURE 3 | The relationship between thalamic [basal ganglia, thalamus (BGT)] and white matter (WM) ^{1}H magnetic resonance spectroscopy (MRS) lactate (Lac)/N-acetylaspartate (NAA) and whole-brain cell death [terminal deoxynucleotidyl transferase dUTP nick end labeling (TUNEL)] **(A,B)**, microglia activation [ionized calcium-binding adapter molecule 1 (Iba1) ramification index] **(C,D)**, and cleaved caspase 3 (CC3) **(E,F)**. All data in the scatterplots were $\log_{10}$ transformed, and the Pearson's correlation coefficients (*r*-values) are illustrated. All values $p < 0.001$. Representative micrographs showing TUNEL, Iba1, and CC3 immunohistochemistry stains in piglets with Lac/NAA <0.39 **(G–I)** and Lac/NAA ≥0.39 **(J–L)** are shown.

TABLE 1 | Pearson's correlation coefficient comparing magnetic resonance spectroscopy (MRS) lactate (Lac)/N-acetylaspartate (NAA), diffusion-weighted imaging (DWI) mean diffusivity and fractional anisotropy at 24 and 48 h and the mean of the two time points with whole-brain terminal deoxynucleotidyl transferase dUTP nick end labeling (TUNEL)-positive count.

	MRS Lac/NAA		DWI Mean Diffusivity		DWI Fractional Anisotropy	
	r	*p*-value	*r*	*p*-value	*r*	*p*-value
24 h BGT region	0.709	<0.001	−0.488	<0.001	0.424	<0.001
48 h BGT region	0.661	<0.001	−0.635	<0.001	0.240	0.065
Mean BGT region	0.722	<0.001	−0.615	<0.001	0.523	<0.001
24 h WM region	0.669	<0.001	−0.511	<0.001	0.452	<0.001
48 h WM region	0.729	<0.001	−0.633	<0.001	0.495	<0.001
Mean WM region	0.748	<0.001	−0.635	<0.001	0.342	0.005

All values were log_{10} transformed prior to correlation analysis. Correlation is significant if $p < 0.01$ (corrected with Bonferroni correction where $p < 0.05$ is considered significant). BGT, basal ganglia and thalamus; WM, white matter.

TABLE 2 | Histology cell counts using a clinical threshold for lactate (Lac)/N-acetylaspartate (NAA) of 0.39.

	Whole-Brain TUNEL Count		*p*-value	Whole-Brain Iba1 Ramification Index		*p*-value	Whole-Brain CC3		*p*-value
	Lac/NAA <0.39	Lac/NAA ≥0.39		Lac/NAA <0.39	Lac/NAA ≥0.39		Lac/NAA <0.39	Lac/NAA ≥0.39	
BGT voxel at 24 h	18.2 (SD 2.96)	109 (SD 2.03)	<0.001	1.96 (SD 1.30)	0.88 (SD 2.08)	<0.001	25.8 (SD 4.94)	4.89 (SD 4.94)	<0.001
BGT voxel at 48 h	15.1 (SD 2.84)	83.4 (SD 2.42)	<0.001	2.05 (SD 1.29)	1.05 (SD 2.05)	<0.001	27.9 (SD 3.75)	6.78 (SD 4.83)	0.001
Mean BGT voxel	15.2 (SD 2.56)	103 (SD 2.12)	<0.001	1.94 (SD 1.29)	0.96 (SD 2.13)	<0.001	25.0 (SD 3.47)	5.82 (SD 5.19)	0.001
WM voxel at 24 h	15.9 (SD 3.26)	84.7 (SD 2.27)	<0.001	1.87 (SD 1.61)	1.11 (SD 1.96)	0.004	24.2 (SD 4.76)	7.71 (SD 4.39)	0.008
WM voxel at 48 h	12.2 (SD 2.61)	58.3 (SD 3.15)	<0.001	2.09 (SD 1.36)	1.29 (SD 1.96)	0.003	27.4 (SD 2.23)	10.7 (SD 5.90)	0.076
Mean WM voxel	11.3 (SD 2.27)	71.6 (SD 2.75)	<0.001	2.04 (SD 1.29)	1.17 (SD 1.99)	0.003	33.0 (SD 2.37)	8.08 (SD 5.41)	0.001

Values shown are the geometric mean and standard deviation (SD). Using this threshold, we showed significant differences in cell counts for cell death [terminal deoxynucleotidyl transferase dUTP nick end labeling (TUNEL)] and microglial activation [ionized calcium-binding adapter molecule 1 (Iba1) ramification index] in the piglets. Correlation is significant if $p < 0.01$ (corrected with Bonferroni correction where $p < 0.05$ is considered significant). BGT, basal ganglia and thalamus; WM, white matter.

cells/mm^2 (SD 2.12); mean BGT Lac/NAA <0.39, mean TUNEL count = 15.2 cells/mm^2 (SD 2.56); $p < 0.001$].

Lactate/N-Acetylaspartate to Ionized Calcium-Binding Adapter Molecule 1

Iba1 ramification index was used to assess microglial activation. Activated microglia become ameboid with fewer processes, represented by a lower ramification index. There was a strong negative correlation between mean Lac/NAA and whole-brain Iba1 ramification index (**Figures 3C,D**). The negative correlation was strongest with the mean BGT voxel ($r = -0.786$, $p < 0.001$) but also present in the mean WM voxel ($r = -0.632$, $p < 0.001$).

Using a Lac/NAA threshold of 0.39, we noted significant differences in the Iba1 ramification index between piglets at all time points and voxels ($p < 0.001$) (**Table 2**, **Figures 3H,K**). Lac/NAA ≥0.39 was associated with lower Iba1 ramification (mean BGT Lac/NAA ≥0.39, Iba1 ramification index 0.96 vs. 1.94 with Lac/NAA <0.39) ($p < 0.001$).

Lactate/N-Acetylaspartate to Cleaved Caspase 3

The correlation between Lac/NAA and CC3 was negative in the BGT voxel ($r = -0.636$; $p < 0.001$) but was weaker in the WM voxel ($r = -0.495$; $p < 0.001$) (**Figures 3E,F**).

Lac/NAA ≥0.39 was associated with lower CC3 counts at 24 h (CC3 count 4.89 vs. 25.8 cells/mm^2, $p < 0.001$) and 48 h scans (CC3 count 6.78 vs. 27.9 cells/mm^2, $p < 0.01$) in the BGT voxel. The CC3 count was also significantly lower with Lac/NAA ≥0.39 at 24 h in the WM voxel (CC3 count 7.71 vs. 25.0, $p < 0.01$) (**Table 2**, **Figures 3I,L**).

Magnetic Resonance Spectroscopy Metabolite Peak Ratios to Terminal Deoxynucleotidyl Transferase dUTP Nick End Labeling

Pearson's correlation coefficients were deduced to compare other proton MRS metabolite ratios with whole-brain TUNEL count (**Table 3**). We observed strong positive correlations between the total whole-brain TUNEL count and mean BGT Lac/Cho ($r = 0.765$, $p < 0.001$) and BGT Lac/Cr ($r = 0.765$, $p < 0.001$). There was a lesser correlation in the corresponding WM voxels (WM Lac/Cho $r = 0.701$, $p < 0.001$; Lac/Cr 0.671, $p < 0.001$). There was a weak correlation between BGT NAA/Cho ($r = -0.530$, $p < 0.01$) and BGT NAA/Cr ($r = -0.565$, $p < 0.001$) with TUNEL. There was no correlation between TUNEL and Cho/Cr (BGT voxel, $r = 0.019$, $p = 0.88$; WM voxel, $r = -0.051$, $p = 0.68$).

TABLE 3 | Pearson's correlation coefficient comparing magnetic resonance spectroscopy (MRS) metabolite ratios with whole-brain terminal deoxynucleotidyl transferase dUTP nick end labeling.

		r	*p*-value
Mean Lac/NAA	BGT	0.722	<0.001
	WM	0.748	<0.001
Mean Lac/Cho	BGT	0.765	<0.001
	WM	0.701	<0.001
Mean Lac/Cr	BGT	0.766	<0.001
	WM	0.671	<0.001
Mean NAA/Cho	BGT	−0.530	<0.001
	WM	−0.565	<0.001
Mean NAA/Cr	BGT	−0.565	<0.001
	WM	−0.624	<0.001
Mean Cho/Cr	BGT	0.019	0.877
	WM	−0.051	0.684

Correlation is significant if $p < 0.01$ (corrected with Bonferroni correction where $p < 0.05$ is considered significant). BGT, basal ganglia and thalamus; Cho, choline; Cr, creatine; Lac, lactate; NAA, N-acetylaspartate; WM, white matter.

When compared with other metabolic ratios Lac/NAA was most consistent in yielding similarly strong correlation coefficient values in the BGT and WM voxels.

Diffusion-Weighted Imaging to Terminal Deoxynucleotidyl Transferase dUTP Nick End Labeling

The correlation between DWI MD and TUNEL was negative (mean DGM MD to TUNEL $r = 0.615$, $p < 0.001$; mean WM MD to TUNEL $r = -0.635$, $p < 0.001$) as illustrated in **Figures 4A**,**B**; however, the correlation was not as a strong as between Lac/NAA and TUNEL-positive cells (**Table 3**). The correlation between FA and TUNEL was weak at 24 and 48 h (mean DGM $r = 0.523$, $p < 0.001$; mean WM $r = 0.342$, $p < 0.01$) (**Figures 4C,D**; **Table 1**). Representative T2-weighted images (T2W), MD and FA maps are shown in **Figures 4E–J**.

DISCUSSION

^{1}H MRS Lac/NAA peak area ratio correlated with overall TUNEL-positive cell death and microglial activation in a piglet model of term perinatal brain injury. Compared to other MRS metabolite ratios and DWI, Lac/NAA demonstrated the best correlation to TUNEL-positive cell death at 24 and 48 h. This concurs with studies in cooled infants with NE where BGT Lac/NAA peak area ratio has a high level of accuracy for outcome prediction compared to other MR methods (8, 9). Using the same Lac/NAA peak area ratio threshold of 0.39 identified in clinical settings (8), we demonstrate significant differences in TUNEL-positive cells and microglial activation. These data support the translational relevance of Lac/NAA in preclinical and clinical neuroprotection studies. In our piglet model, we observed strong correlations between BGT Lac/Cr and Lac/Cho and whole-brain TUNEL; however, these were not consistent in the WM MRS voxel (21–23).

The combined increased lactate and reduced NAA on MRS (translating to a high Lac/NAA peak area ratio) suggest brain mitochondrial impairment and impaired oxidative metabolism during "secondary energy failure." It is possible that this ongoing injury may be amenable to late therapies and thus is an important measure to direct therapies. Woo et al. (24) previously demonstrated a correlation between MRS lactate and NAA with TUNEL-positive cells in a rat model. In this normothermic, middle cerebral artery occlusion model, Lac/Cr increased immediately after reperfusion, whereas NAA/Cr decreased 9 h after injury. There was a strong correlation between Lac/Cr and NAA/Cr at 24 h, and both these metabolite ratios correlated with TUNEL in the basal ganglia. Interestingly, Lac/Cr did not correlate with brain infarct volume at 4 weeks, which they argued was due to using a single voxel that may not reflect whole-brain injury. In our study, we show that Lac/NAA in both the deep gray matter and WM correlates with brain cell death across eight brain regions. Our data concur with those from a lamb model of birth asphyxia involving umbilical cord occlusion; there was a strong correlation between TUNEL in the thalamus and deep gray matter and Lac/NAA at 72 h (25). Our study goes further as we investigated relationships between both TUNEL cell death and neuroinflammation in a variety of perinatal injuries and neuroprotective interventions.

Lac/NAA peak ratio in our piglet studies represents more precisely Lac+threonine/total NAA. Mitra et al. (8) describes the optimization of metabolite fitting with the inclusion of threonine in the spectra. Threonine is an amino acid present in the brain, and the resonance of its methyl groups overlaps with that of lactate on the spectra at 1.3 ppm. The addition of threonine in the spectra fit is important in the accurate quantification of lactate (26).

The source and exact mechanism of raised cerebral lactate remain unknown. Both neurons and astrocytes produce lactate in hypoxic conditions *in vitro* (27). Lactate is a product of anaerobic respiration, produced by lactate dehydrogenase from pyruvate regenerating NAD+ for glycolysis. In traumatic brain injury (TBI) models (28, 29), it is thought that lactate reflects the redox state of NADH/NAD+. NADH is a product of glycolysis and the Krebs cycle, which is oxidized in the electron transport chain of the mitochondria to build a proton gradient for ATP production. Following HI, mitochondrial failure and disruption of the electron transport chain lead to the buildup of NADH and reduction in ATP levels. As a result, the equilibrium may shift toward lactate and NAD+ production to rebalance the intracellular NADH/NAD+ ratio. Pellerin and Magistretti (30) proposed the astrocyte to neuron lactate shuttle (ANLS) model whereby lactate, generated by astrocytes through their high glycolytic metabolism capacity, is shuttled to neurons *via* monocarboxylate transporters (MCTs) and metabolized in neurons to pyruvate as an alternative fuel to glucose. In a rat study of severe traumatic brain injury, uncoupling of the ANLS was associated with disruption in the neuronal uptake of lactate (31), thereby contributing to the rise in lactate. This suggests that where neurons are too damaged to utilize the lactate produced

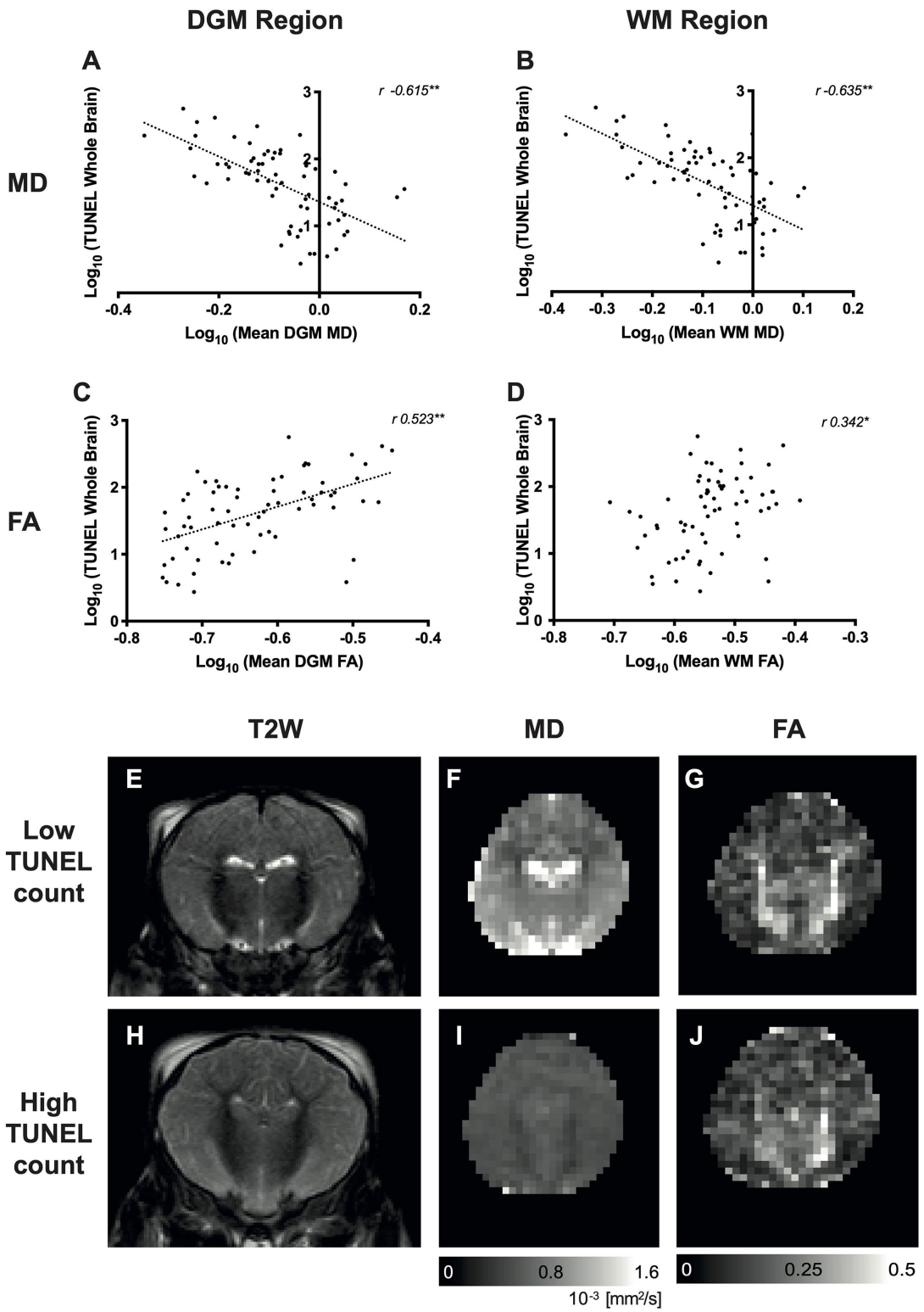

FIGURE 4 | Relationship between diffusion-weighted imaging (DWI) and whole-brain cell death [terminal deoxynucleotidyl transferase dUTP nick end labeling (TUNEL)-positive cells]. Scatterplots showing the correlation between whole-brain TUNEL and average mean diffusivity (MD) **(A,B)** and fractional anisotropy (FA) **(C,D)** localized in the deep gray matter (DGM), white matter (WM) regions. Data were $\log_{10}$ transformed, and the Pearson's correlation coefficients (*r*-values) are illustrated. $^{*}p < 0.01$, $^{**}p < 0.001$. Representative T2-weighted images (T2W), MD and FA maps are shown for a piglet with low TUNEL-positive counts (**E–G**, respectively) and high TUNEL-positive counts **(H–J)**.

by astrocytes, i.e., uncoupling of neuronal and glial metabolism, high extracellular levels of lactate would accumulate, explaining the association between high lactate and poor outcome (29). Other proposed mechanisms of elevated lactate include increased phagocytes (which exhibit increased anaerobic activity), gliosis, altered Na^+/H^+ buffer system (32, 33), and influx of lactate from other injured tissues (34).

There is increasing interest in the role of lactate as a neuroprotective agent. In adults with traumatic brain injury, administration of ^{13}C-labeled lactate *via* the microdialysis catheter and simultaneous collection of the microdialysates, with ^{13}C NMR analysis, revealed ^{13}C labeling in glutamine, consistent with lactate metabolism in the TCA cycle (31, 35). Interestingly, Roumes et al. (36) recently demonstrated the neuroprotective effect of exogenous lactate administration in a neonatal HI rat model. Rice-Vannucci P7 rats that received intraperitoneal injection of lactate following unilateral carotid ligation exhibited a significant reduction in the volume of high-signal intensity brain lesions on DWI and reduced severity of cytotoxic edema as demonstrated by higher apparent diffusion coefficient (ADC) values compared to animals that received 0.9% sodium chloride. Interestingly, rats with HI injury that received three daily injections of lactate performed as well as sham animals without brain injury in sensorimotor and memory neurobehavioral tests. It was proposed that the uptake of lactate by astrocytes, transported *via* the ANLS to neurons, provided an alternative source of energy, thereby sparing the limited glucose for use in the pentose phosphate pathway for glutathione production, a potent reactive oxygen species (ROS) scavenger. Lactate dehydrogenase inhibition using oxamate negated the neuroprotective effects of lactate, demonstrating a role of lactate in neuronal energy metabolism and a link to its neuroprotective properties. A reduction in ROS production was also observed in animals treated with lactate, which was lost when co-administrated with oxamate. We did not perform co-localization immunohistochemistry in all our studies; however, in study 1 (11), co-labeling with TUNEL and glial fibrillary acidic protein (GFAP) in the sensorimotor cortex demonstrated that the majority of TUNEL-positive cells did not co-localize with GFAP, suggesting that the dying cells were not astrocytes. The increased brain lactate that we observe in the most damaged brains after HI may thus reflect astrocytic activity to provide lactate for neuronal needs and an uncoupling of the ANLS.

NAA is a metabolite produced by aspartate N-acetyl transferase and found in neurons. NAA is transported from neurons to oligodendrocytes where it is metabolized into aspartate and acetate and used for energy production and myelin synthesis, respectively (37). NAA has been described as a surrogate marker of neuronal density, integrity, and metabolic activity (38) and of neuronal viability (39). Reduction in absolute concentration of NAA (9) and relative peak ratio of NAA (40), measured with MRS, alone predicts poor neurodevelopmental outcomes in babies with NE (23, 40). Lally et al. (9) reported the predictive accuracy of absolute [NAA] for 2-year cognitive, language, and motor outcomes (AUC 0.99), although Lac/NAA peak area ratio was also highly predictive (AUC 0.94). In our current study, the correlation between NAA/Cho and NAA/Cr with TUNEL was negative but weak compared to ratios that included lactate; this is supported by clinical studies showing NAA/Cho and NAA/Cr are less predictive in neurodevelopmental outcomes compared to Lac/NAA (21–23), although this may be due to inconsistencies in Cho and Cr measurement (39, 40).

We noted a negative correlation between DWI MD and TUNEL-positive cells in the brain. In babies with NE, MD pseudonormalizes at around 7 days in non-cooled infants or 10 days in infants who received HT (41). Our findings in our preclinical model and in babies with NE concur with the experience in a comparative stroke study, where MRS has been shown to better predict outcomes compared with MD. In this study, recovery to normal values of ADC occurred despite the subsequent infarction of tissue, whereas NAA levels continued to show a decline in the same area, thus reflecting tissue injury more accurately (42). Nevertheless, in clinical studies of NE, lower DWI-MD is associated with adverse neurodevelopmental outcomes (41, 43). FA may have more utility in the prediction of outcome as pseudonormalization does not occur; however, we showed poor correlation with TUNEL-positive cell death, which concurs with results from the TOBY Xe neuroprotection study in babies, where FA added little extra to Lac/NAA in accurately predicting neurodevelopmental outcome (10).

In our experience, although highest levels of Lac are seen in the first few days after birth, brain Lac persists for months in babies with adverse outcome after NE; this persisting brain Lac is associated with abnormal MRI and brain alkalosis (32, 44). In our study, piglets were scanned at 24–48 h, which is earlier than in clinical studies of NE [mean age 8.4 days (9) and 6 days (40), respectively]. Therefore, in our preclinical studies, the Lac component in Lac/NAA may have more influence on prediction than NAA in the early post HI period. Wu et al. (34) demonstrated significantly higher cerebral Lac levels early after HI in infants with moderate to severe encephalopathy, which progressively reduced over several days. It is likely that, in the early phase after injury, Lac levels drive the predictive accuracy, whereas in the later phases, the reduction in NAA drives the predictive accuracy (NAA reduction occurs more gradually than the acute Lac rise) (32). A further advantage of combining Lac/NAA peak area ratio is that they depend on both metabolite T2 relaxation times and concentrations, both of which are pathologically modulated, and hence injury severity prediction is improved (39).

Microglia are one of the first inflammatory cells to be activated following HI (45). We used Iba1 ramification index to quantify the morphology of the microglia. At rest, microglia are highly ramified cells with multiple processes sensing the environment (46). Once activated, microglia exhibit a larger body and fewer processes, measured histologically by a reduction in the ramification index. We demonstrated a strong correlation between the degree of microglial activation (Iba1 ramification index) and Lac/NAA, particularly in the BGT, supporting Lac/NAA as a biomarker for neuroinflammation. The role of microglia in secondary energy failure includes cytokine release, metalloproteinase production, breakdown of the blood–brain barrier, leukocyte infiltration, and ultimately further

brain injury (46). We have previously shown that piglets with LPS sensitization 4 h prior to hypoxia resulted in an increase in mortality and overall brain cell death (TUNEL-positive cells), particularly in the internal capsule, periventricular WM, and sensorimotor cortex (14). In addition, microglial activation can persist for many years after insult, and it has been proposed that this pathological activation leads to altered neurogenesis and synaptogenesis (47) and persisting brain Lac.

We observed a poor correlation between Lac/NAA and CC3, and this relationship was unexpectedly negative. This finding concurs with our previous neuroprotection studies where we see little relation between CC3 and other markers of injury severity, particularly TUNEL-positive cells (11). The scatterplots indicate several outliers and a non-linear relationship. The reason for this disconnect between CC3 and brain injury markers is likely to be related to several factors including: (i) cell death occurring by processes independent of caspase, such as necrosis, necroptosis, and autophagy; (ii) sexually dimorphic cell death pathways; as our piglets included only males (in whom cell death occurs through caspase-independent routes such as poly(ADP-ribose) polymerase (PARP)-dependent cell death pathways), CC3 will be a poor marker of cell death (48); (iii) LPS can cause an increase in CC3 without resulting in cell death (49, 50), reflecting the alternative non-apoptotic functions of CC3 (51); (iv) most piglets in this study were treated with HT, which inhibits caspase 3 activation (52).

There are limitations to this study. These data were retrospective and obtained from different studies with differing insults and neuroprotective interventions. However, this is also a strength of the study as the strong correlation of Lac/NAA to TUNEL-positive cells supports the validity of this biomarker across perinatal brain injury which is frequently multifactorial and heterogeneous in nature. In this study, some animals were cooled for 12 h, rather than 24 h (17). This was justified as we develop the model to reflect the clinical situation where cooling is partially effective as in babies with NE; furthermore, the efficacy of HT over 12 h cooling has previously been demonstrated (53). Studies lasted only 48 h after HI, and as mentioned, this early phase will reflect higher Lac levels. In addition, according to the resolution of the DWI derived parameter maps (MD and FA), partial volume effects that could bias our result could not be excluded.

In conclusion, we describe a strong correlation between MRS Lac/NAA and TUNEL-positive cells and microglial activation across WM and gray matter in male piglets after a range of perinatal insults and neuroprotective interventions. These preclinical data concur with clinical studies that have demonstrated the utility of BGT Lac/NAA as a surrogate marker that best predicts outcome in NE and can be used to expedite early-phase clinical neuroprotection trials in NE.

DATA AVAILABILITY STATEMENT

The datasets generated for this study are available on request to the corresponding author.

ETHICS STATEMENT

The animal study was reviewed and approved by UCL Ethics Committee.

AUTHOR CONTRIBUTIONS

RP organized and analyzed the data and drafted the manuscript with the help of KM. KM, AA-B, CM, IL, and TM undertook the experiments. CM undertook microscopy and cell quantification and organized the histology results. MS and AB scanned the piglets and collected MRS and DWI data. XG assisted with MR physics aspects of the study and reviewed the manuscript. NR obtained funding for the studies, designed the studies, and reviewed the manuscript. All authors reviewed the manuscript and approved the final version as submitted and agreed to be accountable for all aspects of the work.

FUNDING

These studies were funded by the Medical Research Council MR/M006743/1, Chiesi Pharmaceuticals (research grant), and Action Medical Research for Children (GN2295).

ACKNOWLEDGMENTS

We thank Debbie Kraus for statistical support and Mariya Hristova for her assistance with histology preparation and fluorescent microscopy. This work was undertaken at University College London Hospitals/University College London, which received a proportion of funding from the UK Department of Health's National Institute for Health Research Biomedical Research Centres funding scheme.

SUPPLEMENTARY MATERIAL

The Supplementary Material for this article can be found online at: https://www.frontiersin.org/articles/10.3389/fneur.2020.00883/full#supplementary-material

REFERENCES

1. Gale C, Statnikov Y, Jawad S, Uthaya SN, Modi N, Group BIew. Neonatal brain injuries in England: population-based incidence derived from routinely recorded clinical data held in the National Neonatal Research Database. *Arch Dis Child Fetal Neonatal Ed*. (2018). 103:F301–6. doi: 10.1136/archdischild-2017-313707
2. Jacobs SE, Berg M, Hunt R, Tarnow-Mordi WO, Inder TE, Davis PG. Cooling for newborns with hypoxic ischaemic encephalopathy. *Cochrane Database Syst Rev*. (2013) 2013:CD003311. doi: 10.1002/14651858.CD003311.pub3

3. Azzopardi D, Strohm B, Marlow N, Brocklehurst P, Deierl A, Eddama O, et al. Effects of hypothermia for perinatal asphyxia on childhood outcomes. *N Engl J Med.* (2014) 371:140–9. doi: 10.1056/NEJMoa1315788
4. Shankaran S, Laptook AR, Ehrenkranz RA, Tyson JE, McDonald SA, Donovan EF, et al. Whole-body hypothermia for neonates with hypoxic-ischemic encephalopathy. *N Engl J Med.* (2005) 353:1574–84. doi: 10.1056/NEJMcps050929
5. Eklind S, Mallard C, Leverin AL, Gilland E, Blomgren K, Mattsby-Baltzer I, et al. Bacterial endotoxin sensitizes the immature brain to hypoxic–ischaemic injury. *Eur J Neurosci.* (2001) 13:1101–6. doi: 10.1046/j.0953-816x.2001.01474.x
6. Nelson KB, Willoughby RE. Infection, inflammation and the risk of cerebral palsy. *Curr Opin Neurol.* (2000) 13:133–9. doi: 10.1097/00019052-200004000-00004
7. Tann CJ, Nakakeeto M, Willey BA, Sewegaba M, Webb EL, Oke I, et al. Perinatal risk factors for neonatal encephalopathy: an unmatched case-control study. *Arch Dis Child Fetal Neonatal Ed.* (2018) 103:F250–6. doi: 10.1136/archdischild-2017-312744
8. Mitra S, Kendall GS, Bainbridge A, Sokolska M, Dinan M, Uria-Avellanal C, et al. Proton magnetic resonance spectroscopy lactate/N-acetylaspartate within 2 weeks of birth accurately predicts 2-year motor, cognitive and language outcomes in neonatal encephalopathy after therapeutic hypothermia. *Arch Dis Child Fetal Neonatal Ed.* (2019) 104:F424–32. doi: 10.1136/archdischild-2018-315478
9. Lally PJ, Montaldo P, Oliveira V, Soe A, Swamy R, Bassett P, et al. Magnetic resonance spectroscopy assessment of brain injury after moderate hypothermia in neonatal encephalopathy: a prospective multicentre cohort study. *Lancet Neurol.* (2019) 18:35–45. doi: 10.1016/S1474-4422(18)30325-9
10. Azzopardi D, Chew AT, Deierl A, Huertas A, Robertson NJ, Tusor N, et al. Prospective qualification of early cerebral biomarkers in a randomised trial of treatment with xenon combined with moderate hypothermia after birth asphyxia. *EBioMedicine.* (2019) 47:484–91. doi: 10.1016/j.ebiom.2019.08.034
11. Robertson NJ, Martinello K, Lingam I, Avdic-Belltheus A, Meehan C, Alonso-Alconada D, et al. Melatonin as an adjunct to therapeutic hypothermia in a piglet model of neonatal encephalopathy: a translational study. *Neurobiol Dis.* (2018) 121:240–51. doi: 10.1016/j.nbd.2018.10.004
12. Robertson NJ, Faulkner S, Fleiss B, Bainbridge A, Andorka C, Price D, et al. Melatonin augments hypothermic neuroprotection in a perinatal asphyxia model. *Brain.* (2013) 136(Pt. 1):90–105. doi: 10.1093/brain/aws285
13. Lingam I, Meehan C, Avdic-Belltheus A, Martinello K, Hristova M, Kaynezhad P, et al. Short-term effects of early initiation of magnesium infusion combined with cooling after hypoxia-ischemia in term piglets. *Pediatr Res.* (2019) 86:699–708. doi: 10.1038/s41390-019-0511-8
14. Martinello KA, Meehan C, Avdic-Belltheus A, Lingam I, Ragab S, Hristova M, et al. Acute LPS sensitization and continuous infusion exacerbates hypoxic brain injury in a piglet model of neonatal encephalopathy. *Sci Rep.* (2019) 9:10184. doi: 10.1038/s41598-019-46488-y
15. Broad KD, Fierens I, Fleiss B, Rocha-Ferreira E, Ezzati M, Hassell J, et al. Inhaled 45-50% argon augments hypothermic brain protection in a piglet model of perinatal asphyxia. *Neurobiol Dis.* (2016) 87:29–38. doi: 10.1016/j.nbd.2015.12.001
16. Lorek A, Takei Y, Cady E, Wyatt J, Penrice J, Edwards A, et al. Delayed ("secondary") cerebral energy failure after acute hypoxia-ischemia in the newborn piglet: continuous 48-hour studies by phosphorus magnetic resonance spectroscopy. *Pediatr Res.* (1994) 36:699–706. doi: 10.1203/00006450-199412000-00003
17. Robertson NJ, Lingam I, Meehan C, Martinello KA, Avdic-Belltheus A, Stein L, et al. High-dose melatonin and ethanol excipient combined with therapeutic hypothermia in a newborn piglet asphyxia model. *Sci Rep.* (2020) 10:3898. doi: 10.1038/s41598-020-60858-x
18. Yushkevich PA, Piven J, Hazlett HC, Smith RG, Ho S, Gee JC, et al. User-guided 3D active contour segmentation of anatomical structures: significantly improved efficiency and reliability. *Neuroimage.* (2006) 31:1116–28. doi: 10.1016/j.neuroimage.2006.01.015
19. Conrad MS, Sutton BP, Dilger RN, Johnson RW. An *in vivo* three-dimensional magnetic resonance imaging-based averaged brain collection of the neonatal piglet (Sus scrofa). *PLoS ONE.* (2014) 9:e107650. doi: 10.1371/journal.pone.0107650
20. Ito D, Tanaka K, Suzuki S, Dembo T, Fukuuchi Y. Enhanced expression of Iba1, ionized calcium-binding adapter molecule 1, after transient focal cerebral ischemia in rat brain. *Stroke.* (2001) 32:1208–15. doi: 10.1161/01.STR.32.5.1208
21. Thayyil S, Chandrasekaran M, Taylor A, Bainbridge A, Cady EB, Chong WK, et al. Cerebral magnetic resonance biomarkers in neonatal encephalopathy: a meta-analysis. *Pediatrics.* (2010) 125:e382–95. doi: 10.1542/peds.2009-1046
22. Alderliesten T, de Vries LS, Staats L, van Haastert IC, Weeke L, Benders MJ, et al. MRI and spectroscopy in (near) term neonates with perinatal asphyxia and therapeutic hypothermia. *Arch Dis Child Fetal Neonatal Ed.* (2017) 102:F147–52. doi: 10.1136/archdischild-2016-310514
23. Shibasaki J, Aida N, Morisaki N, Tomiyasu M, Nishi Y, Toyoshima K. Changes in brain metabolite concentrations after neonatal hypoxic-ischemic encephalopathy. *Radiology.* (2018) 288:840–8. doi: 10.1148/radiol.2018172083
24. Woo CW, Lee BS, Kim ST, Kim KS. Correlation between lactate and neuronal cell damage in the rat brain after focal ischemia: an *in vivo* 1H magnetic resonance spectroscopic (1H-MRS) study. *Acta Radiol.* (2010) 51:344–50. doi: 10.3109/02841850903515395
25. Aridas JD, Yawno T, Sutherland AE, Nitsos I, Ditchfield M, Wong FY, et al. Detecting brain injury in neonatal hypoxic ischemic encephalopathy: closing the gap between experimental and clinical research. *Exp Neurol.* (2014) 261:281–90. doi: 10.1016/j.expneurol.2014.07.009
26. Choi C, Coupland NJ, Kalra S, Bhardwaj PP, Malykhin N, Allen PS. Proton spectral editing for discrimination of lactate and threonine 1.31 ppm resonances in human brain *in vivo*. *Magn Reson Med.* (2006) 56:660–5. doi: 10.1002/mrm.20988
27. Sonnewald U, Wang AY, Schousboe A, Erikson R, Skottner A. New aspects of lactate metabolism: IGF-I and insulin regulate mitochondrial function in cultured brain cells during normoxia and hypoxia. *Dev Neurosci.* (1996) 18:443–8. doi: 10.1159/000111439
28. Stovell MG, Mada MO, Helmy A, Carpenter TA, Thelin EP, Yan JL, et al. The effect of succinate on brain NADH/NAD. *Sci Rep.* (2018) 8:11140. doi: 10.1038/s41598-018-29255-3
29. Carpenter KL, Jalloh I, Hutchinson PJ. Glycolysis and the significance of lactate in traumatic brain injury. *Front Neurosci.* (2015) 9:112. doi: 10.3389/fnins.2015.00112
30. Pellerin L, Magistretti PJ. Glutamate uptake into astrocytes stimulates aerobic glycolysis: a mechanism coupling neuronal activity to glucose utilization. *Proc Natl Acad Sci USA.* (1994) 91:10625–9. doi: 10.1073/pnas.91.22.10625
31. Lama S, Auer RN, Tyson R, Gallagher CN, Tomanek B, Sutherland GR. Lactate storm marks cerebral metabolism following brain trauma. *J Biol Chem.* (2014) 289:20200–8. doi: 10.1074/jbc.M114.570978
32. Robertson NJ, Cox IJ, Cowan FM, Counsell SJ, Azzopardi D, Edwards AD. Cerebral intracellular lactic alkalosis persisting months after neonatal encephalopathy measured by magnetic resonance spectroscopy. *Pediatr Res.* (1999) 46:287–96. doi: 10.1203/00006450-199909000-00007
33. Uria-Avellanal C, Robertson NJ. Na^+/H^+ exchangers and intracellular pH in perinatal brain injury. *Transl Stroke Res.* (2014) 5:79–98. doi: 10.1007/s12975-013-0322-x
34. Wu TW, Tamrazi B, Hsu KH, Ho E, Reitman AJ, Borzage M, et al. Cerebral lactate concentration in neonatal hypoxic-ischemic encephalopathy: in relation to time, characteristic of injury, and serum lactate concentration. *Front Neurol.* (2018) 9:293. doi: 10.3389/fneur.2018.00293
35. Carpenter KL, Jalloh I, Gallagher CN, Grice P, Howe DJ, Mason A, et al. (13)C-labelled microdialysis studies of cerebral metabolism in TBI patients. *Eur J Pharm Sci.* (2014) 57:87–97. doi: 10.1016/j.ejps.2013.12.012
36. Roumes H, Dumont U, Sanchez S, Mazuel L, Blanc J, Raffard G, et al. Neuroprotective role of lactate in rat neonatal hypoxia-ischemia. *J Cereb Blood Flow Metab.* (2020). doi: 10.1177/0271678X20908355. [Epub ahead of print].
37. Rosko L, Smith VN, Yamazaki R, Huang JK. Oligodendrocyte bioenergetics in health and disease. *Neuroscientist.* (2018) 25:334–43. doi: 10.1177/1073858418793077
38. Schmitz B, Wang X, Barker PB, Pilatus U, Bronzlik P, Dadak M, et al. Effects of aging on the human brain: a proton and phosphorus MR spectroscopy study at 3T. *J Neuroimaging.* (2018) 28:416–21. doi: 10.1111/jon.12514

39. Cheong JL, Cady EB, Penrice J, Wyatt JS, Cox IJ, Robertson NJ. Proton MR spectroscopy in neonates with perinatal cerebral hypoxic-ischemic injury: metabolite peak-area ratios, relaxation times, and absolute concentrations. *Am J Neuroradiol.* (2006) 27:1546–54.
40. Sijens PE, Wischniowsky K, Ter Horst HJ. The prognostic value of proton magnetic resonance spectroscopy in term newborns treated with therapeutic hypothermia following asphyxia. *Magn Reson Imaging.* (2017) 42:82–7. doi: 10.1016/j.mri.2017.06.001
41. Bednarek N, Mathur A, Inder T, Wilkinson J, Neil J, Shimony J. Impact of therapeutic hypothermia on MRI diffusion changes in neonatal encephalopathy. *Neurology.* (2012) 78:1420–7. doi: 10.1212/WNL.0b013e318253d589
42. Igarashi H, Suzuki Y, Huber VJ, Ida M, Nakada T. N-acetylaspartate decrease in acute stage of ischemic stroke: a perspective from experimental and clinical studies. *Magn Reson Med Sci.* (2015) 14:13–24. doi: 10.2463/mrms.2014-0039
43. Ancora G, Testa C, Grandi S, Tonon C, Sbravati F, Savini S, et al. Prognostic value of brain proton MR spectroscopy and diffusion tensor imaging in newborns with hypoxic-ischemic encephalopathy treated by brain cooling. *Neuroradiology.* (2013) 55:1017–25. doi: 10.1007/s00234-013-1202-5
44. Robertson NJ, Cowan FM, Cox IJ, Edwards AD. Brain alkaline intracellular pH after neonatal encephalopathy. *Ann Neurol.* (2002) 52:732–42. doi: 10.1002/ana.10365
45. Millar LJ, Shi L, Hoerder-Suabedissen A, Molnár Z. Neonatal hypoxia ischaemia: mechanisms, models, and therapeutic challenges. *Front Cell Neurosci.* (2017) 11:78. doi: 10.3389/fncel.2017.00078
46. Rocha-Ferreira E, Hristova M. Antimicrobial peptides and complement in neonatal hypoxia-ischemia induced brain damage. *Front Immunol.* (2015) 6:56. doi: 10.3389/fimmu.2015.00056
47. Fleiss B, Gressens P. Tertiary mechanisms of brain damage: a new hope for treatment of cerebral palsy? *Lancet Neurol.* (2012) 11:556–66. doi: 10.1016/S1474-4422(12)70058-3
48. Charriaut-Marlangue C, Besson VC, Baud O. Sexually dimorphic outcomes after neonatal stroke and hypoxia-ischemia. *Int J Mol Sci.* (2017) 19:61. doi: 10.3390/ijms19010061
49. Burguillos MA, Deierborg T, Kavanagh E, Persson A, Hajji N, Garcia-Quintanilla A, et al. Caspase signalling controls microglia activation and neurotoxicity. *Nature.* (2011) 472:319–24. doi: 10.1038/nature09788
50. Villapol S, Bonnin P, Fau S, Baud O, Renolleau S, Charriaut-Marlangue C. Unilateral blood flow decrease induces bilateral and symmetric responses in the immature brain. *Am J Pathol.* (2009) 175:2111–20. doi: 10.2353/ajpath.2009.090257
51. Abraham MC, Shaham S. Death without caspases, caspases without death. *Trends Cell Biol.* (2004) 14:184–93. doi: 10.1016/j.tcb.2004.03.002
52. Zhou T, Lin H, Jiang L, Yu T, Zeng C, Liu J, et al. Mild hypothermia protects hippocampal neurons from oxygen-glucose deprivation injury through inhibiting caspase-3 activation. *Cryobiology.* (2018) 80:55–61. doi: 10.1016/j.cryobiol.2017.12.004
53. Hellström-Westas L, Rosén I, Svenningsen NW. Predictive value of early continuous amplitude integrated EEG recordings on outcome after severe birth asphyxia in full term infants. *Arch Dis Child Fetal Neonatal Ed.* (1995) 72:F34–8. doi: 10.1136/fn.72.1.F34

Conflict of Interest: The authors declare that the research was conducted in the absence of any commercial or financial relationships that could be construed as a potential conflict of interest.

frontiers in Neurology

ORIGINAL RESEARCH
published: 06 October 2020
doi: 10.3389/fneur.2020.540878

Involvement of CXCL1/CXCR2 During Microglia Activation Following Inflammation-Sensitized Hypoxic-Ischemic Brain Injury in Neonatal Rats

Meray Serdar[1], *Karina Kempe*[1], *Ralf Herrmann*[1], *Daniel Picard*[2], *Marc Remke*[2], *Josephine Herz*[1], *Ivo Bendix*[1], *Ursula Felderhoff-Müser*[1] *and Hemmen Sabir*[1,3,4]*

[1] *Department of Pediatrics I/Neonatology and Experimental Perinatal Neurosciences, University Hospital Essen, University Duisburg-Essen, Essen, Germany,* [2] *Department of Pediatric Oncology, Hematology, and Clinical Immunology, Medical Faculty, Heinrich Heine University, Düsseldorf, Germany,* [3] *Department of Neonatology and Pediatric Intensive Care, Children's Hospital University of Bonn, Bonn, Germany,* [4] *German Center for Neurodegenerative Diseases (DZNE), Bonn, Germany*

Background: Microglia are key mediators of inflammation during perinatal brain injury. As shown experimentally after inflammation-sensitized hypoxic ischemic (HI) brain injury, microglia are activated into a pro-inflammatory status 24 h after HI involving the NLRP3 inflammasome pathway. The chemokine (C-X-C motif) ligand 1 (CXCL1), and its cognate receptor, CXCR2, have been shown to be involved in NLRP3 activation, although their specific role during perinatal brain injury remains unclear. In this study we investigated the involvement of CXCL1/CXCR2 in brain tissue and microglia and brain tissue after inflammation-sensitized HI brain injury of newborn rats.

Methods: Seven-day old Wistar rat pups were either injected with vehicle (NaCl 0.9%) or *E. coli* lipopolysaccharide (LPS), followed by left carotid ligation combined with global hypoxia (8% O_2 for 50 min). Pups were randomized into four different treatment groups: (1) Sham group ($n = 21$), (2) LPS only group ($n = 20$), (3) Veh/HI group ($n = 39$), and (4) LPS/HI group ($n = 42$). Twenty-four hours post hypoxia transcriptome and gene expression analysis were performed on *ex vivo* isolated microglia cells in our model. Additionally protein expression was analyzed in different brain regions at the same time point.

Results: Transcriptome analyses showed a significant microglial upregulation of the chemokine CXCL1 and its receptor CXCR2 in the LPS/HI group compared with the other groups. Gene expression analysis showed a significant upregulation of CXCL1 and NLRP3 in microglia cells after inflammation-sensitized hypoxic-ischemic brain injury. Additionally, protein expression of CXCL1 was significantly upregulated in cortex of male pups from the LPS/HI group.

Conclusion: These results indicate that the CXCL1/CXCR2 pathway may be involved during pro-inflammatory microglia activation following inflammation-sensitized hypoxic-ischemic brain injury in neonatal rats. This may lead to new treatment options altering CXCR2 activation early after HI brain injury.

Keywords: newborn, HIE, brain, infection, inflammation, microglia, chemokine

OPEN ACCESS

Edited by:
Julie Wixey,
The University of Queensland, Australia

Reviewed by:
Ryuta Koyama,
The University of Tokyo, Japan
Stephanie Miller,
The University of Queensland, Australia

***Correspondence:**
Hemmen Sabir
hemmen.sabir@ukbonn.de

Specialty section:
This article was submitted to Pediatric Neurology, a section of the journal Frontiers in Neurology

Received: *06 March 2020*
Accepted: *31 August 2020*
Published: *06 October 2020*

Citation:
Serdar M, Kempe K, Herrmann R, Picard D, Remke M, Herz J, Bendix I, Felderhoff-Müser U and Sabir H (2020) Involvement of CXCL1/CXCR2 During Microglia Activation Following Inflammation-Sensitized Hypoxic-Ischemic Brain Injury in Neonatal Rats. Front. Neurol. 11:540878. doi: 10.3389/fneur.2020.540878

INTRODUCTION

Globally perinatal asphyxia is one of the leading causes of neonatal mortality and long-term morbidity, including mental dysfunctions and cerebral palsy (1). Perinatal asphyxia may lead to neonatal encephalopathy (NE), most likely due to hypoxia-ischemia (HI). To date therapeutic hypothermia (TH) is the standard treatment for hypoxic-ischemic encephalopathy (HIE) with a short therapeutic time-window of 6 h (2). However, almost half of all cooled asphyxiated newborns do not benefit from the treatment (1). As early specific biomarkers are yet not available, early identification of non-responders to TH is not possible. In low- and middle-income countries, where NE rates are significantly higher, the introduction of TH was unsuccessful in decreasing mortality (3). Therefore, the etiology of NE in this population appears to be different. Perinatal infection is an independent risk factor for adverse neurological outcome in term newborns (4). Clinically, it has been shown that infection rates in asphyxiated newborns are significantly higher, compared with the general newborn population (5). Experimentally, we have previously established a newborn animal model of inflammation-sensitized hypoxic-ischemic brain injury in newborn rats. In this model, we found that TH is not neuroprotective (6, 7). This possibly explains the clinical finding, that TH is ineffective in low- and middle-income countries where the prevalence of perinatal infections is higher. Therefore, we need to better understand the pathophysiology underlying inflammation-sensitized hypoxic-ischemic brain injury to explain why TH may be ineffective in this setting.

Hypoxia-ischemia triggers activation of microglia, the resident immune cells of the central nervous system (CNS) (7, 8). In our recent study modeling inflammation-sensitized HI brain injury an upregulation of pro-inflammatory cytokines in microglia 24 h post injury was shown (9). This indicates, that microglia are activated into a pro-inflammatory phenotype early after inflammation-sensitized hypoxia-ischemia. However, the underlying pathways and mechanisms leading to this pro-inflammatory state in the newborn brain are still unknown.

Chemokines are inflammatory mediators, which are released following different brain injuries (inflammation, trauma, hypoxia-ischemia) (10). The chemokine (c-x-c motif) CXCL1 is a chemoattractant for T cells, monocytes, and neutrophils in the brain (11) after binding to its specific CXCR2 receptor. It has been shown, that CXCL1 is essential for the production of reactive oxygen species, which in turn modulate further inflammation (12, 13). One cardinal response to toxic stimuli in the brain is the assembly and activation of inflammasomes. The most defined inflammasome is NLRP3 (nucleotide-binding domain, leucine-rich repeat protein 3), which is activated in neonatal brain injury either due to inflammation (*E.coli* lipopolysaccharide (LPS)) or HI (14, 15). Activation of the NLRP3 inflammasome induces cleavage and therefore activation of interleukin (IL)-18 and IL-1β from its preforms. We have previously shown that NLRP3 gene expression is significantly upregulated in different brain regions (cortex and hippocampus) in our animal model (9). Therefore, we hypothesized that microglia mediated pro-inflammatory cytokine release may be regulated through the CXCL1-NLRP3 pathway following inflammation-sensitized hypoxic-ischemic brain injury in neonatal rats. As previously shown *in vitro* CXCL1 activates the NLRP3 inflammasome through binding to the CXCR2 receptor (13). Here, we investigated the expression of NLRP3 and CXCL1 in microglia and brain tissue in our animal model, aiming to confirm the involvement of CXCL1/CXCR2 in our animal model which may lead to new treatment options for inflammation-sensitized HI brain injury.

MATERIALS AND METHODS

Animals and Experimental Procedure

All animal experiments were performed in accordance to the Animal Research: Reporting of *in vivo* Experiments (ARRIVE) guidelines with government approval by the State Agency of Nature, Environment and Consumer Protection North Rhine-Westphalia, Germany. Seven-day-old (P7) Wistar rat pups of both genders were used in all our experiments. All pups were kept at the central animal laboratory of the University Hospital Essen, Germany with 12:12 dark: light cycle at an environmental temperature 21°C with food and water *ad libitum*. As previously described, all animals were randomized across litter gender and observers blinded to the different treatments (6, 7, 9, 16).

Temperature during handling and experimental procedures was monitored in sentinel pups not further allocated to the different treatment groups. All rat pups were kept on a servo-controlled mat (CritiCool, MTRE, Yavne, Israel) during separation from their dams, controlled by the sentinel pup via a rectal temperature probe (IT-21, Physitemp Instruments, Clifton, NJ, United States) continuously maintaining nesting temperature of P7 rats (17) or treatment temperatures during experiments (see below). In our experimental setup, four groups were included: (1) sham group, underwent sham surgery (incision of the neck under isoflurane anesthesia (2% isoflurane) without further operation) ($n = 21$), (2) LPS group, received an intraperitoneal injection (i.p.) of lipopolysaccharide solution (LPS) (*Escherichia coli* lipopolysaccharide O55:B5, Sigma; 0.1 mg/kg) and underwent a sham surgery ($n = 20$), (3) Veh/ HI group, received an injection of 0.9% NaCl, underwent left sided ligation of the common carotid artery under isoflurane anesthesia and were thereafter exposed to hypoxia (8% O_2) for 50 min at a rectal temperature (T_{rectal}) of 36°C—resulting in a mild HI injury as previously described (9) ($n = 39$) and (4) LPS/ HI group, received injection of 0.1 mg/kg LPS and treated with unilateral ligation and exposed to hypoxia as above ($n = 42$). Immediately after the HI insult, pups were kept at T_{rectal} of 37°C for 5 h, as in our previous studies (6–9, 17). After the treatment period, pups were immediately returned to their dam. At 24 h post-HI/sham period, all animals were sedated with chloralhydrate, decapitated, and brain tissue removed, dissected into regions of interest and frozen in liquid nitrogen (**Figure 1**, **Table 1**).

Magnetic Activated Cell Sorting (MACS) of CD11 b/c Positive Microglia

Twenty four hours after hypoxia-ischemia or sham-operation CD11b/c positive microglia were isolated via

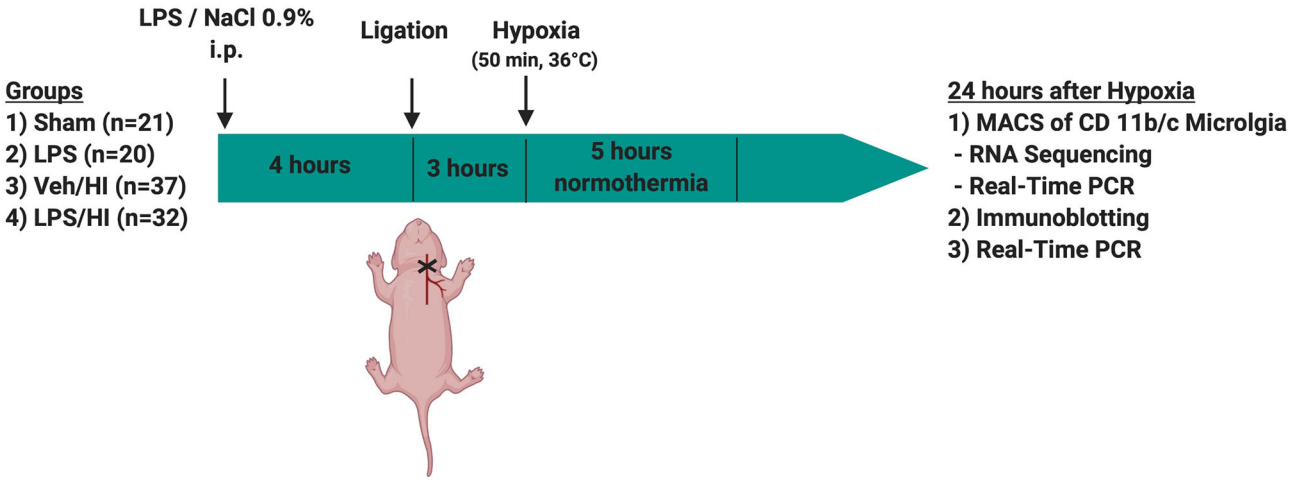

FIGURE 1 | Experimental time course. 7 day old rats (P7) were randomized in 4 different treatment groups. Rats were either injected with NaCl 0.9% or LPS intraperitonally (i.p.) 4 h prior to unilateral ligation of the common carotid artery. Following ligation, rats were exposed to hypoxia (8% O_2) for 50 min before being treated with normothermia (37°C) for 5 h and thereafter returned to their dam. Twenty-four hours after hypoxia brains were extracted and either used for MACS or Immunoblotting.

TABLE 1 | Total number of animals used in this study.

Experimental group	CD11 b/c sorted Microglia RNA [n (m:f)]		Whole brain protein [n (m:f)]	Whole brain RNA [n (m:f)]
	RNA sequencing	Real time PCR		
SHAM	5 (3: 2)	4 (2:2)	7 (4:3)	5 (3: 2)
LPS	5 (3: 2)	4 (2:2)	5 (4:1)	6 (4: 2)
Veh/ HI	10 (3: 7)	8 (5:3)	9 (4:5)	10 (3: 7)
LPS/ HI	8 (3: 5)	8 (5:3)	8 (4:4)	8 (3: 5)

A total of 110 rats were used in this study. For each analysis rats were randomized between litter and gender (m = male, f = female). 52 animals were used for magnetic cell sorting, 29 animals for whole brain protein analyses and 29 animals were used for whole brain RNA analyses.

magnetic activated cell sorting according to our previous study (9). In groups (1) and (2) entire brains (including ipsi-/contralateral hemispheres) were used for analysis (n = 9 per group), while in groups (3) and (4) ipsilateral hemispheres were pooled to get a workable concentration of microglia (n = 18 animals in group (3) and n = 16 animals in group (4) with 2 hemispheres pooled per sample). The brain tissues were mechanically and enzymatically dissociated by using the Neural tissue dissociation kit by Miltenyi Biotech, followed by myelin removal according the manufacturer's instructions (Miltenyi Biotech, Bergisch Gladbach, Germany). Afterwards the cell suspension was incubated with anti-CD11b/c coupled microbeads followed by magnetic separation of CD11b/c positive microglia. The purity of magnetically sorted microglia was confirmed with immunocytochemistry for the microglia marker Iba1 (data not shown). Microglia were used for all further analyses, except of immunoblotting.

RNA Sequencing and Gene Set Analysis

We used n = 5 animals in groups (1) and (2), whereas, we used pooled ipsilateral hemispheres of two animals in groups (3) (n = 10) and (4) (n = 8) to get a workable concentration. RNA was isolated using Trizol (Thermo Scientific, Germany) and 500 ng total RNA was processed using the TruSeq RNA Sample Preparation v2 Kit (low-throughput protocol; Illumina, San Diego, USA) to prepare the barcoded libraries. Libraries were validated and quantified using DNA 1000 and high-sensitivity chips on a Bioanalyzer (Agilent, Boeblingen, Germany); 7.5 pM denatured libraries were used as input into cBot (Illumina), followed by deep sequencing using HiSeq 2500 (Illumina) for 101 cycles, with an additional seven cycles for index reading. Fastq files were imported into Partek Flow (Partek Incorporated, Missouri, USA). Quality analysis and quality control were performed on all reads to assess read quality and to determine the amount of trimming required (both ends: 13 bases 5'and 1 base 3'). Trimmed reads were aligned against the rn6 genome using the STAR v2.4.1d aligner. Unaligned reads were further processed using Bowtie 2 v2.2.5 aligner. Aligned reads were combined before quantifying the expression against the ENSEMBL (release 84) database by the Partek Expectation-Maximization algorithm using the counts per million normalization. Genes with missing values and with a mean expression less than one were filtered out. Finally, statistical gene set analysis was performed using a t-test to determine differential expression at the gene level ($p < 0.05$, fold change ±2). Partek flow default settings were used in all analyses.

Real-Time PCR

The RNA of *ex vivo* isolated microglia was isolated by using the RNeasy mini kit from Qiagen according to the distributed instructions. First strand complementary DNA was synthesized using the total RNA of the cells and TaqMan reverse transcription reagents (Applied Biosystems/ Thermo

Fisher Scientific, United States). Analysis was performed 24 h after HI injury. We used $n = 4$ animals in groups (1) and (2), whereas we used pooled ipsilateral hemispheres of two animals in groups (3) and (4) ($n = 8$ animals) to get a workable concentration. Additionally, RNA of whole brains was isolated by using the RNeasy mini kit from Qiagen according to the distributed instructions and following procedures as before, for modulation of CXCL1 expression. We used $n = 5$ animals in group (1), $n = 6$ animals in group (2), $n = 10$ animals in group (3), and $n = 8$ animals in group (4). Animals of both genders were used. The expression of the inflammasome cryopyrin (NLRP3) (RN04244620_m1; Life Technologies, Germany) and the chemokine (C-X-C) ligand (Rn00578225_m1; Life Technologies, Germanys) was analyzed. As reference gene we used the Beta-2-microtubuline (B2M, Rn00560865_m1; Life technologies, Germany). Measurements were performed in duplicates and repeated two times for each sample. Target gene expression was quantified according to the $2^{\Delta\Delta}$CT method (18). Sham-operated animals served as reference group, as results were normalized to the sham group.

Immunoblotting

For Western-Blot analysis we used $n = 29$ animals [$n = 7$ in group (1), $n = 5$ in group (2), $n = 9$ in group (3), $n = 8$ in group (4)]. Pups were transcardially perfused with PBS and brain regions were prepared using a standard matrix for uniformity as previously described (9) (ASI Instruments Inc., Warren, MI, United States). We used whole cortex, hippocampus and thalamus for further analyses. Western-Blotting was performed as previously described (16, 19), with adaptions in epitope detection. 12.5% gel membranes were loaded with 40 µg of each sample per lane and were blocked with 5% non-fat dry milk in Tris-buffered saline, 0.1% Tween-20 (TBST, Sigma Aldrich, USA) and incubated overnight (4°C) with the following primary antibodies: polyclonal goat anti C-X-C motif chemokine 1 (1:1,000, Thermo Fisher, Germany, catalog number PA5-86508), polyclonal rabbit anti-NLRP3 (1: 5,000, Abcam, Germany, catalog number ab214185), polyclonal rabbit CXCR2 (1:5,000, Abcam, Germany, catalog number ab65968), and polyclonal mouse anti β-Actin antibody (1:20,000, Sigma, Germany). Horseradish peroxidase-conjugated secondary anti mouse (1:5,000) or anti-rabbit (1:2000, both DAKO, Denmark) antibodies were used. All antibodies were diluted in 5% non-fat dry milk in TBST. Antibody binding was detected by using enhanced chemiluminescence (GE Healthcare Life Sciences, Germany). For visualization and densitometric analysis, ChemiDoc™ XRS+ imaging system and ImageLab software (Bio-Rad, Germany) were used.

Statistical Analysis

Graphical data are presented as median values with boxplots including the 25% and the 75% percentile. Data were analyzed using GraphPad Prism 6 (GraphPad Software, United States). Differences between groups were determined by one-way analysis of variance (one-way ANOVA) followed by Bonferroni *post hoc* test for multiple comparison. p-values < 0.05 were considered as statistically significant.

RESULTS

In total 2 experiments were performed using a 4-group design, as stated above. Out of the 122 animals used in our 4-group design, mortality was highest in the LPS/HI group. In total 12 animals died during hypoxia, 2/39 from group (3) and 10/42 from group (4), leaving 110 rat pups for further analysis. The high mortality in the LPS/HI group has been expected and reported in our previous studies (6, 7, 9).

Genome-wide Profiling of Pre-sensitized CD11 b/c Sorted Microglia 24 h After Inflammation-Sensitized Hypoxia Ischemia

In our previous study we showed that microglia polarize into a pro-inflammatory phenotype 24 h post HI after pre-exposure to LPS (9). To further investigate this pro-inflammatory polarization, we performed a transcriptomic profiling of microglia cells in our model 24 h post HI. After RNAseq we focused on gene sets of neutrophil migration and neutrophil degranulation, as this clustered gene set showed significant differences in the LPS/HI group compared with all other groups. Also, they are strongly associated with microglia (20). We used a total of 26 genes of interest, as illustrated in a heatmap (**Figure 2**). We observed a clear upregulation of the CXCR2 and CXCL1 genes in the LPS sensitized HI group compared with the other groups, especially compared with the control group. CXCR2 is a chemokine receptor, which is stimulated by the chemokine CXCL1. Based on the findings and documented results of our previous study (9), we proposed an activation of the inflammasome NLRP3 through a stimulation of the CXCR2 receptor. To verify this hypothesis, we quantified the level of gene expression of the chemokine CXCL1 in CD11b/c positive microglia via RT-PCR, as CXCL1 gene regulation was also significantly upregulated in the LPS/HI group. We determined a significant upregulation of CXCL1 in the LPS/HI group compared with the sham group ($p = 0.0008$) and LPS group ($p = 0.0182$) using RT-PCR.

Activation of the Inflammasome NLRP3 in Microglia After LPS-Sensitized Hypoxic-Ischemic Brain Injury

The NLRP3 inflammasome induces a cleavage of IL-18 and IL-1β, leading to further inflammation by microglia (21). We have previously shown an upregulation of the NLRP3 gene expression in hippocampus and cortex of the LPS/HI group compared with the other three groups (9). However, the modulation of NLRP3 had not been assessed on a cellular level in sorted CD11b/c microglia yet. Therefore, we analyzed the expression of NLRP3 in microglia via RT-PCR and determined a significantly increased expression in the LPS/HI group compared with the Sham group ($p = 0.0031$) (**Figure 3**).

Inflammation Sensitized Hypoxia-Ischemia Increases the CXCL1 Protein-Expression in Cortex of Male Pups

As gene expression levels do not fully represent protein expression levels, we analyzed the protein expression of

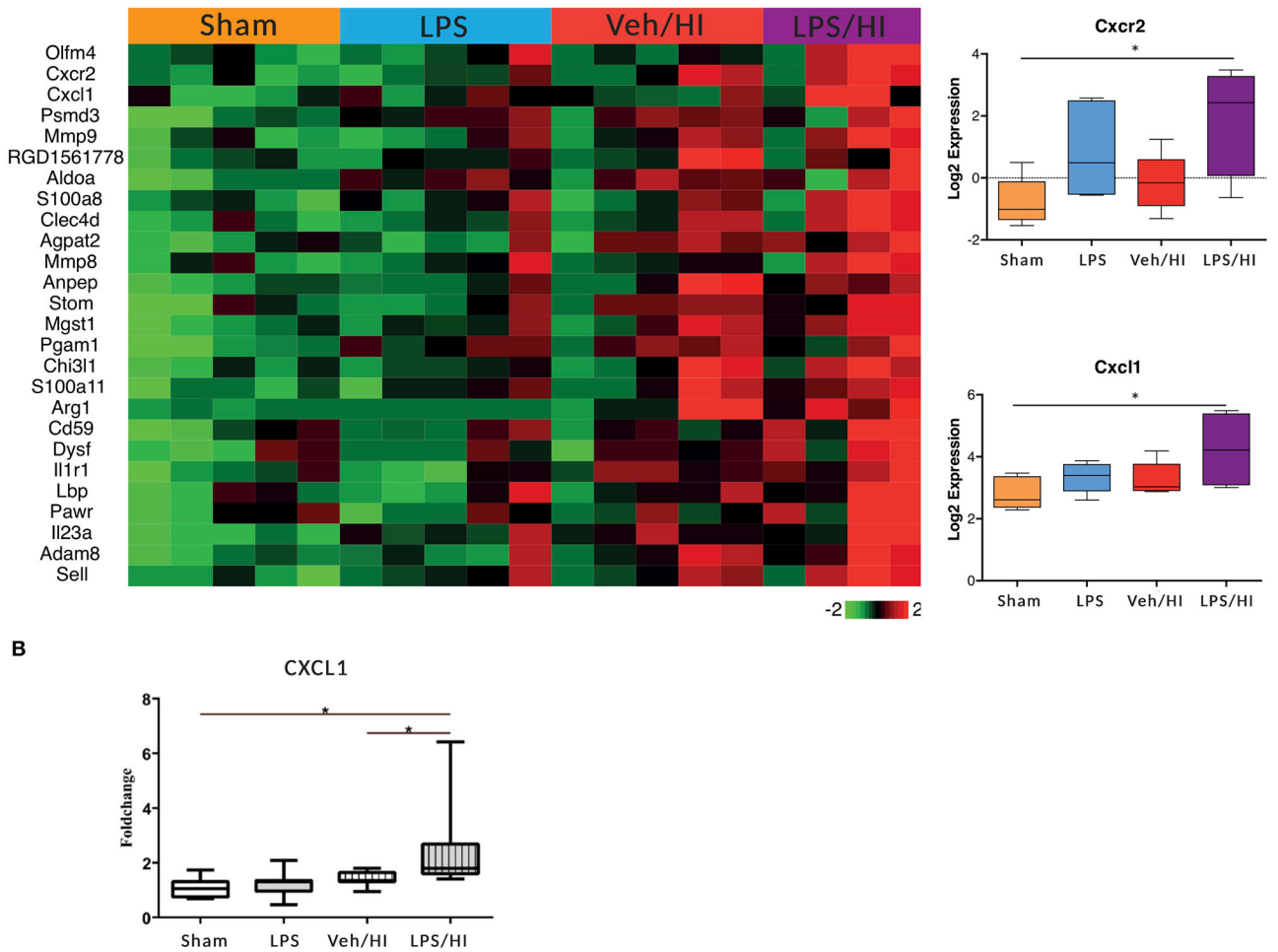

FIGURE 2 | Significant upregulation of several genes especially CXCL1/CXCR2 in inflammation-sensitized HI injury. Twenty-four hours after hypoxia CD11 b/c sorted microglia were used for transcriptome-analysis (RNA-sequencing). The most prominent 26 genes of neutrophil migration and neutrophil degranulation are depicted in a heatmap of each individual group. CXCL1 (ligand to CXCR2) and CXCR2 were significantly upregulated after inflammation-sensitized hypoxic ischemic-brain injury **(A)**. Modulation of CXCL1 expression was confirmed via real time PCR and revealed a significant upregulation after inflammation-sensitized hypoxic ischemic-brain injury **(B)**. $n = 5$ animals in Sham and LPS groups (whole brains), $n = 10$ animals in Veh/HI group and $n = 8$ animals in LPS/HI group (2 pooled ipsilateral brain hemispheres per sample). $^*p < 0.05$.

CXCL1, CXCR2 and NLRP3 in the cortex, hippocampus and thalamus. For CXCL1, we observed no significant modulation in the individual groups as shown in **Figure 4**. Therefore, we investigated gender differences showing that in LPS-sensitized male pups the protein expression of CXCL1 is significantly increased 24 h after inflammation-sensitized hypoxia-ischemia compared with the Sham group ($p = 0.0099$). However, this gender-specific effect was only seen in the cortex and not in the hippocampus or thalamus. For CXCR2 and NLRP3, we did not observe any differences in the LPS-sensitized hypoxia-ischemia groups within the different brain areas and there was no gender differences (**Figures 5**, **6**).

DISCUSSION

Up to now TH is the only established standardized neuroprotective treatment for neonatal encephalopathy following perinatal asphyxia. As treatment success might be influenced by different co-morbidities, the subgroup of non-responders to TH needs to be further investigated. In an experimental setup of inflammation-sensitized hypoxic-ischemic brain injury TH has failed to be neuroprotective (6, 7). To improve the understanding for the lack of neuroprotection from TH, we aim to focus on the underlying mechanisms leading to increased inflammation in our established model of inflammation-sensitized HI brain injury. As we have previously

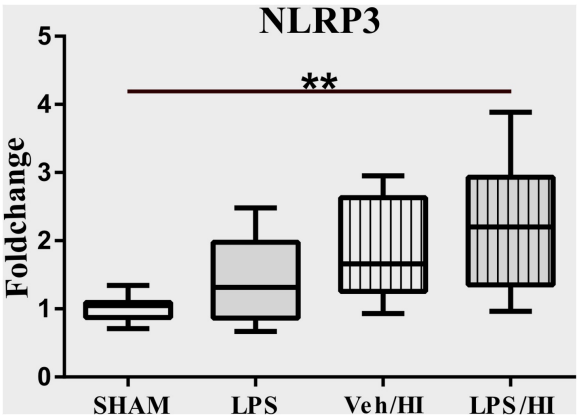

FIGURE 3 | LPS-sensitized hypoxic-ischemic brain injury induces an upregulation of the NLRP3 inflammasome in microglia. Twenty-four hours after HI magnetic sorted microglia were analyzed for the NLRP3-expression via real time PCR. $n = 4$ animals in Sham and LPS groups (whole brains), $n = 8$ animals in Veh/HI and LPS/HI groups (2 pooled ipsilateral brain hemispheres per sample). $^{**}p < 0.01$.

shown, microglia are activated into a pro-inflammatory phenotype early after inflammation-sensitized HI (9). In the current study, we show that the chemokine CXCL1 and its receptor (CXCR2) are upregulated and therefore may be involved in the pro-inflammatory response of microglia in our model. In addition, expression of the NLRP3 inflammasome is upregulated in microglia after inflammation-sensitized HI brains. As it has been shown that NLRP3 is regulated by the chemokine CXCL1 and its specific receptor CXCR2, we assume that CXCL1/CXCR2 is involved during the pro-inflammatory activation of microglia and that this activation also involves NLRP3 upregulation in microglia following inflammation-sensitized HI brain injury.

Only fifty percent of cooled asphyxiated newborns benefit from TH, whereas the others develop mild to severe motor-cognitive deficits in later life (1). Perinatal infection can lead to perinatal asphyxia and also neonatal infection rates are much higher in asphyxiated newborns (5, 22). Comparable with a clinical single-center experience (23), TH is not neuroprotective in our established model of inflammation-sensitized HI brain injury (6, 7). Therefore, there is an urgent need of neuroprotective treatments in the setting

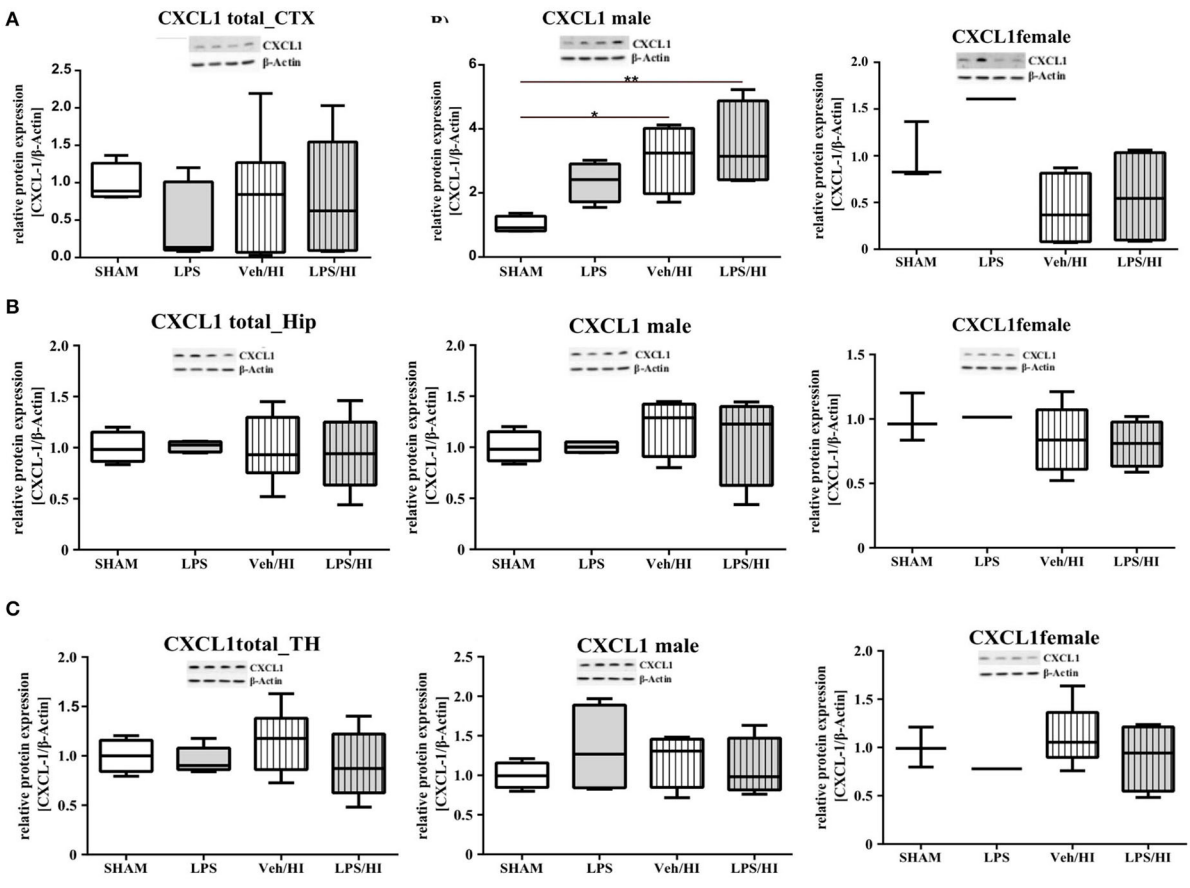

FIGURE 4 | CXCL1 protein expression in different brain regions after inflammation-sensitized hypoxic-ischemic brain injury. Twenty-four hours after hypoxia-ischemia the expression of CXCL1 protein is not regulated in cortex **(A)**, hippocampus (HIP) **(B)** or thalamus (TH) **(C)** from animals of both genders (Sham $n = 7$, LPS $n = 5$, Veh/HI $n = 9$, LPS $n = 8$). A significant upregulation is determined in cortex of males after inflammation-sensitized hypoxic-ischemic brain injury **(A)**, whereas there was no gender specific upregulation in hippocampus **(B)** or thalamus **(C)** (Sham $n = 4$ males, LPS $n = 4$ males, Veh/HI $n = 4$ males, LPS $n = 4$ males). $^{*}p < 0.05$, $^{**}p < 0.01$.

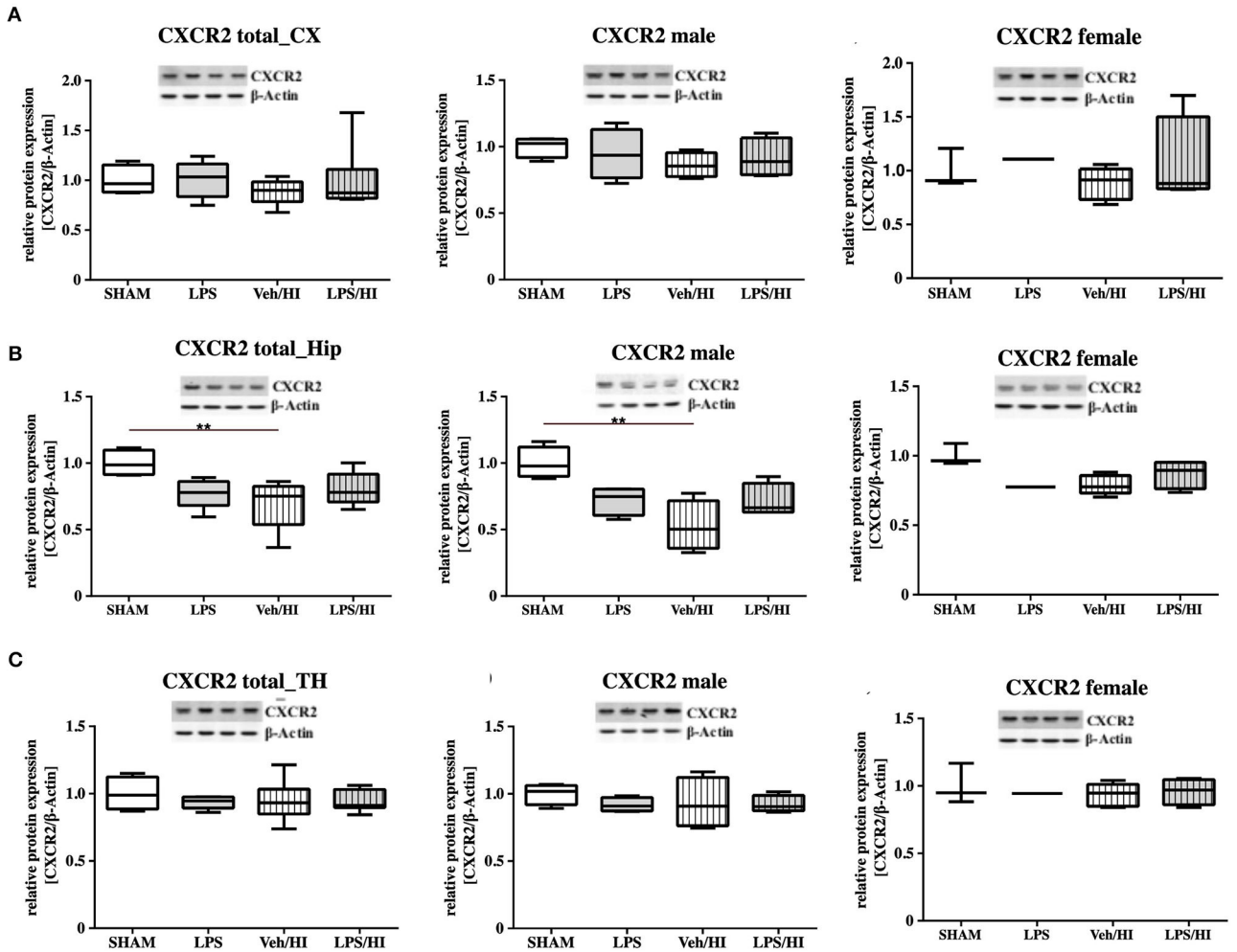

FIGURE 5 | CXCR2 protein expression in different brain regions after inflammation-sensitized hypoxic-ischemic brain injury. Twenty-four hours after hypoxia-ischemia the expression of CXCR2 protein is not regulated in cortex (CX) **(A)**, hippocampus (HIP) **(B)** or thalamus (TH) **(C)** from animals of both genders (Sham $n = 7$, LPS $n = 5$, Veh/HI $n = 9$, LPS $n = 8$). A significant downregulation is determined in hippocampus of males after hypoxic-ischemic brain injury **(B)**, whereas there was no difference in the inflammation-sensitized hypoxic-ischemic brain injury groups (Sham $n = 4$ males, LPS $n = 4$ males, Veh/HI $n = 4$ males, LPS $n = 4$ males). $^{**}p < 0.01$.

of inflammation-sensitized HI brain injury, presenting as neonatal encephalopathy. To identify new treatment options the underlying mechanisms, need to be analyzed. As previously shown, brain ischemia triggers a series of events that cause resident microglia to become activated and develop macrophage-like capabilities (24, 25). Microglia activation can be defined by two different phenotypes; a pro-inflammatory phenotype indicated as M1 and an anti-inflammatory phenotype indicated as M2. In the context of neonatal brain injury, it has already been shown that M1/M2 specific genes are upregulated in a time dependent manner (26) and that early M1 activation might be crucial in developing neonatal HI brain injury (27, 28). Recently, we determined an early upregulation of pro-inflammatory cytokines in different brain regions (cortex and hippocampus) in our model of LPS-sensitized HI brain injury, mainly produced by activated microglia (9). Additionally, we hypothesized that the NLRP3 inflammasome is involved in the inflammatory response of microglia in our model (9). Inflammasomes are activated during pathogenic stimulation including NLRPs (13, 29, 30). NLRP3, the most intensively studied inflammasome, has been shown to be involved in many neurological diseases in adults, such as multiple sclerosis, Alzheimer's disease and Parkinson's disease (31). It is a caspase-1 activating multi-protein complex regulating the cleavage of the interleukins 18 and 1β, which are associated with pro-inflammatory processes (32). Previously, we detected an activation of the NLRP3 inflammasome 24 h after hypoxia in selected brain regions (cortex and hippocampus) of inflammation-sensitized newborn rats. We believe, that the upregulation of NLRP3 in brains of the LPS/HI group is involved in the activation of M1 microglia, as we detected a microglia specific secretion of IL-1β (9). Therefore, we analyzed the NLRP3 gene expression in CD11b/c sorted microglia of brains from individual groups in the present study. We found an upregulation of NLRP3 gene expression

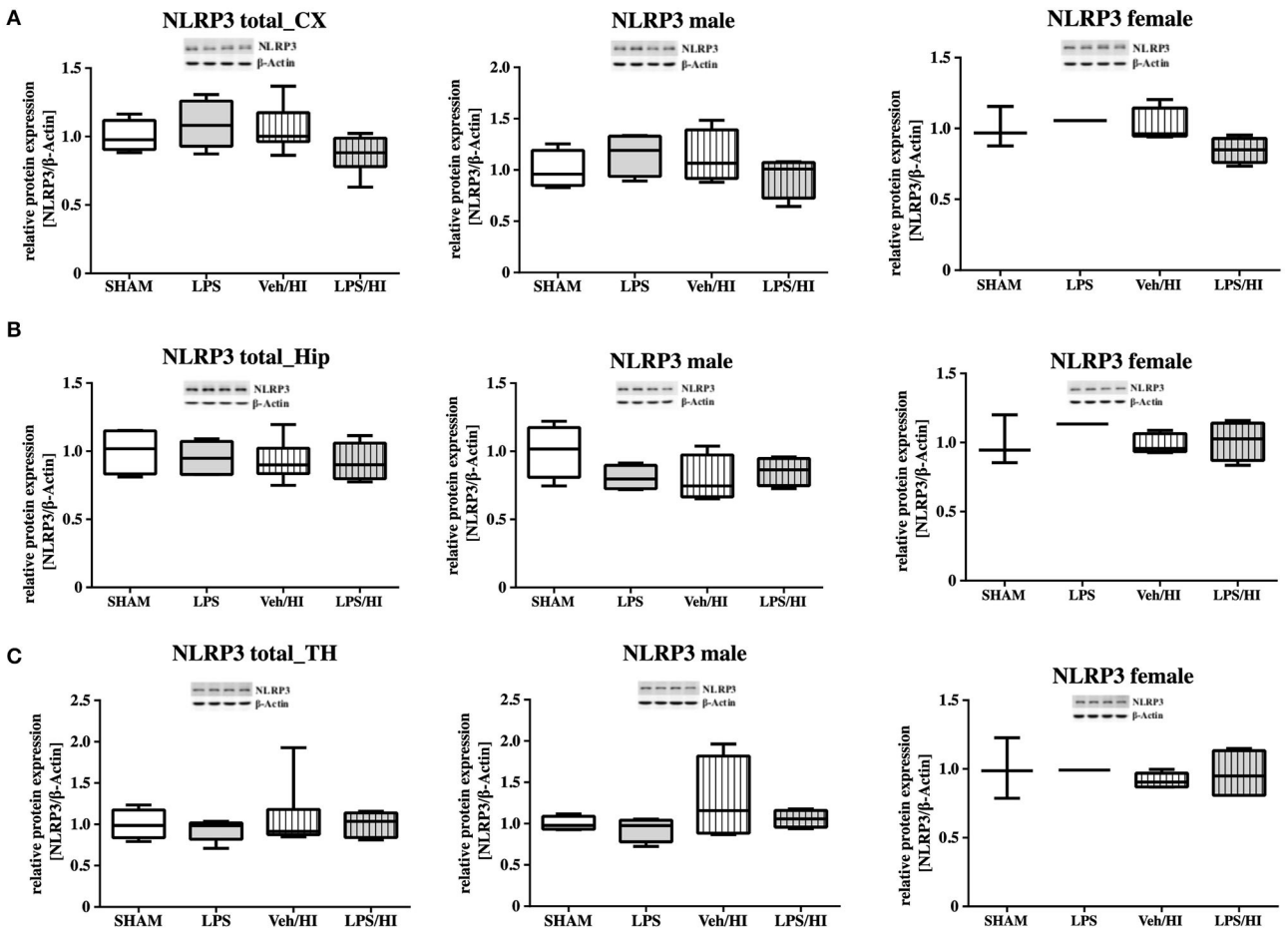

FIGURE 6 | NLRP3 protein expression in different brain regions after inflammation-sensitized hypoxic-ischemic brain injury. Twenty-four hours after hypoxia-ischemia the expression of NLRP3 protein is not regulated in cortex (CX) **(A)**, hippocampus (HIP) **(B)** or thalamus (TH) **(C)** from animals of both genders (Sham $n = 7$, LPS $n = 5$, Veh/HI $n = 9$, LPS $n = 8$). There was no gender differences in any of the groups or analyzed brain regions (Sham $n = 4$ males, LPS $n = 4$ males, Veh/HI $n = 4$ males, LPS $n = 4$ males).

following inflammation-sensitized HI brain injury, suggesting an involvement of the NLRP3 inflammasome as one potential regulatory pathway in LPS-sensitized HI brain injury. Several possible mechanisms activating the NLRP3 inflammasome have been described. The stimulation of Toll-like receptor 4 through LPS triggers the translocation of nuclear factor kappa B into the nucleus and induces the expression of pro-inflammatory genes in microglia involving the NLRP3 inflammasome (33, 34), indicating its role during CNS inflammation. In order to find out which signaling cascades are involved in the pro-inflammatory response of microglia in the LPS/HI group, we investigated the transcriptomic profile of *ex vivo*-isolated microglia from the defined experimental groups. We observed a significant upregulation of different gene clusters. One cluster were gene sets involved in neutrophil migration and neutrophil degranulation. We therefore focused on this set of genes, as neutrophil migration and neutrophil degranulation have been shown to be microglia associated following neonatal brain injury (28). According to our hypothesis that the induced inflammatory process in our model is due to the activation of the NLRP3 inflammasome, we looked at targets which are associated with the activation of the NLRP3 inflammasome. We observed a significant increase of the chemokine receptor CXCR2 in the LPS/HI group compared with the other groups. As previously described in the literature of adult animal models, interaction between CXCL1 and CXCR2 can modulate the activation of the NLRP3 inflammasome (13). However, its function in neonatal brain injury is still unclear and has not been studied under normothermic or hypothermic conditions yet. We investigated the gene expression of the ligand CXCL1 in microglia and showed a significant upregulation in the LPS/HI group comparable with the increased expression of the NLRP3. To clarify whether the modulation of CXCL1 gene expression in the LPS/HI group is also associated with its modulation on protein level, we performed Western-Blot analysis in different brain regions. However, as we performed Western-Blot analysis in brain lysates and not isolated microglia, we determined no different protein regulation between the treatment groups in any of the analyzed brain regions. Region-specific differences in chemokine or inflammasome activation have also been shown by other groups, representing variability in different models. Ystgaard et al. found different distribution of NLRP3 gene upregulation in

their newborn mouse model 24 h post hypoxic-ischemic injury, with a significant upregulation in the hippocampus and thalamus (35). Yellowhair et al. showed that CXCL1/CXCR2 signaling contributes to newborn brain inflammation in an *in-vitro* model of preclinical chorioamnionitis and that blocking the CXCR2 receptor reduces neuroinflammation in different white matter regions (36). Interestingly in our study, we found a gender-specific upregulation of CXCL1 protein level in males in the LPS/HI group compared with the Sham group in the cortex (**Figure 4**). These gender-specific differences might emphasize the findings by Mammun et al., showing inflammatory responses are gender-specific and males are more sensitive to HI brain injury than females (25). This also corresponds to pre-clinical and clinical observations, where males are more sensitive to ischemic insults and have worse outcomes compared to females (37–39). However, this has to be further confirmed in our model.

There are some limitations in our study. First, analyses were performed at a single time point. However, the inflammation process will change over time. Therefore, we need more time-points to understand the time-depended changes in inflammation and to evaluate possible applicable treatments. Second, to analyze if the microglia mediated pro-inflammatory response in the LPS/HI group is regulated specifically through the CXCL1/NLRP3 pathway, we should use a specific antagonist for the CXCR2 receptor, like SB225002, blocking the receptor and the downstream pathway. Furthermore, cell-type specific experimental approaches will be needed to assess the causal relationship between CXCR2 activation and NLRP3 activation and the functional relevance of this pathway for the development of inflammation sensitized hypoxic-ischemic brain injury. Third, although we found gender-specific differences in our western blot results, we were not able to analyze gender differences in our microglia specific analyses, as we used pooled samples of both genders to receive a feasible working concentration of microglia. Therefore, further gender-specific studies need to be performed in our model using microglia, before a gender-specific effect can be assumed. Fourth, we assumed that differences in gene expression would lead to differences in protein expression. However, this is often not the case, as transcription does not automatically lead to translation with the release of proteins (40). Last, we did not include TH in our study. As shown in adult animal models, TH reduces NLRP3 activation and microglia activation after traumatic brain injury (41) or cardiac arrest (42). However, it has been found in a newborn animal study of hypoxic-ischemic encephalopathy, that NLRP3 deficiency increases brain injury (35). Therefore, before we investigate alterations of the CXCR2/NLRP3 pathway under hypothermic conditions, we need to understand the function and role under normothermic conditions.

Our results demonstrate that microglia reveal an early pro-inflammatory response demonstrated by an upregulation of CXCR2, CXCL1 and NLRP3 gene expression following LPS-sensitized HI brain injury in neonatal rats. These findings may contribute to a better understanding of the complex pathophysiology of NE, which is indispensable to develop new treatment options and to improve outcome in asphyxiated newborns, especially in countries with a high prevalence of perinatal infection and associated asphyxia.

DATA AVAILABILITY STATEMENT

The raw data supporting the conclusions of this article will be made available by the authors, without undue reservation, to any qualified researcher.

ETHICS STATEMENT

The animal study was reviewed and approved by State Agency of Nature, Environment and Consumer Protection North Rhine-Westphalia, Germany.

AUTHOR CONTRIBUTIONS

MS and HS have planned and designed the study and have performed the animal experiments. MS, KK, RH, DP, MR, and HS have performed tissue analysis. MS, RH, DP, MR, and HS have analyzed the data. MS, JH, IB, UF-M, and HS have written and corrected the manuscript. All authors contributed to the article and approved the submitted version.

FUNDING

This study was supported by the European Society of Pediatric Research (ESPR), the Elterninitiative Kinderkrebsklinik Düsseldorf e.V., the Deutsche Forschungsgemeinschaft (DFG, German Research Foundation, Project number 422493683), the Bill and Melinda Gates Foundation, and the Federal Ministry of Education and Research (BMBF, grant number 13GW0297).

ACKNOWLEDGMENTS

We would like to thank Mandana Rizazad for technical support during the analysis.

REFERENCES

1. Jacobs SE, Berg M, Hunt R, Tarnow-Mordi WO, Inder TE, Davis PG. Cooling for newborns with hypoxic ischaemic encephalopathy. *Cochrane Database Syst Rev*. (2013) 2013:Cd003311. doi: 10.1002/14651858.CD003311.pub3
2. Gunn AJ, Gunn TR, Gunning MI, Williams CE, Gluckman PD. Neuroprotection with prolonged head cooling started before postischemic seizures in fetal sheep. *Pediatrics*. (1998) 102:1098–106. doi: 10.1542/peds.102.5.1098
3. Robertson NJ, Hagmann CF, Acolet D, Allen E, Nyombi N, Elbourne D, et al. Pilot randomized trial of therapeutic hypothermia with serial cranial ultrasound and 18-22 month follow-up for neonatal encephalopathy in a low resource hospital setting in Uganda: study protocol. *Trials*. (2011) 12:138. doi: 10.1186/1745-6215-12-138
4. Grether JK, Nelson KB. Maternal infection and cerebral palsy in infants of normal birth weight. *Jama*. (1997) 278:207–11. doi: 10.1001/jama.1997.03550030047032

5. Tann CJ, Nakakeeto M, Willey BA, Sewegaba M, Webb EL, Oke I, et al. Perinatal risk factors for neonatal encephalopathy: an unmatched case-control study. *Arch Dis Child Fetal Neonatal Ed*. (2018) 103:F250–f256. doi: 10.1136/archdischild-2017-312744
6. Osredkar D, Thoresen M, Maes E, Flatebo T, Elstad M, Sabir H. Hypothermia is not neuroprotective after infection-sensitized neonatal hypoxic-ischemic brain injury. *Resuscitation*. (2014) 85:567–72. doi: 10.1016/j.resuscitation.2013.12.006
7. Osredkar D, Sabir H, Falck M, Wood T, Maes E, Flatebo T, et al. Hypothermia Does Not Reverse Cellular Responses Caused by Lipopolysaccharide in Neonatal Hypoxic-Ischaemic Brain Injury. *Dev Neurosci*. (2015) 37:390–7. doi: 10.1159/000430860
8. Falck M, Osredkar D, Wood TR, Maes E, Flatebo T, Sabir H, et al. Neonatal systemic inflammation induces inflammatory reactions and brain apoptosis in a pathogen-specific manner. *Neonatology*. (2018) 113:212–20. doi: 10.1159/000481980
9. Serdar M, Kempe K, Rizazad M, Herz J, Bendix I, Felderhoff-Muser U, et al. Early Pro-inflammatory microglia activation after inflammation-sensitized hypoxic-ischemic brain injury in neonatal rats. *Front Cell Neurosci*. (2019) 13:237. doi: 10.3389/fncel.2019.00237
10. Moser B, Willimann K. Chemokines: role in inflammation and immune surveillance. *Ann Rheum Dis*. (2004) 63 Suppl 2:ii84–ii89. doi: 10.1136/ard.2004.028316
11. Semple BD, Kossmann T, Morganti-Kossmann MC. Role of chemokines in CNS health and pathology: a focus on the CCL2/CCR2 and CXCL8/CXCR2 networks. *J Cereb Blood Flow Metab*. (2010) 30:459–73. doi: 10.1038/jcbfm.2009.240
12. Jin L, Batra S, Douda DN, Palaniyar N, Jeyaseelan S. CXCL1 contributes to host defense in polymicrobial sepsis via modulating T cell and neutrophil functions. *J Immunol*. (2014) 193:3549–58. doi: 10.4049/jimmunol.1401138
13. Boro M, Balaji KN. CXCL1 and CXCL2 Regulate NLRP3 inflammasome activation via G-protein-coupled receptor CXCR2. *J Immunol*. (2017) 199:1660–71. doi: 10.4049/jimmunol.1700129
14. Hedtjarn M, Leverin AL, Eriksson K, Blomgren K, Mallard C, Hagberg H. Interleukin-18 involvement in hypoxic-ischemic brain injury. *J Neurosci*. (2002) 22:5910–9. doi: 10.1523/JNEUROSCI.22-14-05910.2002
15. Gustin A, Kirchmeyer M, Koncina E, Felten P, Losciuto S, Heurtaux T, et al. NLRP3 inflammasome is expressed and functional in mouse brain microglia but not in astrocytes. *PLoS ONE*. (2015) 10:e0130624. doi: 10.1371/journal.pone.0130624
16. Serdar M, Herz J, Kempe K, Lumpe K, Reinboth BS, Sizonenko SV, et al. Fingolimod protects against neonatal white matter damage and long-term cognitive deficits caused by hyperoxia. *Brain Behav Immun*. (2016) 52:106–19. doi: 10.1016/j.bbi.2015.10.004
17. Wood T, Osredkar D, Puchades M, Maes E, Falck M, Flatebo T, et al. Treatment temperature and insult severity influence the neuroprotective effects of therapeutic hypothermia. *Sci Rep*. (2016) 6:23430. doi: 10.1038/srep23430
18. Livak KJ, Schmittgen TD. Analysis of relative gene expression data using real-time quantitative PCR and the 2(-Delta Delta C(T)) Method. *Methods*. (2001) 25:402–8. doi: 10.1006/meth.2001.1262
19. Brehmer F, Bendix I, Prager S, Van De Looij Y, Reinboth BS, Zimmermanns J, et al. Interaction of inflammation and hyperoxia in a rat model of neonatal white matter damage. *PLoS ONE*. (2012) 7:e49023. doi: 10.1371/journal.pone.0049023
20. Neumann J, Henneberg S, Von Kenne S, Nolte N, Müller AJ, Schraven B, et al. Beware the intruder: real time observation of infiltrated neutrophils and neutrophil-Microglia interaction during stroke *in vivo*. *PLoS ONE*. (2018) 13:e0193970. doi: 10.1371/journal.pone.0193970
21. Song L, Pei L, Yao S, Wu Y, Shang Y. NLRP3 Inflammasome in Neurological Diseases, from Functions to Therapies. *Front Cell Neurosci*. (2017) 11:63. doi: 10.3389/fncel.2017.00063
22. Tann CJ, Nakakeeto M, Hagmann C, Webb EL, Nyombi N, Namiiro F, et al. Early cranial ultrasound findings among infants with neonatal encephalopathy in Uganda: an observational study. *Pediatr Res*. (2016) 80:190–6. doi: 10.1038/pr.2016.77
23. Wintermark P, Boyd T, Gregas MC, Labrecque M, Hansen A. Placental pathology in asphyxiated newborns meeting the criteria for therapeutic hypothermia. *Am J Obstet Gynecol*. (2010) 203:579.e571–579. doi: 10.1016/j.ajog.2010.08.024
24. Iadecola C, Anrather J. The immunology of stroke: from mechanisms to translation. *Nat Med*. (2011) 17:796–808. doi: 10.1038/nm.2399
25. Al Mamun A, Yu H, Romana S, Liu F. Inflammatory Responses are Sex Specific in Chronic Hypoxic-Ischemic Encephalopathy. *Cell Transplant*. (2018) 27:1328–39. doi: 10.1177/0963689718766362
26. Hellstrom Erkenstam N, Smith PL, Fleiss B, Nair S, Svedin P, Wang W, et al. Temporal characterization of microglia/macrophage phenotypes in a mouse model of neonatal hypoxic-ischemic brain injury. *Front Cell Neurosci*. (2016) 10:286. doi: 10.3389/fncel.2016.00286
27. Cowell RM, Plane JM, Silverstein FS. Complement activation contributes to hypoxic-ischemic brain injury in neonatal rats. *J Neurosci*. (2003) 23:9459–68. doi: 10.1523/JNEUROSCI.23-28-09459.2003
28. Mallard C, Tremblay ME, Vexler ZS. Microglia and neonatal brain injury. *Neuroscience*. (2019) 405:68–76. doi: 10.1016/j.neuroscience.2018.01.023
29. Wen H, Miao EA, Ting JP. Mechanisms of NOD-like receptor-associated inflammasome activation. *Immunity*. (2013) 39:432–41. doi: 10.1016/j.immuni.2013.08.037
30. Guo H, Callaway JB, Ting JP. Inflammasomes: mechanism of action, role in disease, and therapeutics. *Nat Med*. (2015) 21:677–87. doi: 10.1038/nm.3893
31. Strowig T, Henao-Mejia J, Elinav E, Flavell R. Inflammasomes in health and disease. *Nature*. (2012) 481:278–86. doi: 10.1038/nature10759
32. Latz E, Xiao TS, Stutz A. Activation and regulation of the inflammasomes. *Nat Rev Immunol*. (2013) 13:397–411. doi: 10.1038/nri3452
33. O'callaghan JP, Kelly KA, Vangilder RL, Sofroniew MV, Miller DB. Early activation of STAT3 regulates reactive astrogliosis induced by diverse forms of neurotoxicity. *PLoS ONE*. (2014) 9:e102003. doi: 10.1371/journal.pone.0102003
34. Cunha C, Gomes C, Vaz AR, Brites D. Exploring New Inflammatory Biomarkers and Pathways during LPS-Induced M1 Polarization. *Mediators Inflamm*. (2016) 2016:6986175. doi: 10.1155/2016/6986175
35. Ystgaard MB, Scheffler K, Suganthan R, Bjørås M, Ranheim T, Sagen EL, et al. Neuromodulatory effect of NLRP3 and ASC in neonatal hypoxic ischemic encephalopathy. *Neonatology*. (2019) 115:355–62. doi: 10.1159/000497200
36. Yellowhair TR, Newville JC, Noor S, Maxwell JR, Milligan ED, Robinson S, et al. CXCR2 blockade mitigates neural cell injury following preclinical chorioamnionitis. *Front Physiol*. (2019) 10:324. doi: 10.3389/fphys.2019.00324
37. Hill CA, Fitch RH. Sex differences in mechanisms and outcome of neonatal hypoxia-ischemia in rodent models: implications for sex-specific neuroprotection in clinical neonatal practice. *Neurol Res Int*. (2012) 2012:867531. doi: 10.1155/2012/867531
38. Demarest TG, Mccarthy MM. Sex differences in mitochondrial (dys)function: Implications for neuroprotection. *J Bioenerg Biomembr*. (2015) 47:173–88. doi: 10.1007/s10863-014-9583-7
39. Charriaut-Marlangue C, Besson VC, Baud O. Sexually dimorphic outcomes after neonatal stroke and hypoxia-ischemia. *Int J Mol Sci*. (2017) 19:61. doi: 10.3390/ijms19010061
40. Neale DB, Wheeler NC. Gene expression and the transcriptome. In: *The Conifers: Genomes, Variation and Evolution*. Cham: Springer International Publishing (2019). p. 91–117. doi: 10.1007/978-3-319-46807-5_6
41. Zhang F, Dong H, Lv T, Jin K, Jin Y, Zhang X, et al. Moderate hypothermia inhibits microglial activation after traumatic brain injury by modulating autophagy/apoptosis and the MyD88-dependent TLR4 signaling pathway. *J Neuroinflammation*. (2018) 15:273. doi: 10.1186/s12974-018-1315-1
42. Zhou M, Wang P, Yang Z, Wu H, Huan Z. Spontaneous hypothermia ameliorated inflammation and neurologic deficit in rat cardiac arrest models following resuscitation. *Mol Med Rep*. (2018) 17:2127–36. doi: 10.3892/mmr.2017.8113

Conflict of Interest: The authors declare that the research was conducted in the absence of any commercial or financial relationships that could be construed as a potential conflict of interest.

frontiers in Neurology

REVIEW
published: 22 October 2020
doi: 10.3389/fneur.2020.568814

Midkine: The Who, What, Where, and When of a Promising Neurotrophic Therapy for Perinatal Brain Injury

Emily Ross-Munro[1†], Faith Kwa[1,2†], Jenny Kreiner[1], Madhavi Khore[1], Suzanne L. Miller[3], Mary Tolcos[1], Bobbi Fleiss[1,4†] and David W. Walker[1†]*

[1] Neurodevelopment in Health and Disease Research Program, School of Health and Biomedical Sciences, Royal Melbourne Institute of Technology (RMIT), Melbourne, VIC, Australia, [2] School of Health Sciences, Swinburne University of Technology, Melbourne, VIC, Australia, [3] The Ritchie Centre, Hudson Institute of Medical Research, Monash University, Clayton, VIC, Australia, [4] Neurodiderot, Inserm U1141, Universita de Paris, Paris, France

Midkine (MK) is a small secreted heparin-binding protein highly expressed during embryonic/fetal development which, through interactions with multiple cell surface receptors promotes growth through effects on cell proliferation, migration, and differentiation. MK is upregulated in the adult central nervous system (CNS) after multiple types of experimental injury and has neuroprotective and neuroregenerative properties. The potential for MK as a therapy for developmental brain injury is largely unknown. This review discusses what is known of MK's expression and actions in the developing brain, areas for future research, and the potential for using MK as a therapeutic agent to ameliorate the effects of brain damage caused by insults such as birth-related hypoxia and inflammation.

Keywords: midkine, neurotrophins, hypoxia, neuroinflammation, perinatal brain damage, preterm birth

OPEN ACCESS

Edited by:
Carl E. Stafstrom, Johns Hopkins Medicine, United States

Reviewed by:
Dinesh Upadhya, Manipal Academy of Higher Education, India
Diego Iacono, Biomedical Research Institute of New Jersey, United States

****Correspondence:***
David W. Walker
David.Walker@rmit.edu.au

† These authors share first and last authorship

Specialty section:
This article was submitted to Pediatric Neurology, a section of the journal Frontiers in Neurology

Received: *02 June 2020*
Accepted: *18 September 2020*
Published: *22 October 2020*

Citation:
Ross-Munro E, Kwa F, Kreiner J, Khore M, Miller SL, Tolcos M, Fleiss B and Walker DW (2020) Midkine: The Who, What, Where, and When of a Promising Neurotrophic Therapy for Perinatal Brain Injury. Front. Neurol. 11:568814. doi: 10.3389/fneur.2020.568814

INTRODUCTION

The structural and functional development of the brain depends on neurotrophic factors that drive the growth, differentiation, and migration of neural precursor cells. Midkine (MK) and pleiotrophin (PTN) are structurally and functionally related neurotrophic factors and are the only two members of the neurite growth-promoting factor family. MK is called midkine because it was originally identified as a cyto*kine* highly expressed in *mid*-gestation in many organs of the mouse, particularly the kidneys, heart, and brain (1, 2). PTN expression has a different pattern, increasing from birth and persisting into adulthood (3, 4). However, expression of MK in the adult is induced following many forms of injury, and in many forms of cancer (5), where it mediates hypoxic or inflammatory-driven cell response pathways (6, 7). Previous work has demonstrated the potential therapeutic efficacy of MK for repair and regeneration after ischemic brain damage (8) and in seizure (9), and drug addiction-related brain injuries (10). Specifically, MK has been shown to ameliorate cell death, modulate glial reactivity, and enhance proliferation and migration of neural precursor cells (8, 10). MK also promotes hypoxia-induced angiogenesis (11) and serves as a chemoattractant for leukocytes (12). However, the therapeutic potential of MK following injury to the developing CNS has yet to be explored.

In this review, we discuss the spatiotemporal expression of MK and some of its key receptors during neurodevelopment and the function of MK following injury-induced expression. Both highlight the potential for the use of MK as a treatment for perinatal brain damage. We also interrogated gene expression databases to bring together the developmental and

cell specific expression of MK and where possible PTN and their receptors. Perinatal brain damage arises from events such as fetal hypoxia, birth asphyxia, exposure to *in utero* and postnatal inflammation/infection (e.g., chorioamnionitis, sepsis), and/or preterm birth. These global problems in perinatology all too often result in death or life-time disabilities (13, 14), and account for around 2.4% of the total Global Burden of Disease (15). These disabilities include cerebral palsy, mild cognitive deficits, learning difficulties, epilepsy, and pervasive behavioral deficits such as autism spectrum disorders (16). At the present time, the treatment options for perinatally acquired brain damage are very limited. The option for impending preterm birth is intrapartum use of magnesium sulfate preterm birth, but there are no postnatal therapies. The option for term-born infants diagnosed with neonatal encephalopathy (NE) linked to hypoxia-ischemia (HI), (hypoxic-ischemic encephalopathy, HIE) is hypothermia (head alone, or whole-body cooling), which is only effective if commenced within 6 h of birth and requires specialized medical facilities (17, 18). In both cases, lives are saved and outcomes are improved, but the number needed to treat (NNT) for intrapartum use of magnesium sulfate is between 42 and 74 to see a significant reduction in rates of cerebral palsy (18, 19), and the NNT is 7 for hypothermia to see a reduction in mortality and severe morbidity (20), meaning there are still many more infants that need help. This is despite considerable efforts to find adjunct therapies for use with hypothermia (21), and additional therapies for all infants. As such, there remains a strong unmet need for treatments that can be delivered easily and quickly, and over a wider window of time after birth. The focus of this review is to evaluate the potential for MK to meet this need. We surveyed publications listed on PubMed using the search term MK, and then MK coupled with cancer, brain, neuroprotection, infant, neonate, birth, HIE, prematurity, and other terms as shown in **Table 1**. Of the 956 papers captured, only 22 (2.3%) were linked to studies in infants, neonates, brain, and/or birth, 1 was linked to prematurity and preterm birth, and *none* was linked to HIE or other commonly associated conditions of fetal injury such as intrauterine growth restriction. This demonstrates the great paucity of studies of MK in relation to the cause and treatment of perinatally acquired brain injury in the human neonate, despite the clear potential that MK has in this regard that we will outline in this review.

TABLE 1 | Details of the spectrum of publications related to Midkine (MK), highlighting the vast number of works across areas such as cancer, but the striking lack of research in the area of perinatal brain injury (PubMed search, August 20, 2020).

Search term	Number of PubMed hits	Hits relevant to the intended search for MK in perinatal brain injury
Midkine	956 (98 reviews)	–
Midkine AND Cancer	431 (41 reviews)	–
Midkine AND Brain	158 (14 reviews)	–
Midkine AND Neuroprotection	18 (5 reviews)	–
Midkine AND Nanoparticle	8	–
Midkine AND Inflammation	92 (12 reviews)	–
Midkine AND Infant AND Brain	3	1 (22)
Midkine AND Neonatal AND Brain	7	0
Midkine AND Perinatal AND Brain	7	0
Midkine AND Premature or Preterm birth	6	1 (23)
Midkine AND Hypoxic-ischemic Encephalopathy	0	0
Midkine AND Fetal Growth restriction OR intrauterine growth restriction	0	0

MIDKINE PROPERTIES

MK is a secreted, low molecular weight (13–18 kD) basic heparin-binding protein (24). MK has a 46% homology to pleiotrophin (PTN), and both share trophic and cytokine-signaling activities. MK consists of 121 amino acids (25) and is highly endowed with the positively charged basic amino acids-arginine, lysine, and histidine (26). The mRNA and protein of mouse and human MK are similar (27), with the amino acid sequence predicted to have an 83% homology (28). The protein structure of MK is composed of N-terminal and C-terminal halves linked by five disulfide bonds. The C-terminal portion of MK holds a strong conformation-dependent heparin binding site that is needed for full expression of the neurite extension and plasminogen activator activities, but not for promoting cell survival (25, 29). It is noteworthy that the effects of MK on neuronal outgrowth and survival are highly dependent on the sulfate groups (30).

MK binds to highly sulfated structures in the glycosaminoglycan chain of proteoglycans, namely, chondroitin sulfate-E structures and the tri-sulfated structure in heparin sulfate disaccharide units prevalent on the cell surface and within the extracellular matrix (31). In fact, MK protein is the ligand for several receptor-type proteins implicated in various physiological roles as described in **Table 2**. Though this provides an array of potential therapeutic targets, these receptors also have several potential ligands, and this has created difficulty in defining the exact functions of MK.

DEVELOPMENTAL EXPRESSION OF MIDKINE

MK gene expression is regulated by retinoic acid, a derivative of vitamin A (43, 44). MK's role in promoting cell proliferation, differentiation, and mitogenic senescence during development is once it shares with other *trans*-retinoic acid or retinoic-derived gene products (45, 46). The most complete understanding of

TABLE 2 | MK receptor-ligand binding and signaling functions.

MK binding receptors	Biological functions	References
Protein tyrosine phosphatase ζ (PTPZ)	◦ Promotes survival of embryonic neurons ◦ Expressed on LRP6 and apoE receptor 2 (components of reelin, Wnt, and Dickkopf receptors) neurons ◦ Antiapoptotic activity with combined effects of PP1 and PTX—inhibitors of G protein-linked signaling ◦ Promotes migration of embryonic neurons	(32, 33)
Ryudocan (Syndecan-4)	◦ Expressed abundantly in peripheral bundle nerves ◦ Interacts with tissue factor pathway inhibitor ligand ◦ Function in anticoagulant function and inhibits placental cytotrophoblasts	(34)
Syndecan-1	◦ Expressed in brain and spinal cord during earlier gestational period—E10 to E12 ◦ Promotes neurogenesis	(35)
N-syndecan (Syndecan-3)	◦ Interacts with MK during late developmental period—E14 to E16 ◦ Promote neurogenesis	(35)
Low-density lipoprotein receptor-related protein (LRP)	◦ Promotes nucleus translocation ◦ Internalizes MK in the cytoplasm-bound nucleolin, a nucleocytoplasmic shuttle protein ◦ Promotes cell survival	(36)
Neuroglycan C	◦ Promotes CG-4 cells (glial precursors for oligodendrocyte progenitor cells) ◦ Promotes elongation in glial cells	(37)
β-integrins—$\alpha_6\beta1$ integrin and $\alpha_4\beta1$ integrin	◦ $\alpha_4\beta1$ integrin promotes migration of osteoblastic cells ◦ $\alpha_4\beta1$ integrin governs haptotactic migration of osteoblastic cells ◦ Increase tyrosine phosphorylation of paxillin, a key molecule in Crk-II pathway ◦ $\alpha_6\beta1$ integrin promotes neurite outgrowth on embryonic neurons	(38)
Lipopolysaccharide-binding (LBP) receptor—member of low-density lipoprotein receptors	◦ Activates LBP adhesion in the cytoplasm and cell surfaces ◦ Activates and acts as "shuttle protein" in translocating into nucleus ◦ Promotes tumorigenesis process	(39)
Anaplastic lymphoma kinase (ALK)	◦ Mitogenesis-potent proliferation of human endothelial cells from brain microvasculature and umbilical vein ◦ Promotes angiogenesis ◦ Activates Akt phosphorylation by 10-fold, with 2-fold increase in MAPK phosphorylation ◦ Activates NF-κB pathway ◦ Induces insulin receptor-1 to initiate mitogenesis and antiapoptosis ◦ Activates PI3K and MAPK pathways in varying ratio and response in cell types	(40–42)

ALK, anaplastic lymphoma kinase; ApoE, apolipoprotein E; LBP, lipopolysaccharide-binding; LRP, low-density lipoprotein receptor-related protein; MAPK1, mitogen-activated protein kinase 1; MAPK3, mitogen-activated protein kinase 3; NF-kB, nuclear factor kappa-light-chain-enhancer of activated B cells; PTX, paclitaxel; PI3K, phosphatidylinositol-3-kinase; Akt, protein kinase B; PP1, protein phosphatase 1.

the developmental expression of MK and PTN comes from zebrafish and the altricial mouse and rat. In the sections below, we outline this data and highlight what little is known for humans, while also presenting data available from public datasets, as summarized in **Figures 1–5**. In contrast to the staging of developmental events in rodent (and of course zebrafish), in humans, organogenesis occurs predominantly *in utero*. Therefore, it is subject to the influence of the maternal and intrauterine environment, and to the influence of hormones and growth factors released by the placenta (47, 48). In this regard, study of model pregnancies closer to human pregnancy might be very important. For instance, it is known that glucocorticoids negatively regulate MK expression (49). Specifically, glucocorticoids downregulate MK expression in alveolar cells isolated from fetal mouse lungs, and prolonged and exaggerated MK expression occurs in adult mice lacking the glucocorticoid receptor (49). Hence, the observation that MK decreases after mid-gestation in some species might reflect the increased fetal glucocorticoid secretion that occurs toward the end of gestation, a process required for functional maturation of many organs, including the lungs (50, 51), heart (52), and gut (53).

Prenatal Expression

As indicated above, MK is named due to its high expression in mid-gestation. This expression pattern in humans is highlighted in **Figure 1**, but this data is from total cortical extracts, hiding any cell-specific variance. Cell-type specific analysis using RNA-sequencing across fetal and adult time points revealed that across cell-types, MK expression is approximately 10-fold greater in *Mus musculus* (house mouse) when compared to that of humans (**Figure 2**). The most complete ontogenic description of mammalian MK expression comes from rodents (summarized in **Table 3**), for which localization of MK and PTN proteins overlap in the embryonic stages (see also **Figures 2–5**). In the mouse, intense expression of MK mRNA can be detected as early as embryonic day 5 (E5) in the ectoderm and in the allantois and chorion of the placental tissues (54). Then by E8.5, MK expression is found throughout the whole mouse embryo as well as in the extra-embryonic membranes (amnion and yolk sac) (54), and in the placenta at E11.5 (55). Also, in the mouse embryo, strong MK mRNA is present throughout the developing cortical plate at E14.5 and E15.5 (**Figures 3**, **4**), and is also present in the jaw, hindlimb bud, skin, placental capillary endothelial cells, brain, and spinal cord (44) (**Figure 3**).

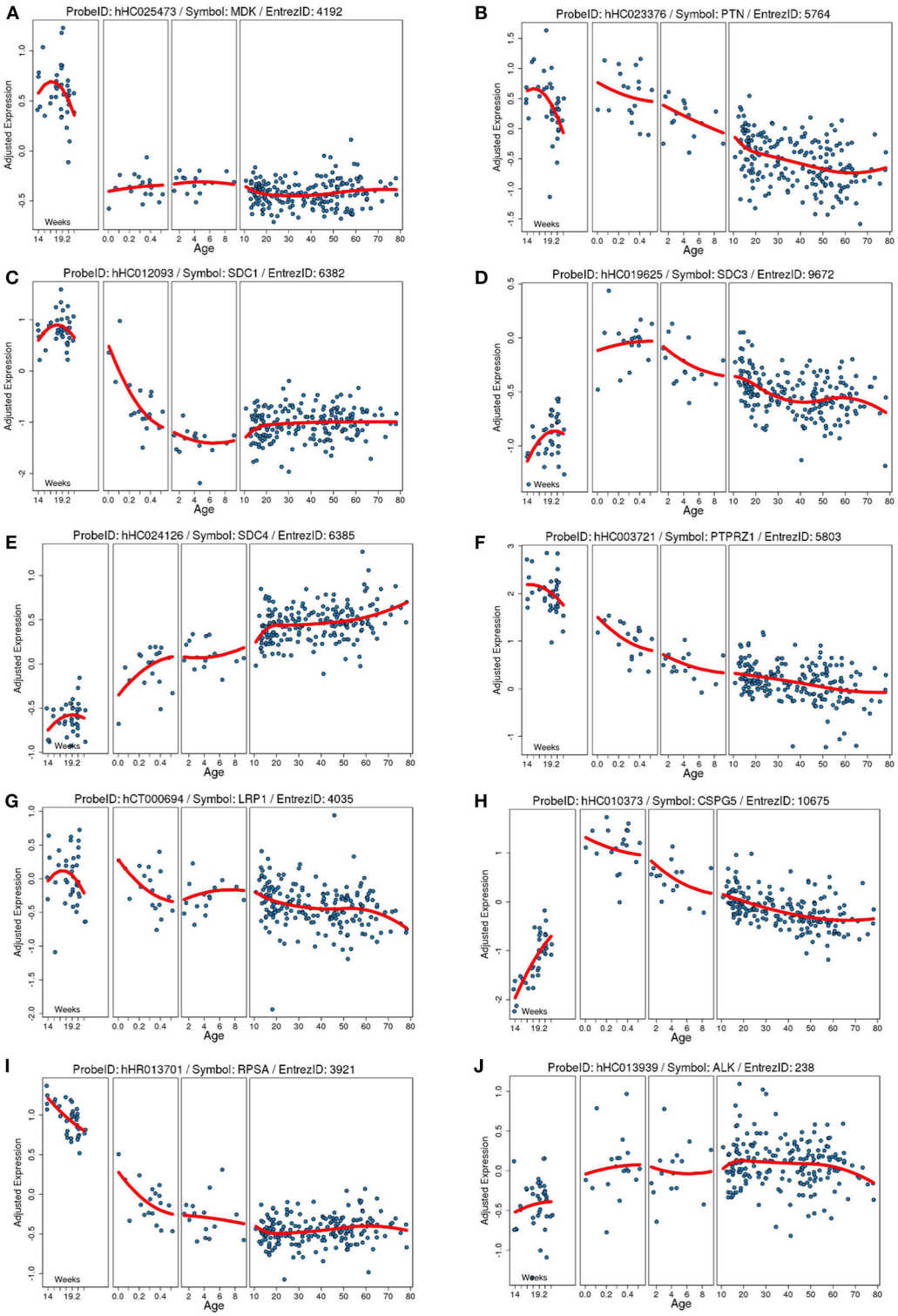

FIGURE 1 | Developmental expression of human mRNA in the cortex for our proteins of interests and known receptors. Each plot shows the gene expression from a frontal cortical sample on the Y axis (age) adjusted to the total average global gene expression across timepoints. Each blue dot is an individual human sample, and the red line is the moving average of gene expression. Age on the Y axis is in weeks of gestation (far right) and then in years after birth. **(A)** Midkine (*MDK*). **(B)** Pleiotrophin (*PTN*). **(C)** Syndecan-1 (*SDC1*). **(D)** Syndecan-3 (*SDC3*). **(E)** Syndecan-4 (*SDC4*). **(F)** Protein tyrosine phosphatase ζ (*PTPRZ1*). **(G)** Low-density lipoprotein receptor-related protein (LRP1). **(H)** Neuroglycan C/chondroitin sulfate proteoglycan 5 (*CSPG5*). **(I)** Laminin binding protein precursor/40S ribosomal protein SA (*RPSA*). **(J)** Anaplastic lymphoma kinase (*ALK*). Data collated from the http://braincloud.jhmi.edu/.

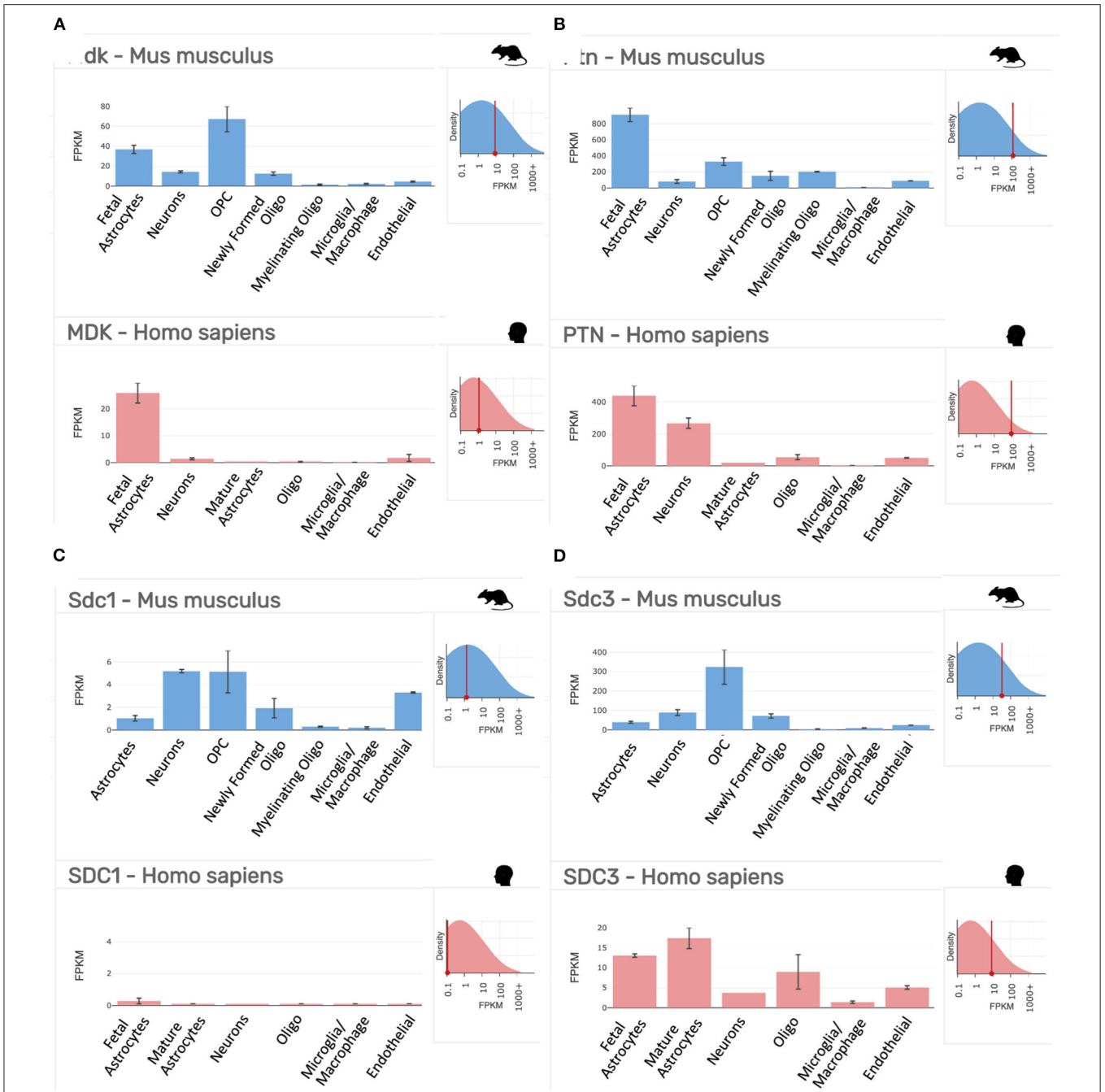

FIGURE 2 | Gene expression profiling data of our targets of interest in purified cell populations from the mouse (*Mus musculus*, blue) and human (*Homo sapiens*, red) at stages of development as indicated. **(A)** Midkine (*Mdk/MDK*). **(B)** Pleiotrophin (*Ptn/PTN*). **(C)** Syndecan-1 (*Sdc1/SDC1*). **(D)** Syndecan-3 (*Sdc3/SDC3*). FPKM, fragments per kilobase of transcript per million mapped reads = the relative expression of a transcript. Top right inset on each panel shows the overall expression of the gene relative to all transcripts in the analysis. Data collated from the http://www.brainrnaseq.org/.

In rats, MK protein immunoreactivity (IR) is found in the ventricular zone of the cerebral vesicle at E10, whereas little PTN-IR is detected here at this time. By E17 in the rat, both MK and PTN-IR emerge radially from the ventricular zone into the telencephalon, and dual expression is most intense in the intermediate zone and subventricular zones beneath the subplate. Moderate expression of MK and PTN is found within the subplate, and most importantly, coexpression in the cortical plate is localized to the radial glial processes (56)–a network that governs migration of postmitotic neurons (57). Expression patterns for MK protein at E17 (4) and MK mRNA at E14.5 and E15.5 are similar (**Figures 3**, **4**).

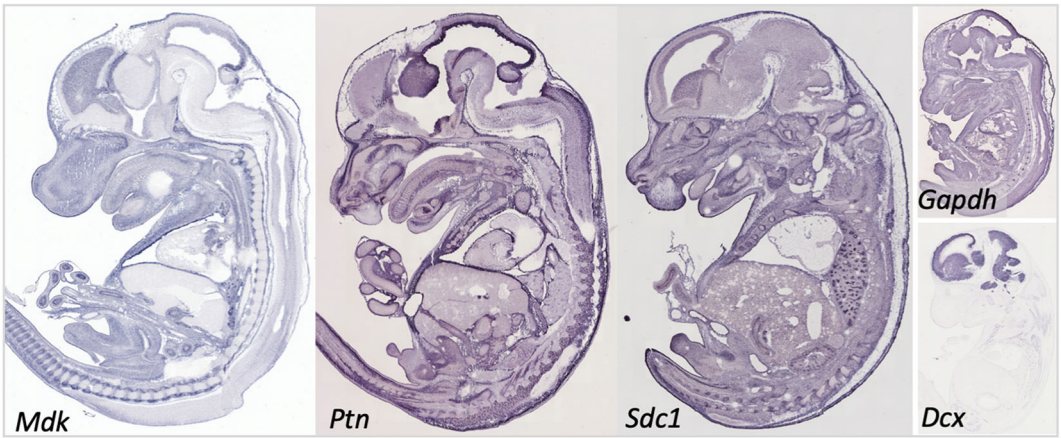

FIGURE 3 | Gene expression in the embryonic day 14.5 mouse embryo for midkine (*Mdk*), pleiotrophin (*Ptn*), and syndecan-1 (*Sdc1*). Data for Syndecan-3 (*Sdc3*) not available. Data for the common reference gene glyceraldehyde 3-phosphate dehydrogenase (*Gapdh)* and the immature neuronal gene doublecortin (Dcx) shown to help understand the relative intensity in our targets. Data collated from Genepaint: https://gp3.mpg.de/.

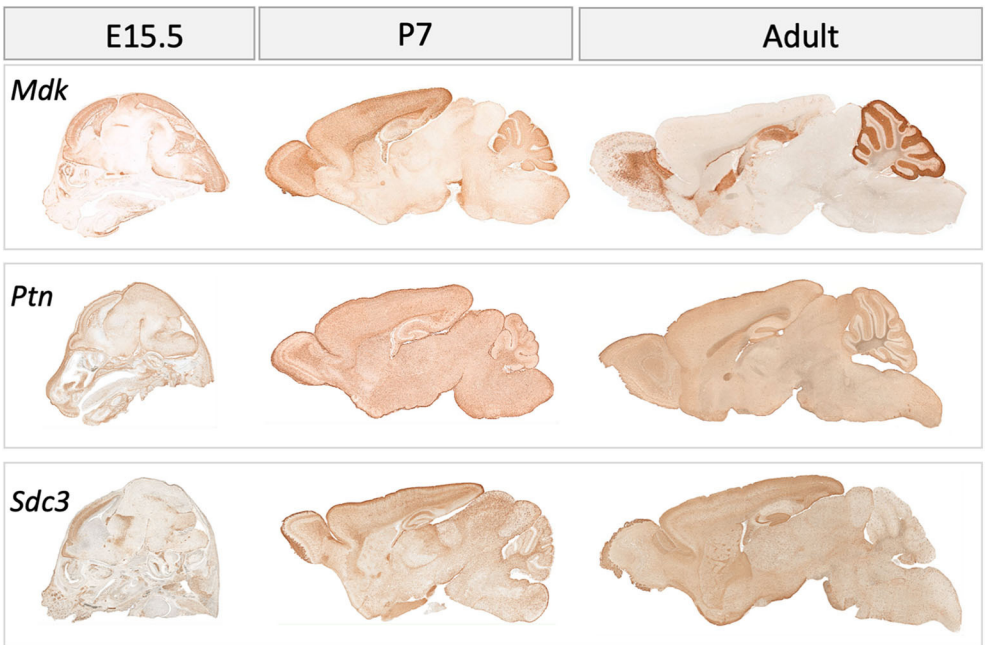

FIGURE 4 | Gene expression in the mouse brain at embryonic (E) day 15.5, postnatal day (P) 7 and in adulthood for midkine (*Mdk*), pleiotrophin (*Ptn*), Syndecan-3 (*Sdc3*). Data for Syndecan-1 (*Sdc1*) not available. Data collated from GENSAT: http://www.gensat.org/index.html.

Of note, in human pregnancies, MK and PTN proteins are present in amniotic fluid in normal mid-term pregnancy, during preterm labor with or without rupture of the membranes, and at term with and without labor (58); the significance is discussed further below.

Postnatal Expression of Midkine

In postnatal life (P7), protein expression for MK in the forebrain of the rat is now largely restricted to the choroid plexus (4). However, there is an obvious discrepancy in this restricted protein expression and mRNA levels, as mRNA data shows that mRNA for MK is still robustly expressed at P7 across the cortex (**Figure 4**). On the other hand, PTN protein shows a distinct spatiotemporal pattern of expression during completion of cortical lamination—corresponding to the inside—out development of the cortex (**Table 3**) (4). Specifically, PTN-IR is localized in the cell surface of neuronal cell bodies and processes and is intensely expressed in the marginal layer at P1, and cortical layer I at P7 and P14. PTN-IR is also robust in the corpus callosum when assessed at P7, localized in the

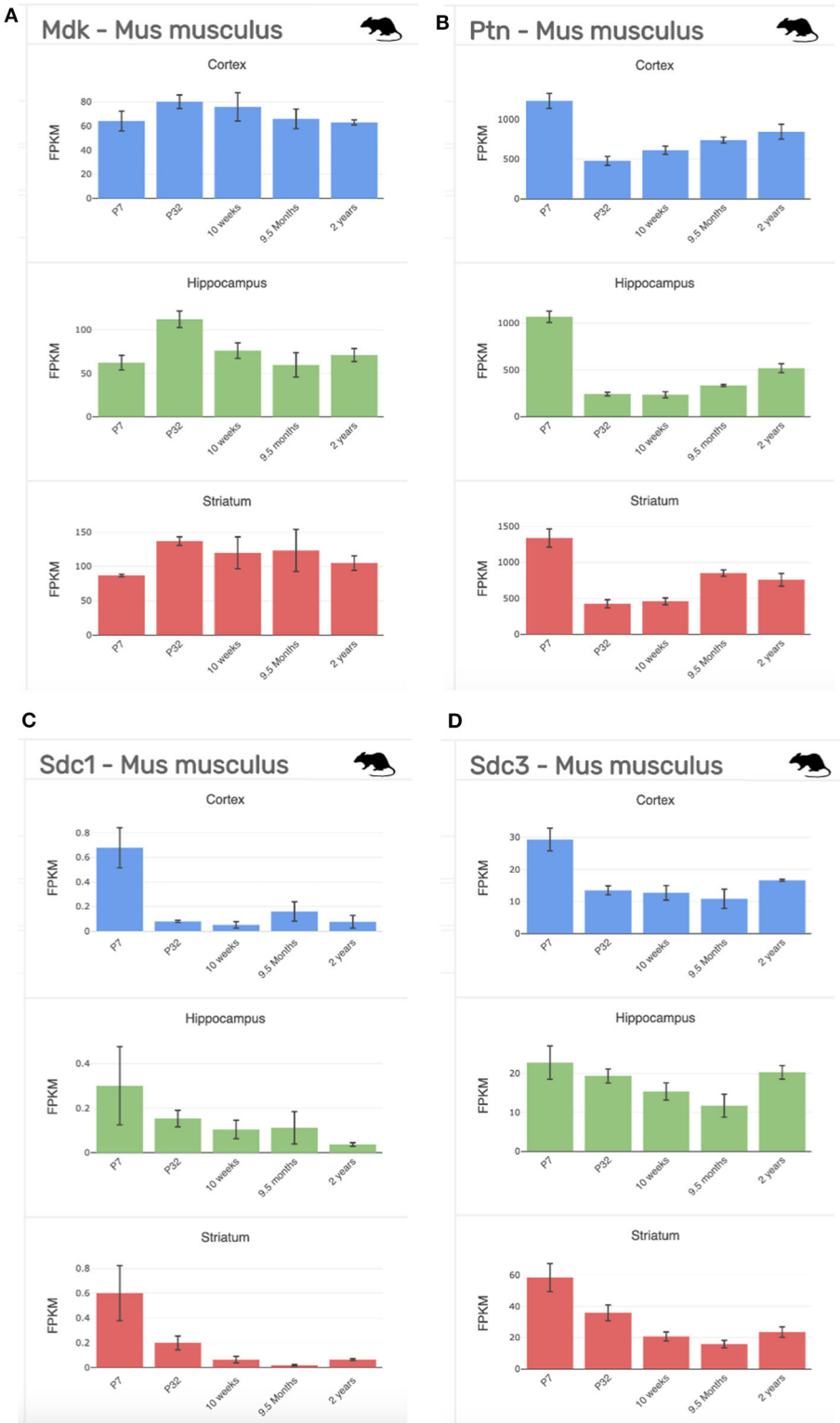

FIGURE 5 | Gene expression profiling data of our targets of interest at stages across development (P7-2 years) and across regions of the brain (cortex, blue; hippocampus, green; striatum, red) from the mouse (*Mus musculus*). **(A)** Midkine (*Mdk*). **(B)** Pleiotrophin (*Ptn)*. **(C)** Syndecan-1 (*Sdc1*); **(D)**. Syndecan-3 (*Sdc3*). FPKM, fragments per kilobase of transcript per million mapped reads = the relative expression of a transcript. Data collated from http://www.brainrnaseq.org/.

TABLE 3 | Developmental expression of MK and pleiotrophin (PTN) in the rat brain.

	Location	Embryonic (E) or postnatal (P) days	PTN expression	MK expression	References
Prenatal cerebral cortex	Ventricular zone	E10	⇧	⇧⇧	(4)
	Ventricular zone	E14	⇧⇧	⇧⇧	
	Preplate	E14	⇧	⇧⇧	
	Ventricular zone and intermediate zone	E17	⇧⇧⇧	⇧⇧⇧	
	Subplate	E17	⇧⇧	⇧⇧	
	Cortical plate	E17 and E18	⇧⇧	⇧⇧	
Postnatal cerebral cortex	Choroid plexus	P7	Not detected	⇧⇧⇧	(4)
	Corpus callosum	P7	⇧⇧⇧	Not detected	
	Cortical plate, marginal layer, and layer V	P1	⇧⇧⇧		
	Layer VI	P1	⇧⇧		
	Layers I, III, and IV	P7	⇧⇧⇧		
	Layers II, V, and VI	P7	⇧⇧		
	Layers I, II, III, V	P14	⇧⇧⇧		
	Layer IV and VI	P14	⇧⇧		
Postnatal cerebellum	PLZ, PM, ML and PCL	P1	⇧⇧⇧	⇧	(3)
	EGL, ML and PCL and WM	P3 and P5	⇧⇧	⇧⇧	
	IGL	P3 and P5	⇧	⇧	
	EGL, ML and PCL and WM	P7	⇧⇧⇧	⇧⇧⇧	
	IGL	P7	⇧	⇧	
	IGL WM	P14	⇧⇧⇧	Not detected	
	ML and PCL	P14	Not detected		

EGL, external granular layer; IGL, internal granular layer; MK, midkine; ML, molecular layer; PTN, pleiotrophin; PMZ, pre-migratory zone; PLZ, proliferative zone; PCL, Purkinje cell layer; WM, white matter.

axoplasm and, to a lesser extent, the surface of callosal fibers. In the forebrain, PTN-IR intensity peaks at P7–P14, consistent with other reports of PTN mRNA peaking at around this age before decreasing progressively into adulthood in humans (**Figure 1**) and in rats (4, 59). Across postnatal life in rats (P7–2 years), mRNA studies indicate that the regional heterogeneity in expression of MK and its associated receptors continues (**Figure 4**).

In the developing rat cerebellum in early postnatal life, MK and PTN protein are coexpressed (3) (see **Table 3**). From P1 to P5, PTN protein expression is found in the cerebellar cortex; at P3, MK protein expression is colocalized with PTN, and MK-IR reaches similar levels to PTN by P5. Most importantly, at P7, intense expression of both proteins is colocalized to neural and glial processes extending downward from the external granular layer, through the molecular layer and Purkinje cell layer, with weaker expression in the internal granular layer but with intense expression in the white matter. This pattern of expression is associated with Bergmann glial processes (3, 60)—a cerebellum-specific radial glial network that mediates migration of postmitotic neurons (61). Expression of MK diminishes from P7 to P14, while PTN-IR becomes restricted to the internal granular layer and the white matter (4). This comprehensive study of MK and PTN protein covered the developmental ages of E17, P7, and P14, but mRNA data for MK in the adult rat cerebellum (**Figure 4**) illustrates a robust expression of MK transcript in the molecular layer that is worth further investigation.

Developmental Importance of MK Expression

During embryonic and early postnatal development in these altricial rodents, both MK and PTN are highly expressed in neurites and glial cell extensions (3, 4) and are key in regulating neurite outgrowth (62–64), earning their membership in the neurite outgrowth family. Co-expression of PTN and MK in the embryonic stages of forebrain development is prominent in regions where cell migration and neurite outgrowth occurs (4), and the same is also true for the postnatal cerebellum, where MK and PTN likely combine to mediate the development of fiber networks (3).

Gene expression and protein studies suggest that MK signaling in the rat embryo occurs predominantly through members of the Syndecan (Synd) family, namely, Synd-1 and Synd-3 (35). Each of the four Synd family members have a specific, developmentally regulated pattern of tissue expression—with high expression of the Synd-1 receptor before birth, which then decreases postnatally, and high expression of the Synd-3 receptor from immediately after birth (**Figures 1–3**) (65). However, both receptor proteins are expressed during mid-gestation, with expression of Synd-1 at E10-12, and Synd-3 at E10-16—implicating both in the early construction of the CNS from the neural tube (66). Despite this, Synd-1 or Synd-3 knockout (KO) mice are viable and fertile (67–69). However, Synd-1 KO mice present with a growth restricted phenotype, being, on average, 15% smaller in weight throughout the first 4 months of life, and this is detected as early as E17.5 (69).

In addition, Synd-3 KO mice exhibit impaired migration of glia and neurons in the cerebral cortex during development, resulting in fewer neurons residing in the superficial cortical laminae when assessed later in adult life (68). Both MK and PTN facilitate neurite outgrowth *in vitro* (43, 70), and so MK and PTN signaling via the Synd-3 receptor during corticogenesis is implicated in axonal/neural migration. Moreover, Synd-3 KO mice exhibit enhanced long-term potentiation in the CA1 region of the hippocampus, resulting in impaired memory formation as assessed using water maze and fear conditioning assays (67).

As outlined in mRNA datasets in **Figure 2**, Synd-3 is more highly expressed than Synd-1 in both *Mus musculus* and humans. More importantly, RNA sequencing suggests that the density of Synd-1 expression is approximately 100-fold less in humans than that of the *Mus musculus*, and this difference is 50-fold less for Synd-3. It is unknown currently if these differences are real (71), and if they are, whether there are differences in protein abundance or stability in humans that counteract any higher expression of the mouse mRNA. Irrespective, it is an example of how results from rodent experiments must be interpreted cautiously considering that this difference may indicate fundamental physiological differences between organisms that prevent simple extrapolation of findings (72).

Difficulties in understanding the specific role of MK come from the fact that MK interacts with several receptors (**Table 2**), each of which have numerous potential ligands, thus limiting the ability to delineate the activity of MK through receptor blockade or KO studies. Also, there are structural and functional similarities and complex feedback loops in actions between MK and PTN. These lead to redundancy, illustrated by the fact that (73), to date, there are no conditional KO mice for MK to provide more nuanced data on functions. Nevertheless, MK KO mice do still show an abnormal phenotype (74). Brain-specific structural abnormalities in MK KO studies include delayed hippocampal development, as shown by a transient abnormal increase in calretinin in the granule cell layer of the dentate gyrus (75). However, at this young adult stage of life for a rat, behavioral analysis unveiled that MK KO mice exhibit increased anxiety and impaired working memory assessed via the elevated plus maze test and y-maze test, respectively. (67), suggesting that MK activity via Synd-3 may serve to modulate hippocampal synaptic plasticity. MK KO mice also exhibit reduced striatal dopamine content, which has been interpreted as an increased vulnerability for development of behavioral disorders such as schizophrenia and autism, and abnormal serum levels of MK have been reported in people with these behaviors (76).

MK/PTN double KO (DKO) mice have been previously produced by cross breeding mice heterozygous for MK and PTN deficiency. DKO mice are born at one third the expected frequency based on Mendelian segregation (77). The authors attributed this to lethality occurring prior to E14.5; however, no histological abnormalities of organ architecture were found at this stage, and an earlier assessment was not made. DKO mice present with a severe postnatally developing growth retardation (50% reduction at 4 weeks of age) not corrected with high-calorie postnatal feeding (77). As mentioned previously, Synd-1 KO mice also present with a growth-restricted phenotype evident as early as E17.5 (69). We speculate that MK and PTN signaling via Synd-1 may be of functional importance during growth and may provide key insights for exploring interventions to ameliorate fetal growth restriction. MK/PTN DKO mice at 4 weeks of age exhibit 40–50% reduction in the spontaneous locomotor activity compared to wild-type (WT) mice, with the difference resolving somewhat to a 20% deficit at 3 months of age (77). Interestingly, MK, KO, and/or PTN KO mice have auditory deficits, but in the case of DKO, the deficit is more severe, consistent with a role for both PTN and MK in regulating the tectorial membrane proteins α- and β-tectorin that are crucial proteins for cochlear development (78).

MK and PTN proteins are present in the amniotic fluid from at least midgestation to birth in normal pregnancies and those disrupted by preterm labor (58). The functional significance and the source of these heparin-binding growth factors in amniotic fluid are unclear. It is known that both MK and PTN are expressed during development of the epithelial-mesenchymal interactions in the fetal lung (2, 49) and gastrointestinal tract (2), and MK is expressed in embryonic mouse keratinocytes in the epidermis (79). As such, MK in the amniotic fluid may be participating in, or be a by-product of, the development of the epithelia of the lung, gastrointestinal tract, and skin. Of course, fetal urine is a major contributor to amniotic fluid, and amniotic MK may also come from the fetal kidney, consistent with the observation that MK is highly and constitutively expressed in the kidney (80) and is involved in kidney nephrogenesis in the fetal rat (81). The human fetus swallows amniotic fluid regularly for at least the last half of pregnancy, and as such, amniotic MK may have a role in promoting development of the luminal epithelium of the gastrointestinal tract. Finally, given the current interest in the use of amniotic stem cells for regenerative repair of perinatal brain damage (82), it is worth investigating if amniotic MK enhances the survival and potential for further differentiation of these cells, as already shown for neurogenic stem cells *ex vivo* (58, 83).

NEUROPROTECTION AND REPAIR

We outline in this section, the primary neuropathological processes occurring in perinatal brain injuries and how these may be influenced by MK. A summary of these processes for encephalopathy of prematurity (EoP) and NE linked to HI is given in **Table 4** together with a summary of proposed MK approaches. The focus of this review is perinatal brain injury, but it is highly likely that MK would also be useful for targeting damaging processes occurring during adult brain injury, such as stroke or traumatic brain injury (8, 87). Injury process do differ by age though, for example, that cell death in the developing brain is more likely to occur via a caspase-dependent process (88) and that microglia are in a "brain building" mode in the developing brain, compared to an adult homeostatic role (89). We wish to highlight that the developmental window in which a perinatal injury occurs is a key determiner of the type of damage that is caused (see **Figure 6**). For example, in preterm born infants, there is a widespread interneuronopathy as these

cells are still migrating throughout the last trimester, a period of development disturbed by their early birth (91, 92). Interneuron damage in neonatal stroke and HIE is limited to the region of frank cell loss (93, 94). A role for HIE in preterm born infants is not conclusively supported (95), but oxygen variability is a likely contributor to injury (96). Also, myelination deficits are predominantly localized in areas such as the posterior limb of the internal capsule and the corona radiata in infants with HIE (97, 98). However, in infants with EoP, white matter injury is diffuse due to the vulnerability of populations of oligodendrocytes across the brain, and this leads to global connectivity deficits (99). Other key factors governing the specific pathogenesis include insult severity, patient population (ethnicity, social demographics), and standards of care/availability of care.

TABLE 4 | An outline of the common neuropathological processes occurring in babies born preterm (with EoP) and those born at term with NE linked to HI (HIE) [as reviewed by (84–86)] and the current available therapies (18–20) and proposed application of MK.

Neuropathology	EoP	NE linked to HI	Potential target for Midkine
Microgliosis	Yes	Yes	Yes
Astrogliosis	Yes, when birth <23 weeks of GA	Yes	Yes
Neuronal death	Limited	Yes	Yes
Oligo. death	In severe cases	Yes	Yes
Oligo. dysmaturation	Yes	No	Yes
Interneuron dysmaturation	Yes	No	Possibly
	Treatments		**Potential midkine therapy**
Description	Magnesium sulfate	Hypothermia	Midkine
Timing/route	At least 1 h before birth, IV	72 h continuous cooling (32–33°C) initiated within 6 h of birth	Acute IV boli, and/or chronic intranasal
Efficacy (NNT)	No change in mortality, decreased CP (74)	Reduced mortality and rates of NDD (7)	To be determined

EoP, encephalopathy of prematurity; NE, neonatal encephalopathy; HI, hypoxia-ischemia; GA, gestational age; Oligo, oligodendrocyte; CP, cerebral palsy; IV, intravenous; NNT, number to treat; NDD, neurodevelopmental disability.

MK Expression Following Injury

Following hypoxic and/or inflammatory injury, there is induction in MK expression. Specifically, MK has been shown to mediate response to injury by suppressing programmed cell death (apoptosis), modulating the glial response, propagating peripheral immune cell recruitment, stimulating angiogenesis, and enhancing proliferation and migration of neural stem cells—all of which will be discussed further below.

The MK gene harbors response elements specific to signals arising from hypoxia and inflammation (6, 40), two conditions that are frequently associated with perinatal brain damage. The hypoxia response element in the promotor region of MK (6) binds with the transcription factor, hypoxia-inducible factor 1α (HIF-1α). MK itself also increases HIF-1α expression creating a positive feedback loop for signal propagation (6). Hypoxic upregulation of MK expression likely explains the MK expression observed in tumors, where higher levels correlate with a worse prognosis (100, 101). The MK promoter region also possesses a putative nuclear factor kappa light-chain enhancer of activated B cells (NFκB) response element (7, 40). Stimuli that induce NFκB activation include reactive oxygen species, proinflammatory cytokines such as tumor necrosis factor α (TNFα) and interleukin-1β (IL-1β), and the bacterial

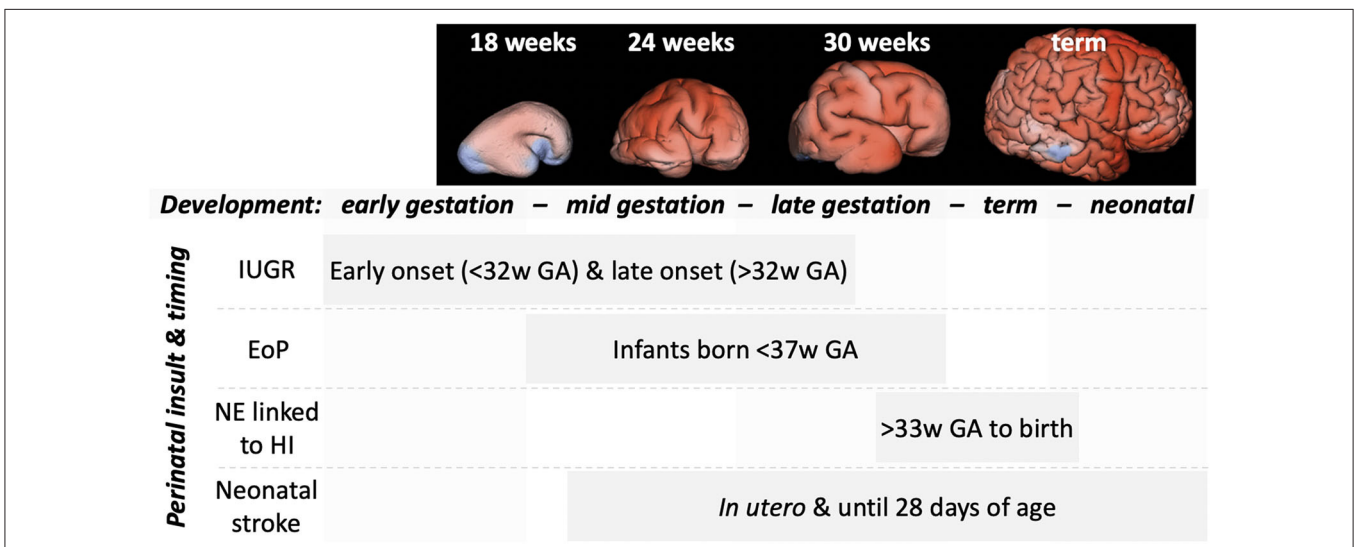

FIGURE 6 | An outline of the timing of the more common perinatal insults relative to gross brain development. MRI panels adapted from Vasung et al. (90). Top, representative MRI reconstructions showing the striking changes in brain development across the weeks of gestational development. Bottom, indications of the timing (weeks of gestational age) of common perinatal insults.

endotoxin, lipopolysaccharide (LPS) (102–105). MK expression can be upregulated during many forms of inflammatory reaction (102–105). Consistent with this, an elegant study that used a prostate adenocarcinoma cell line showed that induction of MK expression following TNFα exposure occurs in an NFκB-dependent manner (7).

Cell Death

Many studies demonstrate that MK is involved in the suppression of apoptosis (9, 106–108). For instance, MK treatment in serum-starved cortical neuronal cultures from E17 rats attenuates expression of caspase-3 via rapid activation of the ERK and Akt pathways by MK (106). This finding is consistent with other *in vivo* evidence that MK has an antiapoptotic effect by downregulating caspase-3 in hepatocellular carcinoma and human meningiomas (107, 108). Furthermore, *in vitro* knockdown of the MK gene using small interfering RNA (siRNA) in gastric cancer cell lines inhibits cell growth, upregulates proapoptotic Bax, downregulates antiapoptotic Bcl-2, increases activity of caspases-3, -8, and -9, and increases release of mitochondrial cytochrome c (109). Cell death occurs in the perinatal brain in response to insults including HI in term infants, and it is often ascribed to apoptotic processes (110, 111), and MK may act to ameliorate these events. However, it is not known if MK interacts with the more recently identified necroptotic pathway—a form of cell death that is initiated using the signal transduction mechanisms of apoptosis, but which culminates with a necrotic phenotype (112, 113). Necroptosis is largely mediated via receptor-interaction protein-1 (113) and is a primary contributor to cell death where it is occurring following perinatal brain injury (114–116). As such, it is now important to assess the potential involvement of MK in necroptosis.

Reactive Gliosis

Microglial activation is almost ubiquitously reported across forms of perinatal brain injury, and a causal role for these processes in injury has been demonstrated across paradigms (117, 118). Conversely, a neuroprotective role for microglia is also shown in other experimental settings (119, 120). It is now generally regarded that microglia play numerous different roles in brain injury, dependent on the nature, severity, and stage of development of the injury, and the timepoint of the analysis (121, 122). Analysis of microglia in MK KO mice has found no significant effects on distribution and morphology in adulthood before or after LPS challenge (123). Another study used fluorescently activated cell sorting (FACS) to phenotype microglia from these mice and observed that $MK^{-/-}$ microglia had higher expression of B7-2 (cluster of differentiation-80), macrophage chemotactic protein-1 (MCP-1), and IL-1β, and these differences were lost once the cells were activated with either LPS or interferon γ (IFNγ) (124).

A pathological role for astrocyte activation becomes apparent in infants older than 28 weeks gestational age, linked to maturation of these supportive glia at that time (125–127). These cells increase production of proinflammatory cytokines and proliferate around focal lesions sites (128, 129). As such, activation of astrocytes is reported in post-mortem studies of infants with encephalopathy of prematurity (126, 130) and infants with NE linked to HI (127, 131). As for microglia, astrocytes also play roles in protecting the brain, with injury leading to increased uptake of glutamate, production of antioxidants, and production of trophic factors [as reviewed by (132)]. Animal studies of brain injury, such as transient cerebral ischemia causing damage to the hippocampal CA1 region in adult male rats (133), and kainic acid-induced epileptic seizure injuries in adult male mice (9), show that reactive astrocytes produce MK. Similarly, astrocytes in autopsied adult human brains express MK 4 days after ischemia (134), and MK is produced by fetal human astrocytes in culture (135). Furthermore, following middle cerebral artery occlusion (stroke model) in the rat, MK expression is induced in the reactive astrocytes localized to the zone surrounding the ischemic tissue at 4 to 14 days following stroke (136). Glial-fibrillary acidic protein (GFAP)-IR astrocytes are not only a source of MK but also produce chondroitin sulfate proteoglycans (CSPGs)—broadly considered to impede neuronal regeneration (137). In a rat model of spinal cord injury, MK treatment overrides the inhibitory effects of CSPG's on neurite outgrowth (138). Specifically, MK treatment significantly improved functional recovery of injured rats as assessed using open field locomotor performance, grip strength, and correct paw placement (138). Importantly, exogenous MK treatment in *in vitro* purified astrocyte and microglia cell cultures did not induce reactive astrocytosis or microgliosis (138).

Adding complexity to the role of MK in modulating reactive gliosis is evidence of the response being stimulus dependent and region specific. For example, amphetamine-induced reactive gliosis (GFAP-IR) is enhanced in the striatum of adult MK KO mice compared to WT; however, hippocampal GFAP-IR is reduced (139). In contrast, adult MK KO mice treated with LPS have reduced striatal GFAP-IR compared to WT—and in the prefrontal cortex, there is a decrease in the perimeter and circularity index of ionized calcium binding adaptor molecule 1 (Iba1; marker of microglia/macrophage) cells in MK KO compared to WT (123). Of interest is that MK enhances migration of microglia/macrophage isolated from the forebrain of newborn mice when assessed *in vitro* (140). As such, MK may contribute to the recruitment of microglia following injury to the developing CNS.

Oligodendrocytes and Myelination

Oligodendrocyte maturation occurs via a highly orchestrated set of sequential processes for which many of the numerous regulatory pathways are known (141). How oligodendrocytes are affected in forms of perinatal brain injuries depends on the timing, nature, and severity of the brain injury (142–145). Very generally, research in post-mortem and preclinical models illustrates that severe injury at any time of development can lead to the death of oligodendrocytes (142). Given the antiapoptotic abilities of MK (outlined above), it may be a valid therapy for this negative outcome of perinatal brain injury. In the preterm brain, where injury is severe enough to cause cell loss, there appears to be a compensatory proliferation, but the newly born oligodendrocyte cells then fail to mature (146). In the cases of moderate/mild injury in the preterm born equivalent brain, this

oligodendrocyte dysmaturation occurs without any appreciable preceding cell death (126, 147). Moderate levels of injury are the most prevalent and only 5% are severe, cystic cases (148).

Receptors for MK (listed in **Table 2**) are found on oligodendrocytes, with complex interactions with other maturation pathways. For instance, Fyn tyrosine kinase-mediated downregulation of Rho activity through activation of p190RhoGAP is crucial for oligodendrocyte differentiation and myelination. MK binds to the extracellular region of the protein tyrosine phosphatase receptor type β/ζ (PTPRZ) that is highly expressed by oligodendrocyte progenitors. Interestingly, p190RhoGAP is also a substrate for PTPRZ indicating that the presence of MK can influence the activity of the p190RhoGAP cascade and, as such, oligodendrocyte maturation. It is worth noting that in the adult brain, there is a pool of oligodendrocyte precursors (OPC) responsible for the homeostatic replacement of mature oligodendrocytes (149) and (attempted) replacement of cells in the case of injury (150). PTN, via its inhibitory actions on PTPRZ, supports this homeostatic self-renewal of the OPC pool (151). In oligodendrocytes, PTPRZ signaling has antagonistic roles for PTN and MK, but it is not yet known if MK plays a role in the maintenance of this OPC pool.

There is little work on the effects of MK on oligodendrocytes directly. Preliminary reports indicate that MK exposure increases oligodendrocyte maturation in an immortalized precursor population (OL1 cells) (152). It has similarly been shown that in the oligodendroglia precursor cell line (CG4), MK acted via the neuroglycan C receptor to stimulate process extension (37). Of note, the authors also overexpressed the neuroglycan C receptor in neuroblastoma cells and were able to induce a similar MK-dependent cytoskeletal arrangement, indicating that this is not necessarily a cell type-specific effect.

Looking for further evidence for a role of MK in oligodendrocyte biology, we note that MK mRNA is increased in the demyelinated white matter of the lumber spinal cord in a mouse model of myelin oligodendrocyte glycoprotein-induced experimental autoimmune encephalopathy (EAE) (153). Subsequent studies of MK's role in EAE (124, 154), including experimental MK therapies, have not reported specific data on the basal or post-insult state of the oligodendrocytes or myelin. However, they have reported a causal link between MK and suppression of regulatory T-cell (Treg) proliferation. We assume that these studies had explored, but had not reported, on the "low hanging fruit" of direct effects of MK on oligodendrocytes or myelin in EAE. So then perhaps the lack of information on any effect of MK on oligodendrocytes in such obvious models itself rules out a significant interaction.

Recruitment of Peripheral Immune Cells

In adult animal models of brain injury, MK facilitates the migration of leukocytes to the site of injury, namely, neutrophils and monocytes/macrophages (12, 140). These immune cells are implicated in modulating repair pathways and positive processes such as angiogenesis (155–157). However, an excessive stimulation of these processes is known to exacerbate brain injury (118, 126, 158–160). In models of perinatal brain damage linked to stroke and moderate systemic inflammation, the role of macrophages is minimal (161, 162), but more significant in models involving HI (160, 163). Under hypoxic conditions, both neutrophils and monocytes isolated from adult human blood transiently express MK, peaking after 4 h of exposure to 1% oxygen (11), and MK-IR is localized to both the cell surface and intracellular cytoplasmic vesicles. Following 6 h of hypoxia, MK expression in neutrophils decreases to near baseline levels. After 20 h of hypoxia, Western blotting techniques revealed that MK expression in monocytes resembles that of normoxic conditions; however, immunostaining for MK showed that the cell membrane is almost completely saturated in MK. However, MK is not detected in the supernatant of neutrophils and monocytes, and so it is assumed that it is not secreted from these cells. Instead, MK may participate in autocrine or cell–cell contact-dependent paracrine signaling pathways. An alternate hypothesis (proposed by 11) is that MK is internalized via endocytosis to prevent an excessive inflammatory response, as for IL-1β and the expression of its decoy receptor, IL-1RII.

MK is involved in extravasation of neutrophils. In neutrophils isolated from adult human blood, MK mediates neutrophil extravasation via interaction with low-density lipoprotein receptor-1 (LRP-1), which, in turn, causes conformational changes in β2 integrins promoting adhesion (12). It is unknown if this mechanism of extravasation is age dependent; however, neutrophil extravasation is impaired in MK KO mice *in vivo* following hindlimb ischemia, and blockade of LRP-1 impairs MK binding to neutrophils *in vitro*–suggesting an important role for MK in neutrophil trafficking. Systemic neutrophil responses are elevated in preterm born infants with brain injury (164), but it is not clear if neutrophils have a significant role in the development of brain injury in these infants (162, 165). In term-born brain injury related to HI, neutrophils are clearly involved in the sequence of events as the injury evolves (166–168), and if one effect of MK was to reduce their transmigration, this could be of significant therapeutic benefit.

The chemoattractant properties of MK for recruitment of peripheral immune cells may explain, in part, the results of a recent study on the examined traumatic brain injury (TBI) in MK KO adult mice (87). Here, MK KO mice had reduced levels of apoptosis at 7 days post-TBI as assessed via cleaved caspase 3 expression and showed improved neurological outcomes at 14 days following TBI. Importantly, MK KO mice had reduced microglial/macrophage Iba1-IR at 3 days post-TBI when compared to WT. Using immunohistochemical markers for the proinflammatory-like or M1 (CD16/32+) and anti-inflammatory-like or M2 (arginase1+) phenotypes at 3 days post-TBI, MK KO mice had fewer M1 CD16/32+ cells in the perilesional site. Furthermore, mRNA levels of other M1 markers (e.g., TNFα, CD11b) were reduced in MK KO compared to WT. Flow cytometry was used to segregate macrophages and microglia, and at 3 days post-TBI, MK KO mice had increased levels of M2 arginase1+ microglia and M2 CD163+ macrophages, but fewer M2 arginase1 + macrophages. Thus, these results suggest that MK modulates neuroinflammation by influencing the polarization of microglia toward the M2 phenotype. However, in the case of TBI, blood–brain barrier (BBB) permeability is significantly increased with effects seen

up to 7 days post injury, facilitating leukocyte trafficking to the brain parenchyma (169). As such, the chemotactic properties of MK may potentiate injury to the adult CNS via amplifying recruitment of peripheral immune cells, and this could explain the reported beneficial effect of MK KO in the adult mouse model of TBI (87). Due to known age-dependent differences in BBB permeability, chemokine function, and leukocyte recruitment following CNS injury (170), it will be important to characterize the effect of MK activity in the context of the developing CNS.

Mast cells are first responders in the response of the brain to experimental HI (171, 172). There is a well-known role for mast cells in adult TBI (173, 174); however, the use of cromoglycate in a P14 rat model has shown that they appear to have no effect on injury outcome (175). A role for these cells in the less developed (preterm) brain, possibly via their lesser known homeostatic secretory roles, is unknown. It is logical that MK may have an impact on developing brain injury as it has striking effects on mast cell activation causing rapid and dose-dependent degranulation (176). Mast cells themselves produce MK, and this expression is increased in people with cystic fibrosis, which is linked to the role of MK as a host defense protein (177).

Finally, MK suppresses Treg proliferation by suppressing the activity of tolerogenic dendritic cells (124, 154). To the best of our knowledge, the role of tolerogenic dendritic cells in perinatal brain injuries is not known. Together with the host of effects on other immune cells, MK may influence perinatal brain injury via these populations.

Angiogenesis

Following HI brain injury in the adult human, a robust angiogenic response occurs within 3–4 days (178). However, several studies indicate that in the neonate, this response is limited and occurs much later, and ischemic tissue presents with severe and chronic signs of vascular degeneration spreading beyond the site of injury (179–181). Indeed, a small study has associated the presence of proangiogenic factors in the serum of asphyxiated neonates with better outcomes (181), and although MK does not appear to be critical for the development of the vascular system (11), MK does promote angiogenesis in certain situations. Angiogenesis is severely compromised in MK KO adult mice subjected to occlusion of the right femoral artery (hindlimb ischemia model) as assessed via immunohistochemistry using markers for proliferation (Ki67) and endothelial cells (CD31) (11). Also, treatment with an antisense oligonucleotide targeting MK impairs angiogenesis in the chick chorioallantoic membrane, and reduces tumor progression *in situ* in hepatocellular carcinoma xenografts in mice (182). Indeed, Synd-1 has been implicated in regulating angiogenesis via activation of $\alpha_v\beta_3$ and $\alpha_v\beta_5$ integrins in human vascular endothelial cells *in vitro*, and in mouse mammary tumors *in vivo*, suggesting that activity of MK via Synd-1 may modulate angiogenesis (183). Promoting angiogenesis supports neural regeneration in a model of neonatal stroke (184), and thus, the angiogenic potential of MK following perinatal brain damage may be relevant for exploring strategies to enhance this response.

Notably, endothelial cells are thought to be a major source of soluble MK (11). MK is localized in the Golgi apparatus of human umbilical vein endothelial cells (HUVECs) following 4 h of hypoxia (1% oxygen), and the supernatant of cultured HUVECs contains increased MK levels after 4 and 20 h of hypoxia. Interestingly, intraperitoneal injection of hypoxia-preconditioned HUVECs in a neonatal rat model of HIE ameliorates neuronal apoptosis, stimulates angiogenesis, and attenuates neurovascular damage in the acute and subacute stages of brain injury—and also improves motor and neuropathological outcomes assessed later in adult life (185). The possibility that the beneficial effects of hypoxia-preconditioned HUVEC treatment may be attributable to the actions of MK is worth further investigation.

As mentioned previously, MK facilitates migration and extravasation of neutrophils and macrophages to sites of tissue injury, and these cells promote angiogenesis (186). Thus, MK's angiogenic role may arise as a result of two primary mechanisms: (i) directly by enhancing growth and proliferation of endothelial cells and (ii) indirectly by recruiting neutrophils and macrophages. With regard to the latter, resident brain microglia/macrophages dominate the site of injury in the acute stages following neonatal HI injury in the neonatal rat (161). Also, microglia have been shown to prevent hemorrhage following focal neonatal stroke in rat pups by modulating the neurovascular response (119). As such, in the context of perinatal brain injury, MK may not only enhance angiogenesis but may also facilitate migration of microglia to the damaged vasculature to preserve BBB integrity. Further work is needed to clarify this.

Proliferation and Migration of Stem Cells and Regeneration

Inflammation and hypoxia have the effect of suppressing neuroglial proliferation in the developing brain (187, 188), although specific effects are linked to the severity of HI [as discussed by (189)]. One important effect of MK is that it promotes neural stem cell proliferation and migration, and MK is strongly expressed in migrating neurons and radial glial processes during development of the cerebral cortex and cerebellum in the rat (4). Injection of MK mRNA into the embryos of zebrafish promotes neurogenesis (190), and expression of MK in neural precursor cells in mice promotes their survival and proliferation (191). Viral-mediated short hairpin (sh) RNA knockdown of MK also significantly reduces sympathetic neuron proliferation (42), where MK-mediated proliferation was shown to occur largely through the receptor anaplastic lymphoma kinase (ALK), as shALK and shMK treatment in sympathetic ganglia resulted in a similar reduction in proliferation (42). In zebrafish, the *ALK* ortholog *leukocyte tyrosine kinase* (*ltk)* is critical for neurogenesis of the developing CNS, where its overexpression increases proliferation of neural progenitors (192). Indeed, MK-mediated cell proliferation via ALK activation has been implicated in many cell types and occurs via activation of downstream signal transduction pathways PI3K and MAPK (41).

Unlike mammals, zebrafish can regenerate photoreceptor neurons (193), providing a platform to assess MK's role in neuronal regeneration. The zebrafish has two species-specific MK genes—*mka* and *mkb* (194). Analysis of retinal development and

regeneration in zebrafish identified that *mka* is highly expressed in stem cells destined to be retinal horizontal cells, and in the outer layer of the retina, a prominent site of stem cell differentiation (195). Importantly, *mka* is transiently expressed in Müller cells in the developing retina—a retina-specific radial glial network (195). Conversely, the zebrafish *mkb* is transcribed in newly postmitotic cells deeply entrenched in the inner retinal layers, and in the amacrine cells and other components in the ganglion cell layer (195). During retinal development, MKA protein is localized in the neuroepithelium and the retinal margin and remains localized in the circumferential marginal zone of the retina (196). Following photolytic death of photoreceptors, *mka* adopts a center-to-peripheral pattern of expression in rods and cones as photoreceptor function regenerates (196). Thus, MK may be a trophic factor critical for development of the retina that also mediates regenerative processes. The developing eye is very sensitive to hypoxia and hyperoxia (197, 198)—consistent with reports of retinal atrophy in human infants following perinatal asphyxia (197) and "retinopathy of prematurity" that occurs due to supraphysiological levels of oxygen (198, 199) and exposure to perinatal inflammation (200). Currently, there is no effective treatment to specifically repair the infant's retina from such damage, and MK may provide the effective therapy needed here. This is further supported by research that showed that intravitreal injection of MK rescued retinal damage induced by exposure to high intensity light in adult rats (201).

In a rat focal brain ischemia model utilizing photoembolism, MK overexpression produced by ipsilateral injection of an adenoviral vector into the lateral ventricle 90 min after injury resulted in proliferation of neuronal stem cells, reduction of infarct volume by ∼33%, and an increase in the number of callosal and subventricular neuronal cells expressing other migratory factors (202). These neuroprotective effects of MK gene transfer persisted beyond the acute phase of infarction. Taken together, there is evidence to support MK's therapeutic potential in enhancing neuronal regeneration following injury to the CNS.

CHALLENGES AND POTENTIAL OF MK TREATMENT IN THE PERINATAL PERIOD

As discussed above, MK has been shown to have diverse actions—in a cell type and developmentally regulated manner. These include effects on neurogenesis, neuronal survival, apoptosis, and glial activation across inflammatory and hypoxic CNS insults. There is an obvious promise for the use of MK in neonates with perinatal brain damage, but careful consideration needs to be made to factors such as patient selection (i.e., HIE with or without exposure to additional inflammatory challenge (203), the mode of MK delivery (systemic, intranasal, intracerebroventricular), and the timing to address the acute, secondary, or tertiary phases of injury (204).

Systemic delivery of MK is appealing because alongside the brain, other organs susceptible to inflammatory and hypoxic damage in preterm and term neonates include the heart, lung, kidney, and skeletal muscles, and in particular the diaphragm [reviewed by (205)]. In term-born infants, a focus was on understanding injury to the brain, but it is important to note that NE can develop secondary to cardiac, pulmonary, hepatic, and renal dysfunction, and is often exacerbated by systemic and cerebral inflammation (206, 207). While brain-specific treatment is an obvious clinical goal, there is the need to protect other vital organs, and it is here that MK might offer benefits in addition to the rescue of brain damage. For example, MK has been shown to be cardioprotective in rodent (208), rabbit (209), and pig (210) models of ischemic myocardial infarct by virtue of both its antiapoptotic and potent angiogenic actions, leading to reduced infarct size, less left ventricular scarring, improved cardiac performance, and overall survival (211). Importantly, the intracardiac injection of MK protein ameliorated heart failure not only when delivered at the time of cardiac ischemia/reperfusion injury but also following a delay of up to 14 days post-infarct (208). This important finding suggests that MK treatment might benefit neonates when given at various times after birth. That is, unlike therapeutic hypothermia where the "window of opportunity" to have an impact on perinatal HIE is only hours after birth (17, 212, 213), MK treatment might not be so time critical. It may be with caution that trials of systemic MK are undertaken though, given the plethora of diverse effects of MK on immune cells that may conflict with supportive recovery and overall health of the infant. The complexity of cross-organ effects is shown in studies where a putative therapy, erythropoietin, used to prevent brain damage in preterm born babies (214–216) has damaging effects on the lung in preterm lambs (217, 218). In the case of term born infants, it is also worth noting that therapies need to be tested in relation to hypothermia, the current standard of care. In this case, careful pharmacokinetics need to be assessed as it has recently been shown that cooling can lead to toxic bioaccumulation of potential neurotherapeutics (219).

The BBB in the healthy neonate is functional and more than capable of excluding circulating factors, as reviewed elsewhere (220). There is no specific evidence of the ability (or not) of MK to cross the BBB, although many neurotrophic factors are known to not penetrate the brain parenchyma sufficiently to facilitate neuroprotection (221). Evidence indicates that many forms of perinatal brain injury open the BBB to varying degrees related to the severity of the insult (162, 222–224). This regionally selective opening of the BBB may then be a useful strategy to deliver MK to the sites of injury while keeping it away from the uninjured parts of the brain. Even so, the many pro- and anti-inflammatory systemic effects of MK might mitigate against it as an effective therapeutic agent but highlights the need for more experimental evidence.

The poor penetration of MK into the brain could be assumed to be reflected in the many experimental studies that use delivery of MK by intracerebroventricular or direct intracranial injection (9). Obviously, this delivery route comes with substantial risks in infants, but it is worth noting that MK administration may be no more complicated than the surgical techniques developed for treating intraventricular hemorrhage or hydrocephalus. For example, the DRIFT procedure, necessitating the placement of two shunts into the infant's brain (225), has been able to improve the cognitive quotient of children with severe intraventricular

hemorrhage by as much as 23 points (226). So, although not ideal, as the future of MK testing proceeds, it may be worth including intracerebroventricular delivery as it might directly target brain injury and avoid the side effects of systemic administration.

Two other approaches for MK delivery are of more obvious value for newborn infants. First, the intranasal route, which has been used to deliver diverse proteins to the brains of neonatal and adult experimental animals (e.g., insulin, IGF1, Fgf2, C3a, EGF, anti-tPA, osteopontin) for protection and repair (104, 227–230). What is lacking here is the experimental data on the distribution of MK after nasal delivery. Second, a route in might be mediated by new nanoparticle. For instance, a polyamidoamine dendrimer has been used to successfully deliver n-acetylcysteine to reduce brain injury in a rabbit model of cerebral palsy induced by hypoxia/ischemia (231, 232). In addition, a poly(lactic-co-glycolic acid)-poly(ethylene glycol) (PLGA-PEG) nanoparticle has successfully increased the delivery of the histone deacetylase inhibitor, curcumin, to the brain in a model of term infant NE related to HI (233). An interesting biomaterials approach involves the engineering of nanoparticles to release their "cargo" in response to tissue damage–in this case–in response to acidosis in the brain subsequent to ischemia (234). This approach is valuable because it reduces possible off-target effects of drug delivery. Indeed, highly targeted effects are possible, as shown by Van Steenwinckel et al. who showed that 3DNA nanocarriers administered intraperitoneally not only cross the BBB but are taken up specifically by microglia and not by liver, bone marrow, or spleen macrophages (118). This enables this 3DNA nanoparticles to target peptides, small molecules, siRNA, and microRNA, and as such, could be used to deliver MK itself or an MK modulator. 3DNA nanoparticles are 200-nm diameter constructs that escape the endosome to enable intracellular delivery of the tagged "cargo," and appear to have no toxicity *in vitro* or *in vivo* (235), and can be tagged with fluorophores for tracking—making them an exciting prospect for future studies.

CONCLUSION

Current methods of preventing or treating perinatal brain damage have low success rates, and as such, there is a need to develop novel therapeutic approaches. The evidence summarized here shows the potential for MK, as an endogenous growth factor and cytokine, to be used to mitigate processes associated with perinatal brain injury such as apoptosis and inflammation, as well the possibility of it inducing increased turnover of the endogenous stem cell pools–neural, cardiac, renal, or muscle. However, many of the experiments discussed above were conducted *in vitro* and a few are conducted *in vivo*. *In vivo* testing is always the key, but given the multitude of cell and developmentally regulated effects of MK, it seems to have even greater importance to prove the validity of MK as a potential therapeutic. It will also be important to understand the roles of MK in animal models of development and injury, which incorporate the maternal–placental–fetal unit, such as the precocial spiny mouse (236, 237), or fetal and newborn sheep (165, 238). Current data predominantly comes from altricial species but given the high levels of MK in the amniotic fluid, there is the possibility that preterm birth causes an MK deficiency, and the effect of prematurity and brain injury in these infants warrants attention. Therefore, further *in vivo* investigations are needed to demonstrate the efficacy of MK, and improved drug delivery platforms are warranted to determine how its therapeutic efficacy and bioavailability can be fully realized in the context of perinatal brain injury.

AUTHOR CONTRIBUTIONS

All authors listed have made a substantial, direct and intellectual contribution to the work, and approved it for publication.

ACKNOWLEDGMENTS

We are grateful for the research support from the Cerebral Palsy Alliance (#PG215) and for the informed discussion from Dr. Graham Robertson (CellMid, Inc., Sydney, Australia). Associate Professor Mary Tolcos is an RMIT Vice Chancellor's Senior Research Fellow and Australian Research Council Future Fellow (FT21500082). Dr. Bobbi Fleiss is an RMIT Vice Chancellor's Research Fellow.

REFERENCES

1. Nakamoto M, Matsubara S, Miyauchi T, Obama H, Ozawa M, Muramatsu T. A new family of heparin binding growth/differentiation factors: differential expression of the midkine (MK) and HB-GAM genes during mouse development. *J Biochem.* (1992) 112:346. doi: 10.1093/oxfordjournals.jbchem.a123903
2. Mitsiadis TA, Salmivirta M, Muramatsu T, Muramatsu H, Rauvala H, Lehtonen E, et al. Expression of the heparin-binding cytokines, midkine (MK) and HB-GAM (pleiotrophin) is associated with epithelial-mesenchymal interactions during fetal development and organogenesis. *Development.* (1995) 121:37–51.
3. Matsumoto K, Wanaka A, Mori T, Taguchi A, Ishii N, Muramatsu H, et al. Localization of pleiotrophin and midkine in the postnatal developing cerebellum. *Neurosci Lett.* (1994) 178:216–20. doi: 10.1016/0304-3940(94)90762-5
4. Matsumoto K, Wanaka A, Takatsuji K, Muramatsu H, Muramatsu T, Tohyama M. A novel family of heparin-binding growth factors, pleiotrophin and midkine, is expressed in the developing rat cerebral cortex. *Brain Res Dev Brain Res.* (1994) 79:229–41. doi: 10.1016/0165-3806(94)90127-9
5. Filippou PS, Karagiannis GS, Constantinidou A. Midkine (MDK) growth factor: a key player in cancer progression and a promising therapeutic target. *Oncogene.* (2020) 39:2040–54. doi: 10.1038/s41388-019-1124-8
6. Reynolds PR, Mucenski ML, Le Cras TD, Nichols WC, Whitsett JA. Midkine is regulated by hypoxia and causes pulmonary vascular remodeling. *J Biol Chem.* (2004) 279:37124. doi: 10.1074/jbc.M405254200
7. You Z, Dong Y, Kong X, Beckett L, Gandour-Edwards R, Melamed J. Midkine is a NF-κB-inducible gene that supports prostate cancer cell survival. *BMC Med Genomics.* (2008) 1:6. doi: 10.1186/1755-8794-1-6

8. Takada J, Ooboshi H, Ago T, Kitazono T, Yao H, Kadomatsu K, et al. Postischemic gene transfer of midkine, a neurotrophic factor, protects against focal brain ischemia. *Gene Ther.* (2005) 12:487–93. doi: 10.1038/sj.gt.3302434
9. Kim YB, Ryu JK, Lee HJ, Lim IJ, Park D, Lee MC, et al. Midkine, heparin-binding growth factor, blocks kainic acid-induced seizure and neuronal cell death in mouse hippocampus. *BMC Neurosci.* (2010) 11:42. doi: 10.1186/1471-2202-11-42
10. Herradón G, Pérez-García C. Targeting midkine and pleiotrophin signalling pathways in addiction and neurodegenerative disorders: recent progress and perspectives. *Br J Pharmacol.* (2014) 171:837–48. doi: 10.1111/bph.12312
11. Weckbach L, Groesser L, Borgolte J, Pagel J, Pogoda F, Schymeinsky J, et al. Midkine acts as proangiogenic cytokine in hypoxia-induced angiogenesis. *Am J Physiol Heart Circul Physiol.* (2012) 303:H429–38. doi: 10.1152/ajpheart.00934.2011
12. Weckbach LT, Gola A, Winkelmann M, Jakob SM, Groesser L, Borgolte J, et al. The cytokine midkine supports neutrophil trafficking during acute inflammation by promoting adhesion via β2 integrins (CD11/CD18). *Blood.* (2014) 123:1887–96. doi: 10.1182/blood-2013-06-510875
13. Lawn JE, Cousens S, Zupan J, Lancet Neonatal Survival Steering T. 4 million neonatal deaths: when? Where? Why? *Lancet.* (2005) 365:891–900. doi: 10.1016/S0140-6736(05)71048-5
14. WHO, UNISEF. *Home Visits for the Newborn Child: A Strategy to Improve Survival*. Geneva (2009).
15. Lee AC, Kozuki N, Blencowe H, Vos T, Bahalim A, Darmstadt GL, et al. Intrapartum-related neonatal encephalopathy incidence and impairment at regional and global levels for 2010 with trends from 1990. *Pediatr Res.* (2013) 74(Suppl. 1):50–72. doi: 10.1038/pr.2013.206
16. Ferriero DM. Neonatal brain injury. *N Engl J Med.* (2004) 351:1985–95. doi: 10.1056/NEJMra041996
17. Gluckman PD, Wyatt JS, Azzopardi D, Ballard R, Edwards AD, Ferriero DM, et al. Selective head cooling with mild systemic hypothermia after neonatal encephalopathy: multicentre randomised trial. *Lancet.* (2005) 365:663–70. doi: 10.1016/S0140-6736(05)17946-X
18. Crowther CA, Middleton PF, Voysey M, Askie L, Duley L, Pryde PG, et al. Assessing the neuroprotective benefits for babies of antenatal magnesium sulphate: an individual participant data meta-analysis. *PLoS Med.* (2017) 14:e1002398. doi: 10.1371/journal.pmed.1002398
19. Conde-Agudelo A, Romero R. Antenatal magnesium sulfate for the prevention of cerebral palsy in preterm infants <34 weeks' gestation: a systematic review and meta-analysis. *Am J Obstet Gynecol.* (2009) 200:595–609. doi: 10.1016/j.ajog.2009.04.005
20. Jacobs SE, Berg M, Hunt R, Tarnow-Mordi WO, Inder TE, Davis PG. Cooling for newborns with hypoxic ischaemic encephalopathy. *Cochrane Database Syst Rev.* (2013) 2013:CD003311. doi: 10.1002/14651858.CD003311.pub3
21. Ellery SJ, Kelleher M, Grigsby P, Burd I, Derks JB, Hirst J, et al. Antenatal prevention of cerebral palsy and childhood disability: is the impossible possible? *J Physiol.* (2018) 596:5593–609. doi: 10.1113/JP275595
22. Bergstrom A, Kaalund SS, Skovgaard K, Andersen AD, Pakkenberg B, Rosenorn A, et al. Limited effects of preterm birth and the first enteral nutrition on cerebellum morphology and gene expression in piglets. *Physiol Rep.* (2016) 4:e12871. doi: 10.14814/phy2.12871
23. Albertine KH, Dahl MJ, Gonzales LW, Wang ZM, Metcalfe D, Hyde DM, et al. Chronic lung disease in preterm lambs: effect of daily vitamin A treatment on alveolarization. *Am J Physiol Lung Cell Mol Physiol.* (2010) 299:L59–72. doi: 10.1152/ajplung.00380.2009
24. Tomomura M, Kadomatsu K, Matsubara S, Muramatsu T. A retinoic acid-responsive gene, MK, found in the teratocarcinoma system. Heterogeneity of the transcript and the nature of the translation product. *J Biol Chem.* (1990) 265:10765–70.
25. Inui T, Bodi J, Kubo S, Nishio H, Kimura T, Kojima S, et al. Solution synthesis of human midkine, a novel heparin-binding neurotrophic factor consisting of 121 amino acid residues with five disulphide bonds. *J Pept Sci.* (1996) 2:28–39. doi: 10.1002/psc.45.o
26. Kadomatsu K, Tomomura M, Muramatsu T. cDNA cloning and sequencing of a new gene intensely expressed in early differentiation stages of embryonal carcinoma cells and in mid-gestation period of mouse embryogenesis. *Biochem Biophys Res Commun.* (1988) 151:1312–8. doi: 10.1016/S0006-291X(88)80505-9
27. Uehara K, Matsubara S, Kadomatsu K, Tsutsui J, Muramatsu T. Genomic structure of human midkine (MK), a retinoic acid-responsive growth/differentiation factor. *J Biochem.* (1992) 111:563–7. doi: 10.1093/oxfordjournals.jbchem.a123797
28. Tsutsui J, Uehara K, Kadomatsu K, Matsubara S, Muramatsu T. A new family of heparin-binding factors: strong conservation of midkine (MK) sequences between the human and the mouse. *Biochem Biophys Res Commun.* (1991) 176:792–7. doi: 10.1016/S0006-291X(05)80255-4
29. Akhter S, Ichihara-Tanaka K, Kojima S, Muramatsu H, Inui T, Kimura T, et al. Clusters of basic amino acids in midkine: roles in neurite-promoting activity and plasminogen activator-enhancing activity. *J Biochem.* (1998) 123:1127–36. doi: 10.1093/oxfordjournals.jbchem.a022052
30. Kurosawa N, Kadomatsu K, Ikematsu S, Sakuma S, Kimura T, Muramatsu T. Midkine binds specifically to sulfatide the role of sulfatide in cell attachment to midkine-coated surfaces. *FEBS J.* (2000) 267:344–51. doi: 10.1046/j.1432-1327.2000.01005.x
31. Muramatsu T. Roles of proteoglycans in reception of the midkine signal. *Trends Glycosci Glycotechnol.* (2001) 13:563–72. doi: 10.4052/tigg.13.563
32. Maeda N, Ichihara-Tanaka K, Kimura T, Kadomatsu K, Muramatsu T, Noda M. A receptor-like protein-tyrosine phosphatase PTPzeta/RPTPbeta binds a heparin-binding growth factor midkine. Involvement of arginine 78 of midkine in the high affinity binding to PTPzeta. *J Biol Chem.* (1999) 274:12474–9. doi: 10.1074/jbc.274.18.12474
33. Sakaguchi N, Muramatsu H, Ichihara-Tanaka K, Maeda N, Noda M, Yamamoto T, et al. Receptor-type protein tyrosine phosphatase zeta as a component of the signaling receptor complex for midkine-dependent survival of embryonic neurons. *Neurosci Res.* (2003) 45:219–24. doi: 10.1016/S0168-0102(02)00226-2
34. Kojima T, Katsumi A, Yamazaki T, Muramatsu T, Nagasaka T, Ohsumi K, et al. Human ryudocan from endothelium-like cells binds basic fibroblast growth factor, midkine, and tissue factor pathway inhibitor. *J Biol Chem.* (1996) 271:5914–20. doi: 10.1074/jbc.271.10.5914
35. Nakanishi T, Kadomatsu K, Okamoto T, Ichihara-Tanaka K, Kojima T, Saito H, et al. Expression of syndecan-1 and−3 during embryogenesis of the central nervous system in relation to binding with midkine. *J Biochem.* (1997) 121:197–205.
36. Shibata Y, Muramatsu T, Hirai M, Inui T, Kimura T, Saito H, et al. Nuclear targeting by the growth factor midkine. *Mol Cell Biol.* (2002) 22:6788–96. doi: 10.1128/MCB.22.19.6788-6796.2002
37. Ichihara-Tanaka K, Oohira A, Rumsby M, Muramatsu T. Neuroglycan C is a novel midkine receptor involved in process elongation of oligodendroglial precursor-like cells. *J Biol Chem.* (2006) 281:30857–64. doi: 10.1074/jbc.M602228200
38. Muramatsu H, Zou P, Suzuki H, Oda Y, Chen GY, Sakaguchi N, et al. alpha4beta1- and alpha6beta1-integrins are functional receptors for midkine, a heparin-binding growth factor. *J Cell Sci.* (2004) 117:5405–15. doi: 10.1242/jcs.01423
39. Salama RH, Muramatsu H, Zou K, Inui T, Kimura T, Muramatsu T. Midkine binds to 37-kDa laminin binding protein precursor, leading to nuclear transport of the complex. *Exp Cell Res.* (2001) 270:13–20. doi: 10.1006/excr.2001.5341
40. Kuo AH, Stoica GE, Riegel AT, Wellstein A. Recruitment of insulin receptor substrate-1 and activation of NF-κB essential for midkine growth signaling through anaplastic lymphoma kinase. *Oncogene.* (2007) 26:859. doi: 10.1038/sj.onc.1209840
41. Stoica GE, Kuo A, Powers C, Bowden ET, Sale EB, Riegel AT, et al. Midkine binds to anaplastic lymphoma kinase (ALK) and acts as a growth factor for different cell types. *J Biol Chem.* (2002) 277:35990. doi: 10.1074/jbc.M205749200
42. Reiff T, Huber L, Kramer M, Delattre O, Janoueix-Lerosey I, Rohrer H. Midkine and Alk signaling in sympathetic neuron proliferation and neuroblastoma predisposition. *Development.* (2011) 138:4699–708. doi: 10.1242/dev.072157
43. Rauvala H. An 18-kd heparin-binding protein of developing brain that is distinct from fibroblast growth factors. *EMBO J.* (1989) 8:2933–41. doi: 10.1002/j.1460-2075.1989.tb08443.x

44. Kadomatsu K, Huang RP, Suganuma T, Murata F, Muramatsu T. A retinoic acid responsive gene MK found in the teratocarcinoma system is expressed in spatially and temporally controlled manner during mouse embryogenesis. *J Cell Biol.* (1990) 110:607–16. doi: 10.1083/jcb.110.3.607
45. Matsubara S, Tomomura M, Kadomatsu K, Muramatsu T. Structure of a retinoic acid-responsive gene, MK, which is transiently activated during the differentiation of embryonal carcinoma cells and the mid-gestation period of mouse embryogenesis. *J Biol Chem.* (1990) 265:9441–3.
46. Muramatsu H, Shirahama H, Yonezawa S, Maruta H, Muramatsu T. Midkine, a retinoic acid-inducible growth/differentiation factor: immunochemical evidence for the function and distribution. *Dev Biol.* (1993) 159:392–402. doi: 10.1006/dbio.1993.1250
47. Miller WL. Steroid hormone biosynthesis and actions in the materno-feto-placental unit. *Clin Perinatol.* (1998) 25:799–817. doi: 10.1016/S0095-5108(18)30084-8
48. Quinn TA, Ratnayake U, Dickinson H, Castillo-Melendez M, Walker DW. The feto-placental unit, and potential roles of dehydroepiandrosterone (DHEA) in prenatal and postnatal brain development: a re-examination using the spiny mouse. *J Steroid Biochem Mol Biol.* (2016) 160:204–13. doi: 10.1016/j.jsbmb.2015.09.044
49. Kaplan F, Comber J, Sladek R, Hudson TJ, Muglia LJ, Macrae T, et al. The growth factor midkine is modulated by both glucocorticoid and retinoid in fetal lung development. *Am J Respir Cell Mol Biol.* (2003) 28:33–41. doi: 10.1165/rcmb.2002-0047OC
50. Ballard PL, Ballard RA. Glucocorticoid receptors and the role of glucocorticoids in fetal lung development. *Proc Natl Acad Sci USA.* (1972) 69:2668. doi: 10.1073/pnas.69.9.2668
51. Bolt RJ, Van Weissenbruch MM, Lafeber HN, Delemarre-Van De Waal HA. Glucocorticoids and lung development in the fetus and preterm infant. *Pediatr Pulmonol.* (2001) 32:76–91. doi: 10.1002/ppul.1092
52. Oakley RH, Cidlowski JA. Glucocorticoid signaling in the heart: a cardiomyocyte perspective. *J Steroid Biochem Mol Biol.* (2015) 153:27–34. doi: 10.1016/j.jsbmb.2015.03.009
53. Nanthakumar NN, Klopcic CE, Fernandez I, Walker WA. Normal and glucocorticoid-induced development of the human small intestinal xenograft. *Am J Physiol Regul Integr Comp Physiol.* (2003) 285:R162–70. doi: 10.1152/ajpregu.00721.2001
54. Fan QW, Muramatsu T, Kadomatsu K. Distinct expression of midkine and pleiotrophin in the spinal cord and placental tissues during early mouse development. *Dev Growth Differ.* (2000) 42:113–9. doi: 10.1046/j.1440-169x.2000.00497.x
55. Obama H, Tsutsui J, Ozawa M, Yoshida H, Yoshida Y, Osame M, et al. Midkine (MK) expression in extraembryonic tissues, amniotic fluid, and cerebrospinal fluid during mouse embryogenesis. *J Biochem.* (1995) 118:88–93. doi: 10.1093/oxfordjournals.jbchem.a124896
56. Wanaka A, Carroll SL, Milbrandt J. Developmentally regulated expression of pleiotrophin, a novel heparin binding growth factor, in the nervous system of the rat. *Brain Res Dev Brain Res.* (1993) 72:133–44. doi: 10.1016/0165-3806(93)90166-8
57. García-Moreno F, Molnár Z. Variations of telencephalic development that paved the way for neocortical evolution. *Prog Neurobiol.* (2020). doi: 10.1016/j.pneurobio.2020.101865. [Epub ahead of print].
58. Jee YH, Lebenthal Y, Chaemsaithong P, Yan G, Peran I, Wellstein A, et al. Midkine and pleiotrophin concentrations in amniotic fluid in healthy and complicated pregnancies. *PLoS ONE.* (2016) 11:e0153325. doi: 10.1371/journal.pone.0153325
59. Li Y-S, Milner P, Chauhan A, Watson M, Hoffman R. Cloning and expression of a developmentally regulated protein that induces mitogenic and neurite outgrowth activity. *Science.* (1990) 250:1690. doi: 10.1126/science.2270483
60. Wewetzer K, Rauvala H, Unsicker K. Immunocytochemical localization of the heparin-binding growth-associated molecule (HB-GAM) in the developing and adult rat cerebellar cortex. *Brain Res.* (1995) 693:31–8. doi: 10.1016/0006-8993(95)00683-H
61. Xu H, Yang Y, Tang X, Zhao M, Liang F, Xu P, et al. Bergmann glia function in granule cell migration during cerebellum development. *Mol Neurobiol.* (2013) 47:833–44. doi: 10.1007/s12035-013-8405-y
62. Kojima S, Inui T, Muramatsu H, Kimura T, Sakakibara S, Muramatsu T. Midkine is a heat and acid stable polypeptide capable of enhancing plasminogen activator activity and neurite outgrowth extension. *Biochem Biophys Res Commun.* (1995) 216:574–81. doi: 10.1006/bbrc.1995.2661
63. Mahoney SA, Wilkinson M, Smith S, Haynes LW. Stabilization of neurites in cerebellar granule cells by transglutaminase activity: identification of midkine and galectin-3 as substrates. *Neuroscience.* (2000) 101:141–55. doi: 10.1016/S0306-4522(00)00324-9
64. Yanagisawa H, Komuta Y, Kawano H, Toyoda M, Sango K. Pleiotrophin induces neurite outgrowth and up-regulates growth-associated protein (GAP)-43 mRNA through the ALK/GSK3beta/beta-catenin signaling in developing mouse neurons. *Neurosci Res.* (2010) 66:111–6. doi: 10.1016/j.neures.2009.10.002
65. Muramatsu H, Zou K, Sakaguchi N, Ikematsu S, Sakuma S, Muramatsu T. LDL receptor-related protein as a component of the midkine receptor. *Biochem Biophys Res Commun.* (2000) 270:936–41. doi: 10.1006/bbrc.2000.2549
66. Hsueh YP, Sheng M. Regulated expression and subcellular localization of syndecan heparan sulfate proteoglycans and the syndecan-binding protein CASK/LIN-2 during rat brain development. *J Neurosci.* (1999) 19:7415–25. doi: 10.1523/JNEUROSCI.19-17-07415.1999
67. Kaksonen M, Pavlov I, Voikar V, Lauri SE, Hienola A, Riekki R, et al. Syndecan-3-deficient mice exhibit enhanced LTP and impaired hippocampus-dependent memory. *Mol Cell Neurosci.* (2002) 21:158–72. doi: 10.1006/mcne.2002.1167
68. Hienola A, Tumova S, Kulesskiy E, Rauvala H. N-syndecan deficiency impairs neural migration in brain. *J Cell Biol.* (2006) 174:569–80. doi: 10.1083/jcb.200602043
69. McDermott SP, Ranheim EA, Leatherberry VS, Khwaja SS, Klos KS, Alexander CM. Juvenile syndecan-1 null mice are protected from carcinogen-induced tumor development. *Oncogene.* (2007) 26:1407. doi: 10.1038/sj.onc.1209930
70. Kaneda N, Talukder AH, Nishiyama H, Koizumi S, Muramatsu T. Midkine, a heparin-binding growth/differentiation factor, exhibits nerve cell adhesion and guidance activity for neurite outgrowth *in vitro*. *J Biochem.* (1996) 119:1150–6. doi: 10.1093/oxfordjournals.jbchem.a021361
71. Li JJ, Bickel PJ, Biggin MD. System wide analyses have underestimated protein abundances and the importance of transcription in mammals. *PeerJ.* (2014) 2:e270. doi: 10.7717/peerj.270
72. Lin S, Lin Y, Nery JR, Urich MA, Breschi A, Davis CA, et al. Comparison of the transcriptional landscapes between human and mouse tissues. *Proc Natl Acad Sci USA.* (2014) 111:17224–9. doi: 10.1073/pnas.1413624111
73. Herradon G, Ezquerra L, Nguyen T, Silos-Santiago I, Deuel TF. Midkine regulates pleiotrophin organ-specific gene expression: evidence for transcriptional regulation and functional redundancy within the pleiotrophin/midkine developmental gene family. *Biochem Biophys Res Commun.* (2005) 333:714–21. doi: 10.1016/j.bbrc.2005.05.160
74. Muramatsu T. Midkine, a heparin-binding cytokine with multiple roles in development, repair and diseases. *Proc Jpn Acad Ser B Phys Biol Sci.* (2010) 86:410–25. doi: 10.2183/pjab.86.410
75. Nakamura E, Kadomatsu K, Yuasa S, Muramatsu H, Mamiya T, Nabeshima T, et al. Disruption of the midkine gene (Mdk) resulted in altered expression of a calcium binding protein in the hippocampus of infant mice and their abnormal behaviour. *Genes Cells.* (1998) 3:811–2. doi: 10.1046/j.1365-2443.1998.00231.x
76. Esnafoglu E, Cirrik S. Increased serum midkine levels in autism spectrum disorder patients. *Int J Neurosci.* (2018) 128:677–81. doi: 10.1080/00207454.2017.1408620
77. Muramatsu H, Zou P, Kurosawa N, Ichihara-Tanaka K, Maruyama K, Inoh K, et al. Female infertility in mice deficient in midkine and pleiotrophin, which form a distinct family of growth factors. *Genes Cells.* (2006) 11:1405–17. doi: 10.1111/j.1365-2443.2006.01028.x
78. Zou P, Muramatsu H, Sone M, Hayashi H, Nakashima T, Muramatsu T. Mice doubly deficient in the midkine and pleiotrophin genes exhibit deficits in the expression of beta-tectorin gene and in auditory response. *Lab Invest.* (2006) 86:645–53. doi: 10.1038/labinvest.3700428
79. Inazumi T, Tajima S, Nishikawa T, Kadomatsu K, Muramatsu H, Muramatsu T. Expression of the retinoid-inducible polypeptide, midkine, in human epidermal keratinocytes. *Arch Dermatol Res.* (1997) 289:471–5. doi: 10.1007/s004030050223

80. Sakamoto K, Kadomatsu K. Midkine in the pathology of cancer, neural disease, and inflammation. *Pathol Int.* (2012) 62:445–55. doi: 10.1111/j.1440-1827.2012.02815.x
81. Vilar J, Lalou C, Duong Van Huyen J-P, Charrin S, Hardouin S, Raulais D, et al. Midkine is involved in kidney development and in its regulation by retinoids. *J Am Soc Nephrol.* (2002) 13:668–76.
82. Li J, Yawno T, Sutherland AE, Gurung S, Paton M, McDonald C, et al. Preterm umbilical cord blood derived mesenchymal stem/stromal cells protect preterm white matter brain development against hypoxia-ischemia. *Exp Neurol.* (2018) 308:120–31. doi: 10.1016/j.expneurol.2018.07.006
83. Prusa AR, Marton E, Rosner M, Bettelheim D, Lubec G, Pollack A, et al. Neurogenic cells in human amniotic fluid. *Am J Obstet Gynecol.* (2004) 191:309–14. doi: 10.1016/j.ajog.2003.12.014
84. Hagberg H, Mallard C, Ferriero DM, Vannucci SJ, Levison SW, Vexler ZS, et al. The role of inflammation in perinatal brain injury. *Nat Rev Neurol.* (2015) 11:192–208. doi: 10.1038/nrneurol.2015.13
85. Hagberg H, David Edwards A, Groenendaal F. Perinatal brain damage: the term infant. *Neurobiol Dis.* (2016). 92(Pt A):102–12. doi: 10.1016/j.nbd.2015.09.011
86. Bokobza C, Van Steenwinckel J, Mani S, Mezger V, Fleiss B, Gressens P. Neuroinflammation in preterm babies and autism spectrum disorders. *Pediatr Res.* (2019) 85:155–65. doi: 10.1038/s41390-018-0208-4
87. Takada S, Sakakima H, Matsuyama T, Otsuka S, Nakanishi K, Norimatsu K, et al. Disruption of Midkine gene reduces traumatic brain injury through the modulation of neuroinflammation. *J Neuroinflammation.* (2020) 17:1. doi: 10.1186/s12974-020-1709-8
88. Zhu C, Wang X, Xu F, Bahr BA, Shibata M, Uchiyama Y, et al. The influence of age on apoptotic and other mechanisms of cell death after cerebral hypoxia–ischemia. *Cell Death Differ.* (2004) 12:162–76. doi: 10.1038/sj.cdd.4401545
89. Matcovitch-Natan O, Winter DR, Giladi A, Vargas Aguilar S, Spinrad A, Sarrazin S, et al. Microglia development follows a stepwise program to regulate brain homeostasis. *Science.* (2016) 353:aad8670. doi: 10.1126/science.aad8670
90. Vasung L, Lepage C, Radoš M, Pletikos M, Goldman JS, Richiardi J, et al. Quantitative and qualitative analysis of transient fetal compartments during prenatal human brain development. *Front Neuroanat.* (2016) 10:11. doi: 10.3389/fnana.2016.00011
91. Panda S, Dohare P, Jain S, Parikh N, Singla P, Mehdizadeh R, et al. Estrogen treatment reverses prematurity-induced disruption in cortical interneuron population. *J Neurosci.* (2018) 38:7378–91. doi: 10.1523/JNEUROSCI.0478-18.2018
92. Stolp HB, Fleiss B, Arai Y, Supramaniam V, Vontell R, Birtles S, et al. Interneuron development is disrupted in preterm brains with diffuse white matter injury: observations in mouse and human. *Front Physiol.* (2019) 10:955. doi: 10.3389/fphys.2019.00955
93. Fowke TM, Galinsky R, Davidson JO, Wassink G, Karunasinghe RN, Prasad JD, et al. Loss of interneurons and disruption of perineuronal nets in the cerebral cortex following hypoxia-ischaemia in near-term fetal sheep. *Sci Rep.* (2018) 8:17686–17613. doi: 10.1038/s41598-018-36083-y
94. Singh R, Kulikowicz E, Santos PT, Koehler RC, Martin LJ, Lee JK. Spatial T-maze identifies cognitive deficits in piglets 1 month after hypoxia-ischemia in a model of hippocampal pyramidal neuron loss and interneuron attrition. *Behav Brain Res.* (2019) 369:111921. doi: 10.1016/j.bbr.2019.111921
95. Gilles F, Gressens P, Dammann O, Leviton A. Hypoxia-ischemia is not an antecedent of most preterm brain damage: the illusion of validity. *Dev Med Child Neurol.* (2018) 60:120–5. doi: 10.1111/dmcn.13483
96. Schmidt BMDM, Whyte RKMB, Roberts RSM. Oxygen targeting in infants born extremely preterm who are small for gestational age: a need for heightened vigilance. *J Pediatr.* (2017) 186:9–10. doi: 10.1016/j.jpeds.2017.02.071
97. Liauw L, Palm-Meinders IH, Van Der Grond J, Leijser LM, Le Cessie S, Laan L, et al. Differentiating normal myelination from hypoxic-ischemic encephalopathy on T1-weighted MR images: a new approach. *AJNR Am J Neuroradiol.* (2007) 28:660–5.
98. Martinez-Biarge M, Diez-Sebastian J, Kapellou O, Gindner D, Allsop JM, Rutherford MA, et al. Predicting motor outcome and death in term hypoxic-ischemic encephalopathy. *Neurology.* (2011) 76:2055–61. doi: 10.1212/WNL.0b013e31821f442d
99. Batalle D, Hughes EJ, Zhang H, Tournier JD, Tusor N, Aljabar P, et al. Early development of structural networks and the impact of prematurity on brain connectivity. *Neuroimage.* (2017) 149:379–92. doi: 10.1016/j.neuroimage.2017.01.065
100. Ikematsu S, Yano A, Aridome K, Kikuchi M, Kumai H, Nagano H, et al. Serum midkine levels are increased in patients with various types of carcinomas. *Br J Cancer.* (2000) 83:701. doi: 10.1054/bjoc.2000.1339
101. Ikematsu S, Nakagawara A, Nakamura Y, Sakuma S, Wakai K, Muramatsu T, et al. Correlation of elevated level of blood midkine with poor prognostic factors of human neuroblastomas. *Br J Cancer.* (2003) 88:1522. doi: 10.1038/sj.bjc.6600938
102. Nadjar A, Combe C, Laye S, Tridon V, Dantzer R, Amedee T, et al. Nuclear factor kappaB nuclear translocation as a crucial marker of brain response to interleukin-1. A study in rat and interleukin-1 type I deficient mouse. *J. Neurochem.* (2003) 87:1024–36. doi: 10.1046/j.1471-4159.2003.02097.x
103. Nijboer CH, Heijnen CJ, Groenendaal F, May MJ, Van Bel F, Kavelaars A. A dual role of the NF-kappaB pathway in neonatal hypoxic-ischemic brain damage. *Stroke.* (2008) 39:2578–86. doi: 10.1161/STROKEAHA.108.516401
104. Yang D, Sun YY, Lin X, Baumann JM, Dunn RS, Lindquist DM, et al. Intranasal delivery of cell-penetrating anti-NF-kappaB peptides (Tat-NBD) alleviates infection-sensitized hypoxic-ischemic brain injury. *Exp Neurol.* (2013) 247:447–55. doi: 10.1016/j.expneurol.2013.01.015
105. Kichev A, Eede P, Gressens P, Thornton C, Hagberg H. Implicating receptor activator of NF-kappaB (RANK)/RANK ligand signalling in microglial responses to toll-like receptor stimuli. *Dev Neurosci.* (2017) 39:192–206. doi: 10.1159/000464244
106. Owada K, Sanjo N, Kobayashi T, Mizusawa H, Muramatsu H, Muramatsu T, et al. Midkine inhibits caspase-dependent apoptosis via the activation of mitogen-activated protein kinase and phosphatidylinositol 3-kinase in cultured neurons. *J Neurochem.* (1999) 73:2084–92. doi: 10.1046/j.1471-4159.1999.02084.x
107. Ohuchida T, Okamoto K, Akahane K, Higure A, Todoroki H, Abe Y, et al. Midkine protects hepatocellular carcinoma cells against TRAIL-mediated apoptosis through down-regulation of caspase-3 activity. *Cancer.* (2004) 100:2430–6. doi: 10.1002/cncr.20266
108. Tong Y, Mentlein R, Buhl R, Hugo HH, Krause J, Mehdorn HM, et al. Overexpression of midkine contributes to anti-apoptotic effects in human meningiomas. *J Neurochem.* (2007) 100:1097–107. doi: 10.1111/j.1471-4159.2006.04276.x
109. Wang Q, Huang Y, Ni Y, Wang H, Hou Y. siRNA targeting midkine inhibits gastric cancer cells growth and induces apoptosis involved caspase-3,8,9 activation and mitochondrial depolarization. *J Biomed Sci.* (2007) 14:783–95. doi: 10.1007/s11373-007-9192-0
110. Thornton C, Leaw B, Mallard C, Nair S, Jinnai M, Hagberg H. Cell death in the developing brain after hypoxia-ischemia. *Front Cell Neurosci.* (2017) 11:248. doi: 10.3389/fncel.2017.00248
111. Truttmann AC, Ginet V, Puyal J. Current evidence on cell death in preterm brain injury in human and preclinical models. *Front Cell Dev Biol.* (2020) 8:27. doi: 10.3389/fcell.2020.00027
112. Alexei D, Junichi H, Megan G, Irene LCE, Olga K, Xin T, et al. Identification of RIP1 kinase as a specific cellular target of necrostatins. *Nat Chem Biol.* (2008) 4:313. doi: 10.1038/nchembio.83
113. Christofferson DE, Li Y, Yuan J. Control of life-or-death decisions by RIP1 kinase. *Annu Rev Physiol.* (2014) 76:129–50. doi: 10.1146/annurev-physiol-021113-170259
114. Northington FJ, Zelaya ME, O'Riordan DP, Blomgren K, Flock DL, Hagberg H, et al. Failure to complete apoptosis following neonatal hypoxia–ischemia manifests as "continuum" phenotype of cell death and occurs with multiple manifestations of mitochondrial dysfunction in rodent forebrain. *Neuroscience.* (2007) 149:822–33. doi: 10.1016/j.neuroscience.2007.06.060
115. Northington FJ, Chavez-Valdez R, Martin LJ. Neuronal cell death in neonatal hypoxia-ischemia. *Ann Neurol.* (2011) 69:743. doi: 10.1002/ana.22419
116. Askalan R, Gabarin N, Armstrong EA, Fang Liu Y, Couchman D, Yager JY. Mechanisms of neurodegeneration after severe hypoxic-ischemic injury in the neonatal rat brain. *Brain Res.* (2015) 1629:94–103. doi: 10.1016/j.brainres.2015.10.020

117. Tahraoui SL, Marret S, Bodenant C, Leroux P, Dommergues MA, Evrard P, et al. Central role of microglia in neonatal excitotoxic lesions of the murine periventricular white matter. *Brain Pathol.* (2001) 11:56–71. doi: 10.1111/j.1750-3639.2001.tb00381.x
118. Van Steenwinckel J, Schang AL, Krishnan ML, Degos V, Delahaye-Duriez A, Bokobza C, et al. Decreased microglial Wnt/beta-catenin signalling drives microglial pro-inflammatory activation in the developing brain. *Brain.* (2019) 142:3806–33. doi: 10.1093/brain/awz319
119. Fernández-López D, Faustino J, Klibanov AL, Derugin N, Blanchard E, Simon F, et al. Microglial cells prevent hemorrhage in neonatal focal arterial stroke. *J Neurosci.* (2016) 36:2881. doi: 10.1523/JNEUROSCI.0140-15.2016
120. Tsuji S, Di Martino E, Mukai T, Tsuji S, Murakami T, Harris RA, et al. Aggravated brain injury after neonatal hypoxic ischemia in microglia-depleted mice. *J Neuroinflammation.* (2020) 17:111–5. doi: 10.1186/s12974-020-01792-7
121. Mallard C, Tremblay M-E, Vexler ZS. Microglia and neonatal brain injury. *Neuroscience.* (2019) 405:68–76. doi: 10.1016/j.neuroscience.2018.01.023
122. McNamara NB, Miron VE. Microglia in developing white matter and perinatal brain injury. *Neurosci Lett.* (2020) 714:134539. doi: 10.1016/j.neulet.2019.134539
123. Fernández-Calle R, Vicente-Rodríguez M, Gramage E, De La Torre-Ortiz C, Pérez-García C, Ramos MP, et al. Endogenous pleiotrophin and midkine regulate LPS-induced glial responses. *Neurosci Lett.* (2018) 662:213–8. doi: 10.1016/j.neulet.2017.10.038
124. Wang J, Takeuchi H, Sonobe Y, Jin S, Mizuno T, Miyakawa S, et al. Inhibition of midkine alleviates experimental autoimmune encephalomyelitis through the expansion of regulatory T cell population. *Proc Natl Acad Sci USA.* (2008) 105:3915–20. doi: 10.1073/pnas.0709592105
125. Gelot A, Villapol S, Billette De Villemeur T, Renolleau S, Charriaut-Marlangue C. Astrocytic demise in the developing rat and human brain after hypoxic-ischemic damage. *Dev Neurosci.* (2009) 31:459–70. doi: 10.1159/000232564
126. Verney C, Pogledic I, Biran V, Adle-Biassette H, Fallet-Bianco C, Gressens P. Microglial reaction in axonal crossroads is a hallmark of noncystic periventricular white matter injury in very preterm infants. *J Neuropathol Exp Neurol.* (2012) 71:251–64. doi: 10.1097/NEN.0b013e3182496429
127. Shiow LR, Favrais G, Schirmer L, Schang AL, Cipriani S, Andres C, et al. Reactive astrocyte COX2-PGE2 production inhibits oligodendrocyte maturation in neonatal white matter injury. *Glia.* (2017) 65:2024–37. doi: 10.1002/glia.23212
128. Vexler ZS, Tang XN, Yenari MA. Inflammation in adult and neonatal stroke. *Clin Neurosci Res.* (2006) 6:293–313. doi: 10.1016/j.cnr.2006.09.008
129. Revuelta M, Elicegui A, Moreno-Cugnon L, Bührer C, Matheu A, Schmitz T. Ischemic stroke in neonatal and adult astrocytes. *Mech Ageing Dev.* (2019) 183:111147 doi: 10.1016/j.mad.2019.111147
130. Supramaniam V, Vontell R, Srinivasan L, Wyatt-Ashmead J, Hagberg H, Rutherford M. Microglia activation in the extremely preterm human brain. *Pediatr Res.* (2012) 73:301–9. doi: 10.1038/pr.2012.186
131. Villapol S, Gelot A, Renolleau S, Charriaut-Marlangue C. Astrocyte responses after neonatal ischemia: the Yin and the Yang. *Neuroscientist.* (2008) 14:339–44. doi: 10.1177/1073858408316003
132. Romero J, Muñiz J, Tornatore TL, Holubiec M, González J, Barreto GE, et al. Dual role of astrocytes in perinatal asphyxia injury and neuroprotection. *Neurosci Lett.* (2014) 565:42–6. doi: 10.1016/j.neulet.2013.10.046
133. Mochizuki R, Takeda A, Sato N, Kimpara T, Onodera H, Itoyama Y, et al. Induction of midkine expression in reactive astrocytes following rat transient forebrain ischemia. *Exp Neurol.* (1998) 149:73–8. doi: 10.1006/exnr.1997.6687
134. Wada M, Kamata M, Aizu Y, Morita T, Hu J, Oyanagi K. Alteration of midkine expression in the ischemic brain of humans. *J Neurol Sci.* (2002) 200:67–73. doi: 10.1016/S0022-510X(02)00134-X
135. Satoh J, Muramatsu H, Moretto G, Muramatsu T, Chang HJ, Kim ST, et al. Midkine that promotes survival of fetal human neurons is produced by fetal human astrocytes in culture. *Brain Res Dev Brain Res.* (1993) 75:201–5. doi: 10.1016/0165-3806(93)90024-5
136. Yoshida Y, Goto M, Tsutsui J, Ozawa M, Sato E, Osame M, et al. Midkine is present in the early-stage of cerebral infarct. *Dev Brain Res.* (1995) 85:25–30. doi: 10.1016/0165-3806(94)00183-Z
137. Teo L, Boghdadi AG, De Souza M, Bourne JA. Reduced post-stroke glial scarring in the infant primate brain reflects age-related differences in the regulation of astrogliosis. *Neurobiol Dis.* (2018) 111:1–11. doi: 10.1016/j.nbd.2017.11.016
138. Muramoto A, Imagama S, Natori T, Wakao N, Ando K, Tauchi R, et al. Midkine overcomes neurite outgrowth inhibition of chondroitin sulfate proteoglycan without glial activation and promotes functional recovery after spinal cord injury. *Neurosci Lett.* (2013) 550:150–5. doi: 10.1016/j.neulet.2013.06.025
139. Vicente-Rodríguez M, Fernández-Calle R, Gramage E, Pérez-García C, Ramos MP, Herradón G. Midkine is a novel regulator of amphetamine-induced striatal gliosis and cognitive impairment: evidence for a stimulus-dependent regulation of neuroinflammation by midkine. *Mediators Inflamm.* (2016) 2016:9894504. doi: 10.1155/2016/9894504
140. Muramatsu H, Yokoi K, Chen L, Ichihara-Tanaka K, Kimura T, Muramatsu T. Midkine as a factor to counteract the deposition of amyloid β-peptide plaques: *in vitro* analysis and examination in knockout mice. *Int Arch Med.* (2011) 4:1. doi: 10.1186/1755-7682-4-1
141. Elbaz B, Popko B. Molecular control of oligodendrocyte development. *Trends Neurosci.* (2019) 42:263–77. doi: 10.1016/j.tins.2019.01.002
142. Silbereis JC, Huang EJ, Back SA, Rowitch DH. Towards improved animal models of neonatal white matter injury associated with cerebral palsy. *Dis Model Mech.* (2010) 3:678–88. doi: 10.1242/dmm.002915
143. Tolcos M, Bateman E, O'Dowd R, Markwick R, Vrijsen K, Rehn A, et al. Intrauterine growth restriction affects the maturation of myelin. *Exp. Neurol.* (2011) 232:53–65. doi: 10.1016/j.expneurol.2011.08.002
144. Penn AA, Gressens P, Fleiss B, Back SA, Gallo V. Controversies in preterm brain injury. *Neurobiol Dis.* (2016) 92:90–101. doi: 10.1016/j.nbd.2015.10.012
145. Tolcos M, Petratos S, Hirst JJ, Wong F, Spencer SJ, Azhan A, et al. Blocked, delayed, or obstructed: what causes poor white matter development in intrauterine growth restricted infants? *Prog Neurobiol.* (2017) 154:62–77. doi: 10.1016/j.pneurobio.2017.03.009
146. Segovia KN, McClure M, Moravec M, Luo NL, Wan Y, Gong X, et al. Arrested oligodendrocyte lineage maturation in chronic perinatal white matter injury. *Ann Neurol.* (2008) 63:520–30. doi: 10.1002/ana.21359
147. Billiards SS, Haynes RL, Folkerth RD, Borenstein NS, Trachtenberg FL, Rowitch DH, et al. Myelin abnormalities without oligodendrocyte loss in periventricular leukomalacia. *Brain Pathol.* (2008) 18:153–63. doi: 10.1111/j.1750-3639.2007.00107.x
148. Back SA, Miller SP. Brain injury in premature neonates: a primary cerebral dysmaturation disorder? *Ann Neurol.* (2014) 75:469–86. doi: 10.1002/ana.24132
149. Yeung MS, Zdunek S, Bergmann O, Bernard S, Salehpour M, Alkass K, et al. Dynamics of oligodendrocyte generation and myelination in the human brain. *Cell.* (2014) 159:766–74. doi: 10.1016/j.cell.2014.10.011
150. Cui QL, Kuhlmann T, Miron VE, Leong SY, Fang J, Gris P, et al. Oligodendrocyte progenitor cell susceptibility to injury in multiple sclerosis. *Am J Pathol.* (2013) 183:516–25. doi: 10.1016/j.ajpath.2013.04.016
151. McClain CR, Sim FJ, Goldman SA. Pleiotrophin suppression of receptor protein tyrosine phosphatase-beta/zeta maintains the self-renewal competence of fetal human oligodendrocyte progenitor cells. *J Neurosci.* (2012) 32:15066–75. doi: 10.1523/JNEUROSCI.1320-12.2012
152. Fujikawa A, Noda M. Role of pleiotrophin-protein tyrosine phosphatase receptor type Z signaling in myelination. *Neural Regen Res.* (2016) 11:549–51. doi: 10.4103/1673-5374.180730
153. Liu X, Mashour GA, Webster HF, Kurtz A. Basic FGF and FGF receptor 1 are expressed in microglia during experimental autoimmune encephalomyelitis: temporally distinct expression of midkine and pleiotrophin. *Glia.* (1998) 24:390–7.
154. Sonobe Y, Li H, Jin S, Kishida S, Kadomatsu K, Takeuchi H, et al. Midkine inhibits inducible regulatory T cell differentiation by suppressing the development of tolerogenic dendritic cells. *J Immunol.* (2012) 188:2602–11. doi: 10.4049/jimmunol.1102346
155. Mikita J, Dubourdieu-Cassagno N, Deloire MS, Vekris A, Biran M, Raffard G, et al. Altered M1/M2 activation patterns of monocytes in severe relapsing experimental rat model of multiple sclerosis. Amelioration of clinical status by M2 activated monocyte administration. *Mult. Scler.* (2011) 17:2–15. doi: 10.1177/1352458510379243

156. MironVE, Boyd A, Zhao JW, Yuen TJ, Ruckh JM. M2 microglia and macrophages drive oligodendrocyte differentiation during CNS remyelination. *Nat Neurosci.* (2013) 16:1211–8. doi: 10.1038/nn.3469
157. Willis EF, Macdonald KPA, Nguyen QH, Garrido AL, Gillespie ER, Harley SBR, et al. Repopulating microglia promote brain repair in an IL-6-dependent manner. *Cell.* (2020) 180:833–46 e816. doi: 10.1016/j.cell.2020.02.013
158. Kaindl AM, Degos V, Peineau S, Gouadon E, Chhor V, Loron G, et al. Activation of microglial N-methyl-D-aspartate receptors triggers inflammation and neuronal cell death in the developing and mature brain. *Ann Neurol.* (2012) 72:536–49. doi: 10.1002/ana.23626
159. Li P, Gan Y, Mao L, Leak R, Chen J, Hu X. The critical roles of immune cells in acute brain injuries. In: Chen J, Hu X, Stenzel-Poore M, Zhang JH, editors. *Immunological Mechanisms and Therapies in Brain Injuries and Stroke.* New York, NY: Springer (2014). p. 9–25. doi: 10.1007/978-1-4614-8915-3_2
160. Hellstrom Erkenstam N, Smith PL, Fleiss B, Nair S, Svedin P, Wang W, et al. Temporal characterization of microglia/macrophage phenotypes in a mouse model of neonatal hypoxic-ischemic brain injury. *Front Cell Neurosci.* (2016) 10:286. doi: 10.3389/fncel.2016.00286
161. Denker SP, Ji S, Dingman A, Lee SY, Derugin N, Wendland MF, et al. Macrophages are comprised of resident brain microglia not infiltrating peripheral monocytes acutely after neonatal stroke. *J Neurochem.* (2007) 100:893–904. doi: 10.1111/j.1471-4159.2006.04162.x
162. Krishnan ML, Van Steenwinckel J, Schang AL, Yan J, Arnadottir J, Le Charpentier T, et al. Integrative genomics of microglia implicates DLG4 (PSD95) in the white matter development of preterm infants. *Nat Commun.* (2017) 8:428. doi: 10.1038/s41467-017-00422-w
163. Smith PLP, Mottahedin A, Svedin P, Mohn CJ, Hagberg H, Ek J, et al. Peripheral myeloid cells contribute to brain injury in male neonatal mice. *J Neuroinflammation.* (2018) 15:301. doi: 10.1186/s12974-018-1344-9
164. O'Hare FM, Watson W, O'Neill A, Grant T, Onwuneme C, Donoghue V, et al. Neutrophil and monocyte toll-like receptor 4, CD11b and reactive oxygen intermediates, and neuroimaging outcomes in preterm infants. *Pediatr Res.* (2015) 78:82–90. doi: 10.1038/pr.2015.66
165. Gussenhoven R, Westerlaken RJJ, Ophelders D, Jobe AH, Kemp MW, Kallapur SG, et al. Chorioamnionitis, neuroinflammation, and injury: timing is key in the preterm ovine fetus. *J Neuroinflammation.* (2018) 15:113. doi: 10.1186/s12974-018-1149-x
166. Palmer C, Roberts RL, Young PI. Timing of neutrophil depletion influences long-term neuroprotection in neonatal rat hypoxic-ischemic brain injury. *Pediatr Res.* (2004) 55:549–56. doi: 10.1203/01.PDR.0000113546.03897.FC
167. Yao HW, Kuan CY. Early neutrophil infiltration is critical for inflammation-sensitized hypoxic-ischemic brain injury in newborns. *J Cereb Blood Flow Metab.* (2019). doi: 10.1177/0271678X19891839. [Epub ahead of print].
168. Mottahedin A, Blondel S, Ek J, Leverin AL, Svedin P, Hagberg H, et al. N-acetylcysteine inhibits bacterial lipopeptide-mediated neutrophil transmigration through the choroid plexus in the developing brain. *Acta Neuropathol Commun.* (2020) 8:4. doi: 10.1186/s40478-019-0877-1
169. Lotocki G, De Rivero Vaccari JP, Perez ER, Sanchez-Molano J, Furones-Alonso O, Bramlett HM, et al. Alterations in blood-brain barrier permeability to large and small molecules and leukocyte accumulation after traumatic brain injury: effects of post-traumatic hypothermia. (Original Article)(Report). *J Neurotrauma.* (2009) 26:1123. doi: 10.1089/neu.2008.0802
170. Mallard C, Ek CJ, Vexler ZS. The myth of the immature barrier systems in the developing brain: role in perinatal brain injury. *J Physiol.* (2018) 596:5655–64. doi: 10.1113/JP274938
171. Jin Y, Silverman AJ, Vannucci SJ. Mast cell stabilization limits hypoxic-ischemic brain damage in the immature rat. *Dev Neurosci.* (2007) 29:373–84. doi: 10.1159/000105478
172. Jin Y, Silverman AJ, Vannucci SJ. Mast cells are early responders after hypoxia-ischemia in immature rat brain. *Stroke.* (2009) 40:3107–12. doi: 10.1161/STROKEAHA.109.549691
173. Stokely ME, Orr EL. Acute effects of calvarial damage on dural mast cells, pial vascular permeability, and cerebral cortical histamine levels in rats and mice. *J Neurotrauma.* (2008) 25:52–61. doi: 10.1089/neu.2007.0397
174. Levy D, Edut S, Baraz-Goldstein R, Rubovitch V, Defrin R, Bree D, et al. Responses of dural mast cells in concussive and blast models of mild traumatic brain injury in mice: potential implications for post-traumatic headache. *Cephalalgia.* (2015) 36:915–23. doi: 10.1177/0333102415617412
175. Moretti R, Chhor V, Bettati D, Banino E, De Lucia S, Le Charpentier T, et al. Contribution of mast cells to injury mechanisms in a mouse model of pediatric traumatic brain injury. *J Neurosci Res.* (2016) 94:1546–60. doi: 10.1002/jnr.23911
176. Hiramatsu K, Yoshida H, Kimura T, Takagi K. Midkine induces histamine release from mast cells and the immediate cutaneous response. *Biochem Mol Biol Int.* (1998) 44:453–62. doi: 10.1080/15216549800201472
177. Nordin SL, Jovic S, Kurut A, Andersson C, Gela A, Bjartell A, et al. High expression of midkine in the airways of patients with cystic fibrosis. *Am J Respir Cell Mol Biol.* (2013) 49:935–42. doi: 10.1165/rcmb.2013-0106OC
178. Krupinski J, Kaluza J, Kumar P, Kumar S, Wang JM. Role of angiogenesis in patients with cerebral ischemic stroke. *Stroke.* (1994) 25:1794–8. doi: 10.1161/01.STR.25.9.1794
179. Svedin P, Guan J, Mathai S, Zhang R, Wang X, Gustavsson M, et al. Delayed peripheral administration of a GPE analogue induces astrogliosis and angiogenesis and reduces inflammation and brain injury following hypoxia-ischemia in the neonatal rat. *Dev Neurosci.* (2007) 29:393–402. doi: 10.1159/000105480
180. Fernández-López D, Faustino J, Derugin N, Vexler ZS. Acute and chronic vascular responses to experimental focal arterial stroke in the neonate rat. *Transl Stroke Res.* (2013) 4:179–88. doi: 10.1007/s12975-012-0214-5
181. Shaikh H, Boudes E, Khoja Z, Shevell M, Wintermark P. Angiogenesis dysregulation in term asphyxiated newborns treated with hypothermia. *PLoS ONE.* (2015) 10:e0128028. doi: 10.1371/journal.pone.0128028
182. Dai L-C, Wang X, Yao X, Lu Y-L, Ping J-L, He J-F. Antisense oligonucleotide targeting midkine suppresses *in vivo* angiogenesis. *World J Gastroenterol.* (2007) 13:1208–13. doi: 10.3748/wjg.v13.i8.1208
183. Beauvais DM, Ell BJ, McWhorter AR, Rapraeger AC. Syndecan-1 regulates α v β 3 and α v β 5 integrin activation during angiogenesis and is blocked by synstatin, a novel peptide inhibitor. *J Cell Biol.* (2009) 184:i12. doi: 10.1083/JCB1845OIA12
184. Dzietko M, Derugin N, Wendland MF, Vexler ZS, Ferriero DM. Delayed VEGF treatment enhances angiogenesis and recovery after neonatal focal rodent stroke. *Transl Stroke Res.* (2013) 4:189–200. doi: 10.1007/s12975-012-0221-6
185. Lee Y-C, Chang Y-C, Wu C-C, Huang C-C. Hypoxia-preconditioned human umbilical vein endothelial cells protect against neurovascular damage after hypoxic ischemia in neonatal brain. *Mol Neurobiol.* (2018) 55:7743–57. doi: 10.1007/s12035-018-0867-5
186. Lingen MW. Role of leukocytes and endothelial cells in the development of angiogenesis in inflammation and wound healing. *Arch Pathol Lab Med.* (2001) 125:67–71. doi: 10.1043/0003-9985(2001)125<0067:ROLEC>2.0.CO;2
187. Stolp HB, Turnquist C, Dziegielewska KM, Saunders NR, Anthony DC, Molnar Z. Reduced ventricular proliferation in the foetal cortex following maternal inflammation in the mouse. *Brain.* (2011) 134:3236–48. doi: 10.1093/brain/awr237
188. Smith PL, Hagberg H, Naylor AS, Mallard C. Neonatal peripheral immune challenge activates microglia and inhibits neurogenesis in the developing murine hippocampus. *Dev Neurosci.* (2014) 36:119–31. doi: 10.1159/000359950
189. Young SZ, Taylor MM, Bordey A. Neurotransmitters couple brain activity to subventricular zone neurogenesis. *Eur J Neurosci.* (2011) 33:1123–32. doi: 10.1111/j.1460-9568.2011.07611.x
190. Yokota C, Takahashi S, Eisaki A, Asashima M, Akhter S, Muramatsu T, et al. Midkine counteracts the activin signal in mesoderm induction and promotes neural formation. *J Biochem.* (1998) 123:339–46. doi: 10.1093/oxfordjournals.jbchem.a021942
191. Zou P, Muramatsu H, Miyata T, Muramatsu T. Midkine, a heparin-binding growth factor, is expressed in neural precursor cells and promotes their growth. *J Neurochem.* (2006) 99:1470–9. doi: 10.1111/j.1471-4159.2006.04138.x
192. Yao S, Cheng M, Zhang Q, Wasik M, Kelsh R, Winkler C. Anaplastic lymphoma kinase is required for neurogenesis in the developing central nervous system of Zebrafish. *PLoS ONE.* (2013) 8:e63757. doi: 10.1371/journal.pone.0063757

193. Vihtelic TS, Hyde DR. Light-induced rod and cone cell death and regeneration in the adult albino zebrafish (*Danio rerio*) retina. *J. Neurobiol.* (2000) 44:289–307. doi: 10.1002/1097-4695(20000905)44:3<289::AID-NEU1>3.0.CO;2-H
194. Winkler C, Schafer M, Duschl J, Schartl M, Volff JN. Functional divergence of two zebrafish midkine growth factors following fish-specific gene duplication. *Genome Res.* (2003) 13:1067–81. doi: 10.1101/gr.1097503
195. Calinescu AA, Vihtelic TS, Hyde DR, Hitchcock PF. Cellular expression of midkine-a and midkine-b during retinal development and photoreceptor regeneration in zebrafish. *J Comp Neurol.* (2009) 514:1–10. doi: 10.1002/cne.21999
196. Gramage E, D'cruz T, Taylor S, Thummel R, Hitchcock PF. Midkine-a protein localization in the developing and adult retina of the zebrafish and its function during photoreceptor regeneration. *PLoS ONE.* (2015) 10:e0121789. doi: 10.1371/journal.pone.0121789
197. Luna B, Dobson V, Scher MS, Guthrie RD. Grating acuity and visual field development in infants following perinatal asphyxia. *Dev Med Child Neurol.* (1995) 37:330–44. doi: 10.1111/j.1469-8749.1995.tb12011.x
198. Chen ML, Guo L, Smith LE, Dammann CE, Dammann O. High or low oxygen saturation and severe retinopathy of prematurity: a meta-analysis. *Pediatrics.* (2010) 125:e1483–92. doi: 10.1542/peds.2009-2218
199. Hellström A, Smith LEH, Dammann O. Retinopathy of prematurity. *Lancet.* (2013) 382:1445–57. doi: 10.1016/S0140-6736(13)60178-6
200. Dammann O, Brinkhaus MJ, Bartels DB, Dordelmann M, Dressler F, Kerk J, et al. Immaturity, perinatal inflammation, and retinopathy of prematurity: a multi-hit hypothesis. *Early Hum Dev.* (2009) 85:325–9. doi: 10.1016/j.earlhumdev.2008.12.010
201. Unoki K, Ohba N, Arimura H, Muramatsu H, Muramatsu T. Rescue of photoreceptors from the damaging effects of constant light by midkine, a retinoic acid-responsive gene product. *Invest Ophthalmol Vis Sci.* (1994) 35:4063–8.
202. Ishikawa E, Ooboshi H, Kumai Y, Takada J, Nakamura K, Ago T, et al. Midkine gene transfer protects against focal brain ischemia and augments neurogenesis. *J Neurol Sci.* (2009) 285:78–84. doi: 10.1016/j.jns.2009.05.026
203. Osredkar D, Thoresen M, Maes E, Flatebø T, Elstad M, Sabir H. Hypothermia is not neuroprotective after infection-sensitized neonatal hypoxic–ischemic brain injury. *Resuscitation.* (2014) 85:567–72. doi: 10.1016/j.resuscitation.2013.12.006
204. Fleiss B, Gressens P. Tertiary mechanisms of brain damage: a new hope for treatment of cerebral palsy? *Lancet Neurol.* (2012) 11:556–66. doi: 10.1016/S1474-4422(12)70058-3
205. Larosa DA, Ellery SJ, Walker DW, Dickinson H. Understanding the full spectrum of organ injury following intrapartum asphyxia. *Front Pediatr.* (2017) 5:16. doi: 10.3389/fped.2017.00016
206. Fleiss B, Tann CJ, Degos V, Sigaut S, Van Steenwinckel J, Schang AL, et al. Inflammation-induced sensitization of the brain in term infants. *Dev Med Child Neurol.* (2015) 57(Suppl. 3):17–28. doi: 10.1111/dmcn.12723
207. Aslam S, Strickland T, Molloy EJ. Neonatal encephalopathy: need for recognition of multiple etiologies for optimal management. *Front Pediatr.* (2019) 7:142. doi: 10.3389/fped.2019.00142
208. Fukui S, Kitagawa-Sakakida S, Kawamata S, Matsumiya G, Kawaguchi N, Matsuura N, et al. Therapeutic effect of midkine on cardiac remodeling in infarcted rat hearts. *Ann Thorac Surg.* (2008) 85:562–70. doi: 10.1016/j.athoracsur.2007.06.002
209. Harada M, Hojo M, Kamiya K, Kadomatsu K, Murohara T, Kodama I, et al. Exogenous midkine administration prevents cardiac remodeling in pacing-induced congestive heart failure of rabbits. *Heart Vessels.* (2016) 31:96–104. doi: 10.1007/s00380-014-0569-5
210. Ishiguro H, Horiba M, Takenaka H, Sumida A, Opthof T, Ishiguro YS, et al. A single intracoronary injection of midkine reduces ischemia/reperfusion injury in Swine hearts: a novel therapeutic approach for acute coronary syndrome. *Front Physiol.* (2011) 2:27. doi: 10.3389/fphys.2011.00027
211. Woulfe KC, Sucharov CC. Midkine's role in cardiac pathology. *J Cardiovasc Dev Dis.* (2017) 4:13. doi: 10.3390/jcdd4030013
212. Barks JD. Current controversies in hypothermic neuroprotection. *Semin Fetal Neonatal Med.* (2008) 13:30–4. doi: 10.1016/j.siny.2007.09.004
213. Davidson JO, Wassink G, Van Den Heuij LG, Bennet L, Gunn AJ. Therapeutic hypothermia for neonatal hypoxic-ischemic encephalopathy - where to from here? *Front Neurol.* (2015) 6:198. doi: 10.3389/fneur.2015.00198
214. Juul SE, Mayock DE, Comstock BA, Heagerty PJ. Neuroprotective potential of erythropoietin in neonates; design of a randomized trial. *Matern Health Neonatol Perinatol.* (2015) 1:27. doi: 10.1186/s40748-015-0028-z
215. McDougall ARA, Hale N, Rees S, Harding R, De Matteo R, Hooper SB, et al. Erythropoietin protects against lipopolysaccharide-induced microgliosis and abnormal granule cell development in the ovine fetal cerebellum. *Front Cell Neurosci.* (2017) 11:224. doi: 10.3389/fncel.2017.00224
216. Wassink G, Davidson JO, Dhillon SK, Fraser M, Galinsky R, Bennet L, et al. Partial white and grey matter protection with prolonged infusion of recombinant human erythropoietin after asphyxia in preterm fetal sheep. *J Cereb Blood Flow Metab.* (2017) 37:1080–94. doi: 10.1177/0271678X16650455
217. Polglase GR, Barton SK, Melville JM, Zahra V, Wallace MJ, Siew ML, et al. Prophylactic erythropoietin exacerbates ventilation-induced lung inflammation and injury in preterm lambs. *J Physiol.* (2014) 592:1993–2002. doi: 10.1113/jphysiol.2013.270348
218. Allison BJ, Larosa DA, Barton SK, Hooper SB, Zahra VA, Tolcos M, et al. Dose-dependent exacerbation of ventilation-induced lung injury by erythropoietin in preterm newborn lambs. *J Appl Physiol.* (2019). 126:44–50. doi: 10.1152/japplphysiol.00800.2018
219. Ezzati M, Kawano G, Rocha-Ferreira E, Alonso-Alconada D, Hassell JK, Broad KD, et al. Dexmedetomidine combined with therapeutic hypothermia is associated with cardiovascular instability and neurotoxicity in a piglet model of perinatal asphyxia. *Dev Neurosci.* (2017) 39:156–70. doi: 10.1159/000458438
220. Saunders NR, Liddelow SA, Dziegielewska KM. Barrier mechanisms in the developing brain. *Front Pharmacol.* (2012) 3:46. doi: 10.3389/fphar.2012.00046
221. Houlton J, Abumaria N, Hinkley SFR, Clarkson AN. Therapeutic potential of neurotrophins for repair after brain injury: a helping hand from biomaterials. *Front Neurosci.* (2019) 13:790. doi: 10.3389/fnins.2019.00790
222. Stolp HB, Dziegielewska KM, Ek CJ, Habgood MD, Lane MA, Potter AM, et al. Breakdown of the blood-brain barrier to proteins in white matter of the developing brain following systemic inflammation. *Cell Tissue Res.* (2005) 320:369–78. doi: 10.1007/s00441-005-1088-6
223. Ek CJ, D'Angelo B, Baburamani AA, Lehner C, Leverin AL, Smith PL, et al. Brain barrier properties and cerebral blood flow in neonatal mice exposed to cerebral hypoxia-ischemia. *J.Cereb Blood Flow Metab.* (2015) 35:818–27. doi: 10.1038/jcbfm.2014.255
224. Sobotka KS, Hooper SB, Crossley KJ, Ong T, Schmolzer GM, Barton SK, et al. Single sustained inflation followed by ventilation leads to rapid cardiorespiratory recovery but causes cerebral vascular leakage in asphyxiated near-term lambs. *PLoS ONE.* (2016) 11:e0146574. doi: 10.1371/journal.pone.0146574
225. Whitelaw A, Jary S, Kmita G, Wroblewska J, Musialik-Swietlinska E, Mandera M, et al. Randomized trial of drainage, irrigation and fibrinolytic therapy for premature infants with posthemorrhagic ventricular dilatation: developmental outcome at 2 years. *Pediatrics.* (2010) 125:e852–8. doi: 10.1542/peds.2009-1960
226. Luyt K, Jary S, Lea C, Young GJ, Odd D, Miller H, et al. Ten-year follow-up of a randomised trial of drainage, irrigation and fibrinolytic therapy (DRIFT) in infants with post-haemorrhagic ventricular dilatation. *Health Technol Assess.* (2019) 23:1–116. doi: 10.3310/hta23040
227. Zhuang X, Xiang X, Grizzle W, Sun D, Zhang S, Axtell RC, et al. Treatment of brain inflammatory diseases by delivering exosome encapsulated anti-inflammatory drugs from the nasal region to the brain. *Mol Ther.* (2011) 19:1769–79. doi: 10.1038/mt.2011.164
228. Van Velthoven CT, Sheldon RA, Kavelaars A, Derugin N, Vexler ZS, Willemen HL, et al. Mesenchymal stem cell transplantation attenuates brain injury after neonatal stroke. *Stroke.* (2013) 44:1426–32. doi: 10.1161/STROKEAHA.111.000326
229. Scafidi J, Hammond TR, Scafidi S, Ritter J, Jablonska B, Roncal M, et al. Intranasal epidermal growth factor treatment rescues neonatal brain injury. *Nature.* (2014) 506:230–4. doi: 10.1038/nature12880
230. Tien LT, Lee YJ, Pang Y, Lu S, Lee JW, Tseng CH, et al. Neuroprotective effects of intranasal IGF-1 against neonatal lipopolysaccharide-induced

neurobehavioral deficits and neuronal inflammation in the substantia nigra and locus coeruleus of juvenile rats. *Dev Neurosci.* (2017) 39:443–59. doi: 10.1159/000477898

231. Kannan S, Dai H, Navath RS, Balakrishnan B, Jyoti A, Janisse J, et al. Dendrimer-based postnatal therapy for neuroinflammation and cerebral palsy in a rabbit model. *Sci Transl Med.* (2012) 4:130ra146. doi: 10.1126/scitranslmed.3003162
232. Lei J, Rosenzweig JM, Mishra MK, Alshehri W, Brancusi F, Mclane M, et al. Maternal dendrimer-based therapy for inflammation-induced preterm birth and perinatal brain injury. *Sci Rep.* (2017) 7:6106. doi: 10.1038/s41598-017-06113-2
233. Joseph A, Wood T, Chen CC, Corry K, Snyder JM, Juul SE, et al. Curcumin-loaded polymeric nanoparticles for neuro-protection in neonatal rats with hypoxic-ischemic encephalopathy. *Nano Res.* (2018) 11:5670–88. doi: 10.1007/s12274-018-2104-y
234. Janovak L, Turcsanyi A, Bozo E, Deak A, Merai L, Sebok D, et al. Preparation of novel tissue acidosis-responsive chitosan drug nanoparticles: Characterization and *in vitro* release properties of Ca2+ channel blocker nimodipine drug molecules. *Eur J Pharm Sci.* (2018) 123:79–88. doi: 10.1016/j.ejps.2018.07.031
235. Muro S. A DNA-device that mediates selective endosomal escape and intracellular delivery of drugs and biologicals. *Adv Funct Mater.* (2014) 24:2899–906. doi: 10.1002/adfm.201303188
236. Ireland Z, Dickinson H, Fleiss B, Hutton LC, Walker DW. Behavioural effects of near-term acute fetal hypoxia in a small precocial animal, the spiny mouse (*Acomys cahirinus*). *Neonatology.* (2010) 97:45–51. doi: 10.1159/000227293
237. Ellery SJ, Goss MG, Brew N, Dickinson H, Hale N, Larosa DA, et al. Evaluation of 3K3A-activated protein C to treat neonatal hypoxic ischemic brain injury in the spiny mouse. *Neurotherapeutics.* (2018) 16:231–43. doi: 10.1007/s13311-018-0661-0
238. Yawno T, Sutherland AE, Pham Y, Castillo-Melendez M, Jenkin G, Miller SL. Fetal growth restriction alters cerebellar development in fetal and neonatal sheep. *Front Physiol.* (2019) 10:560. doi: 10.3389/fphys.2019.00560

Conflict of Interest: The authors declare that the research was conducted in the absence of any commercial or financial relationships that could be construed as a potential conflict of interest.

frontiers in Neurology

BRIEF RESEARCH REPORT
published: 23 October 2020
doi: 10.3389/fneur.2020.562510

Raised Plasma Neurofilament Light Protein Levels After Rewarming Are Associated With Adverse Neurodevelopmental Outcomes in Newborns After Therapeutic Hypothermia

Divyen K. Shah[1,2], Ping K. Yip[2], Akif Barlas[1], Pavithira Tharmapoopathy[2], Vennila Ponnusamy[3,4], Adina T. Michael-Titus[2] and Philippa Chisholm[5]*

[1] The Royal London Hospital, Barts Health NHS Trust, London, United Kingdom, [2] The Centre for Neuroscience, Surgery and Trauma, Barts and The London School of Medicine and Dentistry, Blizard Institute, Queen Mary University of London, London, United Kingdom, [3] Centre for Genomics and Child Health, Barts and The London School of Medicine and Dentistry, Blizard Institute, Queen Mary University of London, London, United Kingdom, [4] Ashford and St. Peter's Hospitals NHS Foundation Trust, Chertsey, United Kingdom, [5] Homerton University Hospitals NHS Foundation Trust, London, United Kingdom

OPEN ACCESS

Edited by:
Bobbi Fleiss, RMIT University, Australia

Reviewed by:
Maurizio Elia, Oasi Research Institute (IRCCS), Italy
Ray Koehler, Johns Hopkins University, United States

***Correspondence:**
Divyen K. Shah
d.shah@qmul.ac.uk

Specialty section:
This article was submitted to Pediatric Neurology, a section of the journal Frontiers in Neurology

Received: *15 May 2020*
Accepted: *24 August 2020*
Published: *23 October 2020*

Citation:
Shah DK, Yip PK, Barlas A, Tharmapoopathy P, Ponnusamy V, Michael-Titus AT and Chisholm P (2020) Raised Plasma Neurofilament Light Protein Levels After Rewarming Are Associated With Adverse Neurodevelopmental Outcomes in Newborns After Therapeutic Hypothermia. Front. Neurol. 11:562510. doi: 10.3389/fneur.2020.562510

Aim: To determine the predictive value of plasma neurofilament light protein (NfL) as a prognostic marker for outcomes in babies who have undergone therapeutic hypothermia (TH) for hypoxic ischemic encephalopathy (HIE).

Method: NfL levels from three groups of term newborns were compared: (1) those with mild HIE who did not receive TH, (2) newborns treated with TH who had minimal or no brain injury on MRI, and (3) newborns treated with TH who had substantial brain injury on MRI. Follow-up outcomes were collected from 18 months onward.

Results: Follow-up was available for 33/37 (89%) of children. A cutoff NfL level >436 pg/ml after rewarming (median age 98 h) was associated with adverse outcome with a diagnostic sensitivity 75%, specificity 77%, PPV 75%, and NPV 77%. NfL levels at earlier time points were not predictive of outcome.

Interpretation: This pilot study shows that persistently raised plasma NfL levels after rewarming are associated with adverse outcomes in babies with HIE who have undergone TH.

Keywords: newborn, hypoxic-ischemic encephalopathy, neurodevelopment, neurofilament light protein, therapeutic hypothermia

INTRODUCTION

Mild therapeutic hypothermia (TH) has been shown to be effective in improving outcomes in newborns suffering hypoxic–ischemic encephalopathy (HIE) with a number needed to treat of 7–9 (1) and is a recognized standard of care (2). At present, there are no specific blood biomarkers in clinical use that assist in stratification of severity of encephalopathy and selection for neuroprotection.

Neurofilament light (NfL) is a structural protein present in myelinated axons and is abundant in the central nervous system (CNS). In response to CNS axonal damage

caused by inflammatory, neurodegenerative, traumatic, or vascular injury, the release of NfL sharply increases (3). The NfL that is released reaches the interstitial fluid, which communicates freely with the CSF, and the blood, where its concentration is roughly 40-fold lower than it is in the CSF. Increased concentrations of NfL in blood have been shown in patients with chronic neurodegenerative conditions such as Alzheimer's disease (4) amyotrophic lateral sclerosis (4, 5) and multiple sclerosis (6). As such, the potential role of NfL as a biomarker for brain injury in the context of HIE in newborns remains to be explored more fully.

Previously, we have shown that it is feasible to study NfL levels from newborns (7). We demonstrated that raised plasma NfL levels assessed at three time points from newborns undergoing TH for HIE were associated with cerebral MRI findings predictive of unfavorable outcomes. However, the relationship between plasma NfL and later outcome in this group of patients has yet to be demonstrated. We hypothesize that raised plasma NfL levels during the newborn period are predictive of longer-term adverse outcome in babies with HIE.

METHOD

Term newborns with HIE were recruited between January 2014 and January 2016 from four tertiary neonatal centers as part of the Brain Injury Biomarkers in Newborns Study (BIBiNS): the Royal London Hospital, Homerton University Hospital, Ashford, and St Peter's Hospitals and Southampton University Hospital. This study was carried out with research ethics committee approval (REC reference: 13/LO/17380).

Participants

These recruits have been described previously (7). For the purposes of the NfL study, samples were studied from three groups of newborns from this cohort: (1) consecutively recruited babies with mild acidosis and/or mild HIE (mild HIE group) who did not fulfill standard criteria (8) for TH and were managed conservatively; (2) consecutively recruited babies who underwent TH but had cerebral MRI predictive of adverse outcome as described previously (9) (TH unfavorable MRI group), and (3) consecutively recruited babies who underwent TH but had cerebral MRI predictive of a favorable outcome (TH favorable MRI group).

Blood Sampling

Newborns who had TH for HIE had blood samples taken at three time points: (i) after the infant had reached target temperature (S1), (ii) prior to commencing rewarming (S2), and (iii) after completing rewarming (S3). Infants with mild HIE who did not receive cooling therapy had a single specimen taken (S1). Preparation and analysis of plasma samples has been previously described (7).

Abbreviations: NfL, neurofilament light protein; TH, therapeutic hypothermia.

TABLE 1 | Perinatal characteristics of the mild HIE group compared with all the TH babies in the study.

	Mild No TH	Mod–Severe TH	*p*-value
n	11	26	
Male	5/11	18/26	0.189
Birth weight (g)	3,360 (2,971, 3,987)	3,493 (2,935, 3,800)	0.233
10-min Apgar	9 (8, 9)	5 (4, 7)	0.316
Chest compressions	0/9	10/21	0.023*
Resuscitation with cardiac drugs	0/9	6/25	0.030*
Worst pH in first hour	6.96 (6.91,7.03)	6.89 (6.72, 7.00)	0.096
Worst base deficit in first hour	−15 (−12, −8)	−13.4 (−18.0, −8.4)	0.096
Maternal pyrexia	2/10	0/25	0.482
Chorioamnionitis	0/9	0/24	0.602
Sentinel event	1/11	7/26	0.255
Meconium aspiration	0/10	3/26	0.012*
Blood glucose (<2.6 mmol/l)	0/8	0/17	0.298
Positive blood culture	0/10	1/26	0.009*
Clinical seizures	0/10	20/26	0.000*
Anticonvulsants given	0/10	18/26	0.005*
Inotropes used	0/11	11/26	0.000*

**Denotes significance where p < 0.05. Values with brackets are median (interquartile range).*

Outcomes and Neurodevelopment Assessment

Neurodevelopmental testing was administered by the local centers and were collected as per local follow-up protocols for babies with HIE, as previously described (9). Abnormal outcome was defined as a cognitive or motor composite score <85 (−1 SD) in either cognitive or motor domains, a diagnosis of cerebral palsy or death related to associated causes.

Statistical Analysis

Analysis was carried out using SPSS V25.0 (IBM Corp, Armonk, New York) and GraphPad Prism V7 (GraphPad Software, La Jolla California USA). Continuous variables between groups were compared using Mann–Whitney U and categorical variables using x^2 in SPSS. NfL levels for S1 were positively skewed and thus were log transformed prior to analysis. A receiver operating characteristic (ROC) curve was created in GraphPad Prism, comparing the mild HIE group with TH babies with abnormal outcome. Additionally, TH babies with abnormal outcomes were compared with the TH babies with normal outcomes at timepoints S1, S2, and S3. Cutoff levels for the ROC curves were obtained where sensitivity and specificity were the highest, where a value $p < 0.05$ was highly significant.

RESULTS

Eleven babies were studied in the mild HIE group, 13 in the TH favorable MRI group, and 13 in the TH unfavorable MRI group. The perinatal characteristics of these three groups have already been described in **Table 1** of our previous publication

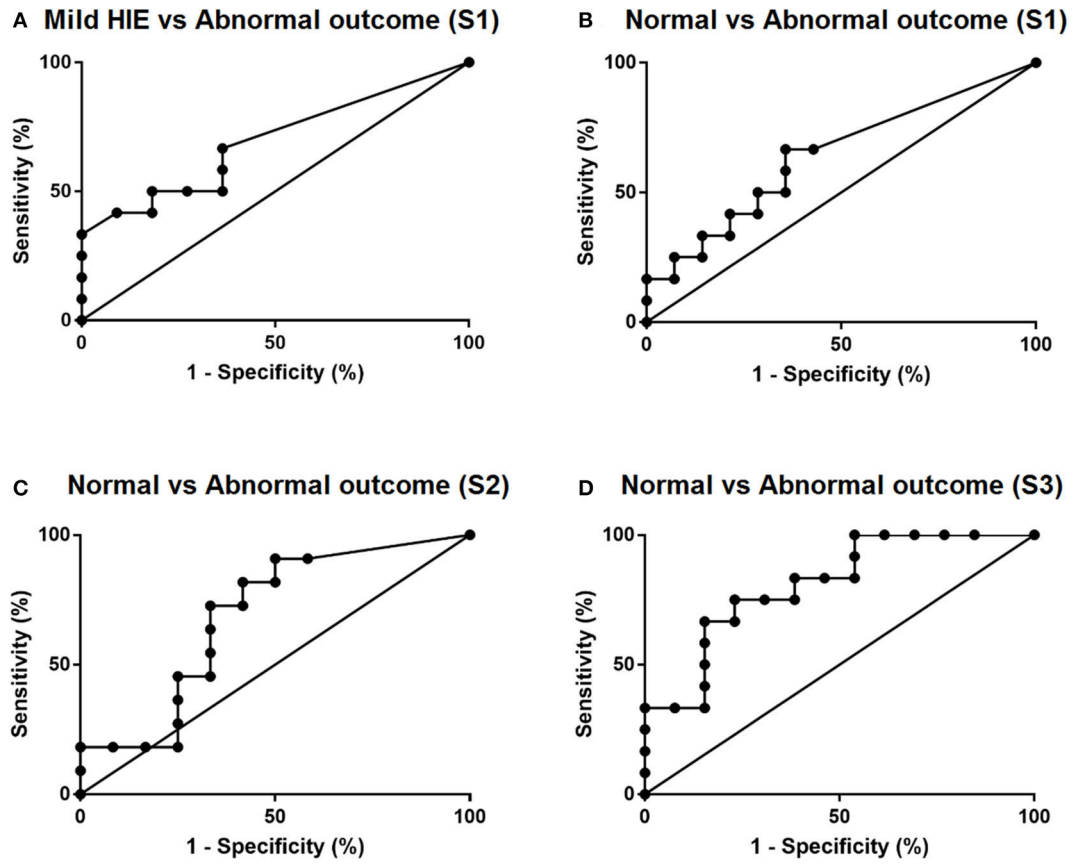

FIGURE 1 | ROC curves of plasma NfL levels. **(A)** Comparison of mild HIE babies vs. cooled babies with abnormal outcomes and **(B–D)** comparison of cooled babies with normal and abnormal outcomes at timepoints S1, S2, and S3 respectively.

TABLE 2 | The predictive value of plasma NfL levels at timepoints S1, S2, and S3 with later neurodevelopment.

Sample	Area under the curve	SE	*p*-value	Cutoff (pg/ml)	Sensitivity (%)	Specificity (%)	PPV (%)	NPV (%)
S1	0.654	0.104	0.156	28	67	63	53	75
S2	0.686	0.115	0.132	166	73	67	67	73
S3	0.808	0.087	0.009	436	75	77	75	77

SE, standard error; PPV, positive predictive value; NPV, negative predictive value.

(7). Perinatal characteristics of babies with mild HIE compared with all the newborns treated with TH combined are shown in **Table 1** in the present publication. Babies who received TH were more likely to have chest compressions, resuscitation with cardiac medication, meconium aspiration, positive blood culture, seizures, anticonvulsants, and use of inotropes ($p < 0.05$).

NfL Levels

NfL levels in the three groups have previously been described (7). The single blood sample from the mild HIE group was obtained at a median age of 24 h. In the cooled babies' samples, S1, S2, and S3 were obtained at median ages of 18, 54, and 98 h, respectively. Only 3/8 babies in the mild HIE group who had outcomes available had a detectable plasma NfL level (83, 156, and 172 pg/ml). Of these three, one child who had high functioning autism with difficulties with social interaction was assigned an abnormal outcome.

Outcomes

Outcomes were available for 33/37 (89%) children, with neurodevelopmental assessment performed at a median age of 2.7 [interquartile range (IQR) 2.0, 3.2] years. Of the 33 babies, 23 had Bayley-III assessments, four had ASQ-3 (Ages and Stages Questionnaire−3) assessments, and six were assigned outcomes by DS based on the follow-up information supplied by the local team. Of the six children with assigned outcomes, three were from the mild HIE group and three had received TH. Only one of the six was in the abnormal outcome category; a baby from the mild HIE group who was diagnosed with features of high functioning autism.

TABLE 3 | Characteristics of babies with cerebral palsy.

Study number	Apgar 10 min	Respiratory support 10 Min	Chest compressions	Worst pH in first hour	Worst base deficit in first hour	Sentinel event	Clinical seizure (Y/N)	PLIC	BGT	WM	Cortex	MRI outcome	S1	S2	S3	CP GMFCS
1	4	Y	Y	6.8	−18	Y	N	2	3	3	3	U	29.394	224.709	674.385	5
2	4	Y	N	6.94	−19.8	N	Y	2	3	3	3	U	0	188.718	1,625.672	5
3	0		Y	7.3		N	Y	2	3	1	1	U	69.941	422.949	1,013.869	3
4	5	Y	Y	6.63	−25.7	N	Y	2	3	2	0	U	2,506.037	2,255.24	4,697.766	5
5		Y	N	6.64	−22	N	Y	2	3	2	1	U	172.529	158.548	334.448	2
6		Y	Y	6.6	−27	N	Y	1	2	1	2	U	0		563.196	5
7	9	Y	N	7	−16.4	N	Y	2	2	3	0	U	148.327	172.168	151.207	4
8	10	N	Y	6.77	−19.7	N	Y	2	2	1	0	U	0	0	511.332	4
9	1	Y	-	6.9	−25.5	N	Y	0	2	3	2	U	412.535	381.27	843.895	3

Y, yes; N, no; U, unfavorable MRI outcome; SE, standard error; PLIC, posterior limb of internal capsule; BGT, basal ganglia and thalami; WM, white matter; CP GMFCS, cerebral palsy gross motor function classification system.

MRI scores noted in Table 3 as adapted from Rutherford et al.

Posterior limb of internal capsule on T1.

0, normal; 1, reduced or asymmetrical signal intensity; 2, severe injury with reversed or abnormal signal intensity bilaterally on T1- and/or T2-weighted images.

Basal ganglia and thalami.

0, normal; 1, mild injury (focal abnormal signal intensity); 2, moderate injury (multifocal abnormal signal intensity); 3,indicates severe injury (widespread abnormal signal intensity).

White matter.

0, normal; 1, mild injury (long T1 and T2 in periventricular white matter only); 2, long T1 and T2 in subcortical WM and or focal punctate lesions or focal infarction; 3, severe widespread abnormalities including long T1 and T2 +/− infarction +/− hemorrhage.

Cortical involvement.

0, normal; 1, mild (1–2 sites cortical highlighting/decreased T1); 2,moderate (3 sites involved); 3, severe (more than three sites).

Three children in the mild HIE groups were lost to follow-up, and one child in the TH favorable MRI group was not available, detailed as below.

Outcomes were available for 8/11 children in the mild HIE group. Seven of these children had normal outcomes. One child, who had high-functioning autism with difficulties with social interaction, was assigned an abnormal outcome. Outcomes were available for 12/13 in the TH favorable MRI group. One child was discharged from follow-up at 5 months as he was thought to be doing well, and no further follow-up data was available. Of the other 12, 11 children had a normal outcome and one had an abnormal outcome. This child had normal motor findings but severe impairment in cognition and language in keeping with other features of autism. Outcomes were available for all 13 children in the TH unfavorable MRI group. Of these, two had normal and 11 abnormal outcomes. Of these 11, nine had a diagnosis of cerebral palsy.

Diagnostic Accuracy of Plasma NfL Levels in Prediction of Outcomes

To assess the diagnostic value of plasma NfL levels in predicting later neurodevelopment, ROC curves were constructed, along with cutoff levels of plasma NfL for each sampling time (**Figure 1**). The area under the curve (AUC) for each blood sample showed that plasma NfL is a variable classifier of neurodevelopmental outcome (**Table 2**). A cutoff of 436 pg/ml at timepoint S3 was strongly predictive of later neurodevelopmental outcome with an AUC 0.81, $p = 0.009$, sensitivity = 75%, and specificity = 77%. Of the nine children who developed cerebral palsy, all nine had detectable NfL levels and seven had levels >436 pg/ml (**Table 3**).

DISCUSSION

In this paper, we provide additional data to complement our previous work in which we have demonstrated the feasibility of using NfL levels as a biomarker of brain injury in term newborns who have undergone TH. We demonstrate that a cutoff level >436 pg/ml after rewarming was associated with abnormal outcome with a diagnostic sensitivity 75%, sensitivity 77%, PPV 75%, and NPV 77%.

Thus far, this is the first study to examine the relationship between serial plasma NfL levels in newborns undergoing TH and later neurodevelopmental outcome in newborns. Toorell et al. (10) highlighted the importance of NfL as an early predictive marker in asphyxia from cord blood. Our study comparing levels from babies with mild HIE who are not cooled with those from cooled babies with substantial brain injury on MRI as well as babies with relatively normal cerebral MR imaging shows that plasma NfL levels rise during the period of TH (7), and the present work shows that NfL levels after the rewarming period, taken at days 4–5 (median age of 98 h in this group), are predictive of later outcomes.

Various novel blood biomarkers of brain injury have been investigated in newborns with HIE (11); however, as yet none has been established in clinical practice.

We chose to explore NfL levels as researchers at our institute, and others have found levels raised in other neurological conditions (5, 12, 13). In cases of severe traumatic brain injury (TBI) in adults, plasma NfL levels were shown to correlate with 12-month follow-up outcomes with an AUC of 0.70, with an AUC of 0.99 at admission to detect TBI. Rodent studies in mild TBI have shown that NfL levels are robustly detectable in younger rodents; however, plasma NfL levels were markedly reduced in older rodents, making NfL a potential biomarker in the younger population (14). Mattsson et al. showed that high plasma NfL levels correlated with poor cognition and Alzheimer's disease-related brain atrophy, with an AUC of 0.87 (15). In comparison to these conditions, the brain injury observed in newborn HIE is arguably a less heterogeneous entity than TBI; is thought to be associated with an acute generalized hypoxic–ischemic insult to a relatively immature brain; and follows a shorter disease time course than conditions such as Alzheimer's disease. We speculate that these differences may account for the difference in NfL cutoff levels that we note in the babies compared to these other groups.

Our work has a number of limitations. As a pilot feasibility study, the numbers are small and the study is not adequately powered to detect smaller differences. Also, we do not have NfL levels from cord blood or earlier samples from babies prior to commencing TH. As the samples are obtained once TH is already established, the role of TH in attenuating NfL levels cannot be excluded. Of the three sequential samples studied, as only NfL levels from the last sample (obtained after rewarming) at a median age of 98 h are significantly associated with outcome, we postulate that NfL levels are unlikely to provide an early biomarker for selection of newborns for neuroprotection but may assist with identifying infants who will benefit from additional treatments in the post-acute period, as they become available. A larger cohort study is required with serial sampling commencing at earlier time points.

CONCLUSION

We have demonstrated in this pilot study that it is feasible to study plasma NfL as a biomarker of brain injury in newborns and that levels after rewarming correlate with later outcomes in newborns who have undergone TH for moderate to severe HIE. As such, NfL may be a candidate biomarker for neuroprotective interventions in the post-acute period, once these are available. A larger prospective cohort study is required.

DATA AVAILABILITY STATEMENT

The raw data supporting the conclusions of this article will be made available by the authors, without undue reservation.

ETHICS STATEMENT

The studies involving human participants were reviewed and approved by Bromley Research Ethics Committee. Written informed consent to participate in this study was provided by the participants' legal guardian/next of kin.

AUTHOR CONTRIBUTIONS

DS conceptualized and designed the study, designed the data collection sheets, recruited patients for the study, performed the data analysis, drafted the initial manuscript, approved of the final manuscript as submitted, and the principal investigator, had full access to all the data in the study and takes responsibility for the integrity of the data and the accuracy of the data analysis. PY conceptualized and designed the study, performed the laboratory analysis, assisted with the data analysis, assisted in preparing the manuscript, and approved the final manuscript. AB coordinated the neurodevelopmental follow-up, assisted in preparing the manuscript, and approved the final manuscript. PT performed the data analysis, assisted in preparing the manuscript, and approved the final manuscript. VP recruited patients for the study, assisted in preparing the manuscript, and approved the final manuscript. AM-T provided intellectual input, assisted in preparing the manuscript, and approved the final manuscript. PC coordinated the neurodevelopmental follow-up, provided intellectual input, assisted in preparing the manuscript, and approved the final manuscript. All authors contributed to the article and approved the submitted version.

FUNDING

We are grateful to the Barts Charity, London, UK and the NIHR Brain Injury Healthcare Technology Cooperative for providing funding support toward this study.

ACKNOWLEDGMENTS

We are grateful to the families who participated in this study and thank the medical and nursing staff on the neonatal units for their support. We are grateful to Ms. Nicola Openshaw-Lawrence for assistance with managing the data, Dr. Jane Evanson, and Dr. Olga Kapellou for cerebral MRI interpretation, Ms. Karen Few for data coordination, and Dr. Neelam Gupta for recruiting patients.

REFERENCES

1. Jacobs SE, Berg M, Hunt R, Tarnow-Mordi WO, Inder TE, Davis PG. Cooling for newborns with hypoxic ischaemic encephalopathy. *Cochrane Database Syst Rev.* (2013) 2013:Cd003311. doi: 10.1002/14651858.CD003311.pub3
2. NICE. *Therapeutic Hypothermia With Intracorporeal Temperature Monitoring for Hypoxic Perinatal Brain Injury | Guidance and Guidelines.* London: NICE (2010).
3. Gaetani L, Blennow K, Calabresi P, Di Filippo M, Parnetti L, Zetterberg H. Neurofilament light chain as a biomarker in neurological disorders. *J Neurol Neurosurg Psychiatry.* (2019) 90:870–81. doi: 10.1136/jnnp-2018-320106

4. Rosengren LE, Karlsson JE, Karlsson JO, Persson LI, Wikkelso C. Patients with amyotrophic lateral sclerosis and other neurodegenerative diseases have increased levels of neurofilament protein in CSF. *J Neurochem.* (1996) 67:2013–8. doi: 10.1046/j.1471-4159.1996.67052013.x
5. Lu CH, Macdonald-Wallis C, Gray E, Pearce N, Petzold A, Norgren N, et al. Neurofilament light chain: a prognostic biomarker in amyotrophic lateral sclerosis. *Neurology.* (2015) 84:2247–57. doi: 10.1212/WNL.0000000000001642
6. Gunnarsson M, Malmestrom C, Axelsson M, Sundstrom P, Dahle C, Vrethem M, et al. Axonal damage in relapsing multiple sclerosis is markedly reduced by natalizumab. *Ann Neurol.* (2011) 69:83–9. doi: 10.1002/ana.22247
7. Shah DK, Ponnusamy V, Evanson J, Kapellou O, Ekitzidou G, Gupta N, et al. Raised plasma neurofilament light protein levels are associated with abnormal MRI outcomes in newborns undergoing therapeutic hypothermia. *Front Neurol.* (2018) 9:86. doi: 10.3389/fneur.2018.00086
8. *National Perinatal Epidemiology Unit*. UK TOBY Cooling Register Protocol. Oxford: NPEU (2007).
9. Tharmapoopathy P, Chisholm P, Barlas A, Varsami M, Gupta N, Ekitzidou G, et al. In clinical practice, cerebral MRI in newborns is highly predictive of neurodevelopmental outcome after therapeutic hypothermia. *Eur J Paediatr Neurol.* (2019). doi: 10.1016/j.ejpn.2019.09.005
10. Toorell H, Zetterberg H, Blennow K, Savman K, Hagberg H. Increase of neuronal injury markers Tau and neurofilament light proteins in umbilical blood after intrapartum asphyxia. *J Matern Fetal Neonatal Med.* (2017) 31:2468–72. doi: 10.1080/14767058.2017.1344964
11. Graham EM, Everett AD, Delpech JC, Northington FJ. Blood biomarkers for evaluation of perinatal encephalopathy: state of the art. *Curr Opin Pediatr.* (2018) 30:199–203. doi: 10.1097/MOP.0000000000000591
12. Kuhle J, Nourbakhsh B, Grant D, Morant S, Barro C, Yaldizli O, et al. Serum neurofilament is associated with progression of brain atrophy and disability in early MS. *Neurology.* (2017) 88:826–31. doi: 10.1212/WNL.0000000000003653
13. Gaiottino J, Norgren N, Dobson R, Topping J, Nissim A, Malaspina A, et al. Increased neurofilament light chain blood levels in neurodegenerative neurological diseases. *PLoS ONE.* (2013) 8:e75091. doi: 10.1371/journal.pone.0075091
14. Cheng WH, Stukas S, Martens KM, Namjoshi DR, Button EB, Wilkinson A, et al. Age at injury and genotype modify acute inflammatory and neurofilament-light responses to mild CHIMERA traumatic brain injury in wild-type and APP/PS1 mice. *Exp Neurol.* (2018) 301(Pt A):26–38. doi: 10.1016/j.expneurol.2017.12.007
15. Mattsson N, Andreasson U, Zetterberg H, Blennow K. Association of plasma neurofilament light with neurodegeneration in patients with Alzheimer Disease. *JAMA Neurol.* (2017) 74:557–66. doi: 10.1001/jamaneurol.2016.6117

Conflict of Interest: The authors declare that the research was conducted in the absence of any commercial or financial relationships that could be construed as a potential conflict of interest.

frontiers in Neurology

ORIGINAL RESEARCH
published: 29 April 2021
doi: 10.3389/fneur.2021.657461

Nosological Differences in the Nature of Punctate White Matter Lesions in Preterm Infants

Mariya Malova[1], Elena Morelli[1], Valentina Cardiello[1], Domenico Tortora[2], Mariasavina Severino[2], Maria Grazia Calevo[3], Alessandro Parodi[1], Laura Costanza De Angelis[1], Diego Minghetti[1], Andrea Rossi[2] and Luca Antonio Ramenghi[1]*

[1] Neonatal Intensive Care Unit, IRCCS Istituto Giannina Gaslini, Genoa, Italy, [2] Neuroradiology Unit, IRCCS Istituto Giannina Gaslini, Genoa, Italy, [3] Epidemiology and Biostatistics Unit, IRCCS Istituto Giannina Gaslini, Genoa, Italy

OPEN ACCESS

Edited by:
Julie Wixey,
The University of Queensland, Australia

Reviewed by:
Linda De Vries,
Leiden University Medical Center, Netherlands
Maurizio Elia,
Oasi Research Institute (IRCCS), Italy
Ursula Felderhoff-Müser,
Essen University Hospital, Germany

***Correspondence:**
Mariya Malova
mmalova@libero.it

Specialty section:
This article was submitted to Pediatric Neurology, a section of the journal Frontiers in Neurology

Received: 22 January 2021
Accepted: 31 March 2021
Published: 29 April 2021

Citation:
Malova M, Morelli E, Cardiello V, Tortora D, Severino M, Calevo MG, Parodi A, De Angelis LC, Minghetti D, Rossi A and Ramenghi LA (2021) Nosological Differences in the Nature of Punctate White Matter Lesions in Preterm Infants. Front. Neurol. 12:657461. doi: 10.3389/fneur.2021.657461

Background: The pathogenesis of punctuate white matter lesions (PWMLs), a mild form of white matter damage observed in preterm infants, is still a matter of debate. Susceptibility-weighted imaging (SWI) allows to differentiate PWMLs based on the presence (SWI+) or absence (SWI–) of hemosiderin, but little is known about the significance of this distinction. This retrospective study aimed to compare neuroradiological and clinical characteristics of SWI+ and SWI– PWMLs.

Materials and Methods: MR images of all VLBW infants scanned consecutively at term-equivalent age between April 2012 and May 2018 were retrospectively reviewed, and infants with PWMLs defined as small areas of high T1 and/or low T2 signal in the periventricular white matter were selected and included in the study. Each lesion was analyzed separately and characterized by localization, organization pattern, and distance from the lateral ventricle. Clinical data were retrieved from the department database.

Results: A total of 517 PWMLs were registered in 81 patients, with 93 lesions (18%) visible on SWI (SWI+), revealing the presence of hemosiderin deposits. On univariate analysis, compared to SWI- PWML, SWI+ lesions were closer to the ventricle wall, more frequently organized in linear pattern and associated with lower birth weight, lower gestational age, lower admission temperature, need for intubation, bronchopulmonary dysplasia, retinopathy of prematurity, and presence of GMH-IVH. On multivariate analysis, closer distance to the ventricle wall on axial scan and lower birth weight were associated with visibility of PMWLs on SWI ($p = 0.003$ and $p = 0.0001$, respectively).

Conclusions: Our results suggest a nosological difference between SWI+ and SWI– PWMLs. Other prospective studies are warranted to corroborate these observations.

Keywords: punctate white matter lesions, brain damage, preterm, magnetic resonance imaging, newborn, SWI

INTRODUCTION

Following a noteworthy reduction in the incidence of severe forms of white matter injury in preterm infants, modern research now focuses on mild forms of damage, such as punctate white matter lesions (PWMLs). PWMLs are diagnosed in up to 30% of very preterm infants (1–6) and can be defined upon brain magnetic resonance imaging (MRI) as focal areas of high T1 and/or low T2 signal intensity located in the periventricular white matter (7).

The pathophysiology of PWMLs is still a matter of debate (6, 7). They are often considered ischemic/inflammatory in origin (8, 9); however, since their first description, it has been postulated that at least some punctate lesions can be hemorrhagic (8). These PWMLs are reported to be connected with congested medullary veins, and their pathogenesis could be similar to that of small venous infarcts (9, 10). Susceptibility-weighted imaging (SWI), a recently developed MRI sequence highly sensitive to hemosiderin deposits, can detect hemorrhagic PWMLs (visible as punctate areas of decreased signal, SWI+), distinguishing them from lesions without hemosiderin (not visible, SWI–) (9, 10). In a previous study, we have found evidence regarding the diversified clinical risk factors of SWI+ and SWI– PWMLs, suggesting that these two lesions have different pathogenesis (6).

To corroborate the hypothesis of the different nature of SWI+ and SWI– lesions, the aim of the present study was to further characterize these two types of PWMLs based on their anatomic localization, pattern, and associated clinical factors.

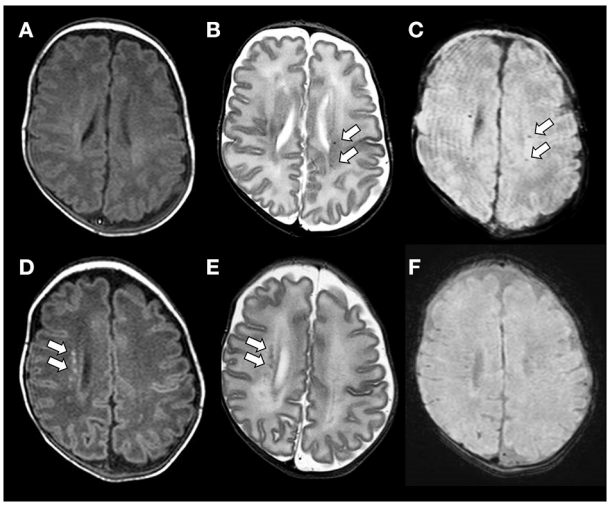

FIGURE 1 | (A–C) Brain magnetic resonance imaging (MRI) performed at the term-equivalent age of an ex-preterm infant born at 25 weeks of gestation showing SWI+ PWMLs. SWI+ lesions are barely detectable on the axial T1-weighed image **(A)**, whereas they are clearly visible as hypointense spots on axial T2-weighted **(B)** and SWI **(C)** sequences. **(D–F)** Brain MRI performed at term-equivalent age of an ex-preterm infant born at 29 weeks of gestation showing SWI– PWMLs. SWI- lesions are more clearly defined on the axial T1-weighted **(D)** than on the axial T2-weighted image **(E)** and are not visible on SWI **(D)**.

MATERIALS AND METHODS

In April 2012, routine brain MRI at term-equivalent age (TEA, between 39 + 0 and 41 + 6 weeks post-menstrual age) was introduced as part of a screening program for prematurity-related lesions in all very low birthweight (VLBW) infants admitted to our department. For the present study, MR images of all VLBW infants scanned consecutively between April 2012 and May 2018 were retrospectively retrieved and reviewed by two neuroradiologists experienced in neonatal neuroimaging (performing more than 200 neonatal brain MRI per year: MS and DT). Infants presenting PWMLs, defined as small areas of high T1 and/or low T2 signal in the periventricular white matter (7), were selected and included in the study. The presence of germinal matrix–intraventricular hemorrhage (GMH–IVH), cerebellar hemorrhage (CBH) and cystic periventricular leukomalacia (PVL) on MRI scans of included subjects was registered. The clinical data of the enrolled patients, including antenatal steroid course, type of delivery, birth weight, gestational age, need for intubation, presence of bronchopulmonary dysplasia (BPD), retinopathy of prematurity (ROP) and of necrotizing enterocolitis (NEC) were retrieved from clinical charts. This retrospective study was approved by the local ethics committee.

Image Acquisition

MRI was performed at TEA during spontaneous sleep using the "feed and wrap" technique. The need for sedation (oral midazolam, 0.1 mcg/kg) to prevent head motion was determined by the neuroradiologist based on the quality of the images after the first sequence and the infants' state of arousal. Hearing protection was used in all patients, and heart rate and oxygen saturation were monitored non-invasively. Scans were performed using a 1.5 Tesla MR system (InteraAchieva 2.6; Philips, Best, The Netherlands) with a dedicated pediatric head/spine coil. Institutional standard MRI protocol in use at the moment of the study included 3-mm thick axial T2- and T1-weighted images, coronal T2-weighted images, sagittal T1-weighted images, axial diffusion-weighted images (b value: 1,000 s/mm^2), and axial SWI. Informed consent, including statements regarding the significance and limitations of MRI at TEA, was obtained in all cases.

Image Analysis

A secondary analysis of MR scans of included subjects was performed by two trained investigators (EM and MM) blinded to the clinical history of the patients. Each PMWL was analyzed separately. In the presence of a low signal on SWI ("black dot"), corresponding to hemosiderin deposits, PWML was defined as SWI+, whereas in the absence of a low signal, it was defined as SWI– (10) (**Figure 1**).

The distance between each lesion and the ventricle was measured on axial (T1 or T2, based on major visibility) and coronal (T2) scans using the "measure" instrument of the PACS visualizer (Carestream Vue Motion, Carestream Health, Inc. 2018). The distance was measured using a straight line perpendicular to the ventricle wall.

Anatomic position on the axial scan of each lesion was determined as defined in the literature (8):

- anterior region (anterior to the frontal horn of the lateral ventricles)
- mid-region (in between or in the centrum semiovale)
- posterior region (posterior to the occipital horn of the lateral ventricles).

Each lesion was then characterized based on the pattern formed with the surrounding lesions [adapted from (7, 8)]:

- cluster (organized in a confluent pattern)
- linear (organized linearly)
- singular (not in proximity with other lesions).

Statistical Analysis

Descriptive statistics were generated for the whole cohort and data were expressed as mean and standard deviation for continuous variables. Median value and range were calculated and reported, as were absolute or relative frequencies for categorical variables. Clinical characteristics were compared using the χ^2 or Fisher's exact test and the Student *t*-test for categorical and continuous variables, respectively. Logistic regression analyses were used, and the results were reported as odds ratio (OR) with their 95% confidence intervals (CIs). The absence of exposure to the factor or the variable that was less likely to be associated with the risk of the lesion was used as the reference for each analysis. Multivariate analysis was then performed, and only variables that proved to be statistically or borderline significant in univariate analysis ($P < 0.08$) were included in the model. The model showing the best fit was based on backward stepwise selection procedures, and each variable was removed if it did not contribute significantly. In the final model a *P*-value of <0.05 was considered statistically significant, and all *P*-values were based on two-tailed tests. Statistical analysis was performed using Statistical Package for the Social Sciences (SPSS) for Windows (SPSS Inc., Chicago, IL).

RESULTS

During the study period, 428 VLBW infants admitted to the Neonatal Intensive Care Unit of IRCSS Istituto Giannina Gaslini underwent brain MRI at TEA. Eighty-one (19%) of them presented with PWMLs and were included in the study. The gestational age at birth of the included subjects ranged between 24 and 34 weeks (mean 28.6 ± 2.1 weeks) and the birth weight ranged between 470 and 1,495 g (mean 1,140 ± 240 g). In 50 infants out of 81 PWMLs were an isolated finding, while remaining 31 patients presented one or more additional prematurity-related brain lesions (GMH-IVH in 26 cases, CBH in 13 and cystic PVL in 6).

A total of 517 PWMLs were registered in 81 patients. Ninety-three lesions (18%) presented a low signal on the SWI sequence, consistent with the presence of hemosiderin deposits, and were therefore classified as SWI+. The remaining 424 lesions (82%) were classified as SWI–.

Clinical parameters distribution in the groups of SWI+ and SWI– lesions are summarized in **Table 1**. SWI+ PWMLs were characterized by lower mean gestational age and birth weight, lower admission temperature, higher frequency of need for intubation, of GMH–IVH, ROP and BPD (all $p < 0.001$).

When anatomic distribution was considered, SWI+ lesions were located significantly closer to the ventricle wall than SWI– lesions both on coronal and axial scans (**Table 2**). On the

TABLE 1 | Clinical parameters in the groups of SWI+ and SWI– PWMLs.

	SWI+ PWMLs (*N* = 93)	SWI– PWMLs (*N* = 424)	*p*-value
Birth weight (gr), mean ± SD	1,000 ± 282	1,202 ± 186	**<0.001**
median (range)	870 (470; 1,495)	1,230 (780; 1,495)	
Gestational age (weeks), mean ± SD	27.4 ± 2.53	29 ± 1.76	**<0.001**
median (range)	28 (24; 34)	29 (25; 34)	
Male gender	43 (46.2%)	221 (52.1%)	0.36
Absent or incomplete antenatal steroid treatment	26 (28%)	164 (38.7%)	0.06
Histological chorioamnionitis*	6 (12%)	68 (23.7%)	0.07
Vaginal birth	31 (33.3%)	152 (35.8%)	0.72
Apgar score at 5° min: mean ± SD	7.8 ± 1.3	8.1 ± 0.9	0.34
Admission temperature: mean ± SD	35.8 ± 0.38	36.2 ± 0.46	**<0.001**
Need for intubation	86 (92.5%)	316 (74.5%)	**<0.001**
GMH-IVH	85 (91.4%)	104 (24.5%)	**<0.001**
Retinopathy of prematurity	64 (68.8%)	159 (37.5%)	**<0.001**
Necrotizing enterocolitis	12 (12.9%)	47 (11.1%)	0.59
Bronchopulmonary dysplasia	41 (44.1%)	33 (7.8%)	**<0.001**

**Data on chorioamnionitis available for 337/517 lesions. PWMLs, punctate white matter lesions; SWI, susceptibility-weighted imaging; GMH–IVH, germinal matrix hemorrhage–intraventricular hemorrhage.*
Bold was used to evidence p < 0.05, corresponding to the statistically significant results.

TABLE 2 | Neuroradiological characteristics of SWI+ and SWI– PWMLs.

	SWI+ PWMLs (*N* = 93)	SWI– PWMLs (*N* = 424)	*p*-value
Distance from the ventricle wall			
Coronal scan (mm), mean ± SD	3.15 ± 1.93	4.79 ± 1.86	**<0.001**
Axial scan (mm), mean ± SD	3.75 ± 1.53	5.22 ± 2.17	**<0.001**
Distribution on the axial plane			
Anterior region	3 (3.2%)	7 (1.7%)	0.39
Mid-region	77 (82.8%)	376 (88.7%)	0.12
Posterior region	13 (14%)	41 (9.7%)	0.26
Patterns of organization			
Linear pattern	70 (75.3%)	258 (60.8%)	**0.009**
Cluster pattern	11 (11.8%)	84 (19.8%)	0.08
Singular lesion	12 (12.9%)	82 (19.3%)	0.18

PWMLs, punctate white matter lesions; SWI, susceptibility-weighted imaging.
Bold was used to evidence p < 0.05, corresponding to the statistically significant results.

TABLE 3 | Results of multivariate analysis including clinical and neuroradiological characteristics of SWI+ and SWI– PWMLs.

	SWI+ PWMLs (*N* = 93)	SWI– PWMLs (*N* = 424)	OR (95%CI)	*p*-value
Distance from the ventricle on axial scan (mm), mean ± SD	3.75 ± 1.53	5.22 ± 2.17	0.73 (0.59–0.89)	**0.003**
Birth weight (gr), mean ± SD	1,000 ± 282	1,202 ± 186	0.994 (0.992–0.996)	**0.0001**

OR, odds ratio; CI, confidence interval; PWMLs, punctate white matter lesions; SWI, susceptibility-weighted imaging.
Bold was used to evidence p < 0.05, corresponding to the statistically significant results.

axial plane, both SWI+ and SWI– lesions were predominantly located in the mid-region as compared with the anterior or posterior region, without significant differences among two types of PWMLs (**Table 2**). Most of the PWMLs were organized in linear pattern, with a significantly higher percentage of SWI+ lesions presenting with this pattern as compared with SWI– lesions (75.3 vs. 60.8%, $p = 0.009$) (**Table 2**).

Multivariate analysis including neuroradiological and clinical parameters showed that the distance from the ventricle on axial plane and birth weight were associated with the type of PWMLs (**Table 3**).

DISCUSSION

In this retrospective study we analyzed anatomic distribution, pattern, and correlation with the clinical data of PWMLs positive and negative on SWI. In our study, 18% of PWMLs presented with decreased signals on the SWI sequence, corresponding to the presence of hemosiderin deposits within the lesion compatible with petechial/hemorrhagic pathogenesis (8, 10). The precise pathologic mechanism behind the development of SWI+ PWMLs remains unknown, but we could speculate that venous sludging and microthrombosis in the medullary veins of the periventricular white matter could play a role, as has been suggested for the pathogenesis of GMH–IVH (11–13). Accordingly, GMH–IVH is more common in babies with inherited thrombophilia; however, we did not investigate any gain-of-function gene mutations like Prothrombin G20210 or Arg506Gln Factor V Leiden, as compared with our previous studies (14). Deep medullary vein congestion has been associated with different patterns of white matter damage in a single-center MRI imaging study (15) as well as in previous observations of infants with GMH–IVH due to cerebral sinovenous thrombosis (16, 17). The hemosiderin deposits within SWI+ PWMLs may act as proinflammatory stimuli for the adjacent white matter as well as interfere with myelination (18, 19).

In this work we observed that SWI+ PWMLs are significantly closer to the ventricular wall, further confirming their possible connection with the congested veins (9). This observation could be explained by the anatomic distribution of the medullary veins flowing vertically into the subependymal veins near the ventricle as well as by their relative immaturity and fragility in a premature infant (20). Interestingly, the distance from the ventricle on axial scan was associated with PWML type independently of clinical parameters.

On the other hand, SWI– PWMLs are distributed further away from the ventricular wall in zones prone to inflammation due to active myelination that are often targeted by cystic PVL (21). A historical work by Leech and Alvord considering the morphologic variations in PVL included the description of focal white matter lesions across the entire depth of the white matter ("Type 1"), with less intense lesions further away from the ventricle (22). Although there is a lack of widespread histological studies of PWML, punctate lesions and PVL are often seen as extremes of the same spectrum (7, 9). Accordingly, the MR T1 signal around developing PVL cavitation is similar in intensity to the signal of SWI– PWMLs. We thus hypothesize that SWI– PWMLs represent the milder form of PVL, sharing its ischemic/inflammatory pathogenesis (9).

Concerning the distribution of PWMLs on the axial scan, in our population, the majority of PWMLs (82.8% of SWI+ and 88.7% of SWI– lesions) were located medially along the lateral ventricles, as reported in the literature (7–9). We did not observe a significant difference in the anatomic distribution between SWI+ and SWI– lesions on the axial scan, although SWI+ lesions were slightly more frequently located frontally and posteriorly compared with SWI– lesions. It remains uncertain whether a different lesion pathophysiology could have contributed to this slight difference, with hemorrhagic lesions being more ubiquitous and not connected with specific inflammation-prone areas of the white matter, such as the corona radiata.

We investigated the distribution patterns of punctate lesions (linear, cluster, or singular), as adapted from previous studies (7, 8). In our study, compared with SWI– lesions, SWI+ lesions were more frequently distributed in the linear pattern (60.8 vs. 75.3%). Similar results were observed by Kersbergen et al., who reported a significant association between the linear appearance of lesions and low signal intensity on SWI. The proximity of SWI+ lesions to the medullary veins, distributed in a comb-shape appearance on axial view could have played a role in this association.

Different clinical factors were investigated in relation to PWMLs; however, only few were found to be significant. These include higher gestational age, greater birth weight, and the presence of IVH grade II or III (4, 23). In our population, GMH-IVH was the most frequent additional prematurity-brain lesion observed, even if in major part of infants PWMLs were an isolated finding. In term infants, congenital heart diseases and surgery for non-cardiac congenital anomalies have been linked to PWMLs (24, 25). We have recently shown that birth weight, absent or incomplete antenatal steroid course, vaginal delivery, and the need for intubation are risk factors of the different types of PWMLs in preterm infants (6). In the present work, we

analyzed the distribution of these and some other clinical factors in the groups of PWMLs visible and not visible on SWI. We observed a significantly lower mean gestational age at birth and a smaller mean birth weight in the SWI+ PWML group than in the SWI– PWML group, with birth weight remaining significant on multivariate analysis. These differences could reflect the higher vulnerability of the extremely premature brain to hemorrhagic lesions (26), including SWI+ PWMLs. Progressive maturation of the medullary veins with growing gestational age could play a protective role as well (18). At the microscopic level, the astrocyte-dependent structural integrity of white matter vessels depends, at least in part, on gestational age (27). It would be interesting to know whether the immature blood–brain barrier in infants with lower gestational ages can favor blood transudation of blood by-products with the subsequent formation of SWI+ PWMLs. However, widespread histological studies on this topic are lacking, partially due to the absence of an animal model.

Accordingly, SWI– PWMLs are associated with higher gestational age and higher birth weight, similar to PVL (9). Specific white matter vulnerability to damage in this phase of maturation could be related to the presence of maturating oligodendrocyte precursors (28) as well as to major microglial activation, with subsequent alterations in myelination and white matter injury (29).

Other clinical factors observed more frequently in SWI+ group, as higher need for intubation, lower admission temperature and more frequent presence of ROP, BPD and GMH-IVH, are probably secondary to lower gestational age and birth weight, even if an association between SWI+ PWML and GMH-IVH has been previously described in the literature (10).

The prognostic significance of PWMLs remains debatable. Some cases seem to be followed by motor disability, cerebral palsy, or altered cognitive performance, while others are accompanied by normal neurodevelopment (2, 4, 5, 7, 30). In a study involving 12 infants with isolated PWMLs followed up until school age, a higher risk of dyspraxia and motor impairment was observed, without increased risk of cognitive impairment (31). In other studies, worse outcome after PWMLs was associated with higher lesion number (2, 4), cluster pattern organization (7), and frontal lobe distribution on axial imaging (5). It would be interesting to investigate the impact on neurodevelopment of PWMLs based on their visibility on SWI, and the related study is ongoing. Our work has several limitations. First, owing to the retrospective design of the study, the findings of our study need to be validated via prospective studies. Furthermore, we studied a very specific population (i.e., VLBW infants); therefore, the extension of our results to other patient groups can be questionable. This is important considering that PWMLs have been described at all gestational ages up to term age (9). In addition, the use of TEA MRI may have limited our ability to identify those PWML disappearing at an earlier stage (7), even if their clinical significance remains to be defined. Finally, the absence of early MRI did not allow us to use diffusion restriction as a marker of PWMLs with possible inflammatory or ischemic origin, as described in the literature (7).

On the other hand, the anatomic dispositions of punctate lesions were analyzed one by one, thereby allowing a more precise characterization of their different anatomic distributions. This represents a potential strength of our study. In addition, the availability of the SWI sequence in all MRIs since 2012 has allowed us to clearly identify PWMLs with the presence of hemosiderin (SWI+) as well as to analyze them separately from SWI– PWMLs.

In conclusion, in this study we observed statistically significant differences between PWMLs visible and not visible on SWI sequence, with closer distance from the ventricle on axial scan and lower birth weight being associated with SWI+ lesions. These observations, together with previously evidenced differences in risk factors, suggest that SWI+ and SWI– PWMLs could represent two distinct nosological entities with potentially different nature. Further prospective studies are warranted to corroborate our findings as well as to define the clinical significance of the two types of PWMLs.

DATA AVAILABILITY STATEMENT

The original contributions presented in the study are included in the article/supplementary material, further inquiries can be directed to the corresponding author/s.

ETHICS STATEMENT

The study was approved by the local ethics committee (Comitato Etico Regione Liguria, Genoa, Italy). Written informed consent to participate in the study was provided by the participant's legal guardian/next of kin.

AUTHOR CONTRIBUTIONS

MM and LR contributed to study planning and design and manuscript writing. MM and EM contributed to the data and imaging analysis and to manuscript writing. VC, LD, DM, and AP contributed to patient recruitment, data collection and analysis, and manuscript writing. MS and DT collected and analyzed MRI data and contributed to manuscript writing. MC performed statistical analysis. AR contributed to interpretation of collected data and to manuscript writing. All authors participated in revising the manuscript and approved the final version before publication.

FUNDING

Funding from Eu-Brain non-profit association supported the present study.

REFERENCES

1. Leijser LM, de Bruïne FT, Steggerda SJ, van der Grond J, Walther FJ, van Wezel-Meijler G. Brain imaging findings in very preterm infants throughout the neonatal period. Part I. Incidences and evolution of lesions, comparison between ultrasound and MRI. *Early Hum Dev.* (2009) 85:101–9. doi: 10.1016/j.earlhumdev.2008.11.010
2. de Bruïne FT, van den Berg-Huysmans AA, Leijser LM, Rijken M, Steggerda SJ, van der Grond J, et al. Clinical implications of MR imaging findings in the white matter in very preterm infants: a 2-year follow-up study. *Radiology.* (2011) 261:899–906. doi: 10.1148/radiol.11110797
3. Tortora D, Panara V, Mattei PA, Tartaro A, Salomone R, Domizio S, et al. Comparing 3TT1-weighted sequences in identifying hyperintense punctate lesions in preterm neonates. *AJNR Am J Neuroradiol.* (2015) 36:581–6. doi: 10.3174/ajnr.A4144
4. Tusor N, Benders MJ, Counsell SJ, Nongena P, Ederies MA, Falconer S, et al. Punctate white matter lesions associated with altered brain development and adverse motor outcome in preterm infants. *Sci Rep.* (2017) 7:13250. doi: 10.1038/s41598-017-13753-x
5. Guo T, Duerden EG, Adams E, Chau V, Branson HM, Chakravarty MM, et al. Quantitative assessment of white matter injury in preterm neonates: association with outcomes. *Neurology.* (2017) 88:614–22. doi: 10.1212/WNL.0000000000003606
6. Parodi A, Malova M, Cardiello V, Raffa S, Re M, Calevo MG, et al. Punctate white matter lesions of preterm infants: risk factor analysis. *Eur J Paediatr Neurol.* (2019) 23:733–9. doi: 10.1016/j.ejpn.2019.06.003
7. Kersbergen KJ, Benders MJ, Groenendaal F, Koopman-Esseboom C, Nievelstein RA, van Haastert IC, et al. Different patterns of punctate white matter lesions in serially scanned preterm infants. *PLoS ONE.* (2014) 9:e108904. doi: 10.1371/journal.pone.0108904
8. Cornette LG, Tanner SF, Ramenghi LA, Miall LS, Childs AM, Arthur RJ, et al. Magnetic resonance imaging of the infant brain: anatomical characteristics and clinical significance of punctate lesions. *Arch Dis Child Fetal Neonatal Ed.* (2002) 86:F171–7. doi: 10.1136/fn.86.3.F171
9. Rutherford MA, Supramaniam V, Ederies A, Chew A, Bassi L, Groppo M, et al. Magnetic resonance imaging of white matter diseases of prematurity. *Neuroradiology.* (2010) 52:505–21. doi: 10.1007/s00234-010-0700-y
10. Niwa T, de Vries LS, Benders MJ, Takahara T, Nikkels PG, Groenendaal F. Punctate white matter lesions in infants: new insights using susceptibility-weighted imaging. *Neuroradiology.* (2011) 53:669–79. doi: 10.1007/s00234-011-0872-0
11. Ghazi-Birry HS, Brown WR, Moody DM, Challa VR, Block SM, Reboussin DM. Human germinal matrix: venous origin of hemorrhage and vascular characteristics. *AJNR Am J Neuroradiol.* (1997) 18:219–29.
12. Ramenghi LA, Supramaniam V, Fumagalli M, Rutherford M. Brain development and perinatal vulnerability to cerebral damage. In: Buonocore G, Bracci R, Weindling M, editors. *Neonatology. A Practical Approach to Neonatal Diseases*. Milan: Springer Italia (2011). p. 1063–73.
13. Tortora D, Severino M, Malova M, Parodi A, Morana G, Sedlacik J, et al. Differences in subependymal vein anatomy may predispose preterm infants to GMH-IVH. *Arch Dis Child Fetal Neonatal Ed.* (2018) 103:F59–65. doi: 10.1136/archdischild-2017-312710
14. Ramenghi LA, Fumagalli M, Groppo M, Consonni D, Gatti L, Bertazzi PA, et al. Germinal matrix hemorrhage: intraventricular hemorrhage in very-low-birth-weight infants: the independent role of inherited thrombophilia. *Stroke.* (2011) 42:1889–93. doi: 10.1161/STROKEAHA.110.590455
15. Arrigoni F, Parazzini C, Righini A, Doneda C, Ramenghi LA, Lista G, et al. Deep medullary vein involvement in neonates with brain damage: an MR imaging study. *AJNR Am J Neuroradiol.* (2011) 32:2030–6. doi: 10.3174/ajnr.A2687
16. Ramenghi LA, Gill BJ, Tanner SF, Martinez D, Arthur R, Levene MI. Cerebral venous thrombosis, intraventricular haemorrhage and white matter lesions in a preterm newborn with factor V (Leiden) mutation. *Neuropediatrics.* (2002) 33:97–9. doi: 10.1055/s-2002-32370
17. Kersbergen KJ, Groenendaal F, Benders MJ, van Straaten HL, Niwa T, Nievelstein RA, et al. The spectrum of associated brain lesions in cerebral sinovenous thrombosis: relation to gestational age and outcome. *Arch Dis Child Fetal Neonatal Ed.* (2011) 96:F404–9. doi: 10.1136/adc.2010.201129
18. Tortora D, Martinetti C, Severino M, Uccella S, Malova M, Parodi A, et al. The effects of mild germinal matrix-intraventricular haemorrhage on the developmental white matter microstructure of preterm neonates: a DTI study. *Eur Radiol.* (2018) 28:1157–66. doi: 10.1007/s00330-017-5060-0
19. Ley D, Romantsik O, Vallius S, Sveinsdóttir K, Sveinsdóttir S, Agyemang AA, et al. High presence of extracellular hemoglobin in the periventricular white matter following preterm intraventricular hemorrhage. *Front Physiol.* (2016) 7:330. doi: 10.3389/fphys.2016.00330
20. Takashima S, Mito T, Ando Y. Pathogenesis of periventricular white matter hemorrhages in preterm infants. *Brain Dev.* (1986) 8:25–30. doi: 10.1016/S0387-7604(86)80116-4
21. Leech RW, Alvord EC Jr. Glial fatty metamorphosis: an abnormal response of premyelin glia frequently accompanying periventricular leukomalacia. *Am J Pathol.* (1974) 74:603–12.
22. Leech, RW, Alvord EC Jr. Morphologic variations in periventricular leukomalacia. *Am J Pathol.* (1974) 74:591–602.
23. Wagenaar N, Chau V, Groenendaal F, Kersbergen KJ, Poskitt KJ, Grunau RE, et al. Clinical risk factors for punctate white matter lesions on early magnetic resonance imaging in preterm newborns. *J Pediatr.* (2017) 182:34–40.e1. doi: 10.1016/j.jpeds.2016.11.073
24. Guo T, Chau V, Peyvandi S, Latal B, McQuillen PS, Knirsch W, et al. White matter injury in term neonates with congenital heart diseases: topology & comparison with preterm newborns. *Neuroimage.* (2019) 185:742–9. doi: 10.1016/j.neuroimage.2018.06.004
25. Stolwijk LJ, Keunen K, de Vries LS, Groenendaal F, van der Zee DC, van Herwaarden MYA, et al. Neonatal surgery for noncardiac congenital anomalies: neonates at risk of brain injury. *J Pediatr.* (2017) 182:335–41.e1. doi: 10.1016/j.jpeds.2016.11.080
26. Sannia A, Natalizia AR, Parodi A, Malova M, Fumagalli M, Rossi A, et al. Different gestational ages and changing vulnerability of the premature brain. *J Matern Fetal Neonatal Med.* (2015) 28 (Suppl. 1):2268–72. doi: 10.3109/14767058.2013.796166
27. El-Khoury N, Braun A, Hu F, Pandey M, Nedergaard M, Lagamma EF, et al. Astrocyte end-feet in germinal matrix, cerebral cortex, and white matter in developing infants. *Pediatr Res.* (2006) 59:673–9. doi: 10.1203/01.pdr.0000214975.85311.9c
28. Buser JR, Segovia KN, Dean JM, Nelson K, Beardsley D, Gong X, et al. Timing of appearance of late oligodendrocyte progenitors coincides with enhanced susceptibility of preterm rabbit cerebral white matter to hypoxia-ischemia. *J Cereb Blood Flow Metab.* (2010) 30:1053–65. doi: 10.1038/jcbfm.2009.286
29. Back SA, Luo NL, Borenstein NS, Levine JM, Volpe JJ, Kinney HC. Late oligodendrocyte progenitors coincide with the developmental window of vulnerability for human perinatal white matter injury. *J Neurosci.* (2001) 21:1302–12. doi: 10.1523/JNEUROSCI.21-04-01302.2001
30. Martinez-Biarge M, Groenendaal F, Kersbergen KJ, Benders MJNL, Foti F, van Haastert IC, et al. Neurodevelopmental outcomes in preterm infants with white matter injury using a new MRI classification. *Neonatology.* (2019) 116:227–35. doi: 10.1159/000499346
31. Arberet C, Proisy M, Fausser JL, Curt M, Bétrémieux P, Tréguier C, et al. Isolated neonatal MRI punctate white matter lesions in very preterm neonates and quality of life at school age. *J Neonatal Perinatal Med.* (2017) 10:257–66. doi: 10.3233/NPM-1691

Conflict of Interest: The authors declare that the research was conducted in the absence of any commercial or financial relationships that could be construed as a potential conflict of interest.

frontiers in Neurology

HYPOTHESIS AND THEORY
published: 02 August 2021
doi: 10.3389/fneur.2021.636740

Plasma Leak From the Circulation Contributes to Poor Outcomes for Preterm Infants: A Working Hypothesis

Yvonne A. Eiby[1]*, *Barbara E. Lingwood*[1,2] and *Ian M. R. Wright*[1,3,4]

[1] Faculty of Medicine, Perinatal Research Centre, Centre for Clinical Research, The University of Queensland, Brisbane, QLD, Australia, [2] Department of Neonatology, Royal Brisbane and Women's Hospital, Brisbane, QLD, Australia, [3] The School of Medicine, Illawarra Health and Medical Research Institute, University of Wollongong, Wollongong, NSW, Australia, [4] Australian Institute of Tropical Health and Medicine, The College of Medicine and Dentistry, James Cook University, Cairns, QLD, Australia

Preterm infants are at high risk of death and disability resulting from brain injury. Impaired cardiovascular function leading to poor cerebral oxygenation is a significant contributor to these adverse outcomes, but current therapeutic approaches have failed to improve outcome. We have re-examined existing evidence regarding hypovolemia and have concluded that in the preterm infant loss of plasma from the circulation results in hypovolemia; and that this is a significant driver of cardiovascular instability and thus poor cerebral oxygenation. High capillary permeability, altered hydrostatic and oncotic pressure gradients, and reduced lymphatic return all combine to increase net loss of plasma from the circulation at the capillary. Evidence is presented that early hypovolemia occurs in preterm infants, and that capillary permeability and pressure gradients all change in a way that promotes rapid plasma loss at the capillary. Impaired lymph flow, inflammation and some current treatment strategies may further exacerbate this plasma loss. A framework for testing this hypothesis is presented. Understanding these mechanisms opens the way to novel treatment strategies to support cardiovascular function and cerebral oxygenation, to replace current therapies, which have been shown not to change outcomes.

Keywords: hypovolemia, blood pressure, premature infant, volume expansion, cerebral blood flow, brain oxygenation, blood volume, preterm infants

OPEN ACCESS

Edited by:
Bobbi Fleiss,
RMIT University, Australia

Reviewed by:
Gorm Greisen,
Rigshospitalet, Denmark
Jeremy D. Marks,
University of Chicago, United States

***Correspondence:**
Yvonne A. Eiby
y.eiby@uq.edu.au

Specialty section:
This article was submitted to Pediatric Neurology, a section of the journal Frontiers in Neurology

Received: *01 December 2020*
Accepted: *09 July 2021*
Published: *02 August 2021*

Citation:
Eiby YA, Lingwood BE and Wright IMR (2021) Plasma Leak From the Circulation Contributes to Poor Outcomes for Preterm Infants: A Working Hypothesis. Front. Neurol. 12:636740. doi: 10.3389/fneur.2021.636740

INTRODUCTION

Preterm infants are at high risk of poor neurodevelopmental outcome. Survival rates of preterm infants have improved with modern care, such that in a recent study across 10 neonatal networks 87% of infants born at 24–30 wk survived (1). However, these improvements in survival have not resulted in a proportional reduction in rates of disability. In preterm infants born at 24–26 weeks in the US, UK and Sweden, 25–40% of survivors have a moderate to severe disability (2). The reasons for impaired brain development are likely multifaceted and include infection (pre and post-natal), cardiopulmonary immaturity contributing to global hypoxia/ischemia and intra-ventricular hemorrhage. However, continuing occurrence of adverse outcomes in preterm infants indicates that some causes and potential interventions remain to be understood.

It is uncertain whether oxygen delivery is adequate during the first days of life. Healthy preterm infants have resting cerebral blood flows averaging 15 mL/100 g/min (range 7–25 mL/100 g/min), this value is 30% lower for ventilated preterm infants (10 mL/100 g/min) whereas, adult values (45–50 mL/100 g/min) are 3–4.5 x higher (3). However, these global measures of flow may mask the vulnerability of white matter as arterial end zones of periventricular white matter are more sensitive to low perfusion pressure than the brain as a whole (3). This selective vulnerability to ischaemia during hypotension means that preterm infants with a blood pressure < 29–30 mmHg, identified by several studies as the threshold below which cerebral autoregulation fails, are likely to have lower flow to white matter than global measures predict (4). But caution is necessary when applying this single blood pressure threshold as maturation-dependent differences in mean blood pressures are observed clinically, such that mean blood pressures increase with gestational age (5). In addition to low perfusion, hypoxemia may occur in individuals with shunts due to delivery of poorly oxygenated blood to the brain (6). Evidence of low cerebral tissue oxygenation, elevated oxygen extraction or low venous oxygen saturation, suggest that in some preterm infants, oxygen extraction is approaching the limit of supply leaving these infants at risk of brain injury (6–8). Infants < 1,250 g who died or had severe neuroradiographic abnormalities had significantly lower average cerebral oxygen saturation than infants that survived without abnormalities (67 vs. 72%; $p = 0.02$) (8). Preterm infants with elevated cerebral oxygen extraction (cFTOE > 0.4) had increased risk of death or brain injury (7). In a small group of preterm infants, cerebral venous saturation was 55% (3). In adults and term infants, cerebral venous oxygen saturation is about 65%, and it has been suggested that the lower values observed in preterm infants may indicate inadequate supply (3). Together these findings support the concept that cardiopulmonary immaturity is a significant contributor to poor neurodevelopmental outcomes in preterm infants.

The traditional approach to supporting cardiovascular function and protecting the brain in preterm infants has focussed on cardiac performance. Standard treatments include crystalloid volume expansion and inotropic support, usually with dopamine or dobutamine. Cochrane reviews indicate that neither treatment has improved long-term neurodevelopmental outcomes (9, 10). Furthermore, there is mounting evidence that both approaches may be associated with poorer outcomes. Extremely preterm infants exposed to antihypotensive therapies had an increased risk of death/neurodevelopmental impairment (OR 1.836, 95% CI 0.709–3.307) even when initial markers of illness were accounted for in the statistical model (11). Despite this, these approaches still form the mainstay of cardiovascular support in clinical practice in preterm infants, as there is no effective alternative approach to fill this therapeutic void. There is a critical need for more effective approaches to cardiovascular support and therefore reduction in brain injury in these very preterm infants. The purpose of this paper is to stimulate discussion about contributors to cardiovascular instability and potential new interventions to address these contributors.

Existing treatment strategies have largely ignored a whole area of cardiovascular physiology – loss of plasma from the circulation, occurring at the capillaries. We propose that specific preterm vulnerabilities at this level lead to hypovolemia, subsequent hypotension and/or low cardiac output and ultimately inadequate cerebral blood flow.

OUR HYPOTHESIS

We propose that, in the preterm infant, high capillary permeability, altered hydrostatic and oncotic pressure gradients, and reduced lymphatic return all combine to increase net loss of plasma from the circulation, resulting in hypovolemia; and that this is a significant driver of cardiovascular instability and poor cerebral oxygenation.

An Old Paradigm Revisited – Hypovolemia Does Occur in PreTerm Infants Soon After Birth

Current belief is that hypovolemia is not a significant contributor to mortality or morbidity in preterm infants. This conclusion is largely based on the ineffectiveness of crystalloid solution for improving outcomes (10). It is assumed that if volume expansion (predominantly with saline) does not improve outcomes, then hypovolemia is not a significant contributor to poor outcomes. We propose that failure of volume expansion with saline does not indicate absence of hypovolemia but is due to the inherent characteristics of the preterm circulation. The capillaries in the preterm infant are significantly more permeable than in the adult, such that saline is retained within the circulation for a very short time (85% lost within 10 min) (12–14) and thus effective volume expansion cannot be achieved with saline. In addition, administration of excessive volumes of saline may lead to accumulation of fluid within the tissue, acidosis and poor outcomes (15–17). Likewise, studies of colloids for volume expansion in preterm infants have failed to improve acute cardiovascular function or long-term outcomes (18–20) as colloids are not effective at increasing blood volume. As for saline, colloids are rapidly lost from the circulation. This is evidenced by a lack of sustained increase in oncotic pressure and/or protein concentration following colloid infusion (20, 21). A similar lack of effect is observed in sick adults where an increase in capillary permeability is cited as a potential cause (22). These studies indicate that permeability of preterm capillaries is so high it allows plasma proteins to rapidly leak out of the circulation. So failure of crystalloids or colloids to improve outcomes is due to their ineffectiveness at increasing blood volume rather than the absence of hypovolemia.

Evidence for Hypovolemia in PreTerm Infants

Early measures of blood volume relied on labeled plasma and dyes and reported higher average values for preterm compared to term infants (83–109 vs. 75–99 mL/kg across multiple studies) (23–26). As a result, current guidelines estimate blood volume to be greater in preterm than term babies, for example 100 vs. 80 mL/kg (27) or 90–95 vs. 80–85 ml/kg (28) (for both preterm

vs. term infants, respectively). However, it has been suggested that these early volume measurements in preterm infants have provided erroneous results due to rapid loss of the small tracers from the circulation (29). More recent studies using larger tracers, have suggested lower blood volumes for preterm infants than previously reported (68.6, 77.9, 72.3, and 71 mL/kg) (29–32). Importantly, the range of blood volumes reported in both these old and newer studies are highly variable, for example 55–134, 46–131, 49–119, 53–105, 45–103 mL/kg. It is possible that babies at the lower end of these ranges are hypovolemic. These low blood volumes may be due to loss of plasma from the circulation. Even in term babies where clinical care has altered less than in preterm babies, large shifts in plasma volume soon after birth have been reported (25, 26, 33).

Echocardiographic evidence of hypovolemia is lacking but this may be due to technical limitations rather than absence of hypovolemia. Even in adults, no echo parameter has been shown to be a reliable predictor of measured hypovolemia (34). We are not aware of any studies that have compared direct measures of blood volume with echo parameters such as atrial and IVC dimensions in neonates.

Studies of delayed cord clamping support early plasma loss. Even after delayed cord clamping, 16% of preterm infants (<32 wk) have a blood volume lower than 63 mL/kg (30). Earlier studies measuring blood volume after DCC show that much of the initial blood volume increase is lost within the first 4 h after birth (35, 36) as predicted by our hypothesis. The resultant increased red cell mass (37) would explain why cerebral hemoglobin concentration is increased but may not be sufficient to counteract the volume effects of plasma loss.

We have conducted extensive studies in preterm piglets at 98/115 d gestation where respiratory requirements, cardiovascular instability, thermoregulation and other factors are similar to a human neonate born at 27 wk gestation (38). We measured blood volume using a large tracer that does not rapidly leak from the circulation. Blood volume 5 h after birth in preterm piglets is significantly lower than in spontaneously born term piglets at 18 h old ($p < 0.001$, **Figure 1**) (39) further supporting that hypovolemia is already present by this time. Parallel data in the same animals indicates an increase in hemoglobin levels in the 6 h after birth (**Figure 2**) suggesting that the low blood volume observed is due to loss of plasma. There is limited data describing changes in hemoglobin levels in human infants in the absence of externally administered fluids however, similar fluid shifts to those seen in the preterm piglet can not be excluded. Our discussions below describe a hypothesis that a similar loss of plasma volume may contribute to poor neurodevelopmental outcomes in some preterm infants.

Consequences of Hypovolemia

We have already demonstrated that preterm piglets are extremely sensitive to low preload and hypovolemia, and unable to maintain blood pressure or cerebral blood flow when blood volume is reduced (40, 41). This is in contrast to term piglets where removal of similar blood volumes/kg also results in reduced blood pressure but not reduced cerebral blood flow (40). These differing responses may be due to immaturity of neurohumoral compensatory systems such as sympathetic and adrenergic control of the circulation, RAAS and the baroreflex (42–48). Thus, hypovolemia in preterm infants due to rapid early loss of plasma may contribute to adverse preterm outcomes.

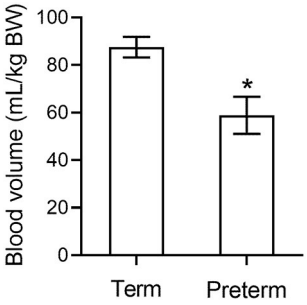

FIGURE 1 | Blood volume in preterm piglets ($n = 26$) is significantly lower than in term piglets ($n = 3$) (39). * indicates $p < 0.001$.

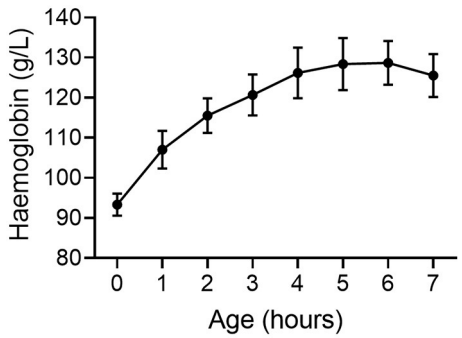

FIGURE 2 | Hemoglobin concentration increases following birth in very preterm piglets ($n = 10$) suggesting a loss of plasma from the circulation and a reduction in blood volume (39). Mean ± SEM.

WHAT ARE THE DETERMINANTS OF PLASMA LOSS AT THE CAPILLARY?

The net movement and type of fluid leaving capillaries is determined by biophysical forces, structural elements and biological moderators, such as inflammation. Multiple biophysical forces affect movement of fluid in or out of the capillary and these are described by the Starling equation:

$$\mathbf{Jv/A = Lp\ \left((P_c - P_i) - \sigma\ \left(\pi_p - \pi_i\right)\right)}$$

where Jv/A = filtration rate/unit area; Lp = filtration co-efficient; P = hydrostatic pressure in capillary or interstitial tissue; σ = reflection co-efficient; π = oncotic pressure of plasma or interstitial fluid. Thus, filtration is determined by capillary permeability in combination with hydrostatic and oncotic pressure gradients. Loss from the circulation is also determined by the rate at which fluid in the tissue is returned to the circulation via the lymphatic vessels. In the fetus, loss from the capillaries is very high but is matched by very high

lymphatic return (49, 50). As a result, plasma volume remains stable. Lymph flow may be operating near capacity, resulting in a system that is close to tipping point. Thus, even small changes in the system (e.g., increased capillary permeability, low oncotic pressure, increased hydrostatic pressure gradient or reduced lymph flow) will result in loss of plasma from the circulation (**Figure 3**). Thus, we hypothesis that the classic Starling equilibrium is thus uniquely disturbed in the preterm infant with the resulting disequilibrium leading to hypovolemia.

Capillary Permeability Is High in PreTerm Infants and Increases With Inflammation

Capillary permeability decreases with developmental maturity. Estimation of blood volume using indocyanine green in human infants consistently reports higher values than hemoglobin subtype dilution, suggesting rapid leakage of the dye out of the vascular space (29). Turnover of albumin from the circulation is 18.4 ± 6.8%/h in term babies (51, 52) which is 3–4 times faster than the 5%/h reported in healthy adults (26, 51). This rapid turnover of albumin indicates a higher rate of capillary leak. In the sheep fetus, intravascular loss of infused saline is 93–94% over the first hour compared to 60–70% in the term newborn (12, 13). In sheep, the fetal whole body capillary filtration coefficient may be 5–6 times that of the adult (14). These values are supported by measures of lymphatic flow that are markedly higher in lambs compared to adults and are higher still in the fetus (49, 50). These very high filtration rates are driven, at least partly, by high capillary permeability.

There is very limited information regarding capillary structure and ultrastructure in preterm infants and how this may contribute to capillary leak and plasma volume loss. Many vessels in the rapidly growing organism are in an angiogenic state and these immature vessels will therefore be more leaky (53). Ultrastructure changes are thought to contribute to capillary leak in adults with conditions such as sepsis or tumors (53–55). Studies assessing capillary ultrastructure in preterm neonates are lacking but whole-body rapid growth necessitates vasculogenesis so it is likely that various aspects of capillary ultrastructure are immature in preterm infants. Investigations of the development of critical structural components such as the calyx, pericytes and gap junctions and these are an essential component to understanding preterm blood volume changes after birth.

Inflammation exacerbates this trans-capillary leak (56). In older children and adults both sepsis and the resultant inflammation contribute to leak as part of septic shock (55). Preterm infants have a vigorous inflammatory response compared to older babies and have a limited ability to produce anti-inflammatory mediators (57). There is an inverse association between gestation (23–28 wk) and blood concentrations of numerous inflammation-related proteins, even on day 1 of post-natal life and in the absence of pre-existing inflammation (57). Other neonatal conditions, such as hypoxic ischemic encephalopathy, are also associated with both increased inflammatory response and capillary leak within the brain parenchyma. It is thus well-established that inflammation causes an increase in capillary permeability at all ages (14). Mathematical modeling suggests the increases in capillary permeability that may occur during mild inflammation would result in up to 5x the rate of plasma loss (58). Therefore, our hypothesis is that in some preterm infants systemic inflammation is contributing to excessive fluid movement into the tissue in the first hours of life.

The Oncotic Pressure Gradient Is Decreased in PreTerm Infants

The oncotic pressure gradient across the capillary membrane is generated by the presence of large protein molecules in the capillary and opposes movement of fluid out of the capillary (**Figure 3**). Preterm infants have low plasma protein levels (19 g/l at 26 wk compared to 31 g/L at term) (59), as do our preterm piglets (25 g/L compared to 48 g/L at term). Low plasma protein levels in preterm infants may limit the trans-capillary oncotic gradient favoring movement of fluid out of capillaries. Numerous clinical studies have shown an association of low plasma protein levels in preterm infants with poor cardiovascular function and adverse outcomes (60, 61). At 24 h of life, very preterm infants with low plasma protein levels had lower blood pressure and longer capillary refill times compared to those with normal plasma protein levels, even after adjusting for gestational age (both $p < 0.001$) (60). Our hypothesis predicts that adverse outcomes in those with low protein levels may be due to the low oncotic pressure gradient contributing to plasma loss and hypovolemia.

The Hydrostatic Pressure Gradient Across the Capillary Increase After Birth

An increase in the hydrostatic pressure gradient across a capillary will increase fluid loss (**Figure 3**). It is unknown whether the hydrostatic pressure gradient increases after birth in preterm infants as measures of tissue pressure and capillary pressure are not feasible. Some reports suggest that the transition from a fetal to neonatal circulation is associated with an increase in blood pressure (62, 63), while others suggest little change at birth (64). It is also unclear if increases in arterial pressure lead to increases in capillary hydrostatic pressure. There may be a decrease in tissue hydrostatic pressure at birth due to removal of the externally applied intra-amniotic fluid pressure of 1–8 mmHg (65). Additionally, the initial high transcutaneous fluid loss that occurs after birth in very preterm infants may act to maintain a low tissue hydrostatic pressure (66). So the hydrostatic pressure gradient between the capillary and the tissue may increase even if capillary pressure is unchanged. Whether this combination of pressure changes will increase the trans-capillary pressure gradient and favor fluid movement out of the circulation into the tissue needs to be addressed in an animal model. Adult mathematical modeling based on the Starling equation of fluid movement suggests that even small changes in blood pressure could result in significant movement of fluid out of the vasculature (58).

When inotropes (or indeed any treatment) are used to increase blood pressure in preterm infants, the increase in driving pressure may increase the hydrostatic pressure gradient across the capillary. This may actually exacerbate fluid loss according

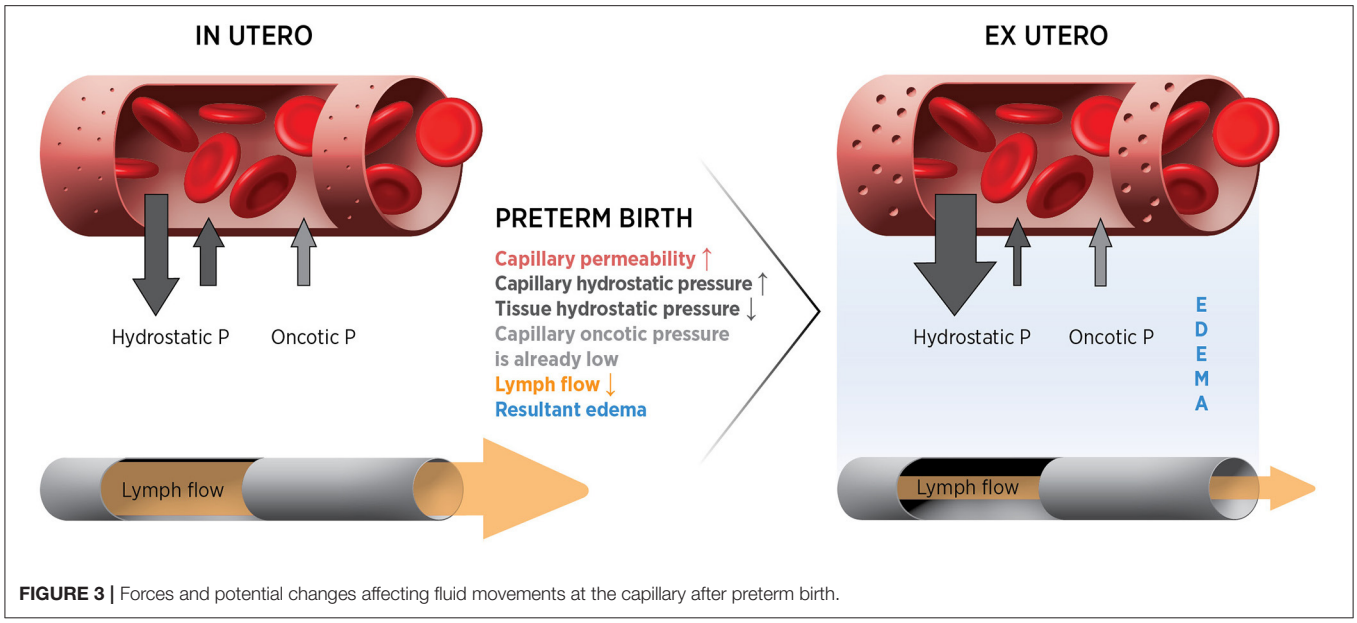

FIGURE 3 | Forces and potential changes affecting fluid movements at the capillary after preterm birth.

the Starling equation (**Figure 3**). Our preterm piglets treated with dopamine had a modest increase in blood pressure, as do preterm infants treated with dopamine. The blood pressure after treatment ended was 7 mmHg below pre-treatment levels. This reduction in blood pressure may be due to an increase in driving pressure produced by dopamine leading to an increase in the hydrostatic pressure gradient across the capillary and thus plasma loss. It needs to be determined if this partly explains why dopamine and dobutamine are ineffective for improving outcomes (9) and why "permissive hypotension" does not result in worse outcomes (67).

Lymphatic Flow May Be Insufficient to Match Plasma Filtration

The interstitial tissue is capable of holding a large fluid volume, as demonstrated by the clinical condition of fetal hydrops. If this fluid is not returned to the circulation, hypovolemia will result. Downstream capillaries are no longer considered to be in a state of sustained reabsorption (68) so fluid balance is critically dependent on adequate lymphatic return. Lymphatic flows in fetal sheep are 2.5–5x higher than in adult sheep (49, 50). This high flow rate in the fetus is adequate to deal with high capillary filtration rates *in utero*. However, it is unclear whether preterm infants may be operating at the upper limit of lymphatic return with little reserve capacity to compensate for the increases in filtration after birth. Indeed, the lymphatic structure and function of preterm infants is largely unknown and warrants investigation.

Iatrogenic factors may further compromise lymphatic return in the *ex utero* preterm. Lymphatic return in fetal sheep is extremely sensitive to increases in intrathoracic pressure which impede flow. Positive pressure support increases intrathoracic pressure and may thus also impede lymph flow, indeed it may cease altogether at intrathoracic pressures only marginally above normal (49). This may, along with increased cardiac output due to improved venous return, contribute to reduction in cardiovascular support required by preterm neonates with the reduced mean airway pressures used in continuous positive pressure rather than ventilator driven support (69, 70). Systemic inflammation, which is common in preterm infants (57), has also been shown to negatively influence lymphatic contraction which is critical to maintaining high flow rates particularly in an immobile population (71). So animal experiments designed to test if either elevated intrathoracic pressure or inflammation limits lymphatic flow are necessary to determine if tissue clearance of fluid is compromised.

DISCUSSION

The evidence presented supports our hypothesis that preterm infants are at high risk of mortality and morbidity because of a unique conjunction of features in the small vessels that make up the majority of the circulatory system. These include that:

- Capillary permeability increases with prematurity, and with inflammation;
- Low plasma protein levels in preterm neonates result in reduced oncotic pressure gradients at the capillary;
- Capillary hydrostatic pressure gradients are increased postnatally in preterm neonates;
- Preterm neonates have impaired postnatal lymphatic flow.

All of these factors would contribute to plasma volume loss resulting in hypotension, and reduced cerebral blood flow and oxygenation in preterm infants. However, it is unclear which factor/s have the greatest influence on plasma loss from the circulation. To test our hypothesis we are undertaking experiments that will provide quantitative assessment of each factor that could drive plasma loss from the circulation and

TABLE 1 | Experiments in preterm and term piglets to test our working hypothesis.

Aspects of hypothesis to test	Data required
Capillary permeability is increased in preterm neonates	Measure permeability as the rate that different sized molecules are lost from the circulation in preterm and term neonates. This will also determine the size required for effective volume expansion.
Capillary permeability is increased with inflammation	Measure the association between inflammation levels and the change in permeability over the 12 h after birth.
Low oncotic pressure gradients are associated with loss of plasma from the circulation	Measure plasma and tissue protein concentrations (oncotic pressure gradient). Is this associated with the change in plasma volume between birth and 12 h old?
Increased capillary hydrostatic pressure gradient in preterm neonates	Estimate hydrostatic pressure gradient by measuring the difference between blood pressure and tissue pressure. Does this correlate with changes in plasma volume?
Reduced lymphatic flow	Does lymphatic flow decrease across the 12 h after birth?
Lymphatic flow is impaired by inflammation	Measure the association between inflammation levels and lymphatic flow across the first 12 h of life.
Lymphatic flow is impaired by high intrathoracic pressure	Measure lymphatic flow during low and high intrathoracic pressure (ventilation induced mean airway pressure).
High plasma loss from the circulation results in edema, hypotension and low cerebral oxygenation	Association between change in plasma/blood volume and edema (tissue water content), blood pressure and cerebral brain oxygenation.
Priority treatment targets	From above experiments, quantitative changes in factors will be used to model the influence of each factor on plasma loss from the circulation.

factors that may reduce lymphatic flow (**Table 1**). These experiments also allow evaluation of resultant edema, hypovolemia, hypotension, and poor cerebral oxygenation. Using preterm piglets delivered when developmentally similar to preterm infants born at 27 wk gestation and cared for using standard intensive care techniques, we are able to observe changes in cardiovascular and lymphatic physiology over the first 12 h of life, when cardiovascular instability typically occurs in preterm infants.

This quantitative data can be used to create a mathematical model of the Starling equation specific to the preterm infant. By expanding this model to include lymphatic return and blood volume we can measure the relative contribution of each factor to identify priority targets for new treatments to effectively support preterm cardiovascular function. Subsequent experiments would then test interventions targeting critical factors identified by the modeling.

1. If high capillary permeability is a major contributor to plasma loss then studies would aim to develop volume expanders large enough to stay within the circulation. Albumin sized volume expanders are not suitable because these leak from the circulation (39) and potentially cause adverse effects. Volume expanders based on larger molecules that remain within the vascular space are likely to be more effective but their use must be tempered by the associated risk. Our proposed permeability studies with different sized molecules will determine the size required for effective volume expansion. We have shown that red blood cell transfusion is effective for increasing blood volume in preterm piglets (72). Early (within 12 h of birth) transfusions as proposed for treatment of anemia of prematurity (73) and could provide an effective form of volume expansion. Understanding the developmental structural changes occurring in the capillaries that underlie these functional changes will identify further possibilities for therapeutic interventions that have not been considered in this vulnerable group. Other more novel target pathways that are known to moderate vascular leak would include targeting Vascular Endothelial Growth Factor (VEGF) mediated leak or modifying the effects of local gasotransmitter-mediated (Nitric oxide, Hydrogen sulfide) capillary leak (74), but appropriate animal and then human studies will be required.
2. If the hydrostatic pressure gradient across the capillary is a major contributor to plasma loss, then studies of the effects of blood pressure targets, "permissive hypotension" and of various inotropic interventions on plasma loss could be conducted. The exact point at which raising the blood pressure is likely to be effective rather than counterproductive is not known (11, 67, 75), nor is the effect of constrictive vs. dilatory inotropes. It is likely to vary by gestation, post-natal age and individual circumstances and that blanket algorithms are not serving our varied clinical populations.
3. Our studies will indicate if decreased lymphatic flow is a major contributor to plasma loss and whether this is due to increased intrathoracic pressure or inflammation. If high intrathoracic pressure is the critical factor then this would support the continued use of lower intrathoracic pressure ventilation strategies. If inflammation is limiting lymphatic flow then there are a number of pharmacological approaches that may be beneficial including corticosteroids or other anti-inflammatory agents, acting to improve lymphatic contraction and potentially also decrease capillary permeability. There is some evidence that administration of low-dose hydrocortisone at 12–48 h after birth results in decreased mortality (76). These

studies would indicate if administration needs to occur at birth in order to prevent early plasma loss. To our knowledge treatment this early has never been trialed.

In summary we propose that a major driver of cardiovascular compromise in the preterm infant is occurring at the level of the microcirculation with a net volume loss that exceeds the ability to compensate. This may lead to both increased mortality and long-term disability and is an urgent area for further research to improve preterm outcomes.

DATA AVAILABILITY STATEMENT

The raw data supporting the conclusions of this article will be made available by the authors, without undue reservation.

ETHICS STATEMENT

The animal study was reviewed and approved by Health Sciences Animal Ethics Committee, The University of Queensland.

AUTHOR CONTRIBUTIONS

All authors contributed to conception and design, statistical analysis and interpretation, wrote and revised the manuscript and approved the submitted version.

FUNDING

This program of research has been funded by the National Health and Medical Research Council of Australia (NHMRC; APP1127142), the Royal Brisbane and Women's Hospital Foundation and The University of Queensland (UQMEI1835189).

ACKNOWLEDGMENTS

The authors acknowledge the support of scientific collaborators Drs. Tracey Bjorkman and Stephanie Miller, our veterinary team, Drs. Cora Lau, Helen Keates and Nicholas Cowling, and veterinary nurses Sharon Moore and Karina Rowe.

REFERENCES

1. Helenius K, Sjörs G, Shah PS, Modi N, Reichman B, Morisaki N, et al. Survival in very preterm infants: an international comparison of 10 national neonatal networks. *Pediatrics.* (2017) 140:e20171264. doi: 10.1542/peds.2017-1264
2. Patel R. Short- and long-term outcomes for extremely preterm infants. *Am J Perinatol.* (2016) 33:318–28. doi: 10.1055/s-0035-1571202
3. Greisen G, Borch K. White matter injury in the preterm neonate: the role of perfusion. *Dev Neurosci.* (2001) 23:209–12. doi: 10.1159/000046145
4. Børch K, Lou HC, Greisen G. Cerebral white matter blood flow and arterial blood pressure in preterm infants. *Acta Paediatr.* (2010) 99:1489–92. doi: 10.1111/j.1651-2227.2010.01856.x
5. Batton B, Li L, Newman NS, Das A, Watterberg KL, Yoder BA, et al. Evolving blood pressure dynamics for extremely preterm infants. *J Perinatol.* (2014) 34:301–5. doi: 10.1038/jp.2014.6
6. Andersen CC, Stark MJ. Haemoglobin transfusion threshold in very preterm newborns: a theoretical framework derived from prevailing oxygen physiology. *Med Hypotheses.* (2012) 78:71–4. doi: 10.1016/j.mehy.2011.09.044
7. Balegar KK, Stark MJ, Briggs N, Andersen CC. Early cerebral oxygen extraction and the risk of death or sonographic brain injury in very preterm infants. *J Pediatr.* (2014) 164:475–80.e1. doi: 10.1016/j.jpeds.2013.10.041
8. Chock VY, Kwon SH, Ambalavanan N, Batton B, Nelin LD, Chalak LF, et al. Cerebral oxygenation and autoregulation in preterm infants (early NIRS study). *J Pediatr.* (2020) 227:94–100.e1. doi: 10.1016/j.jpeds.2020.08.036
9. Osborn DA, Paradisis M, Evans N. The effect of inotropes on morbidity and mortality in preterm infants with low systemic or organ blood flow. *Cochrane Db Syst Rev.* (2007) CD005090. doi: 10.1002/14651858.CD005090.pub2
10. Osborn DA, Evans N. Early volume expansion for prevention of morbidity and mortality in very preterm infants. *Cochrane Database Syst Rev.* (2004) 2004:CD002055. doi: 10.1002/14651858.CD002055.pub2
11. Batton B, Li L, Newman NS, Das A, Watterberg KL, Yoder BA, et al. Early blood pressure, antihypotensive therapy and outcomes at 18-22 months' corrected age in extremely preterm infants. *Arch Dis Child Fetal Neonatal Ed.* (2016) 101:F201–6. doi: 10.1136/archdischild-2015-308899
12. Brace RA. Fetal blood volume responses to intravenous saline solution and dextran. *Am J Obstet Gynecol.* (1983) 147:777–81. doi: 10.1016/0002-9378(83)90036-4
13. Harake B, Power GG. Thoracic duct lymph flow: a comparative study in newborn and adult sheep. *J Dev Physiol.* (1986) 8:87–95.
14. Brace RA, Gold PS. Fetal whole-body interstitial compliance, vascular compliance, and capillary filtration coefficient. *Am J Physiol.* (1984) 247:R800–5. doi: 10.1152/ajpregu.1984.247.5.R800
15. Ewer AK, Tyler W, Francis A, Drinkall D, Gardosi JO. Excessive volume expansion and neonatal death in preterm infants born at 27-28 weeks gestation. *Paediatr Perinat Epidemiol.* (2003) 17:180–6. doi: 10.1046/j.1365-3016.2003.00474.x
16. Reddi BA. Why is saline so acidic (and does it really matter?. *Int J Med Sci.* (2013) 10:747–50. doi: 10.7150/ijms.5868
17. Eisenhut M. Adverse effects of rapid isotonic saline infusion. *Arch Dis Child.* (2006) 91:797. doi: 10.1136/adc.2006.100123
18. Group NT. Randomised trial of prophylactic early fresh-frozen plasma or gelatin or glucose in preterm babies: outcome at 2 years. *Lancet.* (1996) 348:229–32. doi: 10.1016/S0140-6736(95)12506-X
19. Emery EF, Greenough A, Gamsu HR. Randomised controlled trial of colloid infusions in hypotensive preterm infants. *Arch Dis Child.* (1992) 67:1185–8. doi: 10.1136/adc.67.10_Spec_No.1185
20. Bignall S, Bailey PC, Bass CA, Cramb R, Rivers RP, Wadsworth J. The cardiovascular and oncotic effects of albumin infusion in premature infants. *Early Hum Dev.* (1989) 20:191–201. doi: 10.1016/0378-3782(89)90005-4
21. Bhat R, Javed S, Malalis L, Vidyasagar D. Critical care problems in neonates. Colloid osmotic pressure in healthy and sick neonates. C*rit Care Med.* (1981) 9:563–7. doi: 10.1097/00003246-198108000-00001
22. Fleck A, Raines G, Hawker F, Trotter J, Wallace PI, Ledingham IM, et al. Increased vascular permeability: a major cause of hypoalbuminaemia in disease and injury. *Lancet.* (1985) 1:781–4. doi: 10.1016/S0140-6736(85)91447-3
23. Sisson TRC, Whalen LE. The blood volume of infants. *J Pediatr.* (1960) 56:43–7. doi: 10.1016/S0022-3476(60)80287-9
24. Bauer K, Linderkamp O, Versmold HT. Short-term effects of blood transfusion on blood volume and resting peripheral blood flow in preterm infants. *Acta Paediatr.* (1993) 82:1029–33. doi: 10.1111/j.1651-2227.1993.tb12804.x
25. Usher R, Lind J. Blood volume of the newborn premature infant. *Acta Paediatr Scand.* (1965) 54:419–31. doi: 10.1111/j.1651-2227.1965.tb06397.x
26. Steele MW. Plasma volume changes in the neonate. *Am J Dis Child.* (1962) 103:10–8. doi: 10.1001/archpedi.1962.02080020014003
27. Australian National Blood Authority. *Patient Blood Management Guidelines: Module 6 Neonatal and Paedatric, Canberra.* (2016). p. 62. Available online at: https://www.blood.gov.au/pbm-module-6 (accessed July 06, 2021).

28. *World Federation of Societies of Anesthesiologists*. Available online at: https://resources.wfsahq.org/atotw/neonatal-anaesthesia-2-anaesthesia-for-neonates-with-abdominal-wall-defects/ (accessed July 06, 2021).
29. Leipala JA, Talme M, Viitala J, Turpeinen U, Fellman V. Blood volume assessment with hemoglobin subtype analysis in preterm infants. *Biol Neonate.* (2003) 84:41–4. doi: 10.1159/000071442
30. Aladangady N, McHugh S, Aitchison TC, Wardrop CA, Holland BM. Infants' blood volume in a controlled trial of placental transfusion at preterm delivery. *Pediatrics.* (2006) 117:93–8. doi: 10.1542/peds.2004-1773
31. Strauss RG, Mock DM, Johnson KJ, Cress GA, Burmeister LF, Zimmerman MB, et al. A randomized clinical trial comparing immediate versus delayed clamping of the umbilical cord in preterm infants: short-term clinical and laboratory endpoints. *Transfusion.* (2008) 48:658–65. doi: 10.1111/j.1537-2995.2007.01589.x
32. Mock DM, Matthews NI, Zhu S, Burmeister LF, Zimmerman MB, Strauss RG, et al. Red blood cell (RBC) volume can be independently determined in vivo in humans using RBCs labeled at different densities of biotin. *Transfusion.* (2011) 51:148–57. doi: 10.1111/j.1537-2995.2010.02770.x
33. Sisson TR, Whalen LE, Telek A. The blood volume of infants. II. The premature infant during the first year of life. *J Pediatr.* (1959) 55:430–46. doi: 10.1016/S0022-3476(59)80281-X
34. McLean AS. Echocardiography in shock management. *Crit Care.* (2016) 20:275. doi: 10.1186/s13054-016-1401-7
35. Usher R, Shephard M, Lind J. The blood volume of the newborn infant and placental transfusion. *Acta Paediatr.* (1963) 52:497–512. doi: 10.1111/j.1651-2227.1963.tb03809.x
36. Saigal S, O'Neill A, Surainder Y, Chua LB, Usher R. Placental transfusion and hyperbilirubinemia in the premature. *Pediatrics.* (1972) 49:406–19.
37. Tarnow-Mordi W, Morris J, Kirby A, Robledo K, Askie L, Brown R, et al. Delayed versus immediate cord clamping in preterm infants. *N Engl J Med.* (2017) 377:2445–55. doi: 10.1056/NEJMoa1711281
38. Eiby YA, Wright LL, Kalanjati VP, Miller SM, Bjorkman ST, Keates HL, et al. A pig model of the preterm neonate: anthropometric and physiological characteristics. *PLoS ONE.* (2013) 8:e68763. doi: 10.1371/journal.pone.0068763
39. Eiby YA, Wright IMR, Bjorkman ST, Miller SM, Lingwood BE. *A Practical Method for Measuring Blood Volume in Neonatal Pig*s. Marysville, Australia: Fetal and Neonatal Physiological Society (2019).
40. Eiby YA, Shrimpton NY, Wright IMR, Lumbers ER, Colditz PB, Duncombe GJ, et al. Reduced blood volume decreases cerebral blood flow in preterm piglets. *J Physiol.* (2018) 596:6033–41. doi: 10.1113/JP275583
41. Eiby YA, Lumbers ER, Headrick JP, Lingwood BE. Left ventricular output and aortic blood flow in response to changes in preload and afterload in the preterm piglet heart. *Am J Physiol Regul Integr Comp Physiol.* (2012) 303:R769–R77. doi: 10.1152/ajpregu.00010.2012
42. Fyfe KL, Yiallourou SR, Wong FY, Horne RS. The development of cardiovascular and cerebral vascular control in preterm infants. *Sleep Med Rev.* (2014) 18:299–310. doi: 10.1016/j.smrv.2013.06.002
43. Booth LC, Bennet L, Guild SJ, Barrett CJ, May CN, Gunn AJ, et al. Maturation-related changes in the pattern of renal sympathetic nerve activity from fetal life to adulthood. *Exp Physiol.* (2011) 96:85–93. doi: 10.1113/expphysiol.2010.055236
44. Booth LC, Gunn AJ, Malpas SC, Barrett CJ, Davidson JO, Guild SJ, et al. Baroreflex control of renal sympathetic nerve activity and heart rate in near-term fetal sheep. *Exp Physiol.* (2011) 96:736–44. doi: 10.1113/expphysiol.2011.058354
45. Buckley N, Gootman P, Gootman N, Reddy G, Weaver L, Crane L. Age-dependent cardiovascular effects of afferent stimulation in neonatal pigs. *Neonatology.* (1976) 30:268–79. doi: 10.1159/000240931
46. Buckley NM. Maturation of circulatory system in three mammalian models of human development. *Comp Biochem Physiol Physiol.* (1986) 83:1–7. doi: 10.1016/0300-9629(86)90080-0
47. Buckley NM, Brazeau P, Gootman PM. Maturation of circulatory responses to adrenergic stimuli. *Fed Proc.* (1983) 42:1643–7.
48. Lumbers ER, McCloskey DI, Potter EK. Inhibition of Angiotensin II of baroreflex-evoked activity in cardiac vagal efferent nerves in the dog. *J Physiol London.* (1979) 294:69–80. doi: 10.1113/jphysiol.1979.sp012915
49. Brace RA. Thoracic duct lymph flow and its measurement in chronically catheterized sheep fetus. *Am J Physiol.* (1989) 256:H16–20. doi: 10.1152/ajpheart.1989.256.1.H16
50. Johnson SA, Vander Straten MC, Parellada JA, Schnakenberg W, Gest AL. Thoracic duct function in fetal, newborn, and adult sheep. *Lymphology.* (1996) 29:50–6.
51. Parving HH, Klebe JG, Ingomar CJ. Simultaneous determination of plasma volume and transcapillary escape rate with 131 I-labelled albumin and T-1824 in the newborn. *Acta Paediatr Scand.* (1973) 62:248–52. doi: 10.1111/j.1651-2227.1973.tb08100.x
52. Ingomar CJ, Klebe JG. The transcapillary escape rate of T-1824 in newborn infants of diabetic mothers and newborn infants with respiratory distress or birth asphyxia. *Acta Paediatr Scand.* (1974) 63:565–70. doi: 10.1111/j.1651-2227.1974.tb04848.x
53. Park-Windhol C, D'Amore PA. Disorders of vascular permeability. *Annu Rev Pathol.* (2016) 11:251–81. doi: 10.1146/annurev-pathol-012615-044506
54. McDonald DM, Baluk P. Significance of blood vessel leakiness in cancer. *Cancer Res.* (2002) 62:5381–5.
55. Marx G. Fluid therapy in sepsis with capillary leakage. *Eur J Anaesthesiol.* (2003) 20:429–42. doi: 10.1097/00003643-200306000-00002
56. Wiig H, Swartz MA. Interstitial fluid and lymph formation and transport: physiological regulation and roles in inflammation and cancer. *Physiol Rev.* (2012) 92:1005–60. doi: 10.1152/physrev.00037.2011
57. Leviton A, Fichorova R, Yamamoto Y, Allred EN, Dammann O, Hecht J, et al. Inflammation-related proteins in the blood of extremely low gestational age newborns. The contribution of inflammation to the appearance of developmental regulation. *Cytokine.* (2011) 53:66–73. doi: 10.1016/j.cyto.2010.09.003
58. Levick JR, Michel CC. Microvascular fluid exchange and the revised Starling principle. *Cardiovasc Res.* (2010) 87:198–210. doi: 10.1093/cvr/cvq062
59. Cartlidge PH, Rutter N. Serum albumin concentrations and oedema in the newborn. *Arch Dis Child.* (1986) 61:657–60. doi: 10.1136/adc.61.7.657
60. Bonsante F, Ramful D, Samperiz S, Daniel S, Godeluck A, Robillard PY, et al. Low plasma protein levels at birth are associated with poor cardiovascular adaptation and serious adverse outcome in infants with gestational age <32 weeks: the ProHemie study. *Neonatology.* (2017) 112:114–21. doi: 10.1159/000468916
61. Zimmermann B, Francoise M, Germain JF, Lallemant C, Gouyon JB. Colloid osmotic pressure and neonatal respiratory distress syndrome. *Arch Pediatr.* (1997) 4:952–8. doi: 10.1016/S0929-693X(97)86090-3
62. Vrancken SL, van Heijst AF, de Boode WP. Neonatal hemodynamics: from developmental physiology to comprehensive monitoring. *Front Pediatr.* (2018) 6:87. doi: 10.3389/fped.2018.00087
63. Dawes GS. Changes in the circulation at birth. *Br Med Bull.* (1961) 17:148–53. doi: 10.1093/oxfordjournals.bmb.a069890
64. Crossley KJ, Allison BJ, Polglase GR, Morley CJ, Davis PG, Hooper SB. Dynamic changes in the direction of blood flow through the ductus arteriosus at birth. *J Physiol.* (2009) 587:4695–704. doi: 10.1113/jphysiol.2009.174870
65. Weiner CP, Heilskov J, Pelzer G, Grant S, Wenstrom K, Williamson RA. Normal values for human umbilical venous and amniotic fluid pressures and their alteration by fetal disease. *Am J Obstet Gynecol.* (1989) 161:714–7. doi: 10.1016/0002-9378(89)90387-6
66. Taïeb A. Skin barrier in the neonate. *Pediatr Dermatol.* (2018) 35 (Suppl. 1):s5–s9. doi: 10.1111/pde.13482
67. Ahn SY, Kim ES, Kim JK, Shin JH, Sung SI, Jung JM, et al. Permissive hypotension in extremely low birth weight infants (</=1000 gm). *Yonsei Med J.* (2012) 53:765–71. doi: 10.3349/ymj.2012.53.4.765
68. Bhave G, Neilson EG. Body fluid dynamics: back to the future. *J Am Soc Nephrol.* (2011) 22:2166–81. doi: 10.1681/ASN.2011080865
69. Wintermark P, Tolsa JF, Van Melle G, Forcada-Guex M, Moessinger AC. Long-term outcome of preterm infants treated with nasal continuous positive airway pressure. *Eur J Pediatr.* (2007) 166:473–83. doi: 10.1007/s00431-006-0272-3
70. Levesque BM, Kalish LA, LaPierre J, Welch M, Porter V. Impact of implementing 5 potentially better respiratory practices on neonatal outcomes and costs. *Pediatrics.* (2011) 128:e218–26. doi: 10.1542/peds.2010-3265
71. Liao S, von der Weid PY. Inflammation-induced lymphangiogenesis and lymphatic dysfunction. *Angiogenesis.* (2014) 17:325–34. doi: 10.1007/s10456-014-9416-7
72. Eiby YA, Wright IMR, Bjorkman ST, Miller SM, Colditz PB, Stark MJ, et al. Volume expansion with packed RBCs maintains blood pressure and

cerebral oxygenation more effectively than saline in preterm piglets. In: *Forty-Sixth Meeting of the Fetal and Neonatal Physiology Society*. Marysville, Australia (2019).
73. Andersen CC, Karayil SM, Hodyl NA, Stark MJ. Early red cell transfusion favourably alters cerebral oxygen extraction in very preterm newborns. *Arch Dis Child Fetal Neonatal Ed.* (2015) 100:F433–5. doi: 10.1136/archdischild-2014-307565
74. Dyson RM, Palliser HK, Latter JL, Kelly MA, Chwatko G, Glowacki R, et al. Interactions of the gasotransmitters contribute to microvascular tone (Dys) regulation in the preterm neonate. *PLoS ONE.* (2015) 10:e0121621. doi: 10.1371/journal.pone.0121621
75. Dempsey EM, Al Hazzani F, Barrington KJ. Permissive hypotension in the extremely low birthweight infant with signs of good perfusion. *Arch Dis Child Fetal Neonatal Ed.* (2009) 94:F241–4. doi: 10.1136/adc.2007.124263
76. Baud O, Watterberg KL. Prophylactic postnatal corticosteroids: Early hydrocortisone. *Semin Fetal Neonatal Med.* (2019) 24:202–6. doi: 10.1016/j.siny.2019.04.007

Conflict of Interest: The authors declare that the research was conducted in the absence of any commercial or financial relationships that could be construed as a potential conflict of interest.

Advantages of publishing in Frontiers

OPEN ACCESS
Articles are free to read for greatest visibility and readership

FAST PUBLICATION
Around 90 days from submission to decision

HIGH QUALITY PEER-REVIEW
Rigorous, collaborative, and constructive peer-review

TRANSPARENT PEER-REVIEW
Editors and reviewers acknowledged by name on published articles

Frontiers
Avenue du Tribunal-Fédéral 34
1005 Lausanne | Switzerland

Visit us: www.frontiersin.org
Contact us: info@frontiersin.org | +41 21 510 17 00

REPRODUCIBILITY OF RESEARCH
Support open data and methods to enhance research reproducibility

DIGITAL PUBLISHING
Articles designed for optimal readership across devices

FOLLOW US
@frontiersin

IMPACT METRICS
Advanced article metrics track visibility across digital media

EXTENSIVE PROMOTION
Marketing and promotion of impactful research

LOOP RESEARCH NETWORK
Our network increases your article's readership